

Catalog of Apollo 17 Rocks

Volume 1 — Stations 2 and 3 (South Massif)

By Graham Ryder
Lunar and Planetary Institute

Space and Life Sciences Directorate
Solar System Exploration Division
Office of the Curator #87

January 1993



National Aeronautics and
Space Administration

Lyndon B. Johnson Space Center
Houston, Texas

Catalog of Apollo 17 Rocks

Volume 1 — Stations 2 and 3 (South Massif)

By Graham Ryder
Lunar and Planetary Institute

NASA/Johnson Space Center
Houston, Texas 77058 U.S.A.

January 1993

ACKNOWLEDGEMENTS

The work of producing this volume was accomplished in an excellent manner by Anita Dodson (Lockheed), who transformed rough input into professional output and organized the production virtually single-handedly. She remained cheerful through missed deadlines and broken promises about input, and greatly encouraged work to get done under sometimes difficult circumstances.

This volume was conceived and promoted by the Lunar and Planetary Sample Team under various chairmen, and has taken an inordinate number of years to reach fruition. It was produced with the cooperation of John Dietrich and Jim Gooding, successive Lunar Sample Curators. They provided the facilities needed to do the work: office space, computer assistance, and access to the curatorial laboratories, thin sections, and data center, as well as allocation of personnel to the production. I greatly appreciate the help of the data center personnel (alphabetically) Margo Albores, Sue Goudie, Jenny Seltzer, and Lee Smith, who assisted with the data pack and thin section retrieval, and Carol Schwarz and Linda Watts who did some of the proofing.

I thank various people who have provided photographs or unpublished data and other assistance in clarifying some details. In particular, I thank Paul Warren for supplying some photographs and information, Klaus Keil for returning a large number of thin sections, and Odette James for supplying a large number of reprints.

I appreciate the acquiescence of David Black, the Director of the Lunar and Planetary Institute, to my use of time for this project. The Lunar and Planetary Institute operates under NASA Contract # 4574. This volume is Lunar and Planetary Institute Contribution # 805.

CONTENTS

Introduction	v
The Apollo 17 Mission	v
Apollo and Luna Sampling Locations	vi
Apollo 17 Landing Site Region	vii
Apollo 17 Traverse Area	viii
Numbering of Apollo Samples	x
Sample Inventory	xiii
Sample Descriptions	1
References	355

INTRODUCTION

The Catalog of Apollo 17 rocks is a set of volumes that characterize each of 334 individually numbered rock samples (79 larger than 100 g) in the Apollo 17 collection, showing what each sample is and what is known about it. Unconsolidated regolith samples are not included. The catalog is intended to be used by both researchers requiring sample allocations and a broad audience interested in Apollo 17 rocks. The volumes are arranged geographically, with separate volumes for the South Massif and Light Mantle; the North Massif; and two volumes for the mare plains. Within each volume, the samples are arranged in numerical order, closely corresponding with the sample collection stations. The present volume, for the South Massif and Light Mantle, describes the 55 individual rock fragments collected at Stations 2, 2A, 3, and LRV-5. Some were chipped from boulders, others collected as individual rocks, some by raking, and a few by picking from the soil in the processing laboratory.

Information on sample collection, petrography, chemistry, stable and radiogenic isotopes, rock surface characteristics, physical properties, and curatorial processing is summarized and referenced as far as it is known up to early 1992. The intention has been to be comprehensive--to include all published studies of any kind that provide

information on the sample, as well as some unpublished information. References which are primarily bulk interpretations of existing data or mere lists of samples are not generally included. Foreign language journals were not scrutinized, but little data appears to have been published only in such journals. We have attempted to be consistent in format across all of the volumes, and have used a common reference list that appears in all volumes.

Much valuable information exists in the original Apollo 17 Lunar Sample Information Catalog (1973) based on the intense and expert work of the Preliminary Examination Team. However, that catalog was compiled and published only four months after the mission itself, from rapid descriptions of usually dust-covered rocks, usually without anything other than macroscopic observations, and less often with thin sections and a little chemical data. In the nearly two decades since then, the rocks have been substantially subdivided, studied, and analyzed, with numerous published papers. These make the original Information Catalog inadequate, outmoded, and in some cases erroneous. However, that Catalog contains more information on macroscopic observations for most samples than does the present set of volumes. Considerably more detailed information on the

dissection and allocations of the samples is preserved in the Data Packs in the Office of the Curator.

Where possible, ages based on Sr and Ar isotopes have been recalculated using the "new" decay constants recommended by Steiger and Jäger (*Earth Planet. Sci. Lett.* **36**, 359-362); however, in many of the reproduced diagrams the ages correspond with the "old" decay constants. In this volume, mg' or $Mg' = \text{atomic Mg}/(\text{Mg} + \text{Fe})$.

THE APOLLO 17 MISSION

On December 11, 1972, the Apollo 17 lunar excursion module "Challenger," descending from the Command Service Module "America," landed in a valley near the edge of Mare Serenitatis (Figures 1 and 2). It was the sixth and final landing in the Apollo program. Astronauts Eugene Cernan and Harrison Schmitt spent 72 hours at the site, named Taurus-Littrow from the mountains and a crater to the north. The site was geologically diverse, with the mountain ring of the Serenitatis basin and the lava fill in the valley. The main objectives of the mission were to sample very ancient material such as pre-Imbrian highlands distant from the Imbrium basin, and to sample pyroclastic materials believed

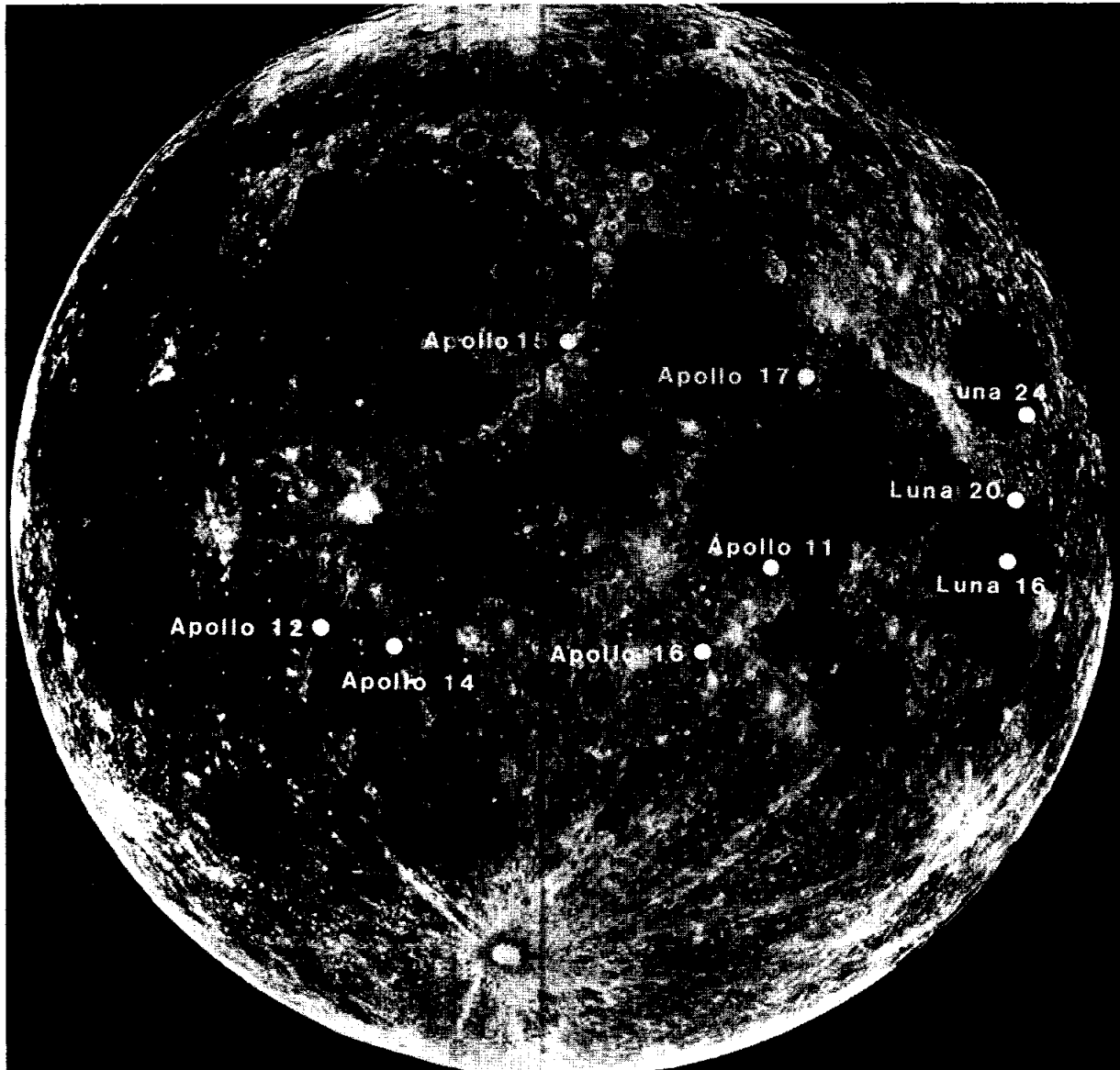


Figure 1: Apollo and Luna sampling sites on the near side of the Moon. S84-31673

pre-mission to be substantially younger than mare basalts collected on previous missions.

The crew spent more than 22 hours on the lunar surface, using the rover to traverse across the mare plains and to the lower slopes of the South and North Massifs, and over a light mantle in the valley that appeared to have resulted

from a landslide from the South Massif. The traverses totalled more than 30 km, and nearly 120 kg of rock and soil were collected (Figure 3). This total sample mass was greater than on any previous mission. An Apollo Lunar Surface Experiments Package (ALSEP) was set up near the landing point. Other experiments and numerous photographs were used to

characterize and document the site. Descriptions of the pre-mission work and objectives, the mission itself, and results are described in detail in the Apollo 17 Preliminary Science Report (1973; NASA SP-330) and the Geological Exploration of the Taurus-Littrow Valley (1980; USGS Prof. Paper 1080), and others listed in the bibliography at the end of this section. Many

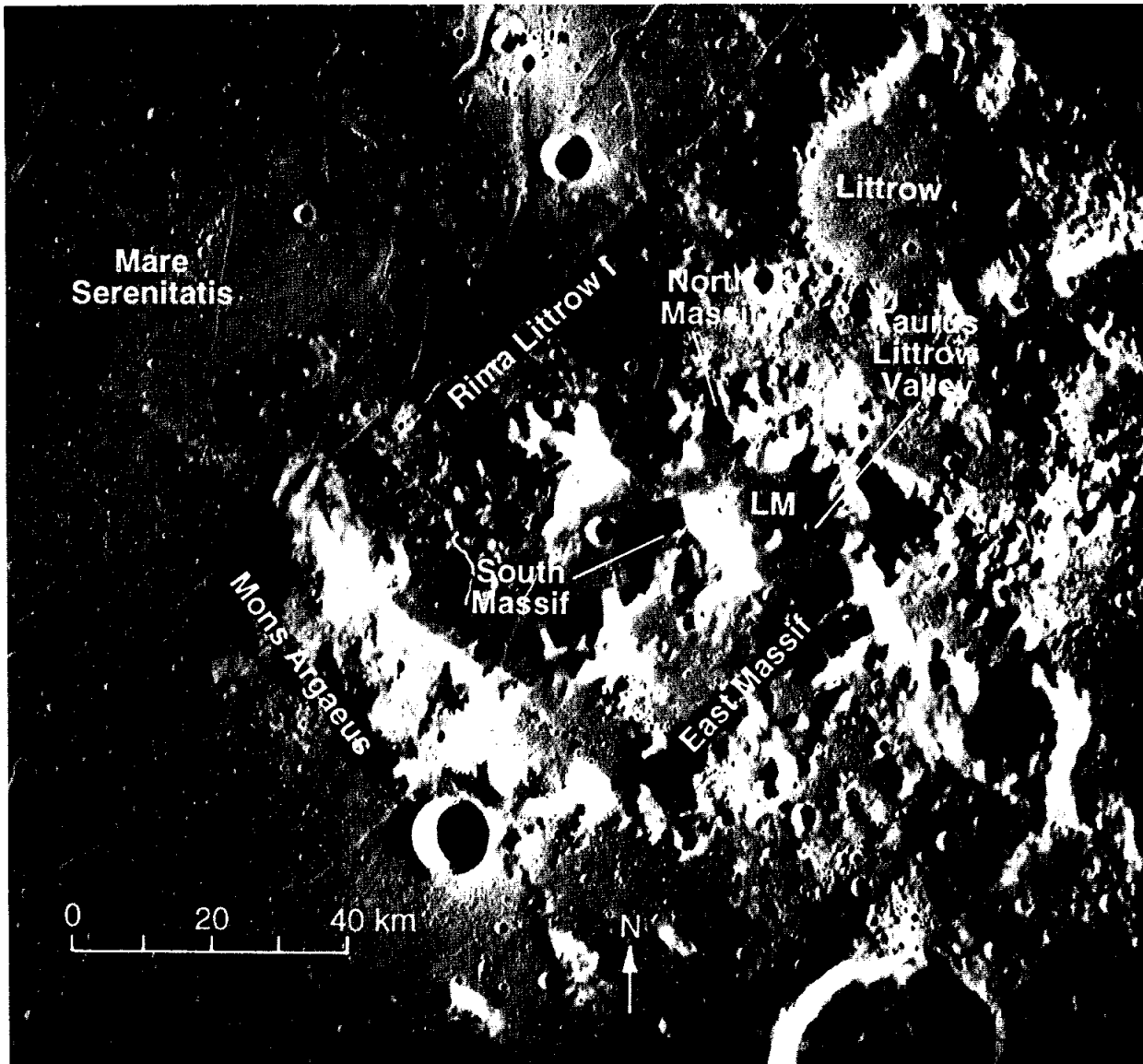


Figure 2: Apollo 17 landing site region showing major geographic features. AS17-M-447

of the rock samples have been studied in detail, and some, particularly massif boulders, have been studied in coordinated fashion in formal consortia.

The valley floor samples demonstrate that the valley consists of a sequence of high-Ti mare basalts that were mainly extruded 3.7 to 3.8 Ga ago. The sequence is perhaps

of the order of 1400m thick. The sequence consists of several different types of basalt that cannot easily be related to each other (or Apollo 11 high-Ti mare basalts) by simple igneous processes, but instead reflect varied mantle sources, mixing, and assimilation. Orange glass pyroclastics were conspicuous, and is the unit that mantles both the

valley fill and part of the nearby highlands. However, they were found to be not considerably younger than other Apollo volcanics, but only slightly younger than the valley fill. These glasses too are high-Ti basalt in composition. The orange glasses occur in the rocks only as components of some regolith breccias.

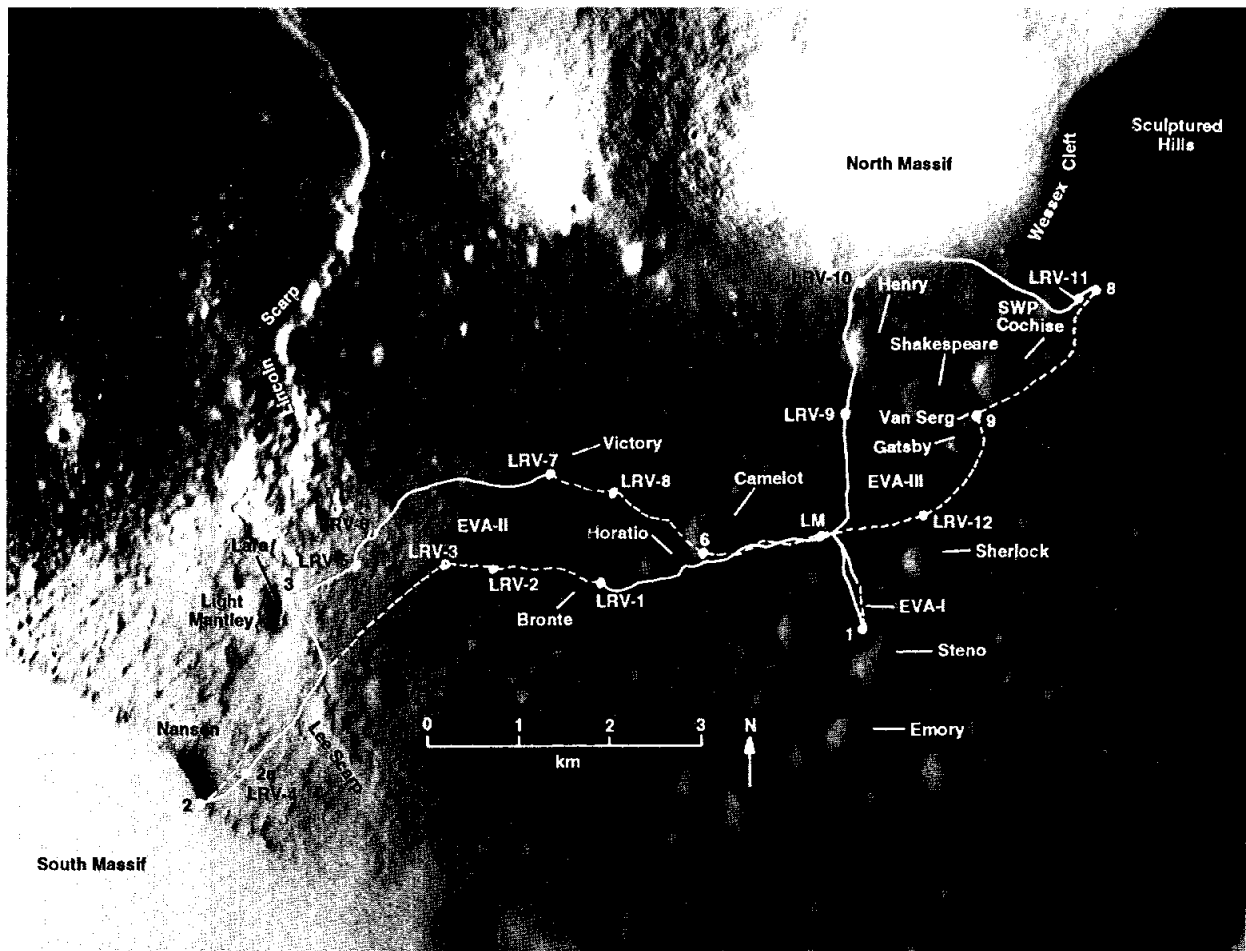


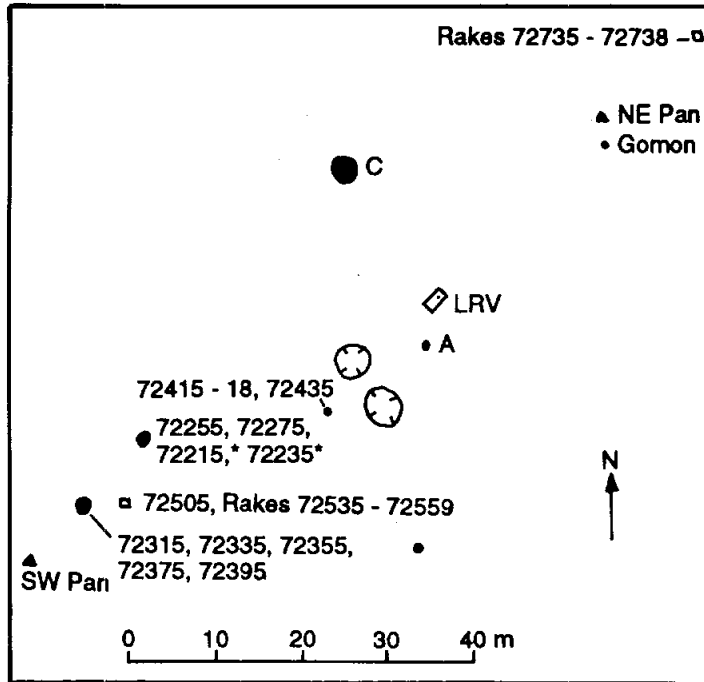
Figure 3: Apollo 17 traverse and sample collection map.

The sampling of the massifs was directed at coherent boulders and some rocks, and are dominated by a particular type of crystalline impact melt breccia. This is found on both massifs, and is characterized by an aluminous basalt composition and a poikilitic groundmass. The samples are widely interpreted as part of the impact melt produced by the Serenitatis basin event itself. A second type of impact melt, dark and aphanitic, is represented only by samples from the South Massif stations. It is similar in

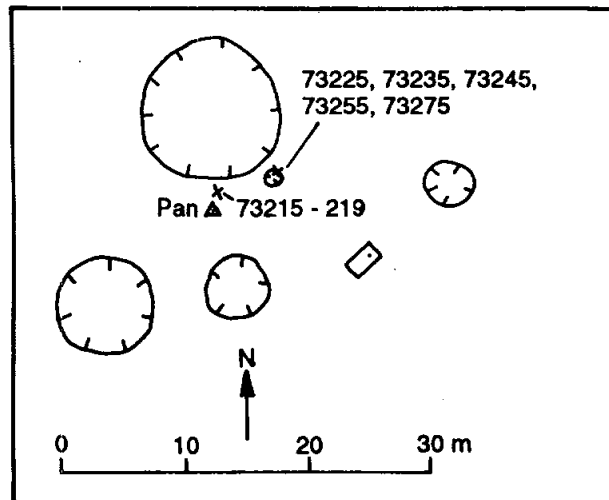
chemistry to first type, but is more aluminous and much poorer in TiO_2 . It contains a much greater abundance and variety of clast types. Opinion still differs as to whether these aphanites are a variant of the Serenitatis melt or represent something distinct. Both aphanitic and poikilitic melts seem to be most consistent with an age of close to 3.87 (± 0.02) Ga. A few rare samples of impact melt have distinct chemistry. Other rock and clasts are pristine igneous rocks, including dunite, troctolite, and norite (some of

which formed meter-sized clasts or individual boulders), as well as more evolved types including gabbros and felsic/granitic fragments. Feldspathic granulites are common as clasts in the melt matrices (both aphanitic and poikilitic) and occur as a few small individual rocks. Geochronology shows that many of these granulites and pristine igneous rocks date back as far as 4.2 and even 4.5 Ga. The purer soils of the South Massif contain more alumina and only half of the incompatible element budget

ROCK SAMPLE COLLECTION SITES



Planimetric Map of Station 2



Planimetric Map of Station 3

Not Shown: 2A (LRV-4) 73145, 73146, 73155, 73156
LRV-5 74115 - 74119

of the dominant impact melt rocks, demonstrating that the massifs, representing pre-Serenitatis material, have a component not well represented in the larger collected samples. Conspicuously absent, and not the "missing" component in the soil, is ferroan anorthosite, common at the Apollo 16 site and widely believed to have formed an early lunar crust.

BIBLIOGRAPHY

Apollo Field Geology Investigation Team (1973) Geologic exploration of Taurus-Littrow: Apollo 17 landing site. *Science* **182**, 672-680

Apollo Lunar Geology Investigation Team (1973) Documentation and environment of the Apollo 17 samples: A preliminary report. U.S. Geological Survey Interagency Report: Astrogeology 71.

Apollo 17 Preliminary Examination Team (1973) Apollo 17 lunar samples: Chemical and petrographic description. *Science* **182**, 659-672

Apollo 17 Preliminary Science Report (1973) National Aeronautics and Space Administration SP-330

Bailey N.G and Ulrich G.E. (1975) Apollo 17 voice transcript pertaining to the geology of the landing site. U.S. Geological Survey Rept. USGS-GD-74-031.

Schmitt H..H. (1973) Apollo 17 report on the valley of Taurus-Littrow. *Science* **183**, 681-690

Wolfe E. W. and others (1981) The geologic Investigation of the Taurus-Littrow valley: Apollo 17 landing site. U.S. Geological Survey Prof. Paper 1080.

NUMBERING OF APOLLO 17 SAMPLES

As in previous missions, five digit sample numbers are assigned each rock (coherent material greater than about 1 cm), the unsieved portion and each sieve fraction of scooped <1 cm material, the drill bit and each drill stem and drive tube section and each sample of special characteristics.

The first digit (7) is the mission designation for Apollo 17 (missions prior to Apollo 16 used the first two digits). As with Apollo 15 and 16 numbers, the Apollo 17 numbers are grouped by sampling site. Each group of one thousand numbers applies to an area as follows:

The first numbers for each area were used for drill stems, drive tubes, and the SESC. Drill stem sections and double drive tubes are numbered from the lowermost section upward.

The last digit is used to code sample type, in conformity with the conventions used for Apollo 15 and Apollo 16. Fines from a given documented bag are ascribed numbers according to:

Sampling Site	Initial Number
LM, ALSEP, SEP, and samples collected between Station 5 and the LM	70000
Station 1A	71000
Station 2 and between it and the LM	72000
Station 3 and between it and Station 2	73000
Station 4 and between it and Station 3	74000
Station 5 and between it and Station 4	75000
Station 6 and between it and the LM	76000
Station 7 and between it and Station 6	77000
Station 8 and between it and Station 7	78000
Station 9 and between it and Station 8	79000

7WXY0	Unsieved material (usually <1 cm)
7WXY1	<1 mm
7WXY2	1-2 mm
7WXY3	2-4 mm
7WXY4	4-10 mm

Rocks from a documented bag are numbered 7WXY5 - 7WXY9, usually in order of decreasing size.

Sample number decades were reserved for the contents of each documented bag. In the cases where the number of samples overflowed a decade, the next available decade was used for the overflow. For example DB 455 contained soil, numbered 71040-71044, and 6 small rocks numbered 71045-71049 and 71075.

Paired soil and rake samples for each sampling area are assigned by centuries starting with 7W500. The soil sample documented bag has the first decade or decades of the century, in conformity with the last digit coding for rocks and fines (as explained above), and the rake sample documented bag uses the following decades. For example, 71500-71509, 71515 were used for the sieve fractions and six rocks from the soil sample in DB 459. Then for the companion rake sample in DB's 457 and 458, 71520 was used for the soil, which was not sieved, and the 38 >1 cm rake fragments were numbered 71535-71539, 71545-71549, etc., to 71595-71597.

In as much as possible all samples returned loose in a sample collection bag or an ALSRC were numbered in a decade. In the cases in which rocks from several stations were put into a single collection bag however, the soil and rock fragments were assigned a decade number that conforms to the site for the largest or most friable rock. The other rocks in the same bag have numbers for their own site, generally in the second or third decade of the thousand numbers for that site.

SOUTH MASSIF ROCK SAMPLE INVENTORY

Sample	Type (a)	Mass grams	Station	Description	Page #
72215	B	379.2	2	Aphanitic impact melt breccia	3
72235	B	61.9	2	Aphanitic impact melt breccia	21
72255	B	461.2	2	Aphanitic impact melt breccia	33
72275	B	3640.	2	Fragmental polymict breccia	55
72315	B	131.4	2	Micropoikilitic impact melt breccia	93
72335	B	108.9	2	Micropoikilitic impact melt breccia	101
72355	B	367.4	2	Micropoikilitic impact melt breccia	105
72375	B	18.2	2	Micropoikilitic impact melt breccia	109
72395	B	536.4	2	Micropoikilitic impact melt breccia	113
72415	B	32.3	2	Cataclastic dunite	127
72416	B	11.5	2	Cataclastic dunite	137
72417	B	11.3	2	Cataclastic dunite	139
72418	B	3.6	2	Cataclastic dunite	147
72435	B	160.6	2	Micropoikilitic impact melt breccia	149
72505	P	3.1	2	Impact melt breccia(?)	161
72535	R	221.4	2	Microsubophitic impact melt breccia	163
72536	R	52.3	2	Microsubophitic impact melt breccia	167
72537	R	5.2	2	Impact melt breccia(?)	171
72538	R	11.1	2	Impact melt breccia(?)	173
72539	R	11.2	2	Microsubophitic impact melt breccia	175
72545	R	4.1	2	Impact melt breccia(?)	179
72546	R	4.9	2	Impact melt breccia(?)	181
72547	R	5.0	2	Impact melt breccia(?)	183
72548	R	29.3	2	Micropoikilitic impact melt breccia	185
72549	R	21.0	2	Micropoikilitic impact melt breccia	189
72555	R	10.5	2	Impact melt breccia(?)	193
72556	R	3.9	2	Impact melt breccia(?)	195
72557	R	4.6	2	Impact melt breccia(?)	197
72558	R	5.7	2	Micropoikilitic impact melt breccia	199
72559	R	27.8	2	Granoblastic impactite	203

Sample	Type (a)	Mass grams	Station	Description	Page #
72705	P	2.4	2	Impact melt breccia	207
72736		28.7	2	Micropoikilitic impact melt breccia	215
72737		3.3	2	Impact melt breccia (?)	219
72738	R	23.8	2	Microsubophitic impact melt breccia	221
73145	P	5.6	2A	Impact melt breccia(?)	225
73146	P	3.0	2A	Cataclastic troctolitic anorthosite	227
73155		79.3	2A	Impact melt breccia	231
73156		3.2	2A	Impact melt breccia or granoblastic impactite	235
73215		1062.	3	Aphanitic impact melt breccia	237
73216		162.2	3	Impact melt breccia	277
73217		138.8	3	Impact melt breccia	281
73218		39.7	3	Impact melt breccia	291
73219		2.9	3	High titanium mare basalt	293
73225	P	3.7	3	Impact melt breccia(?)	295
73235		878.3	3	Aphanitic impact melt breccia	297
73245	P	1.6	3	Granoblastic impactite(?)	309
73255		394.1	3	Aphanitic impact melt breccia	311
73275		429.6	3	Micropoikilitic impact melt breccia	335
73285	P	2.6	3	Glass-coated polymict breccia	343
74115		15.4	LRV-5	Friable regolith breccia	345
74116		12.7	LRV-5	Friable regolith breccia	347
74117		3.7	LRV-5	Friable regolith breccia	349
74118		3.6	LRV-5	Friable regolith breccia	351
74119		1.8	LRV-5	Friable regolith breccia	353

(a) B=sample of boulder R = rake sample P= picked from soil in laboratory

BOULDER 1, STATION 2

Sample 72215; 72235; 72255; 72275

Boulder 1 at Station 2 was one of three boulders sampled on the lower slopes of the South Massif. The immediate area is a strewn boulder field about 50 m above the break in slope at the base of the massif, and has a slope of 5° to 10° to the north (Fig. 1). The boulders probably came to rest on the light deposit after rolling from the upper portions of the massif, although none had tracks leading to them. In the field the light blue-gray color of Boulder 1 appeared to match that of blue-gray materials observed near the top of the west portion of the South Massif (Schmitt, 1973). The boulder lay approximately 35 m southwest of the LRV parking spot (Fig. 1).

Boulder 1, Station 2 is a 2 m boulder with a uniquely foliated or layered structure (Fig. 2). It was embedded in the regolith, projecting 1 m above the soil line, with a well-developed fillet about 30 cm high on the uphill side (fillet material was sampled as 72220, 72240 and 72260). The surface of the boulder had five roughly parallel layers, studded with knobs ranging in diameter from 1 to 15 cm, giving the appearance of being highly eroded. The knobs were reported by the crew to be mostly fine-grained clasts eroded from a more friable fine-grained matrix. The crew also reported dark elongate clasts parallel to the layering, but these are not discernable in the photographs.

Some closely spaced shear planes and open cracks cross-cut the boulder normal to the layering. The surface of the boulder is rough and grainy and has a light, spotty patina of the type that develops on friable materials as they constantly shed small particles (Marvin, 1975).

The astronauts took four specimens from three different layers in the southeast face of the boulder (Fig. 2). All four samples are complex polymict breccias, and show that the boulder is unique in several respects other than its morphology. Each of the samples was a prominent feature on the boulder (Marvin, 1974). 72275 stood up in bold relief at the top; 72235 was a black knob from a

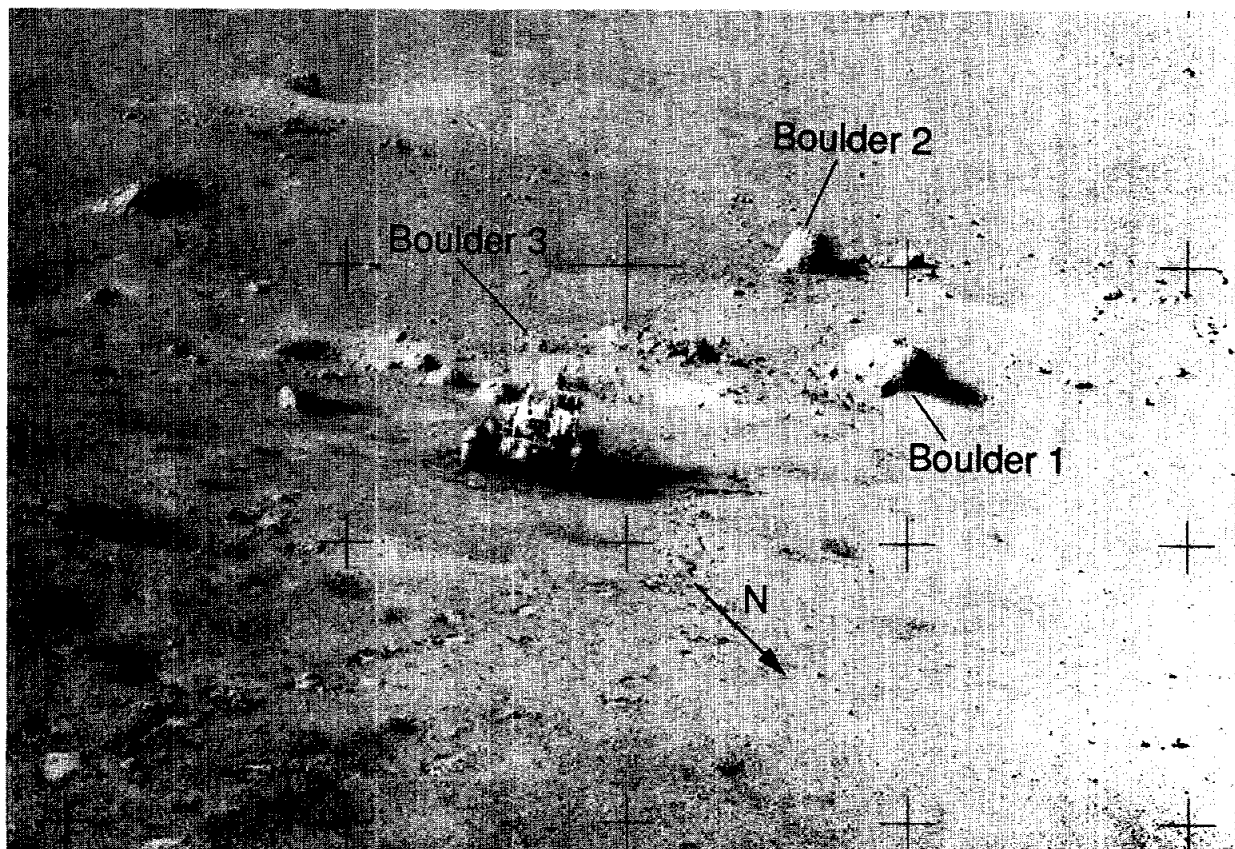


Figure 1: Location of Boulders at Station 2. The view is approximately to the south into the South Massif, showing the horizon at the top of the mountain. The distance from the LRV to the farthest boulder is about 50m. (AS17-138-21072).

lower portion of the same layer; and 72215 and 72255 were gently rounded bulges on two different layers. Most of the studies on all

four samples of Boulder 1 were conducted by the Consortium Indomitabile, led by J.A. Wood (see in particular the Consortium

Indomitabile reports, Vols. 1 and 2, 1974; and the special issue of *The Moon*, Vol. 14, #3/4, 1975).

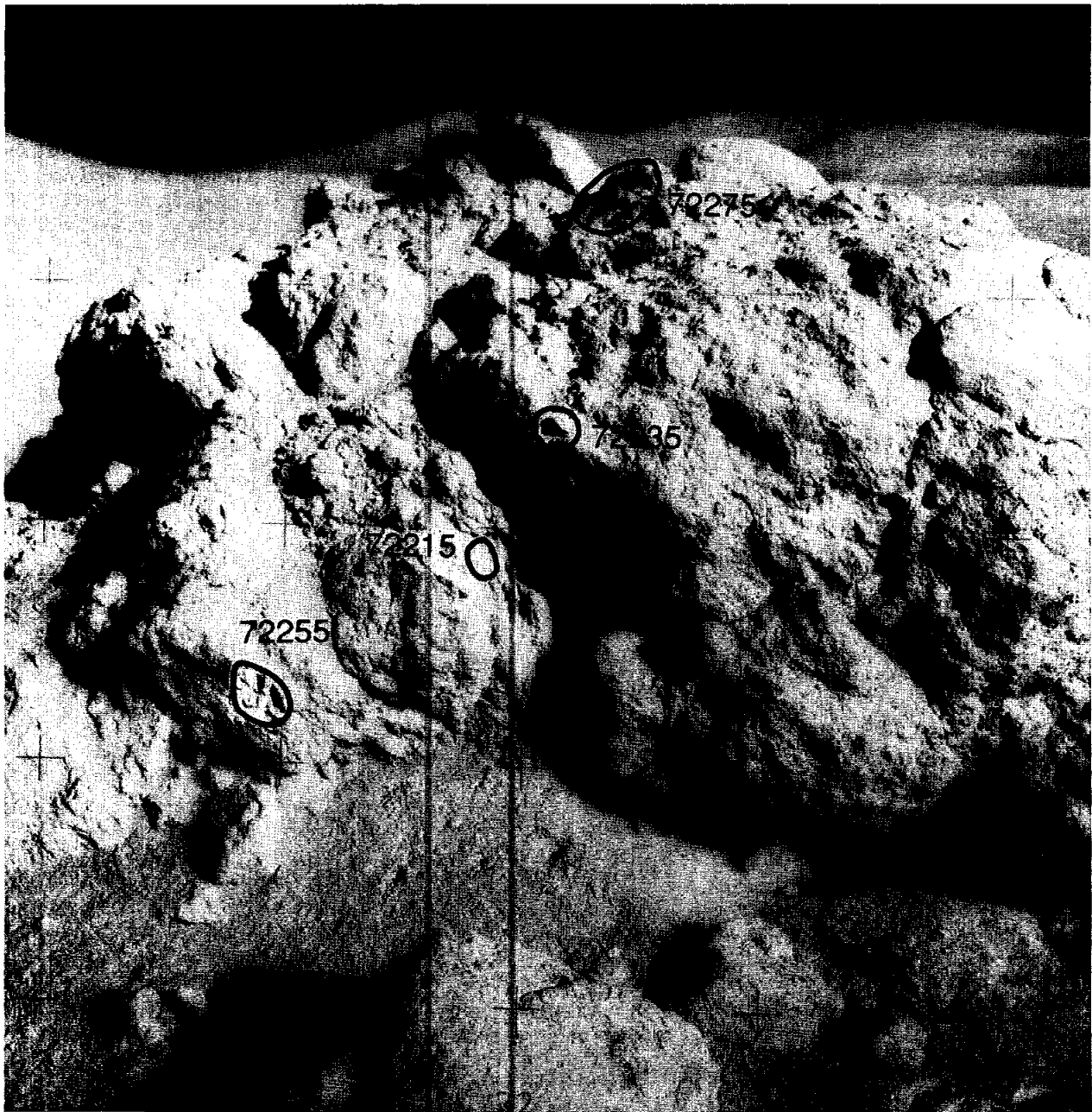


Figure 2: The southeast face of Boulder 1, Station 2 prior to sampling, and showing sampling locations. The foliated/layered morphology of the boulder is clearly visible. The gnomon has a height of 62 cm. (AS17-138-21030).

72215**Aphanitic Impact Melt Breccia**

St. 2, 379.2 g

INTRODUCTION

72215 is an aphanitic, clast-rich impact melt that the crew sampled as a rounded clast in Boulder 1 (see section on Boulder 1, St. 2, Fig. 2). Its groundmass crystallized about 3.83 Ga ago. The sample, which is nearly 10 cm long, is irregularly shaped (Fig. 1), tough, and medium light gray [N5-N6]. The exposed surface had many zap pits with glass linings.

72215 proved to be the most coherent of the four samples collected from Boulder 1. It is a fine-grained, foliated and heterogeneous, medium gray polymict breccia. A few of the clasts in 72215 are more than a

centimeter across (Fig. 1). The clast population comprises a wide variety of lithic and mineral types. The bulk rock has a low-K Fra Mauro composition that is a little more aluminous and a little less titaniferous than the coarser poikilitic Apollo 17 impact melt rocks. Laser Ar-Ar ages show an age of about 3.83 Ga for the crystallization of the groundmass. Sr isotopes did not equilibrate between melt and even tiny clasts, showing that the high temperature period was very short. Rare gas analyses suggest an exposure age of about 42 Ma.

Most of the studies of 72215 were conducted by the Consortium Indomitabile (leader J.A. Wood).

A slab cut lengthwise across the foliation of 72215 (Fig. 2) made a comprehensive petrographic and chemical study possible. Detailed maps of the exterior surfaces and the slab based on the macroscopic observations, as well as descriptions of the sample allocations, were given in Stoesser *et al.* (in CI 2, 1974).

PETROGRAPHY

Specimen 72215 consists of coherent material, with a rounded knob encrusted with a poikilitic anorthositic breccia at one end (Marvin, 1975; CI 2, 1974). LSPET (1973) described the sample as a layered light gray

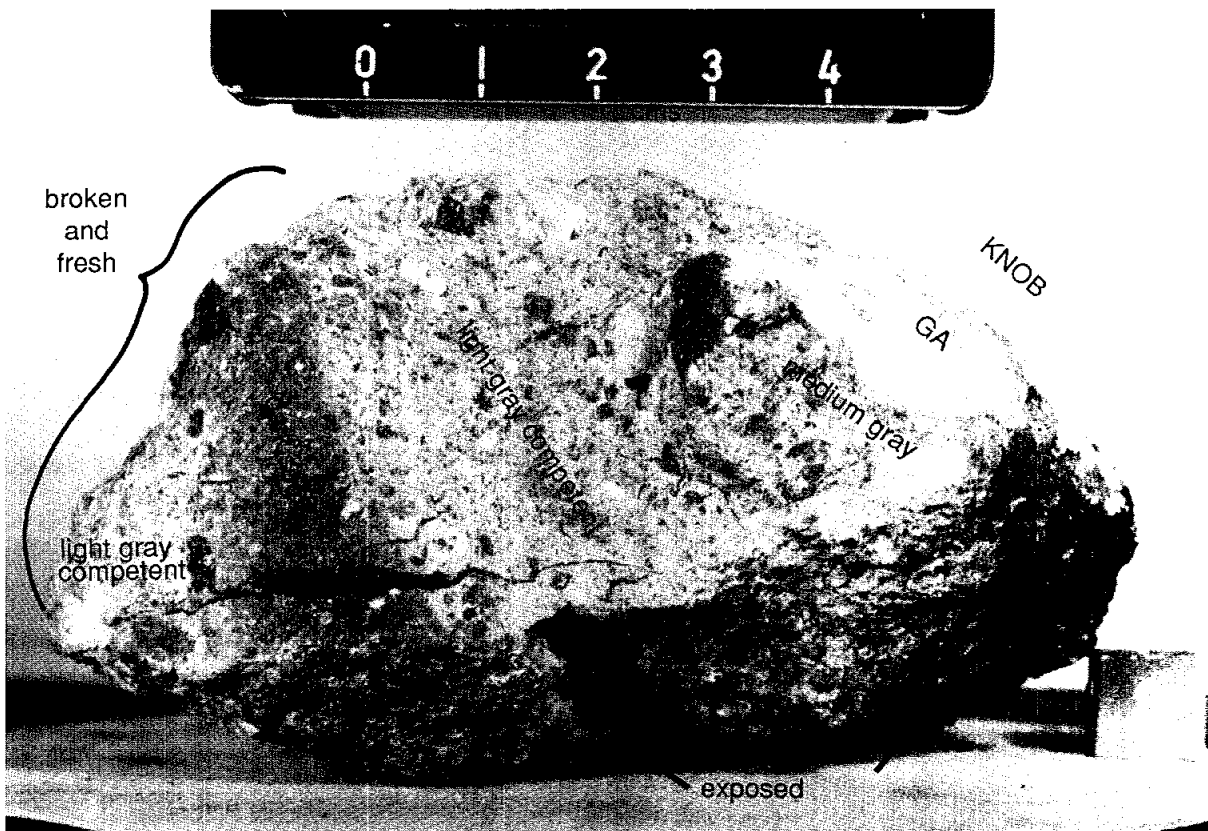


Figure 1: South (arbitrary) face of 72215 prior to slabbing. Most of the upper part visible is the freshly broken surface; the lower part visible was exposed and shows patina and zap pits. S-73-23563.

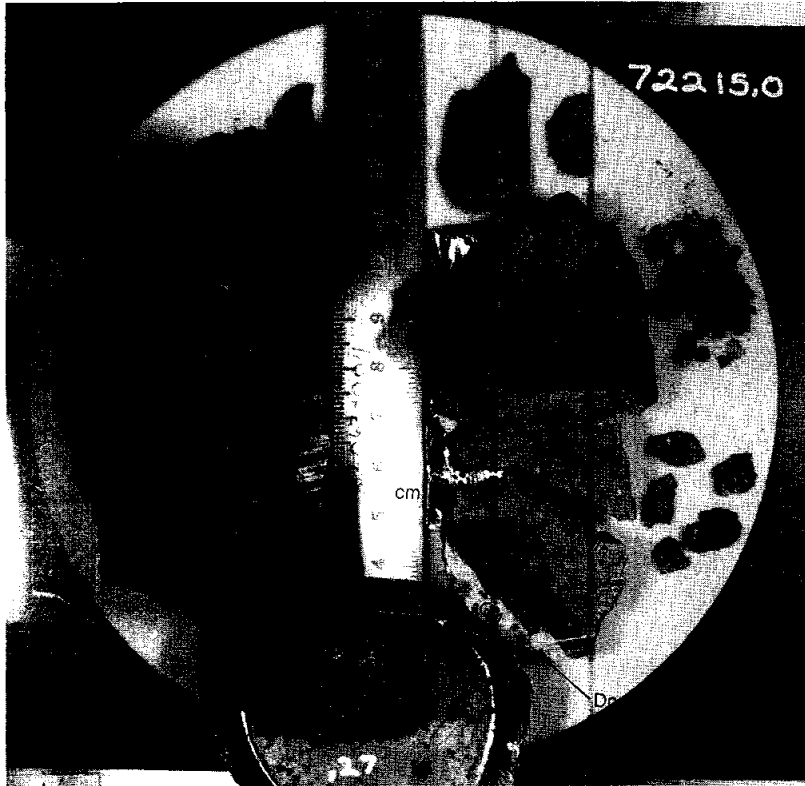


Figure 2: Slab cut from 72215 in 1974. The slab was further subdivided. S-74-21189.

breccia; Simonds *et al.* (1975) listed it as a fragmental breccia (clast-supported); and Stoffler *et al.* (1979) and Knoll *et al.* (1979) included it among their granular crystalline matrix breccias, a product of crystallization of a fragment-laden melt. The most detailed descriptions of the petrography of 72215 are given in Stoesser *et al.* (in CI 2, 1974) and in Ryder *et al.* (1975), although these refer to the sample as metamorphic rather than impact melt (nonetheless noting the obvious shearing, areas of melting, and fluidity of the sample during the high-temperature phase). That the groundmass texture is that of a melt was recognized later (e.g. James, 1977; Stoffler *et al.*, 1979).

The main mass consists of gray breccia that ranges in color from light chalky to dark sugary gray (Figs. 1, 2). The darker material, which is more coherent and uniform than the rest, appears as an irregular band through the matrix,

and as a partial rim on the knob. In thin sections the colors and textures are virtually indistinguishable. Typical matrix is shown in Fig. 3a. It consists of angular to rounded mineral and lithic clasts with a seriate grain-size down to about 20 microns. The host melt material is very fine-grained with pyroxenes and plagioclases less than a few microns across; Simonds *et al.* (1975) quoted less than 5 microns for both phases in the groundmass. In some places the clasts include obvious dark blobs of essentially similar material (Fig. 3b).

Stoesser *et al.* (in CI 2, 1974), on the basis of macroscopic observations and a set of thin sections from the slab that traversed the entire sample, subdivided 72215 into seven domains (Fig. 4). Four domains are melt matrix (referred to by Stoesser *et al.* as dark matrix breccias) and three are cataclastic poikilitic/poikiloblastic feldspathic granulites (referred to by Stoesser *et al.* as cataclastic granulitic and

poikilitic ANT breccias). The latter are essentially large crushed clasts. Most of the sample consists of the melt matrix material.

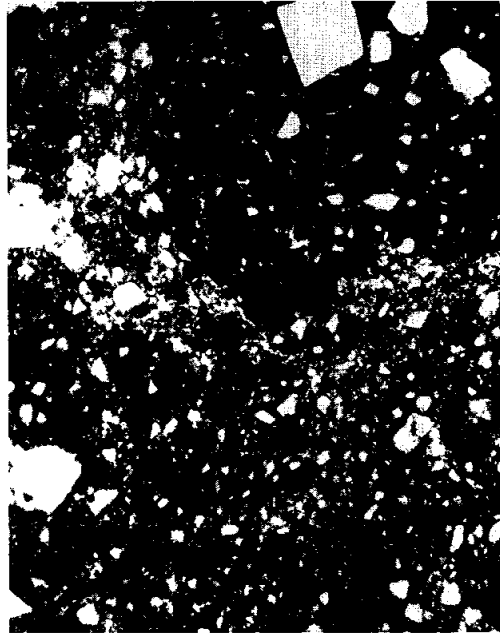
Domains 1-3: Domains 1 and 2 were distinguished because of megascopic differences, with 1 corresponding with dark sugary gray material and 2 corresponding with light sugary gray material. Domain 3 was distinguished from 2 only because of a hiatus in the sampling. All three are very similar in thin sections, consisting of dark melt breccias with a variety of clasts including globby dark clasts of material similar to the matrix itself. The darkest globs are vesicular. In domain 3 the material to the left of the dashed line (Fig. 4) is denser, darker, and more vesicular than that to the right. Defocused beam microprobe analyses of the matrix domains show that all three are very similar in composition (Table 1).

Domain 5: Domain 5 is darker than the others, and has a more vesicular groundmass. In some thin sections it appears to be continuous with the denser portion of domain 3. It is distinct from the other melt domains in its greater abundance of granitic clasts (Table 2). The defocused beam analyses show that the bulk composition of domain 5 is also distinct in being far more potassic (Table 1). Silicate mineral analyses for domain 5 (Fig. 5) show populations similar to those of other Boulder 1 melt matrices.

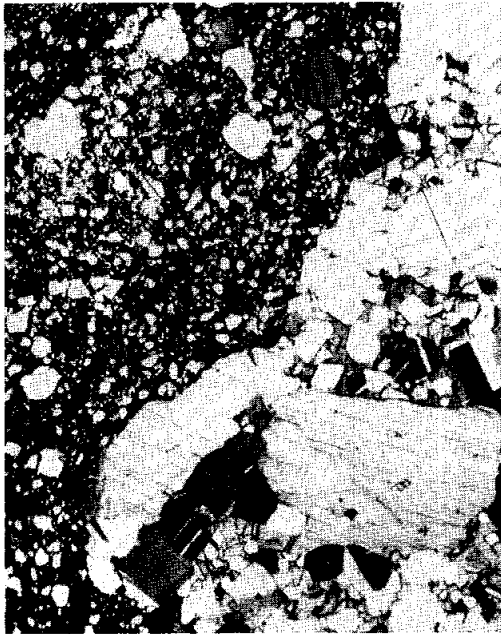
Domains 4 and 7, Cataclastic feldspathic granulite: (cataclastic granulitic ANT breccia of Stoesser *et al.*, in CI 2, 1974; and Ryder *et al.*, 1975). Domain 4 consists of brecciated material that is crushed, fine-grained feldspathic granulite, strung out into a lenticular mass (Fig. 4), and mixed to some degree into domains 3 and 5. Following cataclasis, annealing was sufficient to eliminate porosity. The feldspathic granulite is finer-grained and more heterogeneous than the poikilitic variety in domain 6. A



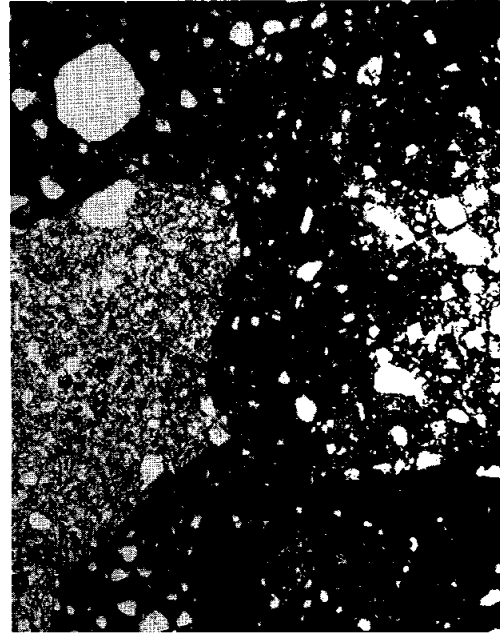
a



b



c



d

Figure 3: Photomicrographs of 72215. All plane transmitted light, all about 1mm width of view.
 a) 72215,184, typical dense dark groundmass, showing fine grain size of matrix and abundance of small clasts.
 b) 72215,193, blobby groundmass in Domain 1.
 c) 72215,107, poikilitic feldspathic granulite (lithology GA) and crushed equivalent that is Domain 6.
 d) 72215,184, basaltic-textured melt clast (left) and feldspathic breccia (right) in Domain 2 groundmass.

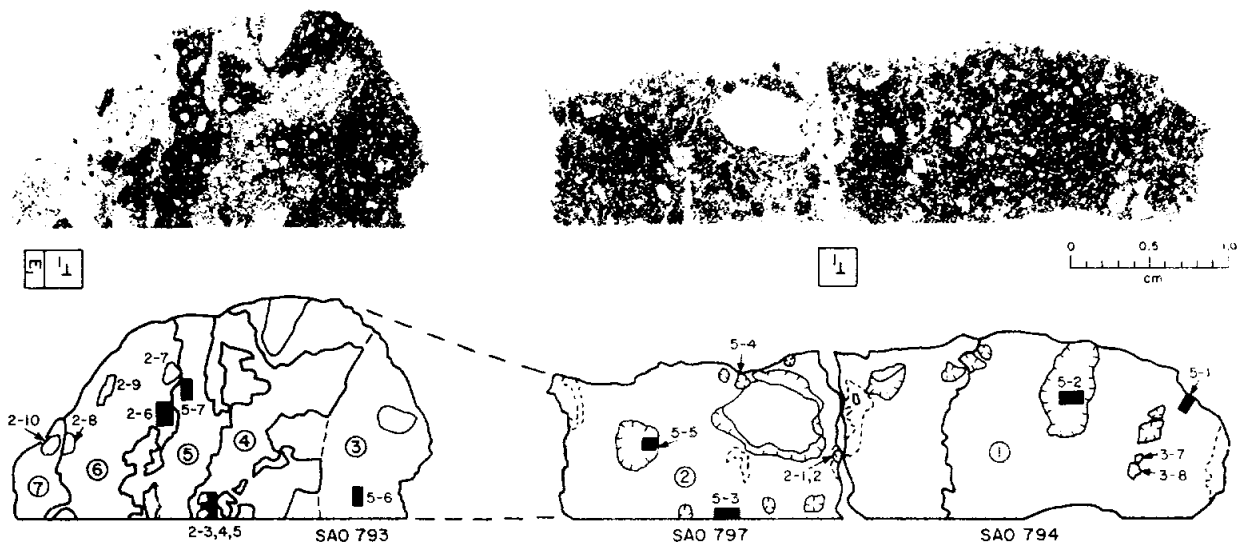


Figure 4: Photographs and sketch maps of traverse through 72215 (from Stoesser *et al.*, in CI 2, 1974), showing domain designations as circled numbers. The knob is to the left.

defocused beam microprobe analysis (Table 1) shows that it is also less feldspathic than domain 6, with a lower mg'. The domain 7 granulite is very similar to that of domain 4, and has a sharp contact with domain 6.

Domain 6, Cataclastic poikilitic feldspathic granulite: (cataclastic poikilitic ANI breccia of Stoesser *et al.*, in CI 2, 1974; also Clast 4). Domain 6 consists mainly of a cataclasized, coarse-grained, poikilitic granulite 3 (Fig. 3c). Equidimensional chadacrysts of plagioclase (An_{90-96}) are embedded in pyroxene oikocrysts ($En_{74-77}Wo_{3.5}$) that are more than 4 mm across. Augite and olivine are present but minor. Some of the plagioclases contain small spherical inclusions of mafic minerals. Modally the granulite is an anorthositic norite, as also shown by the microprobe defocused beam analysis (Table 1). Domain 6 also contains some minor clear brown and finely devitrified glass and finer granulitic material.

Goldstein *et al.* (1976a,b) analyzed metal and cohenite (Fe,Ni)₃C in 72215 melt (from domain 2). They

found an equant bleb of kamacite that contained both carbide (cohenite) and residual taenite. The Ni content of the taenite is higher than that in the metal of iron meteorites; the Ni at the alpha/gamma interface indicates equilibration down to about 500 degrees C.

Stoesser *et al.* (in CI 2, 1974) tabulated a survey of clast populations in the melt domains (Table 2). The populations of each are similar, except that domain 5, which is comparatively darker and more vesicular, has a much higher proportion of granitic clasts. The populations (clasts larger than 0.2 mm) are dominated by feldspathic granulites (~20%), anorthositic breccias (~8%), and plagioclase (including devitrified maskelynite) fragments (~25-40%). Stoesser *et al.* (1974, in CI 2) reported bulk analyses by microprobe defocused beam for several of these clasts (Table 1b); they show a range of compositions with mg' varying from 0.63 to 0.80. Other lithic fragments include various basaltic-textured ones (~2%), granites (4-23%), ultramafics, and norites (less than 2%). Other mineral clasts

include pyroxene, olivine, spinels, and silica phases. Examples of the anorthositic breccia and a basaltic-textured fragment are shown in Fig. 3d. The latter, some of which contain small pink spinels, are probably at least mainly impact melts. Defocused beam analyses show that they are aluminous, olivine-normative fragments (Table 1c).

The granitic clasts in Boulder 1, including those in 72215, were described by Stoesser *et al.* (1975) and Ryder *et al.* (1975), with photomicrographs of some clasts. Those in 72215 show the range of petrographic features typical of those elsewhere in the Boulder. They are characterized by their high K₂O (6-10%) and SiO₂ (70-80%) as shown by defocused beam analyses. Some clasts are glassy, others crystalline, the latter consisting mainly of potash feldspar, silica, plagioclase feldspar, and pyroxenes. Some of those in 72215 show feldspars in the forbidden region of the compositional field (ternary feldspars) (Fig. 6a). Pyroxenes are iron-rich augites and pigeonites.

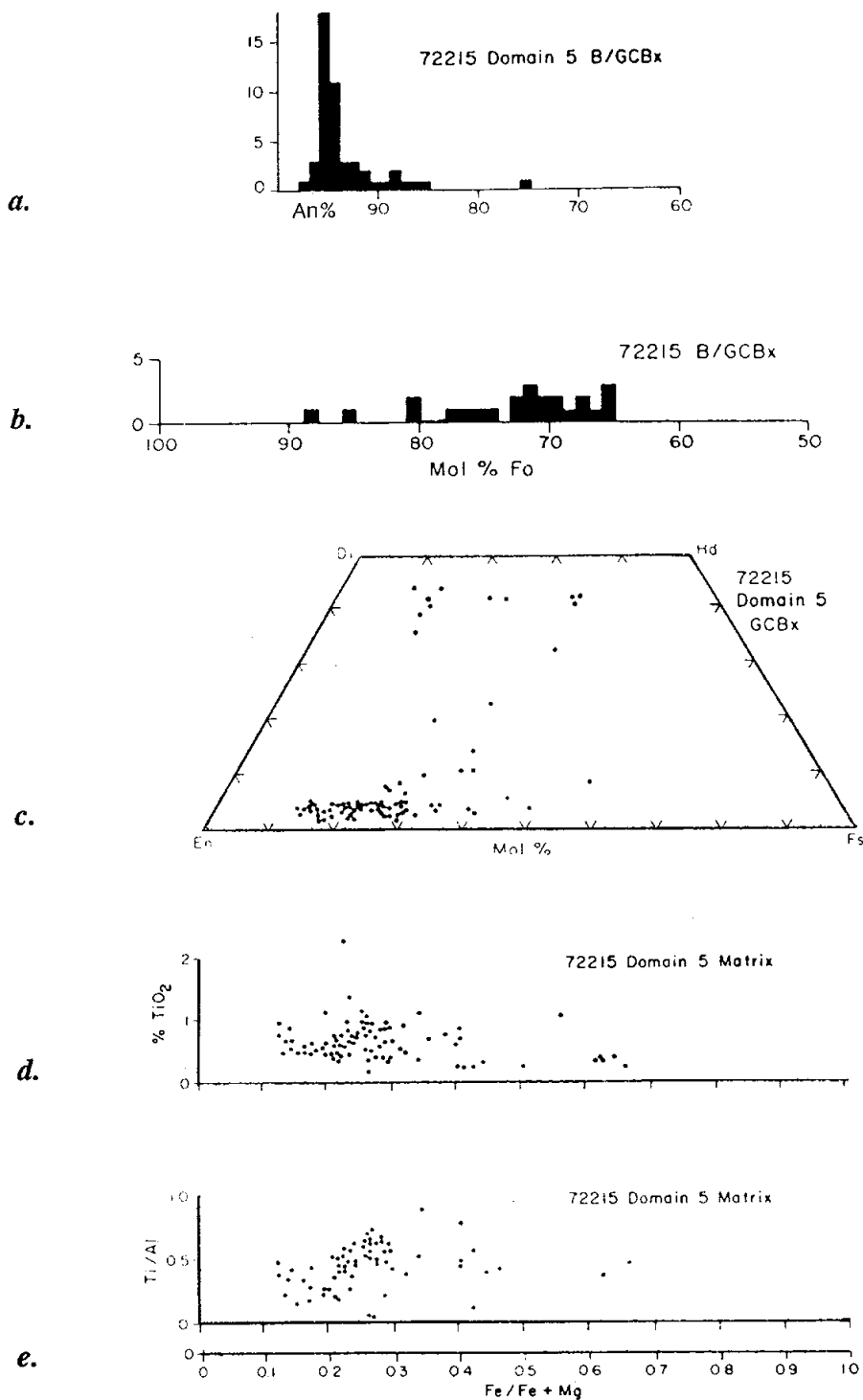


Figure 5: Compositions of plagioclases (a), olivines (b), and pyroxenes (c,d,e) in domain 5 (from Ryder et al., 1975). Most of these analyses are for mineral clasts, rather than for the tiny melt-crystallized phases.

Table 1: Defocused beam analyses of materials in 72215
(from Stoesser *et al.*, in CI 2, 1974).

a) melt matrices (dark matrix breccias).

	1.	2.	3.	4.	5.	6.	7.	
	794	794C10	797	797C4	797C6	793	793	
	matrix dom. 1	vesic. DMB clast	matrix dom. 2	vesic. DMB clast	nonvesic. DMB clast	matrix dom. 3	matrix dom. 5	
WT. % OXIDES								
SiO ₂	46.20	48.04	45.05	45.52	46.78	46.75	48.02	
TiO ₂	0.56	0.79	0.60	0.60	0.58	0.68	0.66	
Al ₂ O ₃	18.30	16.86	19.81	17.38	18.31	19.64	18.79	
Cr ₂ O ₃	0.14	0.15	0.13	0.12	0.18	0.14	0.04	
FeO	8.39	8.30	7.32	8.40	8.86	8.20	8.00	
MnO	0.12	0.11	0.12	0.17	0.12	0.11	0.12	
MgO	11.04	13.46	9.71	14.16	11.39	10.54	7.32	
CaO	12.01	10.80	12.62	11.31	12.10	12.73	11.81	
Na ₂ O	0.51	0.56	0.56	0.55	0.57	0.49	0.77	
K ₂ O	0.21	0.29	0.18	0.21	0.25	0.22	1.02	
BaO	0.03	0.04	0.09	0.14	0.11	0.05	0.09	
P ₂ O ₅	0.24	0.19	0.21	0.19	0.21	0.18	0.34	
TOTAL	97.74	99.58	96.39	98.74	99.47	99.75	97.00	
CIPW NORM								
FO	5.7	5.8	5.8	13.9	7.0	5.7	---	
FA	3.3	2.7	3.3	6.4	4.2	3.3	---	
EN	20.0	25.4	16.8	16.0	18.5	18.2	18.8	
FS	10.6	10.6	8.7	6.6	10.0	9.7	14.2	
WO	4.7	4.1	4.5	4.5	5.1	4.7	5.0	
OR	1.3	1.7	1.1	1.3	1.5	1.3	6.2	
AB	4.4	4.7	4.9	4.7	4.9	4.2	6.7	
AN	48.1	42.8	53.0	44.9	47.0	50.9	46.2	
ILM	1.1	1.5	1.2	1.2	1.1	1.3	1.3	
CHR	0.2	0.2	0.2	0.2	0.3	0.2	0.1	
QTZ	---	---	---	---	---	---	0.6	
COR	---	---	---	---	---	---	---	
AP	0.6	0.4	0.5	0.4	0.5	0.4	0.8	
COMP. NORM MIN.								
OL:	FO	71.2	75.9	71.7	76.0	70.8	71.1	---
PX:	EN	62.1	68.6	61.5	64.1	60.6	61.3	55.4
	FS	25.1	21.8	24.3	20.3	25.0	24.9	31.9
	WO	12.7	9.6	14.2	15.6	14.3	13.7	12.8
PLAG:	OR	2.3	3.4	1.8	2.4	2.7	2.3	10.4
	AB	8.7	10.2	8.9	9.9	9.7	7.8	12.0
	AN	89.0	86.4	89.3	87.7	87.6	89.9	77.6
atomic Mg/(Mg+Fe)		0.701	0.742	0.702	0.750	0.696	0.696	0.619
MgO/(MgO+FeO)		0.568	0.619	0.570	0.628	0.562	0.562	0.478
No. of analyses		14	15	21	11	14	16	15

b) feldspathic breccia ("ANT-suite") clasts.

	1.	2.	3.	4.	5.	6.	7.	8.	9.	10.
	797C2A anorth. breccia clast	797C2B "glassy vein"	793 dom. 4 gran. ANT breccia	793C6 gran. ANT clast	793C7 gran. ANT clast	793 dom. 6 ANT breccia	793C2 poik. ANT clast	793C4 poik. ANT clast	793C1 glass vein in poik. ANT	793C3 gran. ANT clast
WT. % OXIDES										
SiO ₂	45.17	43.68	47.48	46.59	48.41	45.81	46.43	46.26	45.23	47.56
TiO ₂	0.50	1.17	0.79	0.43	0.11	0.61	0.12	0.19	0.11	0.18
Al ₂ O ₃	28.62	23.05	23.14	26.45	22.56	23.93	26.89	25.55	25.45	22.32
Cr ₂ O ₃	0.05	0.05	0.04	0.51	0.07	0.07	0.07	0.10	0.06	0.04
FeO	2.05	5.17	6.63	4.93	7.08	5.83	3.47	4.15	4.19	6.83
MnO	0.06	0.11	0.05	0.07	0.08	0.05	0.06	0.10	0.09	0.15
MgO	2.73	11.48	6.37	5.12	8.17	7.09	6.97	7.76	7.65	7.77
CaO	16.17	13.72	14.76	15.37	13.46	14.72	15.15	14.40	15.49	13.32
Na ₂ O	1.00	0.74	0.58	0.65	0.64	0.46	0.44	0.38	0.50	0.69
K ₂ O	0.31	0.19	0.34	0.17	0.14	0.28	0.08	0.11	0.11	0.33
BaO	0.07	0.09	0.07	0.04	0.06	0.10	0.04	0.03	0.03	0.10
P ₂ O ₅	0.03	0.06	0.66	0.27	0.60	0.39	0.01	n.d.	0.02	0.10
TOTAL	96.77	99.49	100.89	100.59	101.37	99.36	99.74	99.06	98.93	99.39
CPIW NORM										
FO	0.5	18.2	---	0.1	0.1	2.7	2.3	2.5	7.3	2.2
FA	0.2	5.4	---	---	0.1	1.7	0.9	1.0	3.2	1.6
EN	6.4	2.8	15.7	12.6	19.9	13.9	14.1	16.0	8.9	16.3
FS	2.8	0.8	10.8	7.9	12.6	7.7	5.1	6.1	3.6	10.5
WO	3.2	3.7	3.9	2.4	1.9	3.4	1.7	1.6	4.2	3.7
OR	1.9	1.1	2.0	1.0	0.8	1.7	0.5	0.7	0.7	2.0
AB	8.8	6.3	4.9	5.5	5.4	3.9	3.7	3.2	4.3	5.9
AN	75.1	59.4	59.0	68.4	57.5	62.9	71.4	68.3	67.6	57.2
ILM	1.0	2.2	1.5	0.8	0.2	1.2	0.2	0.4	0.2	0.3
CHR	0.1	0.1	0.1	0.7	0.1	0.1	0.1	0.1	0.1	0.1
QTZ	---	---	0.6	---	---	---	---	---	---	---
COR	---	---	---	---	---	---	---	---	---	---
AP	0.1	0.1	1.5	0.6	1.3	0.9	---	---	---	0.2
COMP. NORM. MIN.										
OL: FO	---	82.9	---	---	---	70.4	78.6	77.4	76.6	67.1
PX: EN	56.5	42.7	57.5	60.8	63.8	61.2	72.6	72.5	58.4	59.4
FS	19.0	8.8	30.1	29.1	30.9	25.9	19.8	21.2	17.8	29.2
WO	24.5	48.5	12.4	10.0	5.3	13.0	7.6	6.3	23.7	11.5
PLAG: OR	2.2	1.6	3.0	1.3	1.2	2.0	0.6	0.9	0.9	3.0
AB	10.7	10.0	7.8	7.7	9.0	6.5	5.2	4.7	6.2	9.6
AN	87.1	88.4	89.2	91.0	89.8	91.5	94.2	94.3	92.8	87.4
atomic Mg/(Mg+Fe)	0.704	0.798	0.631	0.650	0.672	0.683	0.781	0.769	0.765	0.670
MgO/(MgO+FeO)	0.571	0.689	0.490	0.509	0.536	0.548	0.667	0.651	0.646	0.532
No. of analyses	7	6	14	8	7	15	20	23	8	15

c) pink spinel troctolite basalts.

WT. % OXIDES	794C1	794C2		
	PSTB	ol-pheno. basalt	FS	
SiO ₂	48.17	43.67	ILM	0.7
TiO ₂	0.36	0.20	CHR	0.1
Al ₂ O ₃	22.30	18.86	QTZ	---
Cr ₂ O ₃	0.05	0.04	COR	---
FeO	4.73	6.73	AP	0.1
MnO	0.07	0.07		
MgO	9.07	17.24	COMP. NORM MIN.	
CaO	14.44	11.31	OL: FO	78.4 82.3
Na ₂ O	0.51	0.39	PX: EN	65.3 66.3
K ₂ O	0.35	0.09	FS	18.0 14.4
BaO	n.d.	n.d.	WO	16.7 19.4
P ₂ O ₅	0.06	0.09	PLAG: OR	3.2 1.0
TOTAL	100.11	98.71	AB	7.1 6.6
			AN	89.7 92.4
CIPW NORM				
FO	2.2	25.1	atomic Mg/(Mg+Fe)	0.773 0.820
FA	0.9	7.8	MgO/(MgO+FeO)	0.657 0.719
EN	19.5	7.7	No. of analyses	12 12

Table 2: Clast populations of 72215 matrices; percentages by volume, in three size categories (from Stoesser *et al.*, in CI 2, 1974).

	DOMAINS 1 + 2				DOMAIN 3				DOMAIN 5			
	0.2-0.5 mm	0.5-1.0 mm	>1.0 mm	TOTALS	0.2-0.5 mm	0.5-1.0 mm	>1.0 mm	TOTALS	0.2-0.5 mm	0.5-1.0 mm	>1.0 mm	TOTALS
ANT suite	(26.1)	(5.5)	(3.7)	(35.3)	(32.6)	(7.7)	(1.5)	(41.8)	(31.9)	(4.3)	(2.6)	(38.8)
ANT breccias	(4.4)	(1.8)	(2.0)	(8.2)	(5.7)	(0.5)	(0.5)	(6.7)	(7.8)	-	-	(7.8)
mafic	0.6	0.2	0.2	1.0	-	-	-	-	-	-	-	-
gabbroic	2.1	1.1	1.2	4.4	4.3	0.5	0.5	5.3	7.8	-	-	7.8
anorthositic	1.7	0.5	0.6	2.8	1.4	-	-	1.4	-	-	-	-
Granulitic ANT	(15.5)	(2.3)	(1.0)	(19.8)	(16.3)	(6.2)	(1.0)	(23.5)	(18.1)	(4.3)	(2.6)	(25.0)
gabbroic	13.6	2.3	0.8	16.7	13.9	6.2	1.0	21.1	16.4	4.3	2.6	23.3
anorthositic	2.9	-	0.2	3.1	2.4	-	-	2.4	1.7	-	-	1.7
Poikiloblastic ANT	0.6	0.3	-	0.9	1.0	-	-	1.0	-	-	-	-
Poikilitic ANT	0.9	0.2	0.2	1.3	5.3	-	-	5.3	2.6	-	-	2.6
Coarse ANT	3.1	0.9	0.5	4.5	4.3	1.0	-	5.3	3.4	-	-	3.4
Unclassified ANT	0.6	-	-	0.6	-	-	-	-	-	-	-	-
Ultramafic particles	2.0	0.2	0.2	2.4	1.4	-	-	1.4	1.7	-	-	1.7
Basalts	(1.6)	(1.1)	(0.9)	(3.6)	(1.4)	-	-	(1.4)	(0.9)	-	-	(0.9)
ol.-norm. pig. bas.	-	0.3	0.5	0.8	-	-	-	-	-	-	-	-
pink sp. troct. bas.	0.9	0.6	0.2	1.7	1.4	-	-	1.4	0.9	-	-	0.9
mafic troct. bas.	0.2	-	-	0.2	-	-	-	-	-	-	-	-
unclassified bas.	0.5	0.2	0.2	0.9	-	-	-	-	-	-	-	-
Microgranites	3.4	0.6	0.2	4.2	8.6	2.4	-	11.0	19.8	3.4	-	23.2
Civet Cat norite	-	-	0.2	0.2	0.5	-	-	0.5	-	-	-	-
Devitrified maskelynite	12.0	1.7	0.3	14.0	8.6	1.4	-	10.0	2.6	-	-	2.6
Glassy clasts	0.2	0.2	-	0.4	-	-	-	-	-	-	-	-
Mineral fragments	(38.3)	(2.1)	-	(40.4)	(31.5)	(2.5)	-	(34.0)	(30.2)	(2.6)	-	(32.8)
Plagioclase	23.4	1.1	-	24.3	16.7	1.0	-	17.7	19.0	2.6	-	21.6
Olivine	4.9	0.2	-	5.1	6.2	0.5	-	6.7	1.7	-	-	1.7
Pyroxene	9.8	0.8	-	10.6	8.1	1.0	-	9.1	9.5	-	-	9.5
Chromite	0.2	-	-	0.2	-	-	-	-	-	-	-	-
Silica phases	-	-	-	-	0.5	-	-	0.5	-	-	-	-
TOTAL %	83.6	11.4	5.5	100.5	84.6	13.0	1.5	100.1	87.1	10.3	2.6	100.0
NO. OF CLASTS	547	72	33	652	177	29	3	209	101	12	3	116

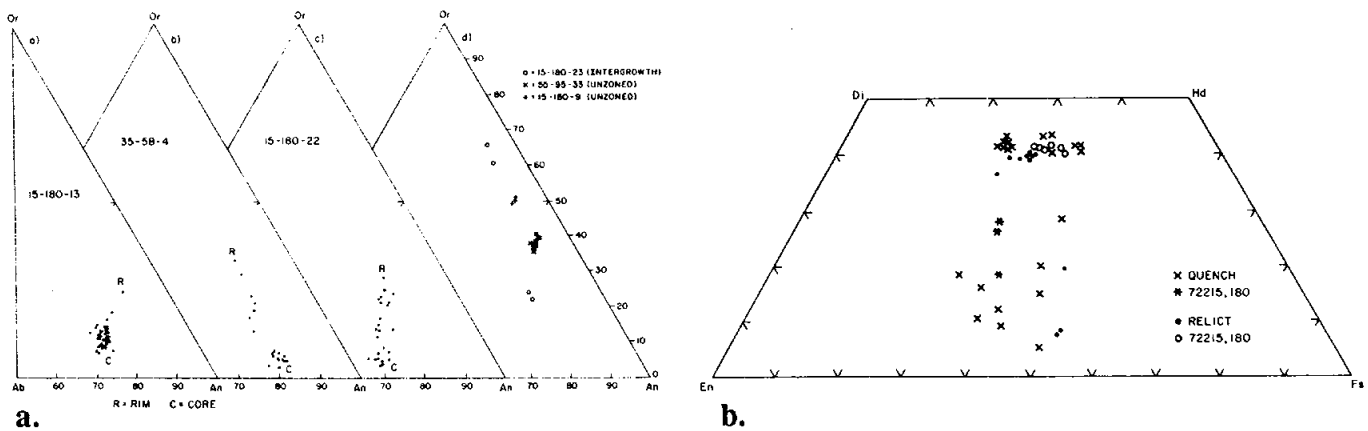


Figure 6: Compositions of minerals in granitic fragments from 72215 and other Boulder 1 samples. a) Plagioclase feldspars. b) Pyroxenes. Ryder et al., 1975.

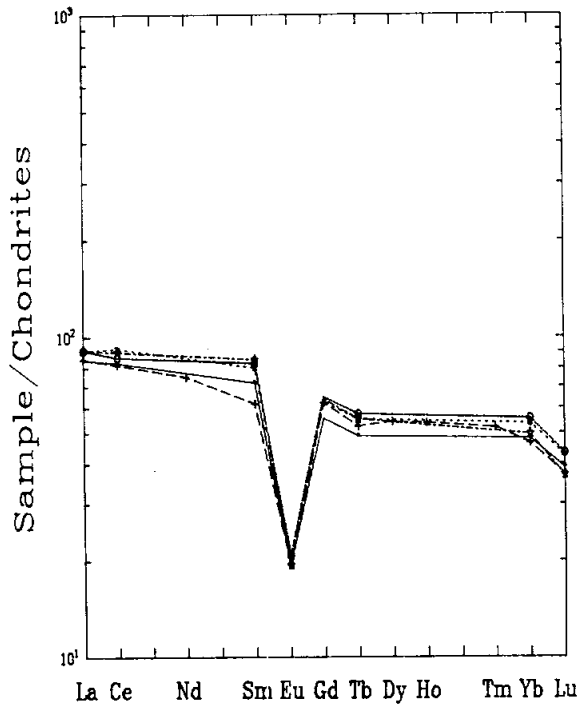


Figure 7: Rare earth element plots of matrices/bulk rock samples of 72215. Solid line and dots = ,64; spaced dotted line = ,60; close dotted line with open circles = ,47; dot-dash line = ,92; all Blanchard et al. (1975). Dashed line and crosses = ,22; Palme et al. (1978).

Spudis and Ryder (1981) showed photomicrographs of clasts in 72215, including granoblastic ones and clasts with accretionary rinds. They noted the differences in clast population of 72215 (and other Boulder 1 samples) from those of the coarser poikilitic melt breccias from the site.

CHEMISTRY

Chemical analyses of bulk melt matrix are reproduced in Table 3, arranged according to sampling domain and description. Rare earths for these analyses are plotted in Fig. 7. Analyses of the poikilitic feldspathic granulite (= anorthositic gabbro, poikilitic ANT breccia, lithology GA, domain 6, and clast 4) are reproduced in Table 4, with the rare earths plotted in Fig. 8. Table 4 also reproduces a partial analysis of an "anorthositic" clast separated from a different area.

Table 3 and Fig. 7 show that all the different colored/textured matrix domains have essentially the same composition. The major elements are in substantial agreement with the compositions determined by microprobe defocused beam analyses (Table 1), except that the latter have slightly lower alumina. Two partial analyses of darker

Table 3: Chemical analyses of matrices/bulk rock samples of 72215.

Split wt %	Slab; average matrix (ordinary breccia OB) Domains 2,3							Slab; dark sugary matrix (DSG) Dom 1			Split wt %
	,64	,40	,22	,39a	,39b	,68a	,68b	,60	,59	,54	
SiO ₂	45.1		46.7					44.9			SiO ₂
TiO ₂	1.0		0.70					0.9			TiO ₂
Al ₂ O ₃	20.7		20.3					21.2			Al ₂ O ₃
Cr ₂ O ₃	0.265		0.243					0.25			Cr ₂ O ₃
FeO	(a) 8.45		10.3					(b) 8.49			FeO
MnO	0.133		0.117					0.12			MnO
MgO	9.81		10.3					11.5			MgO
CaO	12.0		12.5					11.9			CaO
Na ₂ O	0.500		0.475					0.524			Na ₂ O
K ₂ O	0.323		0.214					0.235			K ₂ O
P ₂ O ₅			0.236								P ₂ O ₅
ppm											ppm
Sc	18.9		18.5					18.4			Sc
V											V
Co	23.8		26.9					29.5			Co
Ni	120	154	170					120	158		Ni
Rb		4.88							6.65	5.02	Rb
Sr			160							139.1	Sr
Y			90								Y
Zr			360								Zr
Nb			25								Nb
Hf	9.4		9.11					9.9			Hf
Ba			299								Ba
Th	4.5		3.94	4.298	3.768	4.656	4.327	5.5			Th
U		1.36	1.16	1.185	1.023	1.272	1.179		1.520		U
Cs			0.180						0.216		Cs
Ta	1.4		1.14					1.4			Ta
Pb				2.387	2.122	2.658	2.344				Pb
La	28		28.1					30			La
Ce	73		72.0					81			Ce
Pr											Pr
Nd			45								Nd
Sm	13.0		11.2					14.5			Sm
Eu	1.34		1.34					1.41			Eu
Gd			15.5								Gd
Tb	2.3		2.47					2.6			Tb
Dy			17.2								Dy
Ho			3.77								Ho
Er											Er
Tm			1.56								Tm
Yb	9.6		9.29					10.7			Yb
Lu	1.32		1.26					1.45			Lu
Li			12.2								Li
Be											Be
B											B
C											C
N											N
S			320								S
F			18.8								F
Cl			14.0								Cl
Br		0.0281	0.05						0.0286		Br
Cu											Cu
Zn		1.8							1.6		Zn
ppb											ppb
Au									2.26		Au
Ir									5.02		Ir
I											I
At											At
Ga			3900								Ga
Ge		141							144		Ge
As											As
Se		68							72		Se
Mo											Mo
Tc											Tc
Ru											Ru
Rh											Rh
Pd											Pd
Ag		0.461							0.464		Ag
Cd		3.6							3.0		Cd
In											In
Sn											Sn
Sb		0.66							0.92		Sb
Te		3.32							2.5		Te
W											W
Re		0.372							0.380		Re
Os											Os
Pt											Pt
Hg											Hg
Tl		0.53							0.63		Tl
Bi		0.14							0.32		Bi

(1) (2) (3) (4) (4) (4) (4) (1) (2) (5)

References and methods:

- (1) Blanchard et al. (1974); AAS, INAA
 (2) Higuchi and Morgan (1975a), Morgan et al. (1975), Hertogen et al. (1977); RNAA
 (3) Palme et al. (1978); XRF, MFB, INAA, RNAA
 (4) Nunes and Tatsumoto (1975); IDMS
 (5) Compston et al. (1975); XRF, IDMS
 (6) Jovanovic and Reed (1974, 1975a,b,c,d, 1980); INAA

Notes:

- (a) AAS; INAA = 8.45%
 (b) AAS; INAA = 8.25%
 (c) AAS; INAA = 8.57%
 (d) AAS; INAA = 8.19%
 (e) Poor Th concentration data.
 (f) Combined leach and residue fractions.

Table 3: Continued

Split wt %	Slab; dark sugary breccia (DSG)-----			Slab; light gray breccia (LB)-----				Knob; gray breccia-----		Split wt %
	,61	,51a	,51b	,47	,44	,15a	,15b-1	,15b-2	,92	
SiO ₂				45.1					45.6	
TiO ₂				0.7					0.8	
Al ₂ O ₃				21.4					20.9	
Cr ₂ O ₃				0.251					0.224	
FeO				(c) 8.35					(d) 8.44	
MnO				0.129					0.125	
MgO				11.3					10.1	
CaO				12.0					12.3	
Na ₂ O				0.548					0.504	
K ₂ O				0.195					0.253	
P ₂ O ₅										
ppm										
Sc				18.5					18.5	
V										
Co				31.6					23.0	
Ni				250	146				140	136
Rb					2.83					3.88
Sr										
Y										
Zr										
Nb										
Hf				9.9					9.4	
Ba										
Th				4.8		(c) 4.633	(c) 4.081	5.084	3.1	
U		4.871	4.635		1.32	1.408	1.232	1.369		1.62
Cs		1.315	1.290		0.115					0.198
Ta				1.4					1.3	
Pb		2.936				2.987	2.464	2.716		
La				30					30	
Ce				76					79	
Pr										
Nd										
Sm				15.0					15.4	
Eu				1.44					1.34	
Gd										
Tb				2.7					2.6	
Dy										
Ho										
Er										
Tm										
Yb				11.1					9.9	
Lu				1.47					1.25	
Li										
Be										
B										
C										
N										
S										
F										
Cl										
Br					0.0222				0.0344	
Cu										
Zn					1.7				1.8	
ppb										
Au					2.06				1.76	
Ir					5.34				3.92	
I										
At										
Ga										
Ge					117				124	
As										
Se					49				71	
Mo										
Tc										
Ru	8									
Rh										
Pd										
Ag					0.562				0.466	
Cd					3.8				5.3	
In										
Sn										
Sb					0.64				0.71	
Te					2.4				4.9	
W										
Re					0.397				0.279	
Os	21									
Pt										
Hg										
Tl					0.41				0.46	
Bi					0.29				0.45	
	(6)	(4)	(4)	(1)	(2)	(4)	(4)	(4)	(1)	(2)

Table 3: Continued

Knob; dark sugary breccia.....					
	,100	,104 gray	,104 dk a	,104 dk b	
Split wt %					Split wt %
SiO ₂					SiO ₂
TiO ₂					TiO ₂
Al ₂ O ₃					Al ₂ O ₃
Cr ₂ O ₃					Cr ₂ O ₃
FeO					FeO
MnO					MnO
MgO					MgO
CaO					CaO
Na ₂ O					Na ₂ O
K ₂ O					K ₂ O
P ₂ O ₅	0.57				P ₂ O ₅
ppm					ppm
Sc					Sc
V					V
Co					Co
Ni					Ni
Rb		4.05	44.19	43.98	Rb
Sr		149.7	162.2	161.0	Sr
Y					Y
Zr					Zr
Nb					Nb
Hf					Hf
Ba					Ba
Th					Th
U	3.1				U
Cs					Cs
Ta					Ta
Pb					Pb
La					La
Ce					Ce
Pr					Pr
Nd					Nd
Sm					Sm
Eu					Eu
Gd					Gd
Tb					Tb
Dy					Dy
Ho					Ho
Er					Er
Tm					Tm
Yb					Yb
Lu					Lu
Li	11				Li
Be					Be
B					B
C					C
N					N
S					S
F	129				F
Cl	(f) 58.8				Cl
Br	(f) 0.732				Br
Cu					Cu
Zn					Zn
ppb					ppb
Au					Au
Ir					Ir
I	1.1				I
At					At
Ga					Ga
Ge					Ge
As					As
Se					Se
Mo					Mo
Tc					Tc
Ru					Ru
Rh					Rh
Pd					Pd
Ag					Ag
Cd					Cd
In					In
Sn					Sn
Sb					Sb
Te					Te
W					W
Re					Re
Os					Os
Pt					Pt
Hg					Hg
Tl					Tl
Bi					Bi

(6) (5) (5) (5)

material picked from 72215,104, from the knob area, differ in having extremely high Rb. Possibly these represent domain 5. The melt matrix compositions are similar to those of petrographically similar materials from the other Boulder 1 samples. They are a low-K Fra Mauro composition, (K₂O ~0.2 - 0.3%), and differ from the coarser poikilitic melts at the site in being slightly more aluminous and less titaniferous. The siderophile element ratios are also distinct from those of these coarser melts; Morgan *et al.* (1975) placed 72215 along with other Boulder 1 samples in a meteoritic Group 3L, distinct from the common Group 2 at Apollo 17. However, Blanchard *et al.* (1974, 1975) and Winzer *et al.* (1975) emphasize the similarity of all the melts at the Apollo 17 site.

The data of Jovanovic and Reed (several publications; see Table 1) include analyses for leach and residue fractions for some elements; these are combined for Table 1. They discuss some of their data as suggesting vapor clouds being responsible for the leachable materials, and with varied parents for the non-leachable materials.

RADIOGENIC ISOTOPES

Schaeffer *et al.* (1982a,b) used laser Ar-Ar techniques to determine ages of clasts and to infer the age of the melt in section 72215,144, providing 16 analyses (Table 5). Most of the ages were for plagioclase and felsite ("feldspar-thoid") clasts. The felsite clasts give the youngest ages, averaging 3.83 Ga; the higher ages for the plagioclases range up to 4.02 Ga; some of these plagioclases are in noritic lithic clasts. The age of the felsite clasts, which probably degassed during melting, is the best estimate for the age of the melt groundmass, which is therefore about 3.83 Ga old. (The felsite clasts were preheated to 650 degrees C. The ages are total release, hence K-Ar, of the greater than 650

Table 4: Chemical analyses of poikilitic feldspathic granulate and other anorthositic materials in 72215.

Split wt %	Domain 6 (Clast 4)			Split wt %
	,76	,89	,102	
SiO ₂	44.7			SiO ₂
TiO ₂	0.5			TiO ₂
Al ₂ O ₃	27.3			Al ₂ O ₃
Cr ₂ O ₃	0.126			Cr ₂ O ₃
FeO	(a) 4.80			FeO
MnO	0.067			MnO
MgO	7.19			MgO
CaO	14.9			CaO
Na ₂ O	0.483			Na ₂ O
K ₂ O	0.113			K ₂ O
P ₂ O ₅			0.12	P ₂ O ₅
ppm				
Sc	7.68			Sc
V				V
Co	11.9			Co
Ni	50	56		Ni
Rb		1.48		Rb
Sr			0.86	Sr
Y			164.6	Y
Zr				Zr
Nb				Nb
Hf	2.4			Hf
Ba				Ba
Th	1.30			Th
U		0.52	0.59	U
Cs		0.0516		Cs
Ta	0.310			Ta
Pb				Pb
La	7.3			La
Ce	18.3			Ce
Pr				Pr
Nd				Nd
Sm	3.36			Sm
Eu	1.00			Eu
Gd				Gd
Tb	0.66			Tb
Dy				Dy
Ho				Ho
Er				Er
Tm				Tm
Yb	3.1			Yb
Lu	0.44			Lu
Li			9.2	Li
Be				Be
B				B
C				C
N				N
S				S
F				F
Cl			(b) 10.2	Cl
Br		0.0290	(b) 0.052	Br
Cu				Cu
Zn		1.3		Zn
ppb				
Au		0.793		Au
Ir		2.95		Ir
I			1.6	I
At				At
Ga				Ga
Ge		42.2		Ge
As				As
Se		14.5		Se
Mo				Mo
Tc				Tc
Ru				Ru
Rh				Rh
Pd				Pd
Ag		0.502		Ag
Cd		6.7		Cd
In				In
Sn				Sn
Sb		0.31		Sb
Te		<5.4		Te
W				W
Re		0.187		Re
Os				Os
Pt				Pt
Hg				Hg
Tl		0.59		Tl
Bi		<0.71		Bi

(1) (2) (3) (4)

References:

- (1) Blanchard et al. (1974); AAS, INAA
- (2) Higuchi and Morgan (1975a), Morgan et al. (1975), Hertogen et al. (1977); RNAA
- (3) Jovanovic and Reed (1974, 1975a,b,c,d,1980); INAA
- (4) Compston et al. (1975); IDMS

Notes:

- (a) AAS; INAA = 4.59%
- (b) Combined residue and leach fractions

degrees C fraction. Assuming there is a well-developed plateau above that temperature, the ages are reliable).

Compston *et al.* (1975) reported Rb-Sr isotopic data for whole-rock samples of matrix and an "anorthosite" clast in 72215 (Table 6). The matrix and anorthosite clast fall on a mixing line of about 4.4 Ga, and the Sr isotopes did not equilibrate on the scale of the plagioclase crystals (< 0.1mm). Thus the time for high-temperature assembly was very short. The dark gray matrix fraction has a high Rb content that presumably reflects microgranite. This fraction forms a precise 3.95 +/-0.03 Ga alignment with the anorthosite-depleted matrix fractions and BABI (Fig. 9); this age is a well-determined age for the granites, and is not sensitive to even quite large errors in estimating the Rb/Sr ratio of the granite. These granites are older than the breccia-forming event.

Nunes and Tatsumoto (1975) reported U, Th, Pb isotopic data for 6 matrix samples of 72215, deriving some age parameters (reproduced as Tables 7a,b,c). The data are shown, with other samples from Boulder 1, on Fig. 10, a lead concordia diagram. All data, corrected for blanks and assumed primordial Pb, lie within estimated uncertainty of a 3.9-4.4 Ga discordia line, typical of many lunar highlands rocks. Nunes and Tatsumoto (1975) interpret the 4.4 Ga intersection as merely representing an average of events older and younger than 4.4 Ga, and the 3.9 Ga intersection representing differentiation or metamorphic events at that time. Braddy *et al.* (1975) reported that they measured P and U fission tracks in whitlockites and zircons in 72215, but presented no data or results. They found zircons large enough to date in sections.

Table 5: Laser microprobe data for materials in 72215,144.
Recalculated from Schaeffer *et al.* (1982a,b).

Phase	K%	Ca%	Ar40/39		Age Ga	
K-spar*	3.1	2	35.85+/-0.49		3.905 +/- .040	
Plag	0.27	3	35.68	0.72	3.847	.039
Plag	1.2	6	36.82	0.34	3.897	.027
Plag	0.05	1	38.06	0.88	3.949	.044
Plag	0.10	1	39.85	0.91	4.022	.043
Plag	0.14	6	36.14	2.26	3.867	.103
Plag/comp	0.07	1	36.56	0.61	3.885	.035
Pyroxene	0.03	2	30.49	1.17	3.602	.064
Matrix	0.12	2	32.98	0.33	3.723	.027
Felsite*	6	<10	34.66	0.99	3.847	.042
Felsite*	6	<10	31.10	0.75	3.682	.050
Felsite*	9	<10	35.03	0.60	3.868	.043
Felsite*	3	<10	35.40	1.80	3.885	.088
Felsite*	3	<10	33.77	1.30	3.810	.070
Felsite*	8	<10	34.29	0.55	3.835	.041
Felsite*	5	<10	35.76	0.80	3.899	.050

(Samples degassed at 225 degrees centigrade during bakeout after sample loading)

* = preheated at 650 degrees centigrade

Table 6: Rb-Sr isotopic data for samples from 72215
(Compston *et al.*, 1975).

Sample	Mass mg	Rb ppm	Sr ppm	87Rb/86Sr	87Sr/86Sr
,54 gray	12.0	5.02	139.1	0.1042	0.70572+/-3
,54 anorth	11.2	0.86	164.6	0.01514	0.70006 2
,104 gray	15.8	4.05	149.7	0.0782	0.70424 3
,104 dark gray A	14.7	44.19	162.2	0.7893	0.74534 3
,104 dark gray B	13.9	43.98	161.0	0.7915	0.74513 4

Table 7a: Concentrations of U, Th, and Pb in 72215 samples (Nunes and Tatsumoto, 1975).

Concentrations of U, Th, and Pb in some Apollo 17 whole-rock samples from Boulder 1

Sample	Description	Run	Weight (mg)	Concentrations			²³² Th/ ²³⁸ U	²³⁸ U/ ²⁰⁴ Pb
				U	Th	Pb		
72215,15	Dark clast (GCBx)	C1	46.1	1.408	(4.633)	2.987	(3.40)	2801
72215,15	Light-gray breccia (GCBx)	C1	46.0	1.232	(4.081)	2.464	(3.42)	3227
		C2 ^a	85.5	1.369	5.084	2.716	3.84	1890
72215,51	Sugary dark gray breccia (GCBx)	C1	48.8	1.316	4.871	2.936	3.82	2069
		C2 ^a	98.1	1.290	4.635	^b 3.71	^b	^b
72215,68	Ordinary breccia (GCBx)	C1	55.0	1.272	4.656	2.658	3.78	1010
		C2 ^a	101.8	1.179	4.327	2.344	3.79	2480
72215,39	Ordinary breccia (GCBx)	C1	47.1	1.185	4.298	2.387	3.75	7353
72215,39	Light-gray breccia (GCBx)	C1	41.3	1.023	3.768	2.122	3.81	3322
72275,170	Pigeonite basalt clast (PB)	C1	38.6	1.635	6.255	3.047	3.95	3045

^a Totally spiked sample data; other data were spiked after solution aliquoting.

^b Underspiking and uncertainty in the sample ²⁰⁸Pb/²⁰⁶Pb yielded poor Pb concentration data.

Data in parentheses uncertain owing to poor Th concentration data.

All 72215 samples are competent breccias with colors ranging from black to light-gray.

C=concentration run (GCBx)=gray competent breccia (PB)=pigeonite basalt.

Table 7b: Isotopic composition of Pb in 72215 samples (Nunes and Tatsumoto, 1975).

Isotopic composition of Pb in some Apollo 17 whole-rock samples from Boulder 1

Sample	Description	Run	Weight (mg)	Observed Ratios ^c				Corrected for Analytical Blank ^b			
				²⁰⁶ Pb/ ²⁰⁴ Pb	²⁰⁷ Pb/ ²⁰⁴ Pb	²⁰⁸ Pb/ ²⁰⁴ Pb	²⁰⁸ Pb/ ²⁰⁶ Pb	²⁰⁷ Pb/ ²⁰⁶ Pb	²⁰⁸ Pb/ ²⁰⁶ Pb	²⁰⁷ Pb/ ²⁰⁴ Pb	²⁰⁸ Pb/ ²⁰⁴ Pb
72215,15	Dark clast (GCBx)	P	49.8	1402	786.6	1363	4491	2508	4323	0.5584	0.9625
		C1	46.1	1118	628.7	-	2730	1528	-	0.5596	-
72215,15	Light-gray breccia (GCBx)	P	48.5	1593	837.3	1545	(36540)	(19073)	(34980)	0.5220	0.9573
		C1	46.0	1040	549.3	-	3016	1581	-	0.5226	-
		C2 ^a	85.5	1382	714.6	-	1755	906.1	-	0.5162	-
72215,51	Sugary dark gray breccia (GCBx)	P	47.3	505.7	293.2	498.1	686.0	396.0	668.4	0.5772	0.9744
		C1	48.8	1010	580.1	-	2094	1198	-	0.5720	-
72215,68	Ordinary breccia (GCBx)	C2 ^a	98.1	1059	627.6	-	1219	721.6	-	0.5920	-
		P	37.2	933.0	514.2	902.2	2899	1586	2759	0.5471	0.9520
72215,68	Ordinary breccia (GCBx)	C1	55.0	662.9	366.9	-	979.1	539.3	-	0.5508	-
		C2 ^a	101.8	1716	891.5	-	2311	1199	-	0.5186	-
72215,39	Ordinary breccia (GCBx)	P	38.3	1207	635.2	1180	3952	2066	3815	0.5227	0.9656
		C1	47.1	1629	855.5	-	6892	3599	-	0.5223	-
72215,39	Light-gray breccia (GCBx)	P	39.0	1383	763.3	1332	(11731)	(6432)	(11145)	0.5483	0.9500
		C1	41.3	1096	605.3	-	3197	1756	-	0.5492	-
72275,170	Pigeonite basalt clast (PB)	P	38.9	2360	1079	2387	(34287)	(15592)	(34420)	0.4547	1.0038
		C1	38.6	1299	597.2	-	2672	1220	-	0.4568	-

P = composition run; C = concentration run; (GCBx) = gray competent breccia; (PB) = pigeonite basalt.

^a Totally spiked runs from solid sample splits; other runs were obtained from samples which were divided from solution.

^b Pb blanks ranged from 1.4 to 2.1 ng for the solution aliquoted data and were 1.05 ng for the totally spiked data.

^c Raw data corrected for mass discrimination of 0.15% per mass unit. ²⁰⁸Pb spike contribution subtracted from concentration data.

Data in parentheses subject to extreme error owing to Pb blank uncertainty.

All 72215 samples are competent breccias with colors ranging from black to light-gray.

P. D. NUNES AND M. TATSUMOTO

Table 7c: Age parameters and single-stage ages for 72215 samples (Nunes and Tatsumoto, 1975).

Age parameters and single-stage ages of some Apollo 17 Boulder 1 whole-rock samples

Sample	Description	Run	Atomic ratios corrected for blank and primordial Pb			Single-stage ages $\times 10^4$ yr				
			$\frac{^{208}\text{Pb}}{^{238}\text{U}}$	$\frac{^{207}\text{Pb}}{^{235}\text{U}}$	$\frac{^{207}\text{Pb}}{^{208}\text{Pb}}$	$\frac{^{208}\text{Pb}}{^{232}\text{Th}}$	$\frac{^{206}\text{Pb}}{^{238}\text{U}}$	$\frac{^{207}\text{Pb}}{^{235}\text{U}}$	$\frac{^{207}\text{Pb}}{^{206}\text{Pb}}$	$\frac{^{208}\text{Pb}}{^{232}\text{Th}}$
72215,15	Dark clast (GCBx)	C1P	0.9726	74.73	0.5573	0.2740	4380	4394	4400	4895
		C1	0.9713	74.70	0.5577	—	4375	4393	4402	—
72215,15	Light-gray breccia (GCBx)	C1P	0.9344	67.23	0.5218	0.2612	4253	4288	4304	4690
		C1	0.9317	67.13	0.5226	—	4244	4286	4306	—
72215,51	Sugary dark gray breccia (GCBx)	C2*	0.9299	66.36	0.5131	—	4218	4259	4279	—
		C1P	0.9985	78.47	0.5699	0.2466	4464	4443	4433	4455
72215,68	Ordinary breccia (GCBx)	C1	1.008	79.14	0.5696	—	4493	4451	4432	—
		C1P	0.9657	72.61	0.5453	0.2421	4357	4365	4368	4367
72215,39	Ordinary breccia (GCBx)	C1	0.9596	72.17	0.5455	—	4337	4359	4369	—
		C2*	0.9286	66.09	0.5162	—	4234	4271	4288	—
72215,39	Light-gray breccia (GCBx)	C1P	0.9351	67.22	0.5214	0.2397	4256	4288	4303	4343
		C1	0.9360	67.30	0.5215	—	4259	4288	4303	—
72215,39	Light-gray breccia (GCBx)	C1P	0.9616	72.64	0.5479	0.2395	4343	4365	4375	4340
		C1	0.9596	72.49	0.5476	—	4337	4363	4375	—
72275,170	Pigeonite basalt clast (PB)	C1P	0.8776	55.00	0.4547	0.2228	4061	4087	4100	4065
		C1	0.8747	54.82	0.4545	—	4051	4084	4100	—

* Concentrations determined from totally spiking a separate sample. Concentration and composition splits were divided from perfect solutions prior to spiking for all other analyses.
 All 72215 samples are competent breccias with colors ranging from black to light-gray.
 P—composition run; C—concentration run; (GCBx)—gray competent breccia; (PB)—pigeonite basalt.

U-Th-Pb SYSTEMATICS OF SELECTED SAMPLES FROM APOLLO 17, BOULDER 1, STATION 2

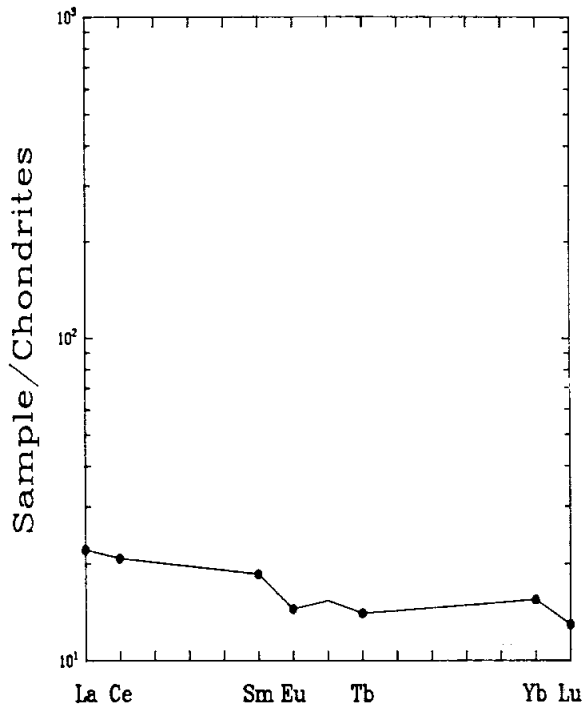


Figure 8: Rare earth element plot for poikilitic feldspathic granulite in 72215. Blanchard et al. (1975).

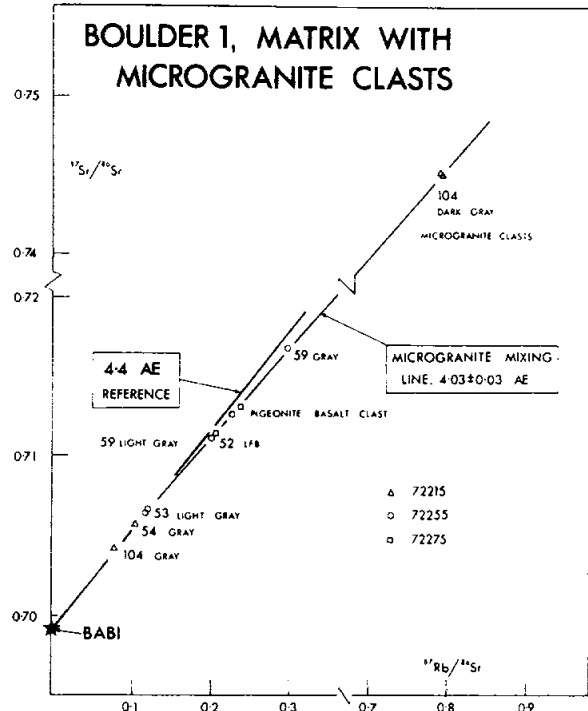
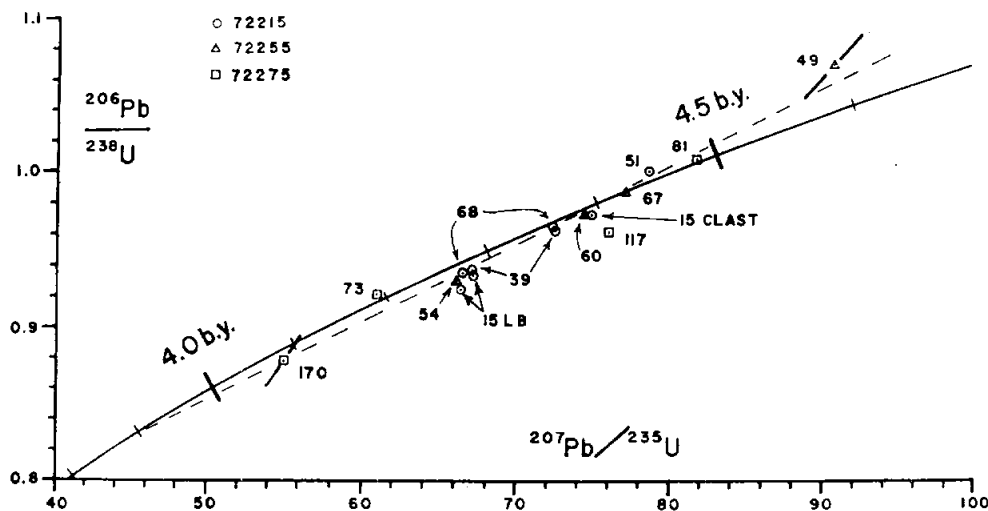


Figure 9: Mixing line defined by 72215,104 dark gray and other samples. The mixing line determines the age of the microgranite, which dominates 72215,104 dark gray, because the microgranites are so radiogenic. The 4.03 Ga age is calculated using the "old" Rb decay constants; using the constant of 1.42×10^{-11} /yr gives 3.95 Ga.



Concordia diagram (Wetherill, 1956) with Boulder 1 data corrected for blanks and primordial Pb. All data for 72215 (circles) and pigeonite basalt clast 72275,170 are from this report; all other 72275 (squares) and 72255 (triangles) data are from Nunes *et al.* (1974a). U/Pb errors of $\pm 2\%$ are shown for the two most extreme analyses, but are omitted from the other data points for clarity. Individual analyses are labelled with their subnumbers. LB=light-gray breccia; b.y.= 10^9 yr. Anorthositic breccia clast 72275,117 is considered to lie outside of error below the 3.9–4.4 b.y. discordia line; all other samples, including matrix sample 72275,73, lie within error of this line.

Figure 10: Concordia diagram for 72215 and other Boulder 1 samples (Nunes and Tatsumoto, 1975).

EXPOSURE AGES

Leich *et al.* (1975) measured the isotopic compositions of the rare gases He, Ne, Ar, Kr, and Xe in three matrix samples from 72215. Trapped gas abundances are very low, with only small to negligible solar wind components. The cosmogenic Kr isotopic spectra give an exposure age of 41.4 ± 1.4 Ma, in good agreement with that of 72255. It is lower than the exposure age of 72275 (52 Ma), probably because of differences in shielding.

PHYSICAL PROPERTIES

Magnetic data for 72215 samples were reported by Banerjee and Swits (1975) and Banerjee and Mellema (1976 a,b,c), with the aim of determining paleointensity (Table 8). The average direction of NRM was the same as that in 72255 and 72275, while the stable components differed in direction.

The Shaw method suggests an averaged large field of 0.41 Oe at 4.0 Ga at Taurus-Littrow. This is similar to the size of the field determined from carbonaceous chondrites; the authors suggest a field of solar origin. Cisowski *et al.* (1977) noted that 72215 did not have hysteresis characterization available, and did not have the minimal requirements of a single phase NRM. Thus, they did not accept the paleointensity measurement as meaningful.

Adams and Charette (1975) and Charette and Adams (1977) obtained reflectance spectra for chips and powders of 72215 (Fig. 11). All the samples have absorption bands near 0.9 and 1.9 microns, from Fe^{2+} in orthopyroxene. The anorthositic gabbro curve (poikilitic feldspathic granulite), 72215,101, is characterized by deep pyroxene and plagioclase Fe^{2+} bands; a high left shoulder at 0.7 microns relative to right shoulder at 1.1 microns; and the absence of any absorption

feature near 0.6 microns. The lighter breccias differ from the darker ones, with the latter (58) having weaker pyroxene and plagioclase bands, more-nearly equal shoulders, and a flatter slope of the continuum.

PROCESSING

The details of the processing of 72215 were given by Marvin in CI 2 (1974), with detailed allocation information. During PET in 1973 a documented chip was used for thin sections, and others were later taken for varied purposes. Marvin and Agrell made detailed surface maps (July 1973). A single saw cut was planned to section all features of interest across the foliation; during sawing (1974) the knob broke from the main slab, producing several subsamples (Fig. 2). Two thin subslabs were cut through the original slab, and devoted to thin sections (Fig. 12).

Table 8: Paleointensity determinations for 72215 samples (Banerjee and Mellema, 1976)

Sample #	Number of determinations	H (Oersted)	s.d	Range (Oersted)
,56	7	0.55	0.10	0.74-0.44
,46	7	0.41	0.17	0.60-0.21
,93	8	0.28	0.07	0.37-0.18

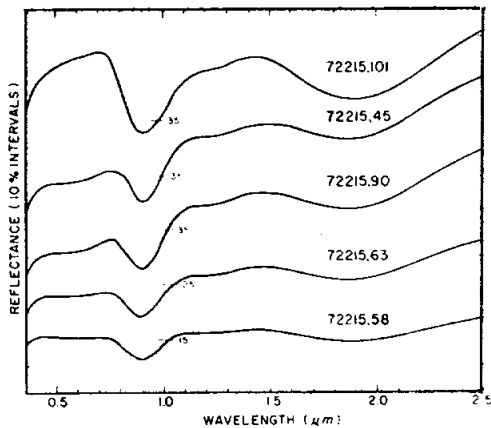


Figure 11: Spectral reflectance diagrams for 72215 samples (Adams and Charette, 1975). ,101 is poikilitic feldspathic granulite (anorthositic gabbro); ,45 and ,90 are light to medium-gray matrix; ,58 is dark matrix; and ,63 is matrix intermediate to dark and light.

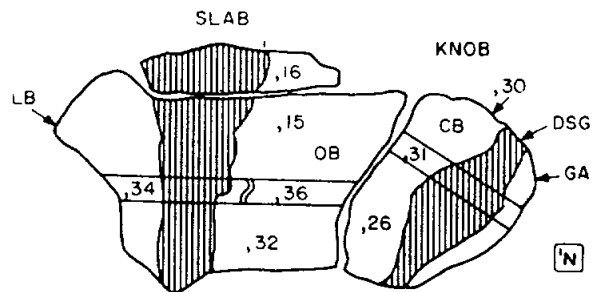


Figure 12: Dissection of the original slab to show the source of the thin section transect (,31; ,36; ,34) and other sample numbers (from Marvin, CI 2, 1974).

72235**Aphanitic Impact Melt Breccia****St. 2, 61.9 g****INTRODUCTION**

72235 is an aphanitic, clast-rich impact melt interlayered with feldspathic clast material that was sampled as a resistant knob on Boulder 1 (see section on Boulder 1, St. 2, Fig. 2). The knob has a patch of adhering medium light-gray [N6-N7] friable matrix similar to 72275 (Fig. 1). 72235 was given the name "Dying Dog" during processing. The knob is about 4 cm across and angular; its dark gray [N3] and very light gray [N8] materials are tough. The exposed surface is brownish gray with a few zap pits.

The dark and light layers of the knob appear to have been crushed and fluidized; veinlets of dark material intrude white layers, and veinlets of white layers intrude the dark material. The dark material is fine-grained, almost glassy looking,

impact melt with numerous clasts. The light material consists of feldspathic granulites, other feldspathic breccias, and other lithic types including plutonic KREEP norite. The aphanitic melt appears to be a low-K Fra Mauro composition, contaminated with meteoritic material. No isotopic or exposure studies have been conducted.

Most of the studies of 72235 were conducted by the Consortium Indomitabile (leader J.A. Wood). A slab was cut perpendicular to the layering in the knob for comprehensive petrographic and chemical study (Fig. 2). Detailed maps of the exterior surfaces and the slab based on macroscopic observations, as well as descriptions of the sample allocations, were given in Stoesser *et al.* (in CI 2, 1974).

PETROGRAPHY

72235 consists of a coherent knob of interlayered dark gray-to-black and white breccias, with a piece of adhering light-gray friable matrix similar to that of 72275 (Marvin, 1975; CI 2, 1974). LSPET (1973) described 72235 as a layered light-gray breccia. Simonds *et al.* (1974) listed it as a fragmental breccia (clast-supported). The most detailed descriptions of the petrography of 72235 are given in Stoesser *et al.* (in CI 2, 1974) and in Ryder *et al.* (1975). When 72235 broke from Boulder 1, it proved to be a clast of roughly layered gray and white breccias almost wholly enclosed within a gray-black, aphanitic rind. Marvin (1975) described the dark and light layers as appearing to have been crushed and fluidized under confining pressure, with the two phases mutually intrusive. The rind varies

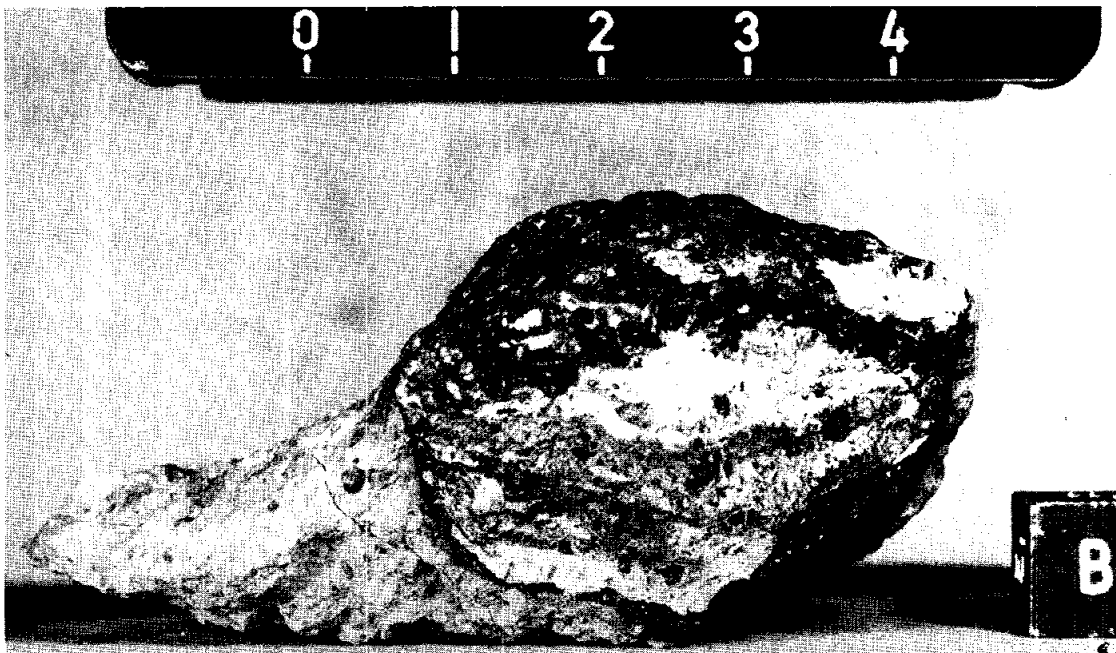


Figure 1: Bottom (arbitrary) face of 72235 prior to slabbing. The topmost visible part was exposed and has patina and zap pits; the remainder is freshly broken. Scale in centimeters. S-73-23589 B.



Figure 2: Cutting of 72235 in 1974. ,13 and ,11 are end pieces; ,6; ,14; and ,15 are matrix pieces that broke away; ,16 is the slab piece. Apart from a thin section from ,6, all further subdivisions and allocations were made from ,16. Scale in centimeters. S-74-20429.

in thickness from less than 1 mm to 5 mm.

The adhering light-gray friable breccia contains numerous angular fragments of aphanitic gray material and a few yellowish patches that are possibly pigeonite basalt. In thin sections it varies from very fine-grained and porous to blobby (Figs. 3a and b). It contains a variety of lithic and mineral fragments but no pigeonite basalts occur in the sections.

In the hand specimen the rind looks markedly darker and more vitreous than any of the interior layers. Macroscopically it appeared as an annealed breccia with several percent small angular inclusions. The white layers appeared to be "cataclastic gabbroic anorthosite" with 10 to 20% yellow and brown mafic crystals plus traces of metal and troilite. The white layers include a few dark gray aphanitic clasts and at least two prominent holocrystalline lithic clasts of coarse mafic silicates.

The set of thin sections from the slab revealed that the central clast is composed of a number of different breccias with a complex structural history. Stoesser *et al.* (in CI 2, 1974) divided it into 6 domains (Fig. 4).

Domain 1—*anorthositic polymict breccia.*

Domain 2—*dense dark matrix breccia (impact melt).*

Domain 3—*white feldspathic granulite breccia.*

Domain 4—*"core" polymict breccia.*

Domain 5—*monomict noritic anorthosite breccia.*

Domain 6—*dark matrix breccia (impact melt).*

Domains 2 and 6 correspond with the rim, and domain 1 lies outside these domains. Domains 3 to 5 are the interior of the knob.

Domain 1: Domain 1 is a feldspathic polymict breccia consisting almost entirely of unshocked mineral fragments of plagioclase and pyroxene, with some fragments of dark melt material and feldspathic granulite. The monomineralic fragments appear to be the crushed remnants of an anorthositic lithology with an average grain size greater than 100 microns and with 10 to 20% mafic silicates. The contact between domains 1 and 2 is sharp.

Domain 2: The rind, domain 2, is the darkest of the melt breccias in 72235, and the least porous. It contains few clasts larger than 0.5 mm, and is poorer in clasts than the other domains (Fig. 3c). A defocused beam analysis indicates its general low-K Fra Mauro composition (Table 1, col. 8) and similarity to other Boulder 1 melts.

Domain 3: Domain 3 is a monomict breccia consisting of fragments of feldspathic granulite in a crushed matrix of itself (Fig. 3d) with a porosity of about 10%. It is similar to other granulites in Boulder 1 except that it appears to contain more ilmenite. Defocused beam analyses indicate that it is chemically similar to domain 5 (Table 2).

Domain 4: The core of 72235 is a complicated polymict breccia consisting of lithic clasts (including melt breccias and feldspathic granulites) and mineral fragments that are crushed and intermixed. The core appears to have been formed in a turbulent environment. Some of the melt breccia clasts are very dark and somewhat vesicular. Defocused beam analyses of such materials show the common low-K Fra Mauro composition (Table 1, cols. 9 and 10), although the core appears to have more titanium.

Domain 5: Domain 5 is a narrow zone (Fig. 4) of monomict breccia containing no polymineralic fragments. The parent consisted of about 75% plagioclase and 25% pyroxene, with small amounts of

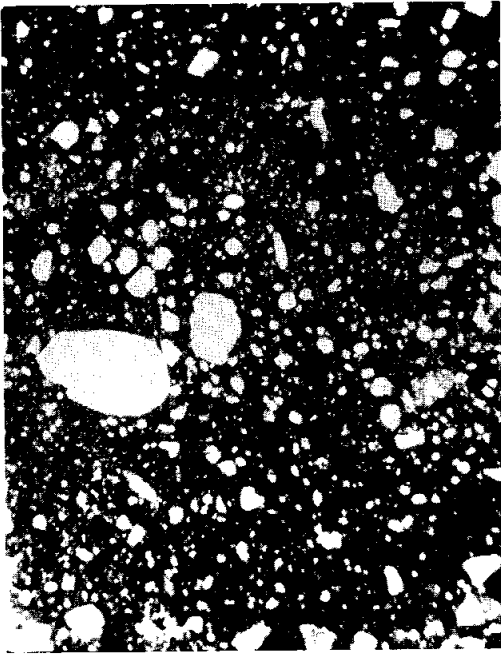


Figure 3: Photomicrographs of 72235; all plane transmitted light, all about 1 mm width of view. a) 72235,9 crushed fragmental fine matrix, dominantly mineral fragments.



Figure 3b: 72235,86 blobby fragmental matrix showing dark melt blobs and mineral fragments.



Figure 3c: 72235,59 rind (domain 2) of knobby clast.

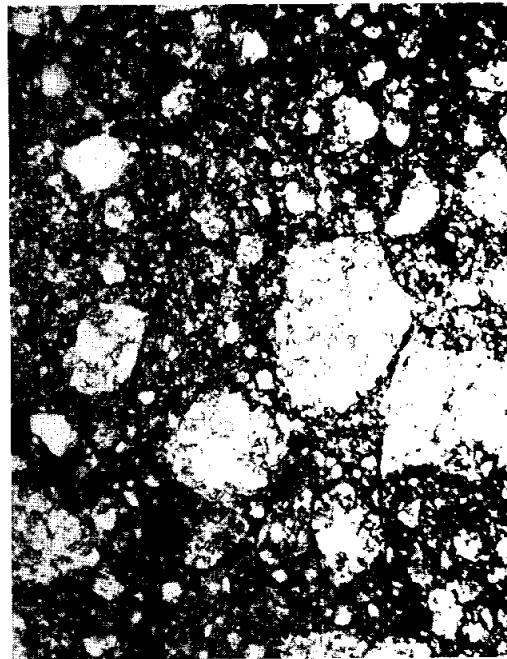


Figure 3d: 72235,61 cataclastic feldspathic granulite (domain 3).

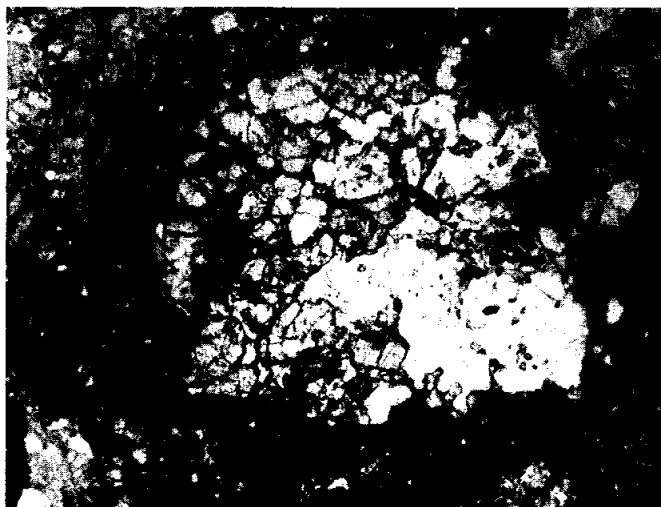


Figure 3e: 72235,52 fragment of KREEP norite.

pink spinel. A defocused beam analysis (Table 2, col. 12) shows that it is very similar to domain 3 feldspathic granulite.

Domain 6: The rind represented by domain 6 is similar to that of domain 2 except that it is a little lighter in color, contains larger clasts, and is slightly more porous.

Stoeser *et al.* (in CI 2, 1974) reported a survey of clast populations in the 72235 melt phases (dark matrix breccias; domains 2, 4, and 6) (Table 3) for clasts larger than 200 microns. Few clasts exceed 1 mm. Compositions of olivines are shown in Fig. 5. The clasts in the melts are dominated by feldspathic materials (varied feldspathic breccias and plagioclase fragments), but there are significant contributions from basaltic (mainly impact melts?) and granitic fragments (see also Spudis and Ryder, 1981). The basaltic fragments include olivine-normative pigeonite-bearing basalts and "troctolitic" fragments bearing pink spinels. Defocused beam analyses of these basaltic fragments are in Table 4. Most of the olivine-normative pigeonite basalts in the boulder are from 72235, and the mineral data given in Fig. 6a are mainly from 72235. The granites were described by Stoeser *et al.*

(1975) and Ryder *et al.* (1975); some mineral data for the granites is given in the catalog section on 72215. They include glassy and holocrystalline varieties.

A distinctive clast in 72235 was a 3 mm fragment of KREEP norite (Fig. 3e) that was yellowish-brown and embedded in feldspathic material. It was recognized macroscopically as distinct, with coarse anhedral brown pyroxene and gray translucent plagioclase (Stoeser *et al.*, in CI 2, 1974). Thin sections show that the KREEP norite consists of equal amounts of plagioclase and pyroxene, with about 1% accessory minerals that are mainly ilmenite and troilite, with a trace of phosphate. The silicate grains occur in interlocking domains up to 1 mm diameter. The compositions of silicate minerals are shown in Fig. 6b. The Or component of the plagioclase is uncommonly high.

Stoeser *et al.* (in CI 2, 1974) note that the textural relations of the materials in 72235 are inconsistent with simple plastering on of a rind to anorthositic material in flight. Both lithologies were fluidized and intermixed with rotation. The origin is somewhat complex.

CHEMISTRY

Chemical analyses for matrix and clast samples are given in Tables 5 and 6, with the rare earths diagrammed in Fig. 7. None of the matrix samples in Table 5 are pure impact melt, but are mixtures of melt and white clast material. ,46 and ,48 are the domain 4 polymict breccia from the interior of the clast; ,11 is the entire end-piece consisting of all the domains. The chemistry is consistent with a mixture of melts similar to those in 72215 and 72255 (as suggested by the defocused beam analyses in Table 1) with dominantly feldspathic granulites. The analysed materials are obviously contaminated with meteoritic siderophiles. The anorthositic breccia (Table 6) is the more pure material of domain 3, feldspathic granulite; it too is obviously contaminated with meteoritic siderophiles. It is far less enriched in incompatible elements than is the bulk rock (Fig. 7).

Higuchi and Morgan (1975) and Morgan *et al.* (1975) placed the meteoritic signature of 72235 in a group 3L with samples from 72215, and distinct from 72235 and 72275. They suggest a heterogeneous impacting body (they assume the siderophiles are derived from a single impacting body).

PROCESSING

72235 was left intact during PET, and was mapped in May, 1973. A chip of dark aphanitic material fell off and was mainly used for thin sections. In 1974 a 1.5 cm thick slab was cut from the center of the large clast, after a chunk of the friable matrix broke away. The main cutting is shown in Fig. 2. The slab ,16 was cut into 3 pieces (Fig. 8). ,28 was used for thin sections, and ,29 for other allocations. The remaining piece ,16 was not allocated.

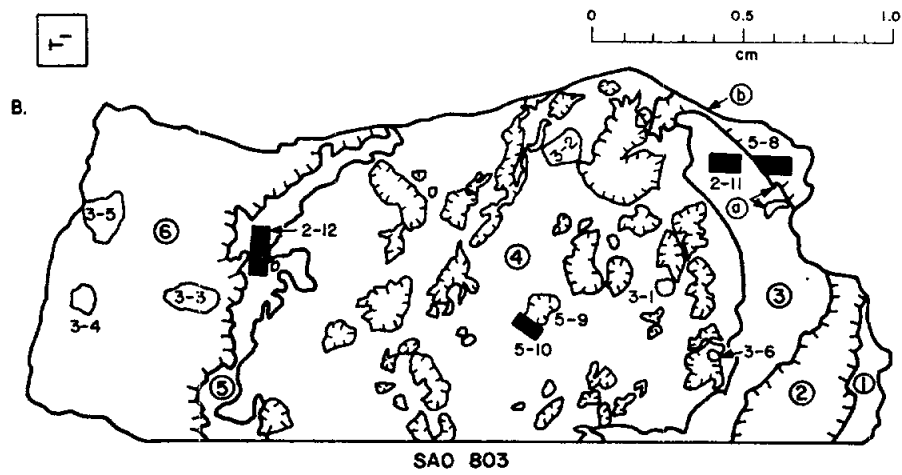
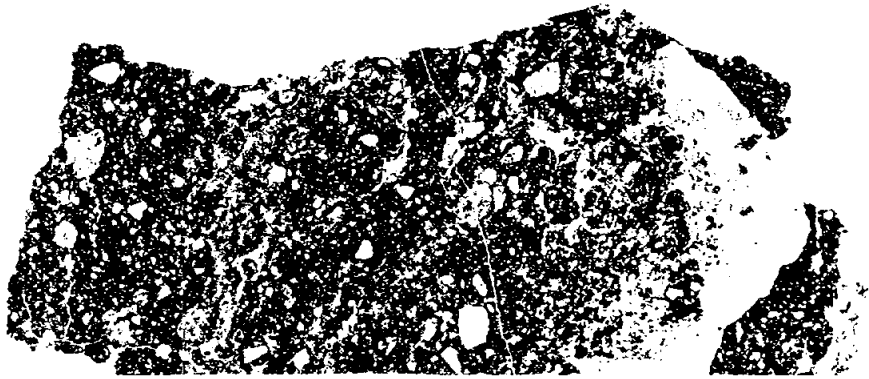


Figure 4: Photograph and sketch map of thin section 72235,59 which is a complete section through the 72235 knob. The circled numbers on the sketch map correspond with the domains. Dark matrix (melt) materials are indicated by barbed lines. From Stoesser et al. (in CI 2, 1974).

Table 1: Microprobe defocused beam analyses of dark matrix materials in 72235
(from Stoesser *et al.*, in CI 2, 1974).

	8.	9.	10.
	803	803C20	803C20
	matrix dom. 2	vesic. DMB clast	DMB rim
WT. % OXIDES			
SiO ₂	45.68	46.71	45.81
TiO ₂	0.70	2.05	0.83
Al ₂ O ₃	21.15	20.11	21.52
Cr ₂ O ₃	0.21	0.25	0.28
FeO	8.00	8.44	7.57
MnO	0.11	0.12	0.13
MgO	8.92	8.99	8.33
CaO	12.19	12.13	12.36
Na ₂ O	0.49	0.68	0.55
K ₂ O	0.25	0.35	0.20
BaO	0.05	0.02	0.03
P ₂ O ₅	0.23	0.29	0.31
TOTAL	97.98	100.17	97.90
CIPW NORM			
FO	3.6	1.8	1.8
FA	2.4	1.1	1.2
EN	17.6	19.8	18.7
FS	10.7	10.7	11.3
WO	1.8	3.2	1.6
OR	1.5	2.1	1.2
AB	4.3	5.8	4.7
AN	55.9	50.7	56.9
ILM	1.3	3.9	1.6
CHR	0.3	0.4	0.4
QTZ	---	---	---
COR	---	---	---
AP	0.5	0.7	0.7
COMP. NORM MIN.			
OL: FO	68.3	70.8	68.5
PX: EN	17.6	64.5	65.3
FS	29.9	26.6	30.0
WO	5.7	8.9	4.7
PLAG: OR	2.4	3.5	1.9
AB	7.3	10.4	7.9
AN	90.2	86.1	90.2
atomic Mg/(Mg+Fe)	0.666	0.655	0.662
MgO/(MgO+FeO)	0.527	0.516	0.524
No. of analyses	27	18	10

Table 2: Microprobe defocused beam analyses of feldspathic interior materials in 72235
(from Stoesser *et al.*, in CI 2, 1974).

	11.	12.
	803	803
	dom. 3 gran. ANT breccia	dom. 5 crushed gab. anorth.
WT. % OXIDES		
SiO ₂	40.43	41.72
TiO ₂	0.15	0.18
Al ₂ O ₃	26.98	27.41
Cr ₂ O ₃	0.08	0.09
FeO	3.84	4.00
MnO	0.04	0.06
MgO	5.85	5.02
CaO	14.35	15.06
Na ₂ O	0.39	0.40
K ₂ O	0.06	0.09
BaO	n.d.	n.d.
P ₂ O ₅	0.04	0.09
TOTAL	92.23	94.13
CPIW NORM		
FO	8.5	5.8
FA	4.4	3.6
EN	3.6	5.0
FS	1.7	2.8
WO	---	0.6
OR	0.4	0.6
AB	3.6	3.6
AN	77.0	77.3
ILM	0.3	0.4
CHR	0.1	0.1
QTZ	---	---
COR	0.3	---
AP	0.1	0.2
COMP. NORM. MIN.		
OL: FO	73.7	69.8
PX: EN	73.7	64.8
FS	26.3	28.0
WO	---	7.1
PLAG: OR	0.5	0.7
AB	4.7	4.6
AN	94.9	94.7
atomic Mg/(Mg+Fe)	0.731	0.690
MgO/(MgO+FeO)	0.604	0.557
No. of analyses	22	21

Table 3: Clast populations of 72235 dark matrix materials. Percentages by volume in three size categories.
(From Stoesser *et al.*, in CI 2, 1974).

	0.2-0.5 mm	0.5-1.0 mm	1.0 mm	TOTALS
ANT suite	(46.4)	(8.6)	(0.2)	(55.2)
ANT breccias	(17.5)	(3.1)	-	(20.6)
mafic	0.4	0.2	-	0.6
gabbroic	13.0	2.3	-	15.3
anorthositic	4.1	0.6	-	4.7
Granulitic ANT	(24.8)	(4.3)	-	(29.1)
gabbroic	22.9	4.3	-	27.2
anorthositic	1.9	-	-	1.9
Poikiloblastic ANT	-	-	-	-
Poikilitic ANT	-	-	-	-
Coarse ANT	3.1	0.4	0.2	3.7
Unclassified ANT	1.0	0.8	-	1.8
Ultramafic particles	1.6	-	-	1.6
Basalts	(1.8)	(0.6)	(0.6)	(3.0)
Ol.-norm. pig. bas.	0.4	0.6	0.6	1.6
Pink sp. troct. bas.	0.8	-	-	0.8
Unclassified	0.6	-	-	0.6
Microgranites	4.5	0.8	-	5.3
Civet Cat norite	0.2	-	-	0.2
KREEP norite	-	-	0.2	0.2
Devitrified maskelynite	10.8	1.2	-	12.0
Glassy clasts	2.3	-	-	2.3
Mineral fragments	(19.8)	(0.4)	-	(20.2)
Plagioclase	12.3	0.2	-	12.5
Olivine	1.8	-	-	1.8
Pyroxene	5.7	0.2	-	5.9
TOTAL %	87.4	11.6	1.0	100.0
NO. OF CLASTS	450	58	5	513

Table 4: Microprobe defocused beam analyses of basaltic textured particles in 72235. Cols. 1-5 are olivine-normative pigeonite basalts; col. 6 is a pink spinel-bearing troctolitic basalt.
(From Stoesser *et al.*, in CI 2, 1974).

	1.	2.	3.	4.	5.	6.
	803C1	803C4	803C7	803C9	803C10	803C5
	quench	ol-pheno.	ol-pheno.	equigran.	suboph.	PSTB
	basalt	basalt	basalt	basalt	basalt	
WT. % OXIDES						
SiO ₂	48.04	46.92	46.17	45.47	45.37	41.80
TiO ₂	0.40	0.84	0.34	0.49	0.23	0.82
Al ₂ O ₃	12.26	11.52	10.99	11.03	14.73	22.89
Cr ₂ O ₃	0.25	1.23	0.28	0.59	0.88	0.05
FeO	15.02	16.51	14.89	16.97	12.75	5.72
MnO	0.25	0.28	0.27	0.27	0.26	0.06
MgO	9.25	13.29	11.91	13.17	10.58	12.91
CaO	12.17	10.26	10.42	10.22	11.45	12.89
Na ₂ O	0.40	0.11	0.22	0.16	0.13	0.51
K ₂ O	0.86	0.07	0.20	0.04	0.08	0.16
BaO	0.05	0.07	0.04	0.05	0.03	0.03
P ₂ O ₅	0.02	0.02	n.d.	0.01	0.02	0.11
TOTAL	98.98	101.12	95.75	98.46	96.51	97.96
CIPW NORM						
FO	3.8	6.1	4.7	8.8	3.8	23.0
FA	4.9	5.8	4.7	9.0	3.6	7.3
EN	17.9	24.0	24.3	20.8	21.9	---
FS	21.1	20.6	22.1	19.2	18.9	---
WO	13.2	8.3	10.2	9.1	7.5	1.7
OR	5.2	0.4	1.2	0.2	0.5	1.0
AB	3.4	1.0	1.9	1.3	1.1	4.4
AN	29.4	30.4	29.7	29.7	40.8	60.7
ILM	0.8	1.6	0.7	0.9	0.4	1.6
CHR	0.4	1.8	0.4	0.9	1.3	0.1
QTZ	---	---	---	---	---	---
COR	---	---	---	---	---	0.1
AP	---	---	---	---	---	0.3
COMP. NORM MIN.						
OL: FO	52.7	60.5	59.0	58.7	60.3	82.1
PX: EN	39.5	51.2	48.7	48.0	51.2	---
FS	35.4	33.4	33.7	33.9	33.7	---
WO	25.1	15.4	17.6	18.1	15.1	---
PLAG: OR	13.5	1.3	3.8	0.7	1.1	1.4
AB	9.4	3.2	6.1	4.5	2.9	7.1
AN	77.1	95.5	90.1	94.7	96.0	91.5
atomic Mg/(Mg+Fe)	0.526	0.589	0.588	0.580	0.596	0.801
MgO/(MgO+FeO)	0.381	0.446	0.444	0.437	0.453	0.693
No. of analyses	16	16	17	17	34	8

Table 5: Chemistry of polymict materials of 72235.

	,46	,11	,40 (black md)	,48
Split wt %				
SiO ₂	44.6			
TiO ₂	0.8			
Al ₂ O ₃	23.1			
Cr ₂ O ₃	0.21			
FeO	7.28			
MnO	0.111			
MgO	9.9			
CaO	13.2			
Na ₂ O	0.514			
K ₂ O	0.20	0.218		
P ₂ O ₅				
ppm				
Sc	15.4			
V				
Co	24.0			
Ni	190		186	195
Rb			8.57	5.10
Sr				
Y				
Zr				
Nb				
Hf	9.5			
Ba				
Th	4.0	4.67		
U		1.15	1.690	1.350
Cs			0.332	0.220
Ta	1.1			
Pb				
La	22.7			
Ce	58			
Pr				
Nd				
Sm	10.6			
Eu	1.25			
Gd				
Tb	2.4			
Dy				
Ho				
Er				
Tm				
Yb	8.9			
Lu	1.20			
Li				
Be				
B				
C				
N				
S				
P				
Cl				
Br			0.134	0.0361
Cu				
Zn			2.0	1.8
ppb				
Au			2.46	2.77
Ir			7.16	7.51
I				
At				
Ga				
Ge			169	124
As				
Se			67	48
Mo				
Tc				
Ru				
Rh				
Pd				
Ag			5.17	0.448
Cd			7.4	3.1
In				
Sn				
Sb			1.13	0.65
Te			3.5	2.2
W				
Re			0.530	0.524
Os				
Pt				
Hg				
Tl			2.80	0.57
Bi			0.26	0.12
	(1)	(2)	(3)	(3)

References and methods:

- (1) Blanchard et al (1975); INAA,AAS - also in Cl(2)
- (2) Truchter et al (1975); g. ray
- (3) Higuehi ad Moyen (1975); RNAA Meyer et al (1975)

Table 6: Chemistry of feldspathic granulite (domain 3) interior clast material from 72235.

	,36	,37
Split wt %		
SiO ₂	44.5	
TiO ₂	0.8	
Al ₂ O ₃	25.8	
Cr ₂ O ₃	0.146	
FeO	6.19	
MnO	0.080	
MgO	8.52	
CaO	14.4	
Na ₂ O	0.42	
K ₂ O	0.11	
P ₂ O ₅		
ppm		
Sc	9.84	
V		
Co	43.7	
Ni	500	307
Rb		1.41
Sr		
Y		
Zr		
Nb		
Hf	2.2	
Ba		
Th	1.6	
U		0.430
Cs		0.0746
Ta	0.5	
Pb		
La	7.2	
Ce	20	
Pr		
Nd		
Sm	3.66	
Eu	0.92	
Gd		
Tb	0.80	
Dy		
Ho		
Er		
Tm		
Yb	2.9	
Lu	0.41	
Li		
Be		
B		
C		
N		
S		
F		
Cl		
Br		
Cu		0.0434
Zn		1.3
ppb		
Au		4.89
Ir		17.6
I		
At		
Ga		
Ge		210
As		
Se		25
Mo		
Tc		
Ru		
Rh		
Pd		
Ag		0.357
Cd		4.4
in		
Sn		
Sb		0.86
Te		2.7
W		
Re		1.19
Os		
Pt		
Hg		
Tl		0.38
Bi		0.33
	(1)	(2)

References and methods:

- (1) Blanchard et al (1975); INAA,AAS also in Cl. (2)
- (2) Higuehi ad Moyen (1975); RNAA Meyer et al (1975)

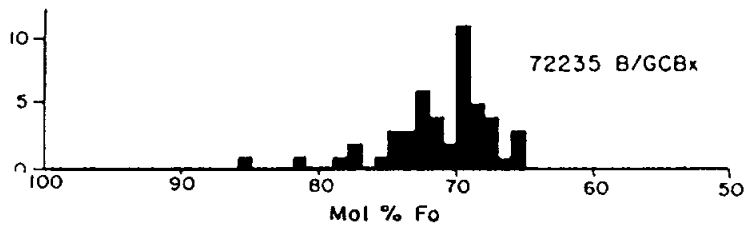


Figure 5: Compositions of olivine in the dark matrix material of 72235. From Ryder et al. (1975).

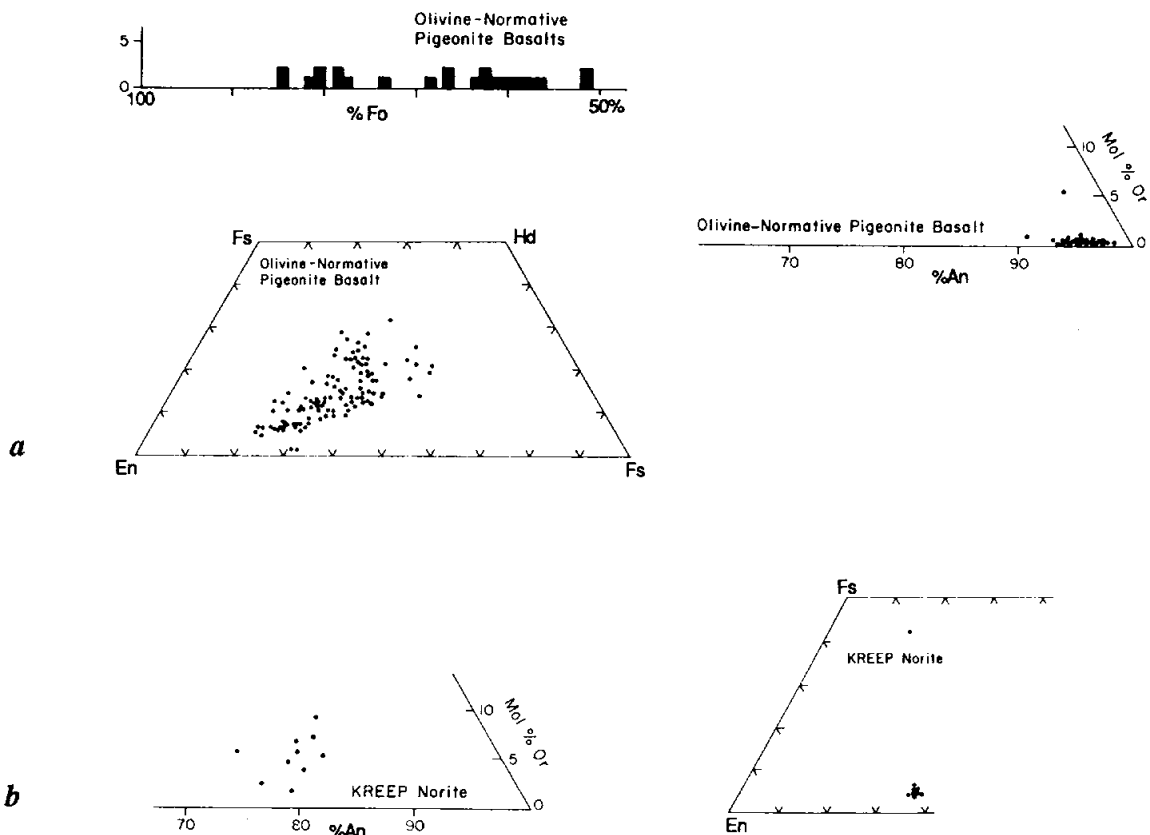


Figure 6: a) Olivine, plagioclase, and pyroxene compositions for olivine-normative pigeonite basalts, mainly from 72235. b) Plagioclase and pyroxene compositions from the KREEP norite clast in 72235. From Ryder et al. (1975).

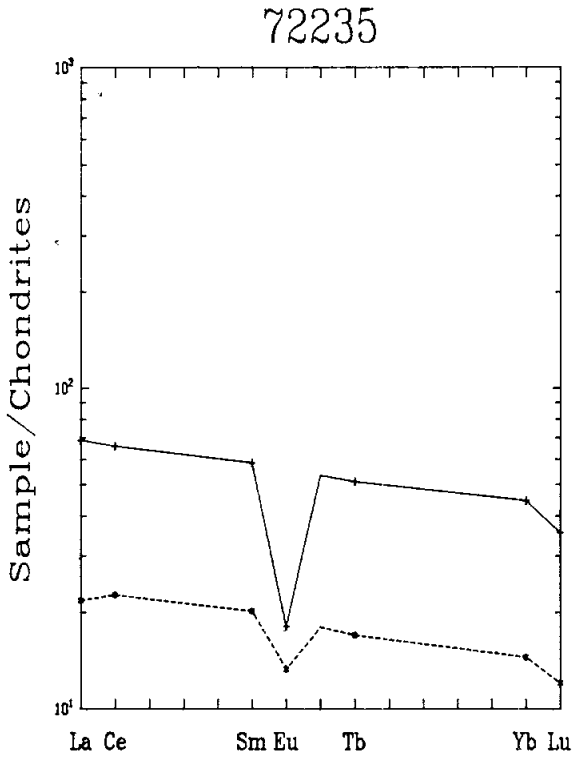


Figure 7: Rare earth elements in polymict breccia (solid line) and feldspathic granulite (dashed line) in 72235. All data from Blanchard et al. (1975).

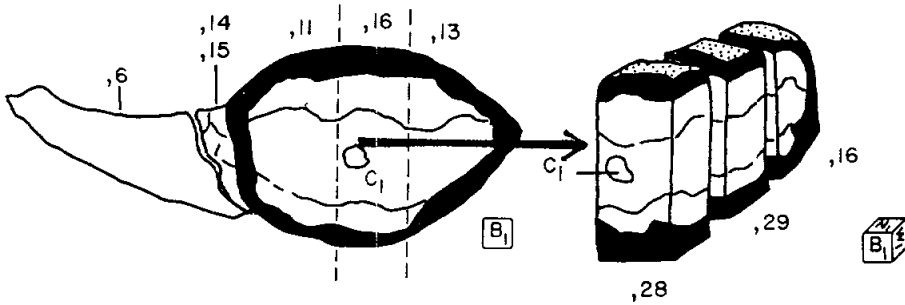


Figure 8: Diagram of cutting of slab and subdivision of slab from 72235 in 1974.

72255**Aphanitic Impact Melt Breccia
St. 2, 461.2 g****INTRODUCTION**

72255 is an aphanitic, clast-rich impact melt that was a rounded mass or bulge on Boulder 1 (see section on Boulder 1, St. 2, Fig. 2). It may have been part of a single large clast in the boulder (Marvin, 1975a). Its groundmass crystallized about 3.8 Ga ago. The sample, slightly more than 10 cm long but only 2.5 cm wide, is subrounded on all faces except for the freshly broken interior (Fig. 1). 72255 is moderately coherent, hetero-

geneous, and polymict, with color varying from medium light gray [N6] to light gray [N5]. The exposed surfaces show a firm dark patina with some zap pits (Fig. 2).

72255 is superficially similar to 72275, but is more coherent. It is fine-grained and heterogeneous, with prominent clasts and a zone rich in chalky white lenses and stringers. The most prominent clast in Fig. 1 is the Civet Cat norite, a 2-cm cataclastic fragment with a relict plutonic texture and a

probable crystallization age of 4.12 Ga. Other clasts include aphanitic melt blobs and fragments, anorthositic breccias, feldspathic granulites, basaltic/troctolitic impact melts, and granites. The melt groundmass has a low-K Fra Mauro composition similar to others in the boulder. Rare gas analyses show an exposure age of about 43 m.y.

Most of the studies of 72255 were conducted by the Consortium Indomitable (leader J.A. Wood). A

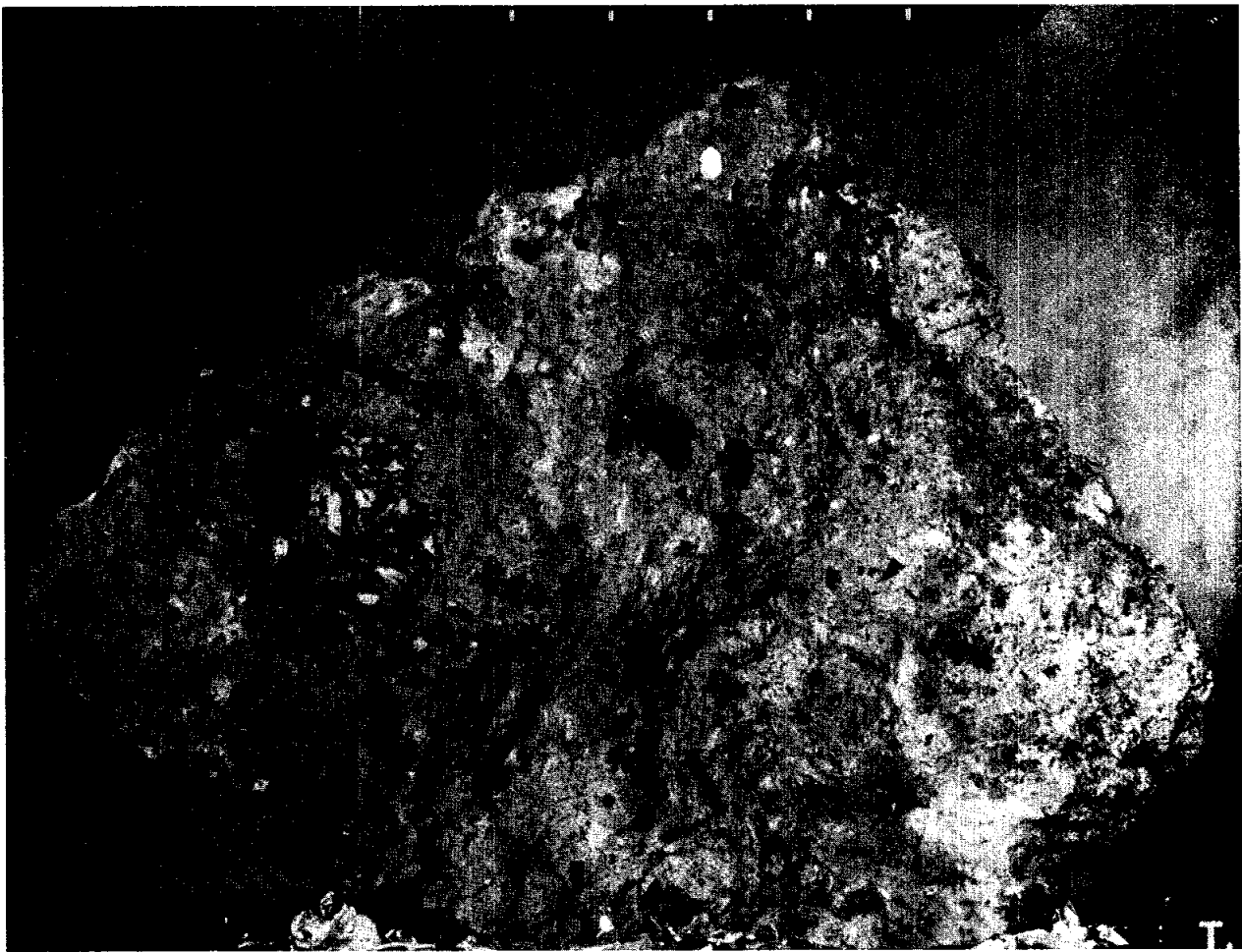


Figure 1: Top (arbitrary) face of 72255, the broken interior. The dashed lines show the location of the cuts for the slab. The prominent clast between the lines is the Civet Cat norite. The area to the right (east) is a zone rich in chalky white lenses and stringers. Scale in cm. S-73-23726B.

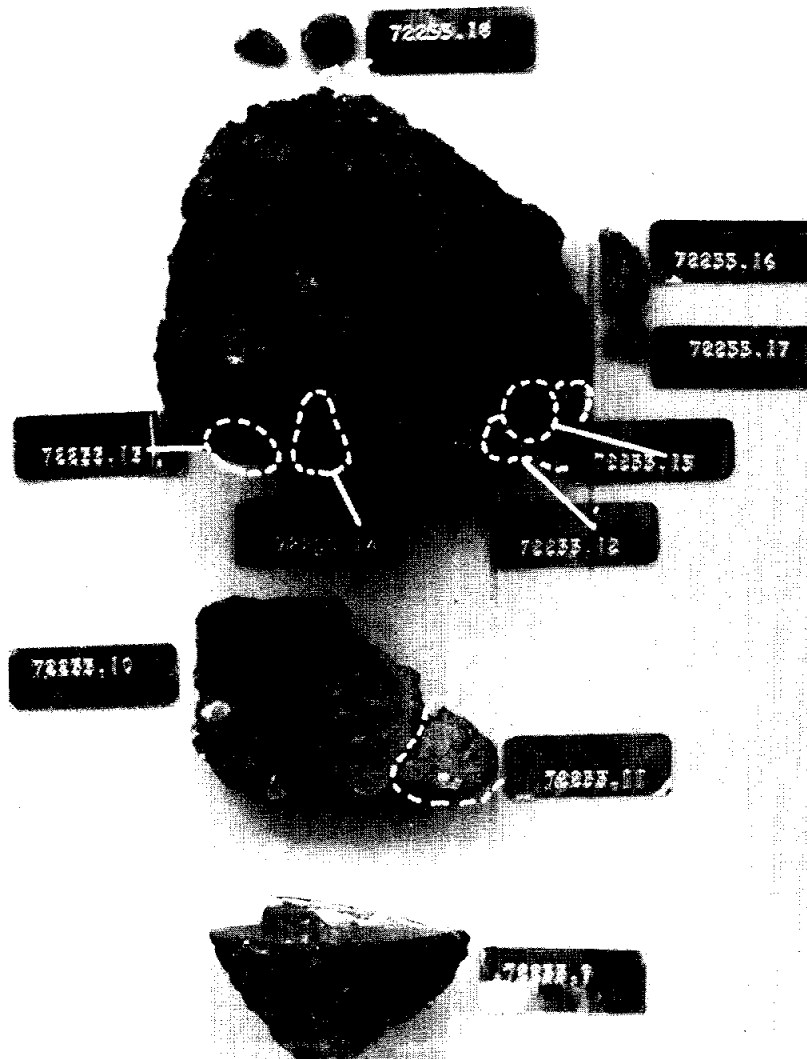


Figure 2: Slab cut from 72255 (center). Lower is west end, upper is main mass, showing exterior patina, and location of other chips. The slab was further dissected. Scale in cm. S-73-32620.

slab was cut across the sample to include the Civet Cat clast (Figs. 1, 2), providing samples for comprehensive petrographic, chemical, and isotopic studies. Detailed maps of the exterior surfaces and the slab based on macroscopic observations, as well as descriptions of the sample allocations, are in Marvin (in CI 1, 1974).

PETROGRAPHY

Specimen 72255 consists of coherent material that is dominantly a dark matrix breccia (Marvin, in CI 1, 1974; 1975a; Stoesser *et al.*, in CI 1, 1974; 1974a,b; Ryder *et al.*, 1975b). Stoesser *et al.* (1974a) suggested about 60% matrix, although what constituted matrix was not clearly defined; it was described as "small monomineralic and lithic clasts in a finely

recrystallized submatrix". The dark breccia material is polymict, with a groundmass that is a fine-grained impact melt (e.g. James, 1977; Spudis and Ryder, 1981). LSPET (1973) listed the sample as a layered light gray breccia. Simonds *et al.* (1974) described 72255 as a clast-supported fragmental breccia, with both matrix feldspars and matrix mafic minerals smaller than 5 microns, and some angular clasts larger than 30 microns. Knoll and Stoffer (1979) described 72255 as having a dark, fine-grained, equigranular crystalline matrix that contains some areas of lighter, coarser-grained matrix.

The thin sections show a melt groundmass similar to that of 72215 (Fig. 3a,b), polymict and dense. The fine material consists of abundant small monomineralic and lithic clasts in a crystalline melt groundmass that consists of plagioclase, pyroxene, and disseminated ilmenite tablets. Magnetic data show that the matrix has about 0.76% metallic iron (Banerjee and Swits, 1975). The monomineralic clasts are plagioclase, olivine, orthopyroxene, clinopyroxene, and sparse-to-trace pink-to-red spinel, chromite, and ilmenite. Compositions of the olivines and pyroxenes are shown in Fig. 4; at least most of the olivines are clasts, not melt-crystallized phases. The olivines include examples more forsteritic than those in the anorthositic and granulitic clasts. The only lithic fragments in the sample with such forsteritic olivine are the basaltic troctolites. The magnesian pyroxenes have no counterpart in any lithic fragments from the boulder. The mineral compositions in 72255 have compositional ranges similar to those in 72215 and the dark breccias in 72275. Ryder (1984a) analyzed olivine fragments in 72255, finding that many have calcium contents high enough (0.05-0.15%) to be consistent with having an origin in shallow, rather than deep, plutonics.

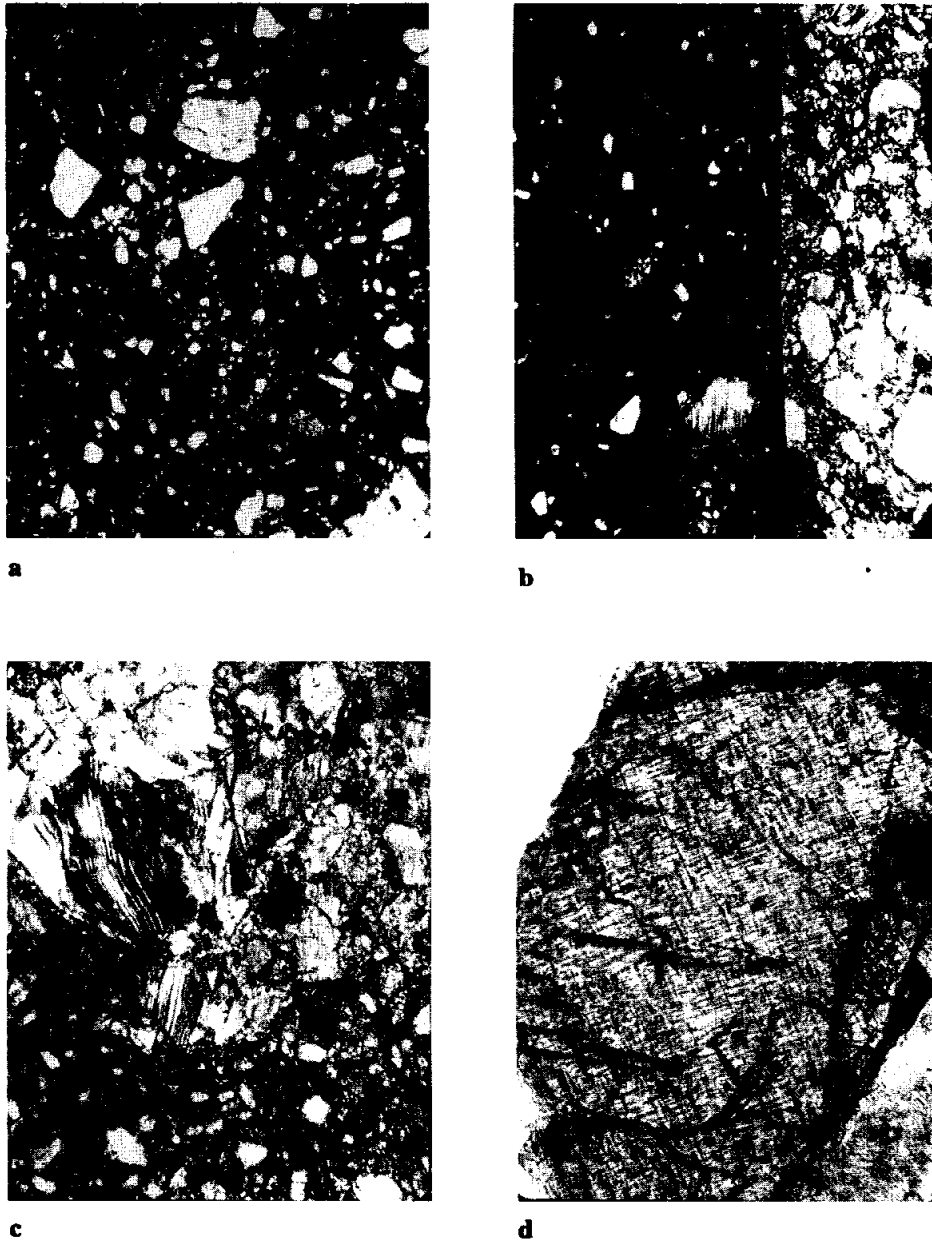


Figure 3: Photomicrographs of materials in 72255. Width of field about 1.5 mm, except for d) which is about 300 microns. Figures a and d are crossed polarizers; b and c plane light.

a) 72255,89; general matrix showing dense dark impact melt with angular to subrounded small mineral and lithic clasts.

b) 72255,130; contact between Civet Cat norite (right) and groundmass (left). The contact is extremely sharp and straight, without evidence of reaction.

c) 72255,123; Civet Cat norite, with deformed plagioclase (top) and crushed orthopyroxene (bottom).

d) 72255,123; orthopyroxene in Civet Cat norite, showing its lineated features.

Table 1: Defocused beam analyses of groundmass of 72255 (Stoeser *et al.*, in CI 1, 1974).

	3 72255, 95 matrix	4 72255, 105 Civet Cat rind
SiO ₂	45.1	46.5
TiO ₂	0.6	0.9
Cr ₂ O ₃	0.2	0.2
Al ₂ O ₃	20.0	21.4
FeO	7.7	8.5
MnO	0.1	0.1
MgO	9.1	9.4
CaO	12.7	12.3
Na ₂ O	0.5	0.3
K ₂ O	0.2	0.2
P ₂ O ₅	0.2	0.4
Total	96.4	100.2
Fo	4.3	1.9
Fa	2.8	1.2
En	17.3	20.8
Fs	10.2	12.1
Wo	4.3	0.8
Or	1.3	1.3
Ab	4.1	2.3
An	53.9	56.5
Ilm	1.1	1.7
Chr	0.2	0.3
Qtz	0.0	0.0
Cor	0.0	0.0
Ap	0.5	0.8

The chemical composition of the groundmass (including small clasts) derived by defocused beam microprobe methods is low-K Fra Mauro basalt (Table 1; see also chemistry section), similar to other samples from the boulder and differing from coarser Apollo 17 impact melts in its lower TiO₂ and higher Al₂O₃. Goswami and Hutcheon (1975) using fission track methods found that U was uniformly distributed on a 10 micron scale. Some of the matrix areas are lighter-colored, and more feldspathic, and contain clasts of dark matrix breccia, visible on the sawn surfaces. In thin sections the dark clasts are difficult to distinguish from the groundmass, and evidently are of very similar material. The groundmass has reacted with the clasts, producing re-equilibration rims up to 15

Table 2: Clast population survey of particles greater than 200 microns in diameter in 72255. Percent by number, not volume. (from Stoeser *et al.*, 1974a).

Clast type	72255
Granulitic ANT breccias	31.3%
Granulitic polygonal anorthosite	6.3
Crushed anorthosite	5.2
Devitrified glass	13.8
Glass shards	—
Ultramafic particles	1.5
Basaltic troctolite	2.2
Pigeonite basalt	—
Other basaltic particles	1.9
Granitic clasts	2.6
"Civet Cat" type norite	0.7
Monomineralic plagioclase	19.3
Monomineralic mafic silicates	14.5
Monomineralic spinel & opaques	0.7
Number of clasts surveyed	269

microns thick around pyroxenes and olivines, and reaction rims around spinels and granite clasts. Some of the granites have partially-melted internally, and all the glasses are devitrified, including those of feldspar composition that were presumably once maskelynite. All these features demand a high temperature (more than 800 or 900 degrees C), but lack of total equilibration shows that the high temperatures were not maintained for long periods.

A wide variety of lithic clasts is present in 72255. The clast population (Table 2) is similar to that in 72275, but lacks the volcanic KREEPy pigeonite basalts. Other basaltic fragments are present. The dark gray melt clasts/blobs are abundant, but the anorthositic clasts are relatively small and rare. Most of the latter are pure white, sugary, and granulitic. The types of material are described in Stoeser *et al.* (in CI 1, 1974; in CI 2, 1974; 1974a,b) and Ryder *et al.* (1975b), mainly without specific identification of those clasts from 72255 except for photomicrographs. The granites were described by Stoeser *et al.* (1975) and Ryder *et al.* (1975a). They include varieties with feldspars in the "forbidden"

compositional field (ternary feldspars), about An₅₅Or₄₀. Defocused beam microprobe analyses of anorthositic breccias, troctolitic basalts, and devitrified glasses are given in Table 3; similarly-produced analyses for a basaltic particle and a granite are given in Table 4. The analysis of the Civet Cat norite in Table 4 is an estimate (see Table caption).

The Civet Cat clast that is conspicuous on the broken face of the sample (Fig. 1, 2) is an angular fragment about 2.5 cm long with light lenses and streaks in a dark groundmass. The rock is a cataclastic norite, essentially biminerale and with a grain size originally of 1 to 4 mm (Stoeser *et al.*, 1974a; Ryder *et al.*, 1975). Orthopyroxene and plagioclase (Figs. 3b, c, d) have very narrow compositional ranges (Fig. 5). The plagioclase (An₉₂₋₉₄Or_{0.5-1.0}) is partially transformed to maskelynite and otherwise deformed (Fig. 3c). The orthopyroxenes (En₇₂₋₇₄Wo₂₋₄) is commonly kinked, and contains abundant small brown plates of ilmenite along the cleavage planes. Rare augite is present as small grains and lamellae. Accessory minerals include cristobalite, baddeleyite, ilmenite, chromite,

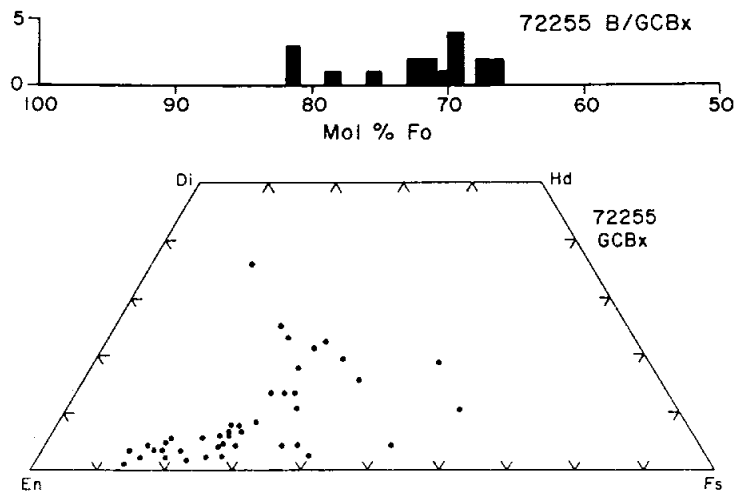


Figure 4: Compositions of monomineralic olivines and pyroxenes in groundmass of 72255 (from Ryder *et al.*, 1975b).

Table 3: Defocused beam analyses of feldspathic granulitic clasts (cols. 1-4), anorthosite breccia (col. 5), polygonal anorthosite (col. 6), troctolitic clasts (cols. 7-9), and devitrified glasses (cols. 10-12) (from Stoesser *et al.*, in CI 1, 1974; Ryder *et al.*, 1975b).

	2 770C7	3 770C12	4 770C24	5 770C27	6 770C26	7 770C37	770C2	770C30	770C77	1 770C10 devitrified glass	2 770C39 devitrified glass	3 770C83 devitrified maskylenite
SiO ₂	43.9	46.2	51.1	44.3	44.9	42.8	42.3	42.5	41.2	44.0	42.4	44.8
TiO ₂	0.1	0.1	0.3	0.2	0.1	0.1	0.3	0.2	0.4	0.4	0.3	0.1
Cr ₂ O ₃	0.0	0.0	tr.	tr.	0.1	tr.	0.3	0.1	0.0	0.1	tr.	tr.
Al ₂ O ₃	25.8	32.2	20.6	23.8	33.9	35.3	16.3	9.8	12.5	25.3	31.6	32.8
FeO	4.1	2.4	6.3	6.4	6.8	0.2	6.5	9.7	13.3	5.0	3.7	0.7
MnO	0.1	tr.	0.1	0.1	tr.	tr.	0.1	0.1	0.2	0.1	0.1	0.1
MgO	5.7	1.0	7.9	11.6	0.8	tr.	25.6	30.5	24.4	12.0	0.7	0.4
CaO	15.8	17.5	12.2	13.6	19.3	19.4	8.7	6.3	7.1	13.9	17.1	18.4
Na ₂ O	0.4	0.6	0.4	0.3	0.4	0.3	0.3	0.3	0.2	0.4	0.3	0.5
K ₂ O	0.1	0.1	0.2	0.1	0.1	0.1	0.1	0.1	0.1	0.1	tr.	0.1
P ₂ O ₅	tr.	tr.	tr.	tr.	tr.	tr.	0.2	0.1	0.1	0.1	tr.	0.2
BaO	tr.	tr.	0.1	0.1	0.1	0.1	0.1	0.1	0.0	0.1	0.1	-
Total	96.0	100.1	99.2	100.5	100.5	98.3	100.8	99.8	99.5	101.3	96.3	98.1
Fo	4.0	0.0	0.0	15.1	0.0	0.0	44.1	50.0	40.5	19.2	0.1	0.0
Fa	2.3	0.0	0.0	6.7	0.0	0.1	8.8	12.8	17.7	6.3	0.5	0.0
En	9.1	2.5	19.8	7.2	2.0	0.0	0.5	4.9	3.5	2.1	1.6	1.0
Fs	4.8	4.4	11.3	2.9	1.3	0.0	0.1	1.2	1.4	0.6	1.1	1.2
Wo	4.3	0.9	2.7	1.6	2.0	1.4	0.0	2.2	0.6	0.7	0.0	1.7
Or	0.7	0.3	0.9	0.6	0.8	0.4	0.5	0.4	0.3	0.8	0.2	0.5
Ab	3.3	5.2	3.3	2.2	3.0	2.6	2.7	2.4	1.8	3.5	2.8	4.0
An	71.3	84.6	54.5	63.3	90.3	94.3	41.9	25.4	33.3	66.0	88.0	89.2
Ilm	0.1	0.1	0.7	0.3	0.2	0.2	0.5	0.4	0.7	0.6	0.2	0.2
Chr	0.0	0.0	0.0	0.0	0.1	0.0	0.4	0.1	0.0	0.2	0.1	0.0
Qtz	0.0	1.8	6.8	0.0	0.3	0.0	0.0	0.0	0.0	0.0	0.0	2.1
Cor	0.0	0.0	0.0	0.0	0.0	0.8	0.3	0.0	0.0	0.0	0.0	0.0
Ap	0.0	0.0	0.1	0.1	0.0	0.1	0.3	0.2	0.2	0.2	0.1	0.0

1 2 3 4 5 6 7 8 9 10 11 12

Table 4: Defocused beam analyses of recrystallized (?) intersertal basalt (col. 1), and a granite (col. 2). Column 3 is an estimate of the composition of the Civet Cat norite, from the mode of 60 +/- 10% orthopyroxene and 40 +/- 10% plagioclase, and using two defocused beam microprobe traverses (2mm x 100 microns) in orthopyroxene- and plagioclase-rich areas whose modes were determined. (from Stoesser *et al.*, in CI 1, 1974).

SiO ₂	47.0	71.2	50.3
TiO ₂	0.4	0.1	1.8
Cr ₂ O ₃	0.2	tr.	0.3
Al ₂ O ₃	14.7	12.7	14.4
FeO	15.1	0.6	9.6
MnO	0.3	tr.	0.3
MgO	7.2	0.1	15.7
CaO	13.9	1.1	7.9
Na ₂ O	0.2	0.2	0.3
K ₂ O	0.1	8.5	0.1
P ₂ O ₅	0.0	tr.	0.0
BaO	0.1	0.6	—
S	—	—	—
Total	99.2	95.1	100.7
Fo	1.2	0.0	0.0
Fa	2.1	0.0	0.0
En	16.5	0.2	39.0
Fs	25.0	1.0	15.1
Wo	12.7	0.0	0.6
Or	0.6	53.3	0.6
Ab	1.6	1.4	2.5
An	39.3	5.8	37.5
Ilm	0.7	0.2	3.4
Chr	0.3	0.0	0.0
Qtz	—	36.8	1.2
Cor	—	1.3	0.0
Ap	—	0.0	0.0
Troi	—	—	—

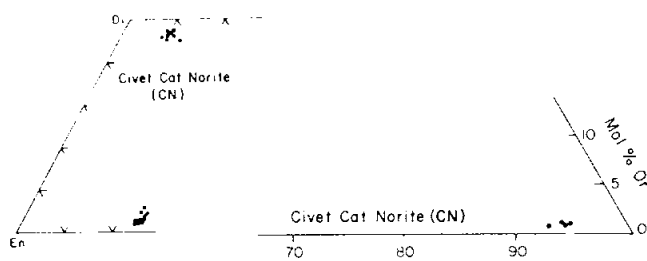


Figure 5: Chemistry of pyroxenes (left) and plagioclases (right) in the 72255 Civet Cat norite. (From Ryder *et al.*, 1975b).

metallic iron, and troilite. An exceptional phase is niobian rutile (Marvin, 1975b); two analyses have 19.7% and 18.5% Nb₂O₅, making it the most Nb-rich mineral analyzed (at least by 1975) in any extraterrestrial sample. Ryder *et al.* (1980a,b) analyzed metal grains in the norite, finding them to be Ni-free, with 2.1 to 4.0% Co. Hansen *et al.* (1979b) plotted data for an Mg-rich plutonic fragment in 72255

(presumably Civet Cat) on diagrams of Mg' (low-Ca px) v. Ab (plag) and Mg' (liquid, calculated from opx) v. Mg' (plagioclase). (The actual data is not tabulated nor its source described.)

The pyroxenes in the Civet Cat norite were studied by Takeda and his group, to assess the thermal history of the lithology and compare it with eucrites (Takeda

and Ishii, 1975; Takeda *et al.*, 1976a,b, 1982; Mori *et al.*, 1980,1982). They used microprobe, x-ray diffraction, and transmission electron microscopy methods. Takeda and Ishii (1975) noted intergranular recrystallization with exsolution of (001) augite from pigeonite well below the pigeonite eutectoid reaction point line; the clinopyroxene inverted to orthopyroxene (Stillwater-type). Takeda *et al.* (1976a,b) reported microprobe analyses for augite (En₄₆Wo₄₄) and orthopyroxene (En₇₃Wo₂), and single crystal diffraction results. The pyroxenes showed very weak reflections of secondary pigeonite, as well as minor augite, with pigeonite having (100) in common with host orthopyroxene. The diffraction spots were diffuse because of shock. Augite was detected as lamellae as well as rare small discrete grains. Mori and Takeda (1980) in single crystal diffraction and TEM studies found diffraction patterns for orthopyroxene similar to those in the Ibbenburen eucrite, but also diffraction spots of pigeonite. Mori *et al.* (1982) and Takeda *et al.* (1982) reinvestigated the pyroxenes using ATEM for comparison with eucrites and other lunar samples, determining the composition of exsolved augite. The pyroxene differs from that in the 78236 lunar norite in that many grains have abundant augite lamellae (although some have very few). The lamellae average 0.2 microns thick, but are as much as 0.4 microns thick. Opaque inclusions are in the lamellae. The host consists of alternate layers of orthopyroxene and clinobronzite; there are abundant fine clinobronzite lamellae or stacking faults up to 20 nm present with (100) in common. In some areas wide clinobronzite slabs intrude the orthopyroxene with a comb-like texture. There are no Guinier-Preston zones. Takeda *et al.* (1982) attribute the presence of the clinobronzite lamellae to shear transformation in shock deformation from impact. The exsolution

lamellae are 20x thicker than those in the Johnstown eucrite, and are a product of cooling at depth before shock. The microprobe opx-aug data suggest last equilibration at 900 degrees C, and the ATEM host-lamellae studies suggest 1000 degrees C, suggesting that the latter results from thermal annealing from the shock event. These authors suggested a model-dependent depth of 10 to 70 km for the equilibration.

The apparent primary texture, the wide pyroxene solvus, the narrow compositional ranges, the Ni-free metal, and the bulk and trace element composition (including lack of meteoritic siderophiles) (see below) are consistent with the Civet Cat norite having been a plutonic igneous rock. James (1982) and James and Flohr (1983) classed the Civet Cat norite with the Mg-norites on the basis of its mineralogy and chemistry.

CHEMISTRY

Chemical analyses for the matrix are given in Table 5; for the Civet Cat norite clast in Table 6; and for other materials in Table 7. Rare earth plots for the matrix are shown in Fig. 6, and for the Civet Cat norite and others in Fig. 7.

The average of the matrix analyses is very similar to those of other melt matrices in Boulder 1, including major and trace element chemistry. However, the small samples analyzed by Blanchard *et al.* (1975, and in CI 1, CI 2) show a range, presumably because of unrepresentative sampling (i.e. varied clast contents). (One sample, a subsplit of ,52, is distinct in chemistry, being less aluminous and more ferrous; it is also lighter in color.) Both Blanchard *et al.* (1975) and Winzer *et al.* (1975a) emphasize the similarity in composition of 72255 with all other Apollo 17 boulder melts, despite the higher alumina and lower titania of 72255. The K abundance

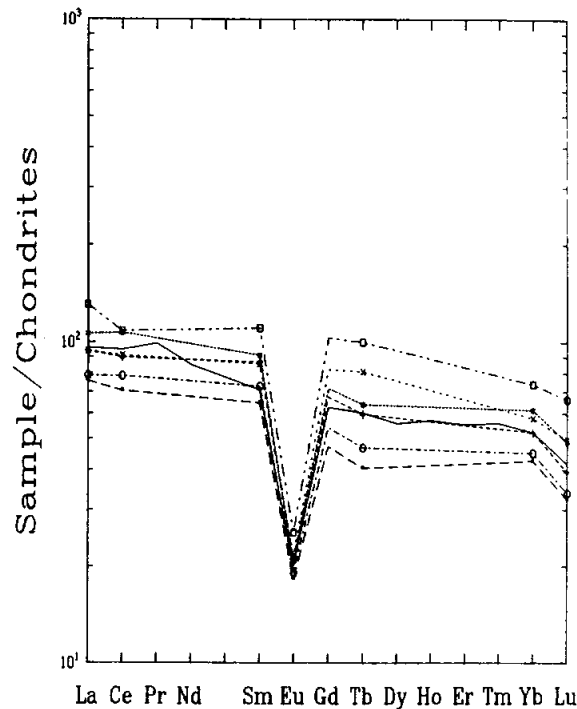


Figure 6: Rare earth element plot for matrix samples of 72255. Solid line without symbols is data of Palme *et al.* (1978); other data is from Blanchard *et al.* (1975, and CI 1, CI 2).

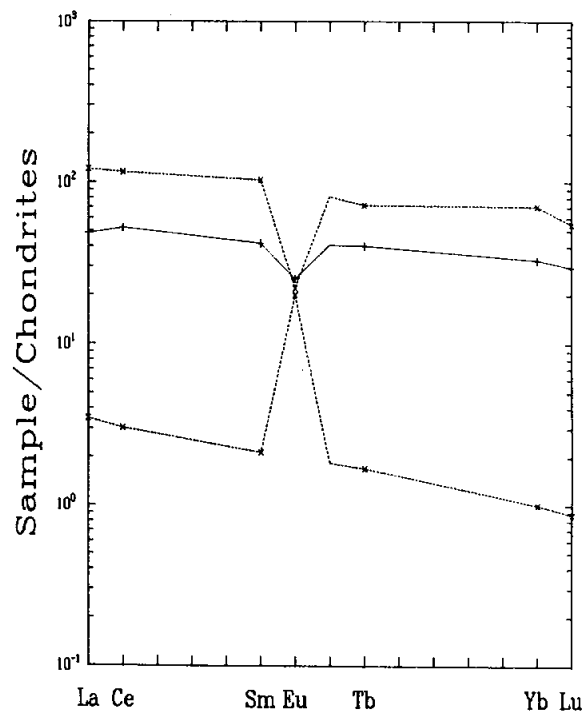


Figure 7: Rare earth element plot for Civet Cat norite (solid line, in center) and the rind (upper dotted line) and core (lower dotted line) of clast #3. All data from Blanchard *et al.*, (1975, and CI 1, CI 2).

Table 5: Chemical analyses of matrix and bulk rock samples of 72255.

	, 2	, 73(a)	, 79(a)	, 52(a)	, 52(d)	, 64(a)	, 69(d)	, 69(a)	, 44	, 83	, 52		
Spillt wt %												Spillt wt %	
SiO ₂		44.8	45.0	49	45.0	45.1	44.7	46	46.72			SiO ₂	
TiO ₂		0.9	0.9	1.4	0.75	0.8	0.8	0.7	0.76			TiO ₂	
Al ₂ O ₃		19.4	20.7	14.5	20.4	21.9	20.5	19.8	20.82			Al ₂ O ₃	
Cr ₂ O ₃		0.630	0.234	0.22	0.232	0.231	0.308	0.46	0.240			Cr ₂ O ₃	
FeO		(b)9.05	(c)8.31	14	(d)8.55	(e)7.42	9.5	9.8	8.1			FeO	
MnO		0.127	0.129	0.163	0.129	0.12	0.108	0.111	0.117			MnO	
MgO		10.5	11.3	9.7	11.3	10.7	10.5	10.4	9.9			MgO	
CaO		11.5	12.0	10.7	12.0	12.4	12.3	12.3	12.56			CaO	
Na ₂ O			0.495	0.584	0.32	0.563	0.496	0.400	0.38			Na ₂ O	
K ₂ O	0.218	0.221	0.393	0.214	0.27	0.231	0.268	0.280	0.25			K ₂ O	
P ₂ O ₅									0.198			P ₂ O ₅	
									0.252				
ppm												ppm	
Sc		15.5	18.2	19.8	18.3	17.3		19.5	18.8			Sc	
V												V	
Co		2530	28.9	28	25.6	26.6		21	24.5			Co	
Ni		7700	260		150	180			150	222	227	Ni	
Rb									4.98	6.85	5.8	Rb	
Sr									151			Sr	
Y									100			Y	
Zr									400			Zr	
Nb									28			Nb	
Hf		9.1	11.2	9.8	10.4	9.9		13.1	10.50			Hf	
Ba									328			Ba	
Tb	4.80	4.4	6.6	5.4		4.3			4.31			Tb	
U	1.28	1.20							1.41	1.820	1.790	U	
Cs									0.18	0.287	0.240	Cs	
Ta			1.5		1.6	1.0			1.27			Ta	
Pb												Pb	
La		25	31	31	35	26		43	31.7			La	
Ce		62	79	80	94	69		95	83.3			Ce	
Pr									11.1			Pr	
Nd									51			Nd	
Sm		11.7	15.7	15.5	16.5	13.2		20	12.86			Sm	
Eu		1.26	1.45	1.49	1.44	1.32		1.76	1.39			Eu	
Gd									15.6			Gd	
Tb		1.9	2.8	3.8	3.0	2.2		4.7	2.83			Tb	
Dy									17.7			Dy	
Ho									4.00			Ho	
Er									11.1			Er	
Tm									1.68			Tm	
Yb		8.55	10.5	11.6	12.3	9.04		14.8	10.50			Yb	
Lu		1.10	1.34	1.69	1.66	1.15		2.25	1.42			Lu	
Li									12.8			Li	
Be												Be	
B												B	
C												C	
N												N	
S									375			S	
F									28.0			F	
Cl									10.2			Cl	
Br									0.03	0.104	0.101	Br	
Cu									3.01			Cu	
Zn									2.43	2.2	2.8	Zn	
ppb												ppb	
Au									2.6	2.95	2.00	Au	
Ir										7.01	5.28	Ir	
I												I	
At												At	
Ga									3660			Ga	
Ge									<100		174	Ge	
As									86			As	
Se										67	77	Se	
Mo												Mo	
Tc												Tc	
Ru												Ru	
Rh												Rh	
Pd									<10			Pd	
Ag										3.03	0.57	Ag	
Cd									<50	6.8	8.1	Cd	
In												In	
Sn												Sn	
Sb										1.74	0.77	Sb	
Te										3.3	4.7	Te	
W									630			W	
Re										0.3	0.503	0.498	Re
Os												Os	
Pt												Pt	
Hg												Hg	
Tl										2.18	1.18	Tl	
Bi										0.67	0.21	Bi	
	(1)	(2)	(3)	(3)	(3)	(3)	(3)	(3)	(3)	(4)	(5)	(5)	

References and methods:

- (1) Fruchter et al. (1975); gamma-ray
- (2) Keith et al. (1974); gamma-ray
- (3) Blanchard et al. (1975); Cl(1), Cl(2); INAA, AAS
- (4) Palme et al. (1978); INAA, RNAA, XRP
- (5) Morgan et al. (1975); Higuchi and Morgan (1975); RNAA C(1).

Table 5: Continued

	.61	.59A(g)	.59B(g)	.59(h)	.53(h)	.53(l)	.67(l)	.54(i)	.60(k)	.52	
Split											Split
wt %											wt %
SiO ₂											SiO ₂
TiO ₂											TiO ₂
Al ₂ O ₃											Al ₂ O ₃
Cr ₂ O ₃											Cr ₂ O ₃
FeO											FeO
MnO											MnO
MgO											MgO
CaO										(e)12.0	CaO
Na ₂ O											Na ₂ O
K ₂ O										(e)0.276	K ₂ O
P ₂ O ₅	0.25										P ₂ O ₅
ppm											ppm
Sc											Sc
V											V
Co											Co
Ni											Ni
Rb		14.95	14.63	9.79	5.69	5.78					Rb
Sr		145.6	141.7	141.2	137.0	141.2				140	Sr
Y											Y
Zr										376	Zr
Nb											Nb
Hf											Hf
Ba										324	Ba
Th							4.222	5.724	6.362		Th
U	1						1.145	1.536	1.663	1.42	U
Cs											Cs
Ta											Ta
Pb							2.478	3.080	3.540		Pb
La											La
Ce											Ce
Pr											Pr
Nd											Nd
Sm											Sm
Eu											Eu
Gd											Gd
Tb											Tb
Dy											Dy
Ho											Ho
Er											Er
Tm											Tm
Yb											Yb
Lu											Lu
Li	11										Li
Be											Be
B											B
C											C
N											N
S											S
P	41										P
Cl	(f)9.1										Cl
Br	(f)0.082										Br
Cu											Cu
Zn											Zn
ppb											ppb
Au											Au
Ir											Ir
I	0.8										I
At											At
Ga											Ga
Ge											Ge
As											As
Se											Se
Mo											Mo
Tc											Tc
Ru											Ru
Rh	>20										Rh
Pd											Pd
Ag											Ag
Cd											Cd
In											In
Sn											Sn
Sb											Sb
Te											Te
W											W
Re											Re
Os	17										Os
Pt											Pt
Hg											Hg
Tl											Tl
Bi											Bi
	(6)	(7)	(7)	(7)	(7)	(7)	(8)	(8)	(8)	(9)	

References and methods:
 (6) Jovanovic and Reed (1975 b,c,d, 1980 a); INAA
 (7) Compston et al (1975); ID/MS
 (8) Nunes et al (1974); ID/MS
 (9) Leich et al (1975); irradiation/MS (K, Ca), others ID/MS

Table 5: Continued

Notes:

(a)	.73 Sawdust .79 Interior Chip .52 White to light gray matrix .52 Gray to medium gray matrix .64 Medium gray material .69 Dark material .69 Dark material
(b)	INAA; AAS = 9.38%
(c)	INAA; AAS = 8.48%
(d)	INAA; AAS = 8.35%
(e)	INAA; AAS = 8.02%
(f)	Combined clast and residue fractions
(g)	Gray fractions
(h)	Light gray fractions
(i)	Dark matrix
(j)	Lighter matrix
(k)	Mixed dark and light matrix
(l)	Revised from Cl(2)

Table 6: Chemical analyses of the Civet Cat norite in 72255.

	,42	,42	,42
Split			
wt %			
SiO ₂	52		
TiO ₂	0.3		
Al ₂ O ₃	15.5		
Cr ₂ O ₃	0.16		
FeO	7.4		
MnO	0.122		
MgO	15.9		
CaO	9.1		(a) 13.0
Na ₂ O	0.33		
K ₂ O	0.08		(a) 0.17
P ₂ O ₅			
ppm			
Sc	13.2		
V			
Co	29		
Ni		4	
Rb		1.27	
Sr			139
Y			
Zr			132
Nb			
Hf	5.5		
Ba			172
Th			
U		0.240	0.45
Cs		0.058	
Ta			
Pb			
La	16		
Ce	46		
Pr			
Nd			
Sm	7.6		
Bu	1.75		
Gd			
Tb	1.9		
Dy			
Ho			
Er			
Tm			
Yb	6.6		
Lu	1.01		
Li			
Be			
B			
C			
N			
S			
F			
Cl			
Br		15.3	
Cu			
Zn		4.5	
ppb			
Au		0.008	
Ir		0.0040	
I			
At			
Ga			
Ge		61	
As			
Se		280	
Mo			
Tc			
Ru			
Rh			
Pd			
Ag		0.76	
Cd		5.8	
In			
Sn			
Sb		0.26	
Te		14.3	
W			
Re		0.0068	
Os			
Pt			
Hg			
Tl		0.30	
Bi		0.30	
	(1)	(2)	(3)

References and methods:

- (1) Blanchard *et al* (1975) and Cl(1), Cl(2); INAA, AAS
 (2) Morgan *et al* (1974, 1975 a, b), Higuchi and Morgan (1975); RNAA, C(1)
 (3) Leich *et al* (1975); irradiation, MS (K, Ca), others ID/MS

Notes:

(a) revised from Cl(2)

Table 7: Chemical analyses of white core and dark rind on clast #3 and other clast material in 72255.

	.45 (a)	.45 (b)	.59 (e)	.53 (f)	.53 (g)
Split					
wt %					
SiO ₂	43.0	45.7			
TiO ₂	0.65	1.2			
Al ₂ O ₃	35.8	19.7			
Cr ₂ O ₃	0.003	0.263			
FeO	(c) 0.13	(d) 9.05			
MnO	0.003	0.136			
MgO	1.43	11.3			
CaO	18.9	11.5			
Na ₂ O	0.631	0.542			
K ₂ O	0.118	0.277			
P ₂ O ₅					
ppm					
Sc	0.45	20.1			
V					
Co	0.33	24.9			
Ni		140			
Rb			1.11	5.52	5.57
Sr			140.6	319.7	190.6
Y					
Zr					
Nb					
Hf	0.10	14.2			
Ba					
Th		6.6			
U					
Ce					
Ta		1.7			
Pb					
La	1.15	40			
Ce	2.68	102			
Pr					
Nd					
Sm	0.39	18.8			
Eu	1.39	1.53			
Gd					
Tb	0.08	3.4			
Dy					
Ho					
Er					
Tm					
Yb	0.202	14.2			
Lu	0.030	1.88			
Be					
B					
C					
N					
S					
F					
Cl					
Br					
Cu					
Zn					
ppb					
Au					
Ir					
I					
At					
Ga					
Ge					
As					
Se					
Mo					
Te					
Ru					
Rh					
Pd					
Ag					
Cd					
In					
Sn					
Sb					
Te					
W					
Re					
Os					
Pt					
Hg					
Tl					
Bi					

References and methods:
 (1) Blanchard et al (1975; CI 1; CI 2); INAA, AAS
 (2) Compston et al (1975, CI 1); ID/MS

Notes:
 (a) white
 (b) black
 (c) INAA
 (d) AAS; INAA = 8.77%
 (e) anorthositic clast
 (f) clear plagioclase
 (g) shocked plagioclase

(1) (1) (2) (2) (2)

of the bulk rock as measured by gamma-ray is lower than that of the matrix samples (Fruchter *et al.*, 1975). Palme *et al.* (1978) noted that their analyses of 72255 and 72215 matrix material were similar to some Apollo 16 samples (i.e. 68516) except for the siderophile elements. Higuchi and Morgan (1975a), Morgan *et al.* (1975), and Hertogen *et al.* (1977) assigned the matrix to their siderophile Group 3H (assigned with 72275 to Crisium by Morgan *et al.*, 1974a,b).

The Civet Cat norite (Table 6; Fig. 6) is quartz-normative, and its chemistry is consistent with it being a cumulate plutonic rock containing 20 to 30% of trapped liquid that would be evolved, approaching KREEP (Blanchard *et al.*, 1975). The norite lacks meteoritic siderophile contamination.

Blanchard *et al.* (1975) analyzed the dark melt rim and the interior white material of clast #3 (45; Table 7, Fig. 7). The rim material is similar to the general matrix; the white material is very anorthositic in major and trace elements, but has a high mg' compared with typical ferroan anorthosites. Rb and Sr analyses for other materials appear to represent varied mixtures of feldspathic material and matrix.

RADIOGENIC ISOTOPES AND FISSION TRACK AGES

Schaeffer *et al.* (1982a,b) used laser Ar-Ar techniques to determine ages of clasts and to infer the age of the melt in section 72255,134, providing 20 analyses (Table 8). Most of the ages were for plagioclase or plagioclase-composite clasts; two were for felsite ("feldsparthoid") clasts. The two felsites, the most K-rich fragments, give ages generally younger than the feldspars. The higher ages for the plagioclases, some of which are in noritic lithic clasts, range up to 4.29 Ga. Schaeffer *et al.* (1982a,b) suggest that the age of the felsite clasts,

which probably degassed during melting, is the best estimate for the age of the melt groundmass, which is therefore about 3.85 Ga, the age of the most precisely dated of the felsites. (The felsite clasts were preheated to 650 degrees C; the ages are total release, hence K-Ar, of the greater than 650 degrees C fraction. Assuming a well-developed plateau above that temperature, the ages are reliable).

Leich *et al.* (1975a) reported Ar-Ar analyses for a matrix sample of 72255 (Fig. 8). Leich *et al.* (1975a) believe that the intermediate-temperature (800 to 1000 degrees C) and the high-temperature (1400 degrees C) plateaus are reliable indicators of the age of the sample; these plateaus give an age of 3.93 Ga. However, the age of the 1000 to 1400 degree release is the one that agrees with the age inferred by

Schaeffer *et al.* (1982a,b), and the Leich *et al.* (1975a) plateaus must be compromised by the plagioclase clasts that did not completely degas.

Compston *et al.* (1975) reported Rb-Sr isotopic data for matrix and small clast samples of 72255 (Table 9). For split ,53 the total rock and plagioclase clasts are well-aligned on a 4.30 +/- 0.24 Ga "isochron" which should be regarded as a mixing line rather than a true isochron (Fig. 9). The clasts are not cogenetic, and the data for 72215 shows that the clasts and matrix did not reach Sr isotopic equilibration, and so 4.30 Ga does not date the assembly of the breccia. Split ,59 materials also fall on a mixing line that is the chance result of mixing unrelated anorthositic material, unidentified old "basaltic" material (i.e. low-K Fra Mauro source

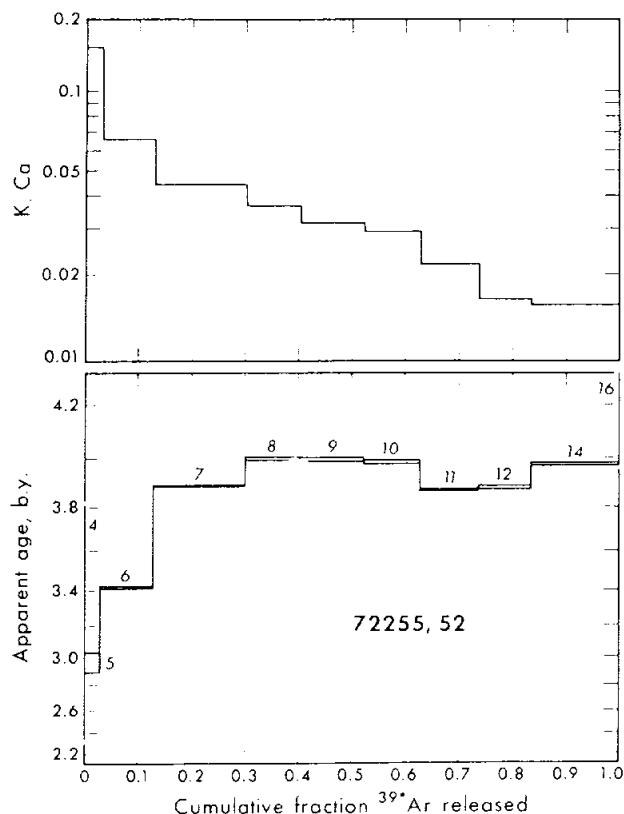


Figure 8: Apparent age and K/Ca data from 72255,52 matrix (Leich *et al.*, 1975a). The ages shown correspond with the "old" decay constant; recalculation shows that the two highest plateaus correspond with 3.93 Ga, and steps 11 and 12 with about 3.83 Ga.

Table 8: Laser microprobe data for materials in 72215,144.
 Recalculated from Schaeffer *et al.*, 1982a,b).

Phase	K%	Ca%	Ar40/39	Age Ga
Plag	0.02	8	37.31+/- 0.333.917 +/- .027	
Plag	0.02	3.4	38.56	1.73 3.970 .076
Plag	0.04	8	33.60	1.28 3.753 .065
Plag	0.02	3.5	36.25	1.73 3.872 .079
Plag-comp	0.09	3.6	47.04	0.62 4.288 .032
Plag-comp*	0.30	<10	43.43	0.99 4.161 .050
Plag-comp	0.05	1.3	43.96	1.00 4.179 .044
Plag-comp*	0.04	<10	37.92	1.42 3.924 .069
Plag-comp	0.04	3	38.72	0.61 3.976 .034
Plag-comp*	0.04	<10	40.07	10.00 4.082 .350
Plag	0.19	15	36.31	0.50 3.874 .032
Plag	0.05	4	40.70	1.52 4.055 .065
Plag-comp	0.12	3	38.85	0.31 3.981 .026
Plag-comp*	0.16	<10	36.02	1.24 3.912 .065
Plag	0.02	3	33.36	0.73 3.740 .041
Matrix	0.10	4	37.02	0.35 3.905 .027
Matrix	0.27	5	34.07	0.19 3.774 .024
Matrix	0.32	12	37.60	0.32 3.929 .027
Felsite*	3.9	<10	34.63	0.57 3.846 .043
Felsite*	2.3	<10	32.75	2.75 3.767 .135

(Samples degassed at 225 degrees centigrade during bakeout after sample loading).

* = preheated at 650 degrees centigrade

Table 9: Rb-Sr isotopic data for samples from 72255
 (Compston *et al.*, 1975)

Sample	Mass mg	Rb ppm	Sr ppm	⁸⁷ Rb/ ⁸⁶ Sr	⁸⁷ Sr/ ⁸⁶ Sr +/-se
,59 gray A	16.2	14.95	145.6	0.2967	0.71693+/-6
,59 gray B	16.8	14.63	141.7	0.2983	0.71695 4
,59 light gray	19.7	9.79	141.2	0.2001	0.71116 4
,59 anorth clast	4.3	1.11	140.6	0.02275	0.70050 8
,53 lt-gy1	29.0	5.69	137.0	0.1198	0.70664 6
,53 lt-gy2	14.0	5.78	141.2	0.1183	0.70642 3
,53 plag 1 (clear)	0.8	5.52	319.7	0.0499	0.70223 11
,53 plag 2 (shocked)	3.1	5.75	190.6	0.0871	0.70450 8

se = internal standard error of mean

,59 gray = plagioclase clasts in opaque matrix

,59 lt gy = plagioclase clasts smaller, subrounded, matrix texture variable

,53 lt gy = coherent uniform matrix with angular plagioclase and small anorthosite clasts

A,B = duplicates from reasonably homogeneous powder

Table 10: Concentrations of U, Th, and Pb in 72255 samples.
(Nunes *et al.*, 1974b)

Sample	Weight (mg)	Concentrations (ppm)				
		U	Th	Pb	$^{232}\text{Th}/^{238}\text{U}$	$^{238}\text{U}/^{204}\text{Pb}$
72255,67 matrix (dark)	132.5	1.145	4.222	2.478	3.81	1,414
72255,54 matrix (light)	98.2	1.536	5.724	3.080	3.85	2,998
72255,60 matrix mixture (dark and light)	196.7	1.663	6.362	3.540	3.95	2,135
72255,49 Civet Cat clast plag.-deficient	51.6	0.3874	1.216	0.9448	3.24	195
72255,49 Civet Cat clast plag.-enriched	35.7	0.2151	—	0.6939	—	177

*Concentration run divided from solution; all other analyses were of splits from crushed solid material obtained prior to spiking.

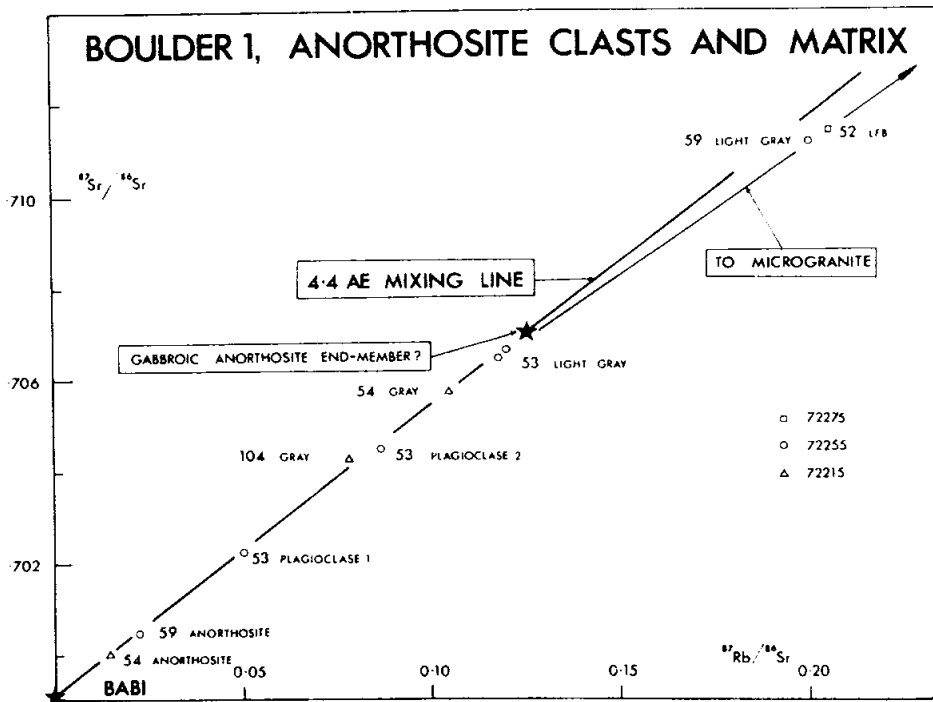


Figure 9: Mixing lines generated by anorthositic clasts within breccia matrix samples and an unidentified gabbroic anorthosite end-member; and between gabbroic anorthosite and microgranite, for 72255 and other Boulder 1 samples. If anorthositic samples are cogenetic, the line marked 4.4 Ae defines their igneous age. Using new decay constants, this line has an age of 4.31 Ga. (See also 72215, Fig. 9).

Table 11: Isotopic composition of Pb in 72255 samples.
(Nunes *et al.*, 1974b)

Sample	Run	Corrected for blank and primordial Pb				Single-stage ages in m.y.			
		$\frac{^{206}\text{Pb}}{^{238}\text{U}}$	$\frac{^{207}\text{Pb}}{^{235}\text{U}}$	$\frac{^{207}\text{Pb}}{^{206}\text{Pb}}$	$\frac{^{208}\text{Pb}}{^{232}\text{Th}}$	$\frac{^{206}\text{Pb}}{^{238}\text{U}}$	$\frac{^{207}\text{Pb}}{^{235}\text{U}}$	$\frac{^{207}\text{Pb}}{^{206}\text{Pb}}$	$\frac{^{208}\text{Pb}}{^{232}\text{Th}}$
72255.67 matrix (dark)	C1P	0.9906	77.36	0.5667	0.2459	4.480	4.486	4.489	4.503
	C1	0.9873	77.22	0.5676	—	4.469	4.484	4.491	—
72255.54 matrix (light)	C1P	0.9321	66.41	0.5170	0.2324	4.285	4.331	4.353	4.281
	C1	0.9317	66.13	0.5151	—	4.284	4.327	4.348	—
72255.60 matrix mixture (dark and light)	C1P	0.9745	74.53	0.5550	0.2349	4.427	4.448	4.458	4.322
	C1	0.9743	74.61	0.5557	—	4.426	4.449	4.460	—
72255.49 Civet Cat clast plag.-deficient	C1P	1.065	92.15	0.6281	0.2499	4.717	4.664	4.641	4.570
	C1	1.069	90.76	0.6159	—	4.732	4.649	4.612	—
72255.49 Civet Cat clast plag.-enriched†	C1P	1.464	147.8	0.7326	—	5.382	5.050	4.916	—
	C1	1.443	169.7	0.8533	—	5.867	5.146	4.865	—

*Note: Concentration and composition splits were divided from solution prior to adding the ^{208}Pb enriched spike. All other analyses were of splits from crushed solid material and the concentration portions were totally spiked prior to dissolution.

†The gross difference between the CP and C only calculations must be because of an heterogeneous splitting of this sample prior to spiking—calculated U/Pb ratios from the concentration only data (i.e. where only the $^{208}\text{Pb}/^{206}\text{Pb}$ ratio from the composition run was utilized) are the most accurate.

Table 12: Age parameters and single-stage Pb ages of 72255 samples.
(Nunes *et al.*, 1974b).

Sample	Weight (mg)	Run	Observed ratios†			Corrected for analytical blank‡				
			$\frac{^{206}\text{Pb}}{^{204}\text{Pb}}$	$\frac{^{207}\text{Pb}}{^{204}\text{Pb}}$	$\frac{^{208}\text{Pb}}{^{204}\text{Pb}}$	$\frac{^{206}\text{Pb}}{^{204}\text{Pb}}$	$\frac{^{207}\text{Pb}}{^{204}\text{Pb}}$	$\frac{^{208}\text{Pb}}{^{204}\text{Pb}}$	$\frac{^{207}\text{Pb}}{^{206}\text{Pb}}$	$\frac{^{208}\text{Pb}}{^{206}\text{Pb}}$
72255.67 matrix (dark)	100.8	P	1,596	908.5	1,526	2,815	1,601	2,682	0.5685	0.9527
	132.5	C*	1,092	624.7	—	1,405	802.5	—	0.5711	—
72255.54 matrix (light)	124.1	P	2,089	1,085	2,023	3,296	1,709	3,186	0.5187	0.9666
	98.2	C*	1,734	898.9	—	2,803	1,449	—	0.5171	—
72255.60 matrix mixture (dark and light)	190.3	P	1,987	1,107	1,909	2,212	1,233	2,128	0.5573	0.9619
	196.7	C*	1,897	1,060	—	2,090	1,166	—	0.5582	—
72255.49 Civet Cat clast plag.-deficient	66.2	P	185.7	120.9	163.5	198.2	128.9	173.3	0.6505	0.8743
	51.6	C*	199.2	127.2	—	217.6	138.6	—	0.6369	—
72255.49 Civet Cat clast plag.-enriched	32.9	P	204.9	153.2	148.8	245.4	183.3	173.3	0.7467	0.7062
	35.7	C*	160.0	138.5	—	180.5	156.4	—	0.8663	—

*Samples totally spiked prior to digestion.

† ^{208}Pb spike contribution subtracted from Pb concentration data.

‡Analytical total Pb blanks ranged from 0.59 to 1.96 ng except for the 75055 composition blank (2.9 ng), and the 74220 concentration blank (2.8 ng).

P = composition data; C = concentration data.

Table 13: Fission track analysis of whitlockite in 72255

(from Goswami *et al.*, 1976a). Track density in $\text{cm}^{-2} \times 10^7$. The table differs from that in Goswami and Hutcheon (1975) in that the observed track density has increased from 30.2 and the row labelled "spallation recoils" has been added, exactly accounting for the increase. Goswami and Hutcheon (1975) also mislabelled the density units as being multiplied by a factor of 10^{-7} instead of 10^7 .

Track contributions	72255*
Observed track density	36.3 ± 1.5
Fe-group cosmic rays	1.0 ± 0.5
Spallation recoils	6.1 ± 0.6
Reactor-induced fission	1.65 ± 0.06
Lunar neutron-induced fission	< 0.15
High-energy cosmic ray-induced fission †	3.3 ± 1.7 $- 1.0$
Spontaneous fission tracks	24.2 ± 1.7 $- 2.2$
Tracks from ^{238}U fission	16.1 ± 1.1 §
Tracks from ^{244}Pu fission	8.1 ± 1.8 § $- 2.4$
Observed $\rho_{\text{Pu}}/\rho_{\text{U}}$	0.51 ± 0.10 $- 0.14$

*Goswami and Hutcheon (1975).

†This work.

‡Assumes Th/U = 12.2.

§C_o = 71 ± 4 ppm; track retention age = 3.96 G.y.

¶C_o = 83 ± 4 ppm; track retention age = 3.98 G.y.

Calculations use the following decay constants: $\lambda_{e^{238}} = 7.03 \times 10^{-17} \text{ yr}^{-1}$ (Roberts *et al.*, 1968); $\lambda_{e^{235}} = 1.55 \times 10^{-10} \text{ yr}^{-1}$ (Jaffey *et al.*, 1971); $\lambda_{e^{244}} = 1.045 \times 10^{-11} \text{ yr}^{-1}$ (Fields *et al.*, 1966); $\lambda_{e^{244}} = 8.50 \times 10^{-9} \text{ yr}^{-1}$ (Fields *et al.*, 1966).

Table 14: Rb-Sr data for the Civet Cat norite in 72255 (Compston *et al.*, 1975).

Rb, Sr, and $^{87}\text{Sr}/^{86}\text{Sr}$ for samples of the Civet Cat clast 72255,41. Total-rock samples are independent fragments rather than homogenized aliquots, so analytical differences are expected due to sampling effects. Mineral separates are grouped with the total-rocks from which they were separated

	Weight (mg)	Rb (ppm)	Sr (ppm)	$^{87}\text{Rb}/^{86}\text{Sr}$	$^{87}\text{Sr}/^{86}\text{Sr} \pm \text{se}^a$
Plagioclase-rich total-rock (1)	5.2	4.20	219.5	0.0552	0.70250 ± 7
Plagioclase-rich total-rock (2)	4.3	3.96	226.5	0.0504	0.70222 ± 3
'Mixed' total-rock (1)	15.8	2.56	101.4	0.0729	0.70348 ± 2
'Mixed' total-rock (2)	14.6	3.02	100.9	0.0864	0.70443 ± 2
Plagioclase (1)	4.5	3.59	224.6	0.0461	0.70203 ± 3
Plagioclase (2)	4.6	3.60	221.2	0.0469	0.70202 ± 3
Plagioclase (3)	3.6	3.29	209.5	0.0453	$(0.70168 \pm 8)^b$
Plagioclase (4)	3.7	2.89	198.0	0.0421	0.70175 ± 3
Pyroxene (green)	8.8	1.09	16.12	0.1956	0.71080 ± 15
Pyroxene (black)	3.7	0.74	22.08	0.0972	0.70518 ± 6
Pyroxene-rich total-rock (1)	15.5	5.68	79.8	0.2053	0.71148 ± 3
Pyroxene-rich total-rock (2)	14.4	5.75	99.7	0.1662	0.70919 ± 4
Plagioclase (5)	5.6	6.67	147.1	0.1309	0.70743 ± 3
Pyroxene (green + black)	4.3	1.80	19.16	0.2721	0.71498 ± 8

^a Internal standard error of mean.

^b Strong anomalous isotopic fractionation – discard.

material), and granitic material (see 72215, Fig. 9 for diagram). U,Th-Pb isotopic data and age parameters for matrix samples were presented by Nunes *et al.* (1974b) (given here as Tables 10, 11, and 12, with data for the Civet Cat norite), and also discussed by Nunes and Tatsumoto (1975). The matrix data plot within error of concordia in a 4.24 to 4.44 Ga range (see 72215, Fig. 10). Although these Boulder 1 data can by themselves be explained by a simple 2-stage U-Pb evolutionary history whereby ~4.5 Ga material was disturbed by ~4.0 Ga event(s), other intermediate events could be masked by the uncertainty of the data. Hutcheon *et al.* (1974b), Braddy *et al.* (1975b), Goswami and Hutcheon (1975), and Goswami *et al.* (1976a,b) used fission tracks to assess the age of a whitlockite grain in the 72255 matrix (Table 13, Fig. 13). Adopting 71 ppm U for the whitlockite, the tracks are in excess of those from ^{238}U alone, and the excess is assumed to result from ^{244}Pu . A $(\text{Pu}/\text{U})_0$ of 0.020 gives an age of 3.90-3.93 Ga for the whitlockite (Hutcheon *et al.*, 1974b); if the ratio is assumed to be the same as that of the St. Severin meteorite, i.e. 0.015, then the age is 3.96 (+0.04, -0.07) Ga. Such a track retention age of the whitlockite most probably refers to the last high-temperature event.

Radiogenic isotopes in the Civet Cat norite clast were investigated by Leich *et al.* (1975a,b) (Ar-Ar), Compston *et al.* (1975) (Rb-Sr), and Nunes *et al.* (1974b) and Nunes and Tatsumoto (1975a) (U,Th-Pb). The Ar-Ar release data are shown in Fig. 10. From 800 to 1200 degrees Centigrade the sample has an apparent-age plateau of 3.93 +/- 0.03 Ga; the plateau includes 57% of the total ^{39}Ar . The 1400 degree centigrade fraction has an age significantly higher (~3.99 Ga) and contains 25% of the total ^{39}Ar . The Ar isotopic data as a whole suggest that the plateau age is reliable, and it is consistent with the disturbances indicated in the Sr

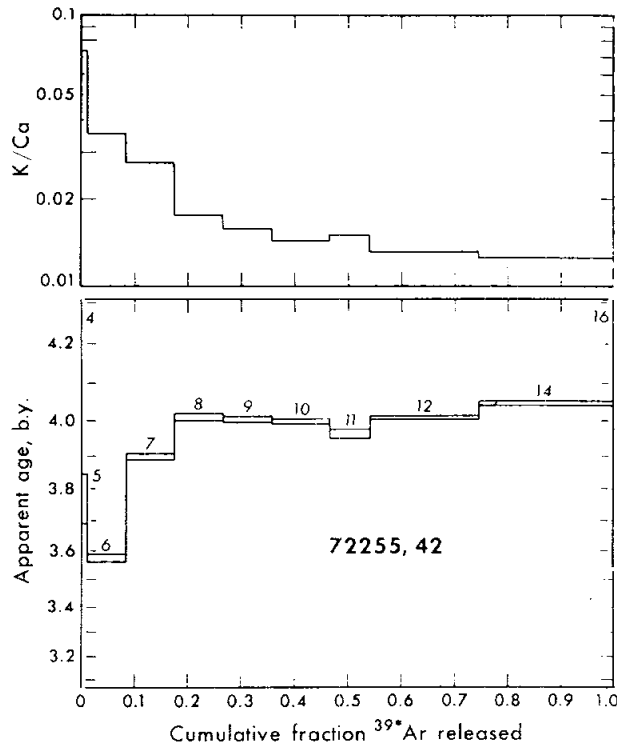


Figure 10: Apparent-age and K/Ca data from 72255,42. (Leich *et al.*, 1975a)

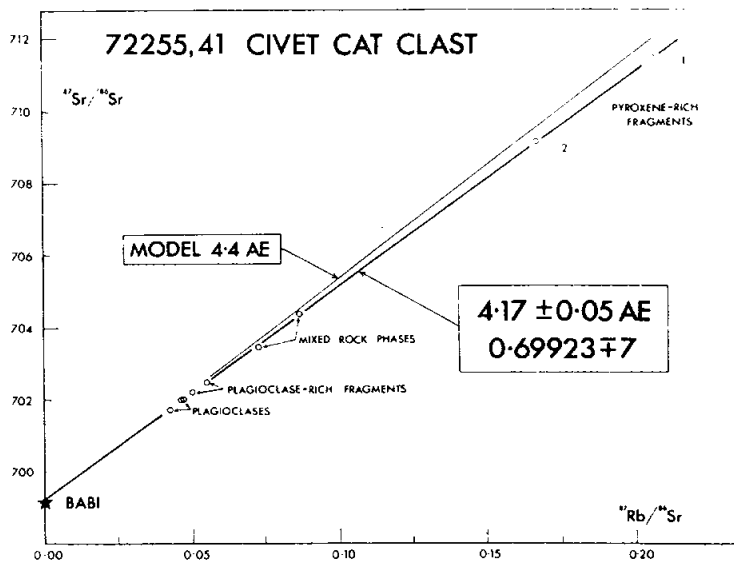


Figure 11: Isochron defined by total-rock fragments and low-Rb plagioclases from the Civet Cat clast (72255,41). The age with new constants is 4.08 Ga; the model line corresponds with 4.31 Ga. (Compston *et al.*, 1975)

and Pb isotopic data. The Rb-Sr isotopic data for the Civet Cat are given in Table 14, and Figs. 11, 12, and 13, and include many mineral separates. The six "bulk" samples alone define a perfectly fitted isochron of 4.10 ± 0.06 Ga, with initial $^{87}\text{Sr}/^{86}\text{Sr}$ of 0.69919 ± 8 (Fig. 11). Compston *et al.* (1975) interpret this age as the igneous crystallization age, because (1) these entities were created during an igneous event (2) the initial Sr isotope ratio is low whereas the Rb/Sr is quite high, and (3) metamorphic equilibration in the sample is limited to smaller volumes. Including the plagioclase separates refines the age to 4.08 Ga. Some separates do not fit the "bulk" isochron (Fig. 12), and the pattern resembles that of response to a younger heating event; however, re-equilibration was not complete on the scale of less than 0.2 mm. An age of 3.81 ± 0.23 Ga approximates the time of mineral disturbance. A detailed discussion is given in Compston *et al.* (1975). Alternatively, if the Civet Cat was not a closed system during re-heating, then those separates richest in Rb might represent Rb gain. Then an alignment of black pyroxene, plagioclase-rich total rocks, and other plagioclases give an age of about 4.36 ± 0.13 for the maximum possible original crystallization age.

The U,Th-Pb isotopic data of Nunes *et al.* (1974b) for the Civet Cat norite are in Table 10. The Civet Cat norite contains excess Pb relative to U, plotting well above concordia. The excess probably reflects transfer of Pb from the matrix, which is relatively Pb-rich, into the clast during breccia formation, although other times are possible. The two analyses are too uncertain to yield an accurate age determination (Nunes and Tasumoto, 1975a).

EXPOSURE AGES:

Leich *et al.* (1975a,b) measured the isotopic compositions of the rare gases He, Ne, Ar, Kr, and Xe in a matrix sample and the Civet Cat norite in 72255. Trapped gas abundances are very low, with only small to negligible solar wind components. The cosmogenic Kr isotopic spectra for the matrix sample gave an exposure age of 44.1 ± 3.3 Ma. (Leich *et al.*, 1975b, tabulated preliminary Kr ages of 44.6 ± 2.9 for the matrix and 36 ± 10 for the Civet Cat, but in Leich *et al.*, 1975a, no Kr age was tabulated for the Civet Cat norite sample because there are large uncertainties in the cosmogenic $^{81}\text{Kr}/^{83}\text{Kr}$ ratio). The age is similar to that of 72215, but lower than the exposure age of 72275 (52 Ma), probably because of differences in shielding. The less-precise Ar-Ca exposure ages (48 Ma for Civet Cat, 56 Ma for matrix, \pm about 25%) are consistent with the Kr age.

Particle track data bearing on exposure were reported by MacDougall *et al.* (1974), Hutcheon *et al.* (1974b), Braddy *et al.* (1975b), Goswami and Hutcheon (1975), and Goswami *et al.* (1976a,b). The track density profile was produced from thick sections 72255,30 and ,32, using SEM and optical methods. The interpretation is complicated by correction for exposure geometry (assumed equivalent to present-day exposure throughout) and uncertainty in the erosive history (assumed as 1 mm/Ma). The external surface of the sample is saturated with craters, suggesting a recent exposure of more than 1 Ma. Hutcheon *et al.* (1974b) using a simple one-stage exposure model calculated an age of 19 ± 2 Ma. The uneven distribution of shock alteration effects could be a complicating factor. Goswami and Hutcheon (1975) added more data (Fig. 14); they found that if normalized to the Kr exposure age of 42 Ma, then agreement at depths

greater than 1 cm was good, but not at less than this depth (Fig. 15). The disagreement could result from small-scale (mm size) cratering event late in the boulder history. MacDougall *et al.* (1974) had placed an upper limit of 15 to 20 Ma on the exposure, but noted that erosion was in any case a problem for interpretation; such track ages do not necessarily date the time that the boulder rolled into its present position, but only some later spalling event.

Yokoyama *et al.* (1974) noted that 72255 was saturated in ^{26}Al , requiring an exposure of at least a few million years.

PHYSICAL PROPERTIES

Magnetic data for 72255 samples were reported by Banerjee *et al.* (1974a,b) and Banerjee and Swits (1975). Samples from the Boulder were oriented with respect to each other (accurate to within about ± 20 degrees). Two samples from 72255 had the same direction (Fig. 16), and within error of those from 72255. The two 72255 samples had the same intensity of 1.2×10^{-5} emu/g. In an attempt to separate stable primary NRM from unstable secondary NRM, the authors attempted thermal demagnetization, avoiding oxidation; however, from the continually decreasing NRM (Fig. 17), it appeared that permanent damage was done to the magnetic carriers and the procedure was unadvisable. AF-demagnetization showed no zig-zag patterns, and the NRM direction after demagnetization in fields at 80 Oe or greater are stable and primary; however, these fields differ in direction from those in 72275 by 130 degrees (Fig. 18). Banerjee and Swits (1975) presented data for paleointensity, suggesting a field of 0.35 Oe, different from those of 72275 and 72215 (suggesting 3 different events, as also suggested by the differing directions of NRM under AF-demagnetization). However, given the problems of

obtaining and interpreting magnetic data for lunar samples then neither the directions nor the intensities can be said to have known meanings (see also discussion by Cisowski *et al.*, 1977).

Adams and Charette (1975) reported spectral reflectance measurements for the 0.35-2.5 micron range for a gray noritic breccia that was heavily contaminated with saw-blade metal (.74). The reflectance curve may be artificially flattened by the presence of the opaque contaminant; it shows little absorption at the 1.9 micron band that results from pyroxene and that is typical of other highland rock samples.

PROCESSING

The details of the initial processing of 72255 were given by Marvin in CI 1 (1974). Three documented pieces had broken away during transport, and partly used for thin sections. The sawing of a 1.5 cm-thick slab (Figs. 1,2) was accomplished in July, 1973. The slab, 72255,10, was removed as a single piece and ,11 broke off along a pre-existing crack. Some chalky white material was sawn from the east tip (.18) and used for thin sections and chemistry, and surface chips were taken from elsewhere on the main mass (Fig. 2). The slab was subdivided, with the main divisions as shown in Fig. 19. Many thin sections were made from slab materials. A second slab and related pieces were cut from the main mass 72255,23 in 1984, but studies of them have only recently commenced.

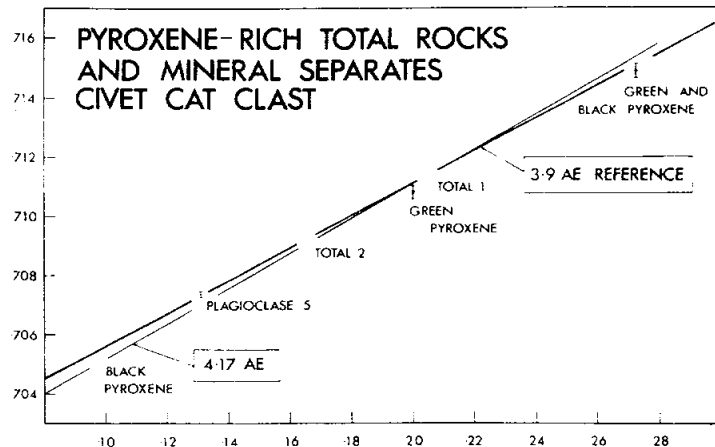


Figure 12: Rb-Sr mineral data for the pyroxene-rich fragments of the Civet Cat clast. With new constants, the "3.9 Ga reference line" corresponds with 3.82 Ga reference, and the 4.17 isochron to 4.08 Ga. The reference isochron corresponds with the time of redistribution of ^{87}Sr and/or Rb after original igneous cooling at 4.08 Ga. (Compston *et al.*, 1975).

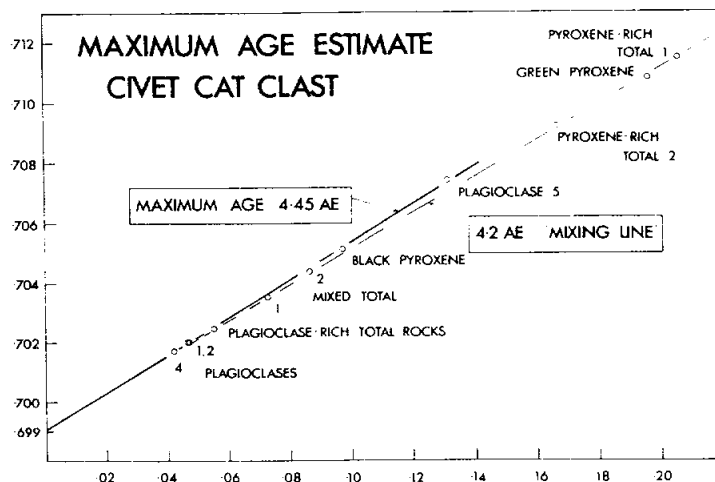


Figure 13: Maximum age estimate for the Civet Cat norite (4.36 Ga with new decay constants). The diagram assumes that new Rb entered the pyroxene-rich component during deformation and shearing at breccia assembly, but that all plagioclase separates and black pyroxene were unaffected. Then the "4.2" Ga (new constants give 4.11 Ga) becomes a mixing line of no simple time significance. (Compston *et al.*, 1975).

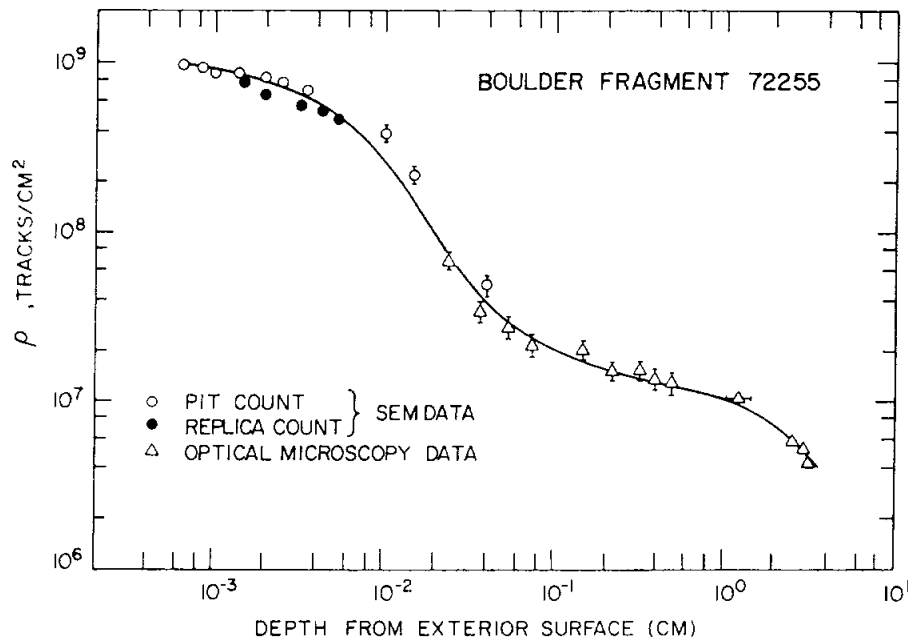


Figure 14: Measured track densities in 72255,30 and ,32 plotted as a function of distance from the exterior surface. SEM and optical data, without normalization. The solid line is the best fit through the data points. (Goswami and Hutcheon, 1975).

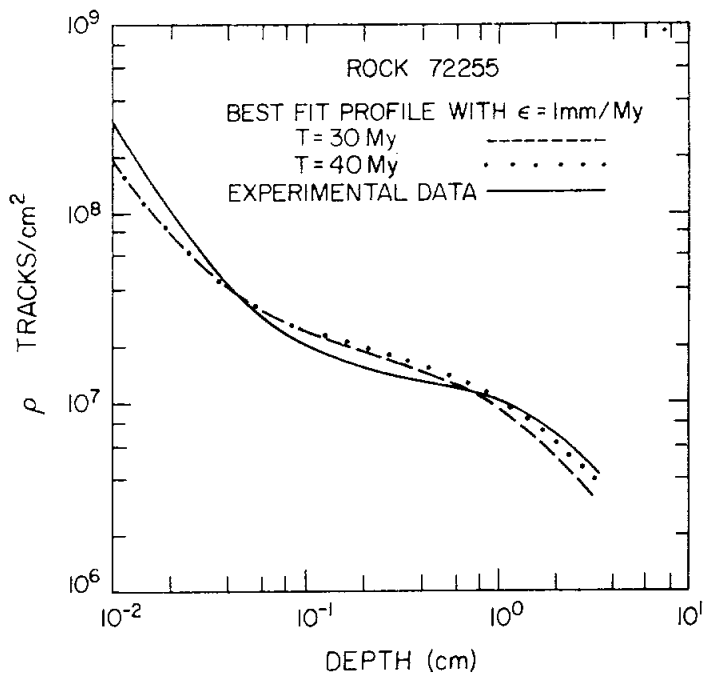


Figure 15: Observed and expected track density profiles for 72255. The solid line is taken from Figure 14; the dotted and dashed lines are calculated for two different exposure ages. (Goswami and Hutcheon, 1975).

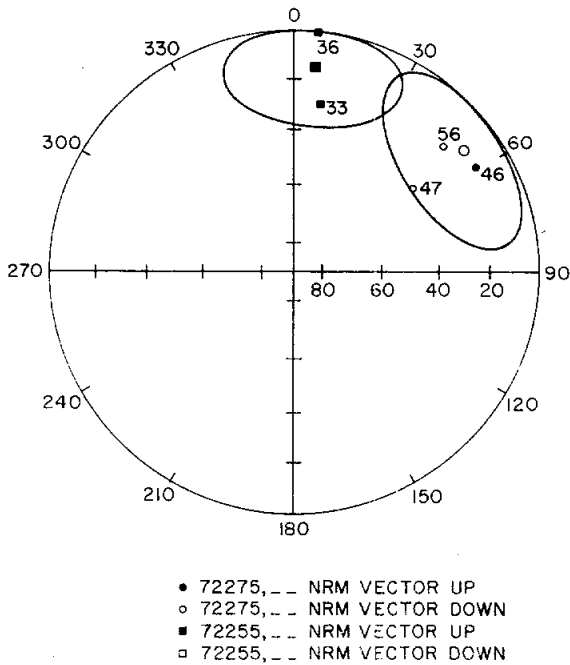


Figure 16: Absolute NRM directions of samples of 72255 and 72275. Average directions for each sample are denoted by the larger symbols. 95% cones of confidence are indicated. (Banerjee et al., 1974a).

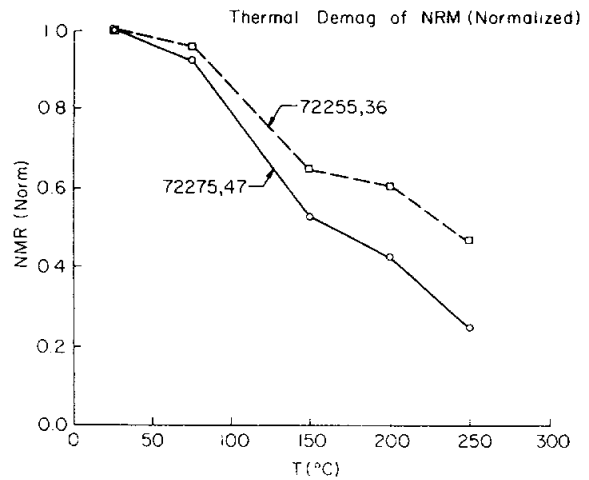


Figure 17: Decay of NRM intensity on thermal demagnetization of 72255 and 72275 samples in zero field and in an H₂-CO₂ gas-buffered furnace. (Banerjee et al., 1974a).

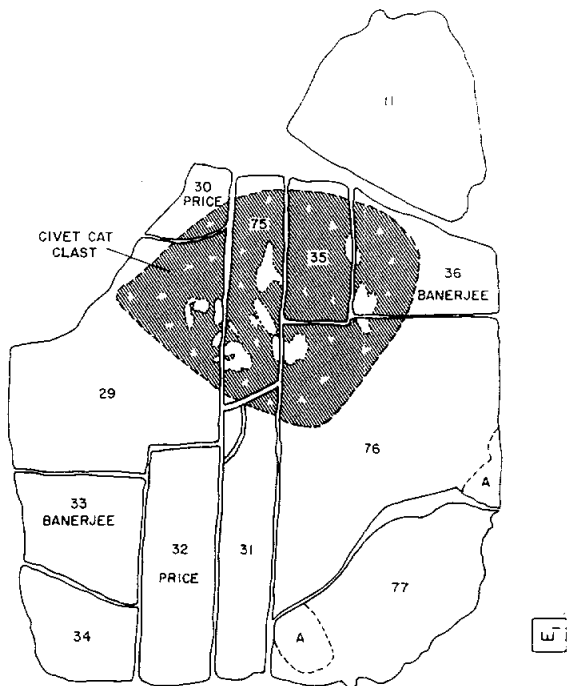


Figure 18: Main subdivisions of the first slab cut from 72255, in 1973 (from Marvin, in CI 1, 1974).

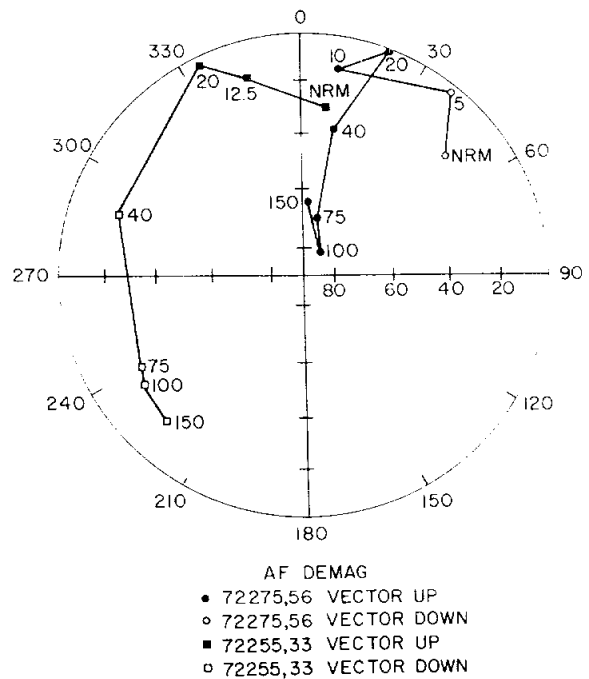


Figure 19: Changes in NRM directions on AF-demagnetization of 72255 and 72275 samples. The numbers refer to peak AF values. The stable direction for 72275 is average of points 75, 100, and 150; that for 72255 for points 75 and 100. (Banerjee et al., 1974a).

72275**Fragmental Polymict Breccia
St. 2, 3640 g****INTRODUCTION**

72275 is a fragmental breccia that may represent the matrix of Boulder 1, although it stood up in bold relief on the top of the boulder (see section on Boulder 1, St. 2, Fig. 2). It is predominantly light gray [N7], fairly friable, and encloses several protruding subrounded coherent knobs. Most such knobs are darker colored (medium gray [N5]). The sample was 17 cm long, and irregularly

shaped with rounded corners. After collection it broke into several pieces (Fig. 1). The exposed surface had a thin patchy brown patina, with a few zap pits on some surfaces (N, E, B). Splashes of black glass covered some of the sample. An opposite face, tilted down toward the boulder, had a powdery covering that was layered and ripple-marked.

72275 is a porous aggregate of angular mineral, devitrified glass,

and lithic fragments constituting a fragmental polymict breccia. The sample is not a regolith breccia. A few of the clasts are more than a centimeter across, including a conspicuous rimmed clast (Figs. 1, and 2) labelled Clast #1 or the Marble Cake clast. Other conspicuous clasts are the Apollo 17 KREEPY basalts (~3.93 Ga old) unique to this sample, many dark melt-matrix breccias, and varied feldspathic granulite and other feldspathic breccias. Numerous rock types,



Figure 1: Reconstructed 72275, with documented pieces mainly on the right, and undocumented pieces in the foreground. The exposed north side shows thin brown patina. Clast #1 (Marble Cake clast) is prominent on the front face. Scale in centimeters. S-73-16077.



Figure 2: Initial slabbing and slab dissection of 72275, leaving irregular surface, and exposing the dark clasts #2 and #3. Clast #1 is to the left. Cubes are 1 inch. S-73-34463.

such as other basalts, granites, and impact melts, are present as smaller fragments. Rare gas analyses suggest an exposure age of about 52 Ma, a little older than 72215 and 72255 and suggesting a two-stage exposure history for the boulder.

Most of the studies of 72275 were conducted by the Consortium Indomitable (leader J. A. Wood). A slab cut across the sample (Fig. 2) in 1973 made a comprehensive

petrographic and chemical study possible. Detailed maps of the exterior surfaces and the slab based on the macroscopic observations, as well as descriptions of the sample allocations, were given in Marvin (in CI 1, 1974) (Fig. 3a, b). Two new slabs parallel to the first were cut in 1984 (Figs. 3c, 4, 5) for new consortium studies (leader L. A. Taylor). They were described by Salpas *et al.* (1985).

PETROGRAPHY

72255 is conspicuously polymict (Figs. 1-5). LSPET (1973) described the sample as a layered light gray-breccia. Simonds *et al.* (1975) listed it as a fragmental breccia. The most detailed descriptions of the petrography of 72275 are given in Stoeser *et al.* (1974a, and in CI 1, CI 2, 1974), Marvin (in CI 1, 1974), and Ryder *et al.* (1975b), who described 72275 as a light gray friable breccia. The Apollo 17 KREEPy basalts were described in particular by Ryder *et al.* (1977) and Salpas *et al.* (1987).

Mapping of the sample before and after slabbing (Marvin, in CI 1, 1974) showed four main lithologic types (Fig. 3a, b)

1) the light gray matrix with minor darker gray zones, appearing as a friable aggregate of mineral and lithic clasts with a range of sizes up to about 0.5 mm. Plagioclase and a few percent brown and yellow mafic silicates were identifiable, with sparse grains of pink or amber spinel, and metallic iron.

2) anorthositic clasts of which the most conspicuous is clast #1 (Marble Cake clast), with a black rim. Smaller white clasts, with and without rims, occur throughout the specimen. Clast #1 is not pure white, but has 10 to 20% yellow mafic silicates, and appears to be a fluidized cataclastic breccia, interlayered with gray breccia and black rim material.

3) Dark gray aphanitic clasts, including clasts #2 and #3, which are hard, resistant dark gray materials (later identified as aphanitic impact melts). These clasts contain small angular fragments and thin white streaks indicating that they are polymict breccias. Small fragments are common in 72275.

4) Basaltic clasts and zones, which are the relics of the Apollo 17 KREEPy basalts. Most of the clasts

are rounded, and consist of white feldspar laths and yellow pyroxene. Most conspicuous are clasts #4 and #5 on the slab pieces. The clasts are embedded in zones of fine-grained basaltic debris, but these zones are difficult to delineate macroscopically. (Other basaltic clasts were later found and mapped on the newer slab cuts by Salpas *et al.*, 1985, 1987).

Three distinct lithologic units in the 1984 surfaces were recognized by Willis (1985). A darker and coarser unit separated two lighter, more fine-grained units. Each is distinct with respect to clast sizes, abundance, and types. One of the lighter units consists mainly of basalts sitting in crushed basalts, whereas the other changes from breccia clasts (mainly dark melt breccias) to basalts towards the interior of the rock. The dark coarse zone consists mostly of dark melt breccia clasts. In all the units the average clast dimension decreases from the first face exposed to the last.

Stoeser *et al.* (1974a, and in CI 1, 1974) and Ryder *et al.* (1975b) considered that the sample had two major lithologic types, that of the gray polymict breccia, and that of the KREEPy basalt (which they referred to as "pigeonite basalt") breccia; the latter forms about 30% of the exposed surfaces. The light-gray friable breccia is composed of porous, poorly-sintered matrix, with angular mineral and lithic clasts (Fig. 6a, b). A clast population survey was tabulated by Stoeser *et al.* (1974a) (Table 1); however, this table omits the dark matrix breccias (the aphanitic melts) that are the dominant clast type. The dark aphanitic melts, which resemble samples 72215 and 72255 in petrography and chemistry, are themselves polymict, containing all the other clast types except for the KREEPy basalts. Materials similar to the Civet Cat norite and granites appear to be dominantly, if not absolutely, confined to the dark aphanitic melts. Neither glass spherules or

Table 1: Population survey of clast types in 72275 light gray matrix, excepting the dark impact melt breccias. % by number, not area. (Stoeser *et al.*, 1974a).

Clast type	72275
Granulitic ANT breccias	48.3%
Granulitic polygonal anorthosite	3.5
Crushed anorthosite	5.1
Devitrified glass	7.9
Glass shards	0.4
Ultramafic particles	1.6
Basaltic troctolite	2.0
Pigeonite basalt	5.1
Other basaltic particles	2.0
Granitic clasts	1.6
"Civet Cat" type nprite	0.4
Monomineralic plagioclase	15.0
Monomineralic mafic silicates	5.5
Monomineralic spinel & opaques	1.2
Number of clasts surveyed	254

ropy glass clasts, nor their devitrified equivalents that are characteristic of regolith breccias, occur in the light-gray friable matrix. The range of mineral fragments (Figs. 7-9) is similar to the range in the dark aphanitic melts (Figs. 9, and 10), with plagioclase, low-Ca pyroxenes, and olivine predominant. Ilmenite, troilite, Fe-metal, pink spinel, chromite, and trace amounts of K-feldspar, silica, zircon, and armalcolite, are present. The differences in lithic clast populations preclude the possibility that the light-gray friable matrix is a crushed version of the dark aphanitic melts. The lack of equilibration rims and lack of extensive sintering suggest that the light-gray matrix was not subjected to high temperatures for any great length of time.

A17 KREEPy Basalts:

The KREEPy basalts, originally referred to as Pigeonite basalts (Stoeser *et al.* in CI 1, 1974, and 1974a,b) occur as fragments and breccia zones in the light gray matrix (Fig. 3a,b). They have not been found in the dark impact melt breccias, nor in any other samples. The brecciated zones consist almost entirely of crushed basalts, and are clots or bands up to 2 cm thick.

(Marvin, in CI 1, 1974; Stoeser *et al.*, in CI 1, 1974). The clasts are rounded, with prominent white feldspar and yellow mafic silicates. Few of the relict basalt fragments are more than a few millimeters across; rare examples reach one centimeter.

Most of the KREEPy basalts clasts have a mesostasis-rich subophitic to intersertal texture (Fig. 6e) (Stoeser *et al.*, CI 1, 1974; CI 2, 1974, 1974a,b; Ryder *et al.*, 1975b, 1977; Irving, 1975; Salpas *et al.*, 1985, 1986a, 1987). Most have a medium grain size (silicates 500-1000 microns), but there is a range down to fine-grained equigranular and glassy vitrophyric varieties, which are less common. The textures are homogeneous, and the fragments contain no xenoliths or other features suggestive of an impact origin for the melt phase. The chemical evidence (below) also suggests that these basalts are volcanic. The range in grain sizes and textures suggests that a sampling of both flow interiors and exteriors was obtained. The dominant subophitic basalts consist of approximately equal amounts of plagioclase and clinopyroxene (mainly pigeonite), with 10% to 30% of a complex fine-grained and opaque mesostasis (Fig. 6e). A

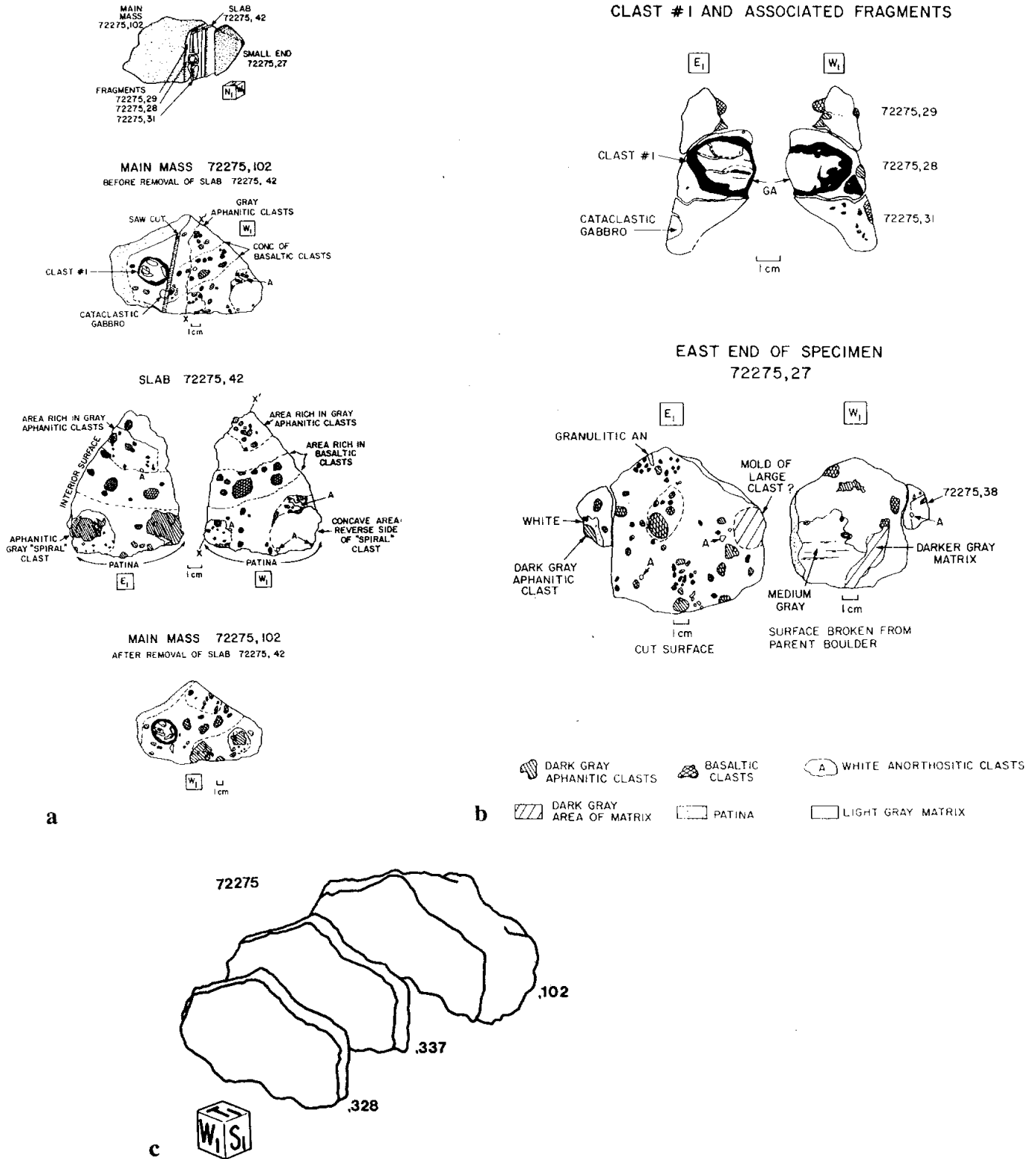


Figure 3: Slabbing and mapping of 72275. a) Sawn surface of the main mass (,102), and the slab (,42). b) Surface of clast #1 and the east end piece (,27). c) 1984 reslabbing of main mass ,102. Cube is 1 inch.

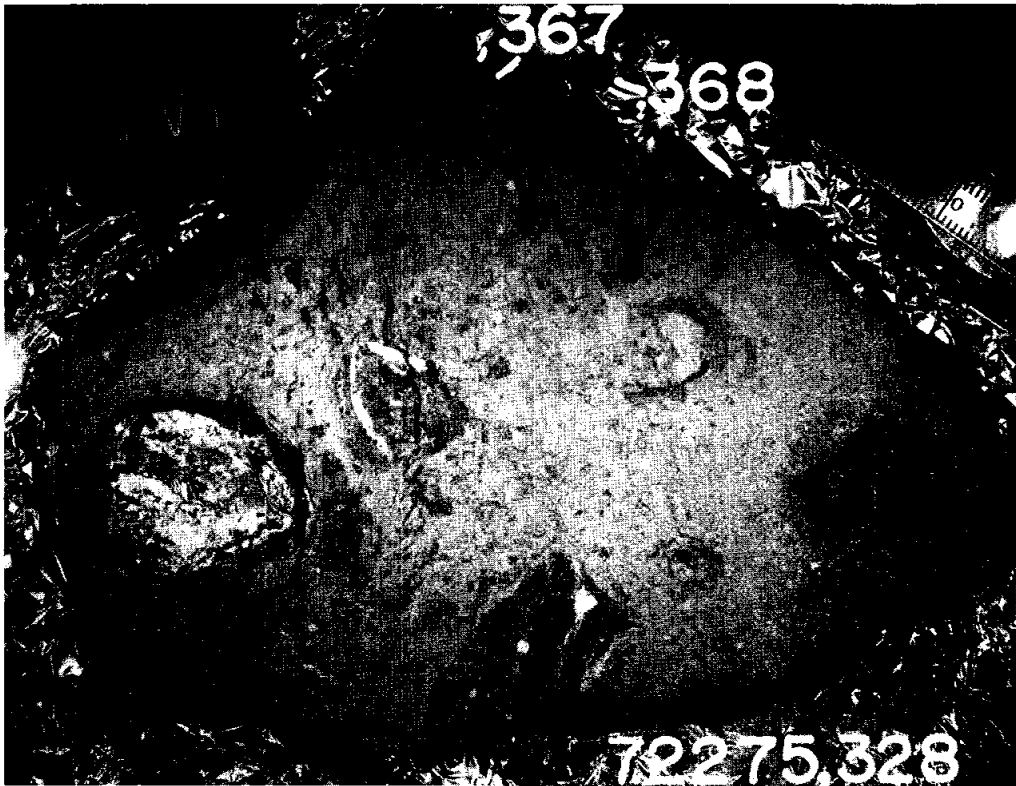


Figure 4: Exposed west face of first 1984 slab (,328) after removing irregular surface left in 1973 slabbing. Most of the surface visible is that exposed in Fig. 2; another large clast has been exposed. Cube is 1 inch; rule scale is centimeters. S-84-45540.



Figure 5: Exposed east face of second 1984 slab (,337) and its subdivisions. There is an obvious lack of large clasts compared with the earlier exposed faces. Cube is 1 inch; rule scale is centimeters. S-84-46145.

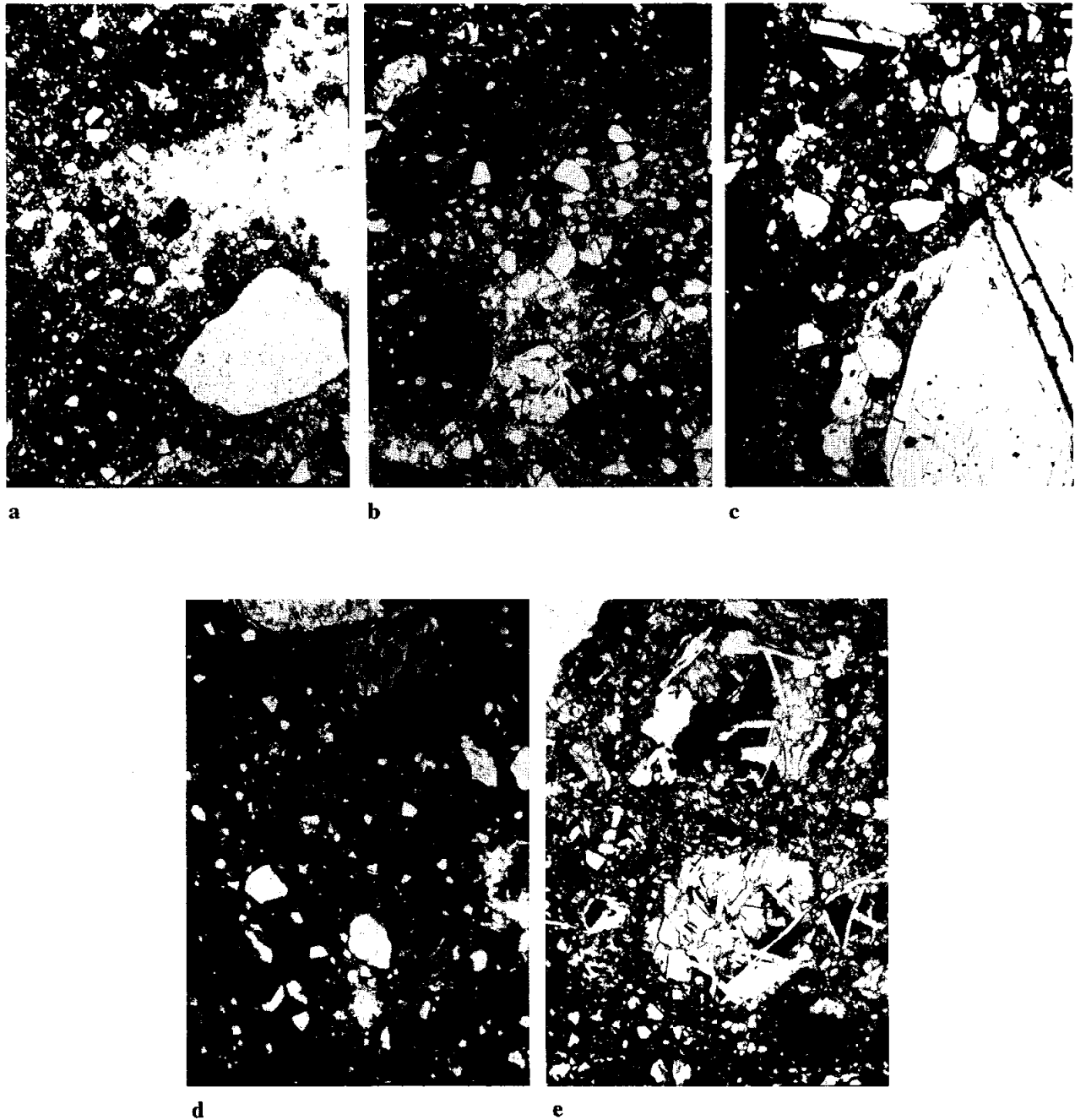


Figure 6: Photomicrographs of 72275. All plane transmitted light except c), crossed polarizers. All about 2mm field of view.

- a) 72275,13: general friable matrix of undocumented chip, showing feldspathic granulite clasts and schlieren (right), clasts or blobs of dark melt matrix breccias, and numerous mineral clasts.
- b) 72275,134: general matrix of 1973 slab near clast #5, showing rounded dark melt breccia pieces, mineral clasts, and small fragments of KREEPy basalts.
- c) 72275,138: anorthositic breccia from the core of clast #1, the Marble Cake clast.
- d) 72275,145: matrix of clast #2, a dark melt breccia.
- e) 72275, 147: clast #5, a monomict breccia or cataclasite of KREEPy basalt.

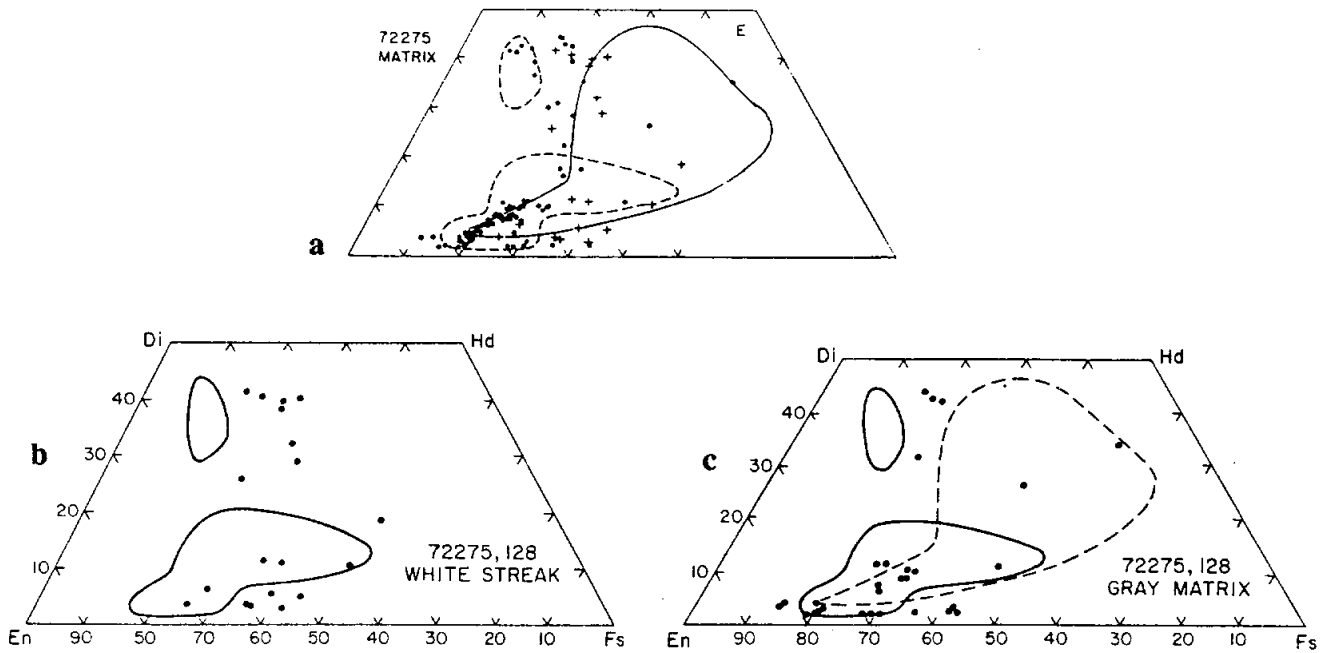


Figure 7: Compositions of pyroxenes in 72275 light gray friable matrix samples. The large outlined area is the range of compositions of pyroxenes in the KREEPy basalts; the smaller outlined areas are the ranges for anorthositic breccias. a) b) are general matrix, c) is a white streak in the matrix in ,128 a) from Stoesser et al. (1974a). b) c) from Stoesser et al. in CI 1, 1974.

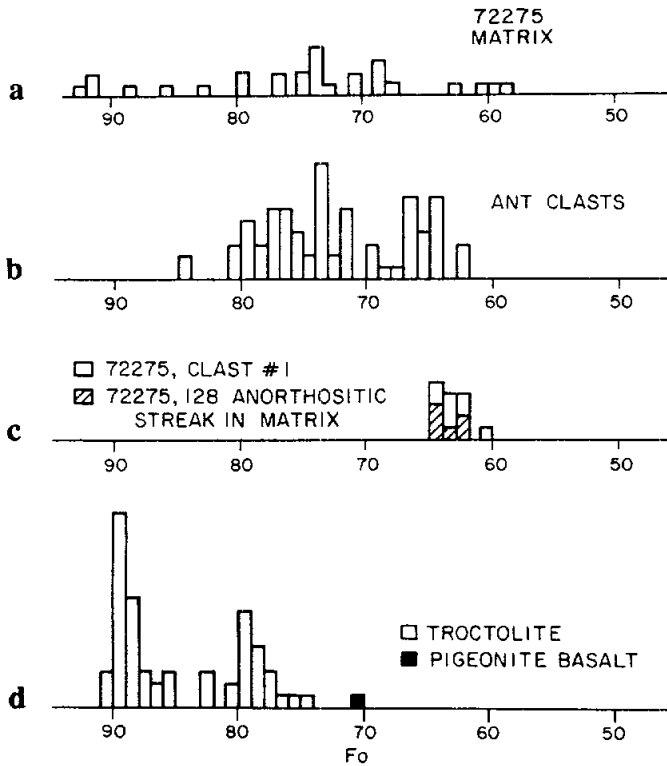


Figure 8: Histograms of olivine compositions in 72275 matrix and clasts. a) monomineralic olivines in general light gray matrix. b) olivines from feldspathic granulite clasts. c) olivines in clast #1 and the white streak in ,128. d) olivines in the troctolitic basalts (impact melts?) and the KREEPy basalts (= pigeonite basalts). Stoesser et al. (1974a).

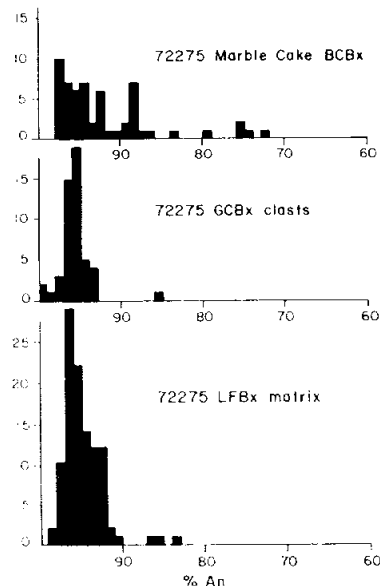


Figure 9: Compositions of olivines in 72275 lithologies. Marble Cake is clast #1; GCBx are the dark impact melt breccias; LFBx is the general light gray matrix. Ryder *et al.* (1975b).

silica mineral (cristobalite?), minor chromite, Fe-metal, and very rare olivine are present outside of the mesostasis. The mesostasis consists of ilmenite, Fe-metal, cristobalite (?), plagioclase, ferroaugite, phosphate, troilite, potash feldspar, zircon, and a Si-rich glass. Both Fe-metal and troilite occur as veins.

The compositions of silicate mineral phases are shown in Figs. 11, 12, and 13, and analyses of metal grains in Fig. 14. Representative microprobe analyses of phases are tabulated in Stoesser *et al.* (in CI 1, CI 2, 1974; 1974b; Ryder *et al.*, 1977). Phases in the relict basalt fragments and the brecciated zones show similar ranges (e.g. Figs. 11, and 12).

Plagioclases, which form an interlocking network of laths, is zoned normally; the trend towards extreme Or-enrichment in plagioclase appears to be unique among lunar samples. Some of the plagioclase borders contain glassy or microcrystalline silicic globules less than 10 microns in diameter, possibly trapped magma. (Ryder *et*

al., 1977) Clinopyroxene, which encloses plagioclases, is elongate to tabular. Many are twinned; none are sector zoned. The first pyroxene to crystallize was Mg-pigeonite; orthopyroxene such as is common in A 15 KREEP basalts is absent. Zoning to more Fe-, Ca-rich pyroxenes is commonly erratic.

The silica polymorph is a late-stage phase, and composes as much as 5% of some clasts. It has the mosaic fracture pattern characteristic of cristobalite. Some grains are laths (poorly-developed) and up to 500 microns long. Chromite is a euhedral to subhedral early-crystallizing phase, most less than 50 microns, that is aluminous and zoned to titanian chromite rims. Olivine is rare, small (less than 300 microns), and a compositional range from Fo69-64. It appears to have survived by enclosure in other silicates. The mesostasis forms interstitial triangular patches several hundred microns across. There is no evidence of immiscibility, although it is heterogeneous, appearing to be more Fe-rich adjacent to pyroxene and more silicic adjacent to plagioclases (Stoesser *et al.*, in CI 1, 1974). The mesostasis rims are not all sharply defined. The bulk composition of the mesostasis is Fe-, Si-, and P-rich, and poor in K compared with many other lunar mesostasis compositions. Fe-metal and (less common) troilite occur in the mesostasis, as veins, and as blebs in early-crystallizing phases. Their low Ni contents are consistent with lack of meteoritic contamination and thus, a volcanic origin for the basalts.

Dark Impact Melt Breccias: Materials originally labelled "dark matrix breccias" (Stoesser *et al.*, in CI 1, 1974) and later gray to black competent breccias (e.g. in Ryder *et al.*, 1975b) are a distinctive feature of 72275. They are the dominant clast material, and occur as discrete clasts and as rinds to, or intermixed with, feldspathic clasts such as feldspathic granulites. They are similar to the dark matrix materials

that form the other Boulder 1 samples 72215 and 72255, and were similarly eventually recognized as aphanitic impact melts (e.g. Ryder and Wood, 1977; Spudis and Ryder, 1981) and not the metamorphosed breccias originally suggested (e.g. Stoesser *et al.*, 1974a, Ryder *et al.*, 1975b).

They are also similar to the Station 3 samples 73215, 73235, and 73255 (e.g. James *et al.*, 1978). The dark breccias were described by Stoesser *et al.*, (1974a,b, and in CI 1, CI 2, 1974), Ryder *et al.* (1977b), and Spudis and Ryder (1981). Most of the dark melt breccias are less than 1 mm, but some are much larger, including Clasts #2 and #3 exposed on the sawn faces (Fig. 2-4). Clast #3 was not allocated, but clast #2 was allocated for petrographic and chemical studies. The Marble Cake clast (clast #1) is a complex rimmed clast (see below). Clasts #1 and #2, and many of the smaller dark breccias, have a "globby" nature, with rounded and irregular outlines (Figs. 2, 4, and 6a, b). In thin sections they are very dark and dense, with a very fine-grained groundmass enclosing a variety of clasts, usually small (Figs. 6a, b, d). The lithic clast population consists of feldspathic granulites, other feldspathic breccias, some basalts and coarser impact melts, and sparse granites. Monomineralic clasts are mainly plagioclase, but olivines and pyroxenes are also common. Some dark clasts have vesicles. The melt matrices are fine-grained, mainly plagioclase and probably pyroxene commonly less than 5 microns, and the melt fraction is probably about 50-70% of the volume. Compositions of monomineralic silicate phases, mainly clasts, are shown in Fig. 9b (plagioclases) and Fig. 10 (olivines and pyroxenes). The range in compositions of mafic minerals is greater than that of anorthositic breccias (e.g. granulites), and indicates that a wide variety of lithologies contributed to the dark melt breccias. However, no fragments of the A 17 KREEPy basalts have been found in these melt breccias. Defocused beam

analyses (Table 2) show that the dark matrix breccias have low-K Fra Mauro basalt compositions similar to those in 72215 and 72255 (see also chemistry section), suggesting a common source, although there is some variation.

Clast #1 (Marble Cake):

The distinctive 3 cm clast visible on the north face (Fig. 1) and after slabbing (Figs. 2-4) was described by Stoesser *et al.* (1974a, and CI 1 and CI 2, 1974), Marvin *et al.* (1974), and Ryder *et al.* (1975b). It consists of a light-colored core (white, with about 10 to 20% yellow minerals) with a dense envelope of dark breccia material that also is crudely interlayered with the core. The rim and the core have been fluidized simultaneously. Part of the clast was thin sectioned and mapped (Fig. 15).

Compositions of mafic mineral phases are shown in Fig. 16. Defocused beam analyses of some clasts are given in Table 3. The dark breccia consists of an aphanitic impact melt, similar to other dark breccias in 72275 except that it is darker, more vesicular, and higher in K and P than most (Table 2, col. 9) (Stoesser *et al.*, in CI 2, 1974). The core material is a complex mix, dominated by a coarse-grained feldspathic lithology that has been crushed (Fig. 6c). Some of its fragments are granulitic, and more than one feldspathic rock type may be present. The parent rock was plagioclase-rich (more than 80%), and contained olivine (Fo₆₀₋₆₈), bronzite, and augite: a cataclastic troctolitic ferroan anorthosite. Ilmenite microgabbros are small igneous (or possibly metamorphic) fragments that are fine-grained and not reported from other lunar samples; they consist of 43-57% plagioclase (An₆₅₋₈₀ Or₅₋₁₅), 25-46% pyroxene (Mg' about 50; see Fig. 16), and 9-18% ilmenite. They also contain minor amounts of cristobalite, troilite, and metallic iron. They are more similar to sodic ferrogabbro fragments at Apollo 16 (Roedder and Weiblen, 1974) than

other samples, but are actually unique. Some exsolved pyroxene fragments that are 200 microns across (hence bigger than those in the ilmenite microgabbros) have a composition similar to those in the ilmenite microgabbros; their source could be a coarser-grained equivalent. Other clast types include an orange glass (spinel troctolite composition), some fine-grained "basalts" with quenched appearance that give the impression of being impact melts, and microgranites. The latter are fairly common.

Feldspathic Breccias:

72275 contains a variety of feldspathic lithic materials ranging from cataclastic ferroan anorthosite-like materials to feldspathic granulites; some of them reach several centimeters long. Apart from the dark melt breccias (in which they are a clast-type), they are the most abundant clasts in 72275; they also occur as discrete fragments in the light gray friable breccia. The feldspathic

clasts were described by Stoesser *et al.* (1974a, and in CI 1, CI 2, 1974), and by Ryder *et al.* (1975b) under the now-obsolete acronym ANT (anorthosite, norite, troctolite). Some are several centimeters in size, and are petrographically similar to those found in other Boulder 1 samples and elsewhere at the Apollo 17 site. Recrystallized varieties (feldspathic granulites, both poikilitic and granulitic in texture) are most common. The compositions range from noritic to troctolitic anorthosites. They have a range of mineral compositions (e.g. Fig. 17), though most individual clasts are fairly well-equilibrated. The ranges are not unlike those reported for other feldspathic highlands breccias; they do not include mafic minerals with Mg' much higher than 0.83, and the plagioclases are dominantly very calcic.

The samples described by Stoesser *et al.* (1974a, and in CI 1, CI 2, 1974) and Ryder *et al.* (1975b)

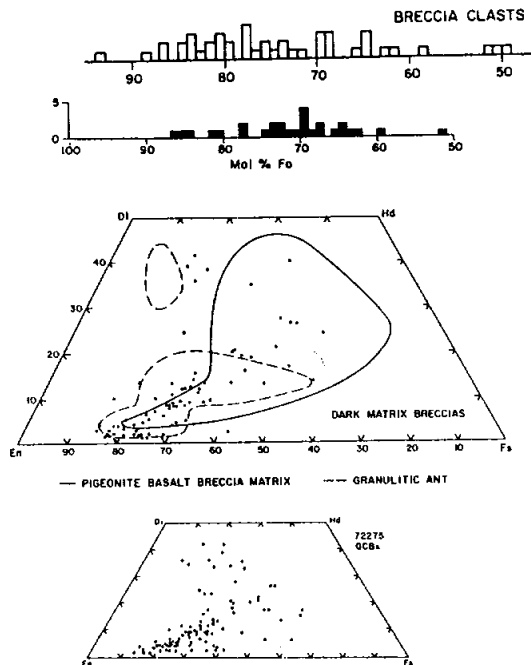


Figure 10: Compositions of olivines (a, b) and pyroxenes (c, d) in dark impact melt breccias (GCBx) in 72275. a) Stoesser *et al.* (1974a), b),d) Ryder *et al.* (1975b), c) Stoesser *et al.*, CI 1.

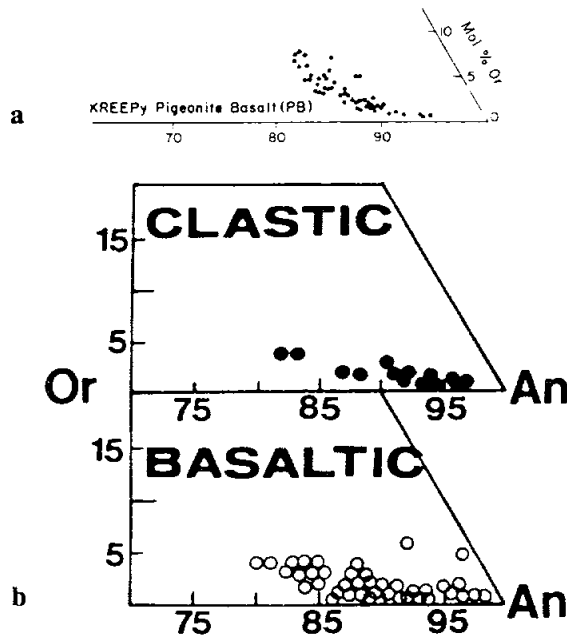


Figure 11: Compositions of plagioclases in A 17 KREEPy basalts. a) Ryder *et al.* (1975b) b) Salpas *et al.* (1985, 1987). Clastic refers to plagioclases in comminuted zones.

were classified as unrecrystallized, granulitic, and poikiloblastic "ANT" breccias. Poikilitic fragments are rare to absent. The unrecrystallized fragments have porous fragmental matrices, and appear to be crushed anorthositic igneous rocks. The dominant part of the core of the Marble Cake clast is one such fragment. The granulitic fragments are characterized by triple point textures typical of recrystallization. Their compositions and textures are varied. Poikiloblastic fragments are distinguished by their small poikilitic pyroxenes enclosing smaller plagioclases, set in a mosaic of much coarser plagioclases; all are fine grained, with even the larger plagioclases rarely more than 200 microns. Salpas *et al.* (1986b, 1987a) described an anorthositic clast from the 1984 slabbing that they referred to as the first Apollo 17 ferroan anorthosite; however, there are other candidates for that honor (including the core of the Marble Cake clast, which is certainly closely related). The small fragment (less than 5 mm) is

monomict, consisting of about 95% anorthite (An_{95.1-97.1}) and 5% pyroxene (augite and pigeonite; Fig. 18). The pyroxene occurs as small (less than 100 micron) grains interstitial to larger plagioclases. Salpas *et al.* (1986b, 1987a) also described six feldspathic granulite clasts from the 1984 slabbing. Their characters are summarized in Table 4. In general they are composed of rounded to angular fragments of plagioclase and olivine in granoblastic or poikiloblastic matrices of plagioclase and pyroxene. The amount of olivine is rather small (<5%). The textures of the granulites suggest that most are brecciated assemblages which were subsequently recrystallized.

72275 also contains small amounts of other lithic clast types, ranging from olivine-normative mare basalt-like fragments, ultramafic particles, troctolitic basalts (probably impact melts), and granitic fragments (Table 1).

CHEMISTRY

A large number of chemical analyses have been made on 72275 matrix and its clastic components, ranging from fairly comprehensive analyses to analyses for one or two elements as part of geochronological studies. The chemical data are given in Tables 5a, b, c (light gray matrix and dark melt breccias), Tables 6a, b (KREEPy basalts), Table 7 (Clast # 1, Marble Cake, lithologies), and Table 8 (feldspathic breccia clasts). The data given by Jovanovic and Reed (several papers) includes some combined leach and residue data.

Light gray friable matrix and dark melt breccias:

The several analyses of bulk friable matrix show some variability at the scale of the rather small samples generally analyzed (less than 50 mg) (Tables 5a, b; Fig. 19). The chemistry differs from that of the dark melt breccias and from other boulder matrices at the Apollo 17 site in being less aluminous and more iron-rich. The chemistry is consistent with a mix of dark melt breccias, feldspathic breccias, and KREEPy basalts. The latter component is seen in the very high Ge content of the matrix (Morgan *et al.*, 1974, 1975), as high Ge is a distinctive character of the KREEPy basalts. The matrix analyses reported by Salpas *et al.* (1987b) are identical in all respects with the KREEPy basalts themselves and these samples must have very low contents of feldspathic granulites or melt breccias. Their abundances of incompatible elements (Fig. 19b) is higher than most other matrix samples and similar to those in the KREEPy basalts (Fig. 20). Of the dark melt breccias, only clast #2 (Table 5c) and the Marble Cake rind (below) were analyzed, apart from the defocused beam microprobe analyses (the defocused beam analysis of clast #2 agrees tolerably well with the atomic absorption analysis except for its higher normative feldspar). The

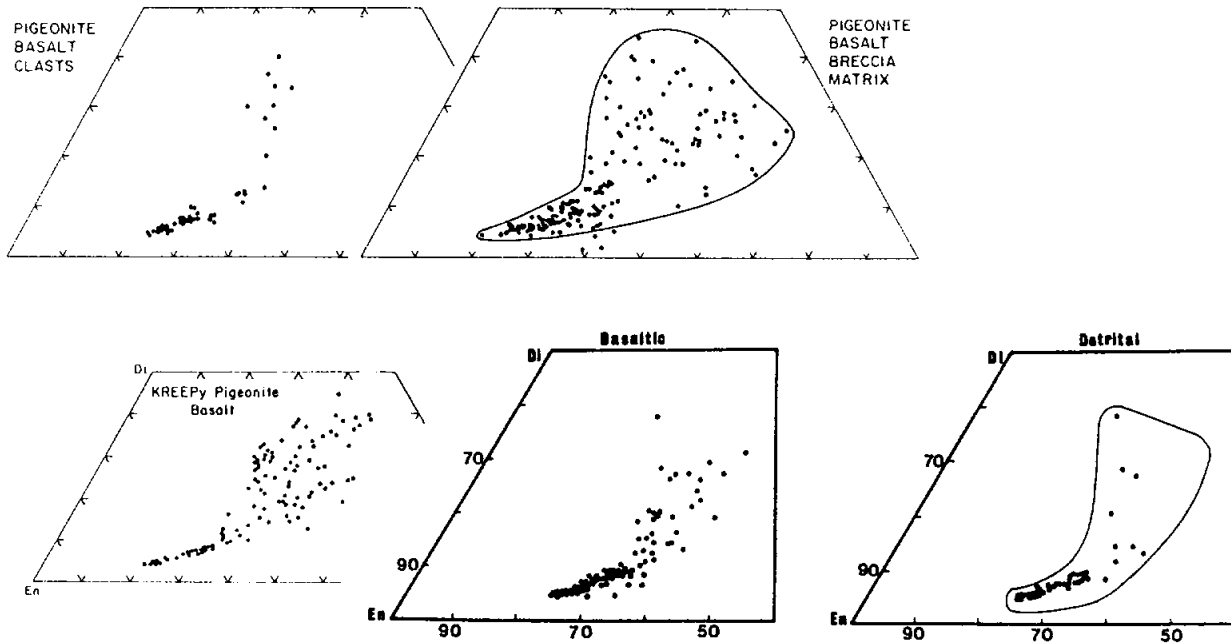


Figure 12: Compositions of pyroxenes in A 17 KREEPy basalts and breccias, plotted on quadrilaterals. a) Stoesser et al. (1974). b) Ryder et al. (1977). c) Salpas et al. (1987)

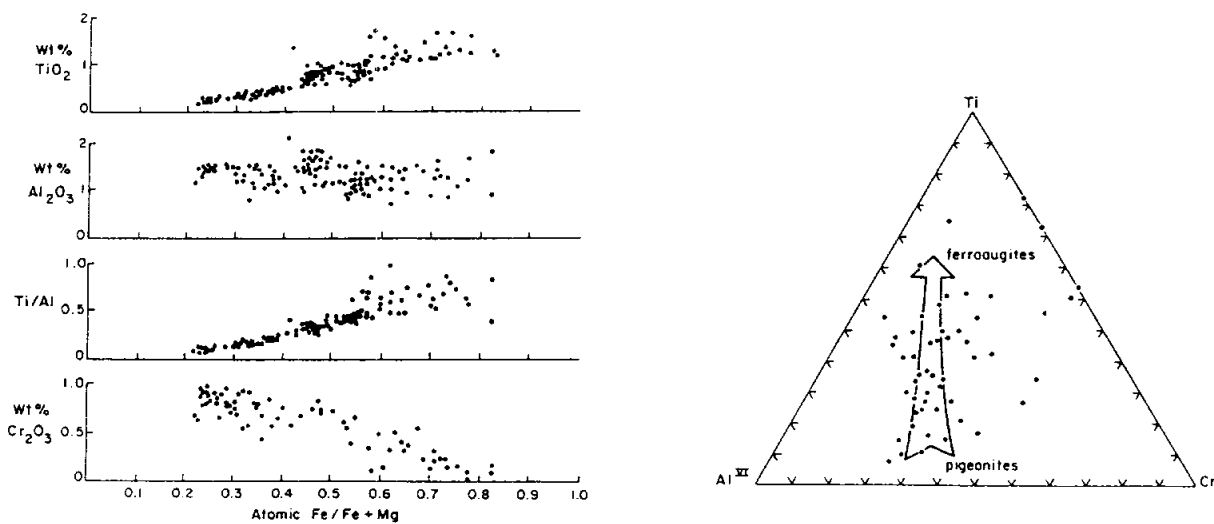


Figure 13: Abundances and ratios of minor elements in pyroxenes in A 17 KREEPy basalts. Arrow indicates direction of crystallization. Ryder et al. (1977).

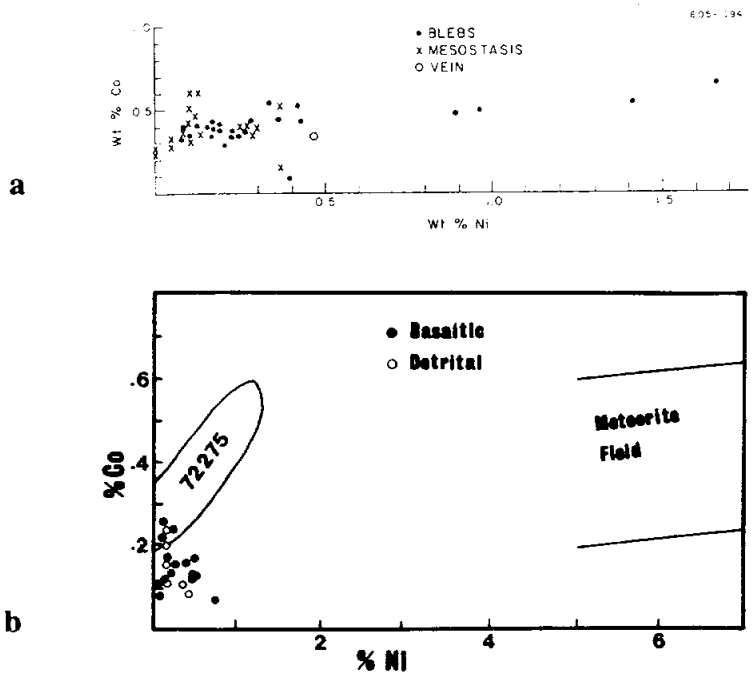


Figure 14: Compositions of metals in A 17 KREEPy basalts. a) Ryder et al. (1977). b) Salpas et al. (1987). In b) field labelled "72275" is taken from a) and the difference is stated by Salpas et al. (1987) to be an analytical problem in the Ryder et al. (1977) study.

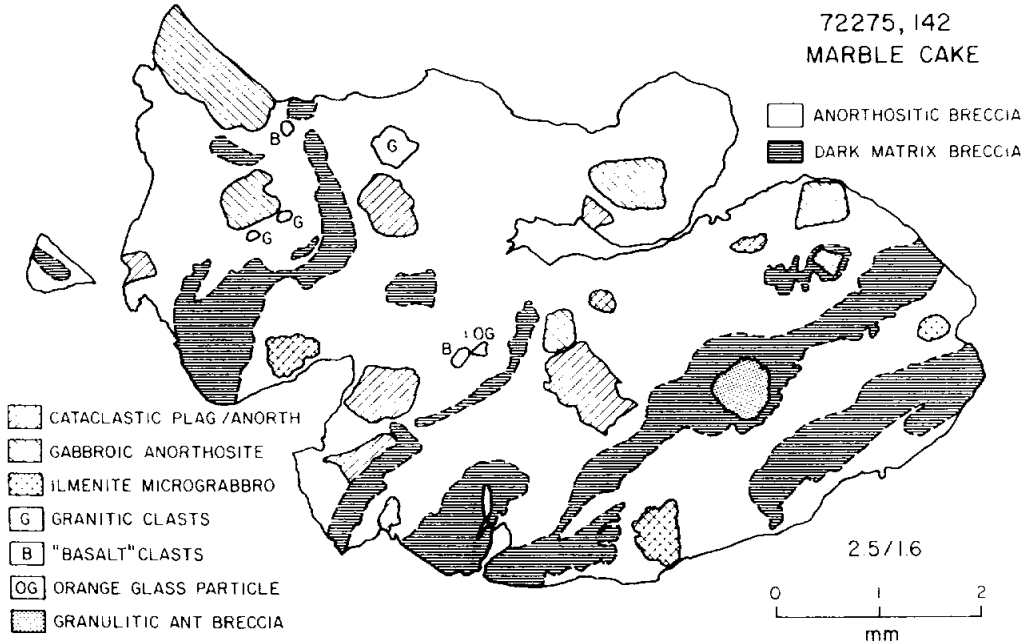


Figure 15: Sketch map of the interior of clast #1 (the Marble Cake clast). The white areas consist of a mixture of finely-crushed gabbroic anorthosite and ilmenite microgabbro. Uncrushed remnants large enough to map are indicated by clast type. Stoesser et al. (in CI 2, 1974) and Marvin et al. (1974).

Table 2: Defocused beam electron microprobe analyses of dark aphanitic melt breccias in 72275.
 Key: 5) 72275,128, average of 10 analyses of 2 clasts. 6) 72275,134, average of 21 analyses of clast. 7) 72275,12, average of 5 analyses of rind around anorthositic clast. 8) Clast #2, average of 15 analyses. 9) Dark melt material of clast #1 (the Marble Cake clast). (Stoeser *et al.*, in CI 1, 1974).

	5	6	7	8	9
	72275, 128 DMB matrix	72275, 134 DMB matrix	72275, 12 vesicular rim	72275, 146 clast #2 matrix	72275, 140 DMB
SiO ₂	49.7	47.7	43.9	47.0	46.6
TiO ₂	1.1	1.1	0.9	1.0	1.3
Cr ₂ O ₃	0.2	0.2	0.2	0.2	0.2
Al ₂ O ₃	18.8	20.3	22.9	22.8	19.6
FeO	10.0	10.6	8.7	8.9	11.0
MnO	0.1	0.2	0.1	0.1	0.2
MgO	9.0	10.0	12.1	8.7	8.2
CaO	11.4	11.5	11.6	12.9	11.4
Na ₂ O	0.5	0.5	0.7	0.6	0.6
K ₂ O	0.3	0.2	0.3	0.2	0.5
P ₂ O ₅	0.5	0.4	0.3	0.5	0.8
Total	101.6	102.7	101.7	102.9	100.4
Fo	0.0	3.4	16.5	4.5	1.6
Fa	0.0	2.7	8.8	3.3	1.5
En	22.0	19.5	6.1	14.8	18.2
Fs	16.3	13.9	3.0	9.9	15.5
Wo	2.1	0.7	0.0	0.8	1.1
Or	2.0	1.3	1.6	1.3	2.9
Ab	3.9	4.2	5.4	4.9	5.5
An	47.5	51.1	55.1	57.4	48.7
Ilm	2.1	2.0	1.6	1.8	2.5
Chr	0.3	0.3	0.3	0.3	0.3
Qtz	2.7	0.0	0.0	0.0	0.0
Cor	0.0	0.0	1.0	0.0	0.0
Ap	1.1	1.0	0.6	1.0	1.8

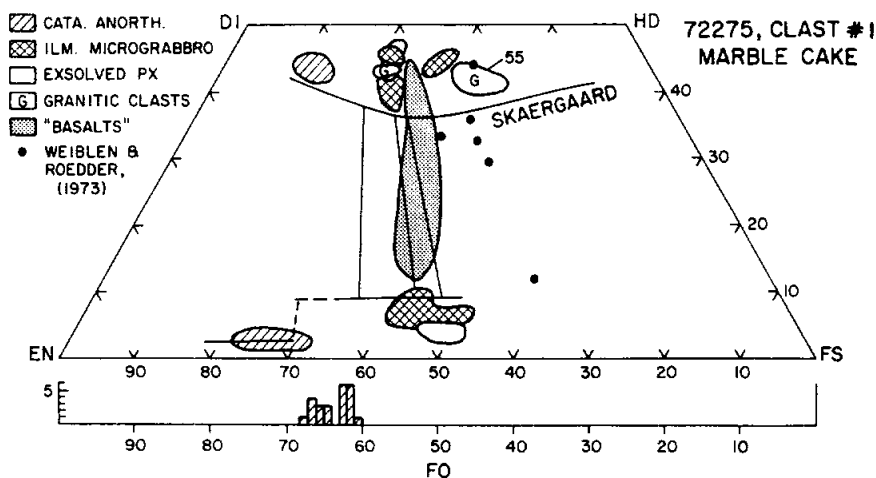


Figure 16: Compositions of pyroxenes and olivines in phases of the interior of clast #1 (the Marble Cake clast) and sodic ferrogabbros for comparison.

Table 3: Defocused beam electron microprobe analyses of four types of clast in the light-colored interior of clast #1 (the Marble Cake clast). (Stoeser *et al.*, in CI 2, 1974).

	1.	2.	3.	4.	5.	6.	
	790C10 anorth. gabbro	790C18 gabbroic anorth.	790C1 ilmenite microgab.	790C2 ilmenite microgab.	790C5 "basalt"	790C6 orange glass	
WT. % OXIDES							
SiO ₂	43.38	41.16	45.89	48.48	47.10	43.20	
TiO ₂	0.08	0.06	4.38	6.59	2.89	0.26	
Al ₂ O ₃	20.87	29.96	14.70	14.54	10.09	13.96	
Cr ₂ O ₃	0.06	0.03	0.05	0.05	0.11	0.05	
FeO	7.85	4.16	11.70	10.01	15.19	8.49	
MnO	0.13	0.04	0.17	0.14	0.19	0.05	
MgO	8.79	3.56	5.67	3.38	7.32	22.87	
CaO	12.70	16.01	12.16	9.42	13.08	8.96	
Na ₂ O	0.28	0.26	0.91	0.85	0.37	0.66	
K ₂ O	0.05	0.05	0.92	0.90	0.25	0.23	
BaO	0.04	0.04	0.11	0.11	0.09	0.04	
P ₂ O ₅	0.02	0.03	0.46	0.42	0.35	n.d.	
TOTAL	94.29	95.43	97.27	95.05	98.02	98.81	
CIPW NORM							
FO	6.1	5.3	---	---	---	38.5	
FA	4.4	4.9	---	---	---	11.3	
EN	14.5	1.8	14.5	8.9	18.7	2.7	
FS	9.6	1.5	14.6	7.7	20.6	0.7	
WO	3.3	---	10.3	4.8	16.1	4.2	
OR	0.3	0.3	5.6	5.6	1.5	1.4	
AB	2.5	2.3	7.9	7.6	3.2	5.6	
AN	58.9	83.1	34.3	35.0	25.8	34.9	
ILM	0.2	0.1	8.6	13.2	5.6	0.5	
CHR	0.1	---	0.1	0.1	0.2	0.1	
QTZ	---	---	2.7	15.8	5.3	---	
COR	---	0.4	---	---	---	---	
AP	0.1	0.1	1.1	1.0	0.8	---	
COMP. NORM MIN.							
OL:	FO	66.5	60.7	---	---	---	83.2
PX:	EN	58.9	60.7	42.0	47.0	39.0	39.2
	FS	29.7	39.3	32.2	31.1	32.1	7.9
	WO	11.4	---	25.8	21.8	28.9	52.9
PLAG:	OR	0.5	0.3	11.5	11.5	5.0	3.3
	AB	4.3	2.9	17.4	16.5	11.0	14.1
	AN	95.3	96.8	71.0	72.0	84.0	82.6
atomic Mg/(Mg+Fe)	0.666	0.604	0.463	0.375	0.462	0.827	
MgO/(MgO+FeO)	0.528	0.461	0.326	0.252	0.325	0.729	
No. of analyses	26	16	12	4	3	1	

clast # 2 analysis is similar to those for 72255 and 72215 dark melt breccias except for slightly higher abundances of incompatible elements (the Marble Cake rind has even higher abundances of incompatible elements). Blanchard *et al.* (1975) described clast #2 as intermediate in chemistry between the rind material and more typical dark melt breccias such as those in 72255.

The 72275 brecciated materials have obvious meteoritic contamination (Morgan *et al.*, 1974, 1975). Morgan *et al.* (1975) grouped the meteoritic materials in 72275 and 72255 as distinct from

those in the other Boulder 1 samples: Group 3H, and 3L for the 72215 and 72235 samples. All are distinct from most other Apollo 17 samples (Group 2). The distinctions are not a result of the high Ge in the KREEPy basalts. Jovanovic and Reed (e.g. 1975c) interpreted their data on some volatile elements as constraining the thermal history of Boulder 1: since consolidation it probably has not been subjected to temperatures greater than 450 degrees C, and vapor clouds from external sources permeated the source regions for the boulder materials.

A 17 KREEPy BASALTS:

Analyses of the KREEPy basalts sampled from the 1973 sawing (clast 5 and probably clast 4) are given in Table 6a, and numerous analyses of small clasts (mainly basaltic breccia) sampled from the 1984 sawing in Table 6b. Most of the latter are partial analyses. The rare earths are shown in Fig. 20. The KREEPy basalt is quartz-normative, with an evolved Mg' similar to some mare basalts, but with elevated rare earths compared with mare basalts. The sample lacks meteoritic contamination (Morgan *et al.*, 1974, 1975). The rare earth elements are KREEP-like, but the heavy rare earths have a slightly steeper slope than other KREEP basalts. These basalts cannot be related to other known KREEP basalts by fractional crystallization or partial melting of common sources. They are quite distinct from the only other volcanic KREEP samples known, the Apollo 15 KREEP basalts (Ryder *et al.*, 1977; Irving, 1975). Ryder *et al.* (1977) discussed the chemistry as being intermediate between mare and KREEP basalts. Salpas *et al.* (1987b) found that the breccias and the actual basalt clasts were indistinguishable in composition. They interpreted their analyses to represent fragments of a single flow or of a series of related flows, with a fairly consistent trend on an Ol-Si-An diagram for the 9 samples that they analyzed more completely (Fig. 21). However, this diagram may be misleading: Some of the variation that they found undoubtedly results from unrepresentative sampling, and the SiO₂ abundances are obtained by difference, not analysis. The trend on the diagram is not that of pyroxene or pyroxene+plagioclase (as the petrography would indicate), but of olivine control; it may be an artifact.

The very high Ge content of the KREEPy basalt is distinctive, and is accompanied by lesser enrichments in Sb and Se (Morgan *et al.*, 1974, 1975).

Clast #1 (Marble Cake clast):

Analyses of both white and dark portions of the Marble Cake clast are given in Table 7, with the rare earth elements shown in Fig. 22. Both phases are polymict, although the white material is dominantly a cataclastic troctolitic anorthosite/feldspathic granulite, and the dark material is dominantly an aphanitic melt breccia. The analysis of the white material probably includes some dark melt component (Blanchard *et al.*, 1975) and presumably ilmenite microgabbros and other lithologies. The rare earth element abundances are higher than expected for anorthositic or granulitic rocks. The dark rim material contains much higher incompatible element abundances than most other dark melts in the boulder; this includes Rb, U, and Th as well as the rare earths. These abundances are higher than their counterparts in the KREEPy basalts and are more similar to the levels in A14 or A15 KREEP. The rim and the core are absolutely distinct in composition; the rim is not melted core, but appears to be plastered on in flight,

as suggested by Stoesser *et al.* (1974a). The rim material contains meteoritic contamination, but no analysis for meteoritic siderophiles was made for the core. The rim siderophiles have ratios corresponding with group 3 siderophiles that characterize other boulder matrix samples.

Feldspathic breccias:

Salpas *et al.* (1987a) provided analyses of an anorthositic clast and six feldspathic granulites obtained from the 1984 sawing (Table 8; Fig. 23). The anorthosite (,350) is similar to other ferroan anorthosites except that its rare earth elements and transition metals are slightly higher than typical; however, the sample mass was only 17 mg. The clast has a positive Eu anomaly and on the basis of the low upper limits on the Ni and Ir abundances, the sample would appear to be uncontaminated with meteoritic material.

The six granulites show a range in alumina from 22.1 to 27.2%, with corresponding variations in Fe, Mg, Sc, and other transition metals. They appear to represent distinct

sources, because they show a range in Mg' consistent with their mineralogy. All are intermediate in major element compositions between ferroan anorthosites and Mg-suite troctolites. Their rare earth element abundances are similar, with fairly flat patterns and mainly small Eu anomalies. All show elevated Ni, Au, and Ir abundances indicative of substantial meteoritic contamination; these elements show abundances higher than in A 16 feldspathic granulites.

STABLE ISOTOPES

Oxygen isotope ratios were measured by Clayton and Mayeda (1975a,b) and Mayeda *et al.* (1975) for a friable matrix sample, both bulk and mineral separates, and for mineral separates from a KREEPy basalt fragment. The bulk breccia, for which $\delta^{18}\text{O}$ (5.80) and $\delta^{17}\text{O}$ (2.94) were measured, falls on the earth-Moon mass fractionation line (Clayton and Mayeda, 1975a,b). A second split of the matrix gave $\delta^{18}\text{O}$ of

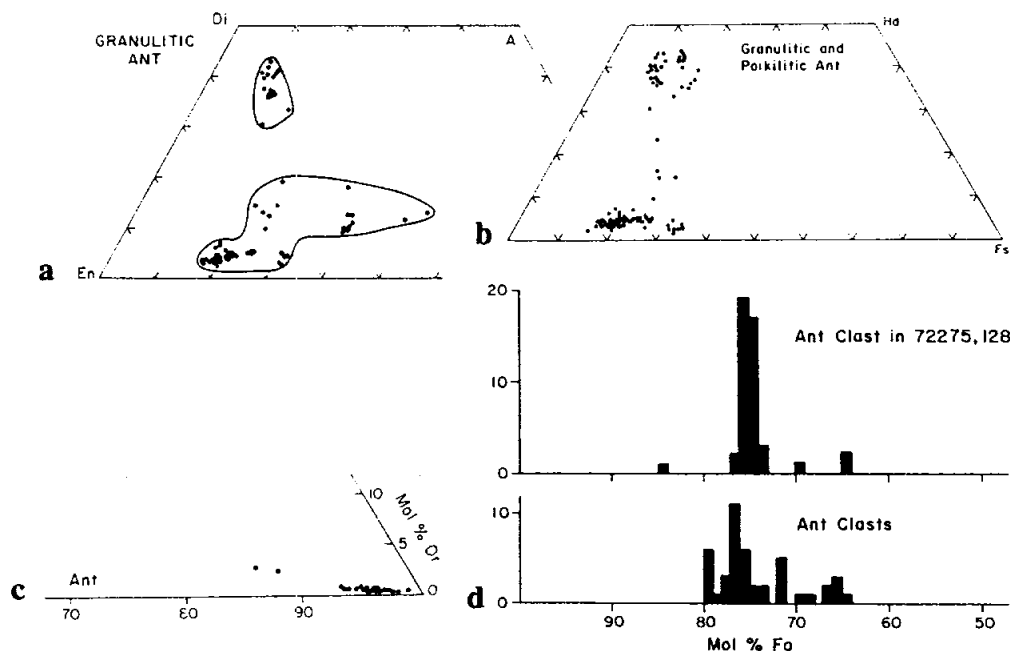


Figure 17: Compositions of silicate mineral phases in feldspathic (mainly feldspathic granulite) breccia clasts in 72275 (and including data for some similar clasts in 72255). a) pyroxenes, Stoesser *et al.* (1974a). b) pyroxenes, Ryder *et al.* (1975b). c) plagioclases, Ryder *et al.* (1975b). d) olivines, Ryder *et al.* (1975b).

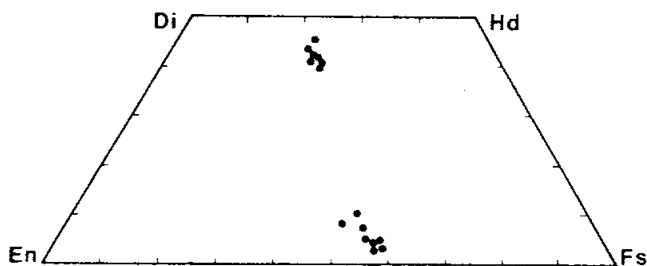


Figure 18: Compositions of pyroxenes in a cataclastic ferroan anorthosite clast (thin section 72275,9018). Salpas *et al.* (1987a).

5.40, with plagioclase at 5.61 and pyroxene at 5.20. The basalt separates gave plagioclase 5.69 and pyroxene 5.35 (Mayeda *et al.*, 1975). The matrix values are at the low end of highlands rocks.

RADIOGENIC ISOTOPES AND GEOCHRONOLOGY

Light gray friable matrix: Compston *et al.* (1975) analyzed a 16.2 mg sample of matrix for Rb and Sr isotopes (Table 9). The data, which are plotted but not specifically discussed by Compston *et al.* (1975), fall on the mixing line

between "gabbroic anorthosites" and microgranites discussed in the section on 72255. These data are fairly similar to those of the KREEPy basalt, which is probably a component of the sample analyzed. Nyquist *et al.* (1974a,b) also analyzed a bulk matrix sample for Rb and Sr isotopes (Table 9), with results similar to those of Compston *et al.* (1975). The Nyquist *et al.* (1975a,b) data correspond to TBABI and TLUNI model ages of 4.13 and 4.15 Ga respectively (original calculation of 4.22 and 4.24 Ga \pm 0.05 using the old decay constant).

Leich *et al.* (1975a, b) attempted to date a friable matrix sample using ^{40}Ar - ^{39}Ar methods. The release diagram (Fig. 24) for this sample (,57) shows an incipient apparent-age plateau that is cut short by a drop-off in the 1000 degree C fractions. The release is broadly similar to that of clast #5 KREEPy basalt (also on Fig. 24). As ,57 is from matrix adjacent to KREEPy basalt clast #4, this matrix sample may be reflecting the pattern for the KREEP basalt. The friable matrix has many components, so a simple, one age release cannot particularly be expected. Leich *et al.* (1975a, b) interpret the pattern as resulting from truncation of the plateau to two temperature steps from outgassing of Fe- or Ti-rich (or both) phases, and state that the data are not adequate for chronological interpretation.

Nunes *et al.* (1974), Nunes and Tatsumoto (1975a), and Tatsumoto *et al.* (1974) reported U,Th-Pb isotopic data and age parameters for 72275 samples, including the friable matrix (72275,73; Table 10). The Pb data plots within error of concordia at about 4.25 Ga (see

Table 4: Petrographic features of 6 feldspathic granulite clasts in 72275 (Salpas *et al.*, 1987a).

INAA/PM:	439/495	355/502	351/9019	397/9021	433/493	none/480
Texture	c-g	g-c	c-g	g-c	c	g-c
Plagioclase						
Mode	46%	66%	59%	57%	76%	52%
Size	< 10-350 μm	< 10-400 μm	< 10-650 μm	< 10-500 μm	< 10-340 μm	< 10-500 μm
An	95.9-97.1	94.1-95.3	95.8-96.4	95.4-96.3	94.8-95.8	95.2-97.3
Pyroxene						
Mode	50%	31%	35%	40%	20%	44%
Size	< 10 μm na					
Olivine						
Mode	1%	3%	5%	1%	2%	2%
Size	40-175 μm	50-150 μm	80-450 μm	100-150 μm	30-45 μm	45-500 μm
Fo	80-82	71-77	63-64	76-77	75-76	75-77
Fe metal						
Mode	3%	< 1%	1%	1%	2%	2%
Size	< 10 μm na	< 10-20 μm see text				

c = cataclastic; g = granulitic; na = not analyzed. Analyzed compositions are for mineral fragments and do not include groundmass minerals that were generally too small for accurate analysis.

Table 5a: Chemical analyses of friable matrix samples from 72275.

	,57	,57	,101	,57	,57	,52	,73	,73	,110	,66	
Split wt %							1	2			Split wt %
SiO ₂	48.6	48	46.2								SiO ₂
TiO ₂	1.2	0.8	0.94								TiO ₂
Al ₂ O ₃	14.7	17.9	18.4								Al ₂ O ₃
Cr ₂ O ₃	0.444	0.25	0.383								Cr ₂ O ₃
FeO	(a)13.8	9.9	(b)11.9								FeO
MnO	0.226	0.12	0.182								MnO
MgO	9.52	11.0	9.9								MgO
CaO	11.0	11.0	11.7		11.8						CaO
Na ₂ O	0.480	0.40	0.49								Na ₂ O
K ₂ O	0.276	0.22	0.265		0.30						K ₂ O
P ₂ O ₅											P ₂ O ₅
ppm											ppm
Sc	44.7	39	30.6								Sc
V											V
Co	30.4	27	226								Co
Ni	75		950	97							Ni
Rb				5.9		8.2					Rb
Sr					112	115.3					Sr
Y											Y
Zr					667						Zr
Nb											Nb
Hf	16.5	14.0	14.1								Hf
Ba					346						Ba
Th	6.1		5.6				5.962	6.285			Th
U				1.500	1.52		1.561	1.672	1.6		U
Cs				0.255							Cs
Ta							3.096	3.451			Ta
Pb											Pb
La	50.5	47	38								La
Ce	130	150	104								Ce
Pr											Pr
Nd											Nd
Sm	24.6	24.5	19.1								Sm
Bu	1.57	1.67	1.46								Bu
Gd											Gd
Tb	3.9	6.1	3.4								Tb
Dy											Dy
Ho											Ho
Er											Er
Tm											Tm
Yb	15.0	15.1	13.3								Yb
Lu	2.01	2.21	1.74								Lu
Li									12		Li
Be											Be
B											B
C											C
N											N
S											S
F									117		F
Cl									29.6		Cl
Br				0.048					0.124		Br
Cu											Cu
Zn				2.7							Zn
ppb											ppb
Au				0.82							Au
Ir				2.26							Ir
I									3.3		I
At											At
Ga											Ga
Ge				406							Ge
As											As
Se				34							Se
Mo											Mo
Tc											Tc
Ru										≤3	Ru
Rh											Rh
Pd											Pd
Ag				0.74							Ag
Cd				13							Cd
In											In
Sn											Sn
Sb				1.17							Sb
Te				4.14							Te
W											W
Re				0.225							Re
Os										1.5	Os
Pt											Pt
Hg											Hg
Tl				0.71							Tl
Bi				0.11							Bi

(1) (1) (1) (2) (3) (4) (5) (5) (6) (6)

References and methods:

- (1) Blanchard et al (1975); AAS; INAA Cl(1) Cl(2)
 - (2) Morgan et al (1974, 1975); RNAA Cl(1) Cl(2)
 - (3) Leich et al (1975); Irradiation/MS (K, Ca) others, ID/MS C(2)
 - (4) Compston et al (1975); ID/MS
 - (5) Nunes et al (1974) Tatsumoto et al, (1974) Cl(1); ID/MS Tab et al (1974).
 - (6) Jovanovic & Reed (1974, a, b 1975) Cl(2); RNAA
- (a) AAS; INAA = 14.2%
 (b) AAS; INAA = 11.8%
 (c) from Wiesmann and Hubbard et al, (1974) gives 0.288%

Table 5a: Continued.

	,90	,2	,2	,71	,2	,108
Split						
wt %						
SiO ₂	47.31			47.54		48.5
TiO ₂	0.94			0.91		0.95
Al ₂ O ₃	16.90			17.01		17.2
Cr ₂ O ₃	0.34	0.343		0.36		0.39
FeO	12.45			11.58		11.4
MnO	0.19			0.18		
MgO	9.47			9.35		8.94
CaO	11.72			11.71		11.6
Na ₂ O	0.35	0.36		0.38		0.40
K ₂ O	0.22	(c)0.276		0.28		0.25
P ₂ O ₅	0.38			0.35		
ppm						
Sc	40					48
V	75					115
Co	37					33
Ni	127			67		120
Rb	4.6	8.97		8.7		6.1
Sr	135	122.7		121		
Y	88			129		160
Zr	545	605		613		485
Nb	24			32		31
Hf		14.6				13.3
Ba	330	350				440
Th		5.29				6.70
U		1.56				1.70
Cs						0.31
Ta						
Pb	<2					4.0
La	35	41.0				42.9
Ce		106				114
Pr						17
Nd		67.4				73
Sm		18.8				21.3
Ba		1.49				1.57
Gd		23.4				24.4
Tb						3.86
Dy		23.2				24.4
Ho						5.85
Er		13.7				15.8
Tm						2.1
Yb	9.2	11.6				13.9
Lu		1.71				2.1
Li	13	13.8				
Be	3.8					
B						
C				23		
N				45		
S			800	860	890	
F						
Cl						
Br						
Cu	5.4					5
Zn	<4		3			
ppb						
Au						
Ir						
I						
At						
Ga	3200					
Ge						
As						
Se						
Mo						
Tc						
Ru						
Rh						
Pd						
Ag						
Cd						
In						
Sn						
Sb						
Te						
W						
Re						
Os						
Pt						
Hg						
Tl						
Bi						

(7) (8) (9) (10) (11) (12)

References and methods:

- (7) Rose *et al* (1974); XRF, OE; etc.
 (8) Hubbard *et al* (1974); Wiesmann & Hubbard (1975); AAS, ID/MS. Nyquist *et al* (1974) a,b.
 (9) LSPET (1973 a,b); XRF
 (10) Moore *et al* (1974, a, b), Moore & Lewis (1976); combustion
 (11) Gibson and Moore (1974 a, b)
 (12) Taylor *et al* (1974); SSMS/microprobe.

Table 5b: Chemical analyses of friable matrix samples from 72275.
All data by neutron activation. Salpas *et al.* (1987b).

	413	417	423
<i>Major Elements (wt %)</i>			
FeO	14.50	15.05	15.16
CaO	10.1	10.3	12.1
Na ₂ O	0.42	0.38	0.37
<i>Trace Elements (ppm)</i>			
Sc	45.7	48.6	49.8
V [‡]	na	na	na
Cr	3062	3088	3255
Mn [‡]	na	na	na
Co	31.3	33.3	35.3
Ni	12	55	<110
Rb	13	12	14
Sr	138	93	<160
Cs	0.37	0.40	0.44
Ba	370	400	400
La	47.9	50.2	52.3
Ce	129	133	139
Nd	80	81	85
Sm	22.2	23.5	25.5
Eu	1.62	1.66	1.68
Tb	4.59	4.97	5.10
Yb	13.5	13.9	13.1
Lu	1.73	1.80	1.90
Zr	600	765	700
Hf	16.4	17.2	17.9
Ta	1.55	1.66	1.58
Th	5.52	5.46	6.01
U	1.30	1.58	1.26
Ir [†]	nd	nd	nd
Au(ppb)	<5	<7	<6
weight (mg)	105.10	123.88	23.59

*SiO₂ by difference.

†nd = not detected (Ir detection limit = 2 ppb).

‡na = not analyzed.

section on 72215, Fig. 10). The high U and Th abundances in 72275,73 suggest that it contains a high proportion of A 17 KREEPy basalt.

A 17 KREEPy basalts:

Compston *et al.* (1975 and in CI 2, 1974) reported Rb-Sr isotopic data for separates of a KREEPy basalt sample, 72275,171, described as a basalt of medium grain size. It was probably a subsample of clast #4; it certainly was not clast #5. The data conform to an internal isochron age of 3.93 +/- 0.04 Ga with an initial ⁸⁷Sr/⁸⁶Sr of 0.69957 +/-14 (Table 11a; Fig. 25a). All the splits fit the isochron within analytical uncertainty. Compston *et al.* (1975) interpret the age to be that of original lava crystallization, before incorporation into the breccia.

Rb-Sr isotopic data for separates of a split ,543 of the KREEPy basalt were reported by Shih *et al.* (1992) (Table 11b). The data yield an isochron age of 4.09 ± 0.08 Ga (new Rb decay constants) and initial ⁸⁷Sr/⁸⁶Sr of 0.69960 ± 0.00012 (Fig. 25b). A subset of whole-rock and 3 separates yields a good linear relationship corresponding with 4.06 ± 0.01 Ga. The age is older than and resolved from that calculated from the data of Compston *et al.* (1975). The initial isotopic ratios agree within uncertainty. Shih *et al.* (1992) infer separate but similar volcanic events. The data scatter around the best fit line and suggest some disturbance. The model age (TLuni) for ,543 is similar to that of other KREEP materials at about 4.3 Ga.

Shih *et al.* (1992) also reported Sm-Nd isotopic data for separates of split ,543. (Table 11c). The data correspond with an age of 4.08 ± 0.07 Ga (Fig. 25c), with all points fitting within uncertainty of the Rb-Sr age (whichever Rb decay constant is used, and whether the whole Sr data set or the subset is used). Shih *et al.* (1992) prefer the old Rb decay constant and suggest that the basalt is 4.08 Ga old, and significantly older than Apollo 15 KREEP basalts. The initial (Epsilon) Nd value relative to CHUR is slightly negative at -0.61 ± 0.23, suggesting derivation from a non-chondritic, low Sm/Nd (light rare earth enriched) source.

Leich *et al.* (1975) provided ⁴⁰Ar-³⁹Ar data for 72275,91, a subsample of the clast #5 KREEPy basalt (Fig. 24). They found the data inadequate for chronological interpretation, mainly because of the drop-off at 1000 degrees C, similar to the friable matrix sample. The highest ages indicated correspond roughly with the Rb-Sr isochron age.

Nunes and Tatsumoto (1975) provided U,Th-Pb isotopic data and age parameters for 72275,170, the same clast analyzed by Compston *et al.* (1975) (Table 12). The data lie within analytical uncertainty of an approximately 3.9 - 4.4 Ga discordia line; varied calculated single-stage ages are in the 4.05 - 4.10 Ga range. However, if the crystallization age is 3.93 Ga (Rb-Sr), then the older ²⁰⁷Pb/²⁰⁶Pb age (4.1 Ga) must result from addition of Pb to the sample. This is presumably from the boulder matrix.

Dark impact melt breccias:

Leich *et al.* (1975a) provided ⁴⁰Ar-³⁹Ar data for the dark melt breccia clast #2, split 72275,83 (Fig. 26a). The drop-off of the intermediate plateau precludes an age determination, although an age of about 3.9 +/- 0.1 Ga is surely suggested by the data.

Table 5c: Chemical analyses of dark melt breccia (clast #2) in 72275.

	,83	,83	,83	,161
Split				
wt %				
SiO ₂	46			
TiO ₂	0.8			
Al ₂ O ₃	19.7			
Cr ₂ O ₃	0.24			
FeO	9.9			
MnO	0.111			
MgO	10.4			
CaO	12.0		11.9	
Na ₂ O	0.30			
K ₂ O	0.25		0.28	
P ₂ O ₅				0.6
ppm				
Sc	28			
V				
Co	30			
Ni		147		
Rb		5.4		
Sr				
Y				
Zr				
Nb				
Hf	13.7			
Ba				
Th				
U		1.840		2.7
Ca		0.255		
Ta				
Pb				
La	41			
Ce	112			
Pr				
Nd				
Sm	18.7			
Eu	1.50			
Gd				
Tb	3.8			
Dy				
Ho				
Er				
Tm				
Yb	12.1			
Lu	1.82			
Li				8
Be				
B				
C				
N				
S				
F				77
Cl				28.9
Br		0.095		0.395
Cu				
Zn		2.4		
ppb				
Au		1.30		
Ir		3.44		
I				1.5
At				
Ga				
Ge		178		
As				
Se		52		
Mo				
Tc				
Ru				6.8
Rh				
Pd				
Ag		0.56		
Cd		26		
In				
Sn				
Sb		1.06		
Te		2.74		
W				
Re		0.334		
Os				10
Pt				
Hg				
Tl		0.62		
Bi		0.12		
	(1)	(2)	(3)	(4)

References and methods:

- (1) Blanchard *et al.* (1975); AAS, INAA C(1) C(2)
(2) Morgan *et al.* (1974, 1975); RNAA Cl(1) Cl(2)
(3) Leich *et al.* (1975); Irradiation/MS Cl(2)
(4) Jovanovic & Reed (1975 a,b,c,d); RNAA Cl(2)

Table 6a: Chemical analyses of A 17 KREEPy basalts made from 1973 slab allocations, plus ,543

	,91	,91	,91	,171 (1)	,171 (2)	,170	,543	
Split wt %								Split wt %
SiO ₂	48							SiO ₂
TiO ₂	1.4							TiO ₂
Al ₂ O ₃	13.5							Al ₂ O ₃
Cr ₂ O ₃	0.46							Cr ₂ O ₃
FeO	15							FeO
MnO	0.156							MnO
MgO	10.0							MgO
CaO	10.5		11.6					CaO
Na ₂ O	0.29							Na ₂ O
K ₂ O	0.25		0.29					K ₂ O
P ₂ O ₅								P ₂ O ₅
ppm								ppm
Sc	61							Sc
V								V
Co	37							Co
Ni		43						Ni
Rb		8.0		6.34	7.53		7.23	Rb
Sr			92	81.1	91.8		89.20	Sr
Y								Y
Zr			625					Zr
Nb								Nb
Hf	18							Hf
Ba			355					Ba
Th						6.255		Th
U		1.500	1.53			1.635		U
Ca		0.355						Ca
Ta								Ta
Pb						3.049		Pb
La	48							La
Ce	131							Ce
Pr								Pr
Nd						65.15		Nd
Sm	23					18.13		Sm
Eu	1.58							Eu
Gd								Gd
Tb	4.5							Tb
Dy								Dy
Ho								Ho
Er								Er
Tm								Tm
Yb	11.9							Yb
Lu	1.75							Lu
Li								Li
Be								Be
B								B
C								C
N								N
S								S
F								F
Cl								Cl
Br		0.044						Br
Cu								Cu
Zn		2.7						Zn
ppb								ppb
Au		0.045						Au
Ir		0.023						Ir
I								I
At								At
Ga								Ga
Ge		1290						Ge
As								As
Se		230						Se
Mo								Mo
Tc								Tc
Ru								Ru
Rh								Rh
Pd								Pd
Ag		0.58						Ag
Cd		8.3						Cd
In								In
Sa								Sa
Sb		2.87						Sb
Te		7.8						Te
W								W
Re		0.0066						Re
Os								Os
Pt								Pt
Hg								Hg
Tl		0.58						Tl
Bi		0.14						Bi

References and methods:

- (1) Blanchard *et al.* (1975); AAS; INAA Cl(1) Cl(2)
- (2) Morgan *et al.* (1974, 1975); RNAA Cl(1) Cl(2)
- (3) Leich *et al.* (1975); Irradiation/MS (K, Ca) other: IDVMS
- (4) Compton *et al.* (1975); IDVMS Cl(2)
- (5) Nunes & Tatemoto (1975); IDVMS
- (6) Shih *et al.* (1992)

Notes:

- ,91 is clast #5
- ,170 and ,171 are probably clast #4.

Table 7: Chemistry of components of clast #1 (Marble Cake clast) of 72275.

	White (An Bx)			Dark (BC Bx)						
	.76	.117	.76	.80	.166(.62) ^a	.81	.80	.80		.168(.62)
Split wt %										Split wt %
SiO ₂	47			47	47					SiO ₂
TiO ₂	1.8			1.8	1.1					TiO ₂
Al ₂ O ₃	23.5			17.9	18.2					Al ₂ O ₃
Cr ₂ O ₃	0.20			0.46	0.27					Cr ₂ O ₃
FeO	7.4			10.3	(b)10.9					FeO
MnO	0.077			0.104	0.167					MnO
MgO	5.24			9.43	9.14					MgO
CaO	14.2		14.6	11.7	11.2		8.5			CaO
Na ₂ O	0.36			0.39	0.63					Na ₂ O
K ₂ O	0.32		0.40	0.47	0.49		0.41			K ₂ O
P ₂ O ₅										P ₂ O ₅
ppm										ppm
Sc	25			34	26.3					Sc
V										V
Co	18.7			28	22.5					Co
Ni					130			122	121	Ni
Rb								11.3	13.0	Rb
Sr			171				151			Sr
Y										Y
Zr			479				908			Zr
Nb										Nb
Hf	14			19.8	25.1					Hf
Ba			361				683			Ba
Th					12.8	13.21				Th
U		0.670	1.60			3.500	3.19	3.100	3.280	U
Cs								0.47	0.50	Cs
Ta					3.5					Ta
Pb		1.410				7.878				Pb
La	48			78	78					La
Ce	131			213	206					Ce
Pr										Pr
Nd										Nd
Sm	22.5			36	36					Sm
Eu	1.81			2.14	2.10					Eu
Gd										Gd
Tb	4.7			7.7	7.7					Tb
Dy										Dy
Ho										Ho
Er										Er
Tm										Tm
Yb	13.9			24	25.4					Yb
Lu	2.04			3.5	3.5					Lu
Li										Li
Be										Be
B										B
C										C
N										N
S										S
F										F
Cl								0.290	0.283	Cl
Br										Br
Cu								2.8	11.7	Cu
Zn										Zn
ppb										ppb
Au								1.16	1.84	Au
Ir								2.54	3.91	Ir
I										I
At										At
Ga										Ga
Ge								137		Ge
As										As
Se								63	72	Se
Mo										Mo
Tc										Tc
Ru										Ru
Rh										Rh
Pd										Pd
Ag								0.93	1.46	Ag
Cd								15	13.9	Cd
In										In
Sn										Sn
Sb								0.94	1.42	Sb
Te								3.46	1.9	Te
W										W
Re								0.233	0.330	Re
Os										Os
Pt										Pt
Hg										Hg
Tl								0.71	1.40	Tl
Bi								0.14	0.59	Bi

References and methods:

- (1) Blanchard et al (1975); AAS, INAA Cl(1) Cl(2)
- (2) Nunes et al (1974); Tatsumoto et al (1974); ID/MS Cl(1)
- (3) Leich et al (1975); Irradiation, MS (K,Ca) and MS/ID (others) Cl(2)
- (4) Morgan et al (1974, 1975); RNAA and Higuchi and Moyen (1975)

Notes:

- (a) Dark separate from interior white.
- (b) AAS; INAA = 10.8%

Cl(1) Cl(2)

Table 8: Partial analyses of six feldspathic granulites and one anorthosite (FAN) from 72275, obtained by neutron activation. Salpas *et al.* (1987a).

	Granulites						FAN
	351A	351B	355A	397	433	439	350
	<i>Major Elements (wt %)</i>						
TiO ₂	0.31	0.32	0.29	0.22	0.15	0.32	na
Al ₂ O ₃	22.1	23.1	27.2	26.2	24.6	26.3	na
FeO	8.87	7.83	4.85	5.71	5.10	4.95	0.485
MgO	11.5	9.9	7.6	7.9	8.0	9.7	na
CaO	11.9	12.6	14.8	14.8	14.2	14.5	19.2
Na ₂ O	0.307	0.316	0.349	0.353	0.362	0.350	0.456
	<i>Trace Elements (ppm)</i>						
Sc	14.97	12.92	8.13	7.81	8.24	7.12	1.12
V	69	65	19	20	24	25	na
Cr	2414	1646	810	842	881	846	46.6
Mn	934	792	489	499	481	462	na
Co	35.1	34.1	27.0	39.3	30.6	52.0	0.440
Ni	250	290	340	455	422	540	< 7
Sr	124	129	157	160	160	163	205
Cs	0.124	0.118	0.164	0.19	0.23	0.10	0.016
Ba	58	55	70	72	87	62	40
La	4.86	3.56	4.04	3.66	4.72	3.76	0.567
Ce	10.9	8.62	9.87	10.1	12.6	10.5	1.48
Nd	7.0	5.5	5.6	5.7	6.2	5.0	< 2.5
Sm	2.04	1.60	1.82	1.56	1.93	1.67	0.228
Eu	0.698	0.713	0.864	0.835	0.860	0.870	0.928
Tb	0.473	0.410	0.456	0.375	0.49	0.381	0.045
Yb	2.05	1.66	1.67	1.69	2.06	1.55	0.125
Lu	0.302	0.242	0.251	0.238	0.292	0.230	0.020
Hf	1.67	1.24	1.46	1.46	1.98	1.22	0.133
Ta	0.266	0.199	0.233	0.302	0.309	0.190	0.015
Th	1.81	1.38	1.18	1.17	2.06	1.02	0.047
U	0.39	0.27	0.30	0.34	0.37	0.19	0.020
Ir (ppb)	9.6	11.3	13.0	16.4	14.0	22.2	nd
Au (ppb)	3.4	3.6	5.0	6.8	6.5	4.3	< 0.8

na = not analyzed.

nd = not detected (Ir detection limit = 2 ppb).

Table 9: Rb-Sr isotopic data for 72275 friable matrix samples.

Sample	Mass mg	Rb ppm	Sr ppm	⁸⁷ Rb/ ⁸⁷ Sr	⁸⁷ Sr/ ⁸⁷ Sr+/-s.e.
a) ,52	16.2	8.20	115.3	0.2053	0.71139 3
b) ,2	52.8	8.97	122.7	0.2115	0.71188 3

a) Compston *et al.* (1975) b) Nyquist *et al.* (1974a,b).

Table 10: U,Th-Pb data and age parameters for 72275 friable matrix and clast #1 (Marble Cake) samples. Nunes *et al.* (1974).

Sample	Weight (mg)	Concentrations (ppm)				
		U	Th	Pb	²³² Th/ ²³⁸ U	²³⁸ U/ ²⁰⁴ Pb
Boulder 1, Station 2						
72275.73 matrix	131.8	1.561	5.962	3.096	3.95	4,284
	150.0	1.672	6.285	3.451	3.89	4,712
72275.81 clast # 1 black rind	31.7	3.500	13.21	7.878	3.90	2,493
72275.117 clast # 1 white interior	50.7	0.670	—	1.410	—	2,445

Sample	Weight (mg)	Run	Observed ratios†			Corrected for analytical blank‡				
			$\frac{^{206}\text{Pb}}{^{204}\text{Pb}}$	$\frac{^{207}\text{Pb}}{^{204}\text{Pb}}$	$\frac{^{208}\text{Pb}}{^{204}\text{Pb}}$	$\frac{^{206}\text{Pb}}{^{204}\text{Pb}}$	$\frac{^{207}\text{Pb}}{^{204}\text{Pb}}$	$\frac{^{208}\text{Pb}}{^{204}\text{Pb}}$	$\frac{^{207}\text{Pb}}{^{206}\text{Pb}}$	$\frac{^{208}\text{Pb}}{^{206}\text{Pb}}$
Boulder 1, Station 2										
72275.73 matrix	162.0	P	1.097	537.1	1.090	1.225	599.3	1.218	0.4893	0.9945
	131.8	C1*	2.715	1,308	—	3.961	1,905	—	0.4811	—
		C2*	3.220	1,545	—	4.556	2,183	—	0.4792	—
72275.81 clast # 1 black rind	53.3	P	1,578	959.2	1,532	1,937	1,176	1,880	0.6072	0.9705
	31.7	C*	1,688	1,000	—	2,521	1,492	—	0.5918	—
72275.117 clast # 1 white interior	83.3	P	902.2	520.8	860.4	1,423	818.2	1,347	0.5752	0.9472
	50.7	C*	920.4	533.3	—	2,361	1,360	—	0.5761	—

Sample	Run	Corrected for blank and primordial Pb				Single-stage ages in m. y.			
		$\frac{^{206}\text{Pb}}{^{238}\text{U}}$	$\frac{^{207}\text{Pb}}{^{235}\text{U}}$	$\frac{^{207}\text{Pb}}{^{206}\text{Pb}}$	$\frac{^{208}\text{Pb}}{^{232}\text{Th}}$	$\frac{^{206}\text{Pb}}{^{238}\text{U}}$	$\frac{^{207}\text{Pb}}{^{235}\text{U}}$	$\frac{^{207}\text{Pb}}{^{206}\text{Pb}}$	$\frac{^{208}\text{Pb}}{^{232}\text{Th}}$
72275.73 matrix	C1P	0.9175	61.26	0.4845	0.2274	4,236	4,250	4,256	4,198
	C1	0.9223	60.95	0.4796	—	4,252	4,245	4,241	—
72275.81 clast # 1 black rind	C1P	1.006	83.88	0.6048	0.2478	4,531	4,568	4,585	4,535
	C1	1.008	81.90	0.5899	—	4,534	4,544	4,548	—
72275.117 clast # 1 white interior	C1P	0.9595	75.60	0.5717	—	4,377	4,463	4,502	—
	C1	0.9620	76.09	0.5740	—	4,385	4,469	4,508	—

Table 11a: Rb-Sr data for KREEPY basalt separates.
Compston *et al.* (1975).

Rb, Sr, and $^{87}\text{Sr}/^{86}\text{Sr}$ analyses for pigeonite basalt 72275,171. Blank levels for these data are 0.035 ng Rb and 0.10 ng Sr. Our mean normalised $^{87}\text{Sr}/^{86}\text{Sr}$ for the NBS987 reference sample is 0.71028 ± 1 (s.e.)

	Weight (mg)	Rb (ppm)	Sr (total) (ppm)	$^{87}\text{Rb}/^{86}\text{Sr}$	$^{87}\text{Sr}/^{86}\text{Sr}$ (\pm s.e.) ^a
Mesostasis	1.48	18.8	122.9	0.4417	0.72489 ± 6
Plagioclase	1.05	1.68	173.3	0.02799	0.70117 ± 4
Pigeonite	1.93	0.427	5.80	0.2127	0.71124 ± 42
Total-rock (1)	11.3	6.34	81.1	0.2260	0.71262 ± 3
Total-rock (2)	11.9	7.53	91.8	0.2370	0.71307 ± 9

^a Internal standard error of mean.

Table 11b: Rb-Sr data for KREEPY basalt separates.
Shih *et al.* (1992).

Sample	Wt. (mg)	Rb (ppm)	Sr (ppm)	$^{87}\text{Rb}/^{86}\text{Sr}$ ^a	$^{87}\text{Sr}/^{86}\text{Sr}$ ^{a,b}	T_{LUNI} (Ga) ^{c,d}
WR	11.16	7.323	89.20	0.2375 ± 12	0.713690 ± 17	4.31 ± 0.02
Plag	2.10	1.040	184.1	0.01634 ± 12	0.700530 ± 19	
Opx	2.76	0.6779	18.95	0.10350 ± 74	0.705463 ± 25	
Opagues	1.04	28.10	96.95	0.8386 ± 49	0.748935 ± 19	
$\rho < 2.75$ ^e	3.50	6.364	199.3	0.09241 ± 48	0.705221 ± 10	
$\rho = 3.3-3.55$	6.94	3.250	21.25	0.4424 ± 23	0.725513 ± 29	
$\rho > 3.55$	2.07	2.859	18.68	0.4428 ± 24	0.725716 ± 19	
NBS 987 ($n = 13$)					0.710251 ± 28 ^f	

^a Uncertainties correspond to last figures and are $2\sigma_m$.

^b Normalized to $^{88}\text{Sr}/^{86}\text{Sr} = 8.37521$ and $^{87}\text{Sr}/^{86}\text{Sr} = 0.71025$ for NBS 987.

^c Calculated for $\lambda(^{87}\text{Rb}) = 0.0139 \text{ Ga}^{-1}$.

^d Model age relative to the LUNar Initial $^{87}\text{Sr}/^{86}\text{Sr}$ (LUNI = 0.69903 of Nyquist *et al.* [21,25]).

^e Density in g/cm^3 for all mineral separates obtained using heavy liquids.

^f Mean value of thirteen measurements made during this investigation; error limits are $2\sigma_p$.

Table 11c: Sm-Nd data for KREEPY basalt separates.
Shih *et al.* (1992).

Sample	Wt. (mg)	Sm (ppm)	Nd (ppm)	$^{147}\text{Sm}/^{144}\text{Nd}$ ^a	$^{143}\text{Nd}/^{144}\text{Nd}$ ^{a,b}	T_{CHONI} (Ga) ^{c,d}
WR	11.16	18.13	65.15	0.16830 ± 17	0.511036 ± 12	4.60 ± 0.01
Plag	2.10	1.549	6.160	0.15203 ± 75	—	
Opx	2.76	2.127	6.394	0.20118 ± 29	0.511943 ± 12	
Opagues	1.04	88.47	326.3	0.16398 ± 17	0.510937 ± 13	
$\rho < 2.75$ ^e	3.50	9.926	37.63	0.15951 ± 17	0.510816 ± 12	
$\rho = 3.3-3.55$	6.94	9.118	30.27	0.18219 ± 18	0.511418 ± 12	
$\rho > 3.55$	2.07	10.10	34.71	0.17607 ± 18	0.511257 ± 12	
Ames Nd Standard ($n = 16$)					0.511088 ± 12 ^f	

^a Uncertainties correspond to last figures and are $2\sigma_m$.

^b Normalized to $^{146}\text{Nd}/^{144}\text{Nd} = 0.724140$ and $^{143}\text{Nd}/^{144}\text{Nd} = 0.511138$ for the Ames Nd metal standard which is equivalent to CIT nNd β standard of Wasserburg *et al.* [15].

^c Calculated for $\lambda(^{147}\text{Sm}) = 0.00654 \text{ Ga}^{-1}$.

^d Model age relative to the CHONdritic Initial $^{143}\text{Nd}/^{144}\text{Nd}$ (CHONI = 0.505893 of Jacobsen and Wasserburg [31]).

^e Density in g/cm^3 for all mineral separates obtained using heavy liquids.

^f Mean value of sixteen Nd standard measurements made during this investigation; ~ 325 ng of Nd standard were used for each measurement; error limits are $2\sigma_p$, as reported in [14].

Table 12: U,Th-Pb data and age parameters for 72275 KREEPy basalt (probably clast #4). Nunes and Tatsumoto (1975a).

Sample	Description	Run	Weight (mg)	Concentrations			²³² Th/ ²³⁸ U	²³⁸ U/ ²⁰⁴ Pb
				U	Th	Pb		
72275,170	Pigeonite basalt clast (PB)	C1	38.6	1.635	6.255	3.047	3.95	3045

Sample	Description	Run	Weight (mg)	Observed Ratios ^a			Corrected for Analytical Blank ^b				
				²⁰⁶ Pb/ ²⁰⁴ Pb	²⁰⁷ Pb/ ²⁰⁴ Pb	²⁰⁸ Pb/ ²⁰⁴ Pb	²⁰⁶ Pb/ ²⁰⁴ Pb	²⁰⁷ Pb/ ²⁰⁴ Pb	²⁰⁸ Pb/ ²⁰⁴ Pb	²⁰⁷ Pb/ ²⁰⁶ Pb	²⁰⁸ Pb/ ²⁰⁶ Pb
72275,170	Pigeonite basalt clast (PB)	P	38.9	2360	1079	2387	(34287)	(15592)	(34420)	0.4547	1.0038
		C1	38.6	1299	597.2	-	2672	1220	-	0.4568	-

P=composition run; C=concentration run; (GCBx)=gray competent breccia; (PB)=pigeonite basalt.
^a Totally spiked runs from solid sample splits; other runs were obtained from samples which were divided from solution.
^b Pb blanks ranged from 1.4 to 2.1 ng for the solution aliquoted data and were 1.05 ng for the totally spiked data.
^c Raw data corrected for mass discrimination of 0.15% per mass unit. ²⁰⁸Pb spike contribution subtracted from concentration data.
 Data in parentheses subject to extreme error owing to Pb blank uncertainty.
 All 72215 samples are competent breccias with colors ranging from black to light-gray.

Sample	Description	Run	Atomic ratios corrected for blank and primordial Pb				Single-stage ages × 10 ⁶ yr			
			²⁰⁶ Pb/ ²³⁸ U	²⁰⁷ Pb/ ²³⁵ U	²⁰⁷ Pb/ ²⁰⁶ Pb	²⁰⁸ Pb/ ²³² Th	²⁰⁶ Pb/ ²³⁸ U	²⁰⁷ Pb/ ²³⁵ U	²⁰⁷ Pb/ ²⁰⁶ Pb	²⁰⁸ Pb/ ²³² Th
72275,170	Pigeonite basalt clast (PB)	C1P	0.8776	55.00	0.4547	0.2228	4061	4087	4100	4065
		C1	0.8747	54.82	0.4545	-	4051	4084	4100	-

^a Concentrations determined from totally spiking a separate sample. Concentration and composition splits were divided from perfect solutions prior to spiking for all other analyses.
 All 72215 samples are competent breccias with colors ranging from black to light-gray.
 P=composition run; C=concentration run; (GCBx)=gray competent breccia; (PB)=pigeonite basalt.

Table 13: Magnetic properties of 72275, 2. Pearce et al. (1974b).

Sample	J _s (emu/g)	X _p (emu/g Oe) × 10 ⁶	X ₀ (emu/g Oe) × 10 ⁴	J _r /J _s	H _c (Oe)	H _r (Oe)	Equiv. wt.% Fe ^o	Equiv. wt.% Fe ⁺⁺	Fe ^o /Fe ⁺⁺
Noritic rocks									
72275,2	1.12	19.0	3.4	.005	35	—	.51	8.72	.059

Table 14: Magnetic properties (hysteresis parameters) of 72275,67.
Brecher *et al.* (1974).

Sample (mass. mg)	72275.67			
	U(35)		O(104)	
<i>T</i> (°K)	300	160	300	160
J_s (emu/g)	1.28	1.19	.877	.93
J_{rs} ($\times 10^3$ emu/g)	.05	.07	.12	.145
χ_0 ($\times 10^4$ emu/g · Oe)	34.6	48.6	34.3	42.3
χ_p ($\times 10^6$ emu/g · Oe)	6.92	6.62	7.86	7.84
H_c (Oe)	72	105	150	185
$m_{Fe^{2+}}$ (wt.%)	.59	.54	.40	.43
$f_{Fe^{2+}}$ (wt.%)	16.1	12.1	16.0	10.5
Fe^0/Fe^{2+}	.036	.045	.025	.04
J_{rs}/J_s	.04	.06	.136	.156
J_s/χ_0	1850	1790	1115	1185

Table 15: Native iron determined from J_s measurement of 72275 samples.
Banerjee and Swits (1975).

Sample No.	J_s (G-cm ³ g ⁻¹)	Fe ⁰ content (wt. %)	Average
72275,46	3.26	1.52	1.69
72275,47 (1)	4.47	2.08	
72275,47 (2)	2.70	1.26	
72275,56	4.09	1.90	

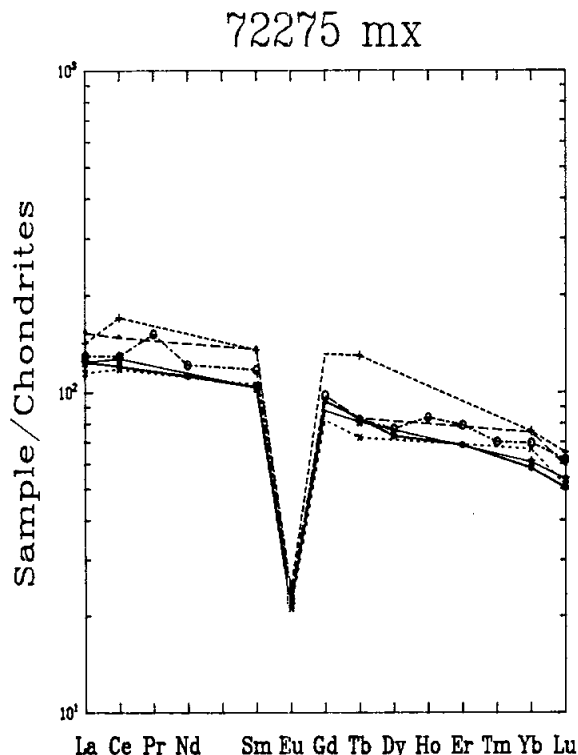


Figure 19a: Abundances of rare earth elements in 72275 friable matrix and dark melt samples. Dark melt breccia clast #2 (.83) is a solid line with + 's, and is similar to typical matrix. The extremely high REE sample (dashed line with + 's) is a split of .57, and is KREEPy basalt rich. Another split of .57 (long dashes) has high light but not heavy rare earths. Split .101 is shortest dashes with x's. A larger sample, .2, is a solid line without added symbols, and .108 is dash-dot with o's. For references, see Tables 5a and 5c.

Clast #1 (Marble Cake):

Leich *et al.* (1975a) provided ^{40}Ar - ^{39}Ar data for the rind (.80) and the interior (.76) of the Marble Cake clast (Figs. 26a, b). Like the other samples discussed above, the data for the interior allow no firm chronological interpretation, although again some age around 3.9 Ga for outgassing is suggested by the data. Leich *et al.* (1975a) however do attach significance to the intermediate plateau for the rind, which gives an age of 3.93 \pm 0.03 Ga (new constants; Fig. 26b).

Nunes *et al.* (1974) provided U,Th-Pb data for both rind (.81) and interior (.117) of the Marble Cake clast (Table 10). The data plot within error of concordia near the 4.5 Ga point.

EXPOSURE AGES AND PARTICLE TRACKS

Leich *et al.* (1975a) tabulated extensive rare gas isotopic data (He, Ne, Ar, Kr, Xe) for 72275 samples: friable matrix (.57), clast #1 (Marble Cake) core (.76) and rind (.80 and .166), and the KREEPy basalt clast #5 (.91). Only .80 shows trapped Ne and Ar components that might be indicative of a small amount of solar wind contamination. ^{81}Kr -Kr exposure ages for four of these samples (KREEPy basalt not included in the exposure tabulations) give a weighted mean of 52.5 m.y., with a 1.3 m.y. standard deviation. This age is about 10 m.y. older than that of samples 72215 and 72255, and indicate different shielding

parameters for boulder samples. Exposure ages from ^{38}Ar , ^{83}Kr , and ^{126}Xe are fairly consistent, but from ^{21}Ne and ^3He are somewhat lower. Exposures calculated from ^{38}Ar -Ca determinations are unreliable (Leich *et al.*, 1975a). Goswami and Hutcheon (1975) studied the particle track record in 72275,44. They found that the extent of shock metamorphism is heterogeneous, and that the sample retained no solar flare tracks. The constituents of the boulder were not exposed to solar radiation prior to the assembly of the boulder and it is not a regolith breccia. Goswami *et al.* (1977a, b) measured track densities in a whitlockite crystal from 72275. With various assumptions, they calculated a track retention age of 3.98 \pm 0.04/-0.06 Ga for the crystal. This age is the age of last significant heating of the crystal, and therefore an upper limit for the age of compaction of the boulder.

PHYSICAL PROPERTIES

Magnetic properties of 72275 friable matrix samples were reported by Pearce *et al.* (1974a, b), Brecher *et al.* (1974), Brecher and Morash (1974), Banerjee *et al.* (1974a, b), and Banerjee and Swits (1975). The data from Pearce *et al.* (1974a, b) is given in Table 13, and that from Brecher *et al.* in Table 14. Native metal contents inferred from J_s measurements by Banerjee and Swits (1975) are in Table 15, and are substantially higher than those inferred for the matrix sample by Pearce *et al.* (1974a, b) or Brecher *et al.* (1974a, b). All measured samples contain much more native metal than do mare samples. Banerjee *et al.* (1974a, b) and Banerjee and Swits (1975) used samples of known mutual orientations (known within about 20 degrees). They found that the average directions of natural remanent magnetism in all the 72255 and 72275 samples were approximately the same (see

diagrams in section on 72255). In an attempt to separate stable primary NRM from unstable secondary NRM, the authors attempted thermal demagnetization, avoiding oxidation; however, it appeared that permanent damage was done to the carriers and the procedure inadvisable. AF-demagnetization showed no zig-zag patterns, and the NRM direction after demagnetization in fields of 80 Oe and greater are stable and primary; however, they differ from those in 72255 by 130 degrees (see diagrams in 72255 section).

Banerjee and Swits (1975) presented data for paleointensity, suggesting a field of about 0.19 Oe, lower than those for 72215 and 72255. However, given the problems of obtaining and interpreting magnetic data for lunar samples, neither the directions nor the intensities can be said to have known meanings. Brecher *et al.* (1974a,b) also tabulated considerable NRM data for 72275 (Table 16), with extensive discussion.

They found a paleointensity similar to that found by Banerjee and Swits (1975). Boulder 1, Station 2 differs greatly in magnetic behaviour from the Station 7 Boulder (sample 77135) analyzed in the same study. The paleomagnetic intensities derived appear to depend directly on thermal history, since drastic changes in magnetic mineralogy and character result from even brief heating cycles at 800 degrees C. Housley *et al.* (1977) in ferromagnetic resonance studies found that 72275,109 had no characteristic FMR intensity.

Adams and Charette (1975) and Charette and Adams (1977) measured the spectral reflectance (0.35 - 2.5 microns) of two samples from 72275 (Fig. 27). 72275,98 is undocumented fines from sawing, and 72275,103 is a surface chip of matrix; both represent general friable matrix. They show the typical absorption bands near 0.9 microns and 1.9 microns that arise from electronic transitions of Fe²⁺ in orthopyroxene, and a broad absorption band near 0.6 microns

that is commonly associated with ilmenite.

PROCESSING

The 1973 processing and sawing was described by Marvin (in CI 1, 1974), and the 1984 processing by Salpas *et al.* (1985). The sample arrived from the Moon with several pieces dislodged from the friable matrix; some of these could be fitted together, but others remained undocumented. Some were used for thin sections and chemical analyses. A slab (.42) was cut (Figs. 2, 3), and subdivided (Fig. 28). Many allocations were made from this slab. The end pieces remained largely untouched. In 1984 two more slabs were cut parallel to the first one (Fig. 3c, 4, and 5) and allocations, mainly of clasts, were made from them.

Table 16: Magnetic properties of 72275,67. Brecher *et al.* (1974a).

Samples (Mass. g)	72275,67 (.932)
NRM ($\times 10^{-5} \frac{\text{emu}}{\text{g}}$)	6.1
IRM _s ⁰ ($\times 10^{-3} \frac{\text{emu}}{\text{g}}$)	4.75
IRM _s ⁰ /NRM	78
TRM ¹ (H _{lab}) $\times 10^{-5} \frac{\text{emu}}{\text{g}}$ (Oe)	3.36 (.087)
TRM ¹ /NRM	.55
H ₀ ¹ (Oe)	0.16
IRM _s ¹ ($\times 10^{-3} \frac{\text{emu}}{\text{g}}$)	48.1
IRM _s ¹ /IRM _s ⁰	10.1
TRM ² (H _{lab}) $\times 10^{-5} \frac{\text{emu}}{\text{g}}$ (Oe)	253 (.63)
TRM ² /NRM	41.5
H ₀ ² (Oe)	.015
IRM _s ² ($\times 10^{-3} \frac{\text{emu}}{\text{g}}$)	128
IRM _s ² /IRM _s ⁰	27

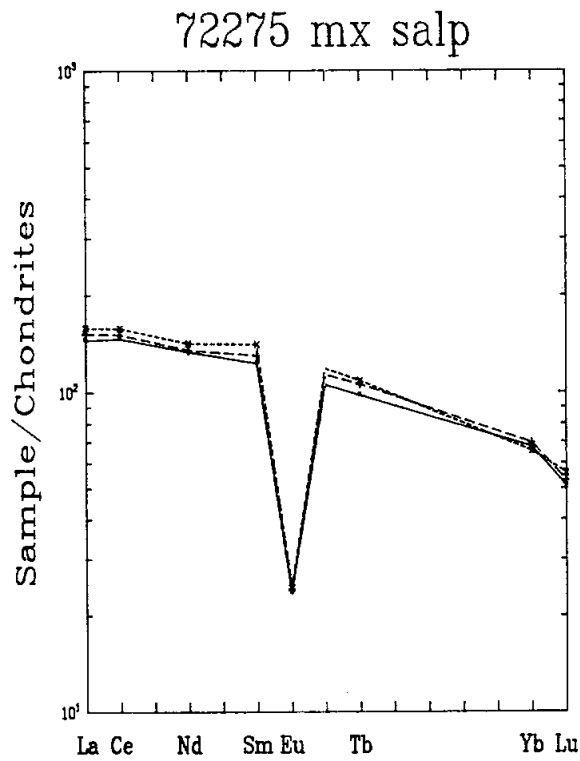


Figure 19b: Abundances of rare earth elements in 72255 friable matrix. These samples are all rich in KREEPy basalts, and may be pure KREEPy basalt breccias. Data from Table 5b (Salpas et al., 1987b).

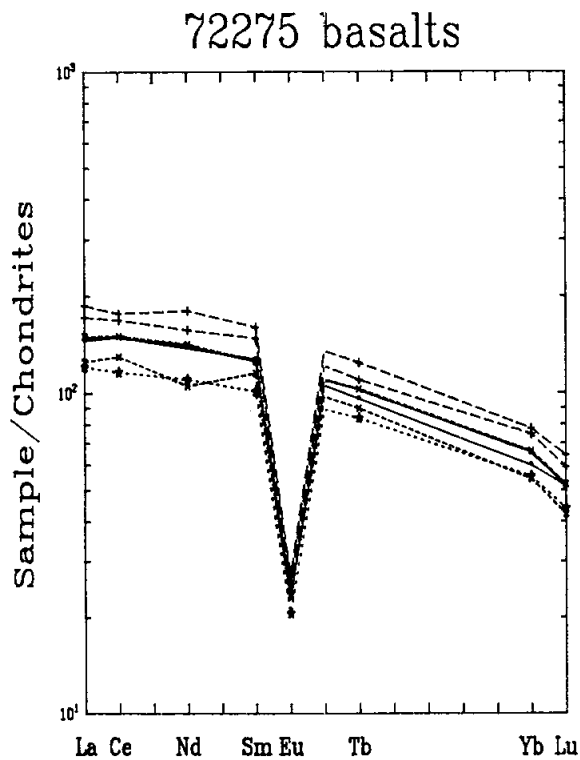


Figure 20: Rare earth elements in samples of KREEPy basalts and KREEPy basalt breccias. 72275,91 is the solid line near the middle of the range (Blanchard et al., 1975). The other five analyses are the two most REE-rich (#357 and 363b), the two most REE-poor (#393 and 359), and one close to an average composition (#347) from Salpas et al. (1987b).

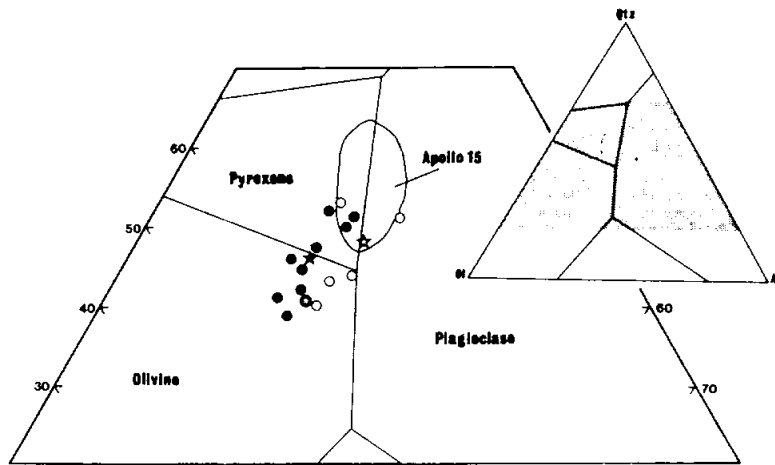


Figure 21: Pseudoquaternary phase diagram (Ol-Si-An) for A 17 KREEPy basalts (Salpas et al., 1987b). The black dots are the 9 analyses that included major elements, with SiO₂ by difference; the filled star is the average of these 9 analyses. The enclosed star is the analysis of Blanchard et al. (1975). The open circles are defocused beam microprobe analyses of Ryder et al. (1977), with their average as an open star.

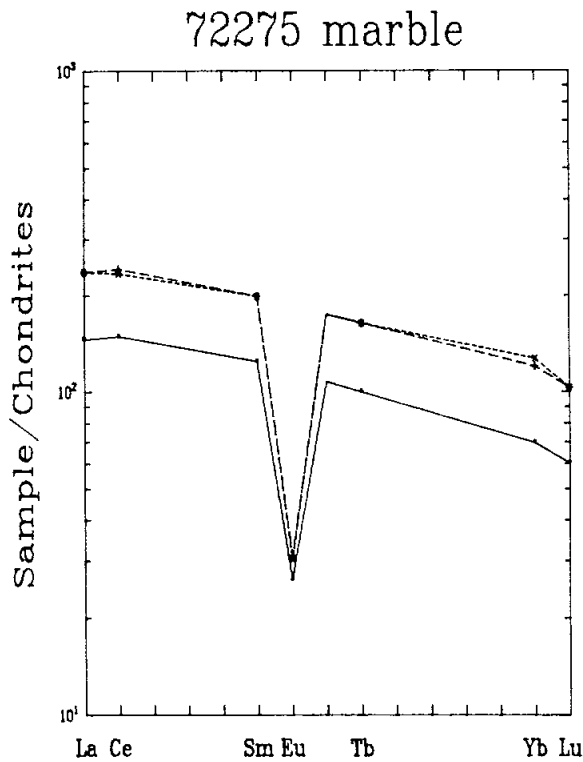


Figure 22: Rare earth elements in lithologies of clast #1 (Marble Cake clast). The two upper plots are for rind materials and are very similar. The lower plot is for the white interior, and probably includes a component of dark rind material. All data from Blanchard et al. (1975).

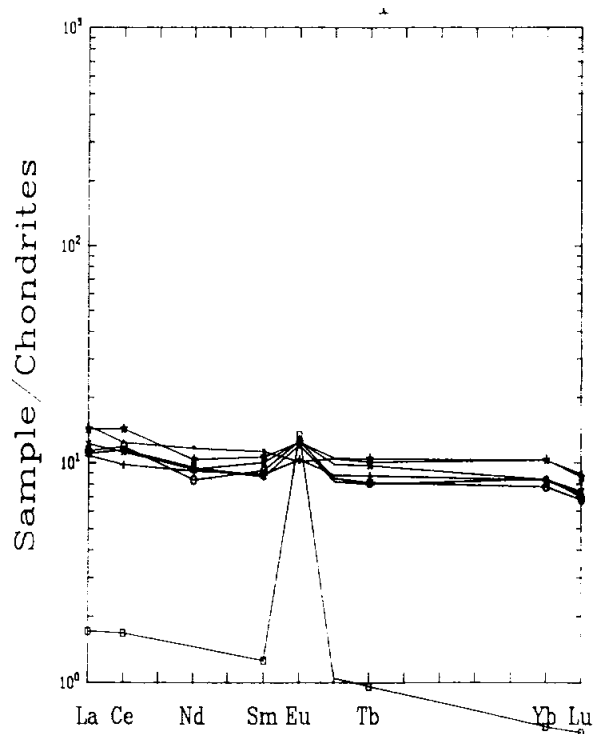


Figure 23: Rare earth elements in six felspathic granulites (top patterns) and a ferroan anorthosite (lower pattern) from 72275. Grid is drawn to conform as closely as possible with other diagrams in this section, so lower pattern falls below grid. Data from Salpas et al. (1987a).

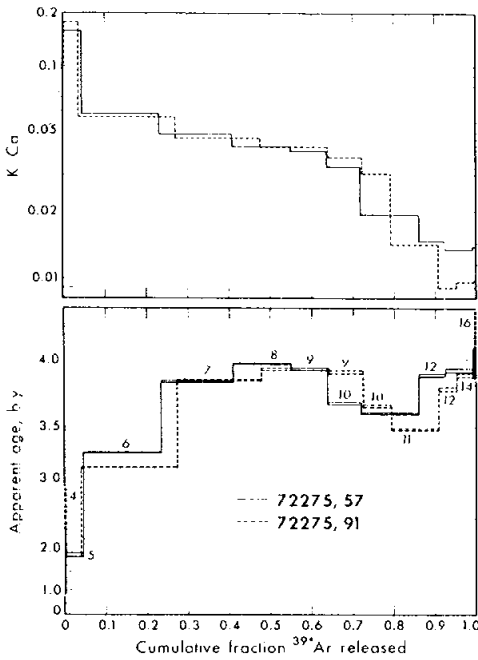


Figure 24: ^{40}Ar release diagram for 72275,57 (friable matrix) and 72275,91 (clast #5, KREEPY basalt). The apparent age scale is calibrated to the old decay constants. *Leich et al. (1975a)*.

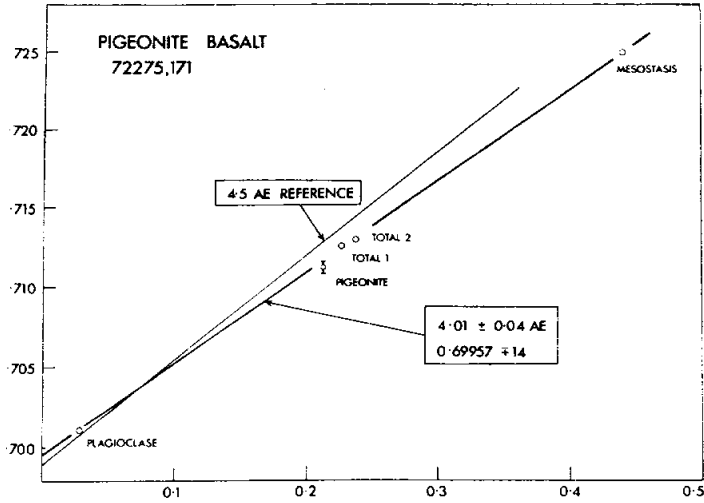


Figure 25a: Rb-Sr internal isochron for 72275 KREEPY basalt (probably clast #4). The age is 3.93 ± 0.04 Ga with the new decay constants. Left hand axis is $^{87}\text{Sr}/^{86}\text{Sr}$; lower axis is $^{87}\text{Rb}/^{86}\text{Sr}$. *Compston et al. (1975)*.

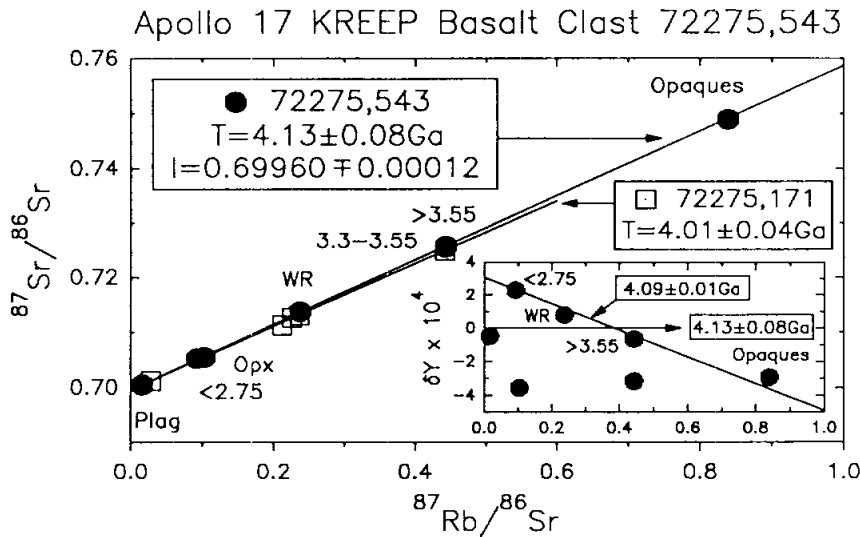


Figure 25b: Rb-Sr isochron for KREEPY basalt sample 72275,543. Ages calculated with old Rb decay constant. *Shih et al. (1992)*.

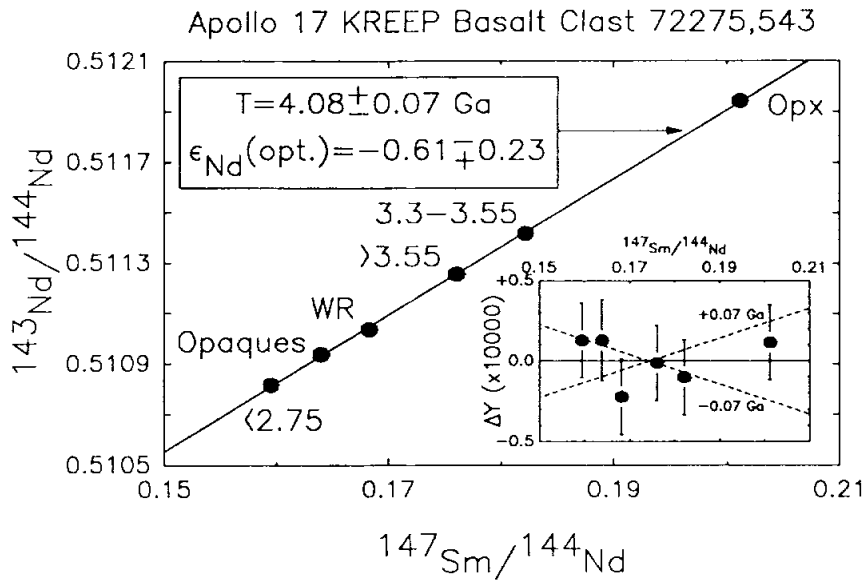


Figure 25c: Sm-Nd isochron for KREEPy basalt sample 72275,543. Shih et al. (1992).

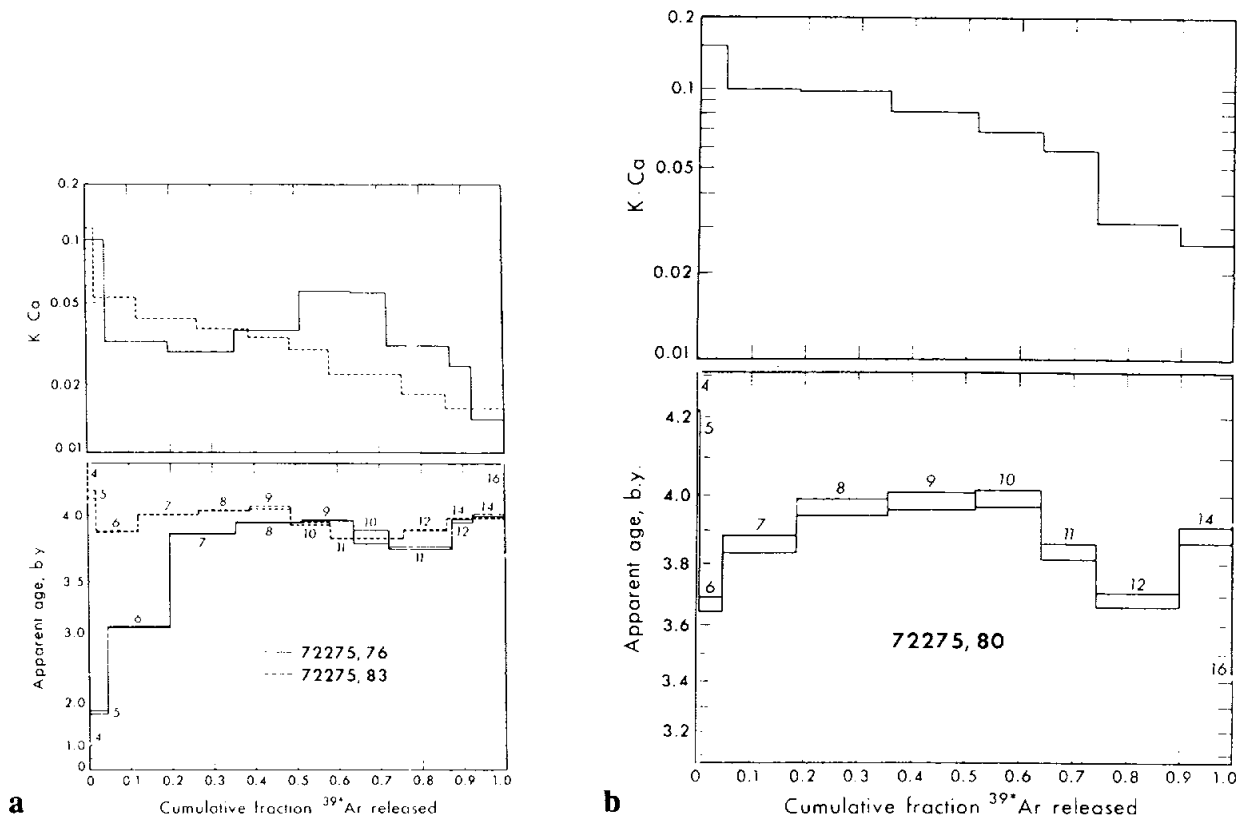


Fig. 26: Apparent ^{40}Ar age and K/Ca for 72275 samples. Age calibrations are with old decay constants. Leich et al. (1975b). a) 72275,76 (Marble Cake interior) and 72275,83 (dark melt breccia clast #2). b) 72275,80 (Marble Cake rind).

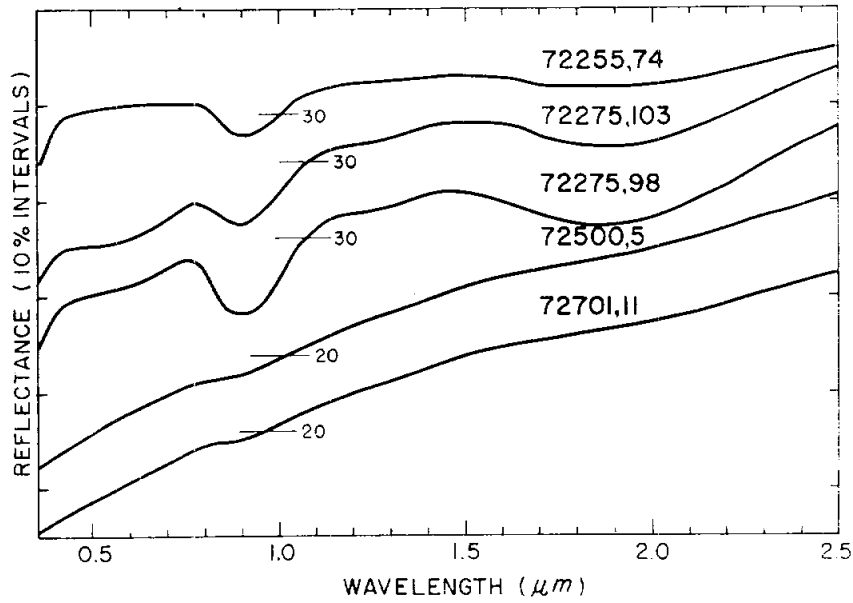


Figure 27: Diffuse reflectance spectra for 72275 and some other A 17 samples. Adams and Charette (1975).

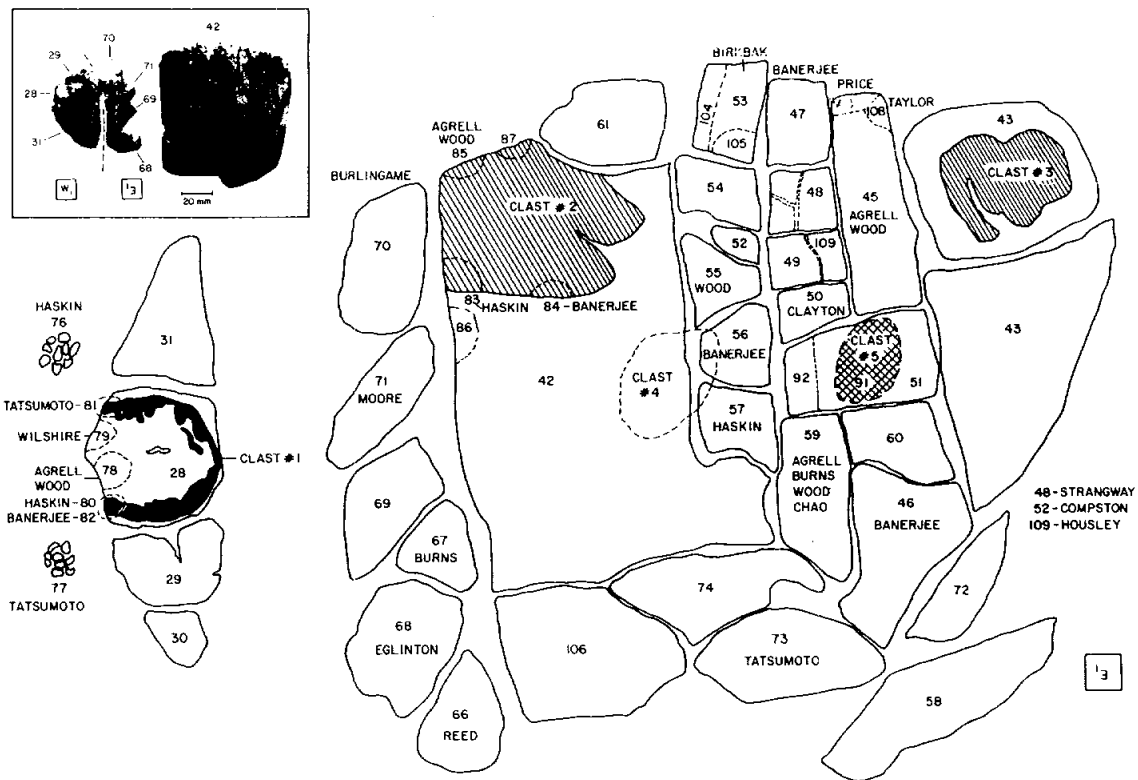


Figure 28: Subdivisions of 1973 slab 72275,42. (Marvin, in CI 2, 1974).

BOULDER 2, STATION 2

Sample 72315, 72335, 72355, 72375, 72395

Boulder 2 at Station 2 was one of three boulders sampled on the lower slopes of the South Massif (see section on Boulder 1, Station 2 for description of area). Boulder 2 lay approximately 50 m southwest of the LRV parking spot. It is greenish-gray or tan gray, and approximately 2 m wide and 2 m high as measured from the lunar surface. It is rounded, and smoother than Boulder 1. Several sets of fractures can be recognized, but no layering is visible. The boulder has a fillet about 25 cm high on its uphill side but overhangs the ground surface on its downhill side (fillet material was sampled as 72320).

The astronauts took 5 samples from Boulder 2 (Fig. 1). During sampling, Schmitt observed a distinctive half-meter patch on the surface that he interpreted as a clast of material similar to the rest of the boulder. Sample 72315 represents this "clast", and 72335 represents the "contact" with the groundmass. 72355, 72375, and 72395 represent normal boulder matrix. Petrographic and chemical studies show that all five samples are virtually identical; the distinctive patch was probably a spall. Each sample has an exterior side (with brown patina and zap pits) and a freshly-exposed interior surface.

Most of the studies of Boulder 2 were made by a loosely-knit Consortium led by the Caltech group (Dymek *et al.* 1976). All are clast-bearing fine-grained impact melts of low-K Fra Mauro with composition similar to others at the Apollo 17 landing site. The boulder is generally interpreted as a piece of an impact melt unit created in the Serenitatis impact at ~3.86 Ga ago. It rolled down the South Massif to its present position about 20 m.y. ago, according to exposure data.



Figure 1. Sampling of Boulder 2, Station 2. The gnomon has a height of 62 cm. (AS137-20913).

72315**Micropoikilitic Impact Melt Breccia
St. 2, 131.4 g****INTRODUCTION**

72315 is a fine-grained, clast-bearing impact melt with a poikilitic texture. Although it was sampled to represent an apparent distinctive half-meter clast (see section on Boulder 2, Station 2), 72315 is identical in all analyzed respects with all other samples from Boulder 2. Although no definitive geochronological data exist, a general assumption is that 72315 crystallized at the same time as other melts of similar petrography and chemistry at the Apollo 17 site, i.e. 3.86 Ga ago. The sample, 10 x 5.5 x 2 cm, is an angular elongate light gray (N7) slab (Fig. 1). It is tough and homogeneous, but with an irregular distribution of clasts and vugs, and there are some penetrative

fractures. Clasts larger than 1 mm compose less than 5% of the rock. The exposed surface (T) of 72315 has many zap pits and the broken surface is hackly (Figs 1, 2, 3). Irregular cavities forming about 10% of the sample range up to 3 mm, although most are much less than 1 mm across; the larger ones have brown pyroxene linings, smaller ones have drusy linings.

72315 is so similar to other samples from Boulder 2 that it will not be described here in detail, but specific studies are referenced. It was studied mainly under a consortium led by the Caltech group (Dymek *et al.*, 1976a), but not in as much detail as 72395. The description of 72395 can be assumed as a description of 72315. Following chipping of a few small pieces of

72315, the sample was sawn to produce mainly two end pieces and two central slabs. These slabs were entirely subdivided and produced oriented samples for track studies.

PETROGRAPHY

All five samples from Boulder 2 are very similar in petrography. Dymek *et al.* (1976a) gave descriptions of the petrography subsequent to a briefer description by Albee *et al.* (1974b) and Dymek *et al.* (1976b). They did not give individual descriptions of the petrography and that practice is for the most part followed here. Thus, for a description and mineral diagrams of 72315 see sample 72395.

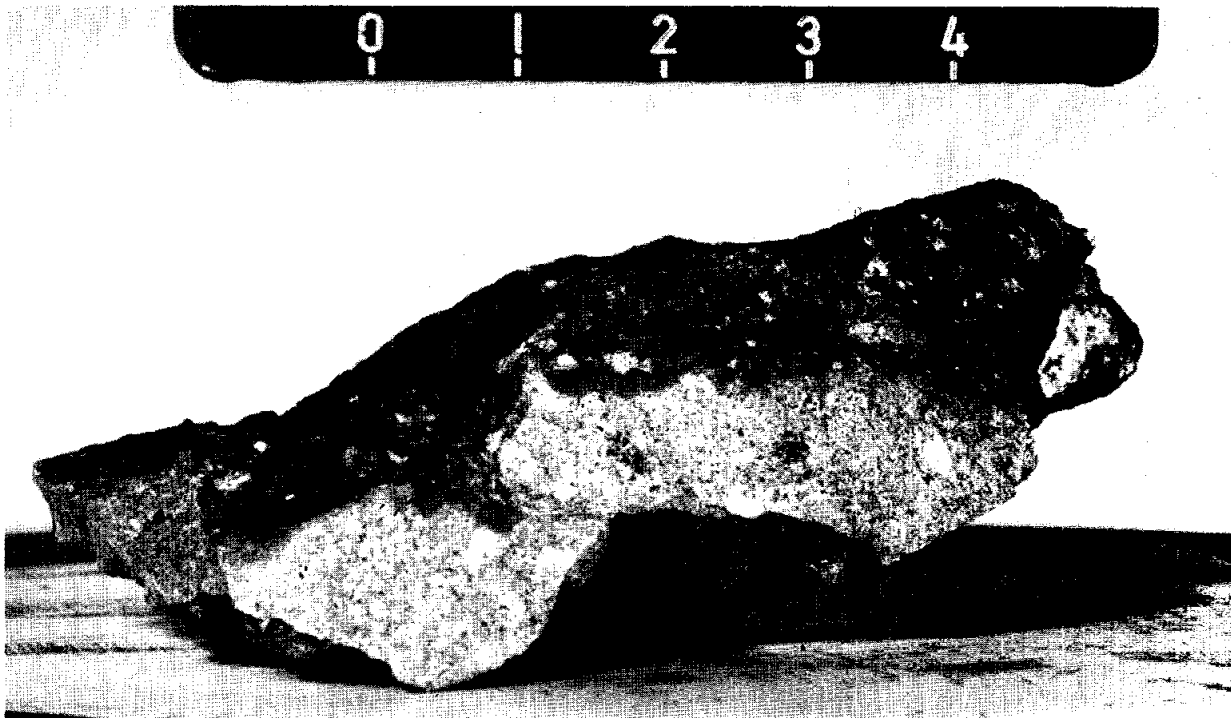
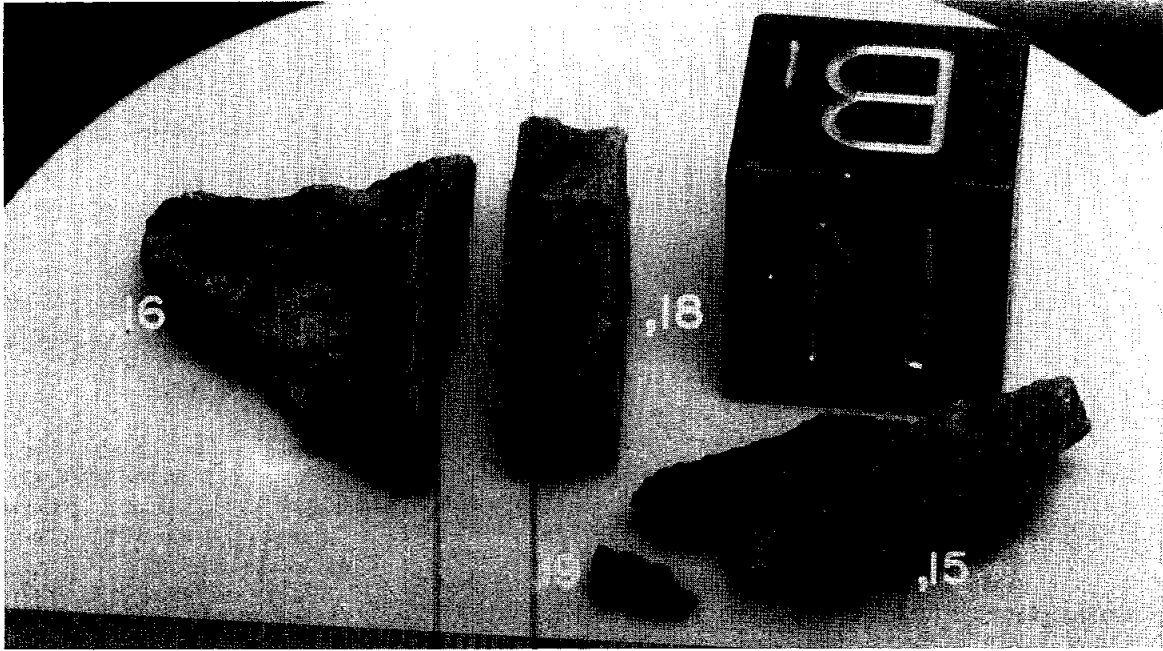
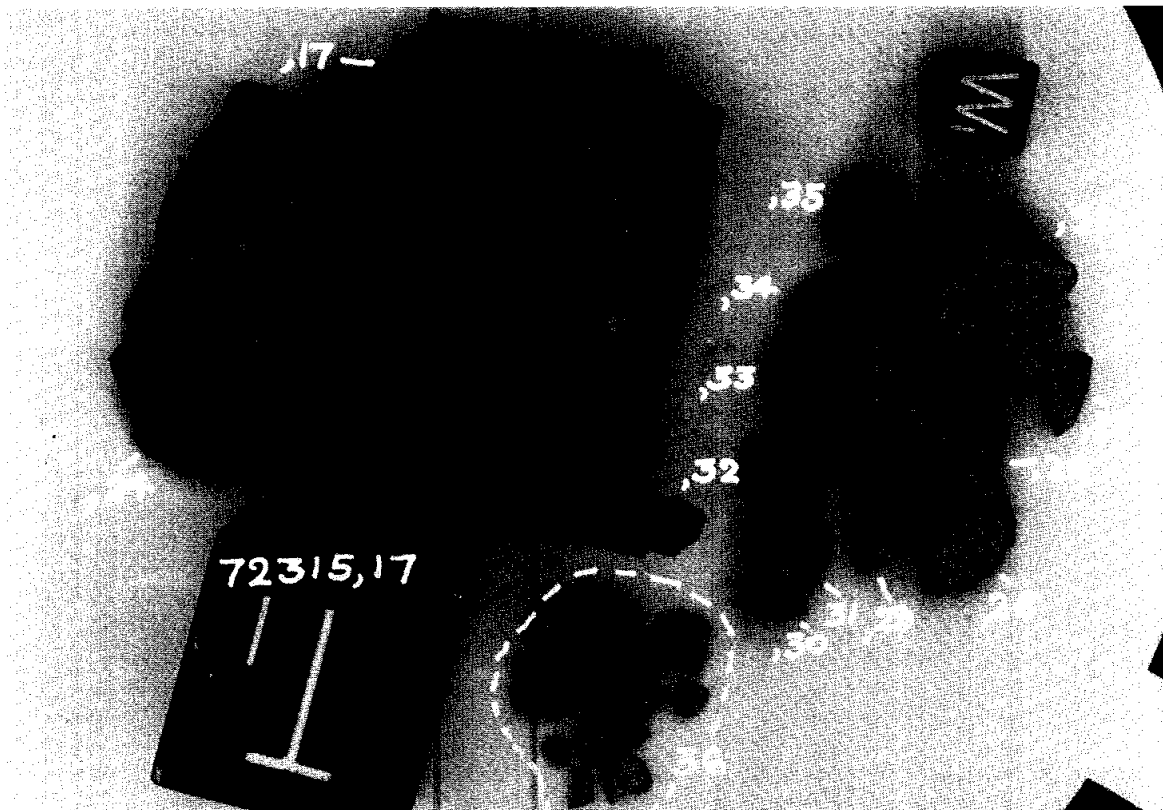


Figure 1: Exposed (top) and broken (lower) surfaces of 72315. The sample is homogeneous, with a few dark and light clasts visible. Scale in centimeters. S-73-18693.



a



b

Figure 2: a) Post-sawing pieces ,16 (W end); ,15 (broken-off N edge); and ,18 (sawn from ,17, and from between ,16 and ,17). Split ,19 fell off ,18. Cube is 2 cm. S-74-15094. b) Post-sawing piece ,17 (E end) and subdivisions of an unnumbered slab cut from it adjacent to ,18. Large cube is 2.54 cm. S-74-17830.

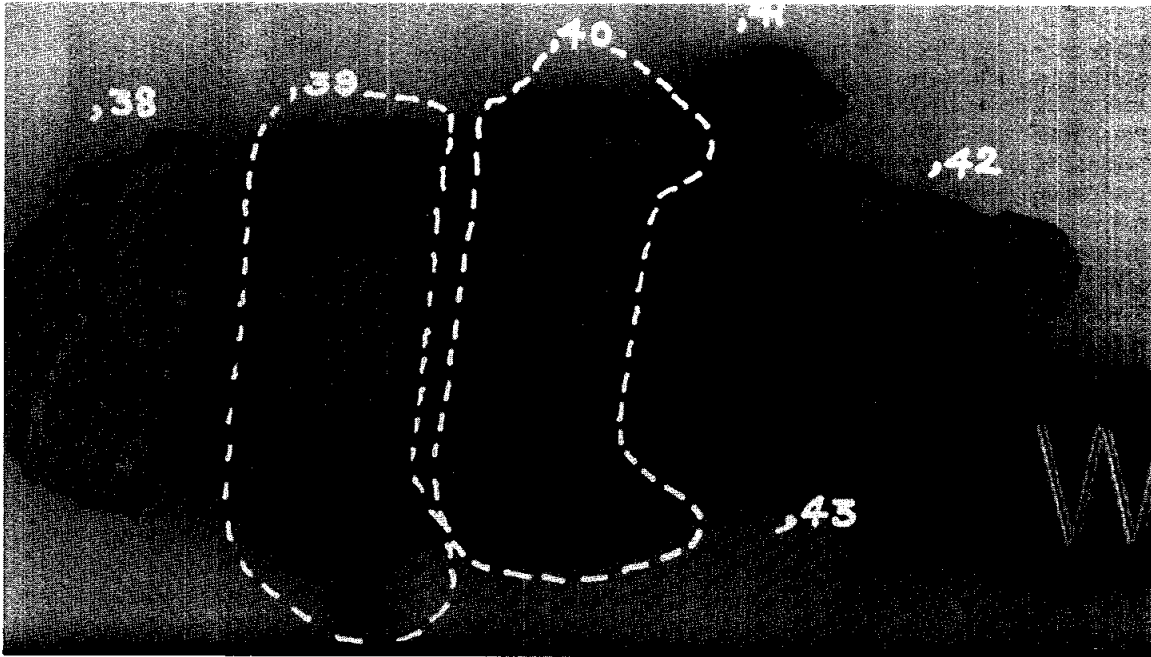
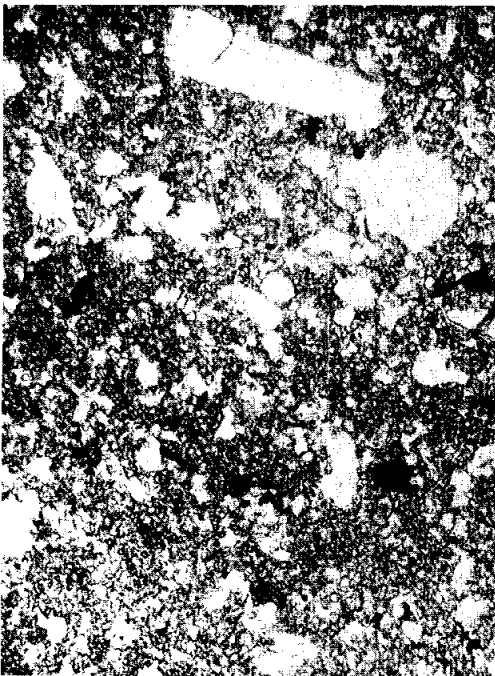
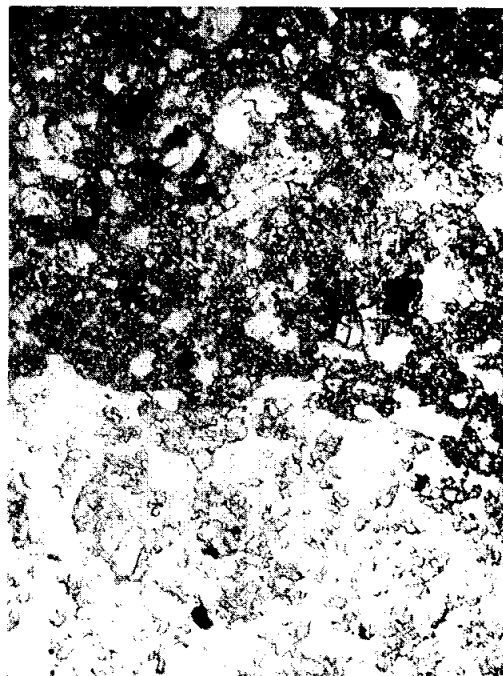


Figure 3: Subdivision of slab ,18. Cube is 1 cm. S-74-17835.



a



b

Figure 4: Photomicrographs of 72315,78. Plane transmitted light, all about 1 mm field of view. a) Melt groundmass and smaller clasts (larger white areas), mainly plagioclases with lesser mafic minerals. Ilmenites are mainly grown in the groundmass. b) Contact between melt (top) and a larger lithic clast of feldspathic granulite (bottom).

The sample is a fine-grained impact melt with a micropoikilitic texture and some small clasts (Fig. 4 and Dymek et al., 1976a). Simonds et al. (1974) referred to it as "clast-rich ophitic" with matrix feldspars and pyroxenes respectively 10 to 40 and 20 to 80 microns long. Photomicrographs of matrix and clasts are given in Dymek et al. (1976a) and Spudis and Ryder (1981). Engelhardt (1979) noted the poikilitic texture and classified the paragenesis as one with ilmenite crystallizing only after pyroxene finished crystallizing.

CHEMISTRY

Chemical analyses of bulk rock (groundmass plus clasts) are given in Table 1 and rare earth elements are plotted in Figure 5 with other data for comparison. Laul and Schmitt (1974a,b,c) and Laul et al. (1974) analyzed both exterior and interior chips which are essentially indistinguishable. The chemistry is similar to that of the other samples from Boulder 2 and other LKFM poikilitic melts from the Apollo 17 landing site; the incompatible element abundances are the lowest among the Boulder 2 samples (Fig. 5).

RADIOGENIC ISOTOPES AND CHRONOLOGY

Tera et al. (1974a) reported Rb and Sr isotopic data for a 24 mg whole-rock split of 72315 without specific discussion. $^{87}\text{Rb}/^{86}\text{Sr}$ (0.1445) and $^{87}\text{Sr}/^{86}\text{Sr}$ (0.70839 \pm 5) correspond with TBABI of 4.44 Ga. Hutcheon et al. (1974b) studied fission tracks in apatite crystals, tabulating densities. Assuming negligible cosmic ray induced fission, the densities correspond with ages of 3.09 Ga and 2.94 Ga; assuming induced fission, the densities correspond with ages of 2.51 Ga and 2.30 Ga (Table 2). These ages are younger than the

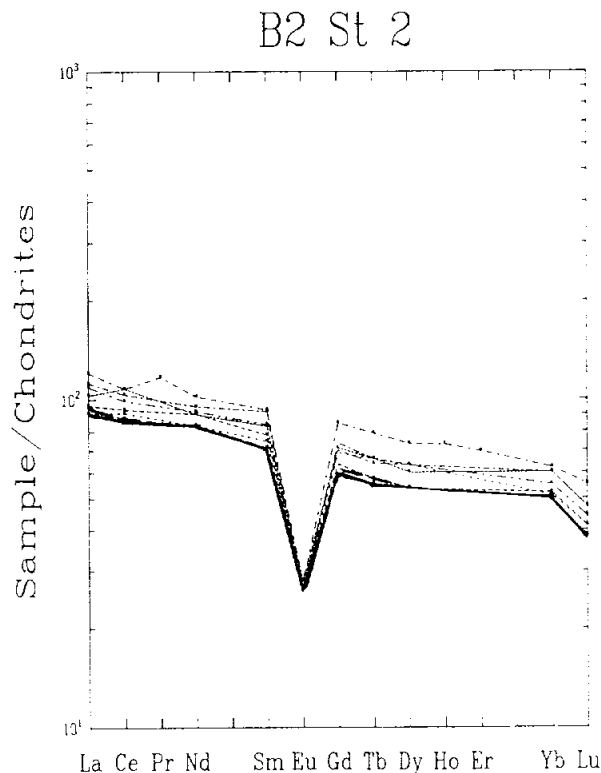


Figure 5: Rare earth elements in splits of 72315 (bold lines) and other Boulder 2, Station 2 samples. 72315 data from Table 1: solid line is ,3; long dashed line is ,4. The two splits are identical for several elements.

probable crystallization age of the rock (about 3.86 Ga) because of thermal fading of tracks over the last 10 to 20 Ma, in which 50 to 60% of tracks have been annealed.

EXPOSURE AGES

Hutcheon et al. (1974a,b,c) and MacDougall et al. (1974) studied cosmic ray tracks in samples from 72315. Hutcheon et al. (1974a) described the collection and sampling of 72315; the studied sample was a column (Fig. 6). The inner side of 72315 was a crevice on the boulder, and with the known orientation, allows the determination of the direction in space from which the particles arrived. The sampling allowed a virtually uneroded Fe spectrum averaged over several hundred thousand years, in the range of

about 1 to about 460 MeV/a.m.u. By tying the intensity of solar flare to that of galactic cosmic rays, an exposure age can be determined assuming production rates. The track density-depth relationships are shown in Figure 7. From these data and the production spectrum of Walker-Yuhas, Hutcheon et al. (1974a) derived an exposure to galactic cosmic rays of about 0.22 Ma, and exposure to solar flares for 0.32 Ma (probably consistent with each other), for an estimated exposure of the crevice for 0.27 Ma. This exposure age is almost certainly unrelated to the time that the boulder rolled down the slope, and reflects only the age of a spall event that removed a large fragment from the surface of the boulder. Surface microcrater counts suggest an exposure age of about 0.15 Ma. Hutcheon et al. (1974b) measured tracks in an unoriented

Table 1: Chemical analyses of bulk samples of 72315.

	,3(c)	,3(c)	,4(d)	,4(d)	17	,3	
Split wt%							Split wt%
SiO ₂			1.4				SiO ₂
TiO ₂	1.4						TiO ₂
Al ₂ O ₃	19.8		19.2				Al ₂ O ₃
Cr ₂ O ₃	0.186		0.187				Cr ₂ O ₃
FeO	8.5		8.5				FeO
MnO	0.111		0.111				MnO
MgO	11		12				MgO
CaO	11.6		11.3				CaO
Na ₂ O	0.61		0.70				Na ₂ O
K ₂ O	0.32		0.35		0.341	0.3166	K ₂ O
P ₂ O ₅							P ₂ O ₅
ppm							ppm
Sc	16		16				Sc
V	50		50				V
Co	21		32	33			Co
Ni	180	180	330	340			Ni
Rb		8.5		9.6		8.21	Rb
Sr		157		165		165.0	Sr
Y							Y
Zr	400		400				Zr
Nb							Nb
Hf	10		10				Hf
Ba	290	(b)320	280	(b)340			Ba
Th	5.2		5.4		4.80		Th
U	1.4	1.58	1.5	1.53	1.53		U
Ce		0.450		0.430			Ce
Ta	1.4		1.4				Ta
Pb							Pb
La	30		31				La
Ce	76		77				Ce
Pr							Pr
Nd	50		50				Nd
Sm	12.8		12.9				Sm
Eu	1.82		1.83				Eu
Gd							Gd
Tb	2.6		2.7				Tb
Dy	17		17				Dy
Ho							Ho
Er							Er
Tm							Tm
Yb	10		10				Yb
Lu	1.3		1.3				Lu
Li							Li
Be							Be
B							B
C							C
N							N
S							S
F							F
Cl							Cl
Br							Br
Cu							Cu
Zn		2.6		2.5			Zn
ppb							ppb
As	3	2.8	4	6.1			As
Ir	5	4.3	10	9.0			Ir
I							I
At							At
Ga							Ga
Ge							Ge
As							As
Se		110		120			Se
Mo							Mo
Tc							Tc
Ru							Ru
Rh							Rh
Pd							Pd
Ag		1.1		0.84			Ag
Cd		(a)300		8.1			Cd
In		0.4		0.5			In
Sa							Sa
Sb		1.3		2.0			Sb
Tb							Tb
W							W
Re		0.43		0.98			Re
Os							Os
Pt							Pt
Hg							Hg
Tl		1.3		0.66			Tl
Bi							Bi
	(1)	(2)	(1)	(2)	(3)	(4)	

References and methods:

- (1) Lual et al (1974) Lual and Schmitt (1974a); INAA.
- (2) Lual et al (1974) Lual and Schmitt (1974 a, c); RNAA.
- (3) Keith et al (1974 a, b); gamma-ray spec.
- (4) Tera et al (1974 a); ID/MS

Notes:

- (a) probably high from contamination, according to authors.
- (b) typographical error, reported as 8d in original papers.
- (c) mostly exterior.
- (d) mostly interior.

interior chip in 72315, located several centimeters from the column sample. Assuming a simple exposure history would suggest an exposure of about 5 Ma, but from the shape of the track density profile in the whole column it can be shown that the boulder has experienced a complicated exposure extending over several million years in an orientation different from that at the present, and that a spall occurred about 0.27 Ma ago (above).

Keith et al. (1974a,b) tabulated count data for cosmogenic nuclides without specific discussion. Yokoyama et al. (1974) used the data of Keith et al. (1974a,b) in discussing ^{22}Na - ^{26}Al relationships. They found the sample to be unsaturated in ^{26}Al , suggesting very short exposure times (of the order of 10^5 years), consistent with the Hutcheon et al. (1974a) results.

PROCESSING

Several early allocations were made from small documented chips (,2 to ,6 and ,11) removed from 72315 prior to sawing. In 1973/4 sawing produced the W end piece ,16 (17.1 g, now stored at Brooks; Fig. 2a) and E end piece,17 (now 70.6 g). Piece ,17 was resawn to produce the slab ,18 (which was subsequently entirely subdivided, Fig. 3) and a second unnumbered slab that was also entirely subdivided (Fig. 2b). During sawing a large piece (,15, 7.8 g) fell off (Fig. 2a). Few of the slab pieces have been used for allocations.

Table 2: Fission track data and calculated ages for apatites in 72315 (Hutcheon et al., 1974b). a=assuming cosmic ray induced fission. b=assuming negligible cosmic ray induced fission.

	72315 Apatite 1	72315 Apatite 2
Uranium content (ppm)	72	78
Total track density (t/cm^2)	1.55×10^8	1.58×10^8
Reactor induced (t/cm^2)	2.82×10^7	3.06×10^7
Cosmic ray (t/cm^2)	3.0×10^6	3.0×10^6
C.R. induced fission* (t/cm^2)	2.82×10^7	3.06×10^7
Age† (m.y.) (a)	2.51×10^9	2.30×10^9
(b)	3.09×10^9	2.94×10^9

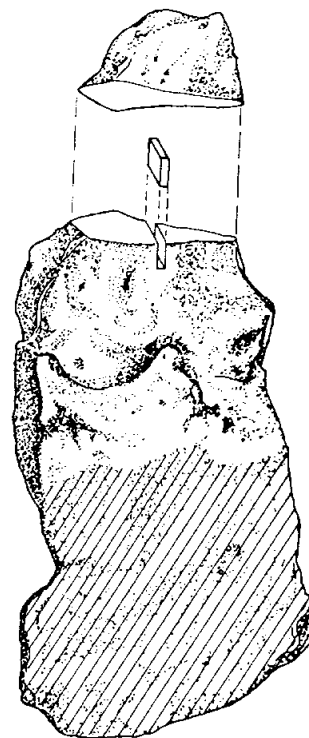


Figure 6: Sketch of the crevice side of 72315, showing the orientation of the track column extending through the sample. Height of the sample is about 10 cm. (Hutcheon et al., 1974a).

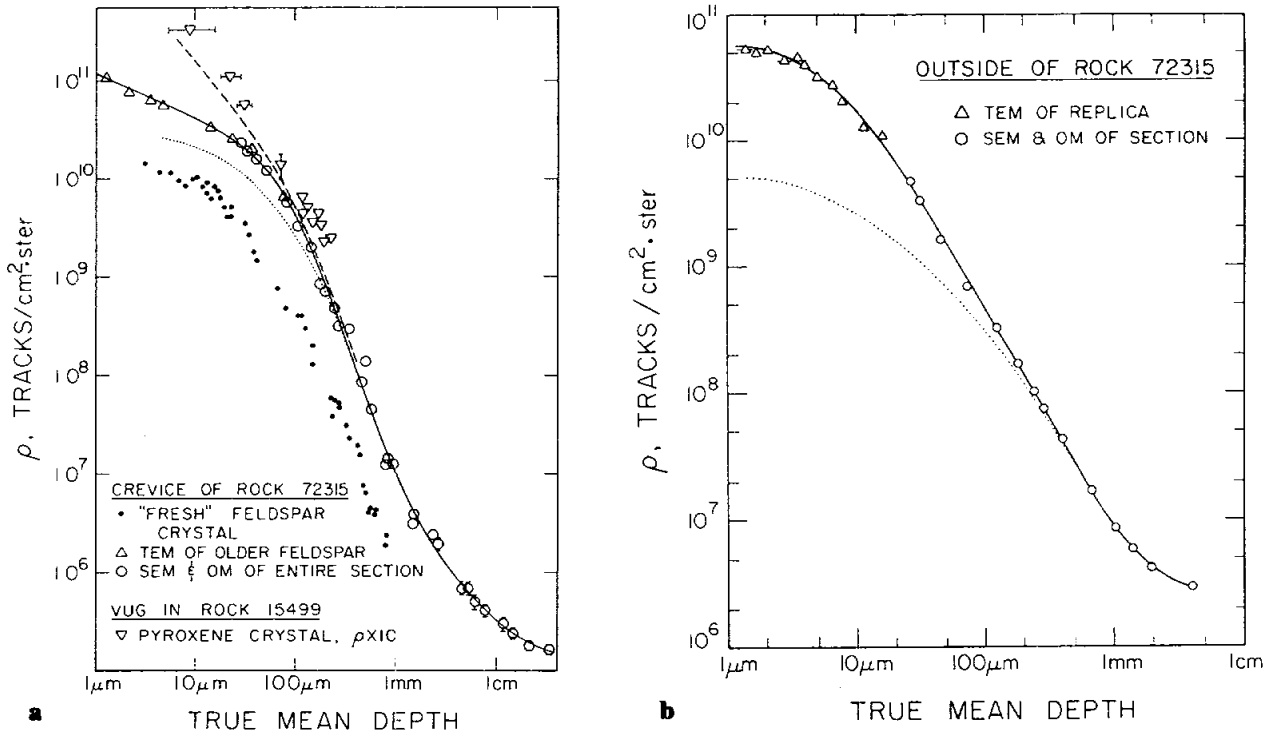


Figure 7: Track density profiles through interior (a) and exterior (b) parts of 72315. Triangles are for TEM measurements and open circles are for SEM measurements. (Hutcheon et al., 1974a).

72335

Micropoikilitic Impact Melt Breccia

St. 2, 106.9 g

INTRODUCTION

72335 is a fine-grained, clast-bearing impact melt with a poikilitic texture. It was collected to sample the contact of the matrix of Boulder 2, Station 2, with an apparent clast, represented by 72315 (see section on Boulder 2, Station 2). However, like 73215, it is identical in all analyzed respects with all other samples from Boulder 2. Nonetheless, the literature about 72335 is distinct in that a granulite clast dominated the early allocations, rather than the matrix, leading to a temporary inference that it was distinct. Although no definitive geochronological data exist, a

general assumption is that 72335 crystallized at the same time as other melts of similar petrography and chemistry at the Apollo 17 site, i.e. 3.86 Ga ago. The sample, 8 x 1.5 x 1.5 cm, is angular and greenish gray (5GY 6/1) (Fig. 1). It is tough, homogeneous, and lacks penetrative fractures. Clasts larger than 1 mm compose less than 10% of the rock. The exposed surface (N,T, part of E) of 72335 has a thin patina and many zap pits. Irregular cavities with drusy crystals form about 30% of the surface; they range up to 1 mm, although most are about 0.2 mm across.

72335 is so similar to other samples from Boulder 2 that it will not be

described here in detail, but specific studies are referenced. It was studied mainly under a consortium led by the Caltech group (Dymek *et al.*, 1976a), but not in as much detail as 72395. The description of 72395 can be assumed as a description of 72335. Following chipping of a few pieces for allocation, the W end of the sample was sawn off (.16; 33.6 g; Fig. 2) and stored at Brooks.

PETROGRAPHY

All five samples from Boulder 2 are very similar in petrography. Dymek *et al.* (1976a)

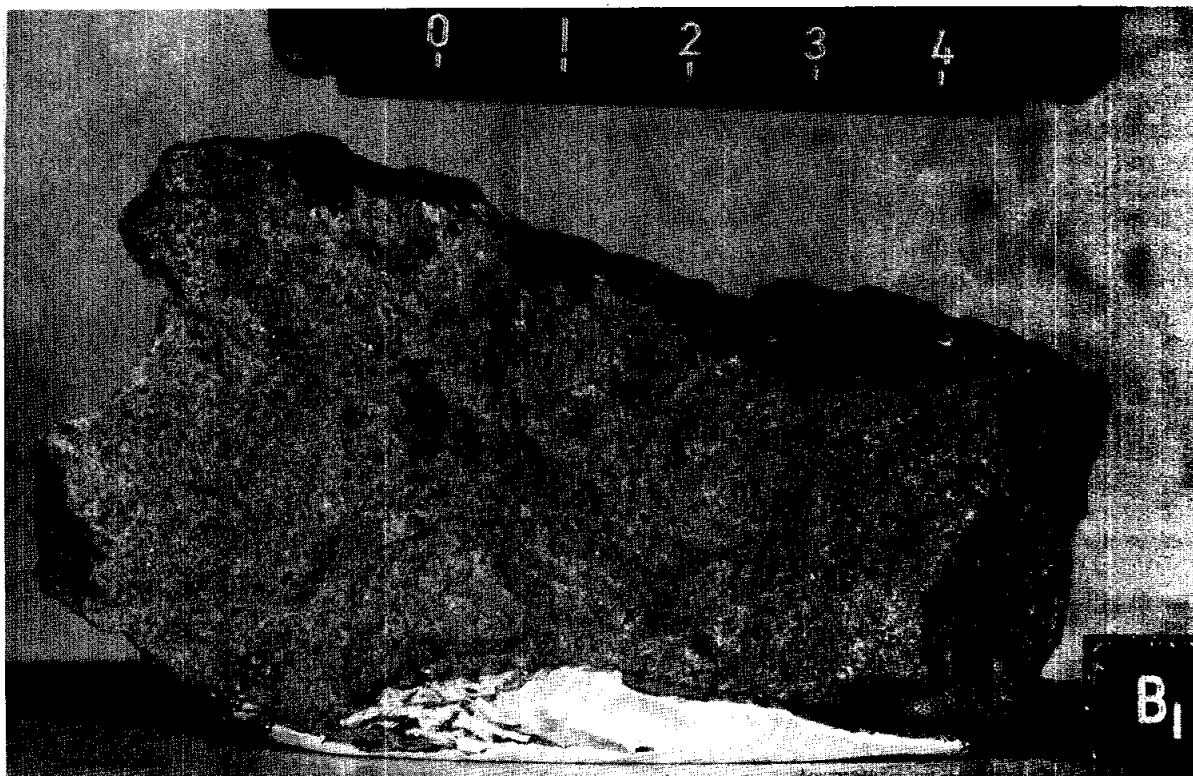


Figure 1: Broken B face of sample 72335, showing irregular vugs and homogeneous character. The exposed surface (at the top) has a darker-colored patina. Scale in centimeters. S-73-23543.



Figure 2: Sawn face of W end piece 72335,16 showing high proportion of vugs. Small divisions on scale are 1 mm. S-76-24377.

gave descriptions of the petrography subsequent to a briefer description by Albee et al. (1974b) and Dymek et al. (1976b). They did not give individual descriptions of the petrography, and that practice is for the most part followed here; thus, for a description and mineral diagrams of 72335 matrix see sample 72395.

Dymek et al. (1976a,c) described the sample, following a briefer description by Albee et al. (1974b). They noted that the earliest allocations had been of a 1-cm clast of a fine-grained, granulitic anorthositic norite (feldspathic granulite), and that the actual matrix was similar to the other Boulder 2 samples (Fig. 3). The description by Simonds et al. (1974) is of the granulitic clast: feldspars 25 to 500 microns and mafic grains 10 to 30 (rarely 100) microns. The paragenesis of Engelhardt (1979) (ilmenite crystallizing later than pyroxene) is for the actual matrix.

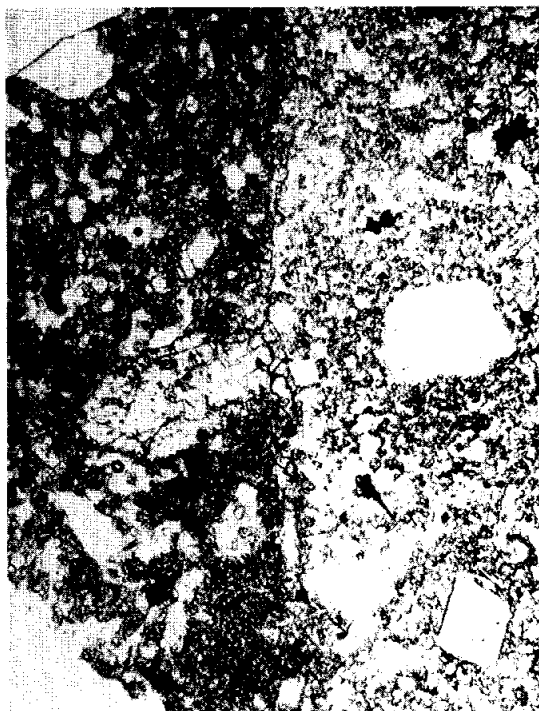


Figure 3: Photomicrograph of 72335,5 showing poikilitic impact melt matrix (left) and feldspathic granulite clast (right). Plane transmitted light. Field of view about 1 mm wide.

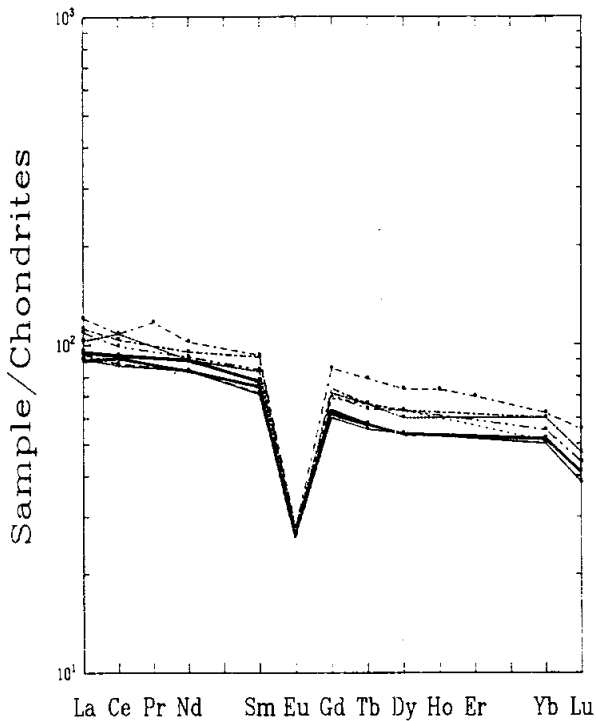


Figure 4: Rare earth element abundances of matrix samples in 72335 (bold lines) with other Boulder 2 data for comparison.

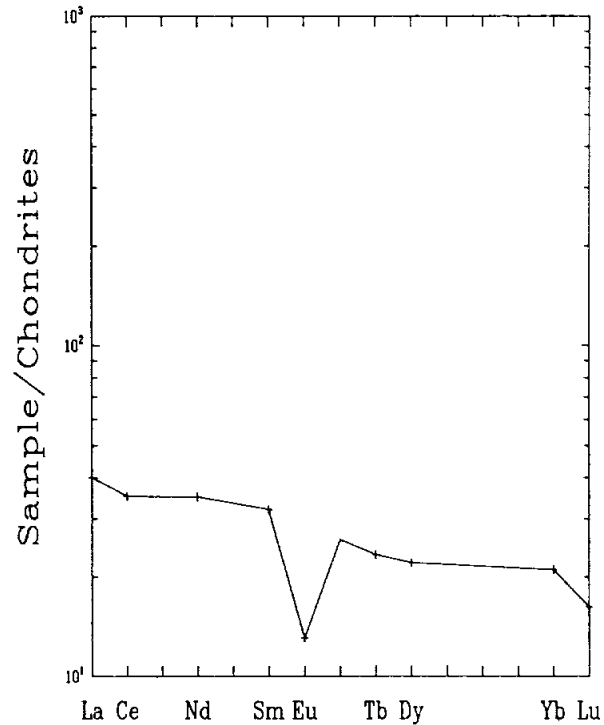


Figure 5: Rare earth element abundances of feldspathic granulite clast in 72335.

CHEMISTRY

Chemical analyses of the matrix and the granulitic clast are tabulated separately (Tables 1 and 2 respectively). The rare earth elements are also plotted separately (Figs. 4 and 5). The chemistry of the matrix is identical with that of other Boulder 2 samples, with rare earths at the lower end of the range (Fig. 4). In the earliest publications (e.g. Laul and Schmitt, 1974a,b), the granulite clast was assumed to represent bulk rock. Later publications (e.g. Laul and Schmitt, 1975) recognize that the first allocations were atypical, but instead of recognizing the presence of a granulitic clast, suggested that the 72335 matrix was heterogeneous. The distinct siderophile ratios of the feldspathic sample (Group 3, cf. Group 2 of the other matrices) was recognized. It is possible that the sample of feldspathic granulite analyzed included matrix contamination, as it

was not specifically sampled as a clast.

RADIOGENIC ISOTOPES AND CHRONOLOGY

Tera et al. (1974a) reported Rb and Sr isotopic data for a split that is probably at least mainly a feldspathic granulite clast, without specific discussion. $^{87}\text{Rb}/^{86}\text{Sr}$ (0.03695) and $^{87}\text{Sr}/^{86}\text{Sr}$ (0.70136 \pm 5) are distinct from those of the matrix of the other Boulder 2 samples and correspond with TBABI of 4.40 Ga.

EXPOSURE

MacDougall et al. (1974) and Hutcheon et al. (1974b) studied a small undocumented chip, supposedly from the surface, for tracks. However, there was no track density gradient discernable on the edge examined. Interior feldspars

showed solar flare track gradients extended over several grains; a maximum density of more than $5 \times 10^8 \text{ cm}^{-2}$ fell to about $3 \times 10^7 \text{ cm}^{-2}$, then rose again. Large variations in track densities occurred adjacent to olivines and feldspars. The results may suggest some irradiation of grains prior to compaction, unusual exposure geometries, or annealing differences.

PROCESSING

A few small chips were first taken for allocations. One of these earlier chips (,2) appears to have been a clast (or dominantly a clast) of feldspathic granulite. Further chipping was made for allocations of the matrix. In 1975, a saw cut was made to remove the W end (,16; 33.6 g, Fig. 2) for remote storage at Brooks.

Table 1: Chemical analyses of bulk rock/matrix of 72335.

Split	,6	,7
wt %		
SiO ₂		
TiO ₂	1.6	1.6
Al ₂ O ₃	18.2	18.3
Cr ₂ O ₃	0.190	0.200
FeO	8.6	8.8
MnO	0.112	0.114
MgO	11	12
CaO	10.7	11.0
Na ₂ O	0.61	0.60
K ₂ O	0.27	0.34
P ₂ O ₅		
ppm		
Sc	16	18
V	50	50
Co	23	26
Ni	200	230
Rb		
Sr		
Y		
Zr	450	450
Nb		
Hf	10	10
Ba	300	300
Th	4.6	4.8
U	1.3	1.3
Cs		
Ta	1.5	1.5
Pb		
La	31.6	30.0
Ce	82	80
Pr		
Nd	54	50
Sm	14.1	13.5
Eu	1.84	1.82
Gd		
Tb	2.7	3.1
Dy	17	20
Ho		
Er		
Tm		
Yb	10.4	10.2
Lu	1.4	1.4
Li		
Be		
B		
C		
N		
S		
F		
Cl		
Br		
Cu		
Zn		
ppb		
Au	4	4
Ir		
	(1)	(1)

References and methods:

(1) Laul and Schmitt (1974); INAA

Table 2: Chemical analyses of a feldspathic granulite clast in 72335.

Split	,2	,2	,2
wt %			
SiO ₂			
TiO ₂	0.60		
Al ₂ O ₃	27.3		
Cr ₂ O ₃	0.100		
FeO	4.8		
MnO	0.060		
MgO	8		
CaO	15.4		
Na ₂ O	0.45		
K ₂ O	0.12		0.1037
P ₂ O ₅			
ppm			
Sc	8.0		
V	30		
Co	25	28	
Ni	330	360	
Rb		2.0	1.882
Sr		145	147.8
Y			
Zr	150		
Nb			
Hf	4.2		
Ba	120	(a)120	
Th	2.4		
U	0.80	0.71	
Cs		0.095	
Ta	0.59		
Pb			
La	13.2		
Ce	31		
Pr			
Nd	21		
Sm	5.8		
Eu	0.90		
Gd			
Tb	1.1		
Dy	7.0		
Ho			
Er			
Tm			
Yb	4.2		
Lu	0.55		
Li			
Be			
B			
C			
N			
S			
F			
Cl			
Br			
Cu			
Zn		1.7	
ppb			
Au	4	5.3	
Ir	12	15	
I			
At			
Ga			
Ge			
As			
Se		67	
Mo			
Tc			
Ru			
Rh			
Pd			
Ag		0.70	
Cd		(b)80	
In		0.8	
Sn			
Sb		1.5	
Te			
W			
Re		1.4	
Os			
Pt			
Hg			0.58
Tl			
Bi			
	(1)	(1)	(2)

Notes:

(a) tabulated as Pd in original reference

(b) authors say probably high as a result of contamination.

References and methods:

(1) Laul and Schmitt (1974a,b,c); Laul et al. (1974); INAA, RNAA

(2) Terra et al. (1974a); ID/MS

72355**Micropoikilitic Impact Melt Breccia
St. 2, 367.4 g****INTRODUCTION**

72355 is a fine-grained, clast-bearing impact melt with a poikilitic texture. It was collected to sample the matrix of Boulder 2, Station 2 (see section on Boulder 2, Station 2). It is identical in all analyzed respects with all other samples from Boulder 2. Although no definitive geochronological data exist, a general assumption is that 72355 crystallized at the same time as other melts of similar petrography and chemistry at the Apollo 17 site, i.e. 3.86 Ga ago. The sample, 10 x 6.5 x 6.5 cm, is blocky/angular and light olive gray (5Y 6/1) (Fig. 1). It is tough,

homogeneous (although apparently less so than other Boulder 2 samples) and has a few non-penetrative fractures. Clasts larger than 1 mm compose less than about 10% of the rock. The exposed surface (mainly N) of 72355 has a patina and many zap pits. Vugs form 3-4% of the rock, with some as large as several millimeters. All have crystal linings, and the larger vugs have larger crystals.

72355 is so similar to other samples from Boulder 2 that it will not be described here in detail, but specific studies are referenced. It was studied mainly under a consortium led by the Caltech group (Dymek *et*

al., 1976a), but not in as much detail as 72395. The description of 72395 can be assumed as a description of 72355. Only a few chips were taken from the sample for allocation and it was never sawn.

PETROGRAPHY

All five samples from Boulder 2 are very similar in petrography. Dymek *et al.* (1976a) gave descriptions of the petrography subsequent to a briefer description by Albee *et al.* (1974b) and Dymek *et al.* (1976b). They did not give individual

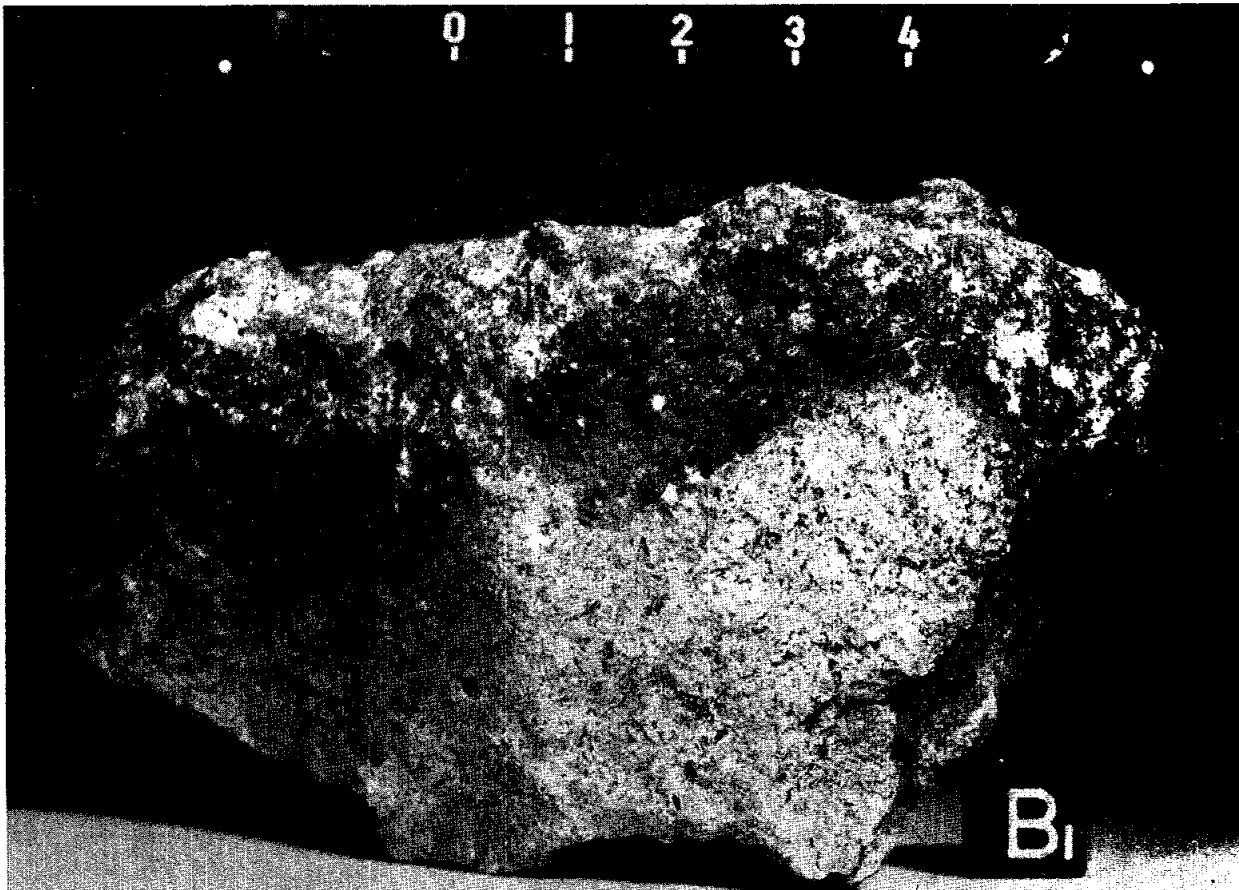


Figure 1: B face of sample 72355. The exposed surface (at the top) has a darker-colored patina; the lower right area is broken surface. Scale in centimeters. S-73-17285.

descriptions of the petrography, and that practice is for the most part followed here; thus, for a description and mineral diagrams of 72355 matrix see sample 72395.

Dymek et al. (1976a,c) described the sample, following a briefer description by Albee et al. (1974b), noting that the matrix was similar to the other Boulder 2 samples (Fig. 2). Simonds et al. (1974) described the sample as clast-rich ophitic, with feldspars 10 to 50 microns and mafic grains 10 to 100 microns, showing a photomicrograph. Engelhardt (1979) tabulated the paragenesis as one with ilmenite crystallizing later than pyroxene.

CHEMISTRY

Chemical analyses of the bulk matrix are given in Table 1, with the rare earth elements plotted in

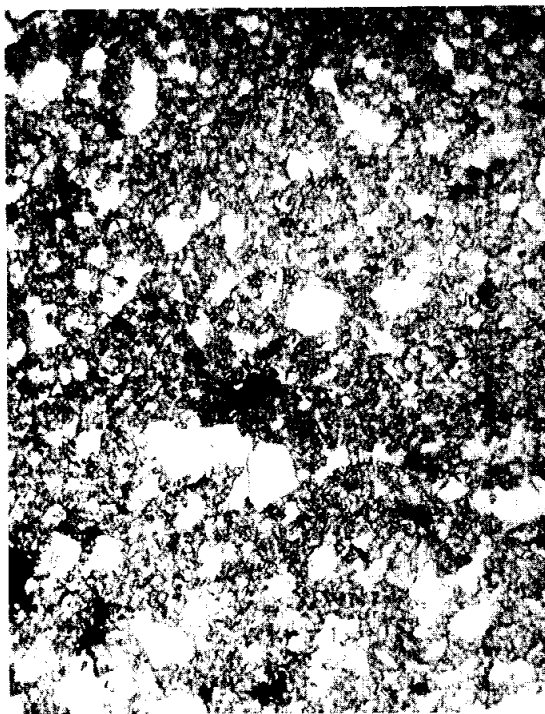


Figure 2: Photomicrograph of 72355,4, showing poikilitic impact melt matrix. Plane transmitted light. Field of view about 1 mm wide.

Figure 3. The chip analyzed by Laul and Schmitt (1974a,b,c) was an exterior chip, but is in any case similar in chemistry to the other Boulder 2 matrix samples. The siderophiles (equivalent to 2.4% chondritic contamination) are assigned to Group 2, correlated with Serenitatis.

RADIOGENIC ISOTOPES AND CHRONOLOGY

Tera et al. (1974a) reported Rb and Sr isotopic data for a matrix split without specific discussion. $^{87}\text{Rb}/^{86}\text{Sr}$ (0.1523) and $^{87}\text{Sr}/^{86}\text{Sr}$ (0.70855 \pm 6) are similar to those of the matrix of the other Boulder 2 samples, and correspond with TBABI of 4.29 Ga.

EXPOSURE

Keith et al. (1974a,b) tabulated cosmogenic nuclide gamma ray count rate data, without specific discussion.

PROCESSING

A few small chips were taken for allocations, but the sample was never sawn or extensively subdivided.

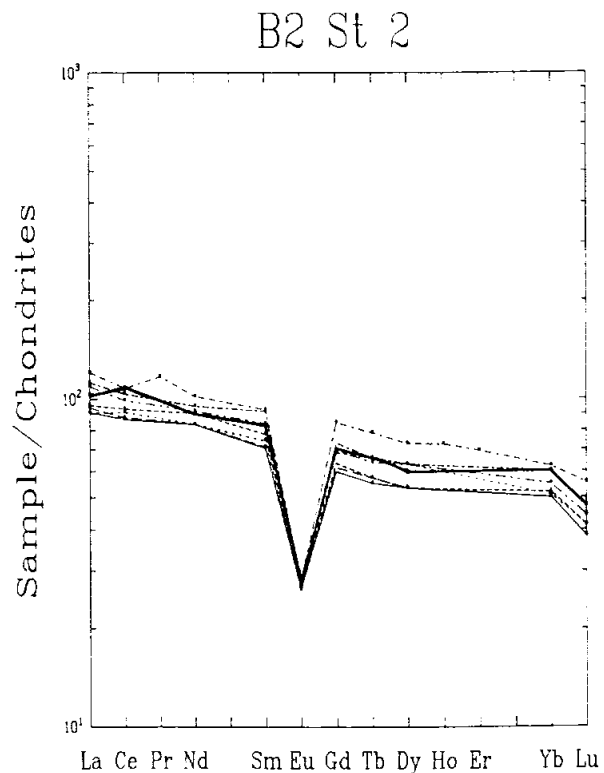


Figure 3: Rare earth element abundances of matrix samples in 72355 (bold line) with other Boulder 2 data for comparison.

Table 1: Chemical analyses of bulk rock/matrix of 72355.

Split	.7	.7	.0	.5	Split
wt %					wt %
SiO ₂					SiO ₂
TiO ₂	1.6				TiO ₂
Al ₂ O ₃	18.8				Al ₂ O ₃
Cr ₂ O ₃	0.193				Cr ₂ O ₃
FeO	8.7				FeO
MnO	0.114				MnO
MgO	12				MgO
CaO	11.1				CaO
Na ₂ O	0.70				Na ₂ O
K ₂ O	0.33		0.304	0.3828	K ₂ O
P ₂ O ₅					P ₂ O ₅
ppm					ppm
Sc	16				Sc
V	50				V
Co	37	34			Co
Ni	340	310			Ni
Rb		8.0		8.65	Rb
Sr		1.57		164.7	Sr
Y					Y
Zr	500				Zr
Nb					Nb
Hf	12				Hf
Ba	280	(a)380			Ba
Th	6.1		5.3		Th
U	1.8	2.00	1.39		U
Cs		0.280			Cs
Ta	1.6				Ta
Pb					Pb
La	34				La
Ce	95				Ce
Pr					Pr
Nd	54				Nd
Sm	15.0				Sm
Eu	1.92				Eu
Gd					Gd
Tb	3.1				Tb
Dy	19				Dy
Ho					Ho
Er					Er
Tm					Tm
Yb	12				Yb
Lu	1.6				Lu
Li					Li
Be					Be
B					B
C					C
N					N
S					S
F					F
Cl					Cl
Br					Br
Cu					Cu
Zn		2.4			Zn
ppb					ppb
Au	3	4.9			Au
Ir	10	7.3			Ir
I					I
At					At
Ga					Ga
Ge					Ge
As					As
Se		75			Se
Mo					Mo
Tc					Tc
Ru					Ru
Rh					Rh
Pd					Pd
Ag		0.87			Ag
Cd		5.1			Cd
In		0.2			In
Sn					Sn
Sb		2.2			Sb
Te					Te
W					W
Re		0.73			Re
Os					Os
Pt					Pt
Hg					Hg
Tl		0.24			Tl
Bi					Bi
	(1)	(1)	(2)	(3)	

References and methods:

- (1) Lail and Schmitt (1974a,b,c); INAA/RNAA
- (2) Keith et al. (1974a,b); Gamma ray spectroscopy
- 3) Tera et al. (1974a); ID/MS

Notes:

(a) listed as Bd in original reference.

72375

Micropoikilitic Impact Melt Breccia

St. 2, 16.16 g

INTRODUCTION

72375 is a fine-grained, clast-bearing impact melt with a poikilitic texture. It was collected to sample the matrix of Boulder 2, Station 2 (see section on Boulder 2, Station 2). It is identical in all analyzed respects with all other samples from Boulder 2. Although no definitive geochronological data exist, a general assumption is that 72375 crystallized at the same time as other melts of similar petrography and chemistry at the Apollo 17 site, i.e. 3.86 Ga ago. The sample, about 4 cm long and the smallest collected from Boulder 2, is angular and green-gray. It has a patina and zap pits on the exposed surface (mainly T), and vugs on the broken surface. Originally the sample was retained as a refrigerated reserve and not studied under binocular microscope, but was later chipped for some allocations.

72375 is so similar to other samples from Boulder 2 that it will not be described here in detail, but specific studies are referenced. It was studied mainly under a consortium led by the Caltech group (Dymek *et al.*, 1976a), but not in as much detail as 72395. The description of 72395 can be assumed as a description of 72375. Only a few chips were taken from the sample for allocation, and it was never sawn.

PETROGRAPHY

All five samples from Boulder 2 are very similar in petrography. Dymek *et al.* (1976a) gave descriptions of the petrography subsequent to a briefer description by Albee *et al.* (1974b) and Dymek *et al.* (1976b). They did not give individual descriptions of the petrography, and that practice is for the most part

followed here; thus for a description and mineral diagrams of 72375 matrix see sample 72395.

Dymek *et al.* (1976a,c) described the sample, following a briefer description by Albee *et al.* (1974b), noting that the matrix was similar to the other Boulder 2 samples (Fig. 2). Simonds *et al.* (1974) merely tabulated the sample as clast-rich ophitic.

CHEMISTRY

Chemical analyses of the bulk matrix are given in Table 1, with the rare earth elements plotted in Figure 3. The chip analyzed was an exterior chip, but is in any case similar in chemistry to the other Boulder 2 matrix samples. The siderophiles are assigned to Group 3, correlated with Serenitatis.

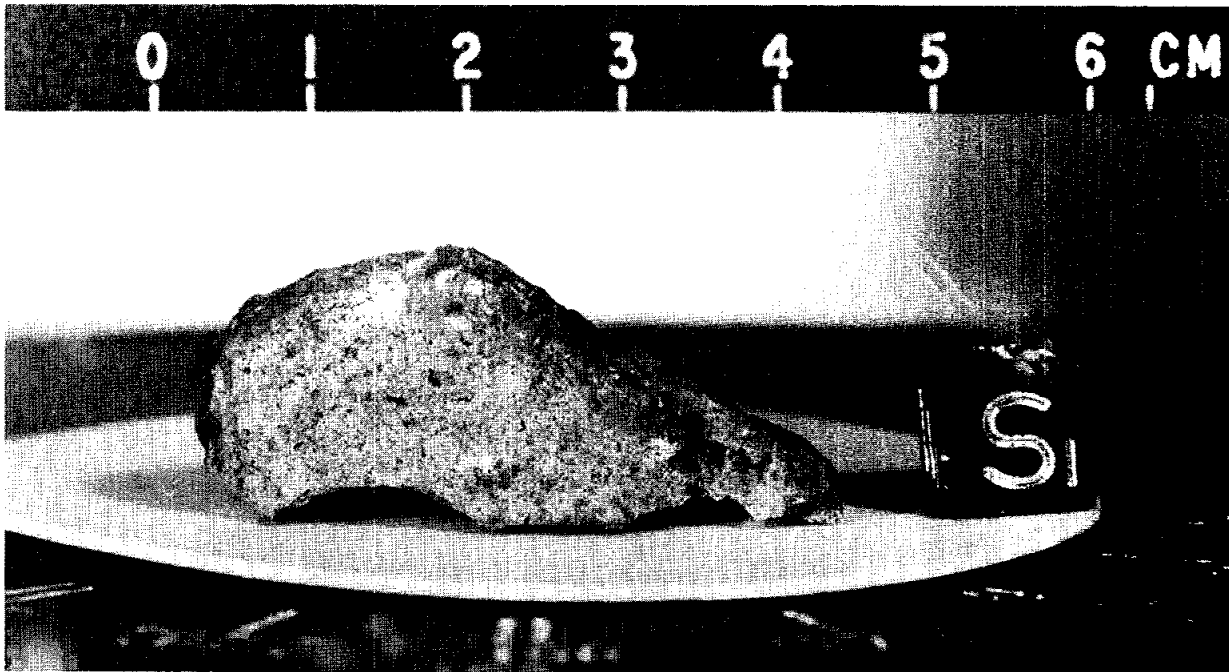


Figure 1: S face of sample 72375. The exposed surface (at the top) has a darker-colored patina; the lower area is broken surface. Scale in centimeters. S-73-15356.

RADIOGENIC ISOTOPES AND CHRONOLOGY

Tera et al. (1974a) reported Rb and Sr isotopic data for a matrix split without specific discussion. $^{87}\text{Rb}/^{86}\text{Sr}$ (0.1173) and $^{87}\text{Sr}/^{86}\text{Sr}$ (0.70632 \pm 6) are similar to those of the matrix of the other Boulder 2 samples and correspond with T_{BABI} of 4.28Ga.

PROCESSING

Three small chips were taken from a single location for allocations, but the sample was never sawn or extensively subdivided.

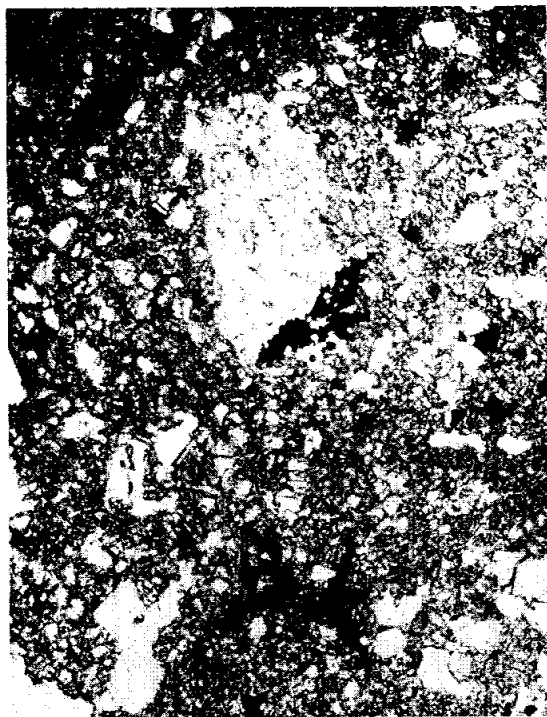


Figure 2: Photomicrograph of 72375,5 showing poikilitic impact melt matrix. Plane transmitted light. Field of view about 1 mm wide.

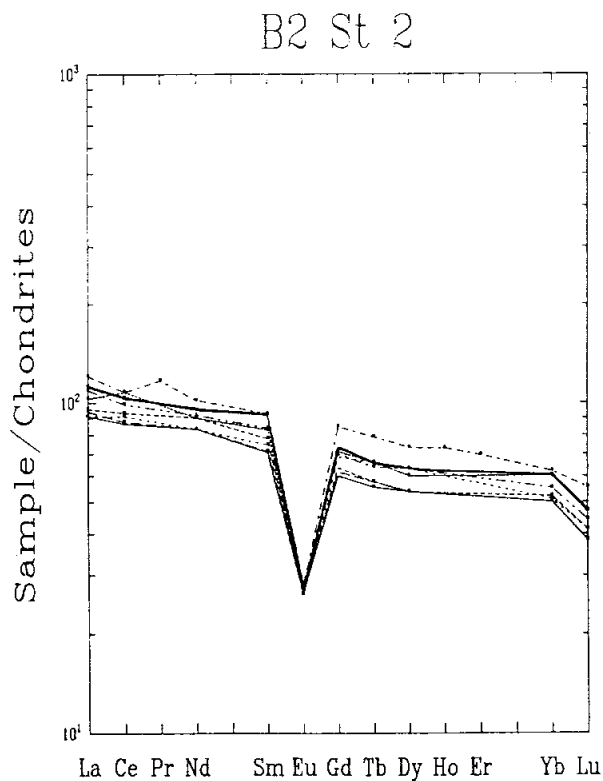


Figure 3: Rare earth element abundances of matrix samples in 72375 (bold line) with other Boulder 2 data for comparison.

**Table 1: Chemical analyses of bulk rock/matrix of
72375.**

Split	,2	,2	,2
wt%			
SiO ₂			
TiO ₂	1.5		
Al ₂ O ₃	18.2		
Cr ₂ O ₃	0.178		
FeO	8.8		
MnO	0.112		
MgO	12		
CaO	10.8		
Na ₂ O	0.67		
K ₂ O	0.27		0.2696
P ₂ O ₅			
ppm			
Sc	15		
V	50		
Co	34	34	
Ni	320	320	
Rb		6.2	6.64
Sr		149	163.5
Y			
Zr	450		
Nb			
Hf	11		
Ba	300	(a)370	
Th	5.7		
U	2.0	1.85	
Cs		0.250	
Ta	1.4		
Pb			
La	37		
Ce	91		
Pr			
Nd	57		
Sm	16.6		
Eu	1.82		
Gd			
Tb	3.1		
Dy	20		
Ho			
Er			
Tm			
Yb	12		
Lu	1.6		
Li			
Be			
B			
C			
N			
S			
F			
Cl			
Br			
Cu			
Zn		2.3	
ppb			
Au	4	5.3	
Ir	10	8.5	
I			
At			
Ga			
Ge			
As			
Se		90	
Mo			
Tc			
Ru			
Rh			
Pd			
Ag		0.82	
Cd		7.2	
In		0.2	
Sn			
Sb		2.2	
Te			
W			
Re		0.84	
Os			
Pt			
Hg			
Tl		0.59	
Bi			

References and methods:

- (1) Laul and Schmitt (1974a,b,c), Laul et al. (1974); INAA/RNAA
(2) Tera et al. (1974a); ID/MS

Notes:

- (a) listed as Bd in original reference.

(1) (1) (2)

72395

Micropoikilitic Impact Melt Breccia

St. 2, 536.4 g

INTRODUCTION

72395 is a fine-grained, clast-bearing impact melt with a poikilitic texture. It was sampled as typical groundmass of Boulder 2, Station 2 (see section on Boulder 2, Station 2, Fig. 1). Although no definitive geochronological data exist, a general assumption is that 72395 crystallized at the same time as other melts of similar petrography and chemistry at the Apollo 17 site, i.e. 3.86 Ga ago. The sample, 12 x 9 x 5.5 cm, is angular, tabular, and light olive gray (N5Y 6/1). It is tough and homogeneous. Its exposed surface (T,N,W) has many zap pits and is

knobby and rounded. The broken surface (S,E,B) is angular and hackly (Fig. 1). Vugs are present on the broken surface, ranging from 0.2 to 2 mm. They tend to be irregular but some are elongate, and many are lined with drusy crystal terminations.

72395 is typical of the samples from Boulder 2, and has only a few clasts larger than a few millimeters. Plagioclases and pale green olivine are the most abundant. The few large lithic clasts are typically fine-grained feldspathic rocks, including granulites. The groundmass contains abundant vesicles smaller than 25 microns, and consists

mainly of plagioclase and pigeonite. The pigeonite forms small oikocrysts (less than 100 microns). The smaller clasts are difficult to distinguish from groundmass phases. The total clast content of the less-than-1-mm fraction is probably 10 to 20%.

Most of the studies of 72395 were conducted under a consortium led by the Caltech group (Dymek *et al.*, 1977). Following chipping of a few small pieces for petrographic study, a slab was cut across 72395 (Fig. 2). Many other small pieces and two larger end pieces were obtained (Fig. 3).

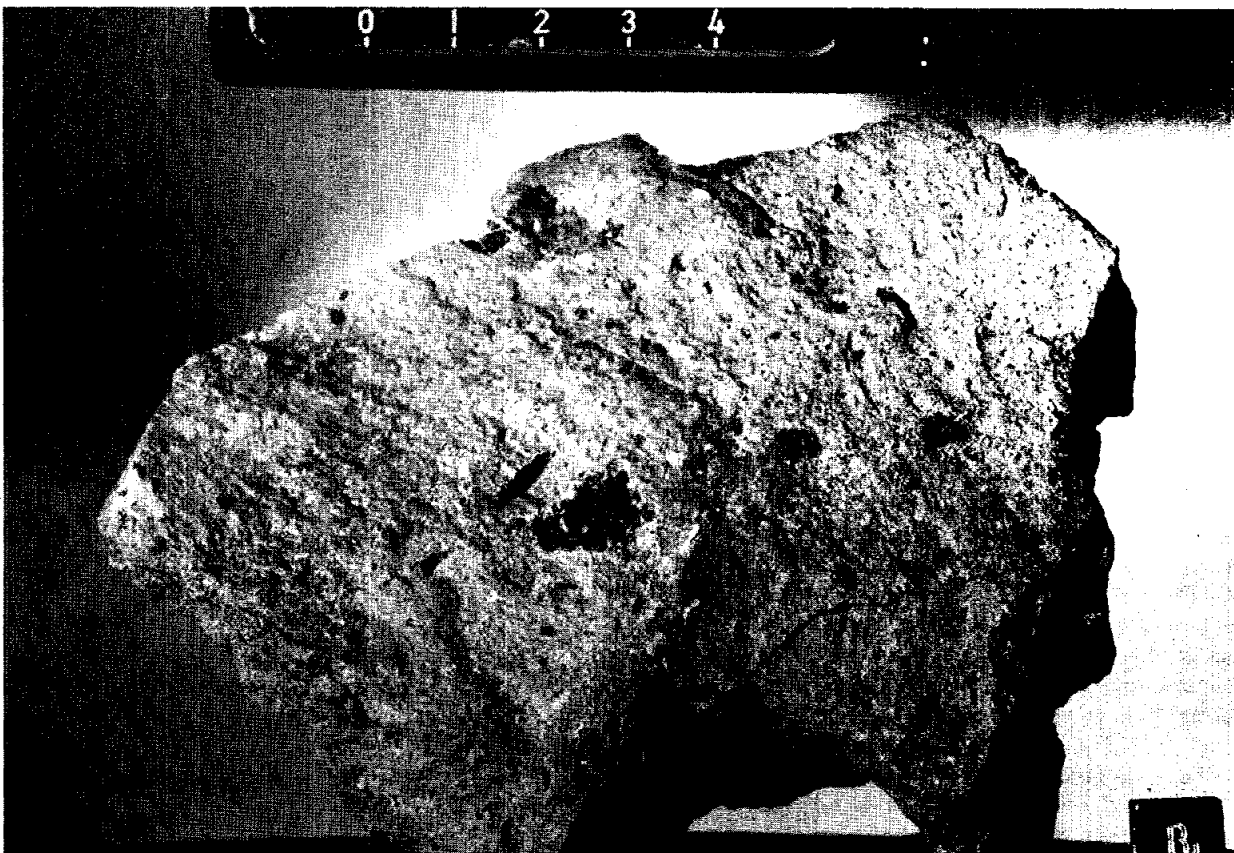


Figure 1: Broken surface of 72395. The sample is homogeneous and structureless, and few clasts are visible at this scale. Slit vesicles are common. The dark feature in the center is a vuggy area lined with pyroxene and plagioclase crystals. Scale in centimeters. S-73-16052.



Figure 2: First cut across 72395. The second cut to produce a slab was made in ,8. Cube is 2.54 cm across. S-76-21619.

PETROGRAPHY

All five samples from Boulder 2 are very similar in petrography. Dymek *et al.* (1977) gave detailed descriptions of the petrography subsequent to the brief description by Albee *et al.* (1974b). They did not give separate descriptions of the petrography, and that practice is for the most part followed here. 72395 has the most thin sections and will be the "type" for description. The mineral diagrams for all 5 samples will be included in this section for ease of comparison.

The samples are rather homogeneous and consist of several percent clasts (1 mm to 1 cm) in a fine-grained crystalline matrix. The

matrix (grains less than 1 mm) is composed of abundant tiny clasts and a groundmass that crystallized from the melt (Fig. 4a) (Dymek *et al.*, 1976a, Simonds *et al.*, 1974). Simonds *et al.*, (1974) referred to these samples as "matrix supported breccias" to emphasize the abundance of fine-grained material. They labelled 72395 as clast-rich ophitic, with matrix feldspars 10 to 40 microns long and matrix mafic minerals 20 to 100 microns across. The texture appears to be distinct from other coarser poikilitic boulders at the Apollo 17 landing site. Dymek *et al.* (1977) drew a distinction between clasts and groundmass at 100 microns grain size. Nonetheless, the distinction of clastic material and melt-crystallized material in the <100

micron fraction is not definite. The total amount of clastic material appears to be about 10 to 20%. Voids, approximately 10% of each sample, are commonly 1 to 25 micron dispersed angular pores, with some slit vesicles up to 250 microns long. Other vugs and vesicular pods are present. In 72395 a few areas consist of pyroxene "shells" enclosing glass of granitic composition; Dymek *et al.* (1977) believe that these represent a residual liquid from the crystallization of the melt, rather than relict clasts.

The groundmass of all samples consists of an interlocking network of tiny pyroxene oikocrysts that enclose abundant chadacrysts of plagioclase. Olivine occurs as

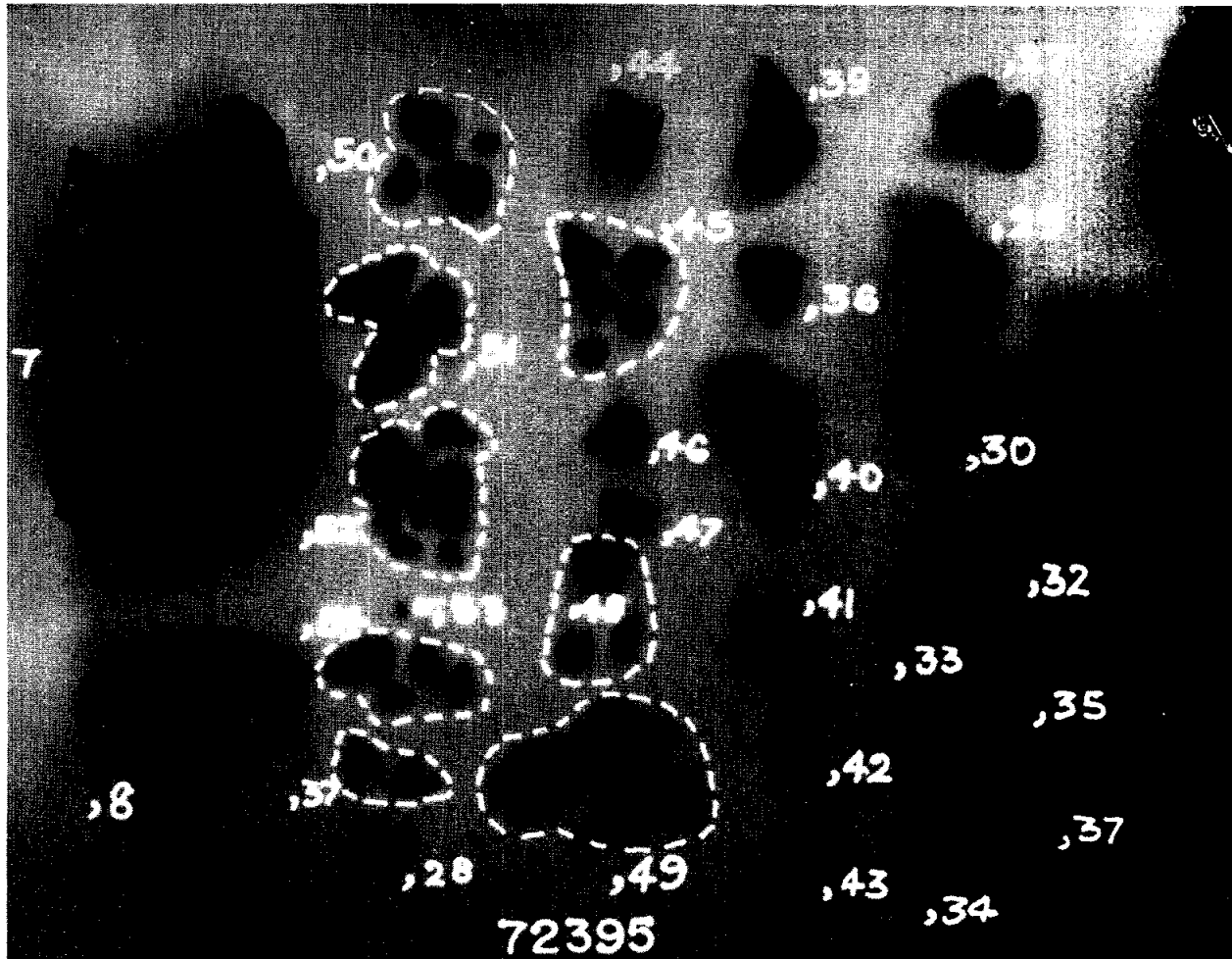


Figure 3: End pieces ,7 and ,8 and numerous smaller pieces of 72395. The slab pieces , 9 and ,10 and other small pieces are not shown. End piece ,7 shows the exterior surface with zap pits. Cube is 2 cm. S-74-15103.

angular, irregularly-shaped grains between the pyroxene oikocrysts and between pyroxene and plagioclase. Ilmenite forms irregularly-shaped grains, up to a few hundred microns long, with a sieve-texture (enclosing pyroxene and plagioclase). Engelhardt (1979) noted that ilmenite started crystallization after pyroxene finished and finished crystallization after pyroxene finished. Ilmenite contains chromite and rutile lamellae and there is some baddelyite at ilmenite margins. There is some K-rich mesostasis. Troilite and lesser Fe-metal are present. According to Dymek *et al.* (1977), the paragenetic sequence was plagioclase followed by olivine, then low-Ca pyroxene, then high-Ca pyroxene. Olivine ceased

at about the same time as high-Ca pyroxene entry, and a reaction relationship of olivine with the melt to produce the low-Ca pyroxene is suggested by resorbed-appearing olivine cores to oikocrysts. Ilmenite and other minor phases completed the crystallization.

Dymek *et al.* (1977) listed the phase abundances, phase compositions, and the bulk-chemical composition (from a microprobe point count) of 72395 (Table 1). The tabulated phase compositions appear to represent those in the melt groundmass, not clasts. Dymek *et al.* (1977) also diagrammed the mineral compositions for the five individual samples, reproduced here as Fig. 5 (plagioclases), Fig. 6 (pyroxenes),

and Fig. 7 (olivines and Fe-Ti oxides), which show the general similarity of the samples. These diagrams do not distinguish clasts from groundmass phases, but they are distinguished on a summary diagram for all rocks, reproduced here as Fig. 8. The majority of the oikocrysts are pigeonite (En₇₅Wo₂ to En₆₅Wo₁₀), with some high-Ca types (En₅₄Wo₂₈ to En₄₅Wo₄₀). The chadacrysts have a small range in composition (An₉₂ to An₈₅), but laths and blocky plagioclases between the oikocrysts have a wider range (An₉₅ to An₇₉). The olivine in the groundmass has a narrow compositional range from Fo₇₂ to Fo₆₈.

Most of the clasts in all the samples are single mineral crystals.

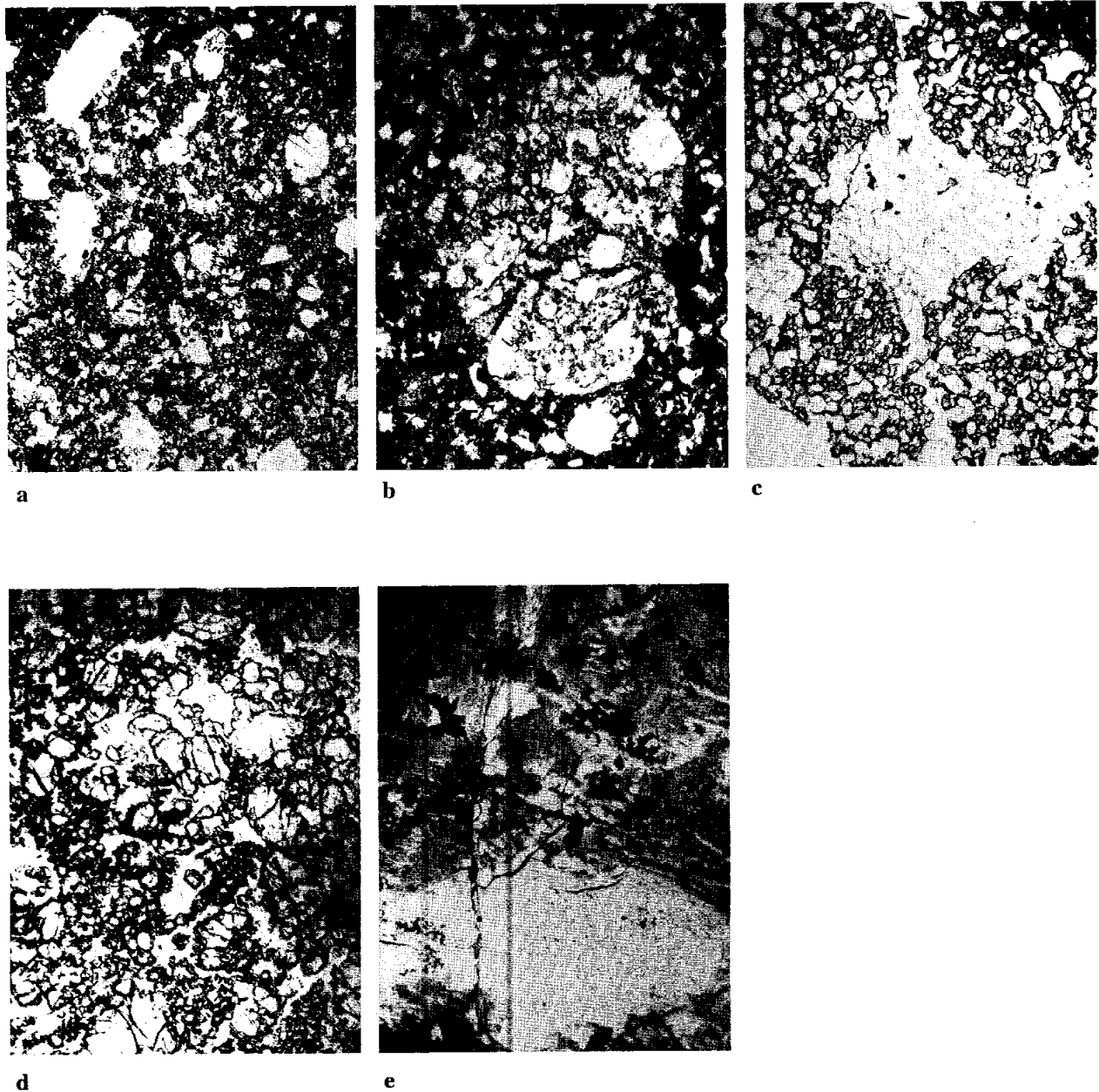


Figure 4: Photomicrographs of 72395,77. All plane transmitted light, all about 1 m field of view. a) Melt groundmass and small clasts (larger white areas), mainly plagioclases with lesser mafic minerals. b) feldspathic granulite clast, evidently a metamorphosed breccia. c) coarser poikilitic feldspathic granulite clast, of less obvious precursor material. Chadacrysts (white) are plagioclases, oikocrysts (darker) are dominantly low-Ca pyroxene. d) mafic granulite e) devitrified plagioclase (grayier areas) and ilmenite (black) in a coarse anorthositic fragment.

Plagioclase is the most abundant, then olivine; low- and high-Ca pyroxene, ilmenite, Fe-Co-Ni metal, and pink spinel clasts are present (Dymek *et al.*, 1976a). They are typically rounded to subangular, and a few show shock effects. Some display rims that are either overgrowths of the same phase or different minerals (coronas). The most prominent coronas are on pink spinels. Clast mineral compositions are included in Figures 5 to 7 for individual rocks, and distinguished on the summary diagram of Fig. 8. The clasts show a much wider range of compositions than do the groundmass minerals. Plagioclase clasts are generally unzoned, but many show conspicuous reaction rims. The most prominent reaction rims are on grains more sodic than the groundmass plagioclases, and many of these sodic rimmed grains have clouded cores. The olivines include many examples zoned to their rims by reaction with the melt, and some are mantled by low-Ca pyroxene. Both high- and low-Ca pyroxenes have overgrowth rims, and typically there is little difference in composition between clast rim and core, but some cores are distinctly more magnesian (Fig. 8); rims tend to have compositions similar to groundmass pyroxenes. Ilmenite and metal clasts typically occur with rounded to amoeboid forms. The ilmenite clasts contain tiny globules of metal, troilite, plagioclase, and pyroxene, unlike any seen in any lithic clast in Boulder 2.

Most of the lithic clasts are of feldspathic highlands lithologies, but there is a range of textures, grain sizes, and compositions. The most abundant group, termed anorthosites by Dymek *et al.* (1977), are typically fine-grained, and most are recrystallized feldspathic granulites (Figs. 4b,c). They grade with increasing mafic content into anorthositic troctolites and norites (Fig. 4d). A few cases are poikilitic, with oikocrysts up to 3 mm. One type of anorthositic fragment was distinguished by

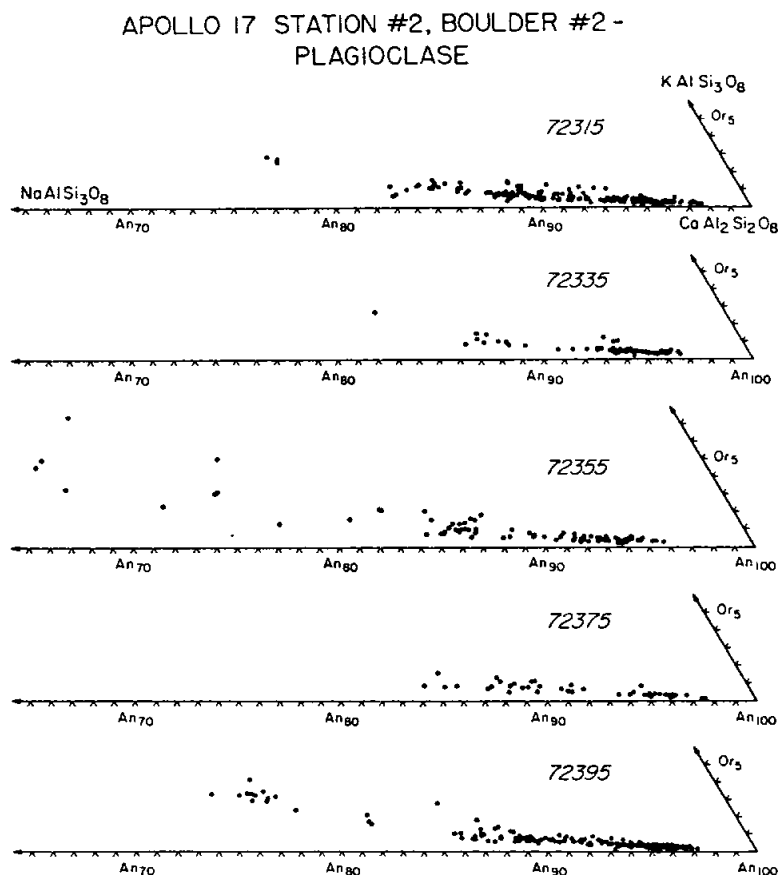


Figure 5: Compositions of plagioclases in 72315, 72335, 72355, 72375, and 72395 (Dymek *et al.*, 1976a).

Dymek *et al.* (1977) for its ilmenite content of up to 10% and its brown coloring; its plagioclases are shocked and partly devitrified (Fig. 4e). A few clasts of gabbro, troctolite, and dunite are present, including one troctolite similar to 76535, though more granulated and recrystallized. The dunites (Fo70-77) are more iron-rich than the dunite 72415.

CHEMISTRY

Chemical analyses of bulk rock (groundmass plus clasts) are given in Table 2; the major element analyses agree well with that derived by Dymek *et al.* (1976a) (Table 1). The rare earth elements are plotted as Figure 9, with other Boulder 2, Station 2 data for comparison. These chemical data

were originally reported with little discussion. The samples have a low-K Fra Mauro basalt composition, similar to many other impact melt samples at the Apollo 17 site. All the Boulder 2 samples are similar; the incompatible element abundances for 72395 are higher than the average. The samples clearly have meteoritic contamination. Laul and Schmitt (1974a) identified the siderophiles with Group 3, attributed to Serenitatis, and again like many other impact melts of low-K Fra Mauro composition at the Apollo 17 site. Jovanovic and Reed (1974a, 1975, 1980), who made analyses of leaches and residues from leaching, identified the Cl (residual)/P₂O₅ ratio with an Apollo 11, 12, and 15 basalt line, but the significance of such an identification is not apparent.

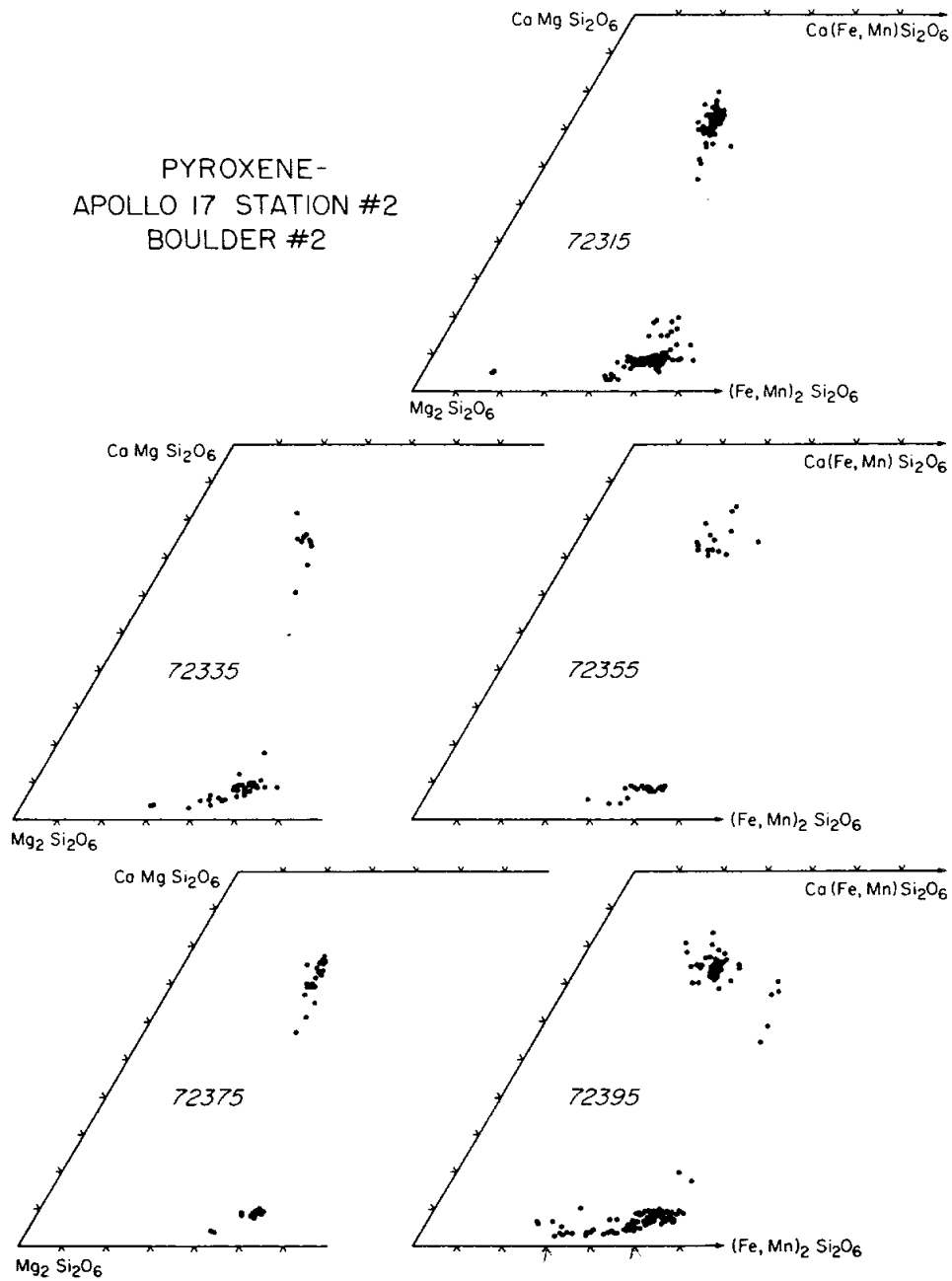


Figure 6: Compositions of pyroxenes in 72315, 72335, 72355, 72375, and 72395 (Dymek et al., 1976a).

Table 1: Phase abundances, "average" phases compositions, and bulk chemical composition derived from point-counting of 72395 (Dymek et al., 1976a).

	Plag.	Low-Ca pyx	High-Ca pyx	Olivine	Ilmenite	Troilite*	Metal*	Ca-Phos.†	Mesostasis	Bulk-composition
Vol.%	56.2 ₁	25.4 ₀	5.9 ₈	8.8 ₅	1.3 ₄	0.1 ₅	0.0 ₈	0.9 ₆	1.0 ₁	Calculated (1307 points)
±1σ	2.0 ₈	1.4 ₁	0.6 ₈	0.8 ₂	0.3 ₂	0.1 ₀	0.0 ₈	0.2 ₇	0.2 ₈	
Wt.%	50.4 ₃	28.4 ₄	6.5 ₆	10.2 ₃	2.0 ₀	0.2 ₃	0.2 ₁	1.0 ₁	0.8 ₃	
P ₂ O ₅	n.a.	n.a.	n.a.	n.a.	n.a.	n.a.	n.a.	43.15	0.08	0.44
SiO ₂	46.67	53.53	50.81	37.66	0.21	n.a.	n.a.	—	57.98	46.47
TiO ₂	0.02	0.90	1.87	0.09	54.16	0.01	<0.01	—	1.82	1.50
Al ₂ O ₃	33.51	0.99	1.95	0.02	<0.01	n.a.	n.a.	—	23.14	17.52
Cr ₂ O ₃	n.a.	0.50	0.64	0.15	0.44	n.a.	n.a.	—	0.03	0.20
CaO	17.78	2.43	18.74	0.16	n.a.	0.08	0.01	54.54	5.29	11.50
MgO	0.09	26.36	17.08	35.76	6.56	0.03	<0.01	—	0.76	12.46
FeO	0.25	15.42	8.65	26.24	37.38	63.17	92.58	—	1.40	8.96
MnO	n.a.	0.19	0.21	0.32	0.46	n.a.	n.a.	—	<0.01	0.11
BaO	<0.01	n.a.	n.a.	n.a.	n.a.	n.a.	n.a.	—	0.90	0.01
Na ₂ O	1.51	0.06	0.17	n.a.	n.a.	n.a.	n.a.	—	0.53	0.79
K ₂ O	0.13	n.a.	n.a.	n.a.	n.a.	n.a.	n.a.	—	7.21	0.13
ZrO ₂	n.a.	n.a.	n.a.	n.a.	0.01	n.a.	n.a.	—	0.07	<0.01
V ₂ O ₃	n.a.	n.a.	n.a.	n.a.	<0.01	n.a.	n.a.	—	n.a.	<0.01
Nb ₂ O ₅	n.a.	n.a.	n.a.	n.a.	0.13	n.a.	n.a.	—	n.a.	<0.01
NiO	n.a.	n.a.	n.a.	<0.01	n.a.	0.04	6.99	—	n.a.	0.02
Co	n.a.	n.a.	n.a.	n.a.	n.a.	<0.01	0.37	—	n.a.	<0.01
S	n.a.	n.a.	n.a.	n.a.	n.a.	38.52	<0.01	—	<0.01	0.09
F	n.a.	n.a.	n.a.	n.a.	n.a.	n.a.	n.a.	2.31	n.a.	0.02
Total	99.94	100.39	100.13	100.40	99.35	101.85	99.96	100.00	99.22	100.22
	An 86.1	Wo 3.3	Wo 33.5	Fo 70.6						
	Ab 13.2	En 69.4	En 45.2	Fa 29.4						
	Or 0.7	Fs 23.1								
	Others	4.2	8.1							
Average—boulder # 2–5 samples										
Vol.%	59.9	22.9	5.8	7.7	1.6	0.1	0.1	0.8	0.9	
Wt.%	54.1	25.8	6.4	9.0	2.5	0.1	0.4	0.9	0.8	

*Elemental abundances; converted to oxides for calculating bulk composition.

†Assumed 1:1 mixture of fluorapatite and whitlockite.

n.a. = Not analyzed.

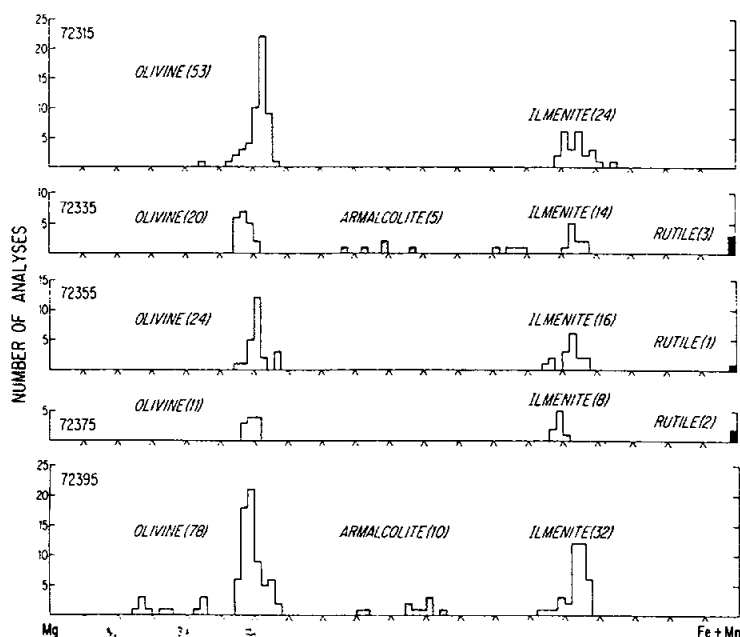


Figure 7: Compositions of olivines and Fe-Ti oxides in 72315, 72335, 72355, 72375, and 72395 (Dymek et al., 1976a).

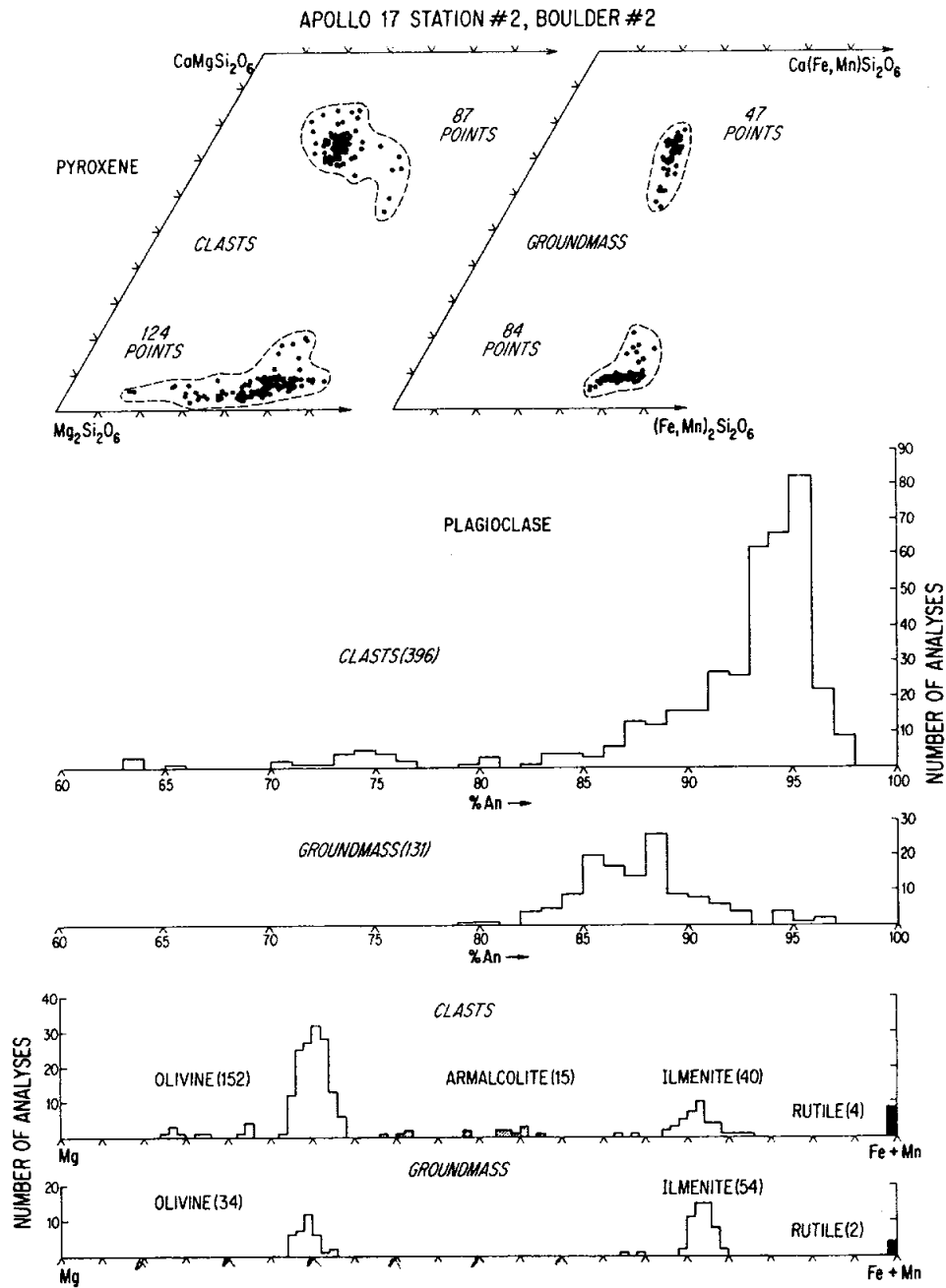


Figure 8: Summary diagram of mineral phases in 72315, 72335, 72355, 72375, and 72395 (Dymek et al., 1976a), distinguishing groundmass phases from clasts.

RADIOGENIC ISOTOPES

Tera *et al.* (1974a) reported U, Th, and Pb isotopic data for a whole-rock split of 72395 (Table 3) without specific discussion. As for other KREEP rocks, μ ($=^{238}\text{U}/^{204}\text{Pb}$) is high, about 2200. The data lie on the same ~ 3.9 - 4.4 Ga concordia curve as most highlands samples, and towards the lower age end as typical of brecciated KREEP rocks (model ages are in the range 4.06 to 4.09 Ga).

EXPOSURE AGES

Hutcheon *et al.* (1974b) and MacDougall *et al.* (1974) studied tracks in a column cut from 72395. Unfortunately the column was oriented parallel to the surface at 3 cm depth, so no depth variations could be measured. No systematic variations in track density occurred along the column. Track densities among adjacent feldspars vary between 2 and $5 \times 10^6 \text{ cm}^{-2}$, far beyond statistical variation. The authors infer that shock erased some tracks about 11 Ma ago. Assuming a single stage irradiation, the maximum track density implies exposure of 27 Ma (from start of track accumulation at 3 cm depth. Fission tracks in an apatite crystal (Table 4) give ages of about 800 Ma, much younger than the probable crystallization age of the sample, suggesting a severe heating, or shock event exceeding 100 kb pressure.

PHYSICAL PROPERTIES

Charette and Adams (1977) measured the spectral reflectivity (0.5 to 2.5 microns wavelength range) of an interior chip of 72395, which they referred to as an "ANT-suite norite". The spectrum shows deep Fe^{2+} bands for pyroxene and plagioclase, with a high left shoulder near 0.7 microns. However, there is no absorption

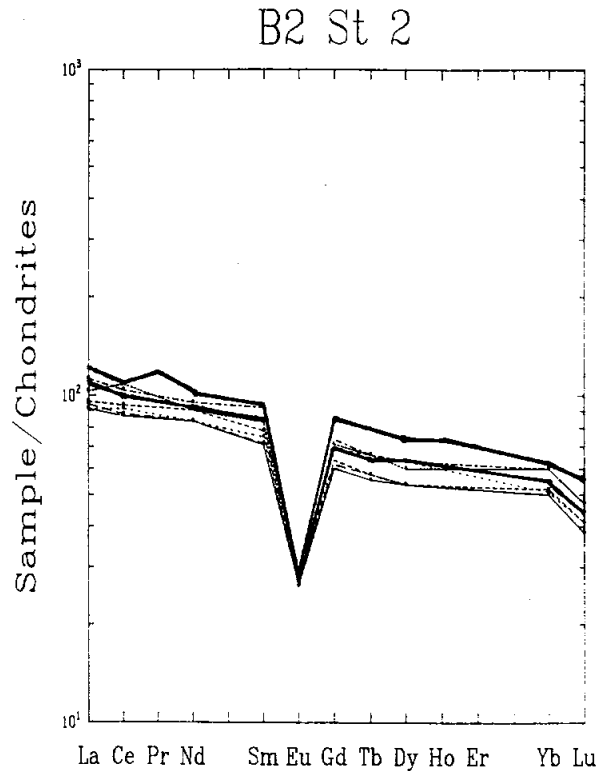


Figure 9: Rare earth elements in splits of 72395 (bold lines) and other Boulder 2, Station 2 samples. 72395 data from Table 2; upper bold line is 72395,46; lower bold line is 72395,3.

band near at 0.6 microns that would be indicative of ilmenite.

Horai and Winkler (1976) measured the thermal diffusivity of a split of 72395 under varied conditions. The sample had a bulk density of 2.539 g/cm^3 and an intrinsic density of 3.073 g/cm^3 . The porosity was 17.4 %. The diffusivity measurements are tabulated in Tables 5 and 6, and diagrammed in Figure 10.

PROCESSING

Following chipping of a few small pieces for petrographic and chemical study, 72395 was sawn into two pieces: ,7 and ,8 (Fig. 2). Between them slab pieces ,9 (29.5g), ,10 (25.2 g), and smaller pieces ,11 to ,26 were cut. Pieces were then chipped from ,8 (now 59.8 g), as shown in Fig. 3. Many allocations were made from both the slab pieces and the fragments from ,8. ,7 is now 251.9 g, and ,8 (stored at Brooks) is now 59.8 g.

Table 2: Chemical analyses of bulk samples of 72395.

Split wt. %	,3	,3	,46	,42	,43	,43	,3
SiO ₂			46.9				
TiO ₂	1.7		1.75				
Al ₂ O ₃	18.7		18.1				
Cr ₂ O ₃	.210		0.2044				
FeO	9.2		9.29				
MnO	.116		0.12				
MgO	12		11.97				
CaO	11.0		11.27				
Na ₂ O	.67		0.694				
K ₂ O	.32		(c) 0.286				
P ₂ O ₅			0.325				
ppm							
Sc	17		18.7				
V	50						
Co	35	33	31.1				
Ni	320	290	260				
Rb		5.3	6.21				
Sr		152	167				
Y							
Zr	400		570				
Nb							
Hf	12		13.7				
Ba	350	(a) 360	386				
Th	5.5		6.05				5.88
U	1.6	1.72	2.06		0.59	1.3	1.67
Ce		0.160	0.190				
Ta	1.6		1.82				
Pb							
La	36		39.7				
Ce	87		95				
Pr			13.1				
Nd	55		61				
Sm	15.2		16.8				
Eu	1.81		1.93				
Gd			21.1				
Tb	3.0		3.7				
Dy	20		23.2				
Ho			5.1				
Er			13.9				
Tm							
Yb	11		12.4				
Lu	1.5		1.88				
Li			24.8				
Be							
B				105			
C							
N			560	770			
S			36				
F			9.90		41		
Cl			.044		(d) 8.4		
Br			3.55		(d) 0.056		
Cu			2.76				
Zn		2.1					
ppb							
Au	5	5.8	4.7				
Ir	10	8.0	11				
I					(e) 1.7		
At							
Ga			4350				
Ge			440				
As			78				
Se		190					
Mo							
Tc							
Ru						17	
Rh							
Pd							
Ag		1.4					
Cd		(b) 170					
In		0.2					
Sn							
Sb		2.1					
Te							
W			750				
Re		0.79	0.2				
Os						9	
Pt							
Hg		0.29					4.4
Tl							
Bi							
	(1)	(1)	(2)	(3)	(4)	(4)	(5)

References and methods:

- (1) Laul and Schmitt (1974); INAA, RNAA
- (2) Wanke et al. (1975a,b); XRF, INAA, RNAA
- (3) Moore et al. (1974a,b); Cripe and Moore (1975)
- (4) Jovanovic and Reed (1974a); RNAA
- (5) Tera et al. (1974a); ID/MS

Notes:

- a) listed by authors as Bd
- b) contamination?
- c) value of 0.2916 also tabulated
- d) residue and leach combined
- e) detected in leach only.

Table 3: U, Th, Pb isotopic data for 72395,3 (Tera et al., 1974).

Sample ^a	Weight mg	Lunar Lead ^{b,c}				α^d		²⁰⁴ Pb ^b blank	$\Delta(^{204}\text{Pb})^b$ blank	²⁰⁴ Pb ^e picomole/g
		²⁰⁸ Pb	²⁰⁷ Pb	²⁰⁶ Pb	²⁰⁴ Pb	comp	conc			
72395,3	9.628	55.58	26.63	59.11	0.0309	1294	1204	0.0185	0.0018	3.20 +0.97

^a Total rock unless otherwise indicated. Acid washed samples designated by L; material removed from sample by acid wash designated by Leach. ^b In picomoles. ^c Corrected for blank with $\alpha = 18.26$, $\beta = 15.46$ and $\gamma = 37.59$. ^d Uncorrected for blank, α values for concentration runs (conc) are corrected for cross contamination from spikes. ^e Magnitude of negative error, corresponding to +100% increase in the blank, is twice the value given for the positive error shown, which corresponds to -50% decrease in the blank.

Sample ^a	²³⁸ U	²³² Th	Th ^b U	²³⁸ U ^b / ²⁰⁴ Pb $\times 10^{-2}$	Model Ages (AE) ^{c,d}			
	nanomole/g	nanomole/g			²⁰⁷ / ²⁰⁶	²⁰⁶ / ²³⁸	²⁰⁷ / ²³⁵	²⁰⁸ / ²³²
72395,3	6.96 ± 0.04	25.34 ± 0.25	3.61 ± 0.04	22 (+33, -5)	4.08	4.06	4.07	4.09

^a Total rock analysis unless otherwise indicated. ^b Atomic ratios. ^c After correction for blank and primordial Pb. Assumed primordial compositions in $\alpha = 9.307$, $\beta = 10.294$ and $\gamma = 29.476$ (50). ^d $\lambda_{238} = 1.5525 \times 10^{-10} \text{ y}^{-1}$, $\lambda_{235} = 9.8485 \times 10^{-10} \text{ y}^{-1}$ and $\lambda_{232} = 4.9475 \times 10^{-11} \text{ y}^{-1}$

Figure 10a: Thermal diffusivity (K) of 72395,14 as a function of temperature T with interstitial gas pressure 1 atm and 10^{-6} torr of air. Horai and Winkler (1976).

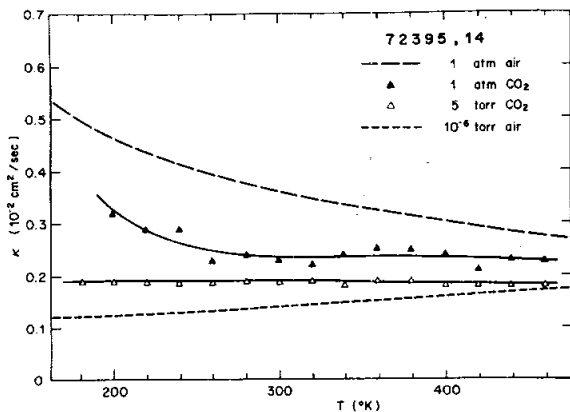
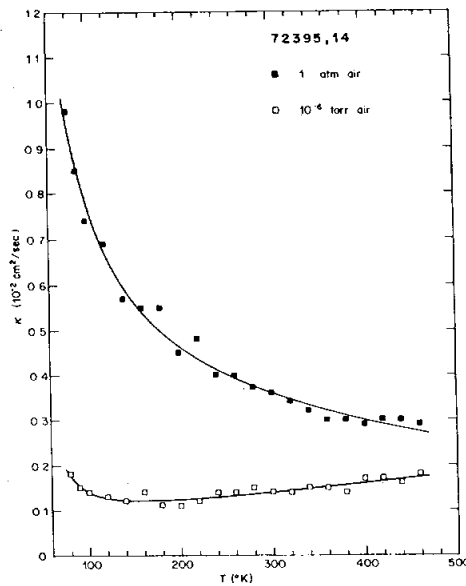


Figure 10b: Thermal diffusivity (K) of 72395,14 as a function of temperature T with interstitial gaseous pressure 1 atm and 5 torr of carbon dioxide. Smoothed curves of K as a function of T with interstitial gas pressure 1 atm and 10^{-6} torr are from Figure 10a. Horai and Winkler (1976).

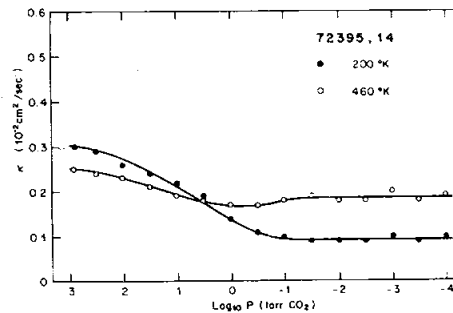


Figure 10c: Thermal diffusivity (K) of sample 72395,14 as a function of interstitial gas pressure P of carbon dioxide at temperatures of 200 degrees and 460 degrees K. Horai and Winkler (1976).

Table 4: Fission track data for an apatite crystal in 72395 (Hutcheon et al., 1974b).

72395 Apatite	
Uranium content (ppm)	108
Total track density (t/cm ²)	8.28 × 10 ⁷
Reactor induced (t/cm ²)	4.22 × 10 ⁷
Cosmic ray (t/cm ²)	3.0 × 10 ⁶
C.R. induced fission* (t/cm ²)	4.22 × 10 ⁷
Age [†] (m.y.) (a)	0
(b)	8.1 × 10 ⁸

Table 5: Thermal diffusivity (K) (cm²/sec) as a function of temperature T (degrees K), $K = A + B/T + C/T^2 + DT^2$. Horai and Winkler (1976).

Sample	Condition	A (10 ⁻² cm ² /sec)	B (cm ² °K/sec)	C (10 ² cm ² °K ² /sec)	D (10 ⁻⁴ cm ² /sec °K ²)
72395,14	1-atm air	0.207	0.488	0.090	-0.203
	10 ⁻⁶ -torr air	0.160	-0.154	0.133	0.190
	1-atm CO ₂	0.816	-2.735	3.638	-0.789
	5-torr CO ₂	0.214	-0.053	0.028	-0.121

Table 6: Thermal diffusivity (in the unit of 10⁻³ cm²/sec) of lunar solid rock samples under atmospheric conditions (a) and under vacuum (b). Horai and Winkler (1976).

	Temperature, degrees K.							
	100	150	200	250	300	350	400	450
a)	7.82	5.67	4.65	4.04	3.61	3.29	3.02	2.79
b)	1.41	1.21	1.24	1.32	1.41	1.50	1.60	1.71

BOULDER 3, STATION 2

Sample 72415; 72416; 72417; 72418; 72435

Boulder 3 at Station 2 was the smallest of three boulders sampled on the lower slopes of the South Massif (see section on Boulder 1, Station 2 for locations). It probably rolled from near the top of the massif. Boulder 3 is an equant, 40 cm subangular block (Fig. 1) with an overall dull blue-gray color. Clasts as large as 10 cm are visible in lunar surface photographs. Three fractures cutting the boulder are recognized, but no well-developed fracture or cleavage sets are visible. The boulder has a poorly-developed fillet.

The boulder contained a prominent 10 cm pale-colored clast; on

several pieces were collected from it. These were later designated as 72415 (two mated pieces), and 72416 to 72418. Astronaut Schmitt recognized the clast as light pastel green material in an even paler matrix, and suggested that it was "olivine and something." Laboratory study showed it to be a unique shocked dunite sample and it has been intensively studied. The matrix of the boulder was also sampled (72435, Fig. 1).

Many of the studies of Boulder 3 samples were made by a loosely-knit consortium led by the Caltech group (Dymek et al., 1975b, 1976a). The matrix is a clast-

bearing, fine-grained impact melt of low-K Fra Mauro composition similar to others at the Apollo 17 landing site. Geochronological data suggest an age of 3.86 Ga, also similar to that of other Apollo 17 low-K Fra Mauro melts, and the matrix is assumed to represent impact melt created in the Serenitatis impact. Strontium isotopic data for the dunite suggest that it crystallized 4.45 Ga ago, and Pb isotopic data are in agreement with such an old age (4.37 to 4.52 Ga).

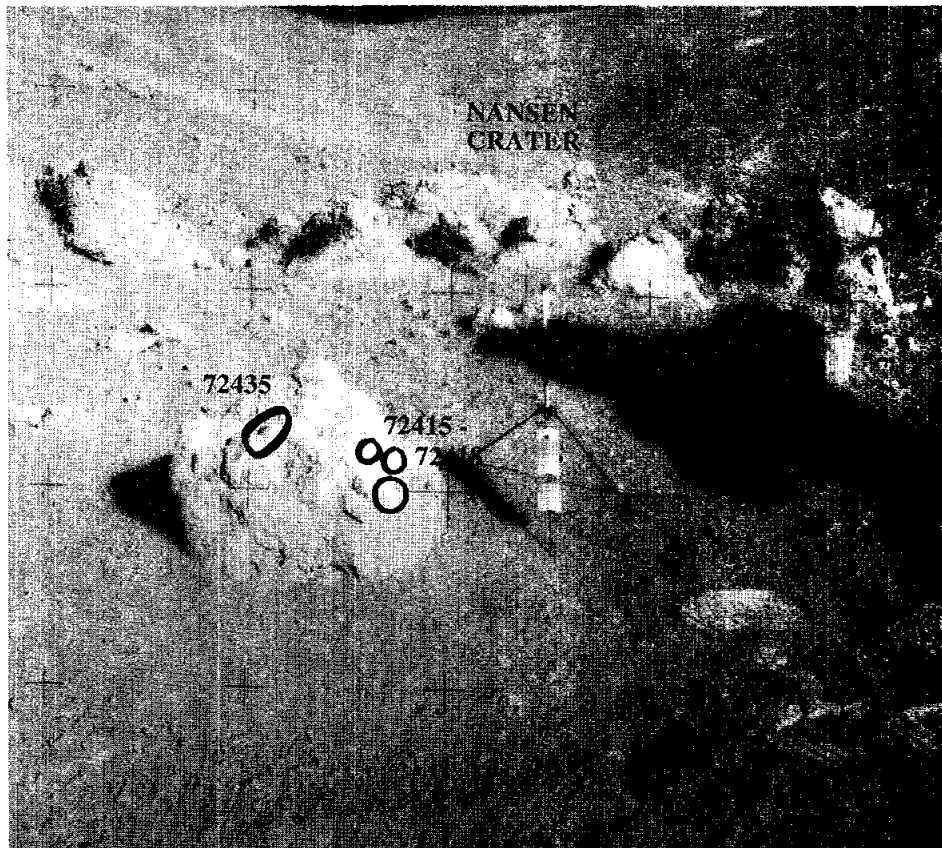


Figure 1: Sampling of Boulder 3, Station 2, with view towards north-west. The photograph was taken prior to sampling, and shows the location of the samples. The total height of the gnomon is 62 cm. AS17-138-21049.

72415

Cataclastic Dunite

St. 2, 32.34 g

INTRODUCTION

72415 is a complexly cataclastic dunite that was collected, along with 72416, 72417, and 72418, to sample a 10 cm clast in the impact melt matrix of Boulder 3, Station 2 (see section on Boulder 3, Station 2, Fig. 1). It was originally a coarse-grained igneous rock consisting mainly of magnesian olivine. Pb isotopic data suggest an igneous age of between 4.37 and 4.52 Ga, in agreement with strontium isotopic analyses of paired sample 72417, which suggest that the dunite crystallized 4.45 Ga ago. It has since suffered a complex history of deformation and excavation. 72415 is a slabby sample consisting of two

homogeneous matched pieces (Fig. 1), originally labelled A and B. Zap pits and a patina are prevalent on the lunar-exposed surfaces of 72415.

The two pieces of 72415 are each about 4 x 2 x 0.8 cm, and pale yellowish to greenish gray (5Y 8/1 to 5GY 8/1). Although the sample appeared to break easily in the lunar sampling, it is tough, and the ease of sampling was a result of a few penetrative fractures. Macroscopically the sample consists of about 30% pale yellow green olivines larger than a millimeter, set in a matrix (65%) of mainly similarly-colored material that is less than 1 mm (mainly less than 0.1 mm) in grain size. A few

of the larger grains appear more grayish, others reddish. In thin section the sample is dominantly olivine with varied aspects of deformation, with some plagioclase, pyroxenes, and Cr-spinel.

Many but not all of the studies of 72415 were conducted under a loosely-knit consortium led by the Caltech group (e.g. Dymek et al., 1975b). Following allocation of small undocumented and documented chips, piece A, the thicker of the two, was sawn in 1974 to produce several pieces for study. Subsequently several other small pieces were taken from varied locations of both piece A and piece B.

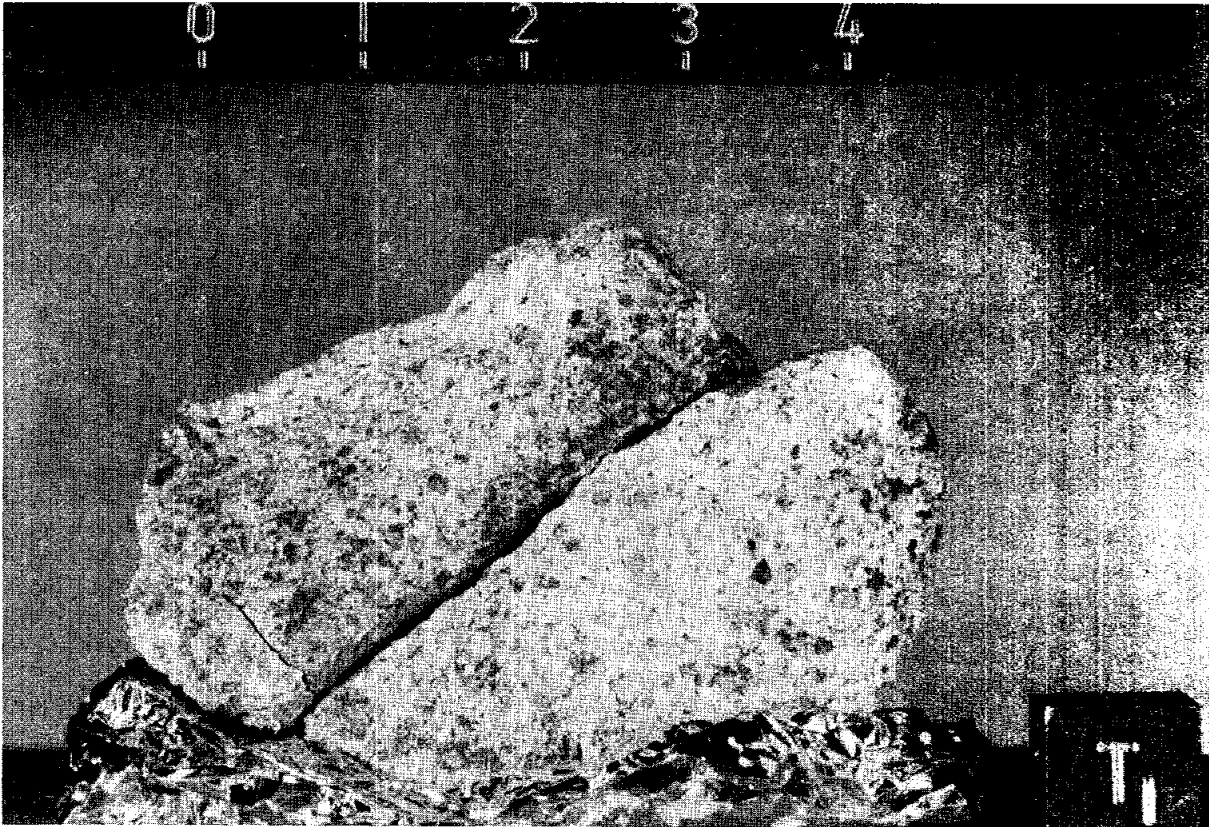


Figure 1: Two matching pieces of 72415 prior to sampling or sawing. Clasts larger than 1 mm are visible. Cube has 1 cm sides. S-73-16199.

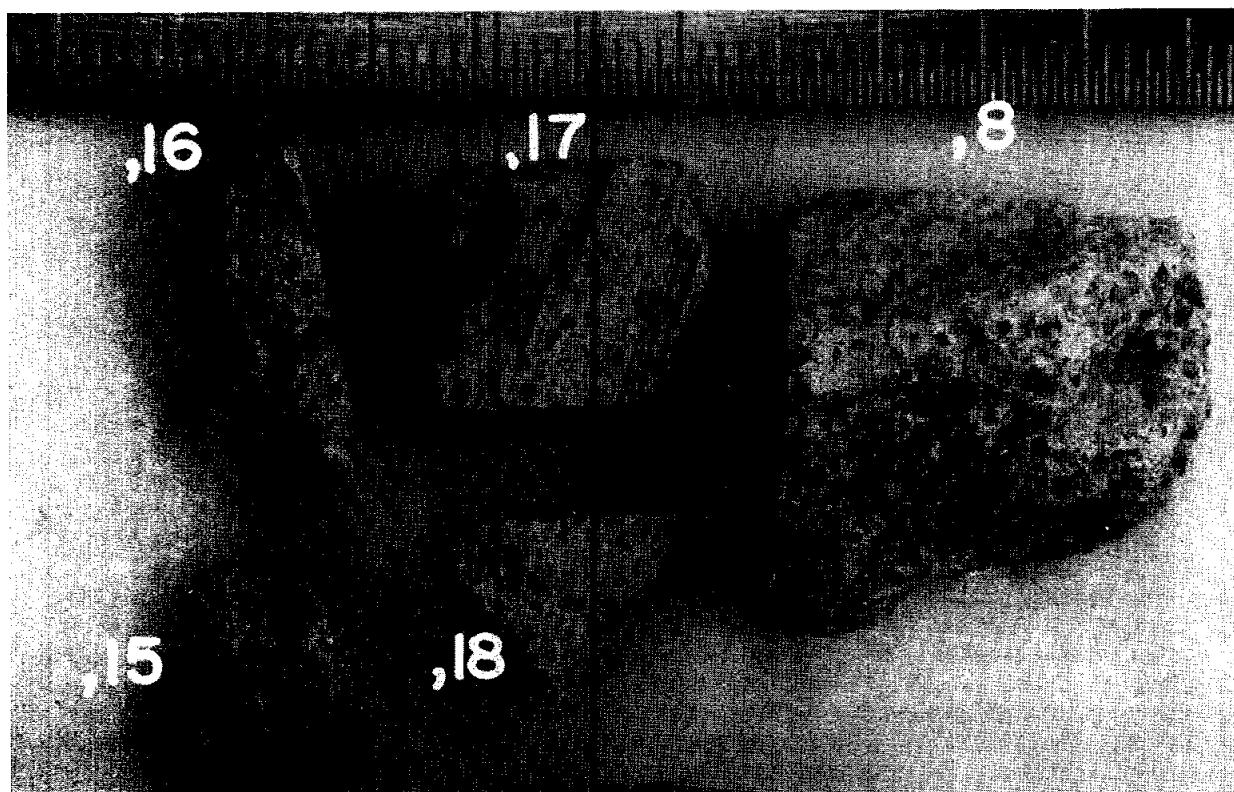


Figure 2: Sawing of one of the main pieces of 72415. An end piece was sawn first, and divided to give ,15 and ,16. A second cut produced a slab that was sawn across to produce ,17 and ,18; the latter was made into thin sections. S74-19014.

PETROGRAPHY

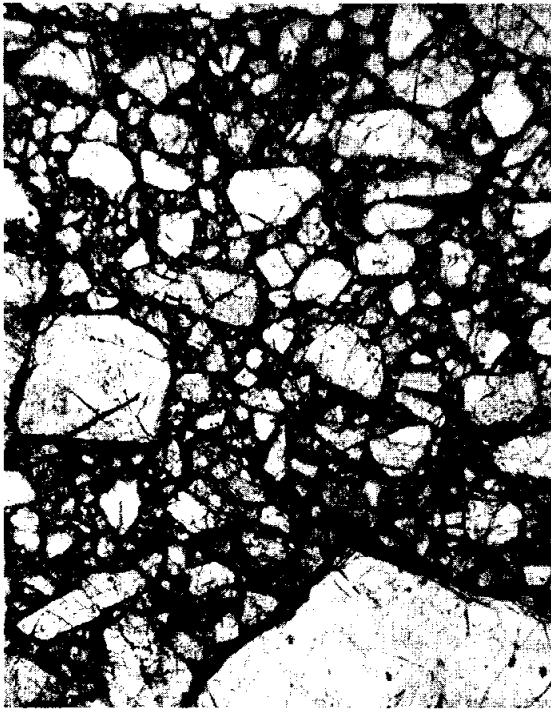
72415 is a cataclasized dunite (LSPET, 1973; Albee et al., 1974a, 1975; Simonds et al., 1974; Stoffler et al., 1979; Ryder 1992a). The Caltech consortium described the petrography of 72415 and 72417 in detail (Albee et al., 1974a, 1975; Dymek et al., 1975b), providing photomicrographs and microprobe data. Because the two samples appear to be virtually identical, the descriptions do not always distinguish them. Most of the thin sections were from 72415 and show a complex history of deformation following original crystallization (Fig. 3).

The mineralogy of the sample was summarized by Dymek et al. (1975b) (Table 1). It consists of 93% olivine, with small amounts of other silicates, and trace amounts of Cr-spinel and metal; there is also extremely rare troilite, whitlockite,

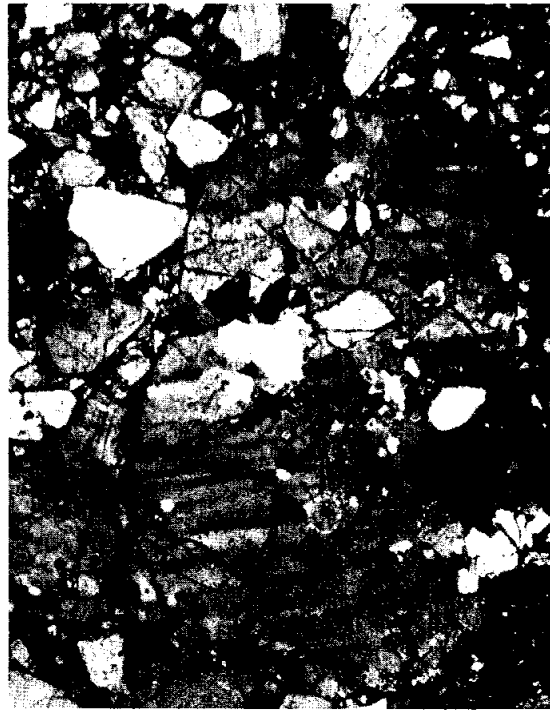
and Cr-Zr armalcolite. The abundance of plagioclase varies significantly among thin sections. The dunite is about 60% angular to subangular clasts of single crystals of olivine up to 10 mm across in a fine-grained matrix that is dominantly olivine (Fig. 3a). The existing texture results mainly from cataclastic crushing, and not from recrystallization at the microscopic scale. Many clasts show subgrains and strain bands (Figs. 3b,c), and many show inclusions that give a cloudy appearance. Some clasts are polygonalized olivine (Fig. 3d). Sparse symplectites consist mainly of chromite and pyroxenes. Fairly common veinlets cutting olivines contain plagioclases as well as olivines. Inclusions, microsymplectites, shock and recrystallization features of olivines, strain bands, and relict grain boundaries are truncated by the cataclasis, showing that they existed prior to that event. On the basis of the mineralogy, James and

Flohr (1982) and James et al. (1982) suggested that the sample was related to Mg-norites rather than Mg-gabbro-norites, but the evidence was not conclusive. The injection of feldspar-rich material of uncertain source was a factor contributing to the problem.

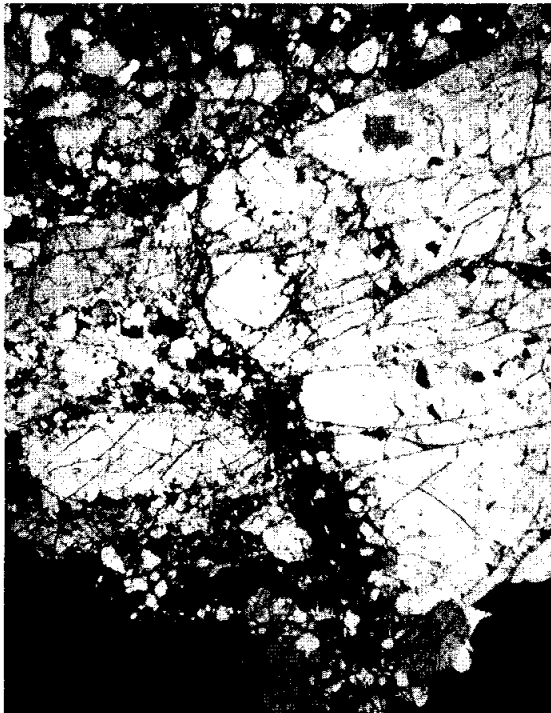
The compositions of silicate and oxide minerals in 72415 and 72417 are shown in Figure 4, and metal compositions in Figure 5 (Dymek et al., 1975b). The olivines show a small range in composition from Fo₈₆₋₈₉, with no systematic variation with petrography. This range was confirmed by Bell et al. (1975). LSPET (1973) gave a range of Fo₈₅₋₉₀ but this is not confirmed by others. Ryder (1984, 1992a) showed that that individual grains were different and zoned over distances of two to three millimeters, and that the range was wider than in dunites from terrestrial plutonic cumulates, the Marjalahti pallasite, or troctolite



a



b



c



d

Figure 3: Photomicrographs of 72415,28 (a,d) and 72415,25 (b,c). All about 1 mm width of view, all crossed polarizers except a) plane transmitted light. a) General view of cataclastic matrix, with olivine clasts in an olivine matrix. Olivines show inclusions and cloudiness, subangular shapes, and varied sizes. b) larger olivine clast showing presence of subgrains and deformation bands. c) larger olivine clast showing subgrains and a veinlet system (mainly lathy plagioclase + olivine). d) general matrix showing lithic clast to left of polygonalized olivine.

76535 (Figs. 6 and 7). He also showed that the calcium in olivines had a substantial range and was higher than in 76535. The zoning is concluded to be an original igneous feature, not a deformation-related one. These data suggest a cooling rate faster than is consistent with deep plutonic processes i.e. shallow cumulate processes.

Ryder (1983) and Bersch (1990) analyzed Ni in the olivines, showing a range from 220-70 ppm, and higher than in 76535 olivines. Bersch (1990) also analyzed precisely for other minor elements in olivines.

The composition of plagioclases varies with petrography, with felty plagioclases tending to be the most calcic (An₉₄₋₉₇), laths zoned from An₉₄₋₉₅, and plagioclase associated with symplectites the most sodic (An₉₁₋₈₉)(Fig. 4). That associated with recrystallized olivines covers a wide range (An₉₅₋₈₉). The pyroxene also varies with petrography (Fig. 4). Those with higher Ca abundances are probably real, not mixtures. The chrome-spinel has a restricted composition (Fig. 4), but that in symplectites is more iron-rich. The metal grains contain high Ni and Co (Fig. 5; data also presented in Dymek et al., 1976a); Ryder et al. (1980a) obtained even higher Ni abundances of 36 to 37%. Analyses of silicate phases by Richter et al (1976a) are similar to those of Dymek et al. (1975b).

The symplectites consist of mainly of Cr-spinel and high-Ca pyroxene; low-Ca pyroxene, olivine, plagioclase, and metal are present in some (Dymek et al., 1975b). Their textures range from granular to vermicular. Albee et al. (1974a,1975) and Dymek et al. (1975b) interpret these intergrowths as late-stage magmatic products, not solid-state reaction products. Bell and Mao (1975) and Bell et al. (1975) described these symplectites as rosettes, and tabulated bulk compositions derived from microprobe data (Table 2). They

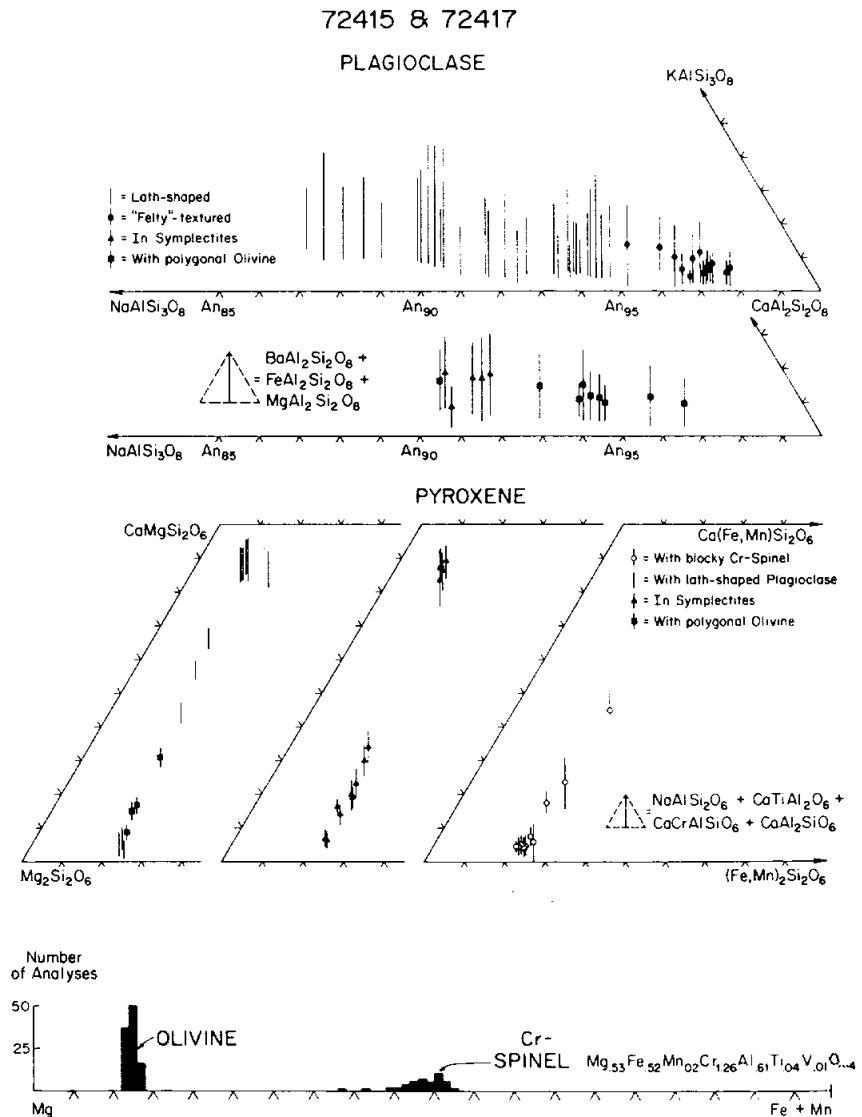


Figure 4: Compositions of silicate minerals and chrome-spinel in 72415 and 72417 (Dymek et al., 1975b).

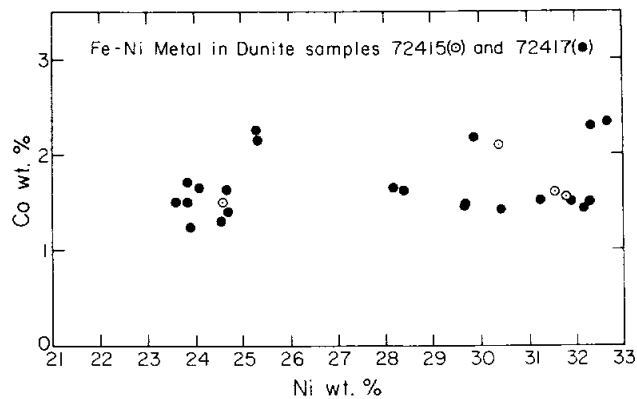


Figure 5: Ni and Co in metal grains in 72415 and 72417 (Dymek et al., 1975b).

Table 1: Phase abundances, "average" phase compositions, and bulk chemical composition, derived from microprobe point counts, of 72415 and 72417 (Dymek et al., 1975b).

	Plag.	Low-Ca pyx	High-Ca pyx	Olivine	Cr- spinel	Metal*	Bulk composition	
Vol.%	4.0 ₃	2.1 ₃	1.0 ₂	92.5 ₂	0.1 ₉	0.0 ₇	Calculated LSPET,	
Wt.%	3.3 ₅	2.1 ₇	1.0 ₀	93.0 ₄	0.2 ₆	0.1 ₇	(4641 Points) 1973	
SiO ₂	44.79	56.05	54.13	40.24	0.04	0.05	40.70	39.93
TiO ₂	< 0.01	0.28	0.11	0.02	1.05	< 0.01	0.03	0.03
Al ₂ O ₃	35.00	0.96	1.22	< 0.01	16.71	n.a.	1.25	1.53
Cr ₂ O ₃	n.a.	0.26	1.11	0.04	51.81	0.54	0.19	0.34
MgO	0.23	32.29	18.40	47.65	10.60	0.01	45.24	43.61
FeO	0.14	6.94	2.71	12.29	19.27	67.65	11.82	11.34
MnO	n.a.	0.15	0.11	0.13	0.58	0.02	0.13	0.13
CaO	19.25	2.24	22.50	0.13	n.a.	0.01	1.04	1.14
Na ₂ O	0.62	0.01	0.05	n.a.	n.a.	n.a.	0.02	< 0.02
K ₂ O	0.09	n.a.	n.a.	n.a.	n.a.	n.a.	0.00 ₃	0.00
BaO	0.04	n.a.	n.a.	n.a.	n.a.	n.a.	< 0.01	—
ZrO ₂	n.a.	n.a.	n.a.	n.a.	< 0.0 ₁	n.a.	< 0.01	< 0.01
V ₂ O ₅	n.a.	n.a.	n.a.	n.a.	0.37	n.a.	< 0.01	—
Nb ₂ O ₅	n.a.	n.a.	n.a.	n.a.	0.05	n.a.	< 0.01	< 0.01
NiO	n.a.	n.a.	n.a.	< 0.01	n.a.	30.42	0.07	0.02
Co	n.a.	n.a.	n.a.	n.a.	n.a.	1.42	< 0.01	—
Total	100.16	99.18	100.34	100.50	100.48	100.14†	100.49	98.07
	An 92.0	Wo 3.0	Wo 41.7	Fo 87.2				
	Ab 5.4	En 84.2	En 49.7	Fa 21.8				
	Or 0.5	Fs 10.4	Fs 4.3					
	Others 2.1	2.4	4.3					

*Elemental abundances. converted to oxides for bulk-composition calculation.

†Includes 0.02 wt.% P.

n.a. = not analyzed.

Table 2: Microprobe analyses in weight % of symplectites in 72415 (Bell et al., 1975). Each analysis is the average of four or five separate analyses made within single symplectites that average 30 microns diameter.

	No.	1	2	8	9	10	12	13	Host olivine
R ¹⁺	Na ₂ O	0.16	0.01	0.00	0.00	0.05	0.01	0.00	0.00
	MgO	16.06	24.72	24.30	19.07	17.80	17.95	21.68	47.52
R ²⁺	FeO	8.17	9.83	9.32	8.29	7.84	8.10	8.21	11.48
	NiO	0.00	0.00	0.00	0.02	0.04	0.04	0.03	0.00
	CaO	14.75	5.36	6.90	12.91	14.55	12.22	12.61	0.12
R ³⁺	MnO	0.21	0.11	0.12	0.13	0.09	0.11	0.04	0.12
	Cr ₂ O ₃	18.02	15.95	15.48	15.90	16.12	17.04	14.23	0.08
R ⁴⁺	Al ₂ O ₃	4.61	3.97	4.16	4.48	4.13	5.36	3.80	0.00
	SiO ₂	37.13	39.59	39.39	38.12	38.05	38.45	38.39	40.71
	TiO ₂	0.46	0.30	0.41	0.34	0.32	0.22	0.17	0.01
Arithmetic total		99.58	99.83	100.09	99.26	98.99	99.50	99.14	100.04

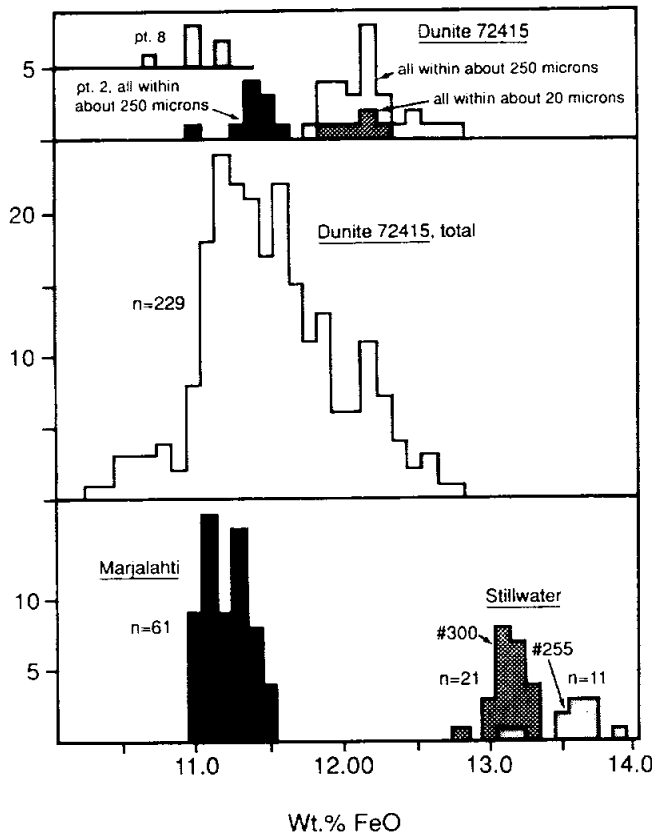


Figure 6: Variation in olivine compositions expressed as FeO wt% in samples of dunite 72415, two Stillwater troctolites, and Marjalahti. Ryder (1992a).

described their detailed occurrences. Bell and Mao (1975) concluded that the bulk compositions of symplectites were equivalent to garnet, and that the symplectites (and the dunite) had formed at high-pressure. Bell et al. (1975) included authors with differing interpretations, although all disagreed with the Dymek et al. (1975b) interpretation of late-stage magmatic products. Two authors continued to prefer the garnet hypothesis, comparing the observations with high-pressure experimental products; two preferred an origin from the diffusion of elements from olivine.

Dymek et al. (1975b) outlined the history of the dunite on the basis of the deformation features and their superpositions. The isotopic data (for 72417) suggest an early igneous origin, with little subsequent disturbance of the isotopic system. Nonetheless, petrographically the sample underwent a complex history. The primary differentiation produced a coarse plutonic cumulate, with olivine and Cr-spinel crystallizing prior to plagioclase, then Cr-spinel, pyroxenes, plagioclase, and metal crystallized from trapped interstitial

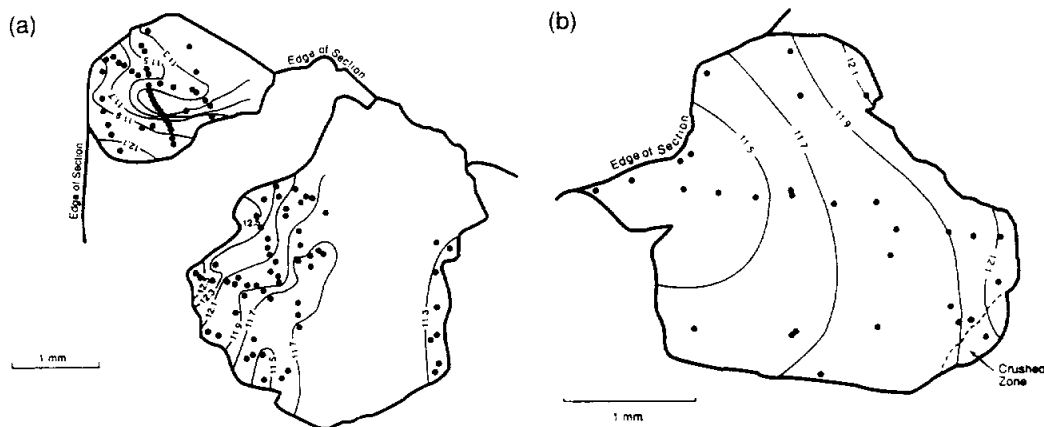


Figure 7: Sketches of zoning in larger olivines in 72415 samples, expressed as contours of FeO wt%. Dots are analytical locations. a) grains in 72415,27; the smaller grain shows a very steep gradient. b) grain in 72415,28. Ryder (1992a).

magma. None of the plagioclase appears to be cumulate. The sample was then shocked to about 330 Kb or more (according to work of Snee and Ahrens, 1975a,b; see below), consistent with an excavation depth of 50 to 150 km, producing maskelynite and a silicic melt from the intercumulus material. However, there are unshocked plagioclase laths that crystallized from that melt. Some recrystallization then took place. A second shock event produced the present observed cataclasis; this took place prior to the incorporation of the clast into the 72435 host melt (although perhaps only seconds before).

Snee and Ahrens (1975a,b)* studied the shock-induced deformation features of 72415 and compared them with the products of experiments. 72415 shows varied shock features, including irregular fractures, planar fractures (single planes and sets), well-defined deformation bands, planar elements, isolated mosaicism, and a few completely recrystallized grains. The orientation of the planar fractures are similar to those observed in experiments of shock from 330 to 440 Kb. Some bipyramid orientations in the sample are not present in the experiment products; similarly, the experimental products do not include recrystallization features.

Richter et al. (1976a,b) made a detailed study of the deformation features in 72415, using SEM as well as microscopic and microprobe techniques, concentrating on the microcracks and micropores. The microstructures show a diverse complex history that is different from any other rocks studied. Healed and sealed cracks are abundant, but open ones are rare. The healed cracks are planes of solid phases and pores; some of the solids are Fe-metal. Symplectites tend to be on or near to microcracks, suggesting a genetic link; microprobe analyses show that Al and Cr are concentrated along

Table 3: Summary of events in the deformation history of 72415 (Richter et al., 1976a).

Crystallization—igneous prehistory
Tectonic cracking
Microcrack annealing, Development of symplectites
Major shock (330–440 kbar—probably confined)
Plagioclase sealed cracks
Annealing
Cataclasis by tectonic process
Excavation by shock
Sintering

cracks even where symplectites are not present. Cracks in olivine are commonly sealed by plagioclase, some of which may be injected shock melt. Others contain abundant micropores (0.1 to 0.4 microns); the micropores have irregular subspherical shapes. Some form subparallel strings, others are random. The open cracks are unlike any others described from lunar rocks, being narrow (0.1 microns) with isolated terminations. The

matrix is cataclastic, and most of its plagioclase is free of shock effects. In contrast with the Dymek et al. (1985b) interpretation, Richter et al. (1976a) note that there is definite sintering (as revealed by the SEM) that produced a highly porous spongy mass in the matrix, with delicate necks preserved. The history as derived by Richter et al (1976a) is shown as Table 3. While consistent with that of Dymek et al. (1975b) it is more detailed. A stage of tectonic deformation followed by slow annealing of cracks and then the development of symplectites took place after igneous crystallization. The major shock deformation that followed was in turn followed by some recovery before the latest cataclasis and some sintering.

Using the mineral chemical data for pyroxenes of Dymek et al. (1975b) and an orthopyroxene-augite geothermometer, Ishii et al. (1976)

derived a temperature of 1120 degrees C for the last equilibration of pyroxenes. Herzberg (1979) estimated a pressure of crystallization of 0 +/- 0.5 Kb using the alumina content of the pyroxenes in the ol+2px+plag assemblage, and assuming a temperature of equilibration of 1000 +/- 50 degrees C estimated from the pyroxene quadrilateral locations. Finnerty and Rigden (1981) in contrast used olivine barometry (from the Ca-content) to derive a pressure of 6.4 to 11.6 Kb (for a temperature estimate of 948–988 degrees C), which they claim is consistent with the depth estimate made by Snee and Ahrens (1975a). However, in the same study they derived a depth estimate for 76535 of 600 km, which seems wholly unrealistic. Clearly these temperature and pressure estimates are inconsistent and unreliable, presumably at least in part because the original igneous crystallization did not produce a totally equilibrated assemblage, and because of the complex history following crystallization.

CHEMISTRY

Chemical analyses are listed in Table 4. The analyses correspond with a magnesian dunite with low abundances of incompatible elements and those compatible with feldspars. There are no analyses for

Table 4: Chemical analyses of bulk rock for 72415

Split	,2	,10	,2	,10b	,31	,33a	,33b
wt %							
SiO ₂	39.93						
TiO ₂	0.03						
Al ₂ O ₃	1.53						
Cr ₂ O ₃	0.34						
FeO	11.34						
MnO	0.13						
MgO	43.61						
CaO	1.14						
Na ₂ O	<0.02						
K ₂ O	0.00						
P ₂ O ₅	0.04						
ppm							
Sc							
V							
Co							
Ni	173	149					
Rb	<0.2	0.045					
Sr	11						
Y	1.1						
Zr	2.6						
Nb	0.3						
Hf							
Ba							
Th							
U		0.0062					
Cs		0.0142					
Ta							
Pb							
La							
Ce							
Pr							
Nd							
Sm							
Eu							
Gd							
Tb							
Dy							
Ho							
Er							
Tm							
Yb							
Lu							
Li							
Be							
B							
C							
N							
S			44				
F							
Cl							
Br		0.0084					
Cu							
Zn	4	2.1		2.4(a)	2.4(a)	2.3(a)	4.1(a)
ppb							
Au		0.255		2.0	0.19	0.35	2.4
Ir		0.0052		2.4	0.023	0.022	0.105
I							
At							
Ga							
Ge		29.8		250	30	71	320
As							
Se		4.9		10	10	5.0	12
Mo							
Tc							
Ru							
Rh							
Pd							
Ag		0.25					
Cd		0.37					
In							
Sn							
Sb		0.47					
Te		<0.036					
W							
Re		0.0048		0.158	<0.04	<0.06	<0.07
Os							
Pt							
Hg							
Tl		0.049					
Bi		0.41					
	(1)	(2)	(3)	(4)	(4)	(4)	(4)

(1) LSPEI (1973), Rhodes (1973); XRF
 (2) Higuchi and Morgan (1975a,b); RNAA.
 (3) Gibson and Moore (1974a,b); combustion.
 (4) Morgan and Wandless (1988); RNAA

Notes:
 (a) erroneously tabulated by authors as ppb

the rare earths. In addition to the tabulated data, Gibson et al. (1977) published a hydrogen abundance of 9.4 ppm without discussion. This abundance is higher than in mare basalts and about twice as high as in impact melts.

The major element analyses are fairly consistent with those for 72417. However, within the Caltech consortium, 72415 appears to have been considered as "normal" and 72417 as comparatively "alkali-rich" (Higuchi and Morgan, 1975a); the tabulated analyses do not support such a distinction, with Higuchi and Morgan (1975a) noting that their "alkali-rich" sample had lower Rb than their "normal" sample. While siderophiles (Ni, Ir, and some others) and some volatiles are high in some subsamples, Higuchi and Morgan (1975a) and Morgan and Wandless (1979) noted that they were not in meteoritic proportions and considered them to be indigenous. Morgan and Wandless (1988) analyzed for siderophile and volatile elements in further small subsamples that were randomly chosen but cannot be considered to be representative whole rocks because of their sizes. The data confirm an indigenous origin for these elements, and suggest a source magma that contained about 6x as high volatile abundances as mare basalts. They also noted that 3 of their subsamples were lower in volatiles and siderophiles than one other in 72415 and than the 72417 subsamples similarly analyzed.

Delano (1980) used the published data for compatible elements to place constraints on their abundance in the parental magma of the dunite.

RADIOGENIC ISOTOPES

Premo and Tatsumoto (1993) reported preliminary Pb-Pb and U-Pb isotopic data for four separates from 72415 (two "whole-rock," one olivine, and one magnetically removed mixture that is mainly

pyroxenes and spinel), summarized in Figure 8. The separates were treated with water-alcohol and very dilute acids to remove secondary Pb components. The Pb from all the separates is very radiogenic (olivine the most radiogenic), but very little Pb is in them so laboratory blank is a significant component in all. With a best-guess blank correction, the magnetic and olivine separates give a minimum age of 4.37 ± 0.23 Ga applicable to the dunite as a whole. The two whole-rocks do not plot together and suggest that WR-2 contains some uncorrected non-radiogenic Pb (above blank). Olivine and WR-1 are most reliable and indicate an age of 4.52 ± 0.06 Ga, older but within error limits of the Rb-Sr age of 72147 (4.45 ± 0.1 Ga). Corrections to align the whole rock and the magnetic separates with olivine are too great to be explained by laboratory chemistry, and suggest pre-preparation contamination, possibly meteoritic. Regardless, the Pb-Pb age is constrained between about 4.37 and 4.52 Ga, assuming the olivine data is unmovable. The data clearly indicates derivation from a high- μ source (>500), similar to results from norite 78235 and 76535 by the same laboratory.

EXPOSURE

Keith et al. (1974a,b) tabulated disintegration counts for cosmogenic radionuclides in 72415, without discussion. Yokoyama et al. (1974) used the ^{26}Al and ^{22}Na data to state that the sample was saturated in ^{26}Al , hence exposed for at least a few million years.

PHYSICAL PROPERTIES

Pearce et al. (1974a,b) tabulated magnetic properties of 72415 (Table 5) with little specific discussion. The metal content is exceptionally low.

Brecher (1975, 1976a) described magnetic anisotropy (high-field saturation and remanence) in 72415 as reflecting the petrographic texture of the sample. Some features with a preferential orientation produced by shock, such as metal decorating planar structures, would certainly produce a magnetic anisotropy. (However, it is not obvious in any petrographic description that there are preferred orientations within 72415; most planar features appear to predate the last cataclasis. This puts Brecher's hypothesis in some doubt in this particular case).

PROCESSING

72415 was created from two pieces that matched (Fig. 1), termed A and B. The first subdivisions were a loose undocumented chip (,1, thin sections); two combined pieces from opposite ends of piece A (,2, chemistry, magnetic); small chips and fragments (,4, unallocated); and an undocumented chip (,6, tracks, no published data). Subsequently piece A was sawn as shown in Figure 2. Sample ,18 was consumed making thin sections. ,17 (4.5 g); and ,16 (1.4 g) remain intact. Small pieces for chemistry, radiogenic isotopes, and thin sections were later taken from ,8; ,15; and ,10 (small chips from piece B), and other small chips allocated for spectral reflectance studies. Piece B (now ,9, 12.3 g) is virtually intact and stored at Brooks. Sample ,8 is now 4.4 g.

Table 5: Some magnetic properties of 72415 (Pearce et al., 1977a).

Sample	J_s (emu/g)	X_p (emu/g Oe) $\times 10^6$	X_0 (emu/g Oe) $\times 10^4$	J_s/J_s	H_c (Oe)	H_{rc} (Oe)	Equiv. wt.% Fe ^o	Equiv. wt.% Fe ⁺⁺	$\frac{Fe^o}{Fe^{++}}$
Dunite clast 72415,2	.064	19.3	.35	—	—	—	.03	8.85	.0033

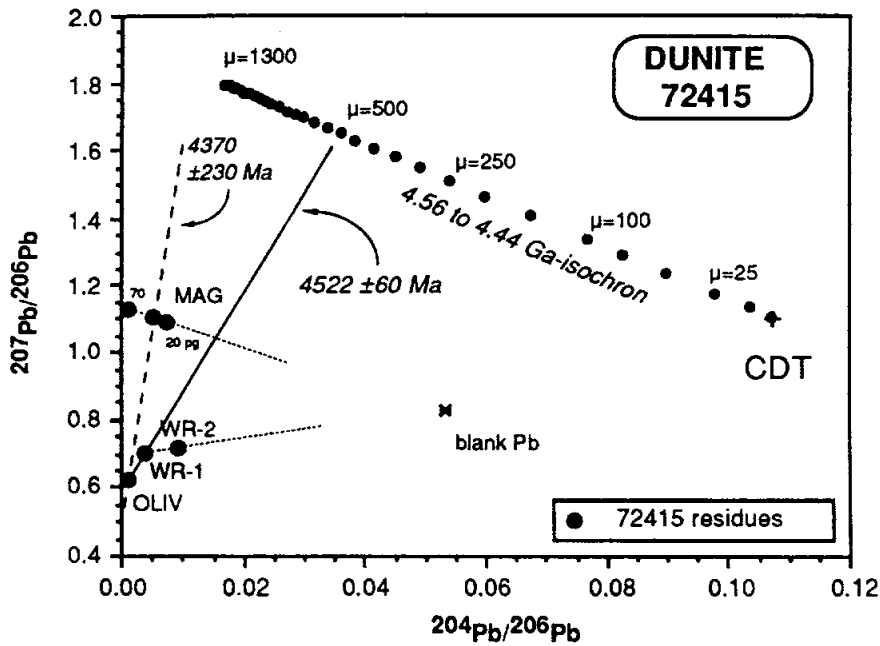


Figure 8: Pb-Pb correlation diagram for lunar dunite 72415 separates. WR-1 and WR-2 are whole-rock samples, OLIV is the olivine separate, and MAG is a magnetic separate consisting mainly of pyroxene and spinel. CDT is Canyon Diablo troilite.

72416

Cataclastic Dunite

St. 2, 11.53 g

INTRODUCTION

72416 is a cataclasized dunite that was collected, along with 72415, 72417, and 72418, to sample a 10 cm clast in the impact melt matrix of Boulder 3, Station 2 (see section on Boulder 3, Station 2, Fig. 1). 72416 is an irregular, slabby piece that measures 2.1 x 1.2 x 0.9 cm, with many zap pits and patina on the one lunar-exposed surface (Fig. 1). It is very similar to 72415 and 72417. 72416 has never been dissected or allocated for study.



Figure 1: Photograph of 72416. The piece is about 2 cm long. Part of photograph S-73-17968.

72417

Cataclastic Dunite

St. 2, 11.32 g

INTRODUCTION

72417 is a complexly cataclastic dunite that was collected, along with 72415, 72416, and 72418, to sample a 10 cm clast in the impact melt matrix of Boulder 3, Station 2 (see section on Boulder 3, Station 2, Figure 1). It was originally a coarse-grained igneous rock consisting mainly of magnesian olivine. Radiogenic isotope analyses suggest that the dunite crystallized 4.45 Ga ago, but has since suffered a complex history of deformation and excavation. 72417 is an irregular, slabby chip, with many zap pits and a patina on the lunar-exposed face (Fig. 1).

72417 is 1.2 x 2.1 x 3.2 cm, and pale yellowish to greenish gray (5Y 8/1 to 5GY 8/1). It is tough, but has a few non-penetrative fractures. It is essentially identical with 72415 both macroscopically and microscopically, consisting dominantly of pale yellow-green olivine fragments in a fine-grained matrix that is also dominantly olivine.

All the early studies of 72417 were conducted under a loosely-knit consortium led by the Caltech group (e.g. Dymek et al., 1975b; Papanastassiou and Wasserburg, 1975a), and the entire sample was allocated to that group for dissection and re-allocation. The details of the dissection are not available, although suballocations to investigators outside of Caltech are documented by mass.

PETROGRAPHY

There are fewer thin sections of 72417 than there are of 72415, and most authors do not distinguish the two samples. Thus the petrographic description of 72415 applies in general to 72417 as well (e.g. Albee

et al., 1974a and Dymek et al., 1975b). However, Dymek et al. (1975b) distinguished the composition of metal grains between the two samples (section on 72415, Fig. 5). Bell et al. (1975) gave two microprobe analyses of olivines that were hosts for symplectites, and gave an average composition derived from microprobe analyses of 3 symplectites; their compositions are roughly similar to those in 72415. They also depicted symplectites in 72417. Dymek et al. (1975b) noted that heavy liquid separations of materials in 72417 included a single grain of ilmenite, a phase not identified in thin sections of 72415 or 72417. Ryder (1984b) suggested on the basis of published olivine compositions that 72417 might be a little more iron-rich than 72415.

Lally et al. (1976a,b) made a very detailed optical and electron petrographic study of deformation, recovery, and recrystallization of 72417. They inferred at least four stages of shock deformation and at least two stages of annealing; at least one heating event may have accompanied the shock deformations. Like the study of Richter et al. (1976a) for 72415, the

interpretation of 72417 by Lally et al. (1976a,b) is consistent with but more detailed than that of Dymek et al. (1975b). High-voltage electron microscopy was used to define the substructure of crystals and matrix grains (latter defined as less than 50 microns). The olivines are moderately deformed, with planar kink boundaries, undulating extinctions, open and healed fractures, and inclusions. Subgrains in large olivine clasts are bounded by dislocations, and the subgrain sizes are very varied. Symplectites occur in planar boundaries. The matrix contains the most highly-deformed grains, but also some recovery and extensive recrystallization. Annealing followed brecciation, and the matrix has genuine porosity and some genuine sintering. Lally et al. (1976a) infer that the fractures observed by Snee and Ahrens (1975a,b) are probably not from the original shock event that produced the subgrains, as most of these recovered, but are from a later event, or even thermal in origin. A lower limit to the shock pressure is given by the presence of maskelynite and plagioclase melts. Most of the dislocations are probably shock-induced, since such

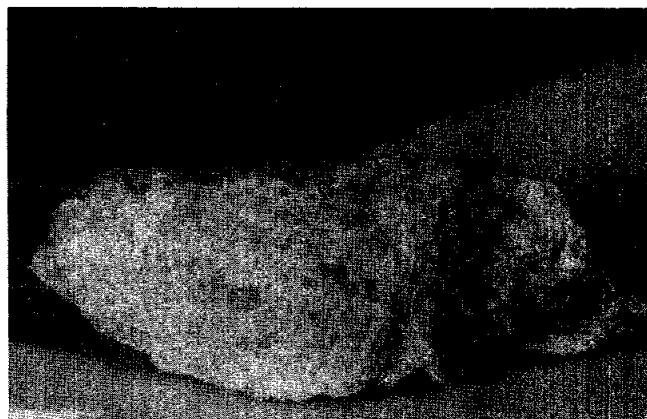


Figure 1: Pre-allocation photograph of 72417. The sample is about 3 cm long. Part of photograph S-73-17968.

fractures rarely occur after crystallization and slow cooling. In large olivine crystals, recovery is dominant; in smaller olivines, there is both recovery and recrystallization; in the matrix, recrystallization is dominant. The smallest olivines must have had the greatest dislocation density.

The history of 72417 as inferred by Lally et al. (1975a) is given in Table 1. Its main difference from that of Dymek et al. (1975b) is the matrix recrystallization, which cannot be seen optically. The recrystallization might result from the inclusion of the dunite in the melt matrix of Boulder 3, Station 2. The large grains of olivine have an unusual heterogeneity of sizes. Shock event IIa (Table 1) produced a coherent rock, with well-recovered and recrystallized olivine and pyroxenes equilibrated at less than 810 degrees C. The present structure of the sample was produced in shock event IIIa, at 50 to 100 kb, without the production of maskelynite.

CHEMISTRY

Among the chemical analyses are for 72417 given in Table 2, none can be particularly said to represent bulk rock. The data from Laul and Schmitt (1975a) in Table 2 are weighted means of 9 different subsamples that were chosen to sample the visual variety of materials composing 72417, and which themselves show a wide range in compositions (Table 3). The 9 subsamples range from 70 to 130 mg. Nonetheless, this mean corresponds reasonably with the analyses given for 72415, and corresponds with a magnesian dunite with low abundances of incompatible and felsic elements. The rare earth elements for the individual samples and the mean are shown in Figure 2; their main feature is the consistent flat pattern of light rare earth elements and changing slope of heavy rare earth elements among subsamples. Laul and Schmitt (1975a,b) attempted to calculate the composition of the parent magma, which in essence

must be enriched in rare earths (cf. chondrites) and comparatively more enriched in light rare earths (e.g. La 14 x chondrites, Lu 7 x chondrites; Fig. 3). However, such calculations are very model dependent. Laul and Schmitt (1975a) explored several possible models, favoring garnet in the history to produce the light rare earth element enrichment. They suggested that the parent magma was a second-stage product, needing a previous history in which the products of melting of a gabbroic anorthosite was mixed with an earlier Mg-rich cumulate in some form of magma pool from which the dunite crystallized. McKay et al. (1979) used the data of Laul and Schmitt (1975a,b) to reinvestigate the composition of the parent magma; using updated coefficients and a trapped liquid model, they suggested a parent magma with rare earth abundances only about half of those of Laul and Schmitt (1975a) but with a similar overall pattern. The inferred magma had Ca/Al less than

Table 1: Mechanical and thermal history of dunite 72417 (Lally et al., 1976a).

Stage	Nature of events	Resulting fabric
I	Initial crystallization, accumulation of dunite; slow cooling.	Coarse-grained; presumably cumulate or modified cumulate texture.
IIa	<i>Shock deformation</i> : plastic deformation of olivine; melting of plagioclase; and injection of plag melt. Introduction of crack porosity.	
IIb	<i>Recovery and local recrystallization</i> : Crystallization of injected plag glass. Sintering of crack porosity.	Texture unknown; probably cohesive and massive.
IIIa	<i>Shock deformation</i> : brecciation, cataclastic deformation; plastic flow especially in fine-grained material. Consolidation (?)	Present breccia fabric; state of consolidation unknown.
IIIb	<i>Recovery and local recrystallization</i> : Possibly responsible for contributing to consolidation.	
IV	<i>Incorporation</i> in melt (72435) of cohesive breccia fragments; heating by melt.	Present breccia texture
V	Excavation of Boulder 3 to present location. Little or no effect on dunite fabric.	Present breccia texture

Table 2: Chemical analyses of "whole rock" 72417 samples.

Split wt %	(a)	,1	,9018a	,9018b	,9018c	,13	,1,1(c)	,1,7(d)	Split wt %
SiO ₂									SiO ₂
TiO ₂									TiO ₂
Al ₂ O ₃	1.3								Al ₂ O ₃
Cr ₂ O ₃	0.34								Cr ₂ O ₃
FeO	11.9								FeO
MnO	0.113								MnO
MgO	45.4								MgO
CaO	1.1								CaO
Na ₂ O	0.0186								Na ₂ O
K ₂ O	0.0030								K ₂ O
P ₂ O ₅									P ₂ O ₅
ppm									ppm
Sc	4.3								Sc
V	50								V
Co	55								Co
Ni	160	411	538	650	314				Ni
Rb		0.027							Rb
Sr	8.2								Sr
Y									Y
Zr									Zr
Nb									Nb
Hf	0.10								Hf
Ba	4.1								Ba
Th									Th
U		0.0028	0.0024	0.0006	0.0051		0.002	0.002	U
Cs		0.0141							Cs
Ta									Ta
Pb									Pb
La	0.15								La
Ce	0.37								Ce
Pr									Pr
Nd									Nd
Sm	0.080								Sm
Eu	0.061								Eu
Gd									Gd
Tb	0.017								Tb
Dy	0.11								Dy
Ho	0.023								Ho
Er									Er
Tm									Tm
Yb	0.074								Yb
Lu	0.012								Lu
Li							2.3		Li
Be									Be
B									B
C									C
N									N
S									S
F									F
Cl								154	Cl
Br		0.0272					6.69(b)		Br
Cu							0.028(b)		Cu
Zn		9.8	2.5	2.1	9.6	2.3			Zn
pph									pph
Au		2.55	3.9	5.1	3.3	3.2			Au
Ir		3.13	0.048	0.050	0.46	<0.010			Ir
I							0.9		I
At									At
Ga		261	349	542	186	270			Ga
Ge									Ge
As		5.1	31	5.4	9.0	3.0			As
Se									Se
Mo									Mo
Tc									Tc
Ru								<3	Ru
Rh									Rh
Pd									Pd
Ag		30.2	14.5	5.0	46				Ag
Cd		0.85	5.2	4.0	26				Cd
In			0.72	0.21	<0.25				In
Sn									Sn
Sb		2.81	1.78		3.4				Sb
Te		0.56							Te
W									W
Re		0.099	0.0007	0.002	0.022	<0.04			Re
Os			<0.043	<0.025	0.71		<0.8	1.2(e)	Os
Pt									Pt
Hg							2.2		Hg
Tl		0.033	0.103	0.101	1.04				Tl
Bi		1.24	2.8	<2	0.89				Bi
	(1)	(2)	(3)	(3)	(3)	(3)	(4)	(4)	

(1) Laul and Schmitt (1975a); INAA, RNAA
 (2) Higuchi and Morgan (1975a,b); RNAA
 (3) Morgan and Wandless (1988); RNAA
 (4) Jovanovic and Reed (1974a,1975c); RNAA

Notes:
 (a) Mass weighted mean of 9 (70-130 mg) samples from different locations of 72417 from Caltech consortium samples.
 (b) combined leach and residue values.
 (c) interior.
 (d) exterior

chondritic, and this and other non-chondritic aspects probably could not be derived by fractional crystallization of a chondritic parent.

Higuchi and Morgan (1975a) and Morgan and Wandless (1979) inferred that the siderophile and volatile elements were of indigenous, not meteoritic, origin. Continued analyses of small subsamples by Morgan and Wandless (1988) showed that the 72417 samples generally had higher siderophiles and volatiles than 72415, and confirmed that the siderophiles were indigenous; for instance, the refractory siderophiles Os, Re, and Ir do not correlate with other siderophiles. Ni, Co, and Ge correlate with each other, suggesting that Ge acted as a siderophile and that all three elements reside mainly in Fe-metal. Morgan and Wandless (1988) infer a source magma for the dunite that had about 6 x the volatiles of a mare basalt.

The data of Jovanovic and Reed (e.g. 1974a) includes separate leach and residue data for Cl and Br. Although most of their data is presented with little discussion, they claim that the Ru/Os ratio is roughly chondritic, but that is a sign of primitiveness rather than contamination. Such a ratio is much lower than that of mare basalts (about 24). For Hg they present some temperature release (<130 degrees C) data.

RADIOGENIC ISOTOPES

Papanastassiou and Wasserburg (1975a,b, 1976b) gave a detailed description of analyses of subsamples of 72417 for Rb and Sr isotopic ratios (Table 4). The subsamples were varied chips and splits of 50 to 150 mg chosen for their distinctive characters, and the analyses included handpicked olivine and symplectite fragments. None specifically represent bulk rock. The data define a precise age

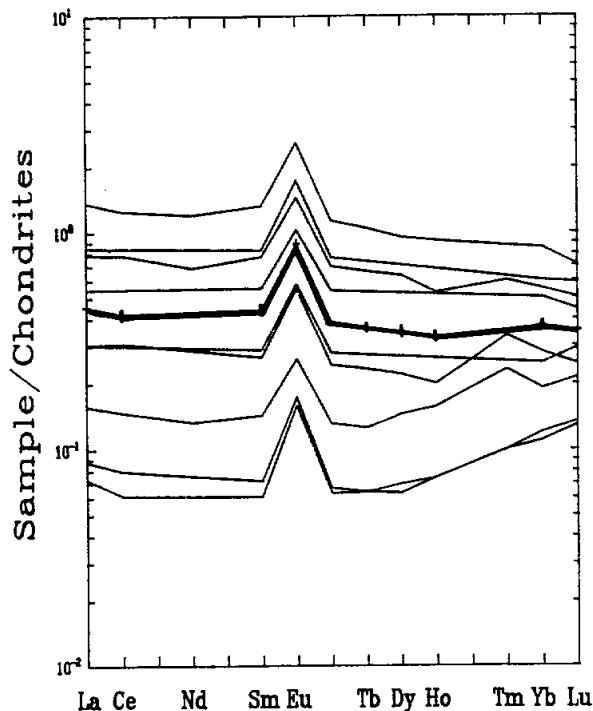


Figure 2: Rare earth elements in small subsamples (70 to 130 mg) of 72417 (lighter lines), from Laul and Schmitt (1975a). The weighted mean is included (heavier line with strokes).

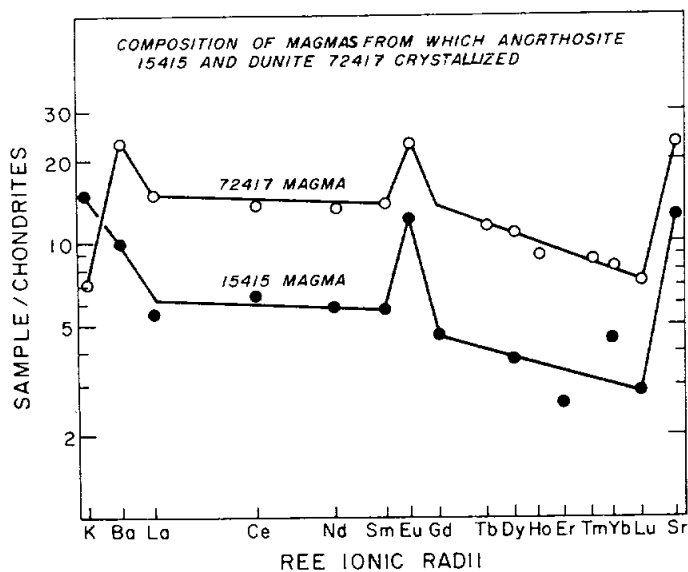


Figure 3: Calculation of abundances of incompatible elements in the parent magma of 72417 according to one of the models of Laul and Schmitt (1975; their Fig. 7), and a calculated parent for anorthosite 15415.

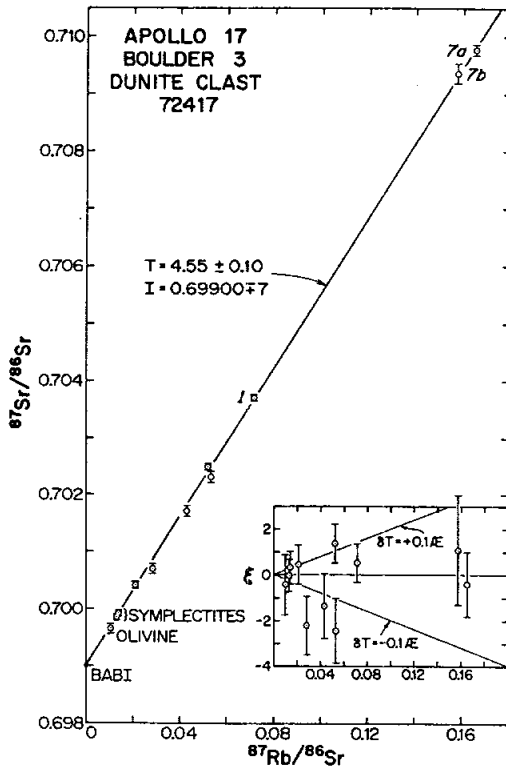


Figure 4: Rb-Sr evolution diagram for mechanically separated samples of the dunite 72417. The age is determined for decay constant for $^{87}\text{Rb} = 1.39 \times 10^{-11}/\text{yr}$; for decay constant for $^{87}\text{Rb} = 1.42 \times 10^{-11}/\text{yr}$, age is 4.47 Ga. Inset shows deviations in parts of 10^4 from the best-fit line (Papanastassiou and Wasserburg, 1975a).

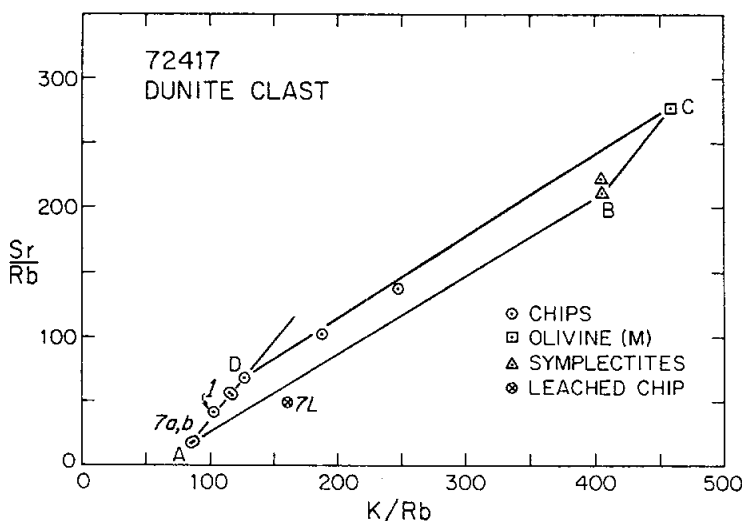


Figure 5: Element correlation diagram for dunite 72417 samples. The distinctly low K/Rb data fall along line AD. These data require the presence of at least three different phases with distinct Rb/Sr values (Papanastassiou and Wasserburg, 1975a).

of 4.47 ± 0.10 Ga (decay constant for $^{87}\text{Rb} = 1.42 \times 10^{-11}/\text{yr}$), with an initial $^{87}\text{Sr}/^{86}\text{Sr}$ of 0.69900 ± 7 (Fig. 4). A few of the points fall slightly off a best fit line. The chips are several millimeters in size, so the data establish the time of isolation of the isotopic systems at this scale. The array is a primary isochron, and is not merely a mixture of two components (Figs. 5 and 6). The variation in Rb/Sr is not attributable to specific phases. The very low K/Rb ratio eliminates contamination as a contributing factor. The data thus define a very ancient crystallization event. The initial $^{87}\text{Sr}/^{86}\text{Sr}$ is indistinguishable from BABI Papanastassiou and Wasserburg (1975a) document the severe effects that leaching of dunite samples with organic liquids has on the Rb/Sr isotopic systems, with preferential removal of Rb and the obliteration of any time information.

Dymek et al. (1975b) quoted ^{40}Ar - ^{39}Ar data from Huneke (pers. comm.) that suggested a complicated release pattern but that indicated Ar loss at 3.89 ± 0.1 Ga (assuming original quote of 3.95 Ga

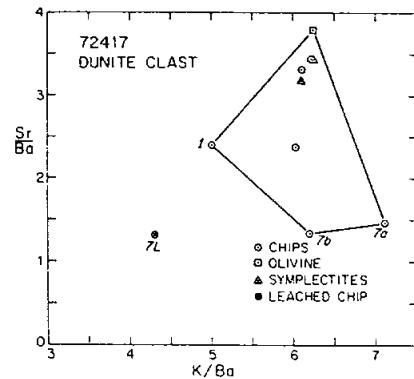


Figure 6: Element correlation diagram for dunite 72417 samples. These data require the presence of at least three different phases. The olivine appears to be sampling phases distinct from the handpicked coarse symplectites. (Papanastassiou and Wasserburg, 1975a).

used the old decay constant), which is the same age as that of the host melt. However, no details were published. Tera et al. (1974b) reported some limited Pb isotopic data that also suggested a somewhat younger age than 4.6 Ga and might indicate a disturbed system. The Pb is distinctly radiogenic.

STABLE ISOTOPES

Clayton and Mayeda (1975a,b) and Mayeda et al. (1975) reported isotopic analyses of oxygen in 72417 splits, with little discussion (Table 5). The delta ¹⁸O values for olivines are in the middle of the range for lunar olivines.

PROCESSING

The sample was entirely allocated to the Caltech group for study and further allocation, and the details of the subdivisions are not generally available. Allocations to investigators outside of Caltech are documented by mass.

Table 3: Chemical analyses of small subsamples of 72417 (70 to 130 mg) from Laul and Schmitt (1975a); the weighted average is included in Table 2.

Sample	Wt. mg	Al ₂ O ₃ %	Al ₂ O ₃ * %	FeO %	MgO %	CaO %	Na ₂ O ppm	K ₂ O ppm	MnO %	Cr ₂ O ₃ %	Sc ppm	V ppm	Co ppm	Ba ppm	Sr ppm	La ppm	Ce ppm	Nd ppm	Sm ppm	Eu ppm	Tb ppm	Dy ppm	Ho ppm	Tm ppm	Yb ppm	Lu ppm	Hf ppm	Ni ppm	Au ppb
11	78	4.0	3.9	11.4	43.0	3.0	430	65	0.109	0.200	5.9	50	43	—	0.45	—	—	0.24	0.18	—	—	—	—	0.17	0.024	0.20	130	—	
1 R	77	—	—	—	—	—	—	—	—	—	—	—	—	8.3	25	0.45	1.1	0.72	0.24	0.18	0.049	0.30	0.064	0.026	0.17	0.024	—	—	—
21	69	2.5	2.2	11.6	42.5	1.6	270	40	0.114	0.290	5.1	80	72	—	0.28	—	—	0.15	0.12	—	—	—	—	0.12	0.020	0.13	550	3.0	
31	135	2.2	2.1	12.0	43.8	1.7	220	40	0.117	0.284	5.3	50	50	—	0.26	—	—	0.15	0.10	—	—	—	—	0.12	0.017	0.1	130	—	
3 R	122	—	—	—	—	—	—	—	—	—	—	—	—	5.1	15	0.26	0.69	0.41	0.14	0.10	0.031	0.20	0.037	0.018	0.11	0.015	—	—	—
41	86	1.6	1.5	11.7	46.9	1.2	160	28	0.116	0.320	4.6	50	50	—	0.18	—	—	0.10	0.071	—	—	—	—	0.07	0.009	<0.05	230	1.5	
51	210	0.90	0.80	12.4	48.7	0.80	100	—	0.114	0.240	4.1	40	60	—	0.10	—	—	0.055	0.042	—	—	—	—	0.07	0.009	<0.05	230	1.5	
5A1	89	—	—	12.4	—	—	80	18	—	0.242	4.1	—	—	—	0.10	—	—	0.050	0.039	—	—	—	—	0.07	—	—	—	1.3	
5AR	89	—	—	—	—	—	—	—	—	—	—	—	—	7.0	5.9	0.10	0.27	—	0.048	0.038	0.011	0.070	0.014	0.010	0.056	0.0084	—	—	—
5B1	108	0.90	0.80	12.3	—	0.82	80	18	0.116	0.240	4.1	40	—	—	0.10	—	—	0.055	0.042	—	—	—	—	0.06	0.009	—	—	—	
61	77	0.90	0.77	12.0	48.1	0.85	100	20	0.116	0.310	4.0	50	54	—	0.10	—	—	0.052	0.040	—	—	—	—	0.05	0.01	<0.04	250	1.0	
71	69	0.41	0.36	11.5	50.0	0.44	70	6-1	0.116	0.116	3.3	40	45	—	0.095	—	—	0.023	0.025	—	—	—	—	0.03	—	—	0.06	100	—
7 R	69	—	—	—	—	—	—	5.3	—	—	—	—	—	0.75	2.2	0.032	0.13	0.080	0.026	0.018	0.0059	0.046	0.011	0.007	0.038	0.0073	—	—	—
81	106	0.40	0.28	11.6	45.3	0.41	30	7-1	0.107	0.300	3.3	40	47	—	0.030	—	—	0.012	0.014	—	—	—	—	0.02	—	<0.04	180	1.4	
8 R	104	—	—	—	—	—	—	5.4	—	—	—	—	—	(2)	1.9	0.029	0.070	—	0.013	0.012	0.0030	0.022	0.0052	0.003	0.022	0.0044	—	—	—
91	118	0.55	0.21	11.7	45.6	0.60	30	7-2	0.110	0.830	4.1	80	84	—	0.023	—	—	0.013	—	—	—	—	—	0.02	—	<0.04	650	4.0	
9 R	117	—	—	—	—	—	—	6.4	—	—	—	—	—	(1.0)	1.2	0.024	0.054	—	0.011	0.011	0.0030	0.020	0.0052	0.003	0.024	0.0046	—	—	—
Mass weighted mean	1.3	1.2	11.9	45.4	1.1	130	24	0.113	0.34	4.3	50	55	4.1	8.2	0.15	0.37	—	0.080	0.061	0.017	0.11	0.023	—	0.074	0.012	0.10	160	—	
Mass weighted mean*	1.2	—	11.4	45.5	1.2	-200	25	-0.11	-0.11	—	—	—	—	4	8.0	—	—	—	—	—	—	—	—	—	—	—	150-410 ^b	0.2-2.5 ^c	
BCR-1	13.7	—	12.3	—	6.9	32000	17000	0.174	—	—	32	420	36	650	330	23.0	53	29	6.70	1.90	1.1	6.30	1.2	0.52	3.40	0.42	4.7	—	—

*1 = INAA, R = RNAA. Errors in INAA are cited by Laul et al. (1974). Overall errors in RNAA are 2-10%.
 Al₂O₃* values are corrected for Cr-spinel (Al₂O₃/Cr₂O₃ = 0.41) from Albee et al. (1974).
^aAlbee et al. (1974).
^bHiguchi and Morgan (1975) values for Ni and Au in two 72415 fragments.
^cLSPET (1973).

Table 4: Analyses of subsamples of 72417 for Rb and Sr isotopic ratios.

Sample ^a	Weight (mg)	K ppm	Ba ppm	Rb ⁸⁶ Sr ⁸⁷ Rb/ ⁸⁶ Sr ^b 10 ⁻⁸ mole/g	⁸⁶ Sr	⁸⁷ Rb/ ⁸⁶ Sr ^b × 10 ²	⁸⁷ Sr/ ⁸⁶ Sr ^c	Sr/Rb ^d	Sr/Ba ^d	K/Rb ^d	K/Ba ^d	Ref. ^e
Chip-1	203	7.3	1.213	0.0830	2.712	7.14	0.70370 ± 6	40.58	2.37	103	6.02	1
-2	255	8.2	1.642	0.0827	3.713	5.19	0.70249 ± 6	55.76	2.40	116	4.99	2
-3	45	9.3	—	0.0931	4.075	5.33	0.70231 ± 10	54.35	—	117	—	2
-4	54	8.9	—	0.0817	4.438	4.29	0.70171 ± 10	67.45	—	127	—	2
-5	53	16.9	2.77	0.1053	8.651	2.838	0.70070 ± 9	102.0	3.31	188	6.10	
-6	170	19.9	3.20	0.0938	10.37	2.110	0.70041 ± 6	137.2	3.44	248	6.22	
-7a ^f	114	4.7	0.664	0.0645	0.910	16.53	0.70977 ± 10	17.53	1.46	85	7.1	
-7b	63	4.9	0.787	0.0661	0.979	15.75	0.70936 ± 17	18.40	1.32	87	6.2	
Sym I-1	125	29.1	4.66	0.0843	15.08	1.304	0.69985 ± 5	222.1	3.43	404	6.24	1
-2	151	31.3	5.14	0.0905	15.38	1.372	0.69992 ± 5	211.0	3.18	405	6.09	2
Olivine	138	10.6	1.70	0.0271	6.074	1.041	0.69965 ± 9	278.3	3.79	458	6.24	2

^aAll samples were obtained by mechanical means only, except chip-1 which was rinsed in acetone prior to crushing.
^bUncertainty in concentrations is 0.4% for Rb and 0.1% for ⁸⁶Sr.
^cErrors correspond to last significant figures and are 2σ_{mean}.
^dElemental ratios are calculated by weight.
^eRef. 1: Albee et al. (1974); Ref. 2: Papanastassiou and Wasserburg (1975).
^fSample 7a represents a quarter split of a homogenized sample after crushing to less than 75 μm; 7b is an eight split of the same original sample.

**Table 5: Oxygen isotopic analyses for samples of
72417 (Clayton and Mayeda, 1975a,b;
Mayeda et al., 1975).**

<u>Split</u>	<u>description</u>	<u>delta ¹⁸O</u>	<u>delta ¹⁷O</u>
,9011	dunite	4.77	2.52
,9011	dunite	5.20	2.55
,9011	mx in dunite	4.82	
,9010	ol in dunite	5.09	

72418

Cataclastic Dunite

St. 2, 3.55 g

INTRODUCTION

72418 is a cataclasized dunite that was collected, along with 72415, 72416, and 72417, to sample a 10 cm clast in the impact melt matrix of Boulder 3, Station 2 (see section on Boulder 3, Station 2, Fig. 1). 72418 is an irregular, slabby piece that measures 1 x 2.5 x 0.4 cm, with many zap pits and patina on the one lunar-exposed surface (Fig. 1). It is very similar to 72415 and 72417, but appears to contain a few exceptionally large spinels (up to 1.5 mm). 72418 has never been dissected or allocated for study.

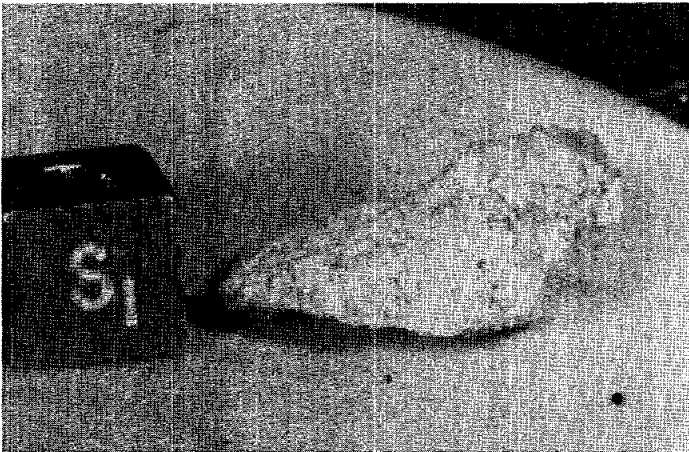


Figure 1: Photograph of 72418. The piece is about 2 cm long. Part of photograph S-73-17968.

72435**Micropoikilitic Impact Melt Breccia
St. 2, 160.6 g****INTRODUCTION**

72435 is a very fine-grained, clast-bearing impact melt with a micropoikilitic texture. It was sampled as typical matrix of Boulder 3, Station 2 (see section on Boulder 3, Station 2, Fig. 1). The sample has a major and trace element chemistry similar to other Apollo 17 low-K Fra Mauro impact melts, and can be assumed to have formed in the Serenitatis event. It is among the finest-grained of such samples. Radiogenic isotopic data on matrix and clasts show that it crystallized close to 3.86 Ga ago, and that matrix and clasts did not totally equilibrate with each other, even for argon. The larger clasts are dominantly feldspathic granulites,

and brecciated dunitic, troctolitic, and noritic fragments.

The sample, consisting of two mated pieces (4 x 5 x 3 cm, and 5 x 4 x 3 cm) is angular, and gray (N4) (Fig. 1). It is commonly referred to as blue-gray (e.g. LSPET, 1973). It is tough but with one penetrative fracture that broke the sample. The sample is homogeneous, except for apparent variation in grain size near some cavities. Clasts up to 1 cm are visible in the sample; larger clasts (including the sampled dunite) were visible in the parent boulder. Clasts larger than 1 mm compose about 5% of the sample. Both clasts and elongate cavities in 72435 are aligned, but most cavities are spherical. Some are as large as 8

mm. Smaller cavities are smooth or drusy; some larger ones have crystal linings. Cavities occupy less than 1% of the sample. The exposed surface (B and W) are knobby, discolored, and rounded, with zap pits. The broken interior is hackly.

Most of the studies of 72395 were conducted under a consortium led by the Caltech group (Dymek et al., 1976a; Papanastassiou and Wasserburg 1975a; Huneke, 1978). Following chipping of two small samples, advantage was taken of the samples breakage to produce a slab with a single saw cut across the large of the ends. This slab was dissected (Fig. 2), and nearly all subsequent allocations were made from this slab.

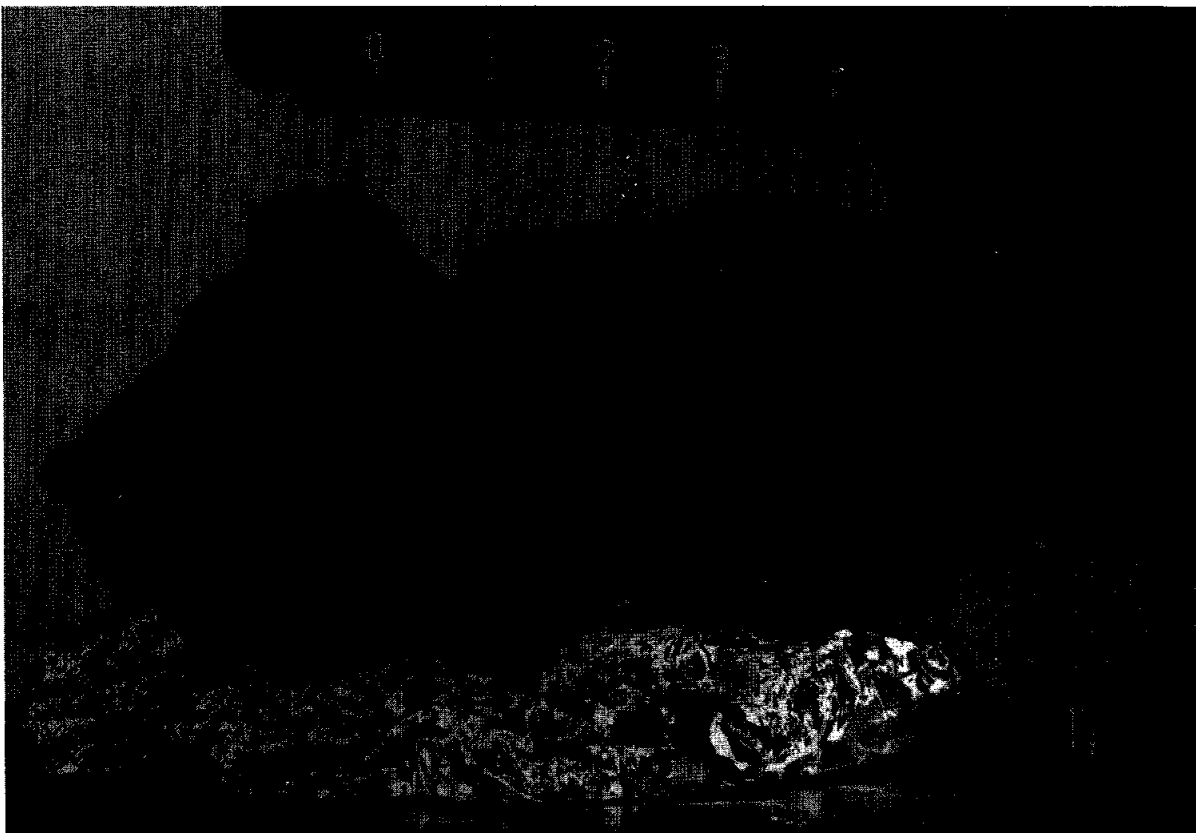


Figure 1: Fractured surface of 72435. Clasts as large as 10 mm are visible, as well as vesicles up to 8 mm (lower center right). Scale in centimeters. S-73-19652.

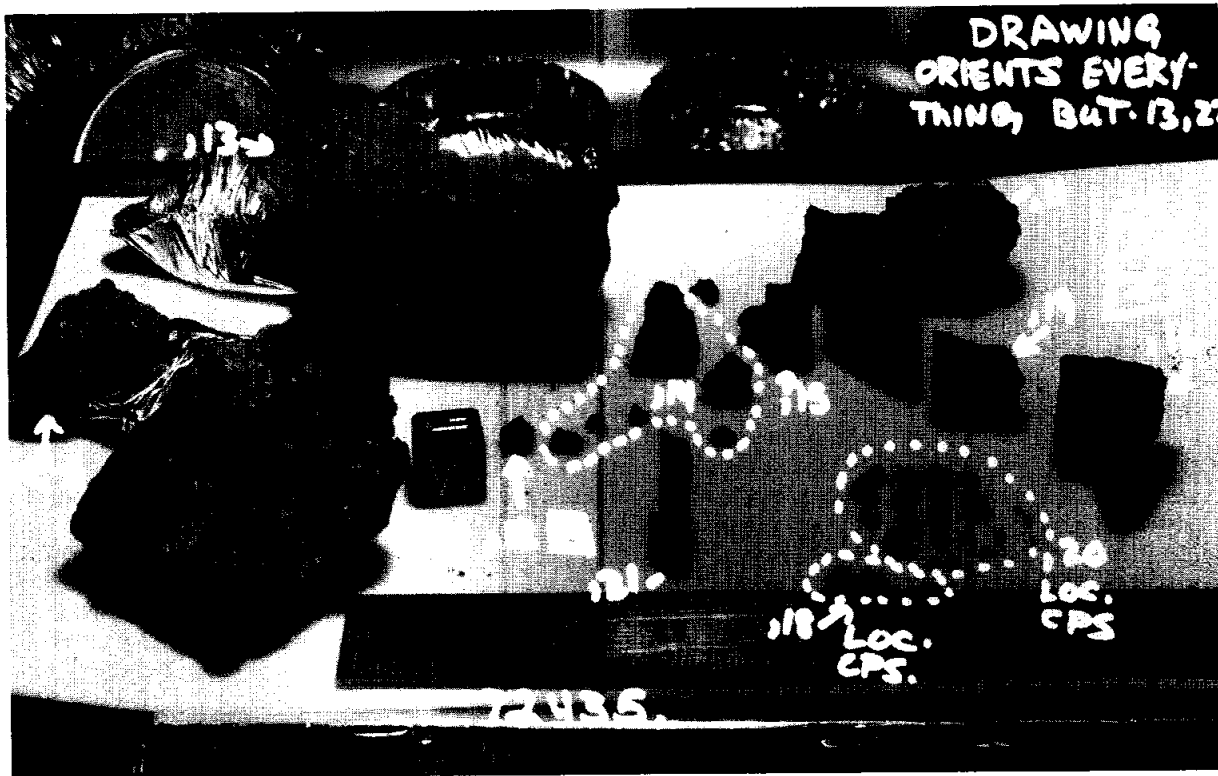


Figure 2: Dissection of 72435 with a single saw-cut across the larger end. Cube is 1 cm across. S-74-23143.

PETROGRAPHY

72435 consists of mineral and lithic clasts in an extremely fine-grained, poikilitic, partially clastic matrix (Dymek et al., 1976a,b). The sample formed as the result of crystallization of a clast-bearing melt produced in an impact. In thin section the matrix has a dark gray appearance resulting from the aphanitic nature (Fig. 3a). The larger clasts are lithic fragments, most less than 2 cm across. The smaller clasts include abundant mineral clasts. According to Dymek et al. (1976a), clasts in the 1 to 20 mm range compose 5 to 10% of the sample. The igneous groundmass has an average grain-size of less than 50 microns (Fig. 3b), and the microclasts have a seriate grain-size distribution. Simonds et al. (1974) referred to 72435 as a crystalline, matrix-supported, micropoikilitic rock with matrix feldspars 5 to 30 microns long and matrix mafic grains 25 to

50 microns long. Chao and Minkin (1974b) noted that 72435 was similar to 77135. Albee et al. (1974) noted that the sample differs from the Boulder 2, Station 2 samples in being blue-gray, having fewer and smaller clasts, and some larger vesicles; they also noted some zones of aligned slit vesicles.

The most detailed petrographic description of both clasts and matrix for 72435 are by Dymek et al. (1976a), who present microprobe data. Further details on a specific spinel-troctolite clast were given by Herzberg (1978), Herzberg and Baker (1980), and Baker and Herzberg (1980a,b). Most of the groundmass is homogeneous, but there are some areas (about 300 microns) that are much finer-grained. Other areas up to 500 microns across contain aggregates of plagioclase laths; these might be either clasts or a type of "synneusis" texture. The groundmass appears to be unaffected by the local alignment

of slit vesicles and clasts. Dymek et al. (1976a) listed the phase abundances, phase compositions, and the bulk chemical composition (from a microprobe point count) of 72435 (Table 1). The tabulated phase compositions appear to represent those of the groundmass, not clasts. These authors also diagrammed the mineral compositions for the sample, reproduced here as Fig. 4 (plagioclases), Fig. 5 (pyroxenes), Fig. 6 (olivines and Fe-Ti oxides), Fig. 7 (spinel), and Fig. 8 (metal). Most of these diagrams include data from dunite 72415-7 for comparison, and distinguish clasts from groundmass phases.

The groundmass consists of fine-grained intergrown pyroxene, plagioclase, olivine, and ilmenite. The mafic silicate grains form tiny oikocrysts (about 10-50 microns across) that enclose tinier grains of plagioclase; most of the ilmenite is interstitial to the oikocrysts (Fig. 3b). Most of the oikocrysts are low-

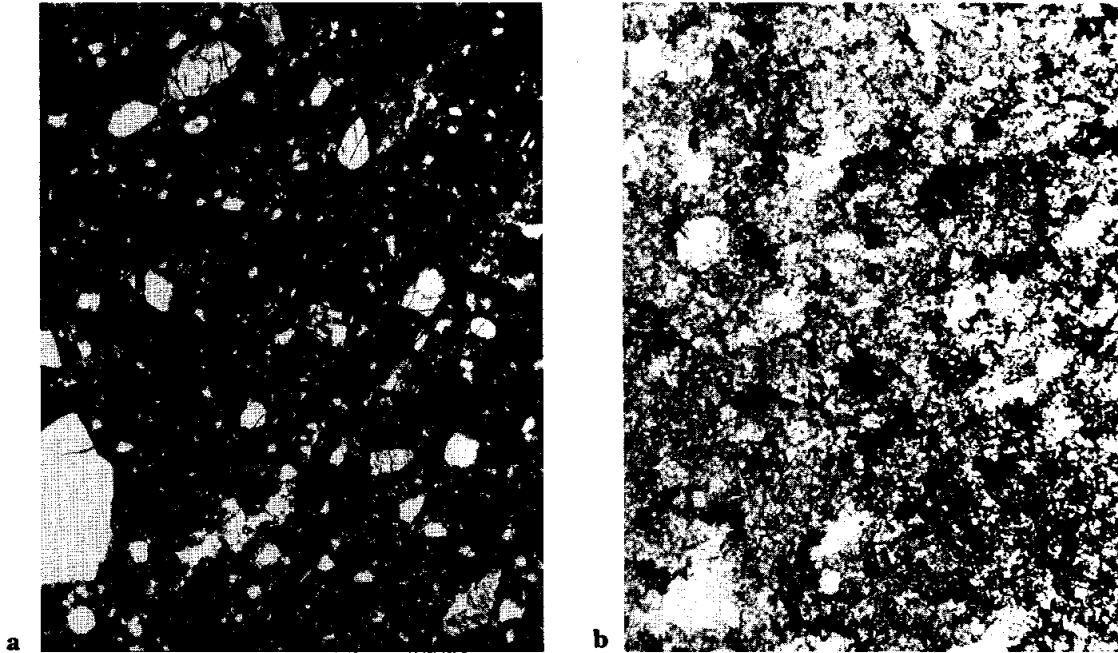


Figure 3: Photomicrographs of 72435,7. Both transmitted light; fields of view about 1 mm (a) and about 300 microns (b). a) shows the dense nature of the groundmass, the subrounded/subangular nature of the clasts, and the small size of most clasts. b) shows the igneous nature of the groundmass, with ilmenite (black) forming interstitially to the mafic oikocrysts, which seem mottled because they are studded with tiny plagioclases.

Figure 4: Compositions of plagioclases in 72435, with groundmass and clast plagioclases distinguished, and data for dunite 72415-7 for comparison (Dymek et al., 1976a).

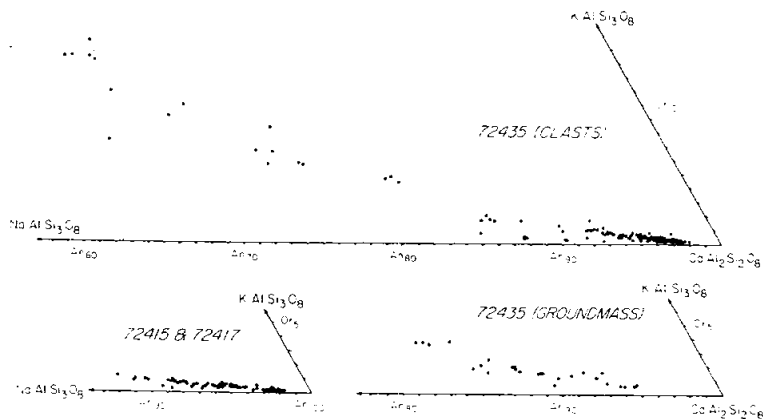


Figure 5: Compositions of pyroxenes in 72435, with groundmass and clast pyroxenes distinguished, and data for dunite 72415-7 for comparison (Dymek et al., 1976a).

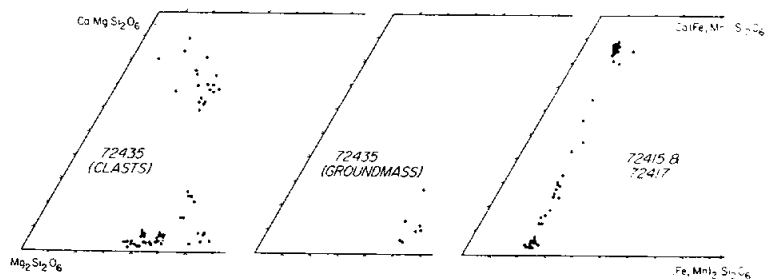


Figure 6: Compositions of olivines in 72435, with groundmass and clast olivines distinguished, and data for dunite 72415-7 for comparison (Dymek et al., 1976a).

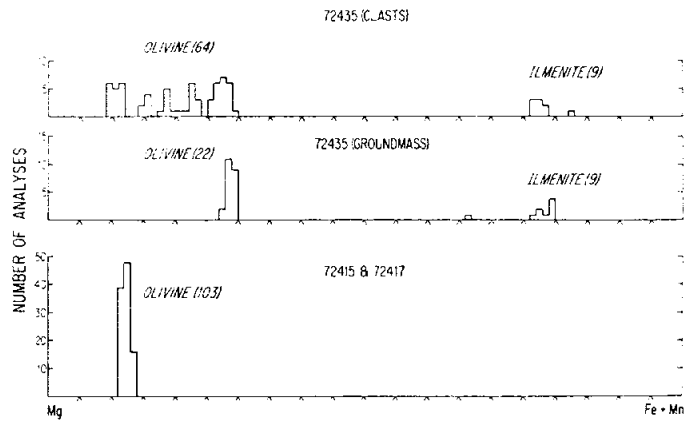


Figure 7: Compositions of spinels in 72435, with groundmass and clast spinels distinguished, and data for dunite 72415-7 for comparison (Dymek et al., 1976a).

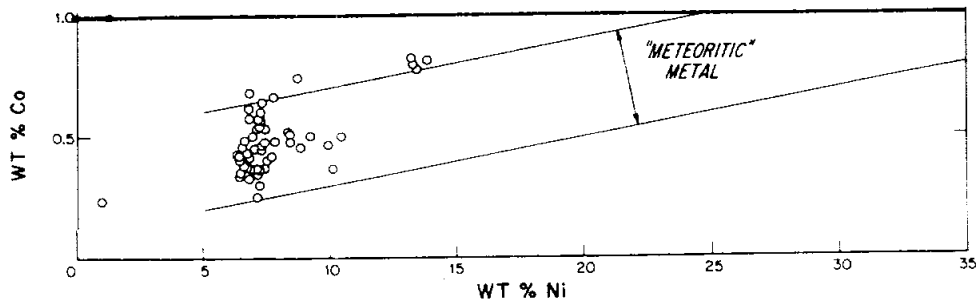
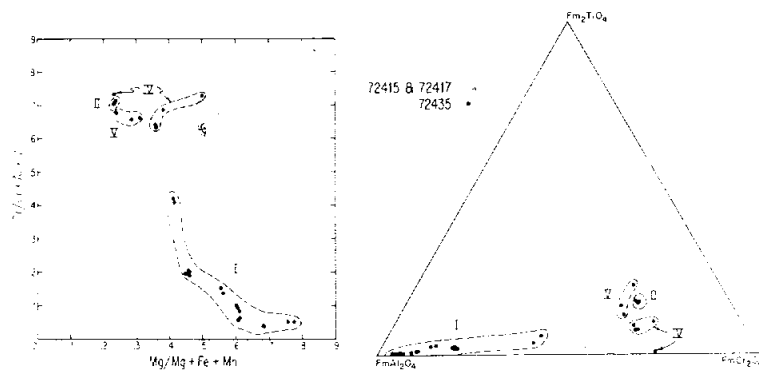


Figure 8: Ni and Co concentrations of metals in 72435 groundmass. Most fall in the "meteoritic" field. (Dymek et al., 1976a).

Table 1: Phase abundances, "average" phase compositions, and calculated bulk chemical composition of 72435,39. (Dymek et al., 1976a).

	Plag.	Low-Ca pyx	High-Ca pyx	Olivine	Ilmenite	Troilite*	Metal*	Ca-Phos.†	Meso- stasis	SiO ₂	Bulk comp.
Vol.%	63.0 _a	21.0 _a	3.8 _a	8.1 _a	1.9 _a	0.0 _a	0.1 _a	0.3 _a	0.9 _a	0.6 _a	Calculated (777 points)
±1σ	2.8 _a	1.6 _a	0.7 _a	1.0 _a	0.5 _a	0.0 _a	0.1 _a	0.1 _a	0.3 _a	0.2 _a	
Wt.%	57.5 _a	23.9 _a	4.2 _a	9.5 _a	2.7 _a	0.0 _a	0.3 _a	0.3 _a	0.7 _a	0.5 _a	
P ₂ O ₅	n.a.	n.a.	n.a.	n.a.	n.a.	n.a.	n.a.	43.15	0.09	n.a.	0.15
SiO ₂	45.46	52.77	51.96	37.71	0.31	<0.1	<0.01	—	64.10	99.93	45.59
TiO ₂	0.09	1.03	1.85	0.10	53.53	n.a.	<0.01	—	1.92	<0.01	1.85
Al ₂ O ₃	34.98	1.39	2.53	<0.01	0.08	n.a.	n.a.	—	16.79	0.48	20.71
Cr ₂ O ₃	n.a.	0.40	0.67	0.10	0.40	n.a.	n.a.	—	<0.01	n.a.	0.14
MgO	0.07	25.33	17.38	36.65	5.98	n.a.	<0.01	—	0.11	0.03	10.49
FeO	0.12	14.87	8.01	26.12	39.12	63.12	91.26	—	1.19	0.04	8.01
MnO	n.a.	0.20	0.19	0.21	0.39	0.05	n.a.	—	0.01	n.a.	0.09
CaO	18.48	3.83	17.88	0.11	n.a.	n.a.	n.a.	54.54	1.28	0.03	12.51
Nb ₂ O ₅	1.12	0.02	0.13	n.a.	n.a.	n.a.	n.a.	—	0.26	<0.01	0.66
K ₂ O	0.21	n.a.	n.a.	n.a.	n.a.	n.a.	n.a.	—	13.31	0.25	0.23
BaO	0.11	n.a.	n.a.	n.a.	n.a.	n.a.	n.a.	—	1.29	0.24	0.07
ZrO ₂	n.a.	n.a.	n.a.	n.a.	<0.01	n.a.	n.a.	—	<0.01	n.a.	<0.01
V ₂ O ₅	n.a.	n.a.	n.a.	n.a.	<0.01	n.a.	n.a.	—	n.a.	n.a.	<0.01
Nb ₂ O ₅	n.a.	n.a.	n.a.	n.a.	0.19	n.a.	n.a.	—	n.a.	n.a.	<0.01
NiO	n.a.	n.a.	n.a.	<0.01	n.a.	<0.01	7.18	—	n.a.	n.a.	0.03
Co	n.a.	n.a.	n.a.	n.a.	n.a.	<0.01	0.58	—	n.a.	n.a.	<0.01
S	n.a.	n.a.	n.a.	n.a.	n.a.	37.25	<0.01	—	n.a.	n.a.	0.03
F	n.a.	n.a.	n.a.	n.a.	n.a.	n.a.	n.a.	2.31	n.a.	n.a.	<0.01
Total	100.63	99.85	100.61	101.01	100.00	100.42	99.02	100.00	100.37	101.01	
	An 89.0	Wo 5.6	Wo 32.4	Fo 71.3							
	Ab 9.8	En 67.8	En 47.9	Fa 28.7							
	Or 1.2	Fs 22.6	Fs 12.7								
	Others	4.0	7.0								

*Elemental abundances; converted to oxides for calculating bulk composition.

†Assumed 1:1 mixture of fluorapatite and whitlockite.

n.a. = Not analyzed.

Ca pyroxenes (En₇₃Wo₂ to En₆₂Wo₁₄); some are high-Ca pyroxenes, and others are olivines (Fo₇₂₋₇₀). Olivine also occurs at oikocryst boundaries. Most of the plagioclase chadacrysts form euhedral laths less than 10 microns across, and compose up to a third of the area of the oikocryst. Orientations are random. Most chadacrysts are An₉₁₋₈₅; laths outside the oikocrysts range from An₉₅₋₈₀. Ilmenite occurs interstitially as bladed grains 1-10 microns wide, and as tiny blebs, some of which are in oikocrysts. The groundmass also contains interstitial troilite, Fe-metal, and areas of K-rich mesostasis with small phosphate grains.

Most of the clasts are single mineral fragments, and include plagioclase, olivine, low-Ca pyroxenes, and much less common high-Ca pyroxene, metal, ilmenite, and spinel. Variation in size, angularity, degree of shock, and composition indicate a variety of sources. They tend to have wider ranges in composition than groundmass phases. Plagioclases

include untwinned and twinned types, ranging from subrounded to subangular, and from subequant to elongate. They vary from unshocked and clear, to shocked with cloudy or undulose extinction features, including feathery/spherulitic aggregates. Zoning is only rarely present. The range in compositions is extremely large (An₅₅Ab₃₀Or₁₅ to An₉₈Ab₂Or_{<1}), and includes compositions both less refractory and more refractory than groundmass plagioclases. Some have reaction rims; rarely plagioclases clasts are extensively resorbed. Most pyroxenes are subequant. They range from very pale green and brown to darker, mottled fragments that are probably shocked. Most are homogeneous in composition, and are at least as magnesian as groundmass grains. Olivines (Fo₉₂₋₇₀) range from strain-free, virtually colorless grains to those with abundant strain bands and partings. Some are zoned; reaction rims are not present, and edge compositions are equivalent to groundmass olivines.

Spinel clasts have spectacular reaction rims.

Most of the lithic clasts in 72435 are feldspathic highlands lithologies, similar to those in Boulder 2, Station 2 samples, and compose several percent of the rock. They have a range of textures, grain sizes, and compositions. Plagioclases in these fragments are generally more calcic than An₉₀. Pyroxenes and olivines have compositions similar to those of the mineral clasts. The lithologies (according to Dymek et al., 1976a) include recrystallized anorthositic, noritic, and troctolitic rocks, poikilitic norites, dunites, and spinel cataclastite. Many of these are feldspathic granulitic breccias, i.e. recrystallized. The dunites resemble 72415-8 samples i.e., coarse-grained. Some fine-grained samples differ in having polygonal textures and are not cataclastites.

Dymek et al. (1976a) noted two spinel cataclastite fragments, a distinctive lithology, and reported mineral analyses. The fragments are friable, and consist of a broken

assemblage of plagioclase (70%; An₉₈₋₉₄), olivine (20%; Fo₇₂), pink spinel (5%), low-Ca pyroxene (1%), and smaller amounts ilmenite, troilite, and Fe-metal. One of the clasts contains a single grain of cordierite (30 microns) as an inclusion in spinel. No high-Ca pyroxene was observed by Dymek et al. (1976a). The major mineral phases are unshocked and clear. Herzberg (1978), Herzberg and Baker (1980), and Baker and Herzberg (1980a,b) further studied the spinel cataclasites in an attempt to define temperatures and pressures of origin from thermodynamic constraints based on experimental data. They provided new mineral composition data (Figs. 9, 10) that is consistent with the Dymek et al. (1976a) data and detailed petrographic descriptions. A summary of the compositions and conclusions based on them is given as Table 2, with the cordierite-bearing (in ,8) and cordierite-free (in ,30) samples distinguished. Ranges in composition of spinels and pyroxenes show that the fragments are not in equilibrium, and some grains may not be indigenous. However, much of the olivine, spinel, and pyroxene may be in equilibrium. The two samples produce different estimates of the pressure, with the cordierite-free sample suggestive of mid- to lower-crust levels, and the cordierite-bearing sample giving negative pressures.

CHEMISTRY

Chemical analyses of bulk rock (groundmass plus clasts) for 72435 are given in Table 3; the major element analyses agree fairly well with that derived by Dymek et al. (1976a) from a microprobe point count (Table 1). The rare earth elements are plotted as Figure 11. These data were reported with little specific discussion. The sample has a low-K Fra Mauro basalt composition, similar in major and trace elements to many other impact melt samples at the Apollo

17 site. It clearly has meteoritic contamination, but the siderophile element data are inadequate to specify a meteoritic group (a la Anders group).

RADIOGENIC ISOTOPES AND GEOCHRONOLOGY

Rubidium and strontium isotopic data for whole-rock samples of 72435 were reported by Nyquist et al. (1974a, b) and Papanastassiou and Wasserburg (1975a, b), and the

latter authors also reported data for splits derived from handpicking of clasts and density separations of a matrix sample. These isotopic data are reproduced in Tables 4 (whole rock) and 5 (separates).

According to Nyquist et al. (1974a), the data lie on a line with other Apollo 17 melt samples with a slope equivalent to an age of 3.94 \pm 0.1 Ga. 72435 has lower Rb than most of these other samples, giving older model ages. Papanastassiou and Wasserburg (1975a) found that

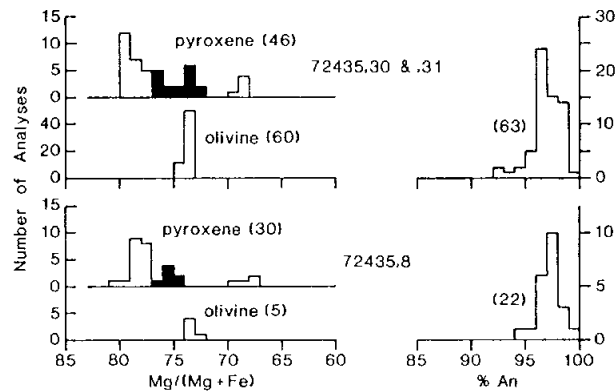


Figure 9: Summary of compositions of low-Ca pyroxene, olivine, and plagioclase in 72435 spinel cataclasites. Number of analyses in parentheses. The compositional range of pyroxenes in apparent equilibrium with coexisting olivine in each field is shaded. 72435,8 is cordierite-bearing; the others are cordierite-free. (Baker and Herzberg, 1980a).

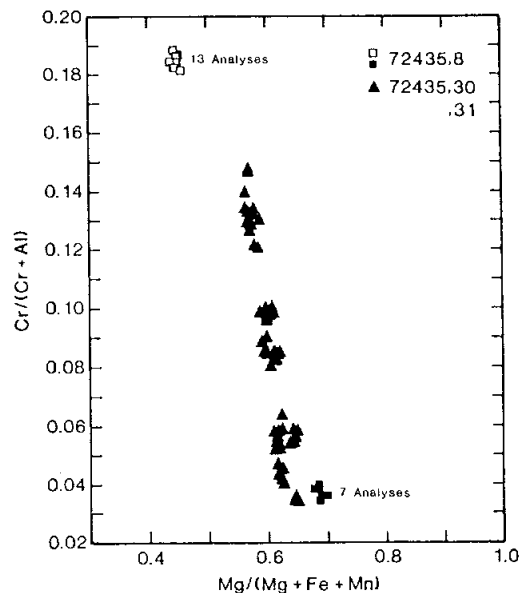


Figure 10: Compositions of spinels in 72435 spinel cataclasites. 72435,8 is cordierite-bearing; the others are cordierite-free. (Baker and Herzberg, 1980a).

Table 2: Pressure-temperature summary for spinel cataclasites in 72435, with summary of relevant mineral compositions. (Baker and Herzberg, 1980a).

72435,30				
Olivine (Fo ₇₃), Orthopyroxene [Mg/(Mg + Fe) = 0.78, Al ₂ O ₃ = 3.83 wt %, Ti/Al = .14], Spinel [Mg/(Mg + Fe) = 0.57 - 0.64, Al/(Al + Cr) = .87 - .94], Plagioclase (An ₉₆)				
Selenothermometer	T(°C)	Depth (km)		
		I	II	
1	1000-1200	≅32	≅12	
2	800-1200	≅28	≅12	
3	680- 810	≅26	≅12	
4	1170-1230	≅32	≅12	
I: from highest Al/(Al + Cr) and Mg/(Mg + Fe) in spinel II: from lowest Al/(Al + Cr) and Mg/(Mg + Fe) in spinel				
72435,8				
Olivine (Fo ₇₅), Orthopyroxene [Mg/(Mg + Fe) = .75, Al ₂ O ₃ ≈ 4 wt %, Ti/Al = 0.11], Cordierite [Mg/(Mg + Fe) = .84], Spinel [Mg/(Mg + Fe) = .45, Al/(Al + Cr) = 0.81], Plagioclase (An ₉₇).				
Selenothermometer	T(°C)	Depth (km)*		
		I	II	
1	700	-6	-12	
2	no solution		?	
3	950-1020	-10	-18	
4	1290-1310	-16	-24	
* 72435.8 is a univariant mineral assemblage. In principle, a specific T and P can be determined. I: from lowest Al ₂ O ₃ in opx II: from highest Al ₂ O ₃ in opx				

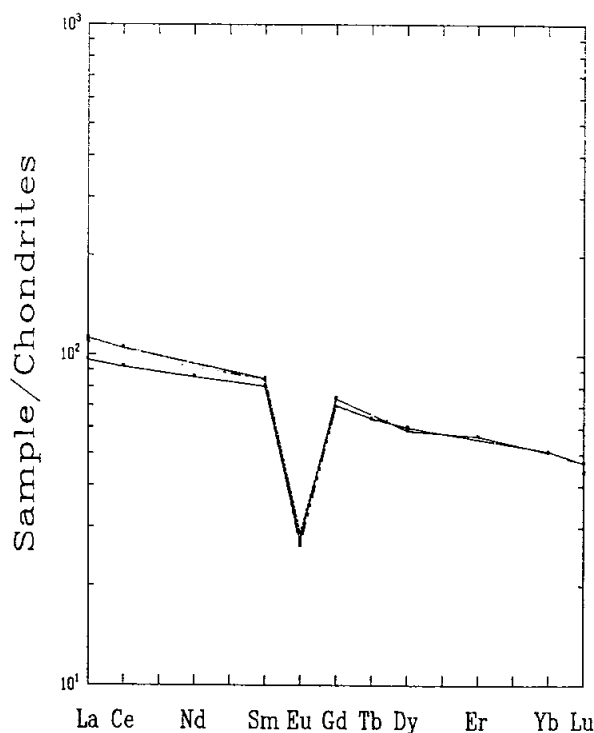


Figure 11: Rare earth elements in splits of 72435. Solid line is ,1 (Hubbard et al., 1974; Nyquist et al., 1974a). Fine dashed line is ,11 (Murali et al., 1977).

Table 3: Chemical analyses of bulk rock for 72435.

Split	,1	,1	,11	,1	,11 T-1	,11 T-2	,11 (a)	Split
wt %								wt %
SiO ₂	45.76							SiO ₂
TiO ₂	1.54		1.5					TiO ₂
Al ₂ O ₃	19.23		17.8					Al ₂ O ₃
Cr ₂ O ₃	0.20	0.1185	0.217					Cr ₂ O ₃
FeO	8.70		10.4					FeO
MnO	0.11		0.112					MnO
MgO	11.63		12					MgO
CaO	11.72		10.4					CaO
Na ₂ O	0.52		0.67					Na ₂ O
K ₂ O	0.23	0.2163	0.23		0.2394	0.2393	0.2131	K ₂ O
P ₂ O ₅	0.27							P ₂ O ₅
ppm								ppm
Sc			17					Sc
V			50					V
Co			31					Co
Ni	112		320					Ni
Rb	3.8	3.93			3.528	3.445	2.762	Rb
Sr	165	171.6			168.0	169.5	165.4	Sr
Y	107							Y
Zr	450	473	430					Zr
Nb	30							Nb
Hf		12.7	11.5					Hf
Ba		334	310					Ba
Th			3.0					Th
U		1.40						U
Cs								Cs
Ta			1.9					Ta
Pb								Pb
La		31.7	37.0					La
Ce		80.6	92					Ce
Pr								Pr
Nd		51.3						Nd
Sm		14.5	15.3					Sm
Eu		1.88	1.98					Eu
Gd		18.3						Gd
Tb			3.0					Tb
Dy		18.6	19					Dy
Ho								Ho
Er		11.3						Er
Tm								Tm
Yb		10.1	10.2					Yb
Lu			1.6					Lu
Li		17.5						Li
Be								Be
B								B
C								C
N								N
S	800			945				S
F								F
Cl								Cl
Br								Br
Cu								Cu
Zn	2							Zn
ppb								ppb
Au			6					Au
Ir			9					Ir
	(1)	(2)	(3)	(4)	(5)	(5)	(5)	

References and methods.

- 1) LSPET (1973); XRF
- 2) Hubbard et al. (1974), Nyquist et al. (1974a); ID/Ms except Na by AAS
- 3) Murali et al. (1977); INAA
- 4) Gibson and Moore (1974a); combustion
- 5) Papanastassiou and Wasserburg (1975a); ID/MS

Notes

(a) matrix adjacent to clast E.

Table 4: Whole-rock Rb-Sr isotopic data for 72435. Ages have been recalculated for new decay constant for ^{87}Rb (decay constant = $1.42 \times 10^{-11} \text{ y}^{-1}$) and are ± 0.06 to 0.09 Ga. Isotopic ratios have not been adjusted for interlaboratory bias.

Reference	Rb ppm	Sr ppm	$^{87}\text{Rb}/^{86}\text{Sr}$	$^{87}\text{Sr}/^{86}\text{Sr}$	T_{BABI}	T_{LUNI}
Nyquist et al. (1974a)	3.93	171.6	0.0662 \pm 6	0.70360 \pm 5	4.63	4.70
Papanastassiou and Wasserburg (1975a)	3.528 3.445 2.762	168.0 169.5 165.4	0.0609 0.0589 0.0484	0.70306 \pm 5 0.70300 \pm 5 0.70245 \pm 6	4.57 4.65 4.88	

Table 5: Rubidium and strontium isotopic data for 72435 whole-rock and separates as reported by Papanastassiou and Wasserburg (1975a). T_{BABI} ages are for a decay constant of $1.39 \times 10^{-11} \text{ y}^{-1}$. The first two and the last rows appear in modified form in Table 4.

Sample ^a	Weight mg	K ^f ppm	Rb ^f 10^{-8} mole/g	$^{88}\text{Sr}^f$ mole/g	$^{87}\text{Rb}/^{86}\text{Sr}$ $\times 10^2$	$^{87}\text{Sr}/^{86}\text{Sr}^g$	$T_{\text{BABI}}(\text{AE})$
Total-1	M 73	1995	4.128	158.0	6.09	0.70306 \pm 5	4.67 \pm 0.06
Total-2	M 35	1944	4.031	159.5	5.89	0.70300 \pm 5	4.75 \pm 0.06
Total-clast A	M 21	755	2.819	126.1	5.21	0.70234 \pm 5	4.50 \pm 0.07
Plag clasts	M 3.4	776	0.879	242.3	0.846	0.69957 \pm 4	—
Density separates (on 2.8 g of matrix)							
2.70 < ρ < 2.80	L 15	—	5.70	260.8	5.10	0.70240 \pm 4	4.67 \pm 0.05
2.60 < ρ < 2.70	L 5.3	7725	25.11	258.5	22.65	0.71318 \pm 4	4.37 \pm 0.02
		2.5 ^e 7350	23.70	257.7	21.45	0.71245 \pm 11	4.38 \pm 0.04
2.40 < ρ < 2.45	L 1.9	2990	12.11	186.6	15.14	0.70828 \pm 6	4.29 \pm 0.03
		1.6 ^e 2440	8.75	168.2	12.13	0.70657 \pm 7	4.37 \pm 0.04
2.35 < ρ < 2.40	L 2.3	2315	7.35	169.0	10.14	0.70540 \pm 5	4.42 \pm 0.03
Density separates (on 48 mg of matrix)							
2.6 < ρ < 2.8	L 2.2	2186	4.46	199.4	5.22	0.70250 \pm 5	4.69 \pm 0.07
2.4 < ρ < 2.5	L 1.6	1886	4.65	142.8	7.60	0.70396 \pm 9	4.57 \pm 0.08
2.8 < ρ < 3.0	L 2.3	2503	6.64	183.1	8.45	0.70448 \pm 5	4.54 \pm 0.02
Clast E							
Plag ^b -1	M 1.2	1148	2.141	174.2	2.867	0.70074 \pm 6	—
-2	M 1.0	1464	2.575	178.2	3.370	0.70111 \pm 9	—
-3	M 3.5	1725	4.495	197.3	5.32	0.70206 \pm 7	—
-4	M 4	1740	5.067	203.1	5.82	0.70239 \pm 4	4.10 \pm 0.05
-5	M 1.6	1584	4.948	180.1	6.41	0.70271 \pm 8	4.07 \pm 0.09
Rim ^c -1	M 2.3	2006	3.893	198.5	4.57	0.70199 \pm 9	4.59 \pm 0.14
-2	M 1.6	2043	4.076	178.7	5.32	0.70246 \pm 7	4.56 \pm 0.09
-3	M 0.8	1930	4.374	174.8	5.84	0.70270 \pm 12	4.44 \pm 0.14
Matrix ^d -1	M 3.9	1776	3.232	155.6	4.84	0.70245 \pm 6	4.98 \pm 0.09

^aSample obtained mechanically [M] or by heavy liquid density separations [L].

^bSamples from the interior of the clast.

^cSamples from pink-grey rim of clast.

^dMatrix sample adjacent to clast E.

^eRepeat analysis.

^fUncertainties in the concentrations: K \pm 1%; Rb \pm 0.4%; ^{88}Sr \pm 0.1%.

^gUncertainties correspond to last significant figures and are $\pm 2\sigma_{\text{mean}}$.

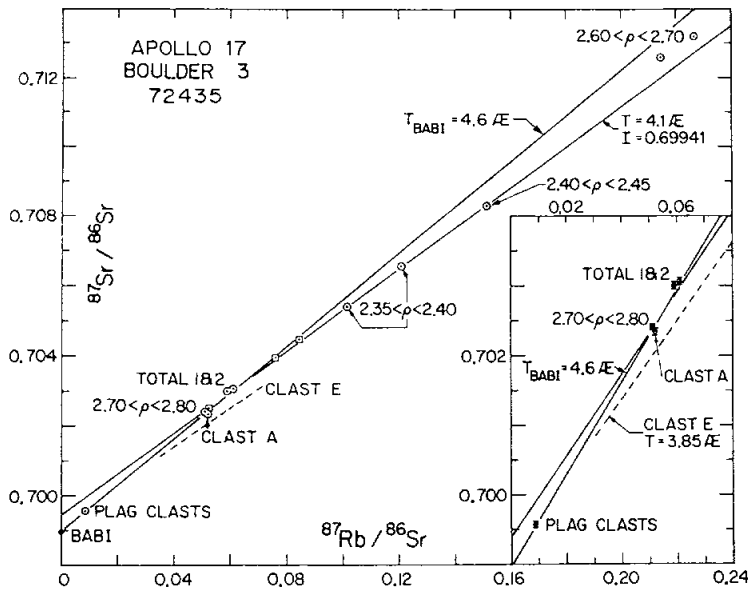


Figure 12: Rb-Sr evolution diagram for materials from 72435 (Papanastassiou and Wasserburg, 1975a). All ages on the diagram are for the old decay constant of $1.39 \times 10^{-11} \text{ y}^{-1}$. Lack of isotopic homogenization at any unique time in the past is obvious (a) for total rocks and clasts and (b) for mineral separates from the finer-grained matrix. The dashed line is for interior samples from clast E.

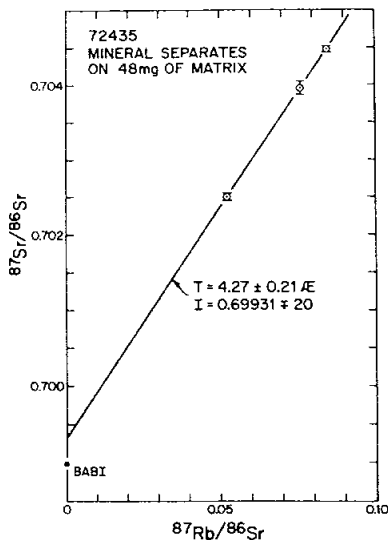


Figure 13: Rb-Sr evolution diagram for mineral separates from a 48 mg matrix sample of 72435 (Papanastassiou and Wasserburg, 1975a). The fit of the data to a straight line could result from mixing of only two phases. The age is for the old decay constant of $1.39 \times 10^{-11} \text{ y}^{-1}$.

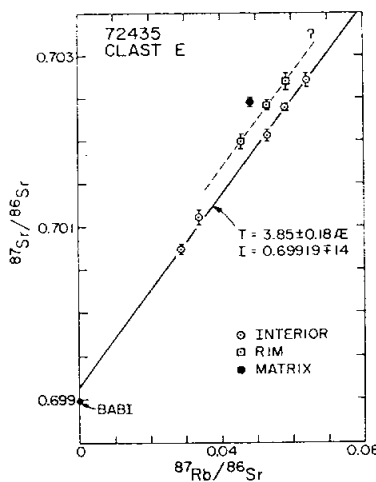


Figure 14: Rb-Sr evolution diagram for clast E from 72435 (Papanastassiou and Wasserburg, 1975a). Interior samples define a straight line (solid) from which rim and adjacent matrix samples are offset. The age (given on the diagram for the old decay constant of $1.39 \times 10^{-11} \text{ y}^{-1}$) has a large uncertainty because of the low spread in Rb/Sr.

the matrix and clasts do not fall on an isochron (Fig. 12); the plagioclases are distinctly non-radiogenic and lie on a whole-rock-BABI line equivalent to 4.5 Ga. Thus there is no Sr isotopic equilibration between matrix and clasts. (However, the paper refers to a Pb isotope study by Tera and Wasserburg that shows Pb equilibration between matrix and plagioclase clasts in 72435 at about 3.8 Ga; the reference given is erroneous). The density separates on the matrix also do not lie on a straight line so the matrix is not homogeneous. Matrix separates for a single 48 mg split fall on a line corresponding to an age of 4.18 ± 0.21 Ga (Fig. 13) but little credence can be given to such an age with the data available, the small spread in Rb/Sr, and the independent data for a younger age for the matrix-forming event. Data for clast E (predominantly plagioclase with a range of compositions) are shown in Figs. 14 and 15, with clast interior, rim, and adjacent matrix shown separately. The clast data correspond with an age of 3.77 ± 0.18 Ga; with large uncertainties resulting from the small spread in Rb/Sr. The adjacent rim and matrix samples fall distinctly off the isochron. Panastassiou and Wasserburg (1975a) could not distinguish whether the age of the clast was primary or metamorphic. The lowest model ages for breccia components are those of separates of clast E at about 3.9 Ga (decay constant $1.42 \times 10^{-11} \text{ y}^{-1}$), and these are maximum ages for breccia formation. The age of clast E itself would indicate a younger age or some disturbance.

Huneke et al. (1977) reported argon isotopic data for 4 combined plagioclase clasts from 72435, totalling 1.5 mg with 530 ppm K. The age is constant at 3.87 ± 0.07 (new constant) over the entire release (Fig. 16), with no suggestion of older ages suggested by the primitive Sr isotopes in 72435 plagioclases. Huneke and Wasserburg (1978) and Huneke (1978) reported further studies on

argon isotopes in two individual clasts (Fig. 17), tabulating release data. One consisting of a plagioclase crystal and 25% matrix (0.4 mg; 1200 ppm K) gave a well-defined age of 3.86 ± 0.04 Ga over the entire release. A large plagioclase crystal (0.6 mg; 190 ppm K) gave a similar age over the first 40% of ^{39}Ar release, then the age rose to 4.04 Ga for the remainder of the release. This plagioclase was incompletely degassed at 3.86 Ga, and 4.04 Ga is a lower limit to its age.

Goswami et al (1976a) reported track data for 72435. The boundary-track method gave preliminary results of an upper limit to compaction less than 4.1 Ga ago. A more precise determination was hindered by a lack of cosmic ray exposure ages, as there was a high background of cosmic ray tracks. No data were presented

PHYSICAL PROPERTIES

Pearce et al (1974a,b) listed the magnetic properties of 72435,1 (Table 6) without specific discussion. The metallic iron contents are similar to other Apollo 17 impact melts and much higher than mare basalts. The metal is coarse-grained with low $J_{\text{rs}}/J_{\text{s}}$.

PROCESSING

The sample was received as two pieces originally numbered as 72435 and 72436; they were combined as 72435 when it was realized that they fitted together. Two small chips (#1; #2) were removed from #0. Advantage was taken of the natural break to produce a slab across the sample with only one sawcut, leaving the large E end #13 (now 71 g), the W end #22 (two broken pieces, 40 g, now at Brooks), and the slab sections (Fig. 2). The slab was subdivided by perpendicular sawcuts and most allocations made

from it. One piece, 11(21 g) was sent for subdivision and study by the consortium led from Caltech. Some matrix pieces were taken from #22 before it was stored at Brooks.

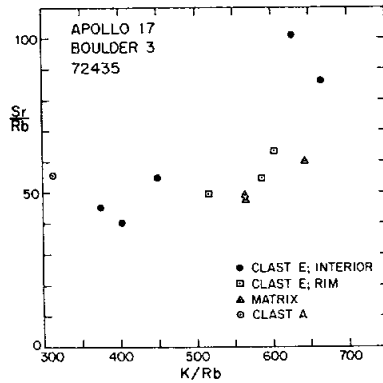


Figure 15: Element correlation diagram for samples from 72435 (Papanastassiou and Wasserburg, 1975a). Samples of clast E require the presence of at least 3 phases; the matrix and clast E rim appear distinct from clast E.

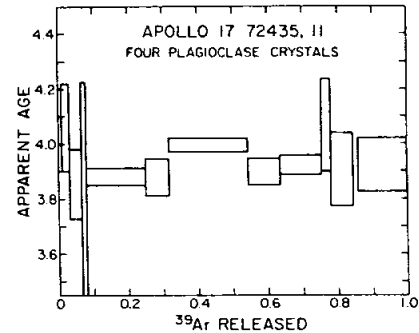


Figure 16: Apparent age of four combined plagioclase crystals from 72435 (Huneke et al., 1977). Age scale is for old decay constants.

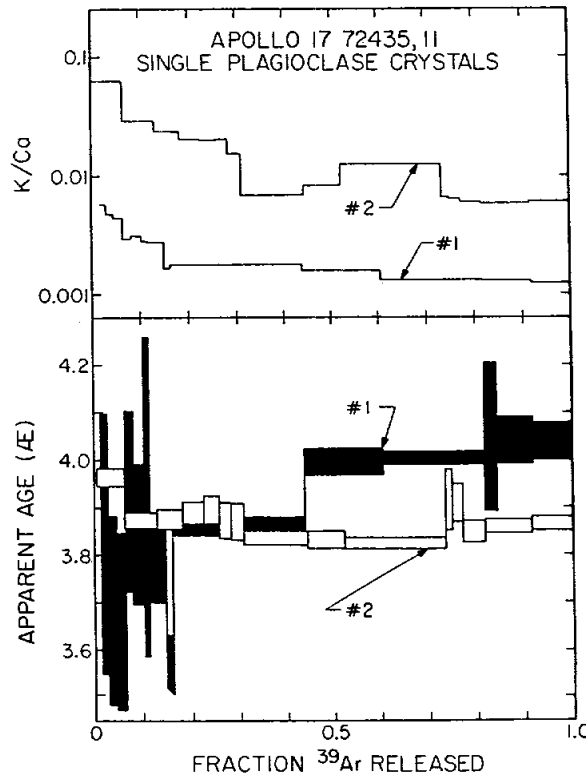


Figure 17: Apparent age of clasts from 72435 (Huneke, 1978). Clast 1 is plagioclase; Clast 2 is plagioclase + 25% matrix. Age scale is for new decay constants.

Table 6: Magnetic properties of 72435,1. Pearce et al (1974a,b)

Sample	J_s (emu/g)	X_p (emu/g Oe) $\times 10^6$	X_0 (emu/g Oe) $\times 10^4$	J_{s1}/J_s	H_c (Oe)	H_{c2} (Oe)	Equiv. wt.% Fe ⁰	Equiv. wt.% Fe ²⁺	$\frac{Fe^0}{Fe^{2+}}$
72435.1	.86	14.9	2.1	.003	19	—	.39	6.83	.058

72505**Impact Melt Breccia (?)****St. 2, 3.09 g****INTRODUCTION**

72505 is an angular tough block (Fig. 1) collected as part of the soil with the first rake sample at Station 2, near Boulder 2. The sample was picked during sieving of soil 72500 as a fragment larger than 1 cm. It has macroscopic characters that suggest that it is an impact melt; identification is uncertain because it has never been allocated or dissected. According to LSIC 17 (1973), 72505 is light gray (N7) to olive gray (5Y 6/1); according to Keil et al. (1974) it is medium dark gray (N4). It is similar in

appearance to several other green-gray breccias from the South Massif that are impact melts (e.g. 72549). Keil et al. (1974) suggested that 72505 was melted or recrystallized. It was originally described as a high grade metaclastic rock, with an equigranular holocrystalline homogeneous fabric (LSIC 17, 1973). The mineralogy was identified as 55% colorless plagioclase, 41% mainly pale gray pyroxene, 3% yellow green olivine, and 1% black opaques. Most grains other than a few clasts are smaller than 200 microns. About 1% of the

volume is crystal-lined vugs, most smaller than about 100 microns. One outer surface is rounded with many zap pits (some of which are also present on parts of adjacent surfaces). The sample is coherent without fractures.



Figure 1: Sample 72505. Small scale divisions in millimeters. S-73-33423.

72535**Microsubophitic Impact Melt Breccia
St. 2, 221.4 g****INTRODUCTION**

72535 is a fine-grained clast-bearing impact melt with a subophitic groundmass texture. Its chemistry is similar to the common low-K Fra Mauro melts that dominate the Apollo 17 highlands samples. It has an exposure age of about 96 Ma and may have been excavated as part of a landslide caused by Tycho secondaries.

72535 was one of several blue-gray breccias (LSIC 17, 1973) collected in the first rake sample from Station 2, adjacent to Boulder 2. It is 7.6 x 6.8 x 5.9 cm, and medium dark gray (N4) (Keil et al., 1974). It is

subrounded (Fig. 1) and coherent, with a few non-penetrative fractures and about 1% small vugs. There are many zap pits and one surface has a thin layer of dark glass. Other surfaces were described by Keil et al. (1974) as granulated. Matrix material (less than 1 mm grain size) was estimated as 92% of the sample.

PETROGRAPHY

The groundmass of 72535 is a very fine-grained crystallized melt, with small clasts quite distinct from the groundmass (Fig. 2). It has some patchiness but is generally

homogeneous. Warner et al. (1977b,c; 1978f) described 72535 as a microsubophitic matrix breccia. Their modal data (Table 1) shows a high proportion of melt groundmass (85%) and a clast population dominated by plagioclase, similar to many other impact melt samples at the Apollo 17 site. Warner et al. (1977b,c; 1978f) described the dark porous groundmass as basaltic-textured, with plagioclase laths less than 30 microns long subophitically enclosed by irregular mafic crystals. Some mafic grains are locally ophitic to micropoikilitic in habit. Opaque minerals (mainly ilmenite) occur as irregular discrete

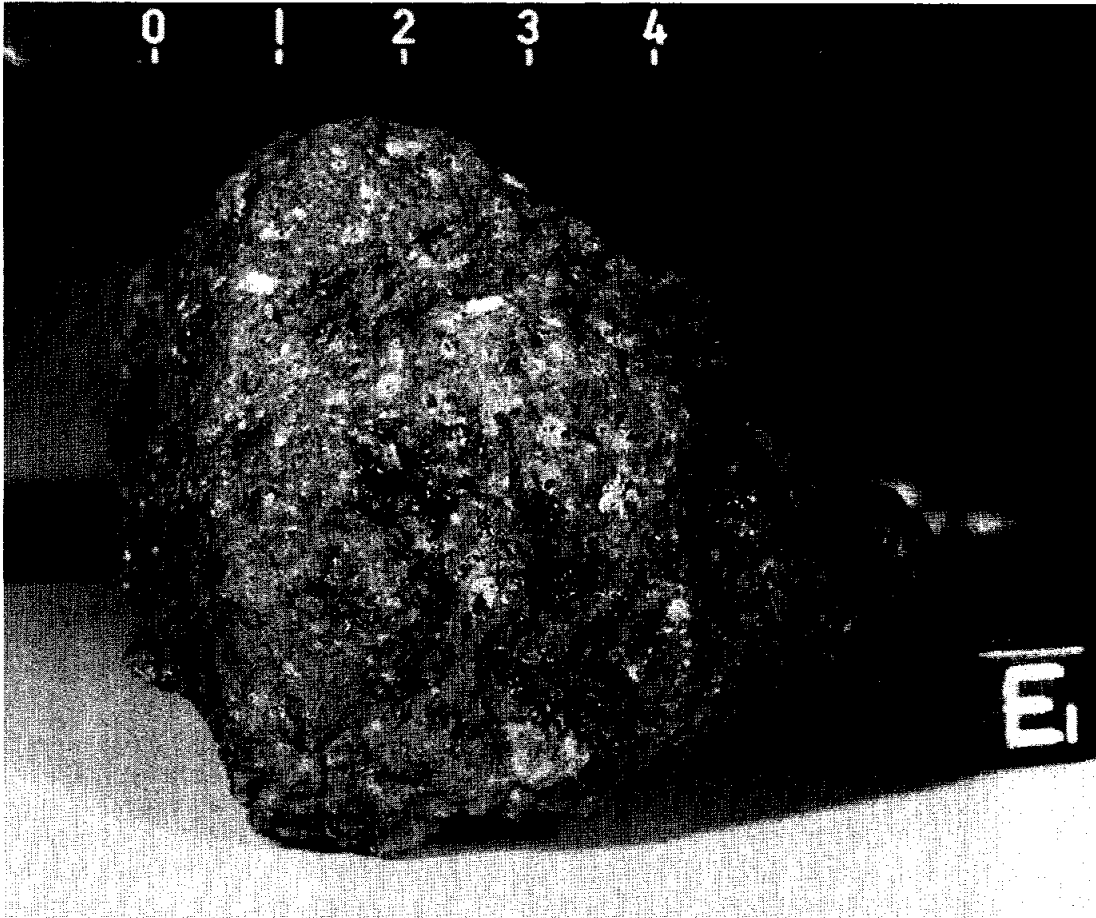


Figure 1: Sample 72535. S-73-20457B. Scale divisions in centimeters.

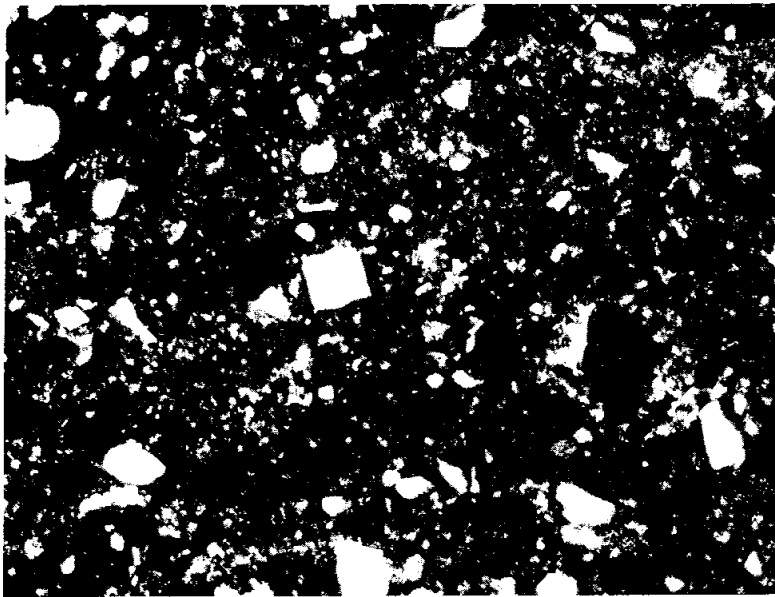


Figure 2: Photomicrograph of 72535,6, showing general groundmass. White phases are plagioclase clasts and some vugs. Plane transmitted light; width of field about 1 mm.

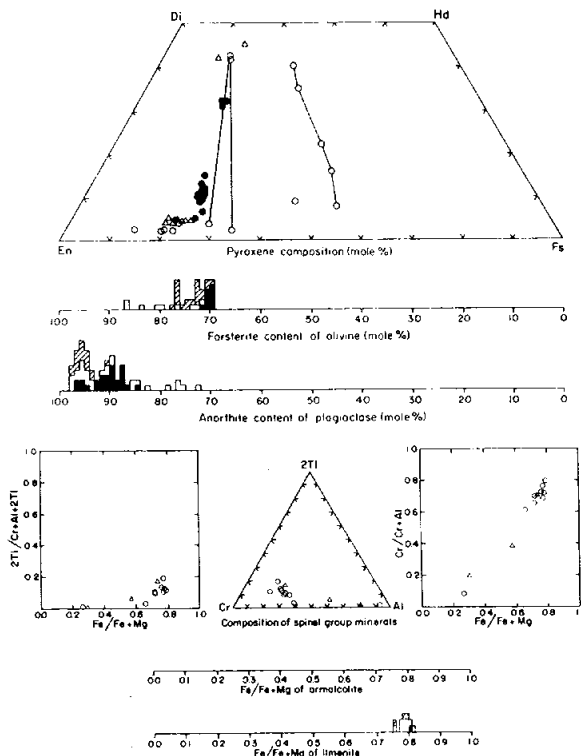


Figure 3: Microprobe analyses of minerals in 72535 (Warner et al., 1978f). Filled symbols = matrix phases. In histograms, open symbols = mineral clasts and cross-hatched = minerals in lithic clasts. In other diagrams, open circles = mineral clasts and open triangles = minerals in lithic clasts.

rods less than 5 microns wide and up to 20 microns long. Tiny grains of Fe-metal and troilite are widely disseminated. Microprobe analyses (Warner et al., 1978f) are shown in Figure 3. The matrix olivines show a narrow range of composition (Fo₆₉₋₇₁), but matrix pyroxenes and plagioclases show a wider range. Engelhardt (1979) tabulated ilmenite paragenetic features, inferring that ilmenite crystallization started after plagioclase but before pyroxene.

Both mineral and lithic clasts tend to be subrounded to subangular. Calcic plagioclases dominate the mineral clasts, and most are smaller than 100 microns; mafic mineral clasts also tend to be more refractory than the groundmass counterparts (Fig. 3). The lithic clasts are common highlands lithologies, including poikilitic norites, granoblastic feldspathic breccias, and several fine-grained crystalline feldspathic breccias. Two lithic fragments are broadly granitic.

CHEMISTRY

A 771 mg sample was analyzed by Laul and Schmitt (1975c) (Table 2; Fig. 4). The chemistry is fairly similar to that of other Apollo 17 impact melts (although K appears to be lower), and Laul and Schmitt (1975c) suggested that 72535 could be a fragment from Boulder 2 Station 2. A microprobe defocused beam analysis for the major elements (Table 3) agrees well with the neutron activation analysis.

RARE GASES AND EXPOSURE

Arvidson et al. (1976) reported Kr and Xe isotopic data for 72535, and a calculated ^{81}Kr -Kr exposure age of 107 ± 4 Ma. The hard Kr and Xe spallation spectra suggested that the sample received little shielding, and the relatively low $(^{131}\text{Xe}/^{126}\text{Xe})_c$ is also

characteristic of simple surface exposure. Assuming single stage exposure, therefore, and correcting for erosion, the exposure age was inferred to be 96 ± 5 Ma. The exposure age is one of a group of similar exposure ages that includes samples from the central crater cluster on the mare plains and may be attributable to secondary cratering from Tycho that created the cluster and caused the light mantle landslide.

PROCESSING

A few exterior chips with total mass less than 2 g were taken in 1974. Sample ,1 was used for thin sections and the chemical analysis, and ,2 for the rare gases. The three small chips composing ,3 remain unallocated.

Table 1: Modal analysis of 72535,6 (Warner et al., 1977b).

72535	
Points counted	3222
Matrix	84.8
Mineral clasts	11.0
Lithic clasts	4.2
Mineral clasts	
Plagioclase	7.1
Olivine/pyroxene	3.7
Opaque oxide	tr
Metal/troilite	0.2
Other	—
Total	11.0
Lithic clasts	
ANT	1.9
Devitrified anorthosite	0.6
Breccia	1.4
Other	0.3
Total	4.2
Percent of matrix (normalized to 100)	
Plagioclase	52.9
Olivine/pyroxene	43.8
Opaque oxide	2.9
Metal/troilite	0.1
Other	0.2

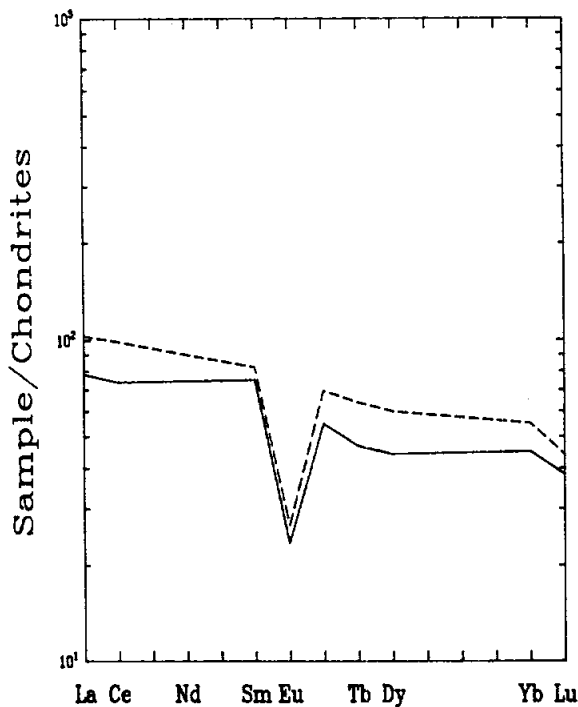


Figure 4: Chondrite-normalized rare earths in 72535,1 (solid line; Laul and Schmitt, 1975c) and average of Boulder 2 at Station 2 (dashed line; Laul and Schmitt, 1974a).

Table 2: Chemical analysis of bulk sample 72535.

Split	.1
<u>wt %</u>	
SiO ₂	
TiO ₂	1.4
Al ₂ O ₃	17.8
Cr ₂ O ₃	0.190
FeO	8.4
MnO	0.099
MgO	11
CaO	11.2
Na ₂ O	0.58
K ₂ O	0.13
P ₂ O ₅	
<u>ppm</u>	
Sc	16
V	40
Co	29.2
Ni	250
Rb	
Sr	
Y	
Zr	400
Nb	
Hf	8.7
Ba	300
Th	3.4
U	
Cs	
Ta	1.2
Pb	
La	25.8
Ce	65
Pr	
Nd	
Sm	13.6
Eu	1.62
Gd	
Tb	2.2
Dy	14
Ho	
Er	
Tm	
Yb	9.0
Lu	1.3
	(1)

Table 3: Microprobe defocused beam analysis of matrix of 72535 (from Warner et al., 1977b).

Split	
<u>wt %</u>	
SiO ₂	47.9
TiO ₂	1.68
Al ₂ O ₃	18.1
Cr ₂ O ₃	0.17
FeO	8.7
MnO	0.13
MgO	10.6
CaO	11.9
Na ₂ O	0.54
K ₂ O	0.07
P ₂ O ₅	0.27
	(Normalized to 100%).

References and methods:

(1) Laul and Schmitt (1975c); INAA

72536**Microsubophitic Impact Melt Breccia
St. 2, 52.3 g****INTRODUCTION**

72536 is a fine-grained clast-bearing impact melt with a subophitic groundmass texture. Its chemistry is similar to the common low-K Fra Mauro melts that dominate the Apollo 17 highlands samples.

72536 was one of several blue-gray breccias (LSIC 17, 1973) collected in the first rake sample from Station 2, adjacent to Boulder 2. It is 2.1 x 2.9 x 5.5 cm and medium dark gray (N4) (Keil et al., 1974). It is subrounded (Fig. 1) and coherent, with a few non-penetrative fractures. It lacks cavities but has many zap pits on most surfaces. It contains more and larger clasts than most other blue-gray breccias.

Matrix material (less than 1 mm grain size) was estimated to compose 94% of the rock (Keil et al., 1974).

PETROGRAPHY

The groundmass of 72536 is a very fine-grained crystallized melt very similar to 72535, with small clasts quite distinct from the groundmass (Fig. 2). It is a little more heterogeneous than 72535, with patches of finer material. Warner et al. (1977b,c; 1978f) described 72536 as a microsubophitic matrix breccia. Their modal data (Table 1) shows a high proportion of melt groundmass (83%) and a clast population dominated by plagioclase, similar to many other

impact melt samples at the Apollo 17 site. Warner et al. (1977b,c; 1978f) described the dark porous groundmass as basaltic-textured, with plagioclase laths less than 30 microns long subophitically enclosed by irregular mafic crystals. Opaque minerals (mainly ilmenite) occur as irregular discrete rods less than 5 microns wide and up to 20 microns long. Tiny grains of Fe-metal and troilite are widely disseminated. Microprobe analyses (Warner et al., 1978f) are shown in Figure 3. Engelhardt (1979) tabulated ilmenite paragenetic features, inferring that ilmenite crystallization started after plagioclase but before pyroxene.

Both mineral and lithic clasts tend to be subrounded to subangular;

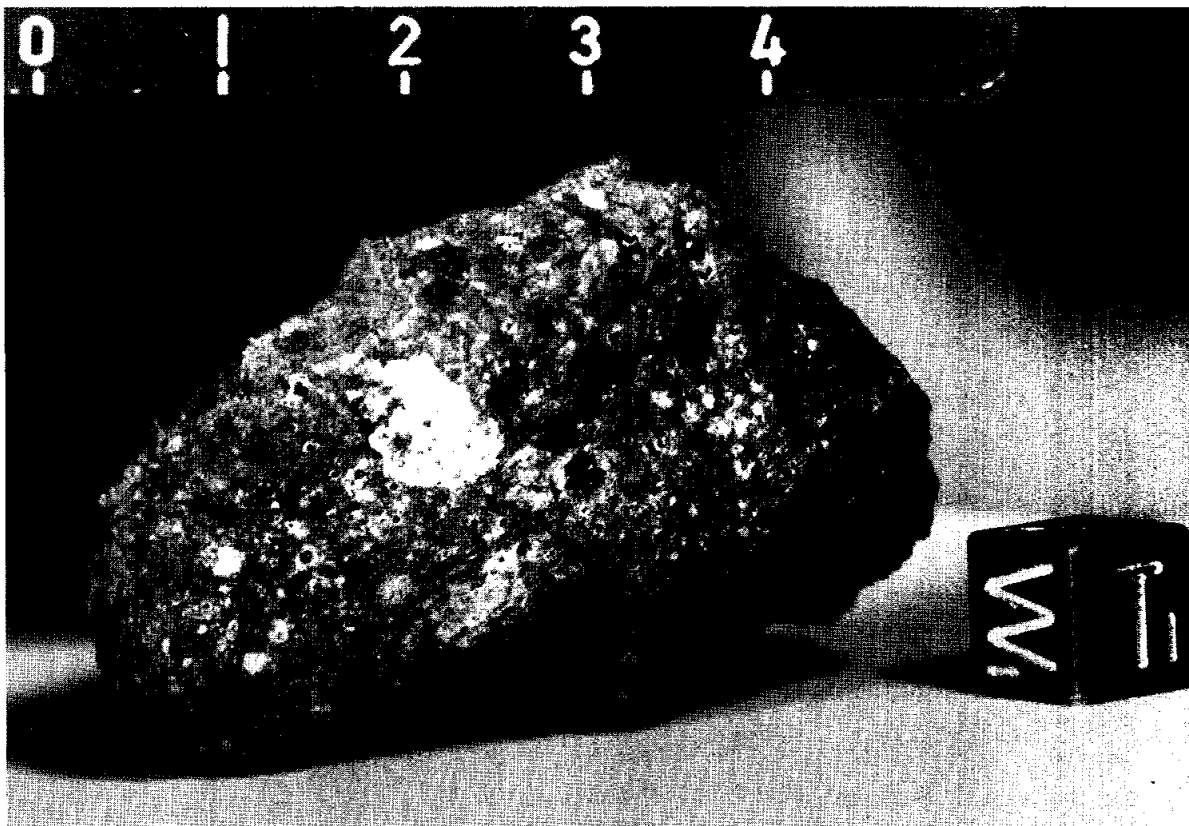


Figure 1: Sample 72536 S-73-20438. Scale divisions in centimeters.

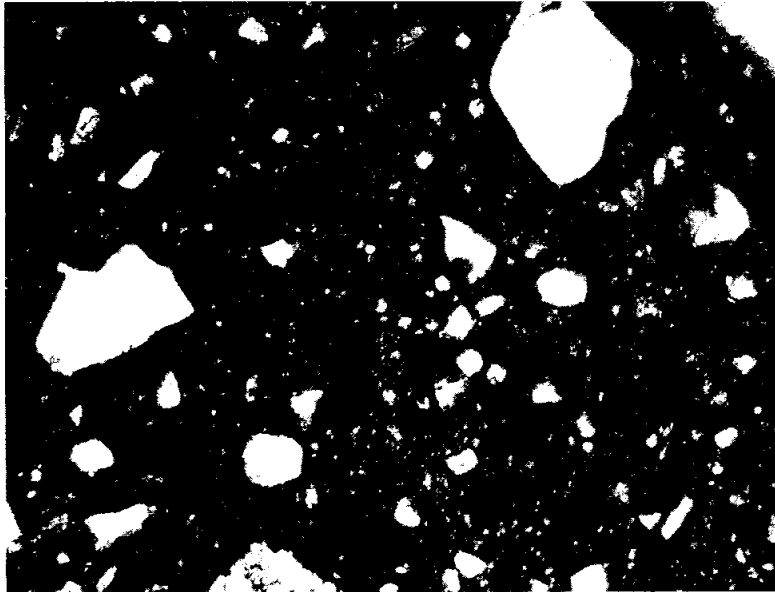


Figure 2: Photomicrograph of 72536,8, showing general groundmass. White phases are plagioclase clasts and some vugs. Plane transmitted light; width of field about 1 mm.

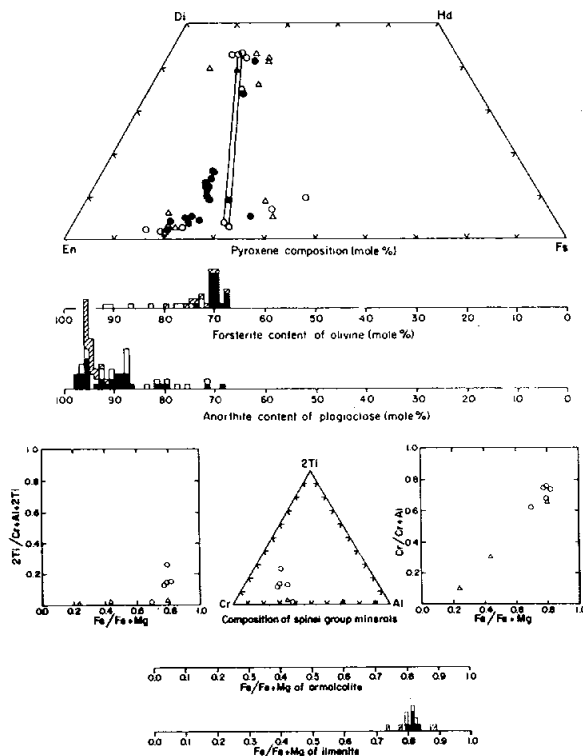


Figure 3: Microprobe analyses of minerals in 72536 (Warner et al., 1978f). Filled symbols = matrix phases. In histograms, open symbols = mineral clasts and cross-hatched = minerals in lithic clasts. In other diagrams, open circles = mineral clasts and open triangles = minerals in lithic clasts.

they tend to be larger than those in other blue-gray breccias. Calcic plagioclases dominate the mineral clasts; mafic mineral clasts also tend to be more refractory than the groundmass counterparts (Fig. 3). Some of the pyroxene contains exsolution lamellae. The lithic clasts are common highlands lithologies, including several fine-grained crystalline feldspathic breccias, a granoblastic anorthosite, devitrified anorthositic material, and a tiny intersertal basaltic fragment. Two lithic fragments are broadly granitic.

CHEMISTRY

A 630 mg sample was analyzed by Murali et al. (1977a) (Table 2; Fig. 4). The chemistry is fairly similar to that of other Apollo 17 impact melts, and demonstrates meteoritic contamination (about 3% C1 equivalent). A defocused beam analysis for the major elements (Table 3) agrees well with the neutron activation analysis.

PROCESSING

A few exterior chips were taken from a single area of the sample in 1974. Chips, 3 were used for the thin section and chemical analysis; other chips remain unallocated.

Figure 4: Chondrite-normalized rare earths in 72536 (solid line; Murali et al., 1977a) and average of Boulder 2 at Station 2 (dashed line; Laul and Schmitt, 1974a).

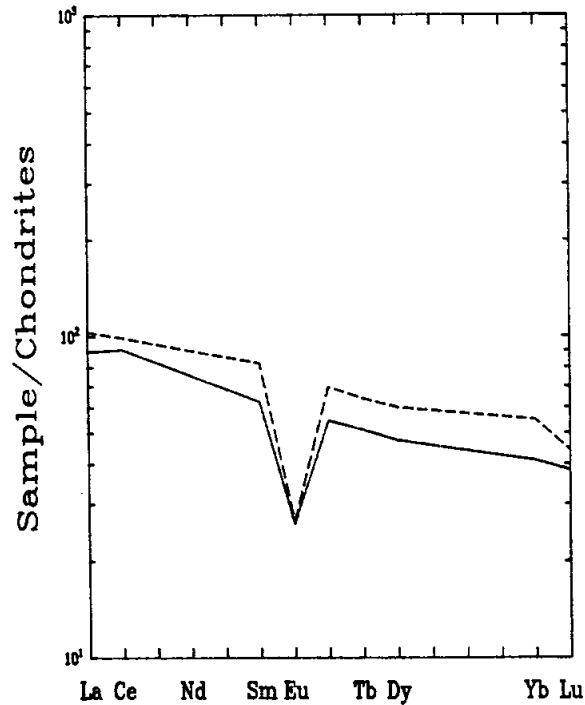


Table 1: Modal analysis of 72536,8 (Warner et al., 1977b).

Points counted	3496
Matrix	82.9
Mineral clasts	12.9
Lithic clasts	4.2
Mineral clasts	
Plagioclase	8.9
Olivine/pyroxene	3.9
Opaque oxide	tr
Metal/troilite	0.1
Other	—
Total	12.9
Lithic clasts	
ANT	2.6
Devitrified anorthosite	1.0
Breccia	0.6
Other	tr
Total	4.2
Percent of matrix (normalized to 100)	
Plagioclase	52.3
Olivine/pyroxene	44.3
Opaque oxide	3.0
Metal/troilite	0.3
Other	tr

Table 2: Chemical analysis of bulk sample 72536.

<u>Split</u>	,3
<u>wt %</u>	
SiO ₂	
TiO ₂	1.4
Al ₂ O ₃	17.1
Cr ₂ O ₃	0.286
FeO	10.0
MnO	0.120
MgO	11
CaO	10.6
Na ₂ O	0.53
K ₂ O	0.21
P ₂ O ₅	
<u>ppm</u>	
Sc	19
V	60
Co	32
Ni	320
Rb	
Sr	
Y	
Zr	320
Nb	
Hf	9.6
Ba	290
Th	2.5
U	
Cs	
Ta	1.5
Pb	
La	29.5
Ce	80
Pr	
Nd	
Sm	11.3
Eu	1.8
Gd	
Tb	2.4
Dy	15
Ho	
Er	
Tm	
Yb	8.2
Lu	1.3
Li	
Be	
B	
C	
N	
S	
F	
Cl	
Br	
Cu	
Zn	
<u>ppb</u>	
Au	1.5
Ir	4
	(1)

Table 3: Microprobe defocussed beam analysis of matrix of 72536 (from Warner et al., 1977b).

<u>wt %</u>	
SiO ₂	46.7
TiO ₂	1.63
Al ₂ O ₃	18.2
Cr ₂ O ₃	0.16
FeO	8.8
MnO	0.13
MgO	11.1
CaO	11.5
Na ₂ O	0.57
K ₂ O	0.21
P ₂ O ₅	0.30
Sum	99.3

References and methods:

(1) Murali et al. (1977a); INAA

72537**Impact Melt Breccia (?)****St. 2, 5.2 g****INTRODUCTION**

72537 is a small block (Fig. 1) collected as part of the first rake sample at Station 2, near Boulder 2. It has macroscopic characters that suggest that it is an impact melt; identification is uncertain because it has never been allocated or

dissected. According to LSIC 17 (1973), 72537 is a blue-gray breccia; according to Keil et al. (1974) it is medium dark gray (N4). It is similar in appearance to several other green-gray breccias from the South Massif that are impact melts (e.g. 72535). The sample is 2.1 x 1.2 x 1.5 cm, subrounded and

coherent, with a few non-penetrative fractures (Fig. 1). Matrix material (grain size less than 1 mm) is about 96% of the sample; the remaining 4% consists mainly of small plagioclase clasts. It has zap pits on most surfaces, but no internal cavities or vugs.

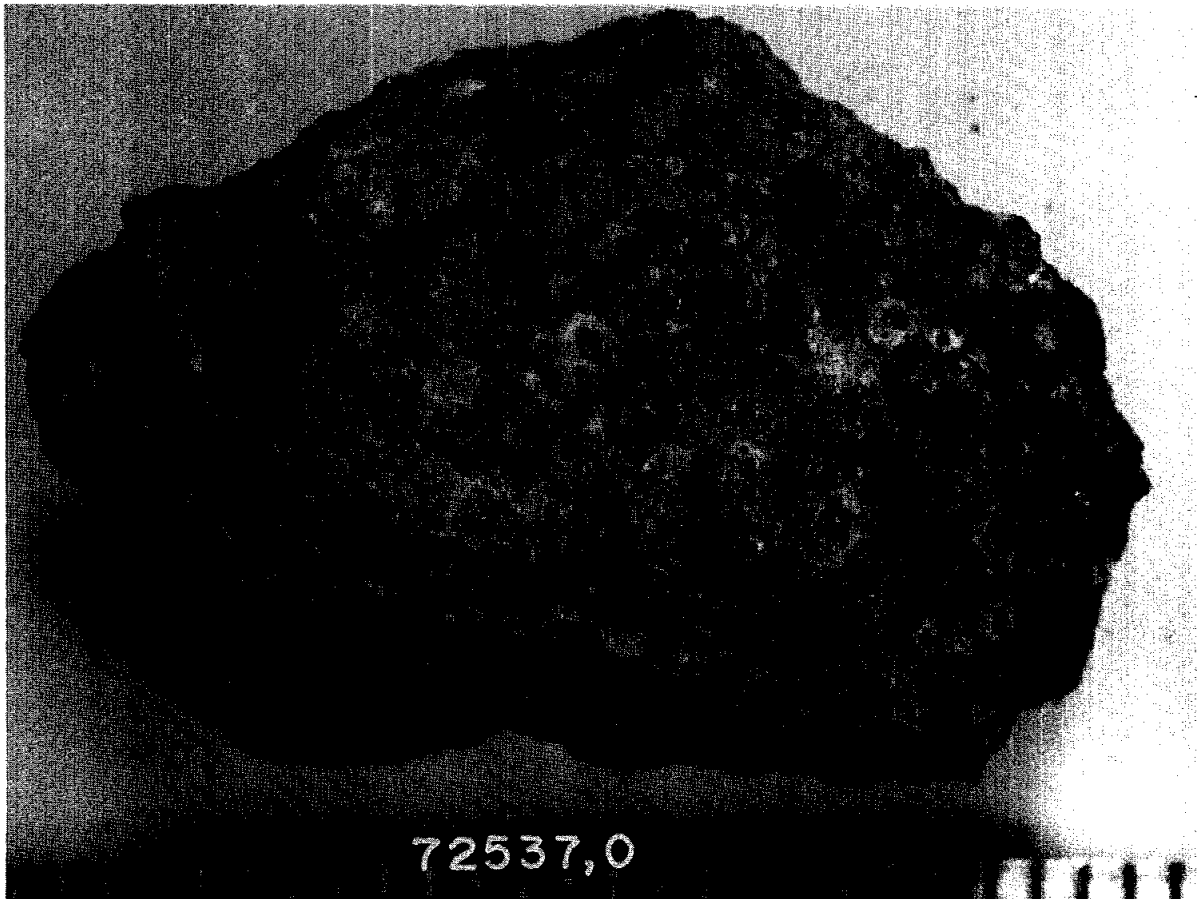


Figure 1: Sample 72537. Small scale divisions in millimeters. S-73-19643.

72538
Impact Melt Breccia (?)
St. 2, 11.1 g

INTRODUCTION

72538 is a small block (Fig. 1) collected as part of the first rake sample at Station 2, near Boulder 2. It has macroscopic characters that suggest that it is an impact melt; identification is uncertain because it has never been allocated or

dissected. According to LSIC 17 (1973), 72538 is a blue-gray breccia; according to Keil et al. (1974) it is dark gray (N4). It is similar in appearance to several other green-gray breccias from the South Massif that are impact melts (e.g. 72535). The sample is 3.3 x 2.1 x 1.6 cm, angular, coherent, and

without fractures (Fig. 1). Matrix material (grain size less than 1 mm) is about 92% of the sample; the remaining 8% consists mainly of small plagioclase clasts. It has zap pits on most surfaces, and small spherical vesicles (about 1%).

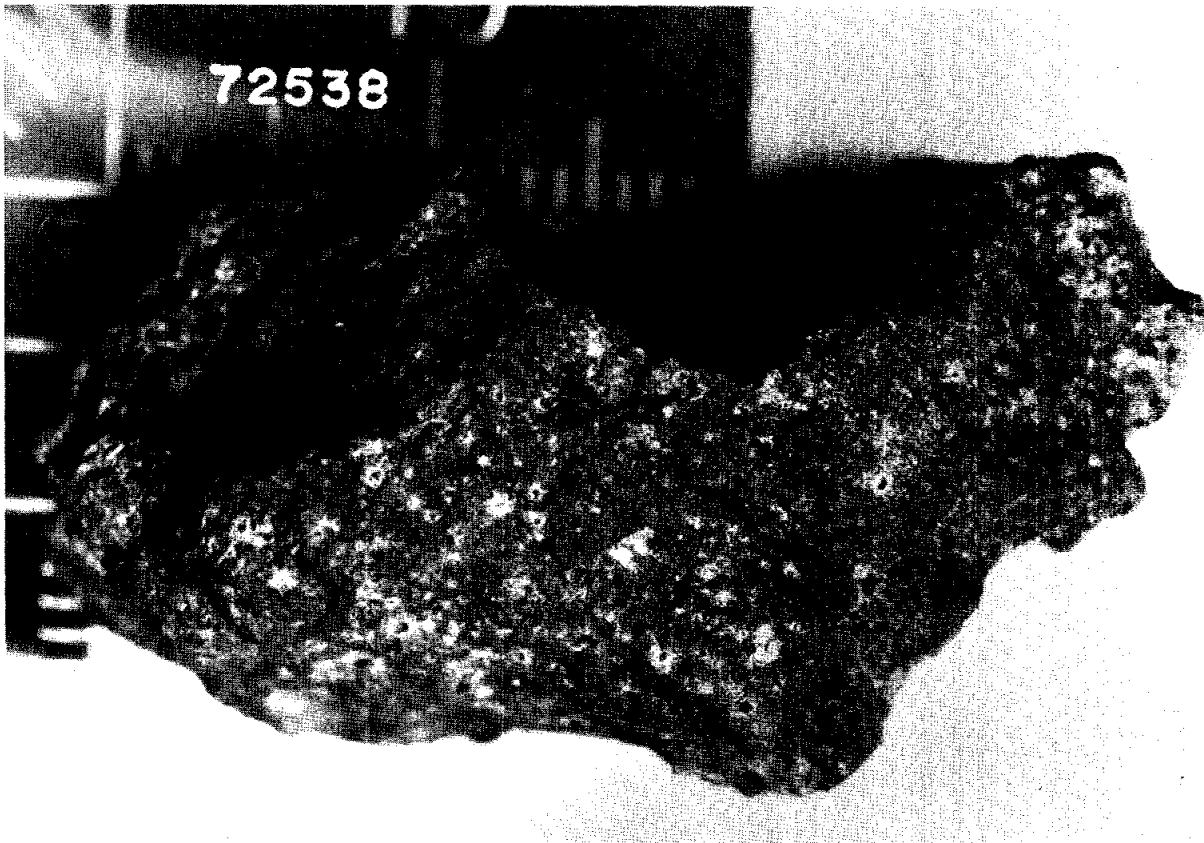


Figure 1: Sample 72538. Small scale divisions in millimeters. S-73-33430.

72539**Microsubophitic impact Melt Breccia
St. 2, 11.2 g****INTRODUCTION**

72539 is a fine-grained clast-bearing impact melt with a subophitic groundmass texture. Its chemistry is similar to the common low-K Fra Mauro melts that dominate the Apollo 17 highlands samples.

72539 was one of several blue-gray breccias (LSIC 17, 1973) collected in the first rake sample from Station 2, adjacent to Boulder 2. It is 2.5 x 2.5 x 1.3 cm and medium dark gray

(N4) (Keil et al., 1974). It is subrounded (Fig. 1) and coherent, with a few non-penetrative fractures. It has about 4% vesicles, and a few zap pits. The clast-matrix contrast is a little sharper than in other blue-gray breccias, partly because the matrix is among the most fine-grained. Matrix material (less than 100 microns grain size) was estimated to compose 91% of the rock (Keil et al., 1974).

PETROGRAPHY

72539 is a very fine-grained crystallized melt, similar to 72535 and 72536 but finer-grained (Fig. 2a). It differs in that the opaque grains are extremely minute (less than 1 micron) and tend to be clustered at the edges of mafic grains. Warner et al. (1977b,c; 1978f) described 72539 as a microsubophitic matrix breccia. Their modal data (Table 1) shows a high proportion of melt groundmass (88%) and a clast population



Figure 1: Sample 72539. S-73-19632. Smallest scale divisions in millimeters.

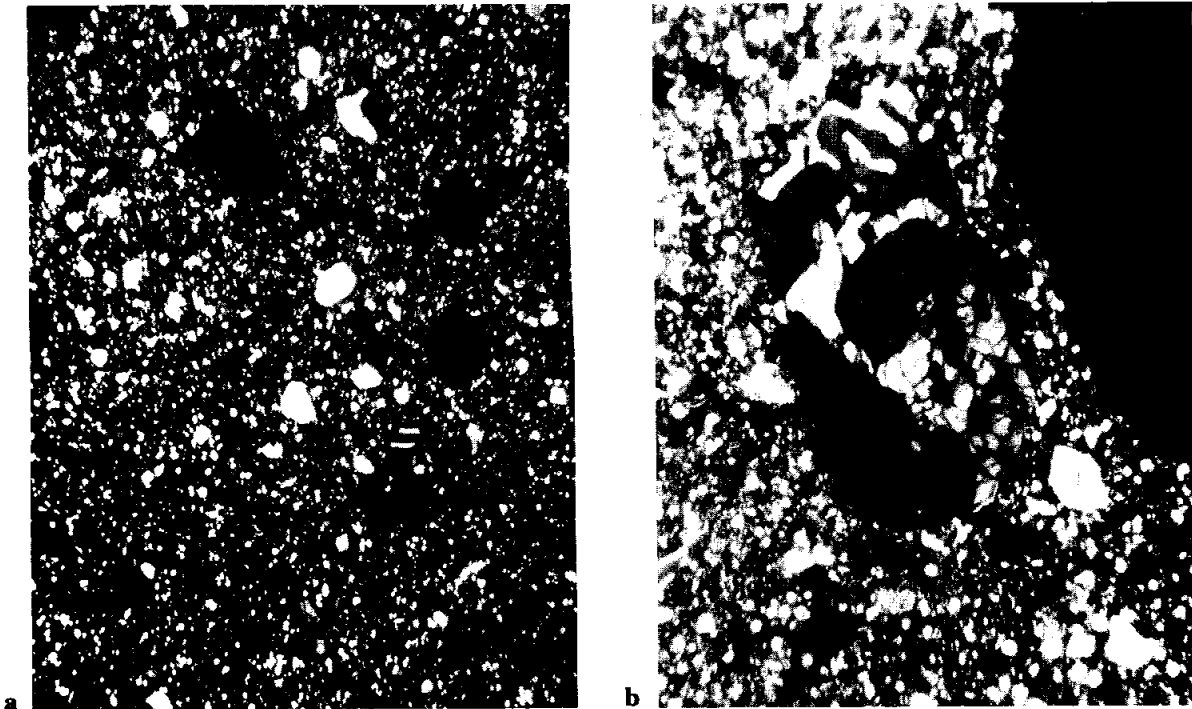


Figure 2: a) Photomicrograph of 72539,5 showing general groundmass. Dark areas are mainly vesicles. Crossed polarized light; width of field about 1 mm. b) Graphic granite fragment (center) and vesicle (upper right) in 72539,5. Crossed polarized light; width of field about 500 microns.

dominated by plagioclase, similar to many other impact melt samples at the Apollo 17 site. Warner et al. (1977b,c; 1978f) described the groundmass as having a well-developed igneous texture. Microprobe analyses (Warner et al., 1978f) are shown in Figure 3. The groundmass olivine, which is prominent and euhedral, has a narrow range of compositions (Fo₇₀₋₇₄). Engelhardt (1979) tabulated ilmenite paragenetic features, inferring that ilmenite crystallization started after plagioclase but before pyroxene.

Plagioclase clasts dominate the mineral fragment population, but pink spinels are present. A variety of feldspathic lithic clasts is present, including poikiloblastic norites and devitrified anorthositic fragments. Several granitic fragments are present, including one prominent one with a graphic

texture (Fig. 2b) that contains a silica phase, a K-feldspar phase, and a ternary feldspar phase (Warner et al., 1977b).

CHEMISTRY

The only analysis is a defocused beam analysis for the major elements (Table 2). The composition is similar to that of many other Apollo 17 impact melts.

PROCESSING

A few exterior chips were taken from a single area of the sample in 1974. Chip ,1 was used for the thin section, which consists of four serial slices. The other chips remain unallocated.

Figure 3: Microprobe analyses of minerals in 72539 (Warner et al., 1978f). Filled symbols = matrix phases. In histograms, open symbols = mineral clasts and cross-hatched = minerals in lithic clasts. In other diagrams, open circles = mineral clasts and open triangles = minerals in lithic clasts.

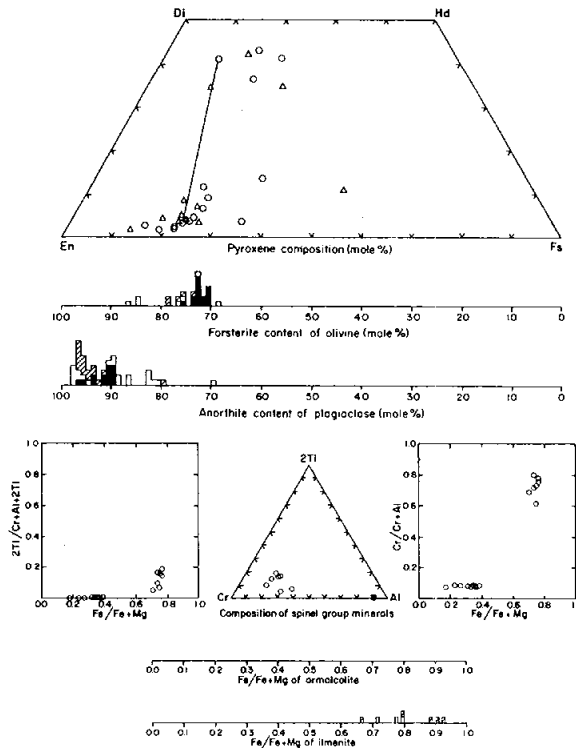


Table 1: Modal analysis of 72539,5 (Warner et al., 1977b).

Points counted	4072
Matrix	87.7
Mineral clasts	7.6
Lithic clasts	4.7
Mineral clasts	
Plagioclase	5.5
Olivine/pyroxene	1.9
Opaque oxide	0.1
Metal/troilite	0.1
Other	tr
Total	7.6
Lithic clasts	
ANT	1.2
Devitrified anorthosite	0.9
Breccia	2.2
Other	0.4
Total	4.7
Percent of matrix (normalized to 100)	
Plagioclase	51.6
Olivine/pyroxene	45.0
Opaque oxide	2.5
Metal/troilite	0.4
Other	0.6

Table 2: Microprobe defocused beam analysis of matrix of 72539 (from Warner et al., 1977b).

wt %	
SiO ₂	47.1
TiO ₂	1.77
Al ₂ O ₃	17.4
Cr ₂ O ₃	0.15
FeO	8.4
MnO	0.12
MgO	11.1
CaO	11.3
Na ₂ O	0.59
K ₂ O	0.16
P ₂ O ₅	0.28
Sum	98.4

72545**Impact Melt Breccia (?)****St. 2, 4.06 g****INTRODUCTION**

72545 is a subrounded coherent block (Fig. 1) measuring 1.7 x 1.2 x 0.8 cm. It was collected as part of the first rake sample at Station 2, near Boulder 2. It is a microbreccia with macroscopic characters that suggest that it is an impact melt; identification is uncertain because it

has never been allocated or dissected. According to LSIC 17 (1973), 72545 is a blue-gray breccia; according to Keil et al. (1974) it is medium dark gray (N4). It is similar in appearance to several other breccias from the South Massif that are impact melts. Keil et al. (1974) described the matrix as resembling that of 72705; the dark

matrix, with grain-size less than 100 microns, constitutes 93% of the rock. Most clasts are plagioclase-rich. 72545 has less than 1% vugs, and lacks zap pits.



Figure 1: Sample 72545, showing prominent plagioclase or feldspathic fragment. Small scale divisions in millimeters. S-73-19625.

72546

Impact Melt Breccia (?)

St. 2, 4.9 g

INTRODUCTION

72546 is a subangular coherent block (Fig. 1) measuring 1.8 x 1.7 x 1.0 cm. It was collected as part of the first rake sample at Station 2, near Boulder 2. It is a microbreccia with macroscopic characters that suggest that it is an impact melt; identification is uncertain because it has never been allocated or dissected. According to LSIC 17 (1973), 72546 is a blue-gray

breccia; according to Keil et al. (1974) it is medium dark gray (N4). It is similar in appearance to several other breccias from the South Massif that are impact melts. The dark matrix, with grain-size less than 1 mm (and mainly less than 100 microns), constitutes 93% of the rock (Keil et al., 1974). Most clasts are plagioclase-rich. 72546 lacks vugs, but has many zap pits on one surface.

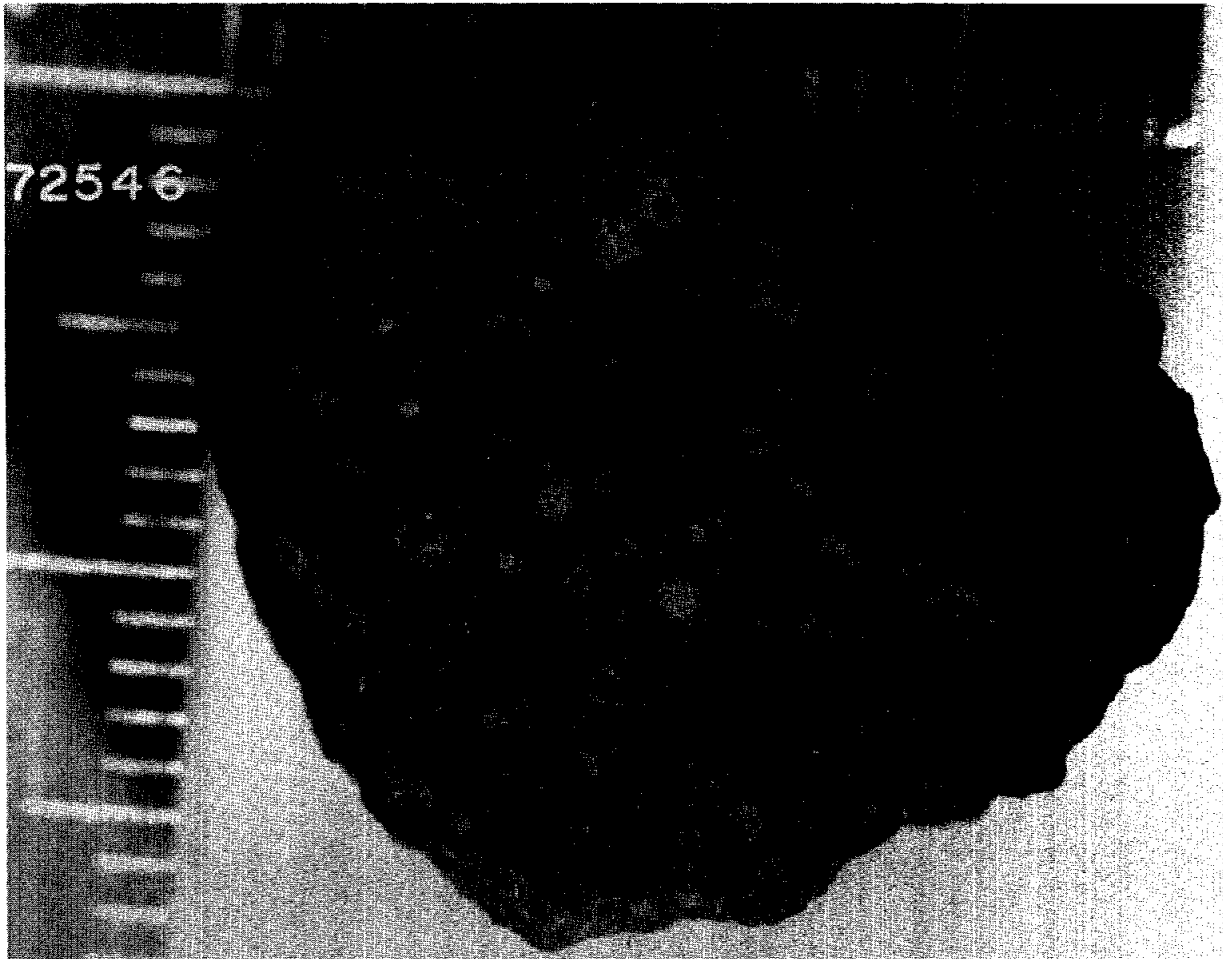


Figure 1: Sample 72546, showing surface with many zap pits. Small scale divisions in millimeters. S-73-33462.

72547**Impact Melt Breccia (?)****St. 2, 5.0 g****INTRODUCTION**

72547 is a subrounded coherent block (Fig. 1) measuring 2.0 x 1.7 x 1.1 cm. It was collected as part of the first rake sample at Station 2, near Boulder 2. It is a microbreccia with macroscopic characters that suggest that it is an impact melt;

identification is uncertain because it has never been allocated or dissected. According to LSIC 17 (1973), 72547 is a blue-gray breccia; according to Keil et al. (1974) it is medium dark gray (N4). It is similar in appearance to several other breccias from the South Massif that are impact melts. The

dark matrix, with grain-size less than 1 mm (and mainly less than 100 microns), constitutes 90% of the rock (Keil et al., 1974). Most clasts are plagioclase-rich. 72547 lacks vugs, but has a few zap pits.

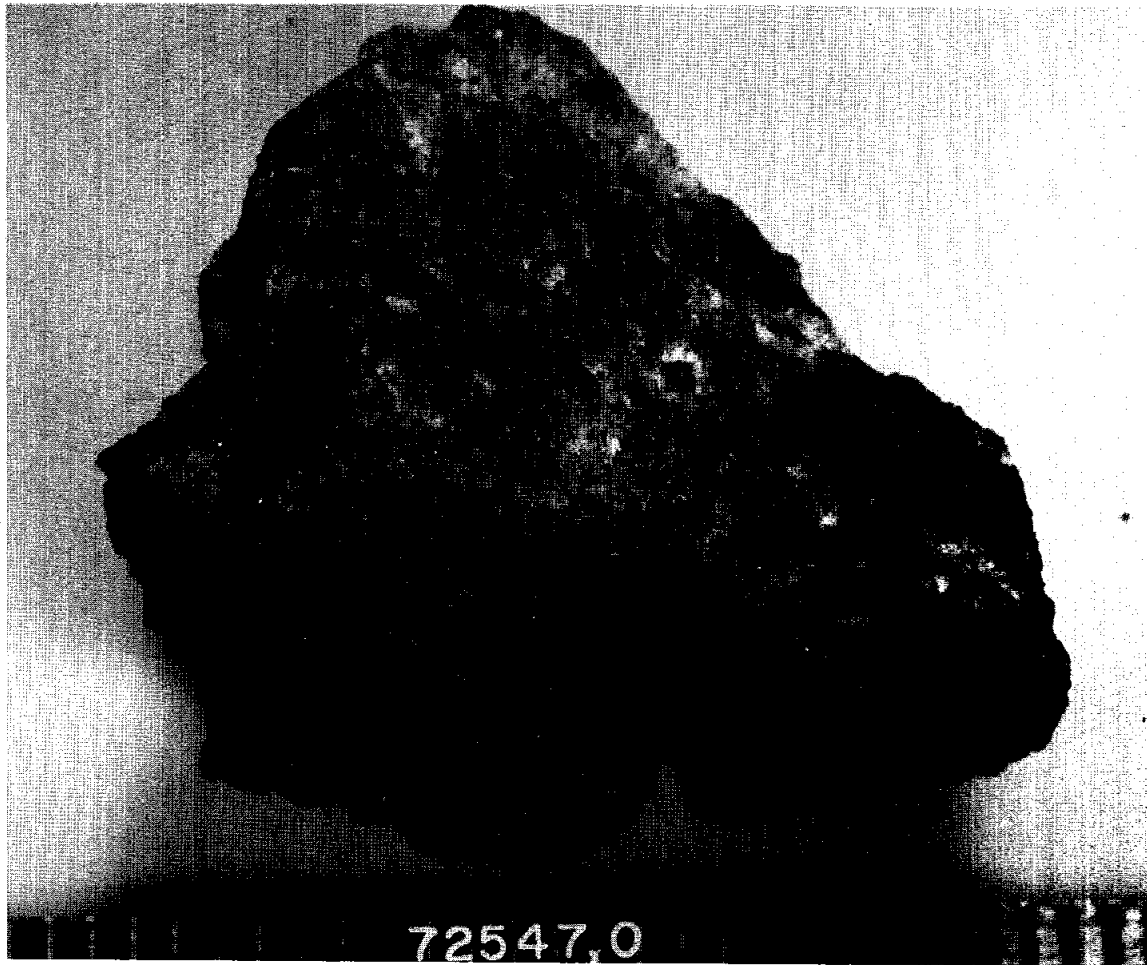


Figure 1: Sample 72547, showing surface with zap pits and patina as well as fresh surfaces. Small scale divisions in millimeters. S-73-19626.

72548**Micropoikilitic Impact Melt Breccia****St. 2, 29.3 g****INTRODUCTION**

72548 is a fine-grained clast-bearing impact melt with a microgranular to micropoikilitic groundmass texture. Its chemistry is similar to the common low-K Fra Mauro melts that dominate the Apollo 17 highlands samples.

72548 was one of several blue-gray breccias (LSIC 17, 1973) collected in the first rake sample from Station 2, adjacent to Boulder 2. It is 4.1 x 2.5 x 2.0 cm and medium dark gray (N4) (Keil et al., 1974). It is subrounded and coherent, with a few non-penetrative fractures; it

broke up during processing (Fig. 1). It lacks cavities, but has a few zap pits. Matrix material (mainly less than 100 micron grain size) was estimated to compose 94% of the rock (Keil et al., 1974). Most of the clast material is feldspathic.

PETROGRAPHY

72548 is a crystallized impact melt containing lithic and mineral clasts (Fig. 2). Warner et al. (1977b,c; 1978f) described 72548 as a microgranular-micropoikilitic matrix breccia. It has a coarser grain size than the microsubophitic

melts represented by 72535. The modal data (Table 1) shows a high proportion of melt groundmass (80%) and a clast population dominated by plagioclase, similar to many other impact melt samples at the Apollo 17 site. The groundmass plagioclase occurs as laths or stubby grains, many with rounded corners; mafic and opaque grains are equant to subequant. Microprobe analyses (Warner et al., 1978f) are shown in Figure 3. The groundmass olivine, which is prominent and euhedral, has a narrow range of compositions (Fo₆₉₋₇₀). Engelhardt (1979) tabulated ilmenite paragenetic

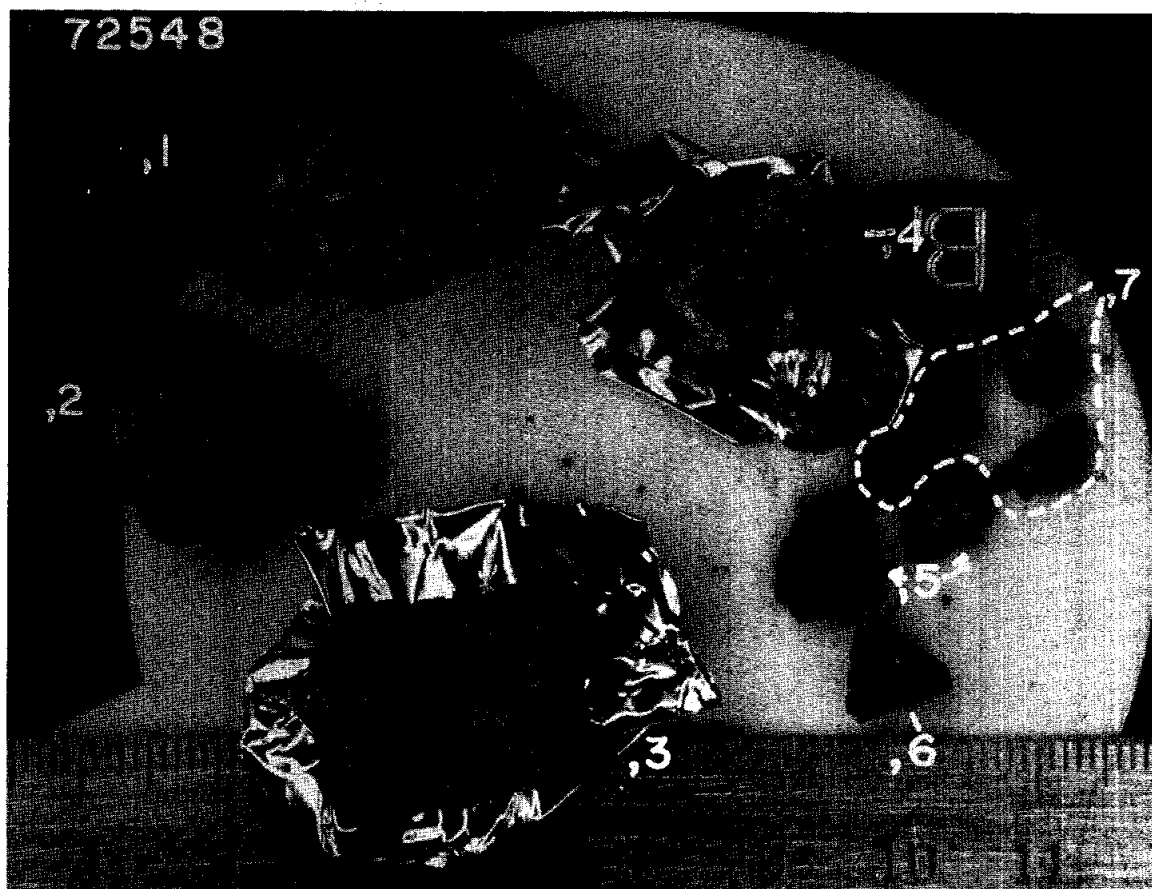


Figure 1: Sample 72548, showing post-processing subdivisions. Smallest scale divisions in millimeters. S-74-19023.

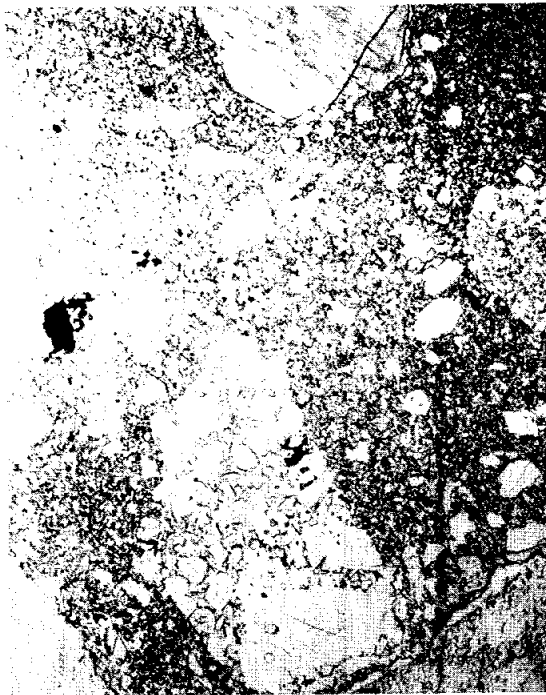


Figure 2: Photomicrograph of 72548,11, showing general groundmass and some larger lithic and mineral clasts. Plane light; width of field about 1 mm.

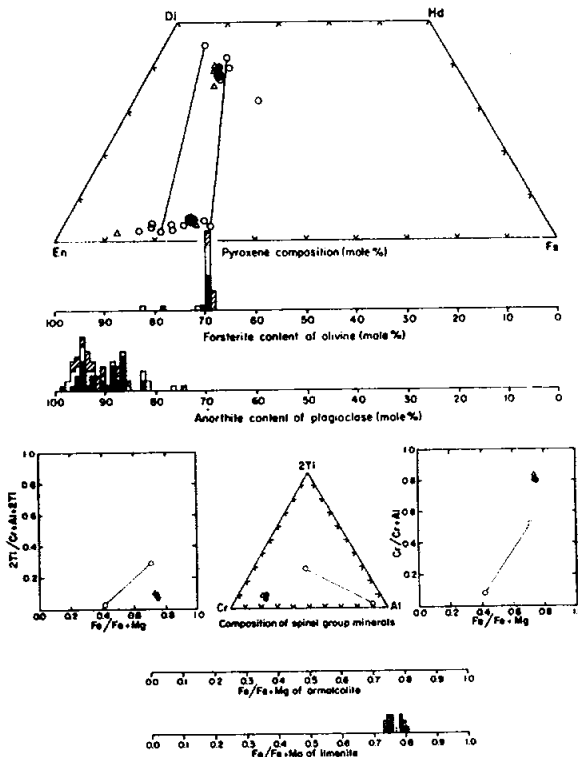


Figure 3: Microprobe analyses of minerals in 72548 (Warner et al., 1978f). Filled symbols = matrix phases. In histograms, open symbols = mineral clasts and cross-hatched = minerals in lithic clasts. In other diagrams, open circles = mineral clasts and open triangles = minerals in lithic clasts.

features, inferring that ilmenite crystallization was simultaneous with plagioclase and pyroxene.

The clasts are more rounded with more evidence of reaction (e.g. coronas) than in the finer-grained, subophitic melts. Plagioclase clasts dominate the mineral fragment population; pink spinels are present. A variety of feldspathic lithic clasts is present, including poikiloblastic norites and devitrified anorthositic fragments.

CHEMISTRY

The only analysis is a defocused beam analysis for the major elements (Table 2). The analysis is similar to that of many other Apollo 17 impact melts, but is slightly more aluminous and thus falls of the plagioclase-pyroxene cotectic in the Ol-Si-An system. However, this is probably a sampling effect.

PROCESSING

The sample was broken into several documented pieces during chipping in 1974 (Fig. 1). The only allocation was the two fragments .5, which were made into two thin sections.

Table 1: Modal analysis of 72548,11 (Warner et al., 1977b).

72548	
Points counted	3595
Matrix	80.4
Mineral clasts	16.4
Lithic clasts	3.2
Mineral clasts	
Plagioclase	10.9
Olivine/pyroxene	5.4
Opaque oxide	tr
Metal/troilite	0.1
Other	—
Total	<u>16.4</u>
Lithic clasts	
ANT	2.3
Devitrified anorthosite	0.3
Breccia	0.4
Other	<u>0.2</u>
Total	<u>3.2</u>
Percent of matrix (normalized to 100)	
Plagioclase	54.4
Olivine/pyroxene	43.3
Opaque oxide	1.7
Metal/troilite	0.1
Other	0.5

Table 2: Microprobe defocused beam analysis of matrix of 72548 (from Warner et al., 1977b).

<i>wt %</i>	
SiO ₂	48.1
TiO ₂	1.47
Al ₂ O ₃	20.3
Cr ₂ O ₃	0.15
FeO	7.4
MnO	0.11
MgO	9.3
CaO	12.1
Na ₂ O	0.60
K ₂ O	0.27
P ₂ O ₅	0.15
Sum	100.0*

*normalized.

72549**Micropoikilitic Impact Melt Breccia
St. 2, 21.0 g****INTRODUCTION**

72549 is a fine-grained clast-bearing impact melt with a microgranular to micropoikilitic groundmass texture. Its chemistry is similar to the common low-K Fra Mauro melts that dominate the Apollo 17 highlands samples.

72549 was one of several green-gray breccias (LSIC 17, 1973) collected in the first rake sample from Station 2, adjacent to Boulder 2. It is 2.8 x 2.5 x 2.4 cm and

medium dark gray (N4) (Keil et al., 1974). It is subrounded and coherent, with no fractures (Fig. 1). It has 1% vugs and a few zap pits. Matrix material (mainly less than 100 microns grain size) was estimated to compose 91% of the rock (Keil et al., 1974). More than half of the clast material in the 1 to 2 mm range is feldspathic, the remainder consists of reddish brown and yellow-green mafic minerals.

PETROGRAPHY

72549 is a crystallized impact melt containing mineral clasts (Fig. 2); lithic clasts are rare. Warner et al. (1977b,c; 1978f) described 72549 as a microgranular-micropoikilitic matrix breccia. It has a coarser grain size than the microsubophitic melts represented by 72535. While it is similar to 72548, the mafic minerals and opaque grains are coarser-grained. The modal data (Table 1) shows a high proportion of melt groundmass (84.3%) and a

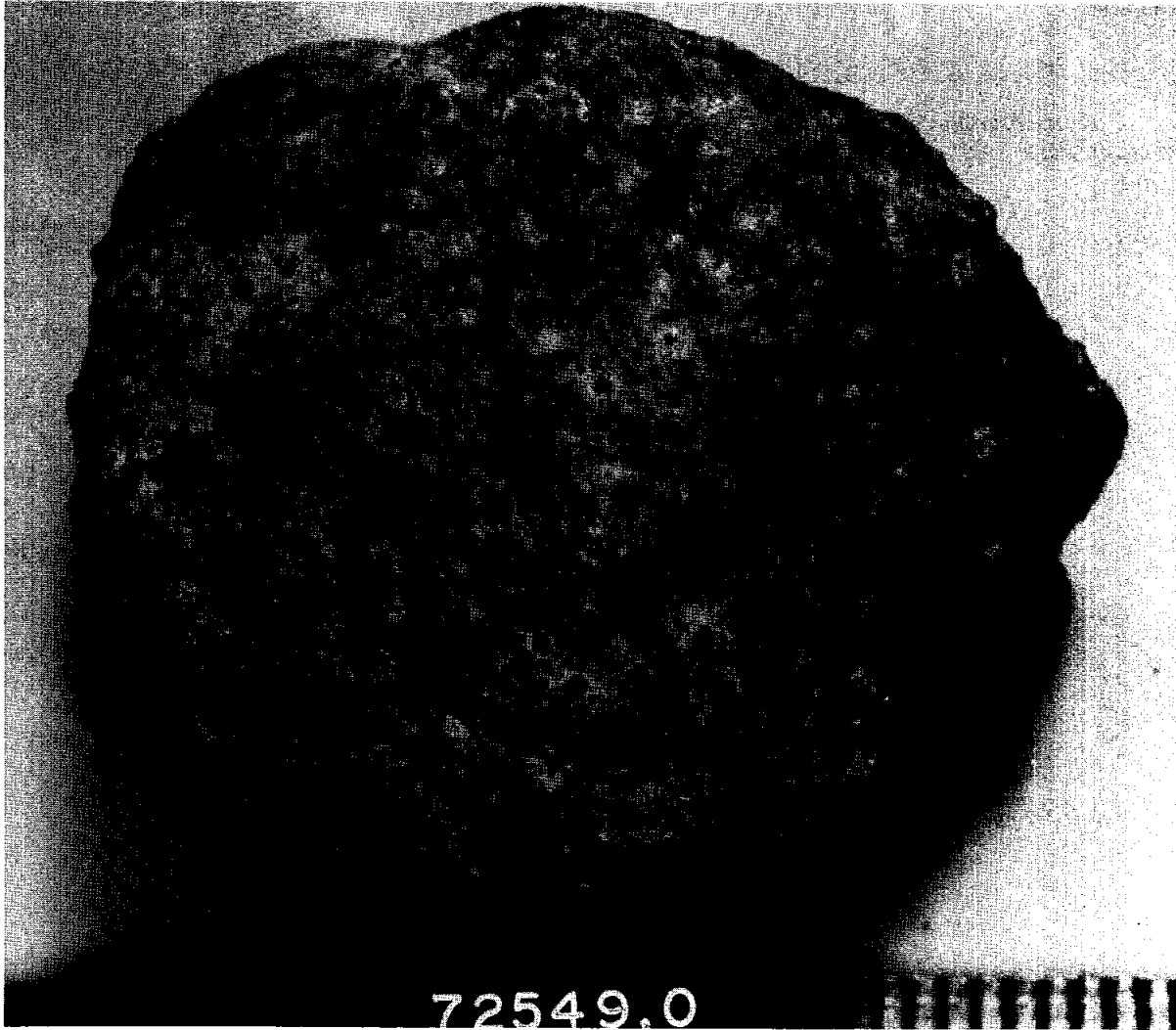


Figure 1: Sample 72549. Smallest scale divisions in millimeters. S-74-19628.

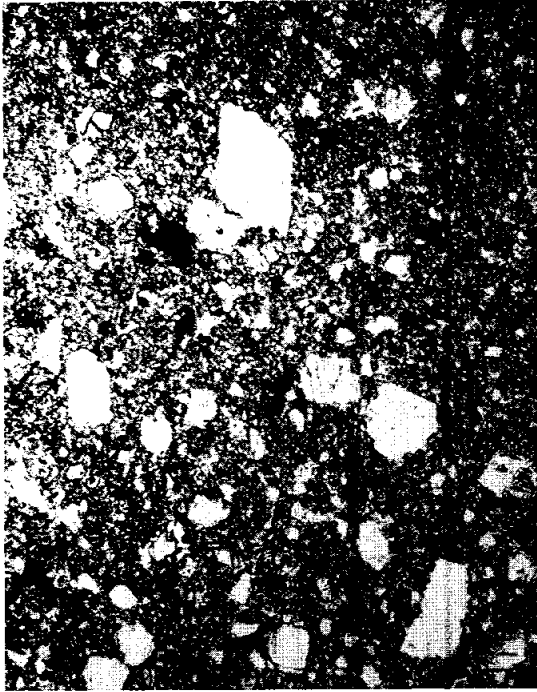


Figure 2: Photomicrograph of 72549,7, showing general groundmass and mineral clasts. Plane light; width of field about 1 mm.

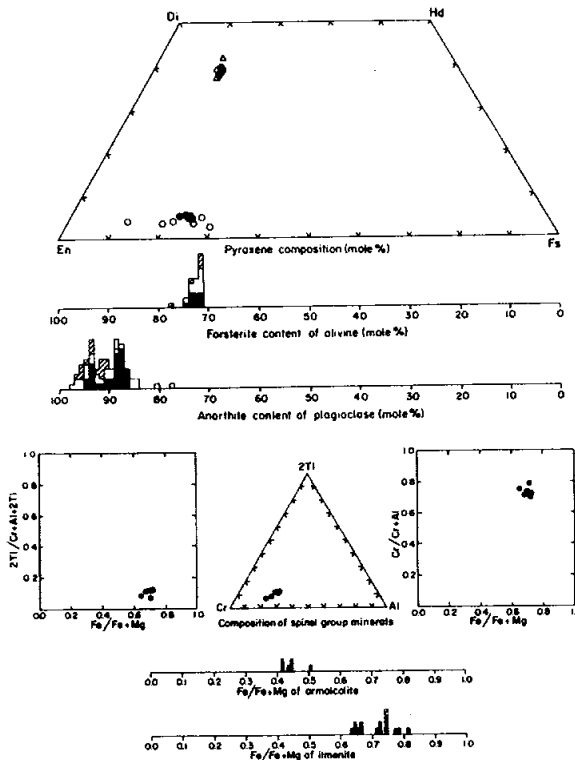


Figure 3: Microprobe analyses of minerals in 72549 (Warner et al., 1978f). Filled symbols = matrix phases. In histograms, open symbols = mineral clasts and cross-hatched = minerals in lithic clasts. In other diagrams, open circles = mineral clasts and open triangles = minerals in lithic clasts.

clast population dominated by plagioclase, similar to many other impact melt samples at the Apollo 17 site. The groundmass plagioclase occurs as laths or stubby grains, many with rounded corners; mafic and opaque grains are equant to subequant. Armalcolite is present. Microprobe analyses (Warner et al., 1978f) are shown in Figure 3. The groundmass olivine, which is prominent and euhedral, has a narrow range of compositions (Fo71-75). The opaque mineral grains are larger than those in 72548. Engelhardt (1979) tabulated ilmenite paragenetic features, inferring that ilmenite crystallization post-dated pyroxene.

The clasts are more rounded with more evidence of reaction (e.g. coronas) than in the finer-grained, subophitic melts. Plagioclase clasts dominate the mineral fragment population. The rare lithic clasts are mostly recrystallized feldspathic and devitrified anorthositic fragments.

CHEMISTRY

The only analysis is a defocused beam analysis for the major elements (Table 2). The analysis is similar to that of many other Apollo 17 impact melts, and falls on the plagioclase-pyroxene cotectic in the Ol-Si-An system.

PROCESSING

The sample was broken into several documented pieces during chipping in 1974. The only allocation was the two fragments, 2 which were made into two thin sections.

Table 1: Modal analysis of 72549,7 (Warner et al., 1977b).

	72549
Points counted	2464
Matrix	84.3
Mineral clasts	14.2
Lithic clasts	1.5
Mineral clasts	
Plagioclase	10.1
Olivine/pyroxene	4.1
Opaque oxide	—
Metal/troilite	tr
Other	—
Total	14.2
Lithic clasts	
ANT	1.0
Devitrified anorthosite	0.2
Breccia	0.3
Other	—
Total	1.5
Percent of matrix (normalized to 100)	
Plagioclase	53.7
Olivine/pyroxene	43.7
Opaque oxide	1.4
Metal/troilite	0.4
Other	0.8

Table 2: Microprobe defocused beam analysis of matrix of 72549 (from Warner et al., 1977b).

wt %	
SiO ₂	48.8
TiO ₂	0.95
Al ₂ O ₃	19.1
Cr ₂ O ₃	0.17
FeO	7.8
MnO	0.11
MgO	11.2
CaO	12.0
Na ₂ O	0.58
K ₂ O	0.27
P ₂ O ₅	0.35
Sum	101.4

72555

Impact Melt Breccia (?)

St. 2, 10.48 g

INTRODUCTION

72555 is a subangular tough block (Fig. 1) collected as part of the first rake sample at Station 2, near Boulder 2. It has macroscopic characters that suggest that it is an impact melt; identification is uncertain because it has never been allocated or dissected. According to

Keil et al. (1974) 72555 is medium dark gray (N4) and 2.6 x 1.8 x 1.7 cm. It is similar in appearance to several other green-gray breccias from the South Massif that are impact melts (e.g. 72549). It is coherent with a few non-penetrative fractures, has about 1% vugs, and lacks zap pits. It consists of about 92% matrix material (mainly less

than a few hundred microns), with a few plagioclase and mafic clasts in the 0.5 to 2 mm range.

72555 has never been dissected or allocated. A reference by Levsky et al. (1981) is a misprint for 72255.

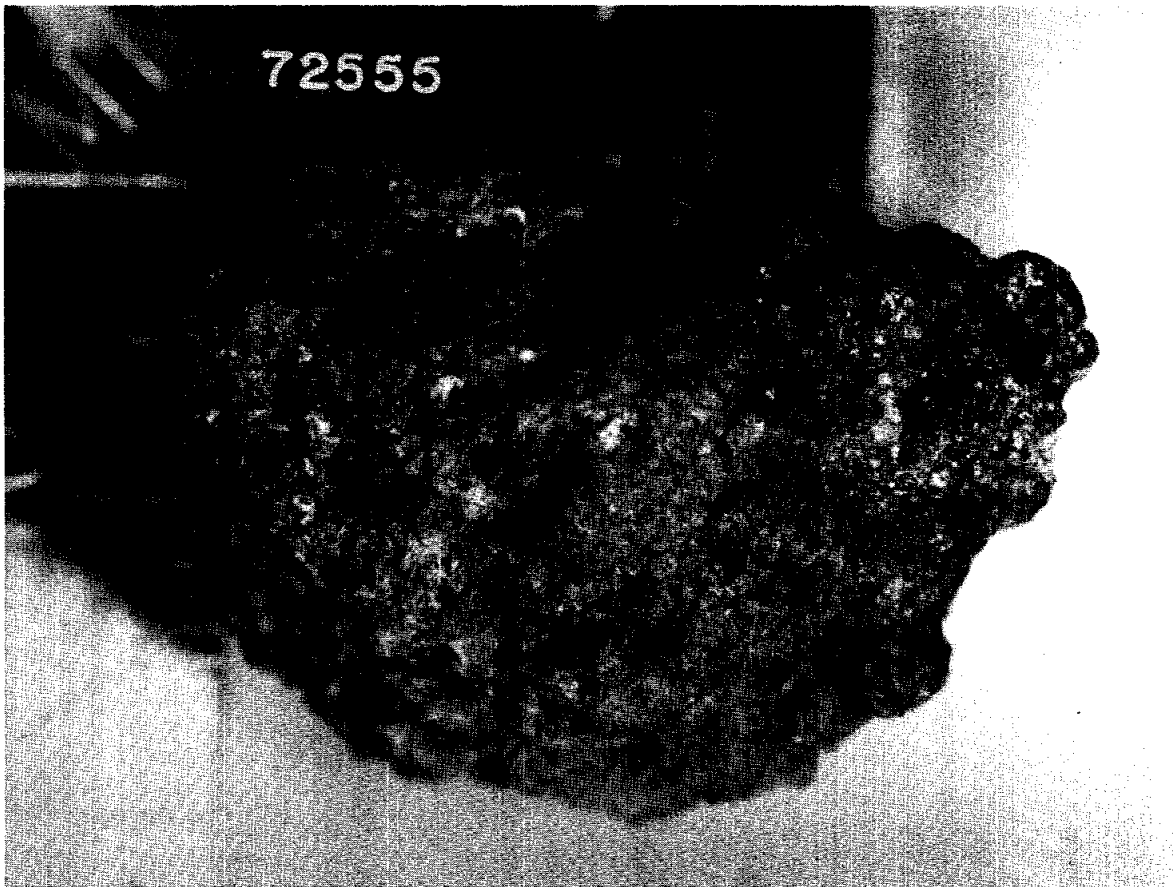


Figure 1: Sample 72555. Small scale divisions in millimeters. S-73-33436.

72556**Impact Melt Breccia (?)****St. 2, 3.86 g****INTRODUCTION**

72556 is a subangular tough block (Fig. 1) collected as part of the first rake sample at Station 2, near Boulder 2. It has macroscopic characters that suggest that it is an impact melt; identification is uncertain because it has never been allocated or dissected. According to

Keil et al. (1974) 72556 is medium gray (N5) and 1.5 x 1.5 x 1.5 cm. It is similar in appearance to several other green-gray breccias from the South Massif that are impact melts (e.g. 72549). It is coherent with no fractures, has about 3% vugs, and a few zap pits. It consists of about 97% matrix material (mainly less than 100 microns), with a few

plagioclase and mafic clasts less than 0.5 mm across. 72556 has never been dissected or allocated, although, 0 consists of a small fragment as well as the main mass.

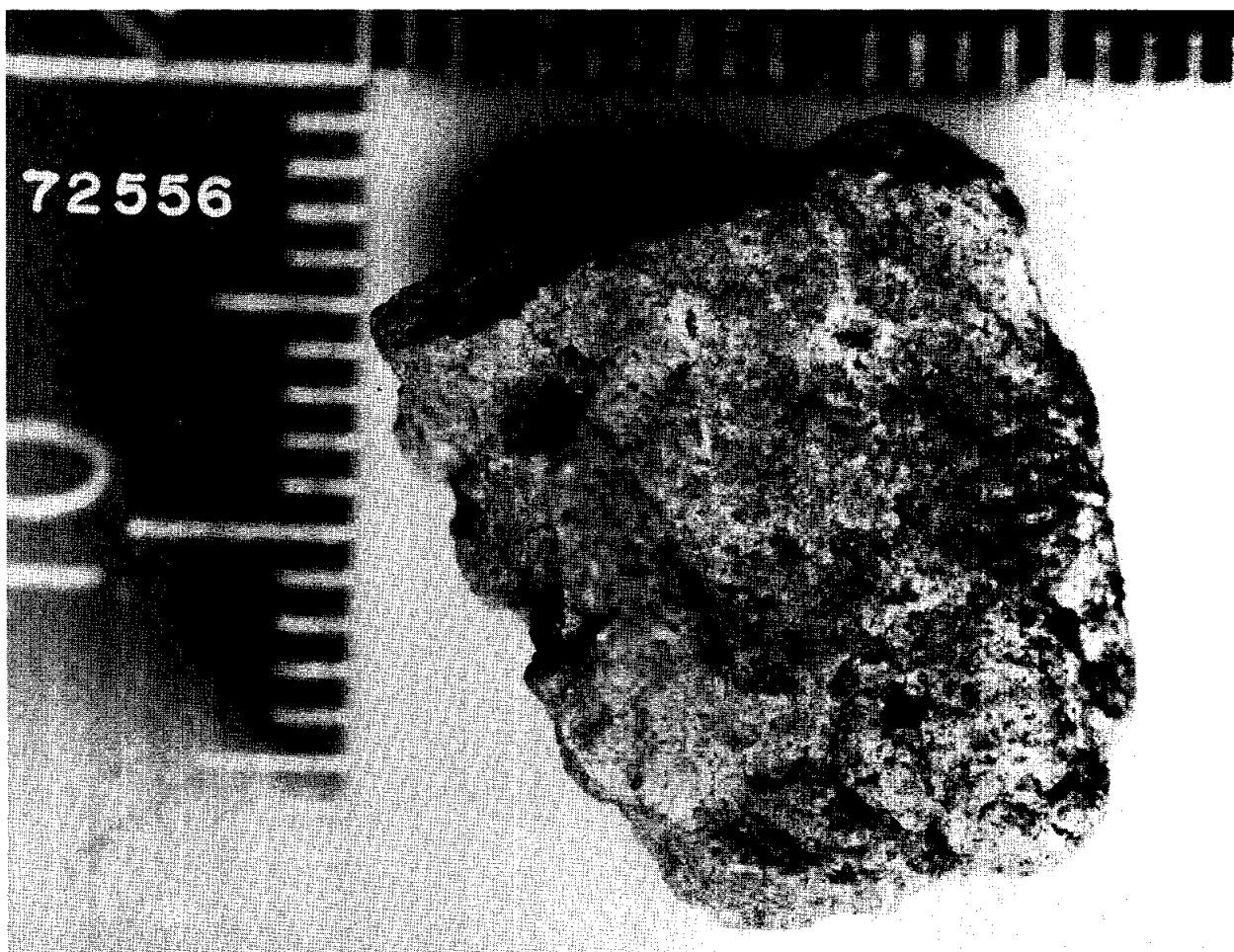


Figure 1: Sample 72556. Small scale divisions in millimeters. S-73-33427.

72557**Impact Melt Breccia (?)****St. 2, 4.56 g****INTRODUCTION**

72557 is a subrounded tough block (Fig. 1) collected as part of the first rake sample at Station 2, near Boulder 2. It has macroscopic characters that suggest that it is an impact melt; identification is uncertain because it has never been

allocated or dissected. According to Keil et al. (1974) 72557 is medium gray (N5) and 2.0 x 1.8 x 1.6 cm. It is similar in appearance to several other green-gray breccias from the South Massif that are impact melts (e.g. 72549). It is coherent with no fractures, has less than 1% vugs, and zap pits on one side. It consists

of about 97% matrix material (mainly less than 100 microns), with a few plagioclase and mafic clasts less than 0.5 to 2.0 mm across. 72557 has never been dissected or allocated.

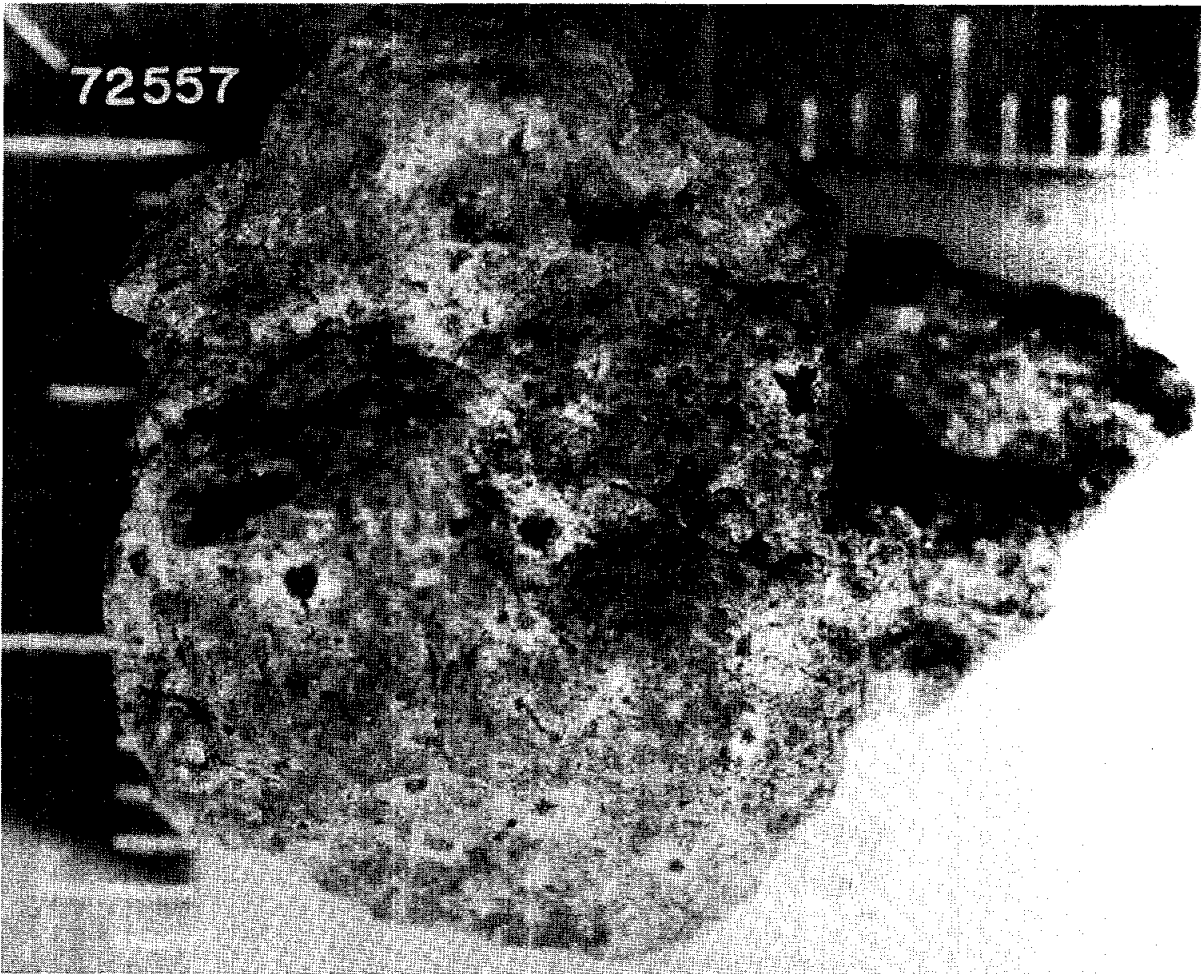


Figure 1: Sample 72557. Small scale divisions in millimeters. S-73-33399.

72558**Micropoikilitic Impact Melt Breccia
St. 2, 5.71 g****INTRODUCTION**

72558 is a fine-grained clast-bearing impact melt. Although its chemistry was reported to differ from most other melts at the Apollo 17 site in being higher in potassium, an unpublished analysis for major and trace elements shows that it is similar to the common low-K Fra Mauro melts that are presumed Serenitatis melts. It was also reported to contain more clastic material than most of the local impact melt samples; possibly

the sampled chip was unrepresentative.

72558 was one of several green-gray breccias (LSIC 17, 1973) collected in the first rake sample from Station 2, adjacent to Boulder 2. It is 1.8 x 1.5 x 1.4 cm and medium gray (N5) (Keil et al., 1974). It is subangular and coherent, with no fractures (Fig. 1). It has a few zap pits and about 1% vugs. Matrix material (mainly less than 100 micron grain size) was estimated to compose 92% of the

rock (Keil et al., 1974). Thin sections show a higher abundance of clasts, and the sample might be more heterogeneous than most melts.

PETROGRAPHY

72558 is a crystallized impact melt containing lithic and mineral clasts (Fig. 2, Table 1). Warner et al. (1977b,c; 1978f) described 72558 as a microgranular-micropoikilitic matrix breccia, similar to 72549 but

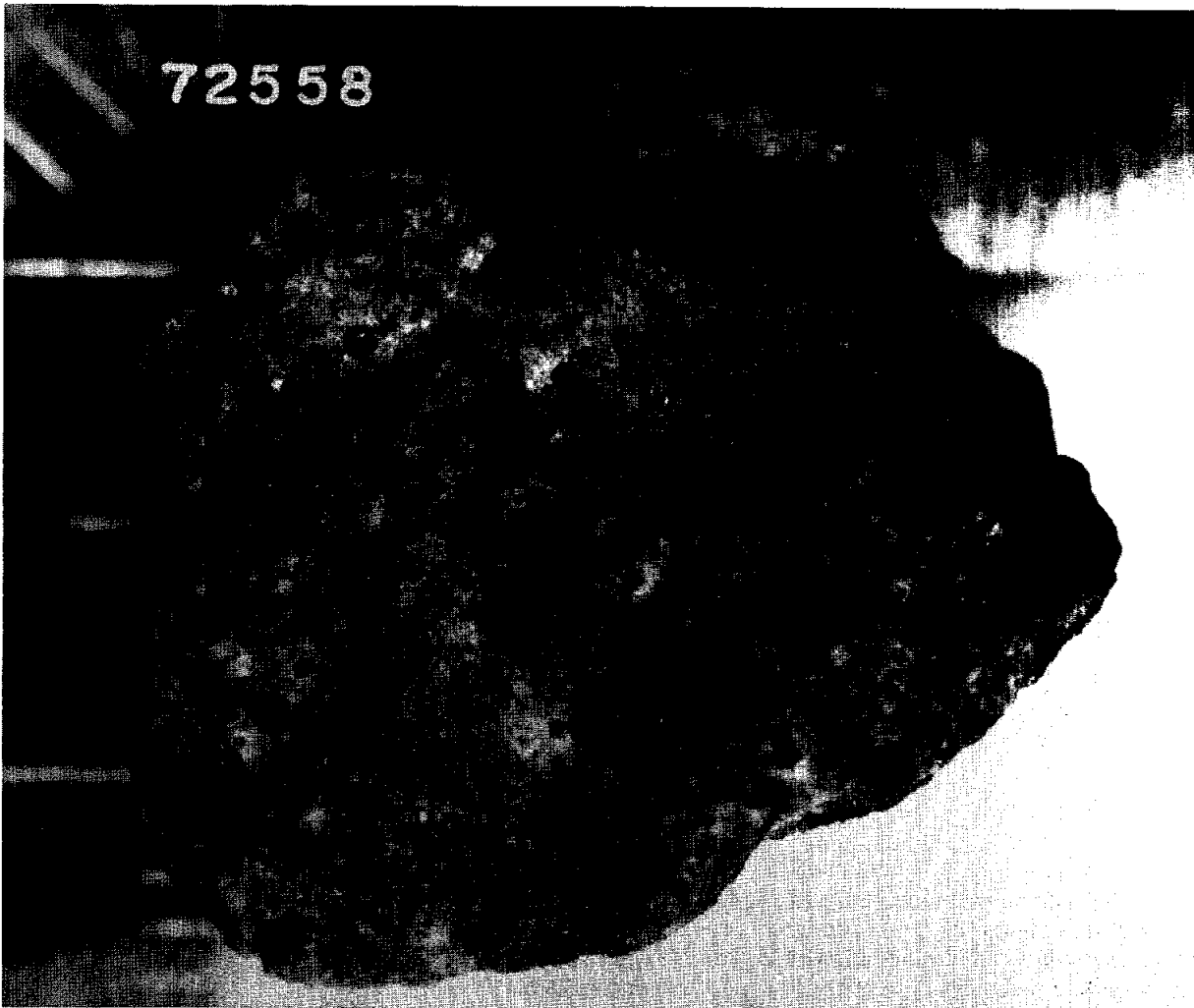


Figure 1: Sample 72558. Smallest scale divisions in millimeters. S-73-33460

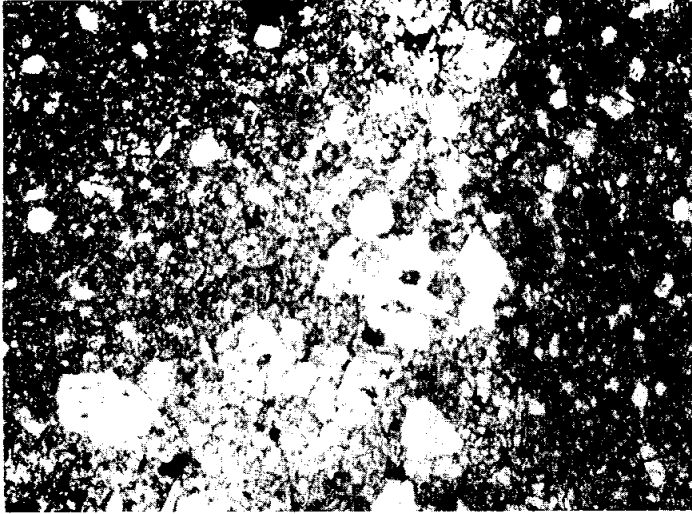


Figure 2: Photomicrograph of 72558,5, showing general groundmass, mineral clasts, and lithic schlieren. Plane light; width of field about 1 mm.

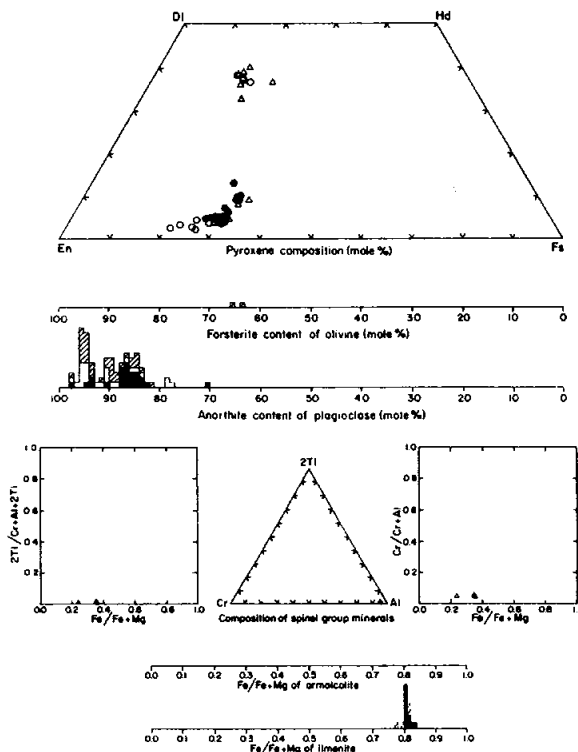


Figure 3: Microprobe analyses of minerals in 72558 (Warner et al., 1978f). Filled symbols = matrix phases. In histograms, open symbols = mineral clasts and cross-hatched = minerals in lithic clasts. In other diagrams, open circles = mineral clasts and open triangles = minerals in lithic clasts.

with mafics almost wholly pyroxene. They distinguished 72258 with 72735 as a high-K KREEP breccia on the basis of the high K_2O (0.57%) evident in the defocused beam analysis (Table 2). However, this is probably not the case (see CHEMISTRY section). Nonetheless, there is a lack of olivine, and several other differences from most local impact melts. The grain size is coarser than that of the microsubophitic melts represented by 72535. The modal data (Table 1) shows a low proportion of melt groundmass (52%), and the clast population is dominated by lithic clasts, unlike most melts. Microprobe analyses (Warner et al., 1978f) are shown in Figure 3; the matrix pyroxenes are more iron-rich than those in other melts, and more varied in composition. There is interstitial K-rich phase. Quite likely, the chip is unrepresentative or possibly even a clast. Engelhardt (1979) tabulated ilmenite paragenetic features, inferring that ilmenite crystallization was simultaneous with plagioclase and pyroxene.

The mineral and lithic clasts almost exclusively appear to be derived from coarse-grained feldspathic rocks. In many cases it is in schlieren or obscurely-defined masses. One plagioclase grain poikilistically encloses several pink spinels.

CHEMISTRY

The only published analysis is a defocused beam analysis for the major elements (Table 2). The analysis is unlike that of most other impact melts from the Apollo 17 site in that it contains higher silica, lower titania, and lower mg^* , but most significantly in its higher K_2O . However, an analysis of a chip for major and trace elements (Ryder, unpublished) shows that 72558 is identical with the common low-K Fra Mauro basalt that is inferred to be the Serenitatis impact melt.

PROCESSING

The sample was broken to produce a few documented pieces during chipping in 1974.. The only original allocation was ,1 which was made into two thin sections. A subsequent allocation was made for chemistry.

Table 1: Modal analysis of 72558,5 (Warner et al., 1977b).

	72558
Points counted	1098
Matrix	51.9
Mineral clasts	9.0
Lithic clasts	39.1
Mineral clasts	
Plagioclase	4.8
Olivine/pyroxene	4.1
Opaque oxide	—
Metal/troilite	0.1
Other	—
Total	9.0
Lithic clasts	
ANT	38.8
Devitrified anorthosite	0.1
Breccia	—
Other	0.2
Total	39.1
Percent of matrix (normalized to 100)	
Plagioclase	53.9
Olivine/pyroxene	40.9
Opaque oxide	1.7
Metal/troilite	0.5
Other	3.0

Table 2: Microprobe defocused beam analysis of matrix of 72558 (from Warner et al., 1977b).

wt %	
SiO ₂	50.2
TiO ₂	0.76
Al ₂ O ₃	19.4
Cr ₂ O ₃	0.16
FeO	8.5
MnO	0.16
MgO	8.7
CaO	11.3
Na ₂ O	0.85
K ₂ O	0.57
P ₂ O ₅	0.25
Sum	100.9

72559

Granoblastic Impactite

St. 2, 27.8 g

INTRODUCTION

72559 is a subrounded, partly subangular tough block (Fig. 1) collected as part of the first rake sample at Station 2, near Boulder 2. Its petrography and chemistry show that it is a feldspathic impactite, unique among individual South Massif samples. According to LSIC Apollo 17 (1973) and Keil et al. (1974) 72559 is light olive gray (5Y 6/1) and 3.4 x 2.3 x 1.6 cm. It was singled out as distinct macroscopically among the rake samples, of which it is one of the largest as well as most obviously feldspathic. Keil et al (1974)

identified it as a cataclastic anorthosite. Macroscopically it appeared to be virtually all plagioclase, but thin sections show about 75% feldspar. 72559 is coherent with a few non-penetrative fractures, has no vugs, and some zap pits (LSIC Apollo 17, 1973 states many; Keil et al., 1974, states few).

PETROGRAPHY

72559 is a granoblastic feldspathic impactite with a fine-grained groundmass (Fig. 2) and is a recrystallized anorthositic norite. It

has a partly poikiloblastic texture and some apparent relict lithic clasts. Petrographic descriptions were given by Warner et al. (1977c, 1978c, 1978f), and Nehru et al. (1978); the latter is the more detailed. The texture and homogeneous mineral chemistry of 72559 is most consistent with an origin of brecciation of a source consisting only of related feldspathic igneous rocks followed by thermal metamorphism.

According to Nehru et al. (1978), 72559 contains (in volume %) plagioclase (74.5), olivine (14.4), orthopyroxene (10.2), and

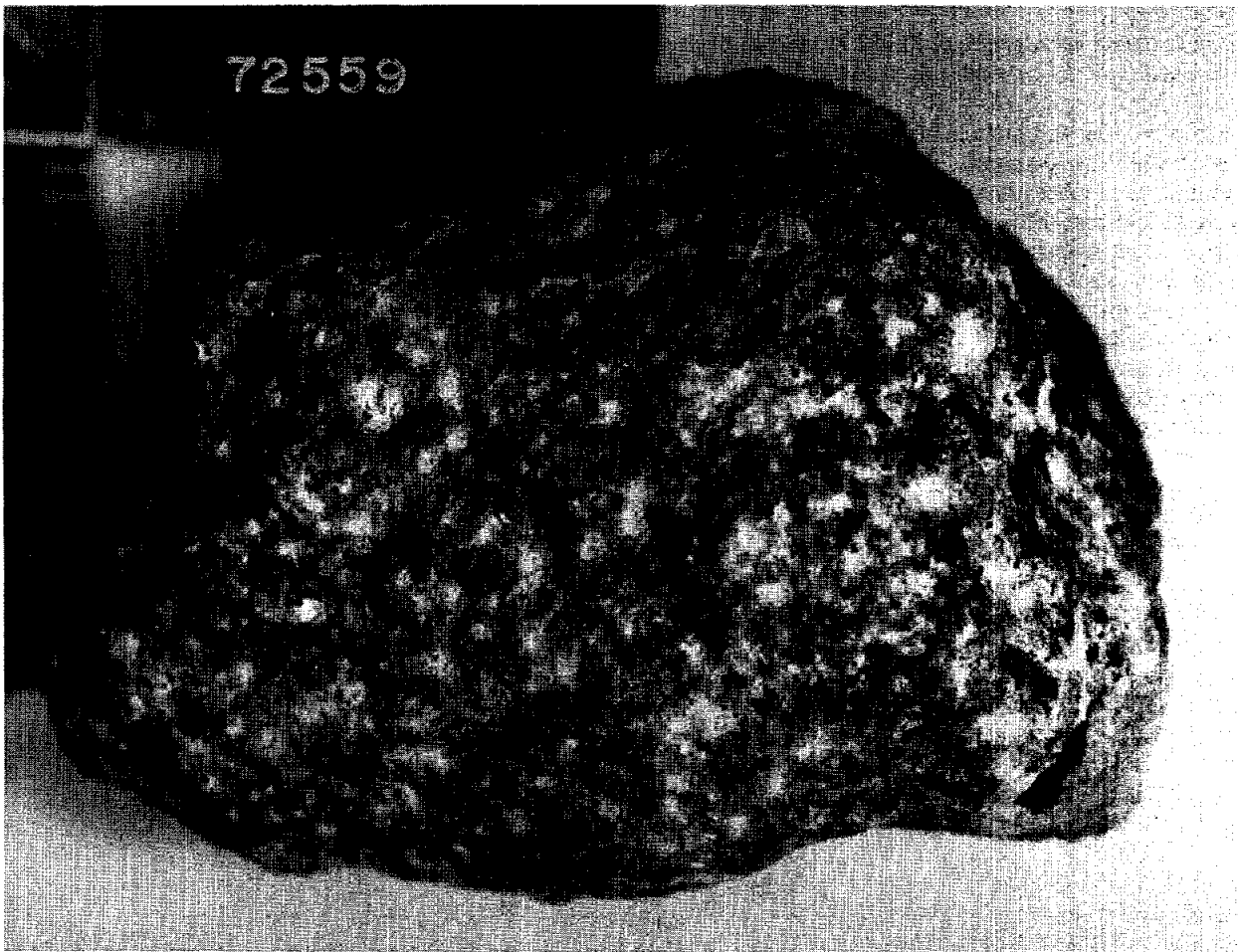


Figure 1: Sample 72559 prior to chipping. Small scale divisions in millimeters. S-73-33433.

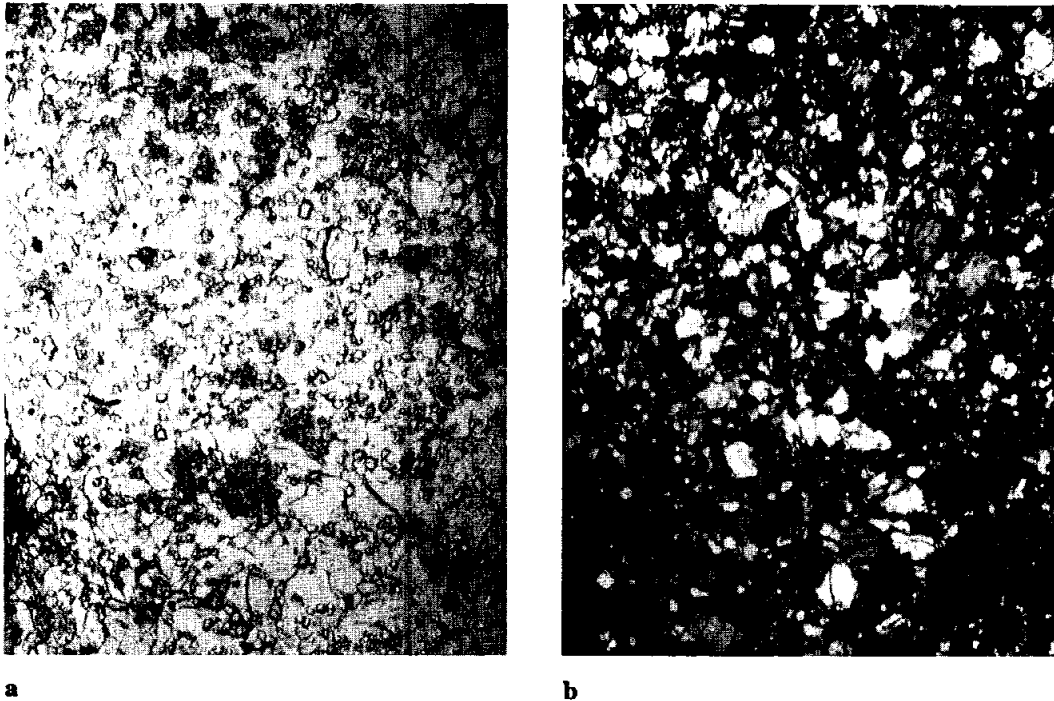


Figure 2: Photomicrograph of 72559,10, showing typical texture. Field of view about 1mm wide. a) plane transmitted light. b) crossed polarized light.

accessories (0.9); that include high-Ca pyroxene, Mg-Al-spinel, chromite, armalcolite, ilmenite, zircon, K-feldspar, metal, and troilite. Larger grains of plagioclase and olivine are set in a fine-grained granoblastic groundmass of plagioclase, olivine, and orthopyroxene (Fig. 2). Orthopyroxene is partly poikiloblastic. Microprobe analyses are given in Fig. 3, with representative analyses in Table 1. The silicate minerals are very homogeneous (An_{98.96}; Fo₈₁; En_{79.81}Wo_{3.4}) but the opaque oxides show ranges. Two areas (each about 1 mm²) are apparently lithic clasts; one is almost 100% plagioclase i.e. an anorthosite, with a granoblastic texture; the other is a troctolite. The mineral compositions of the lithic clasts are the same as in the matrix.

The textural evidence and mineralogical evidence suggest that a fairly homogeneous KREEP-free source was brecciated and thermally metamorphosed. The opaque oxides may represent

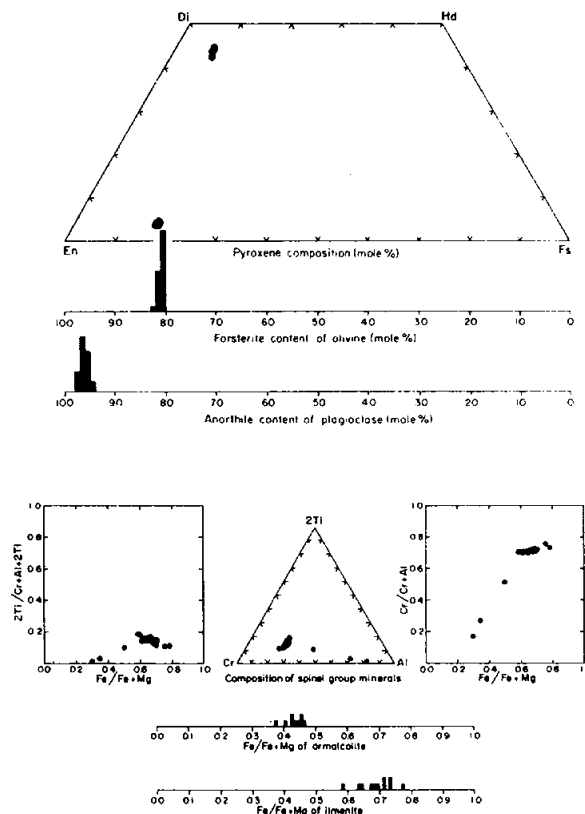


Figure 3: Microprobe analyses of mineral phases in 72559,10 (Warner et al., 1978f; Nehru et al., 1978).

Table 1: Representative analyses of silicates in 72559 (Nehru et al., 1978). 1) large plagioclase. 2) matrix plagioclase. 3) large olivine. 4) matrix olivine. 5) matrix orthopyroxene. 6) matrix clinopyroxene.

	1	2	3	4	5	6
SiO ₂	43.3	44.1	39.3	39.5	54.7	51.0
TiO ₂	n.a.	n.a.	0.07	<0.05	0.78	1.86
Al ₂ O ₃	35.2	35.1	<0.01	<0.01	1.29	2.63
Cr ₂ O ₃	n.a.	n.a.	<0.05	0.05	0.45	0.67
FeO	0.07	0.24	17.8	17.3	10.7	5.0
MgO	0.05	0.06	41.8	41.9	29.2	16.5
CaO	19.8	19.4	0.08	0.13	1.87	21.2
Na ₂ O	0.32	0.44	n.a.	n.a.	n.a.	n.a.
K ₂ O	0.12	0.15	n.a.	n.a.	n.a.	n.a.
Total	98.9	99.5	99.1	98.9	99.0	98.9
An	96.5	95.2				
Ab	2.8	3.9				
Or	0.7	0.9				
Fo			80.7	81.2		
Fa			19.3	18.8		
En					80.0	47.8
Fs					16.4	8.1
Wo					3.7	44.1

trapped liquid in originally cumulate rocks, whereas most of the silicates represent cumulus phases. The homogeneity of the minerals could represent either original igneous plutonic homogeneity or metamorphic equilibration. The pyroxenes do not show exsolution, but the coexisting high-Ca and low-Ca phases suggest re-equilibration at 950-1000 degrees C. The range in composition of the oxides is preferred by Nehru et al (1978) to represent the original igneous variation rather than reaction, except for the Mg-Al spinels.

CHEMISTRY

Two analyses are reproduced in Table 2, and the rare earths are shown in Fig. 4 (with average LKFM from Boulder 2 at Station 2 for comparison). The two analyses are reasonably consistent, and show that the rock is a magnesian anorthositic troctolite, with considerable meteoritic contamination and lack of a KREEP component. The chemistry is fairly typical for a feldspathic granulitic impactite, with low rare earths and a positive Eu anomaly,

quite distinct from the LKFM melt rocks. Warren and Wasson (1978) noted some discrepancies in their analysis (<250 mg) with that of Murali et al. (1977a) (605 mg) that they attributed mainly to non-representative sampling.

PROCESSING

In 1974 a few chips were removed from one end of 72559. Two small pieces (,1) were allocated and used for a thin section and for chemistry. In 1977 fragments constituting ,2 were allocated for chemistry and three further thin section. Four small chips constituting ,3 remain in storage, as well as the main mass ,0 (26.5 g).

Table 2: Chemical analyses of 72559.

Split	,5	,1
wt%		
SiO ₂	42.4	45
TiO ₂	0.2	<0.2
Al ₂ O ₃	28.5	25.2
Cr ₂ O ₃	.14	0.130
FeO	4.7	5.3
MnO	0.05	0.055
MgO	8.41	10
CaO	15.3	13.7
Na ₂ O	.35	0.30
K ₂ O	0.1	0.093
P ₂ O ₅		
ppm		
Sc	6.5	5.5
V		20
Co	37.1	32
Ni	494	470
Rb		
Sr		
Y		
Zr		
Nb		
Hf	1.3	1.4
Ba	70	59
Th	0.77	0.3
U	0.23	
Ce		
Ta		0.41
Pb		
La	3.2	3.4
Ce	8.3	6.4
Pr		
Nd		
Sm	1.27	1.3
Eu	0.8	0.74
Gd		
Tb	0.3	0.2
Dy		2
Ho		
Er		
Tm		
Yb	1.58	1.5
Lu	0.23	0.23
Li		
Be		
B		
C		
N		
S		
F		
Cl		
Br		
Cu		
Zn	5.4	
ppb		
Au	26.7	5
Ir	13.6	16
I		
At		
Ga	3930	
Ge	119	
As		
Se		
Mo		
Tc		
Ru		
Rh		
Pd		
Ag		
Cd	27000	
In	2600	
Sn		
Sb		
Te		
W		
Re		
Os		
Pt		
Hg		
Tl		
Bi		
	(1)	(2)

References and methods:

- (1) Warren and Wasson (1978); INAA, RNAA, except majors mainly microprobe fused bead
 (2) Murali et al. (1977a); Nehru et al. (1978); INAA, except SiO₂ from modal proportions

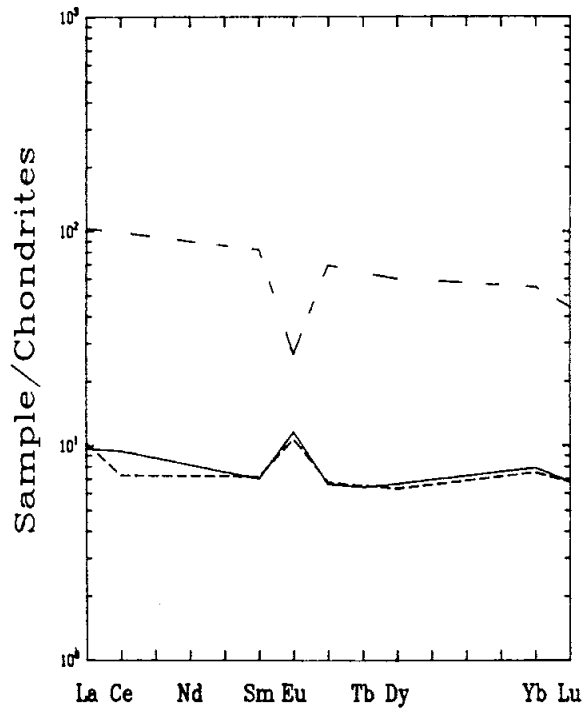


Figure 4: Rare earth elements in two samples of 72559 (bottom) and typical LKFM from Station 2 boulders (upper). Solid line from Warren and Wasson (1978), short-dash line from Murali et al. (1977a). (LKFM, wide dash line).

72705

Impact Melt Breccia St. 2, 2.39 g

INTRODUCTION

72705 is a vesicular impact melt that is probably a fine-grained variant of the common Apollo 17 LKFM composition such as forms Boulders 2 and 3 at the sample station. It contains two conspicuous white clasts, the investigated one of which is a cataclasized troctolitic anorthosite with flame-textured plagioclases.

72705 was picked from the soil collected with the the second rake sample from Station 2, on the southeast rim of Nansen crater. 72705 was described as a miscellaneous sample in LSIC

Apollo 17 (1973), consisting of "one-half crushed anorthosite and one-half black glass. The glass is highly dust-coated." According to Keil et al. (1974), 72705 is 1.6 x 1.0 x 0.7 cm, and medium dark gray (N4). It is subangular (Fig. 1) and coherent, with a few non-penetrative fractures, about 1% small vugs, and no zap pits. Matrix material (less than 1 mm grain size) appeared to be a devitrified glass and was estimated as 90% of the sample; the remainder appeared as white plagioclase clasts up to 3 mm across. The two white clasts became more conspicuous on breaking the sample.

PETROGRAPHY

72705 has a fine-grained mainly crystalline melt matrix that consists dominantly of plagioclase, pyroxene, some olivine, and cryptocrystalline or possibly glassy interstitial material. It contains conspicuous spherical vesicles, and is clast-rich (Fig. 2). The groundmass appears similar to that of 76035, one of the finest-grained of the Apollo 17 LKFM samples, except that the olivine microphenocrysts in 72705 are not so well developed. Warren and Wasson (1979), however, described the matrix as cataclastic,

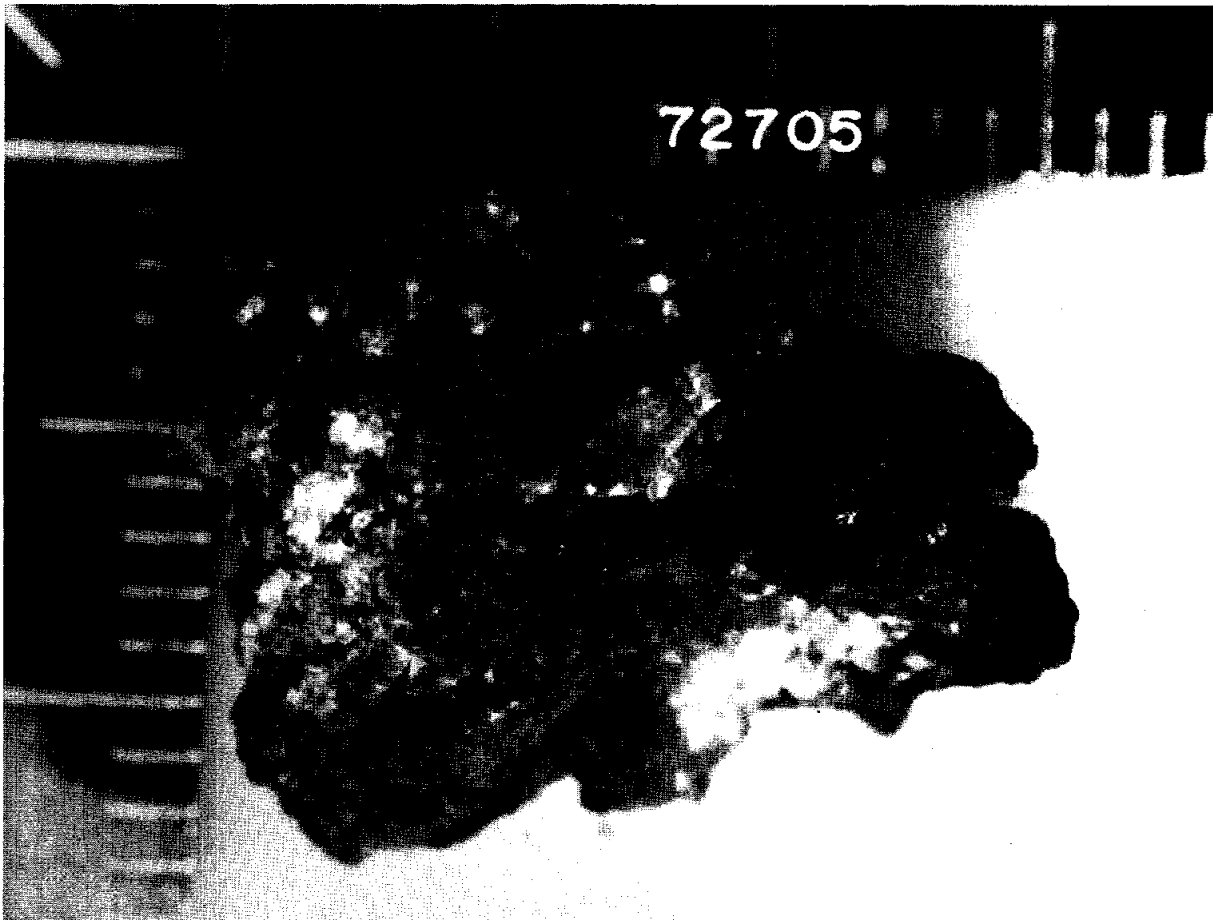


Figure 1: Sample 72705. S-73-33444. Smallest scale divisions in millimeters.

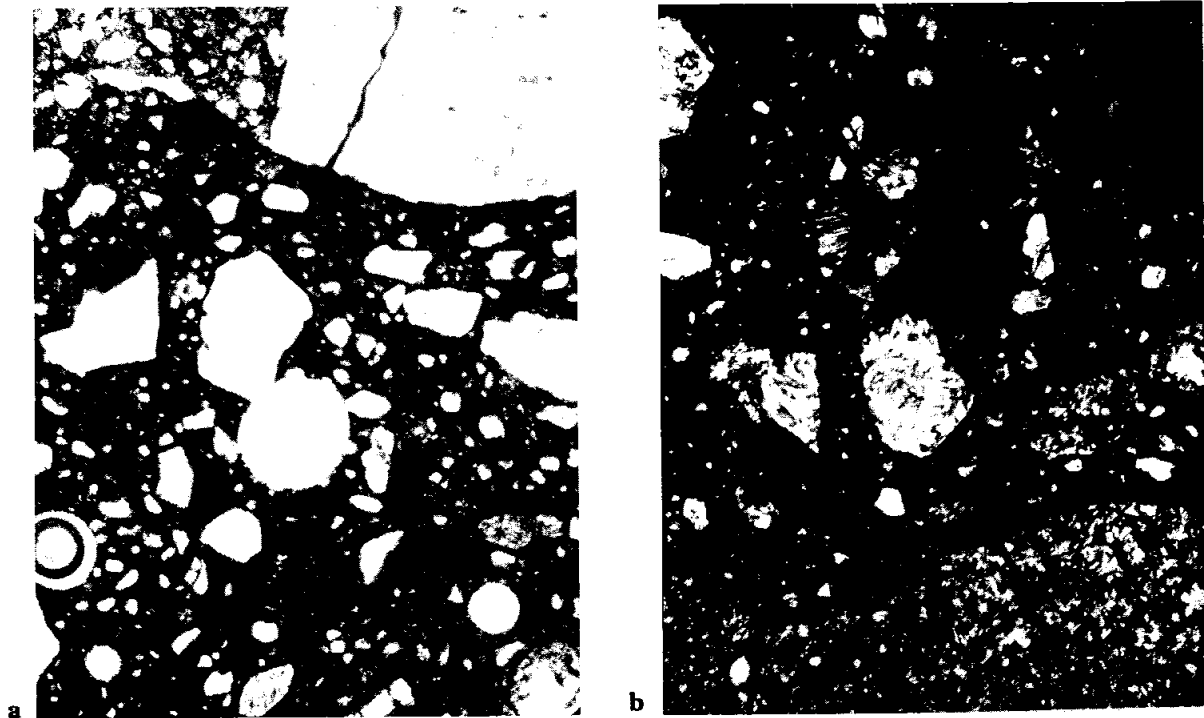


Figure 2: Photomicrograph of 72705,4, showing vesicular dark groundmass and flame-textured plagioclase in clast A. Width of field about 1 mm. a) plane-transmitted light. b) crossed polarizers.

inconsistent with Warren (1979), who had described it as granulitic.

The mineral clasts include both very rounded and very angular varieties. Warren and Wasson (1979) analyzed silicate mineral fragments, and found them all to be olivines and plagioclases with compositions identical with those in the white lithic clast they analyzed (Fig. 3 and below). Nearly all of the plagioclases also have a flame-texture identical with those in the lithic clast.

72705 was investigated mainly because of its white clasts. Two were identified on breaking the sample, and labelled A and B. Thin sections show only matrix and clast A. Part of clast A is shown in Fig. 2. It consists mainly of plagioclase, which has a flame-texture normally assumed to be indicative of devitrified maskelynite, and some olivine. The clast was cataclitized, leaving plagioclase relics up to 2 mm across. Both cataclasis and maskelynitization occurred prior to breakup of the clast and its

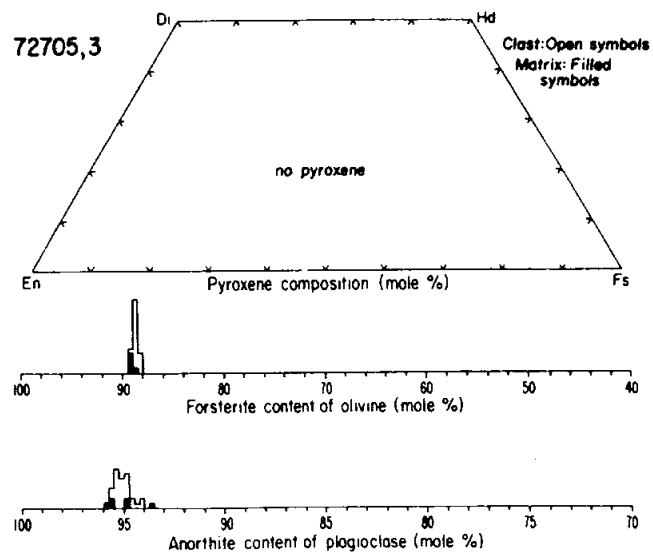


Figure 3: Microprobe analyses of minerals in clast A and the matrix of 72705 (Warren and Wasson, 1979).

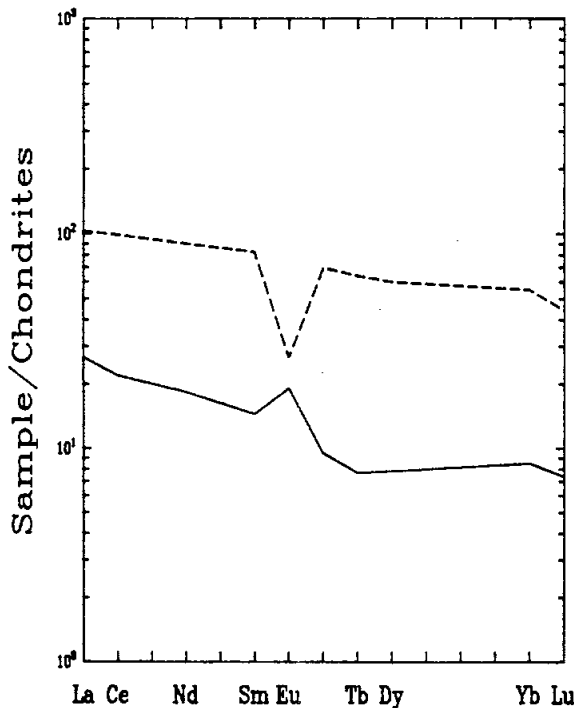


Figure 4: Chondrite-normalized rare earths in clast A (72705,1, solid line), with typical Apollo 17 LKFM (dashed line) for comparison.

immersion in the melt, which left the clast with a fragmental porous interior and a baked and sintered border against the melt. Clast A was described by Warren (1979) and Warren and Wasson (1979) who identified the cataclasis as preceding maskelynitization. They found that the clast was about 2/3 plagioclase and 1/3 olivine, with each phase of very restricted composition (about An₉₅, Fogg; Fig. 3). They found no pyroxene, but that a trace of Cr-spinel is present. They interpreted clast A as essentially a pristine igneous lithology that had been cataclasized.

CHEMISTRY

A chemical analysis of clast A, made on a 75 mg subsample, is reproduced in Table 1, with the rare earth elements plotted in Fig. 4. No analysis has been made of the melt groundmass of 72705. Clast A is normatively a troctolite (61% feldspar, 38% olivine, in good agreement with the mode, given the small size of both the thin section and the analyzed split). It is free of

meteoritic siderophile contamination, and its rare earth element pattern is fractionated compared with KREEP; thus the sample is considered to be a pristine igneous lithology by Warren (1979) and Warren and Wasson (1979). Its mineral chemistry is like that of troctolite 76535.

PROCESSING

The sample was not chipped until 1978, when it was investigated for its white material rather than its dark matrix. 72705 was broken to reveal two white clasts (A and B). A small chip of pure clast A (.1) was used for chemical analysis and for a tiny thin section; a chip (.2) consisting of matrix and a little of clast A was used to make thin sections ,3 and ,4. Clast A probably had an original mass of about 0.5 g. The remainder of clast A occurs with matrix in ,0 (0.97 g). Clast B occurs with matrix in ,5 (1.1 g).

Table 1: Chemical analysis of clast A in 72705.

Split	.1*
wt %	
SiO ₂	42.2
TiO ₂	
Al ₂ O ₃	23.8
Cr ₂ O ₃	0.134
FeO	4.0
MnO	0.040
MgO	16.8
CaO	12.6
Na ₂ O	0.305
K ₂ O	0.064
P ₂ O ₅	
ppm	
Sc	2.6
V	
Co	2.5
Ni	18
Rb	
Sr	16(a)
Y	
Zr	190
Nb	
Hf	1.6
Ba	170
Th	0.32
U	0.12
Cs	
Ta	0.062
Pb	
La	8.8
Ce	19.3
Pr	
Nd	1.1
Sm	2.62
Eu	1.32
Gd	
Tb	0.36
Dy	
Ho	
Er	
Tm	
Yb	1.7
Lu	0.25
Li	
Be	
B	
C	
N	
S	
F	
Cl	
Br	
Cu	
Zn	1.9
ppb	
Au	0.170
Ir	0.016
I	
At	
Ga	3400(a)
Ge	11
As	
Se	
Mo	
Tc	
Ru	
Rh	
Pd	
Ag	
Cd	3.0
In	1.3
Su	
Sb	
Te	
W	
Re	
Os	
Pt	
Hg	
Tl	
Bi	

References and methods:

1) Warren (1979), Warren and Wasson (1979); INAA, RNAA, microprobe fused bead; except (a) updated by Warren and Kallemeyn (1984).

Notes: * incorrectly labelled as 72075,1 on one data line in Warren (1979).

(1)

72735**Impact Melt Breccia (High-K)****St. 2, 51.1 g****INTRODUCTION**

72735 is a fine-grained clast-bearing impact melt. Its chemistry differs from the common low-K Fra Mauro melts that dominate the Apollo 17 highlands samples in having much higher K and other incompatible element contents, and a lower Mg/Fe. It also contains more clastic material than most of the local rake impact melt samples.

Of the four samples of the second rake sample from Station 2, on the southeast rim of Nansen crater, 72735 was the only one described as a green-gray breccia by LSIC 17 (1973). 72735 is 4.2 x 3.5 x 3.0 cm and medium dark gray (N4) (Keil et al., 1974). It is subrounded and coherent, with a few non-penetrative fractures (Fig. 1). It has a few zap pits on all sides, and about 5% vugs. Matrix material

(mainly less than 100 microns grain size) was estimated to compose 94% of the rock (Keil et al., 1974), with the clasts mainly appearing to be plagioclase. LSIC 17 (1973) estimated clasts about 1mm across as less than 1% of the rock.

PETROGRAPHY

72735 is a crystallized impact melt containing lithic and mineral clasts (Fig. 2, Table 1). Warner et al. (1977b,c; 1978f) described 72735 as a microgranular-micropoikilitic matrix breccia, similar to 72549 but with mafics almost wholly pyroxene. They distinguished 72735 with 72558 as a high-K KREEP breccia (however, see 72558 CHEMISTRY) on the basis of the high K_2O (0.89%) evident in the defocused beam analysis (Table 2; confirmed by the INAA analysis,

Table 3). However, apart from the lack of olivine, there are several other differences from most other local impact melts; the overall appearance is like some of the Boulder 1, Station 2 samples. The grain size is finer than that of the other supposed high-K breccia 72558. The modal data (Table 1) shows a low proportion of melt groundmass (73%), and the clast population is dominated by lithic clasts, unlike most melts. Microprobe analyses (Warner et al., 1978f) are shown in Figure 3; the matrix pyroxenes are more iron-rich than those in other melts, and more varied in composition. There is an interstitial K-rich phase. Engelhardt (1979) tabulated ilmenite paragenetic features, inferring that ilmenite crystallization followed that of pyroxene.

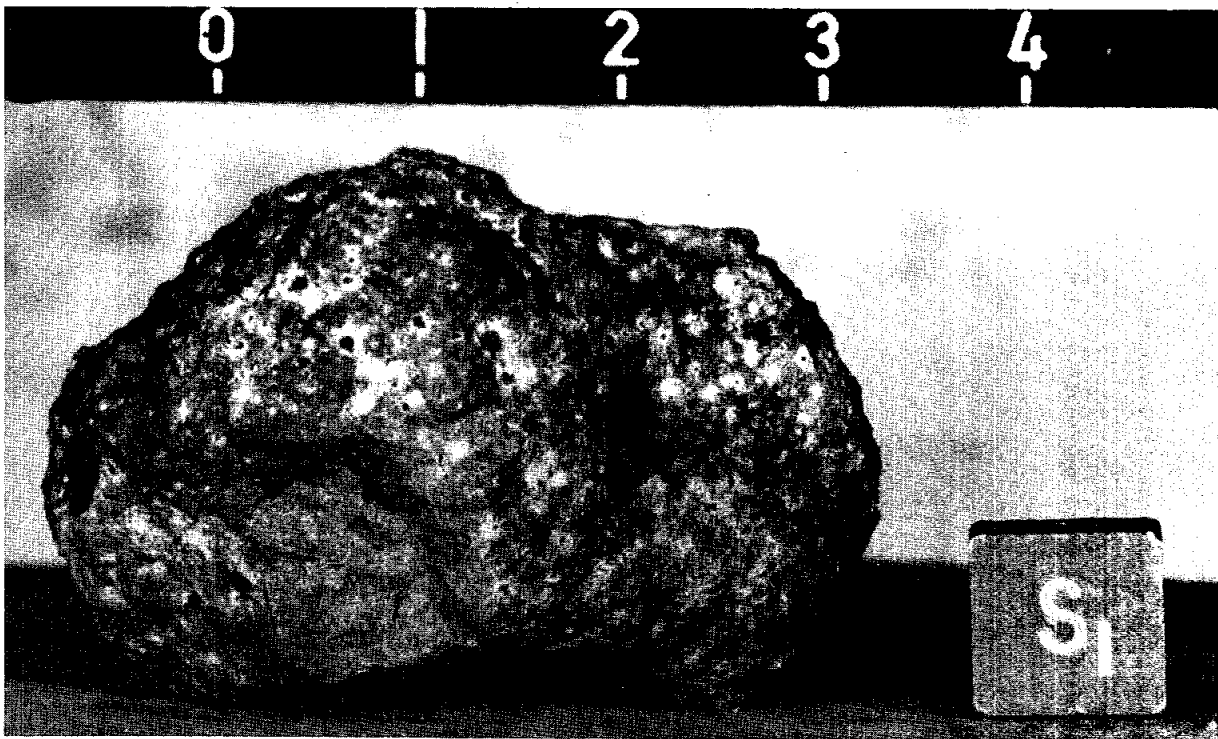


Figure 1: Sample 72735. Scale divisions in centimeters. S-73-19444.

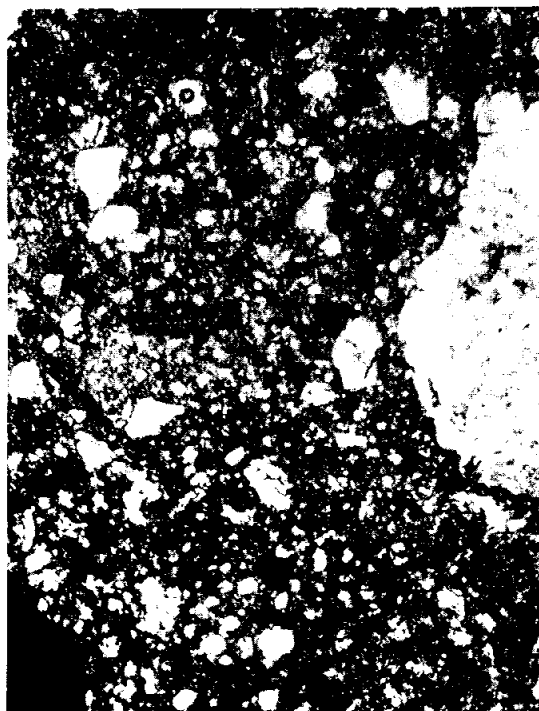


Figure 2: Photomicrograph of 72735,12, showing general groundmass, mineral clasts, and a lithic fragment. Plane light; width of field about 1 mm.

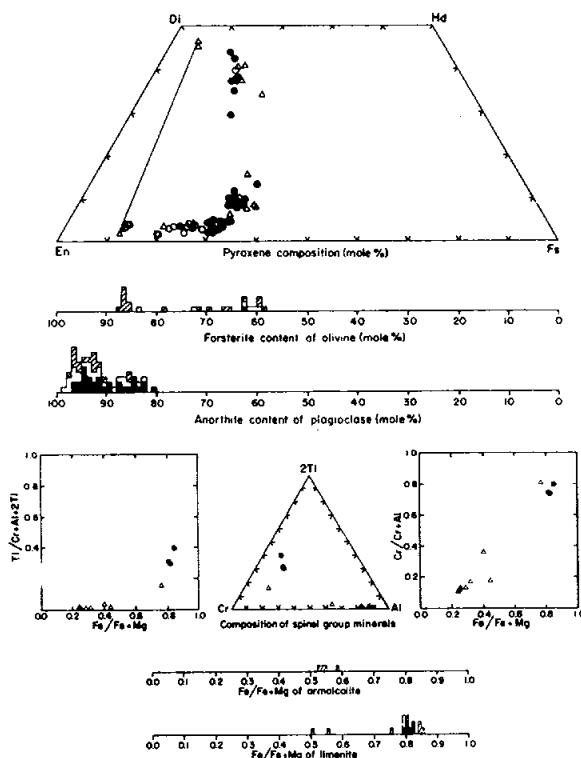


Figure 3: Microprobe analyses of minerals in 72735 (Warner et al., 1978f). Filled symbols = matrix phases. In histograms, open symbols = mineral clasts and cross-hatched = minerals in lithic clasts. In other diagrams, open circles = mineral clasts and open triangles = minerals in lithic clasts.

The mineral and lithic clasts almost exclusively appear to be derived from coarse-grained feldspathic rocks. Some of the larger ones include troctolitic varieties. Warner et al. (1977b) described and depicted two troctolitic clasts larger than 1 mm as being the only two highlands feldspathic clasts in their Apollo 17 melt samples to have preserved an original igneous texture. One has a cumulate texture, with olivines (Fo_{86-87}) poikilitically enclosed by plagioclase (An_{92}), with trace pink spinel, ilmenite, and chromite. The other is basically of basaltic texture, with olivines similar to the first described clast but smaller plagioclases (An_{91-96}), and pyroxenes as well as several trace phases. Microprobe analyses of the phases in these clasts are shown in Fig. 3. Bulk compositions determined by defocused beam microprobe analyses (Warner et al., 1977b) indicate that they are of picritic composition.

CHEMISTRY

A chemical analysis of a 574 mg split by INAA is reproduced as Table 3. The major elements agree reasonably well with those of the defocused beam analysis (Table 2). 72735 is unlike all other impact melts from the Apollo 17 site in that it contains higher silica, lower titania, and lower Mg/Fe, but most significantly higher K_2O and other incompatible element abundances. However, Murali et al (1977b) did not remark on the difference of 72735 from other melt samples. The rare earth element pattern is that of KREEP (Fig. 4). The Ir abundance is extremely high, and unusually so given the comparatively low Ni abundance.

PROCESSING

The sample was chipped in one area to produce a few documented pieces in 1974. Six small chips were divided into ,2 and ,3.; and a larger chip (,4) was taken adjacent to them. These remain unallocated. Two small chips were combined as ,1 and used for chemical analysis and to make thin section ,12.

Table 1: Modal analysis of 72735,5 (Warner et al., 1977b).

	72735
Points counted	2827
Matrix	72.9
Mineral clasts	12.7
Lithic clasts	14.3
Mineral clasts	
Plagioclase	8.0
Olivine/pyroxene	4.7
Opaque oxide	tr
Metal/troilite	—
Other	—
Total	12.7
Lithic clasts	
ANT	10.6
Devitrified anorthosite	2.4
Breccia	1.3
Other	tr
Total	14.3
Percent of matrix (normalized to 100)	
Plagioclase	52.7
Olivine/pyroxene	42.2
Opaque oxide	1.2
Metal/troilite	0.3
Other	3.6

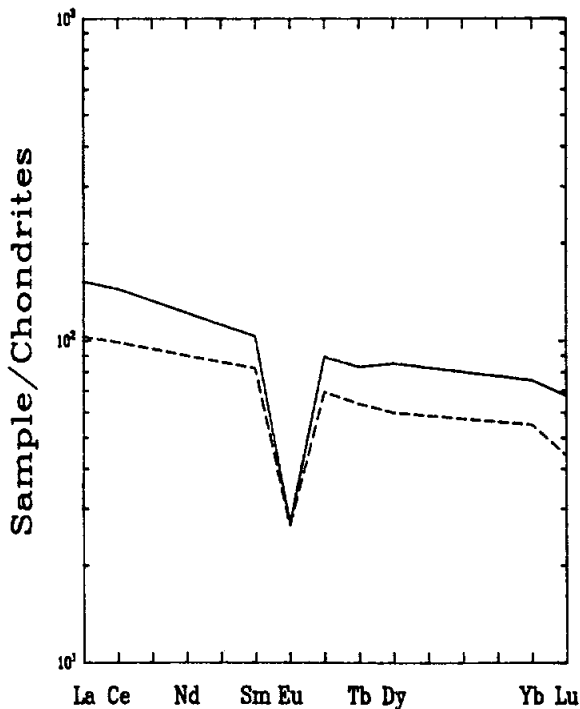


Figure 4: Plot of rare earth elements in 72735,1 (solid line) with typical A17 LKFM as represented by average Boulder 2 Station 2 samples (dashed line).

Table 2: Microprobe defocused beam analysis of matrix of 72735
(from Warner et al., 1977b).

<u>wt %</u>	,12
SiO ₂	50.1
TiO ₂	0.67
Al ₂ O ₃	20.2
Cr ₂ O ₃	0.18
FeO	7.9
MnO	0.12
MgO	8.1
CaO	11.5
Na ₂ O	0.68
K ₂ O	0.89
P ₂ O ₅	0.32
Sum	100.7

Table 3: Chemical analysis of 72735,1

<u>Split</u>	,1
<u>wt %</u>	
SiO ₂	
TiO ₂	0.7
Al ₂ O ₃	18.0
Cr ₂ O ₃	0.184
FeO	9.3
MnO	0.12
MgO	9
CaO	10.2
Na ₂ O	0.54
K ₂ O	0.73
P ₂ O ₅	
<u>ppm</u>	
Sc	16
V	40
Co	17
Ni	91
Rb	
Sr	
Y	
Zr	880
Nb	
Hf	23
Ba	560
Th	2.9
U	
Cs	
Ta	2.3
Pb	
La	50.2
Ce	127
Pr	
Nd	
Sm	18.7
Eu	1.87
Gd	
Tb	3.9
Dy	27
Ho	
Er	
Tm	
Yb	15.1
Lu	2.3
Li	
Be	
B	
C	
N	
S	
F	
Cl	
Br	
Cu	
Zn	
<u>ppb</u>	
Au	
Ir	110

(1)

References and methods:

(1) Murali et al.(1977a); INAA

72736**Micropoikilitic Impact Melt Breccia****St. 2, 28.7 g****INTRODUCTION**

72736 is a fine-grained clast-bearing impact melt with a microgranular to micropoikilitic groundmass texture. Its chemistry is similar to the common low-K Fra Mauro melts that dominate the Apollo 17 highlands samples.

72736 was one of two tan breccias (LSIC 17, 1973) collected in the second rake sample from Station 2. It is 5.0 x 2.6 x 1.8 cm and medium dark gray (N4) (Keil et al., 1974). It is subangular and coherent, with few, non-penetrative, fractures, although the sample broke in half (Fig. 1). It has 1% vugs, and many zap pits. Matrix material (mainly less than 100 microns grain size) was estimated to compose 95% of the rock (Keil et al., 1974). Nearly all of the clast material in the 1 to 2 mm range is feldspathic.

PETROGRAPHY

72736 is a crystallized impact melt containing mineral clasts (Fig. 2) similar to 72549 but slightly finer-grained. The texture is somewhat blotchy, with finer-grained areas such as are apparent in Fig. 2a; these areas are not clasts. Lithic clasts are rare, although two larger ones (2 mm) constitute much of the thin section .9. Warner et al. (1977b,c; 1978f) described 72736 as a microgranular-micropoikilitic matrix breccia. It has a coarser grain size than the microsubophitic melts represented by 72535. The modal data (Table 1) shows a lower proportion of melt groundmass (72.2%) than other melt samples because of the two large clasts. The mineral clast population is dominated by plagioclase, similar to many other impact melt samples at the Apollo 17 site; two pink

spinel with reaction coronas are in the thin section.

The groundmass plagioclase occurs as laths or stubby grains, many with rounded corners; mafic and opaque grains are equant to subequant. Microprobe analyses (Warner et al., 1978f) are shown in Figure 3. The groundmass olivine, which is prominent and euhedral, has a narrow range of compositions (Fo₇₁₋₇₅). Engelhardt (1979) tabulated ilmenite paragenetic features, inferring that ilmenite crystallization post-dated pyroxene.

The clasts are more rounded with more evidence of reaction (e.g coronas) than in the finer-grained, subophitic melts. Plagioclase clasts dominate the mineral fragment population. The two larger lithic clasts are a flame-textured devitrified anorthosite (Fig 2b) and a microgranular breccia.

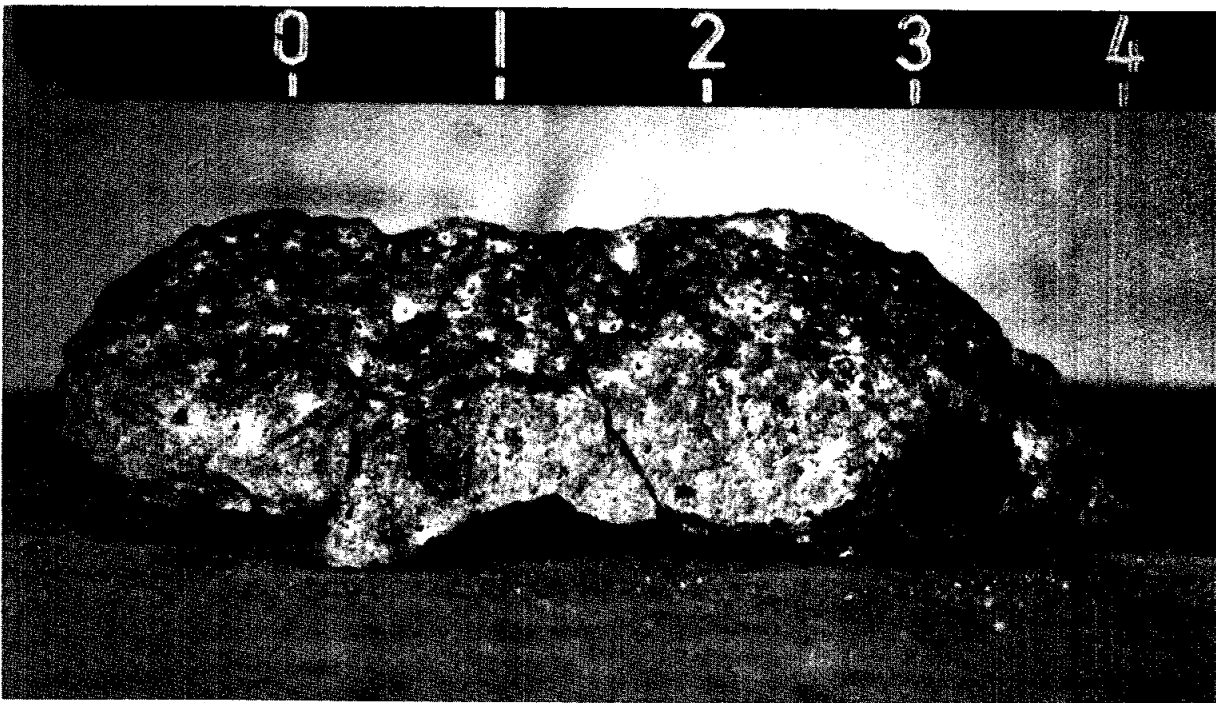


Figure 1: Sample 72736. Scale divisions in centimeters. S-73-19436.

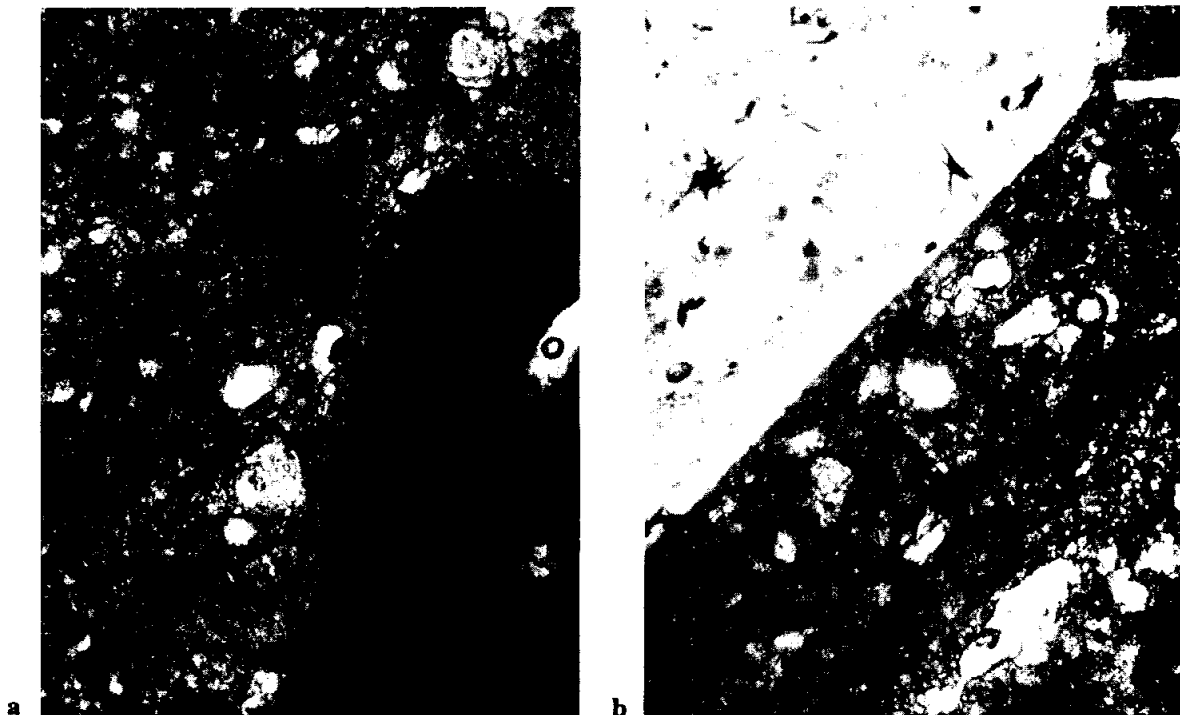


Figure 2: Photomicrographs of 72736,9, showing general groundmass and mineral clasts. Plane light; width of field about 1 mm. a) shows blotchy groundmass, with ilmenite needles growing across apparent boundaries. b) shows sharp contact of flame-textured anorthositic clast with the groundmass.

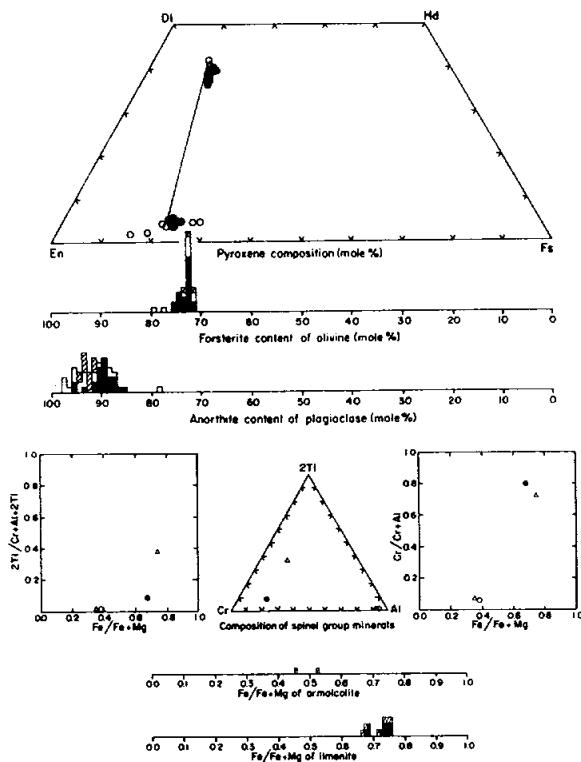


Figure 3: Microprobe analyses of minerals in 72736 (Warner et al., 1978f). Filled symbols = matrix phases. In histograms, open symbols = mineral clasts and cross-hatched = minerals in lithic clasts. In other diagrams, open circles = mineral clasts and open triangles = minerals in lithic clasts.

CHEMISTRY

The only analysis is a defocused beam analysis for the major elements (Table 2). The analysis is similar to that of many other Apollo 17 impact melts (although apparently lower in TiO_2), and falls on the plagioclase-pyroxene cotectic in the OI-Si-An system.

PROCESSING

The sample broke into two pieces (.5 and .6) before chipping in 1974. Chips .2 and .3 (each consisting of two fragments) were taken from .5. Only .2 was used, producing thin sections .9 and .10.

Table 1: Modal analysis of 72736,7 (Warner et al., 1977b).

72736	
Points counted	3097
Matrix	72.2
Mineral clasts	12.0
Lithic clasts	15.8
Mineral clasts	
Plagioclase	8.1
Olivine/pyroxene	3.8
Opaque oxide	tr
Metal/troilite	0.1
Other	—
Total	<u>12.0</u>
Lithic clasts	
ANT	0.9
Devitrified anorthosite	7.8
Breccia	7.1
Other	tr
Total	<u>15.8</u>
Percent of matrix (normalized to 100)	
Plagioclase	50.3
Olivine/pyroxene	46.2
Opaque oxide	2.1
Metal/troilite	0.6
Other	0.8

Table 2: Microprobe defocused beam analysis of matrix of 72736 (from Warner et al., 1977b).

<u>wt %</u>	
SiO ₂	47.5
TiO ₂	0.67
Al ₂ O ₃	19.3
Cr ₂ O ₃	0.16
FeO	7.7
MnO	0.13
MgO	11.6
CaO	11.9
Na ₂ O	0.72
K ₂ O	0.26
P ₂ O ₅	0.27
Sum	100.2

72737**Impact Melt Breccia (?)****St. 2, 3.3 g****INTRODUCTION**

72737 was one of two tan breccias (LSIC 17, 1973) collected in the second rake sample from Station 2. It is 1.5 x 1.1 x 1.1 cm and medium gray (N5) (Keil et al., 1974). It is subrounded and coherent, with few non-penetrative fractures (Fig. 1). It has less than 1% vugs, and a few

zap pits. Matrix material (mainly less than 100 microns grain size) was estimated to compose 93% of the rock (Keil et al., 1974). Most of the clast material in the 1 to 2 mm range is feldspathic.

Macroscopically it appears to be very similar to 72736. The sample has never been divided or allocated.

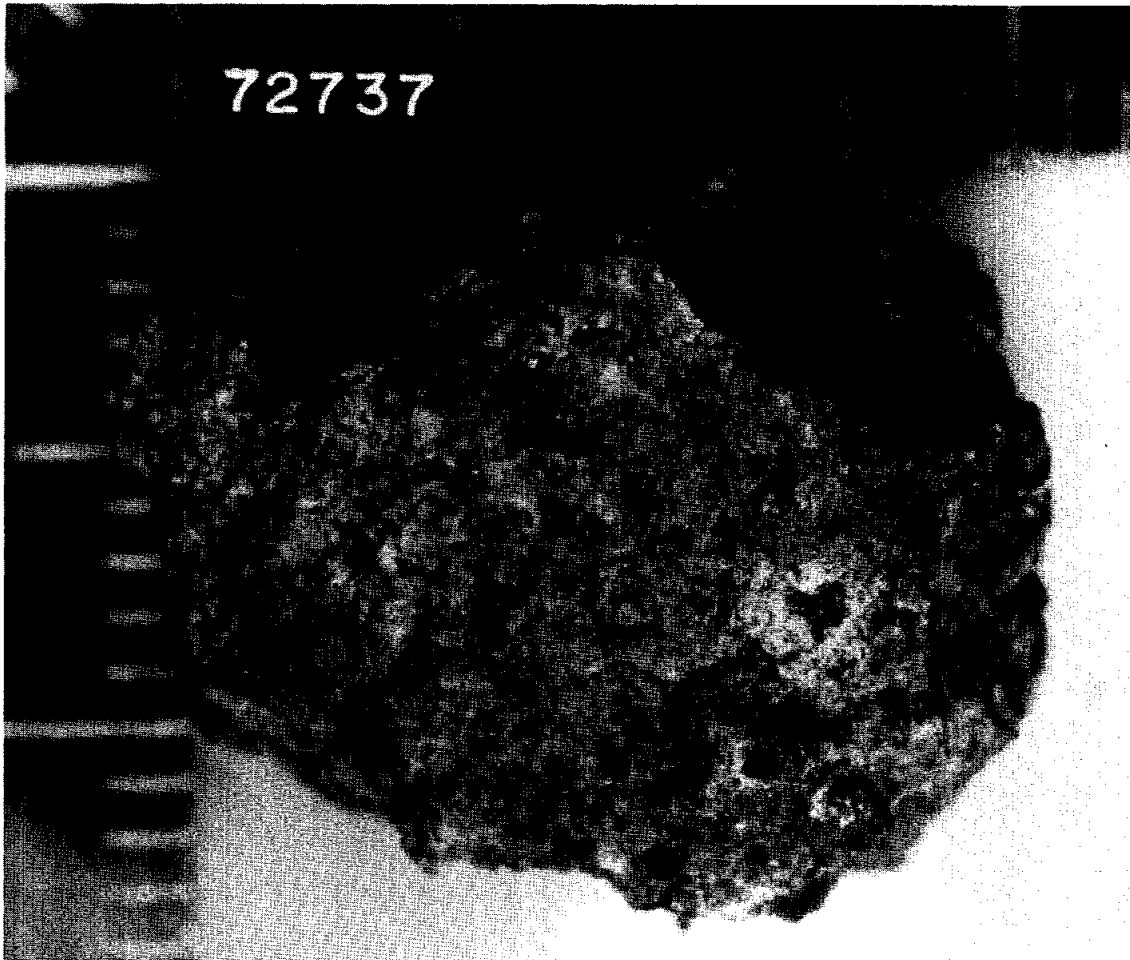


Figure 1: Sample 72737. Smallest scale divisions in millimeters. S-73-33448.

72738

Microsubophitic Impact Melt Breccia

St. 2, 23.8 g

INTRODUCTION

72738 is a fine-grained clast-bearing impact melt with a subophitic groundmass texture. Its chemistry is similar to the common low-K Fra Mauro melts that dominate the Apollo 17 highlands samples.

72738 was the only blue-gray breccia (LSIC 17, 1973) collected in the second rake sample from Station 2. It is 3.8 x 2.9 x 2.5 cm and medium dark gray (N4) (Keil et al., 1974). It is subangular (Fig. 1) and coherent, with no fractures and a few vugs. There are no zap pits. Matrix material (less than 1 mm grain size) was estimated as 90% of the sample, with plagioclase and lithic clasts dominating the remainder. Splitting attempted to include a 6 mm clast, but the

allocated material either has little of this clast or it is identical with the groundmass.

PETROGRAPHY

The groundmass of 72738 is a very fine-grained crystallized melt, with small clasts quite distinct from the groundmass (Fig. 2). It is generally homogeneous, and slightly finer-grained than 72535. Warner et al. (1977b,c; 1978f) described 72738 as a microsubophitic matrix breccia. Their modal data (Table 1) shows a high proportion of melt groundmass (87%) and a clast population dominated by plagioclase, similar to many other impact melt samples at the Apollo 17 site. Warner et al. (1977b,c; 1978f) described the dark porous groundmass as basaltic-textured,

with plagioclase laths less than 30 microns long subophitically enclosed by irregular mafic crystals. Microprobe analyses (Warner et al., 1978f) are shown in Figure 3. The matrix olivines show a wider range of compositions than the other subophitic samples studied by Warner et al. (1978f) (Fo71-79). Engelhardt (1979) tabulated ilmenite paragenetic features, inferring that ilmenite crystallization started after plagioclase but before pyroxene.

Both mineral and lithic clasts tend to be subrounded to subangular. Calcic plagioclases dominate the mineral clasts, and most are smaller than 100 microns; mafic mineral clasts also tend to be more refractory than the groundmass counterparts but quite a few are less refractory (Fig. 3). The rare lithic

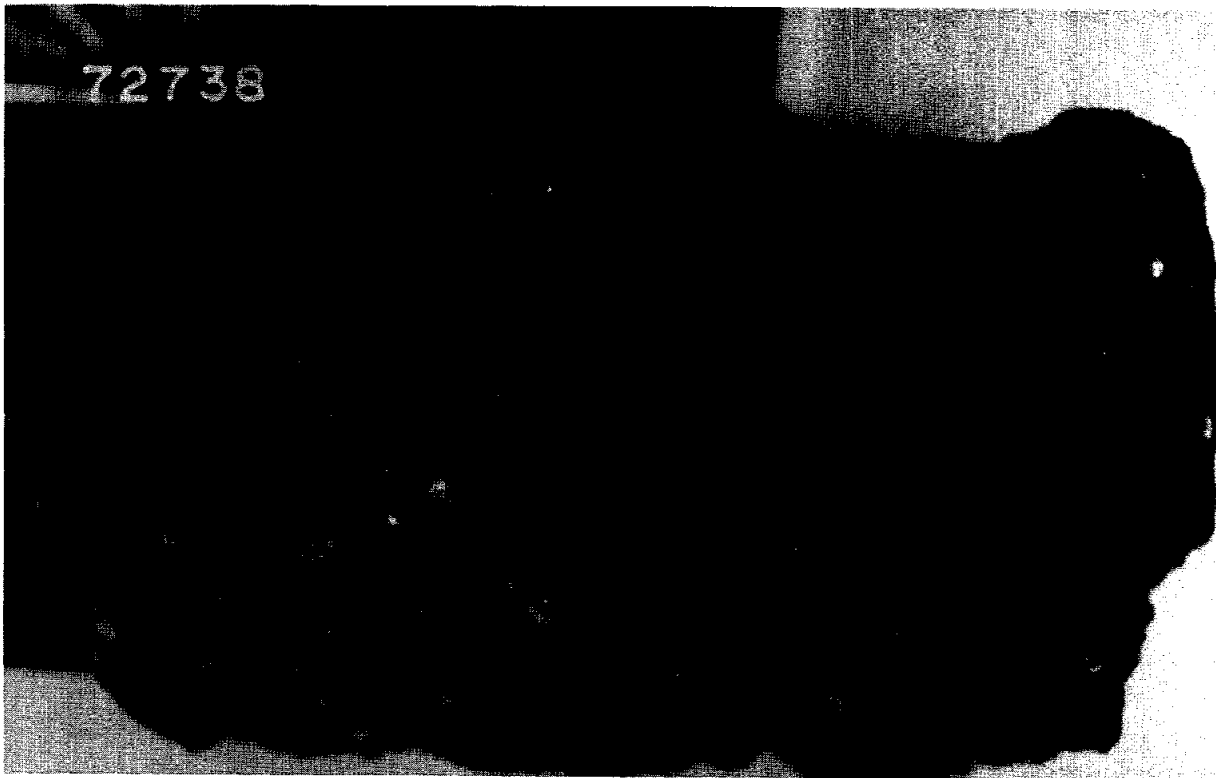


Figure 1: Sample 72738. S-73-33454. Smallest scale divisions in millimeters.

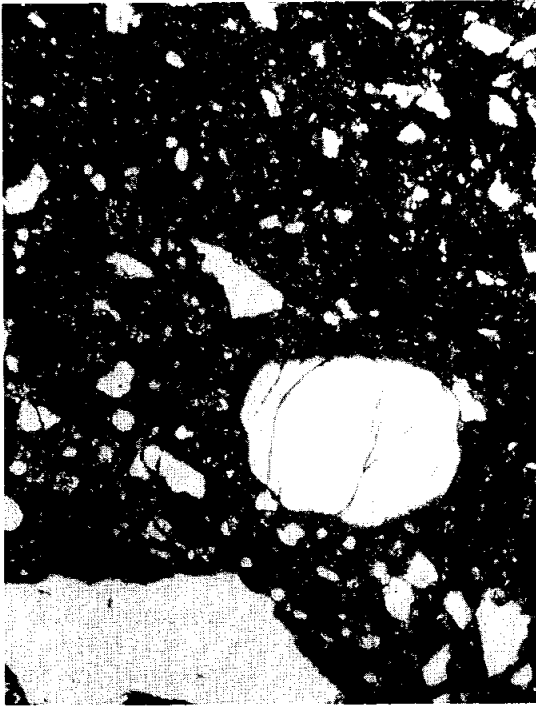


Figure 2: Photomicrograph of 72738,15, showing general groundmass. White phases are plagioclase clasts and some vugs. Plane transmitted light; width of field about 1 mm.

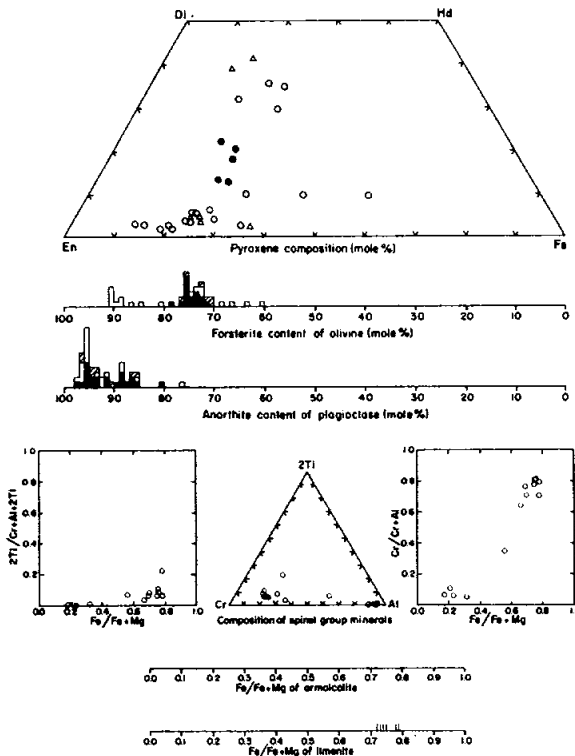


Figure 3: Microprobe analyses of minerals in 72738 (Warner et al., 1978f). Filled symbols = matrix phases. In histograms, open symbols = mineral clasts and cross-hatched = minerals in lithic clasts. In other diagrams, open circles = mineral clasts and open triangles = minerals in lithic clasts.

clasts are mainly fine-grained anorthositic materials. The sampling was intended to sample a 6 mm clast but such a clast is not apparent in the 5 serial slices that compose the thin section (,15).

CHEMISTRY

A 413 mg sample was analyzed by Murali et al. (1977a) (Table 2; Fig. 4). The chemistry is fairly similar to that of other Apollo 17 impact melts, although it is a little lower in incompatible elements. A microprobe defocused beam analysis for the major elements (Table 3) agrees well with the neutron activation analysis except for being lower in FeO. If the sample included the 6 mm clast that was targeted, then the clast may have a composition similar to the bulk rock; alternatively, it may be responsible for the analysis having lower incompatible elements than the Boulder 2 groundmass.

PROCESSING

72738 was sawn to provide samples, and was entirely subdivided. The W end piece is 14 g, and the E end piece is 1.8 g. The slab produced was subdivided into several pieces, with .5 remaining as 3.8 g. Piece ,9, described as having a 6 mm clast composing 15% of it, was allocated for chemical analysis and subsequent thin sectioning; but no hint of clast/groundmass differences was given in reports. Other pieces were not allocated.

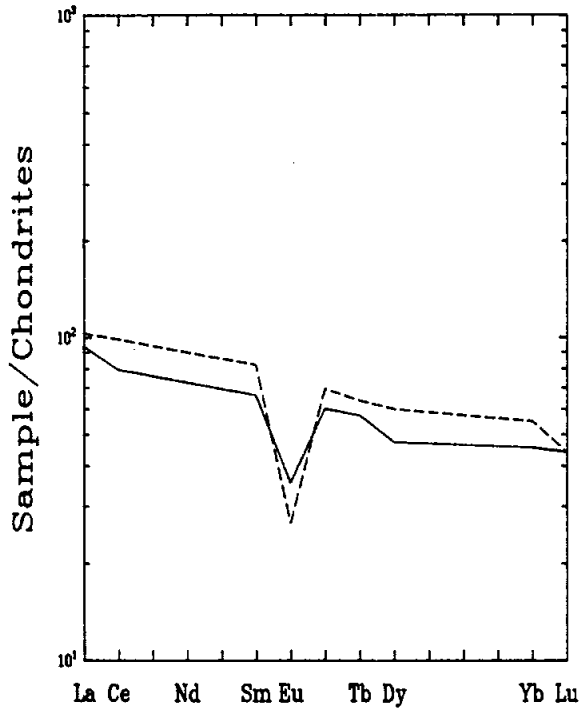


Figure 4: Chondrite-normalized rare earths in 72738,1 (solid line; Murali et al., 1977a) and average of Boulder 2 at Station 2 (dashed line; Laul and Schmitt, 1974a).

Table 1: Modal analysis of 72738,6 (Warner et al., 1977b).

	72738
Points counted	2561
Matrix	86.9
Mineral clasts	10.1
Lithic clasts	3.0
Mineral clasts	
Plagioclase	7.1
Olivine/pyroxene	2.9
Opaque oxide	tr
Metal/troilite	0.1
Other	tr
Total	10.1
Lithic clasts	
ANT	1.6
Devitrified anorthosite	0.4
Breccia	0.5
Other	0.5
Total	3.0
Percent of matrix (normalized to 100)	
Plagioclase	50.8
Olivine/pyroxene	43.9
Opaque oxide	2.4
Metal/troilite	0.2
Other	2.7

Table 2: Chemical analysis of bulk sample 72738.

<u>Split</u>	,9
<u>wt %</u>	
SiO ₂	
TiO ₂	1.3
Al ₂ O ₃	18.5
Cr ₂ O ₃	0.176
FeO	10.2
MnO	0.113
MgO	10
CaO	11.3
Na ₂ O	0.89
K ₂ O	0.25
P ₂ O ₅	
<u>ppm</u>	
Sc	17
V	40
Co	28
Ni	220
Rb	
Sr	
Y	
Zr	380
Nb	
Hf	10.5
Ba	350
Th	3.1
U	
Cs	
Ta	11
Pb	
La	31.0
Ce	70
Pr	
Nd	
Sm	12.0
Eu	2.45
Gd	
Tb	2.7
Dy	15
Ho	
Er	
Tm	
Yb	9.1
Lu	1.5
<u>ppb</u>	
Au	2
Ir	6
	(1)

Table 3: Microprobe defocused beam analysis of matrix of 72738 (from Warner et al., 1977b).

<u>wt %</u>	
SiO ₂	46.4
TiO ₂	1.69
Al ₂ O ₃	18.7
Cr ₂ O ₃	0.16
FeO	8.0
MnO	0.11
MgO	10.1
CaO	11.8
Na ₂ O	0.82
K ₂ O	0.23
P ₂ O ₅	0.27
Sum	98.3

References and methods:

(1) Murali et al. (1977a); INAA

73145

Impact Melt Breccia (?)

St. 2A (LRV-4), 5.6 g

INTRODUCTION

73145 was picked from soil sample 73140 taken from the bottom of a 15cm-deep trench on the landslide or avalanche from the South Massif, 600 m NE of Nansen Crater. The tough sample is slabby and angular (Fig. 1), with dimensions of 2.5 x 2.0 x 1 cm. It is medium dark gray (N4) and

homogeneous, with about 75% being fine-grained matrix and about 25% being small plagioclase clasts. Its appearance is similar to homogeneous impact melts, with its groundmass described as possibly diabasic in LSIC 17 (1973). It lacks zap pits and cavities. It does have some irregular fractures on which euhedral pyroxenes are visible.

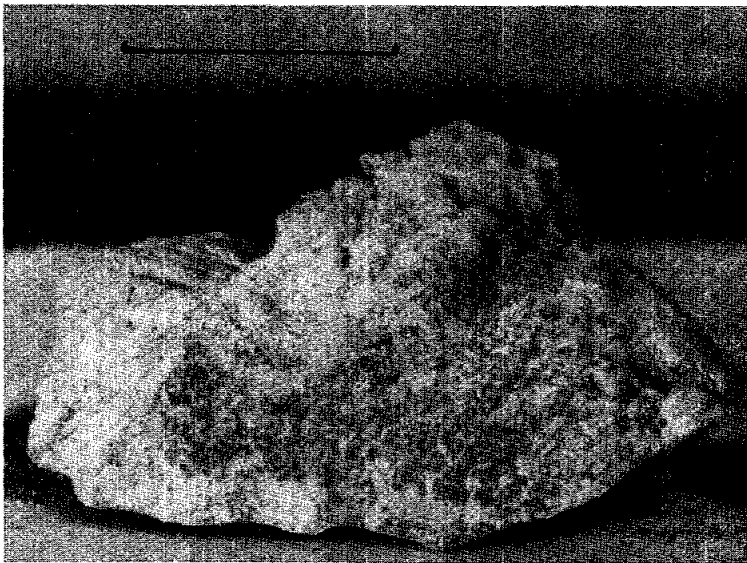


Figure 1: Sample 73145. Scale bar 1 centimeter. Part of S-73-21776.

73146**Cataclastic Troctolitic Anorthosite
St. 2A (LRV-4), 3.0 g****INTRODUCTION**

73146 was picked from soil sample 73140, taken from the bottom of a 15cm-deep trench on the landslide or avalanche from the South Massif, 600 m NE of Nansen Crater. It is a troctolitic anorthosite that is probably chemically igneous although cataclasized and partly recrystallized.

The sample is subangular and blocky (Fig. 1), and very light gray (N8). It is tough and homogenous. It was described in LSIC 17 (1973) as an anorthosite, consisting of about half plagioclase clasts (up to 2 mm) and half white matrix (less than 100 microns), with only about 2% pale green mafic minerals. However the chips eventually taken show a higher percentage of green material in the form of bands; these are olivine-rich bands.

PETROGRAPHY

73146 consists mainly of plagioclase, with schlieren of olivine-rich material (Fig. 2a,b). The plagioclase consists of

fragments up to 2 mm across but with a seriate size range. Individual olivine fragments are rarely as large as 100 microns. The appearance is generally that of a cataclastic rock, but the tough sample has been partly recrystallized, and in some areas bonded by a melt. The plagioclase fragments contain numerous chains of uncertain nature (Fig. 2c), although at least some of them include opaque phases; the interstitial melt has crystallized plagioclases without such chains, but with tiny mafic grains that give the spotted appearance in Fig. 2c. Most of the olivine fragments are clear, but varied inclusions occur in some. One vermicular chromite growth occurs in one olivine in thin section ,3.

Warren and Wasson (1979) and Wasson et al. (1979) gave a mode of 85% plagioclase, 15% olivine, and a trace of low-Ca pyroxene, roughly consistent with their chemical norm for two tiny sections. They noted problems with the mode in that the olivines are concentrated in one corner (however, they imply that the

LSIC (1973), estimate of 2% mafic phases is an underestimate; without further knowledge of the essential sampling strategy such an implication is unsubstantiated). Microprobe analyses by Warren and Wasson of the silicate phases are shown in Fig. 3; the magnesian nature of the olivines (F₀₈₅₋₈₇) show that the sample is not a member of the ferroan anorthosite suite, whatever its plagioclase abundance. The small range in compositions of the silicate phases consistent with the sample being an igneous troctolite, cataclasized and perhaps modally unrepresentative.

CHEMISTRY

A chemical analysis of a small chip (104 mg) is given in Table 1. The incompatible elements are low and extremely fractionated relative to KREEP (Fig. 4). The Ir concentration of less than 3×10^{-4} times C1 chondrites leave little doubt that the sample is pristine igneous (Warren and Wasson, 1979). However, the Ni abundance is high for such a feldspathic igneous fragment, suggesting that the olivines may contain unusually high Ni (several hundred parts per million) among lunar magnesian suite rocks.

PROCESSING

In 1978 one end of the sample was chipped. The piece so derived was further chipped to produce 4 small pieces and some finer material. Two adjacent of these pieces were designated ,1 and ,2; both contained about half of green-rich bands. ,1 (0.11 g) was used for chemistry and to make a small thin section, while ,2 (0.10 g) was used to make two small thin sections. The other pieces remain with ,0 (total 2.7 g).

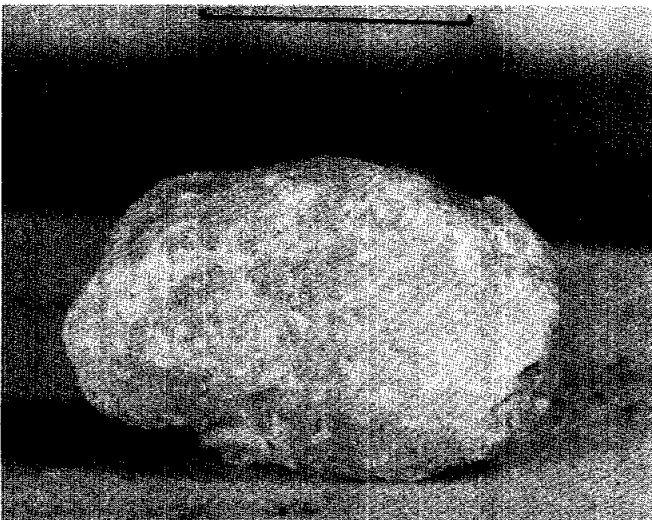


Figure 1: Sample 73146. Scale bar 1 centimeter. Part of S-73-21776.

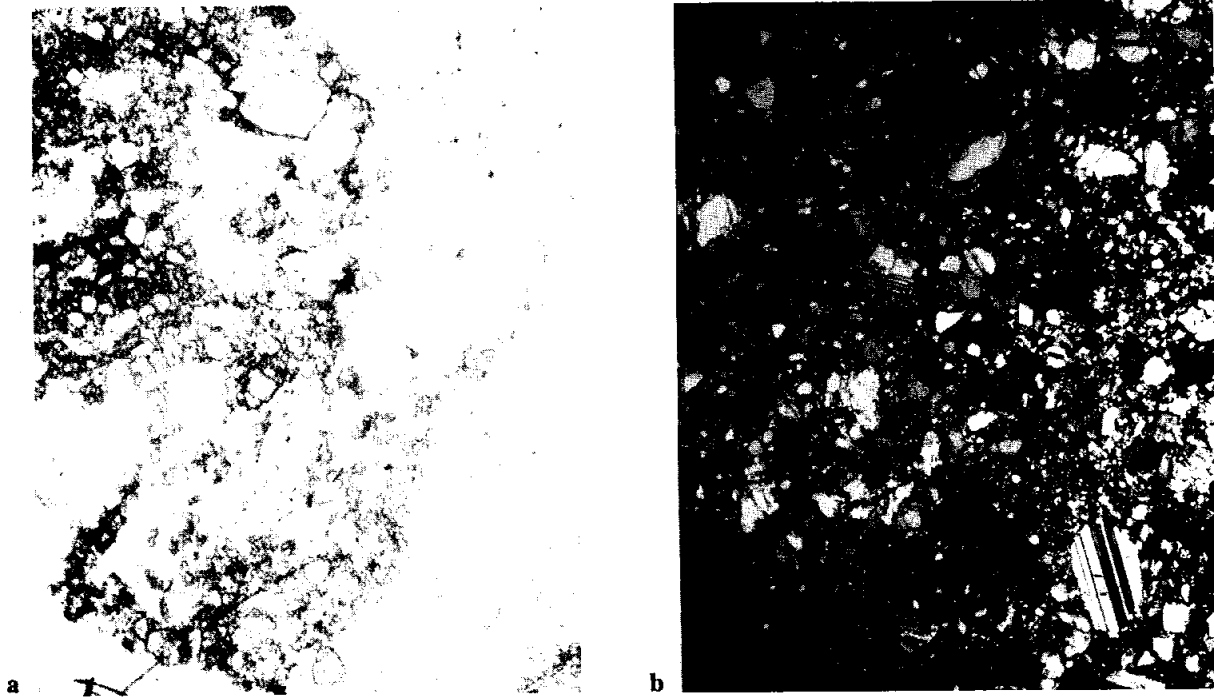


Figure 2: Photomicrographs of 73146,3. a)b) general view, width of field 2 mm, showing streaks of olivine-rich material and overall feldspathic nature. a) plane light b) crossed polarizers. c) feldspathic area showing relics with numerous chains and tiny mafics in the main fine groundmass that appears to be a mixture of melt and small plagioclase clasts. Width of field about 400 microns, plane transmitted light.



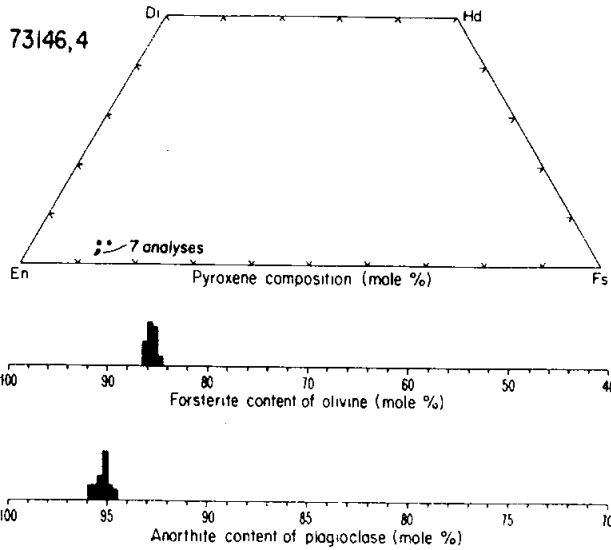


Figure 3: Microprobe analyses of silicate minerals in 73146,4; from Warren and Wasson (1979).

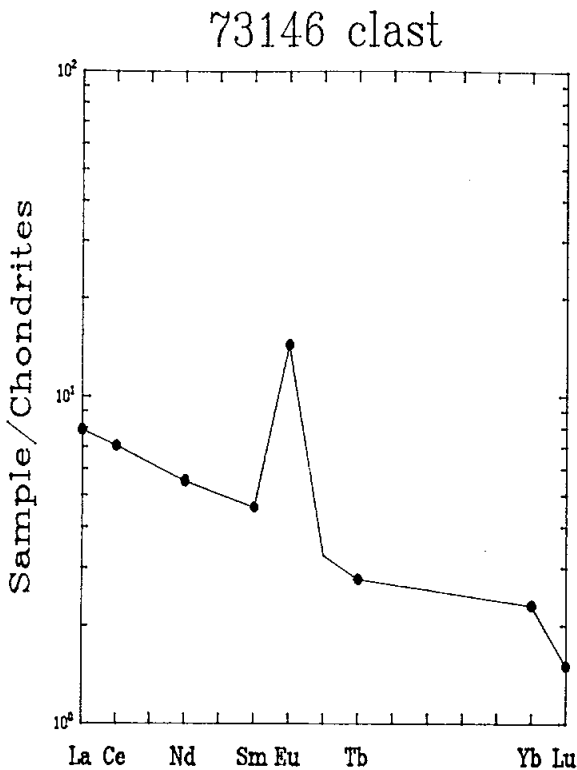


Figure 4: Plot of rare earth elements in 73146,1 (Data from Warren and Wasson, 1979; Warren et al., 1979).

Table 1: Chemical analysis of bulk rock 73146.

Split	.1
wt %	
SiO ₂	43.0
TiO ₂	
Al ₂ O ₃	30.1
Cr ₂ O ₃	0.04
FeO	2.3
MnO	0.022
MgO	7.7
CaO	16.2
Na ₂ O	0.34
K ₂ O	0.058
P ₂ O ₅	
ppm	
Sc	1.01
V	
Co	8.7
Ni	100
Rb	
Sr	190
Y	
Zr	
Nb	
Hf	0.27
Ba	58
Th	0.17
U	
Cs	
Ta	
Pb	
La	2.6
Ce	6.2
Pr	
Nd	3.3
Sm	0.83
Eu	0.99
Gd	
Tb	0.13
Dy	
Ho	
Er	
Tm	
Yb	0.46
Lu	0.051
Li	
Be	
B	
C	
N	
S	
F	
Cl	
Br	
Cu	
Zn	9.4
ppb	
Au	0.690
Ir	0.130
I	
At	
Ga	3.2
Ge	39
As	
Se	
Mo	
Tc	
Ru	
Rh	
Pd	
Ag	
Cd	13
In	16
Sn	
Sb	
Te	
W	
Re	
Os	
Pt	
Hg	
Tl	
Bi	

(1)

References and methods:
 (1) Warren and Wasson (1979), Warren et al. (1979),
 Warren and Kallemeyn (1984); INAA, RNAA, MFB.

73155

Impact Melt Breccia St. 2A (LRV-4), 79.3 g

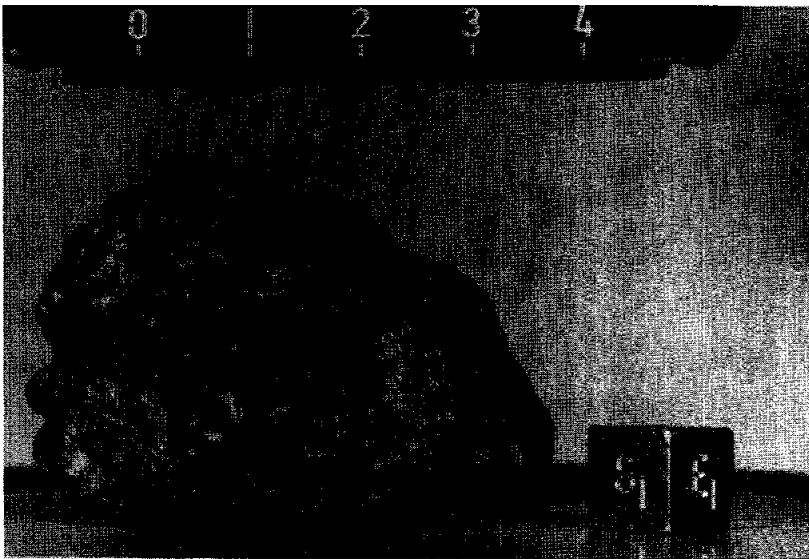
INTRODUCTION

73155 was scooped up on the landslide or avalanche from the South Massif, 600 m NE of Nansen Crater. It lay on the surface, only slightly impressed into the regolith. The sample is rather heterogeneous, with a medium dark gray (N4) color. It consists of about 85% fine-

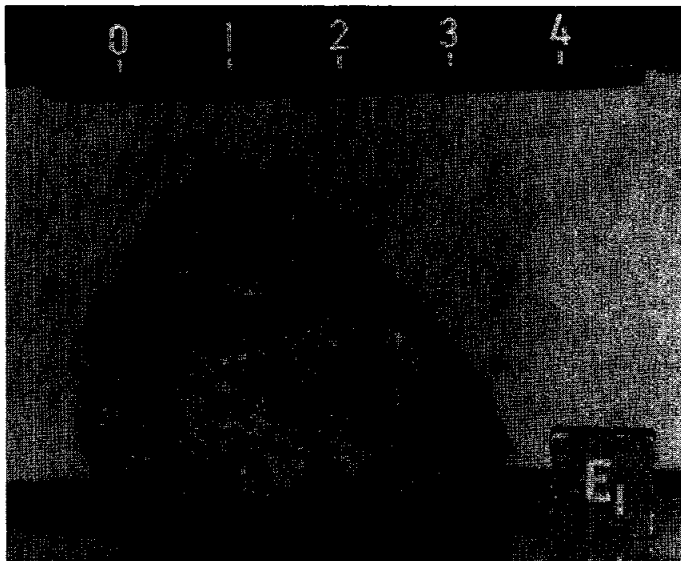
grained matrix that appears to correspond with fine-grained impact melt in the thin sections, and the remainder mainly lithic clasts. Unpublished analyses show that the melt matrix has a typical Apollo 17 low-K Fra Mauro composition, similar to those poikilitic melt rocks commonly inferred to be the Serenitatis melt.

A prominent clast-type is a crushed igneous gabbro, and coarse granoblastic impactite is also common.

73155 is blocky and subrounded (Fig. 1), and tough; it has a few penetrative fractures. It was described as metaclastic in LSIC 17 (1973). It has many zap pits on several sides and a few on all of the others. It has less than 1% cavities, mostly as irregular slits, with some vugs up to 2 mm across. The clast abundances are difficult to estimate because of the zapping of all the surfaces and indistinct borders of many clasts. One prominent zap pit was targeted for sampling. The matrix was described in LSIC 17 (1973) as very fine-grained, with a salt-and-pepper texture. One large clast (12 x 7 mm) was fine-grained yellowish-gray and equigranular. The lithic clasts appear to be dominantly fine-grained with a variety of colors (mainly varieties of gray) and shapes. Mineral clasts larger than 0.5 mm compose only 2 or 3% of the rock.



a



b

Figure 1: Sample 73155, pre-splitting. Scale bars 1 centimeter. a) S-73-23887B b) S-73-23888B.

PETROGRAPHY

The thin sections, made from one chip, indicate that the fine-grained groundmass of 73155 is a clast-rich impact melt (Fig. 2a). The melt fraction has a rather equigranular and regular grain-size (less than 20 microns). It consists of plagioclase, mafic minerals, Ti-oxides, metal, and other minor phases. The melt penetrates and separates some of the larger clasts. The clast population is varied. In the thin sections the dominant clast is an unusual lithology that consists of schlieren made of plagioclase and pyroxene in subequal amounts; clinopyroxene is more common than pigeonite (Ryder 1992b). The clinopyroxene is distinctly riddled with inclusions of sulfide and

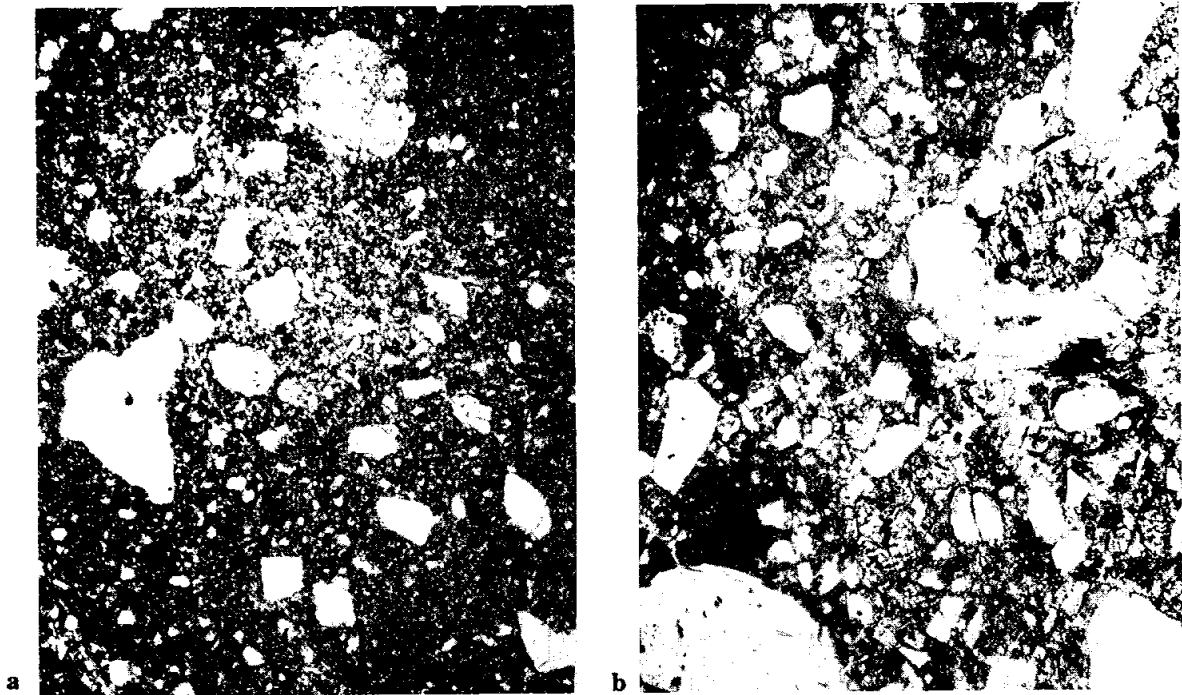
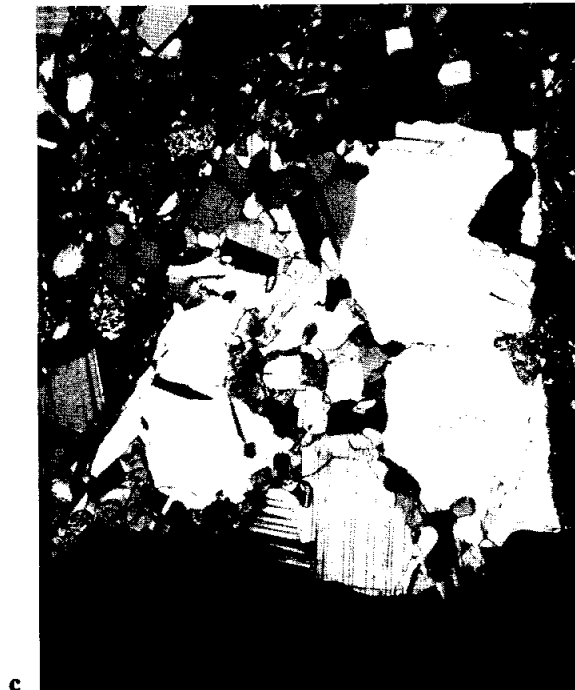


Figure 2: Photomicrographs of 73155, all widths of field about 2 mm. a) general melt groundmass of 73155,30, showing very fine and homogeneous groundmass and small mineral and lithic clasts; plane transmitted light. b) plagioclase-pyroxene-glass schlieren (gabbro) (right) adjacent to melt matrix (left) in 73155,29. The clast is spread out into wide cataclased zones or schlieren that may not be perfectly monomict. The phase with dark inclusions is augite; plane transmitted light. c) clast of granoblastic impactite in 73155,30, presumptively that referred to by Bickel and Warner (1978c) and Steele et al.(1980) and Steele and Smith (1980).



silicic glass with potash feldspar. The pigeonite contains exsolved lamellae of clinopyroxene. The pyroxenes are fairly evolved and zoned (Fig. 3) with some reaction at their edges. The plagioclase includes sodic compositions (An82) as well as anorthite. Other phases present include ilmenite and silica, and both colorless and brown glass (Fig. 2b). The schlieren is partly mixed with matrix and possibly with granoblastic impactite.

The only other published references to 73155 are to granoblastic impactite; such material does occur in the thin section, and either is part of the lithology with the fayalitic olivine(?) or is intimately mixed with it in the sections. Such granoblastic impactite in thin section 73155,30 was referred to by Bickel and Warner (1978c) (without description) and by Steele and Smith (1980) and Steele et al. (1980). The latter analyzed trace elements in plagioclase with the ion probe; the revised data (in Steele et al., 1980) lists plagioclase with 13 ppm Li, 6.8 mol % Na, 330 ppm Mg, 965 ppm K, 260 ppm Ti, 250 ppm Sr, and 125 ppm Ba. These abundances are generally quite distinct from those of plagioclases in ferroan anorthosites, and similar to those in some other feldspathic impactites. The clast analyzed is presumptively that shown in Fig. 2c.

CHEMISTRY

Major and trace element analyses, as yet unpublished (Ryder), show that the melt groundmass has a composition similar to that of the generally accepted Serenitatis melt sheet such as represented by the Station 6 boulders. Analysis of a small chip of the igneous gabbro shows that it is an evolved gabbro with high K_2O (0.87 wt%) but with low abundances of other incompatible elements. The rare earth elements have a fairly flat chondrite-normalized pattern (about 25x chondrites) with a small positive Eu anomaly.

PROCESSING

Processing in 1974 was targeted first to sample a prominent zap pit. Chipping created two pieces, but was stopped because one of the visible fractures started to widen drastically. Chip ,2 (0.30 g) was stored. Chip ,1 (0.67 g) had the zap pit, which was made into potted butts ,26 and ,27. They have apparently not been studied. The remainder was made into 4 serial thin sections, ,28 to ,31, leaving a large potted butt (0.61 g). Some further processing in 1992 produced small chips for chemical and petrographic studies.

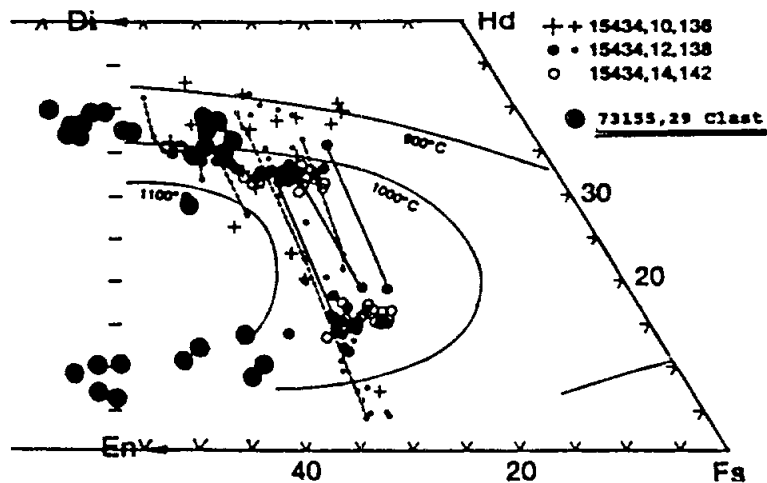


Figure 3: Compositions of pyroxenes in gabbro schlieren in 73155,29, with pyroxenes from evolved Apollo 15 rocks for comparison. (Ryder, 1992b).

73156

Impact Melt Breccia or Granoblastic Impactite

St. 2A (LRV-4), 3.2 g

INTRODUCTION

73156 was scooped up with 73155 on the landslide or avalanche from the South Massif, 600 m NE of Nansen Crater. However, it does not look like 73155 and was probably not a part of it. The tough sample is wedge-shaped and angular (Fig. 1), with dimensions of 1.5 x 1 x 1 cm. It is light gray and

homogeneous, with a very fine grain size (99% less than 0.2 mm). Most appears to be granoblastic plagioclase and a mafic silicate(?). There are a few zap pits on all surfaces, with white, pale green, and dark glass linings. There are a few cavities at one end with projecting crystals of plagioclase, and the sample has a few penetrative fractures. Apart from it

being a fine-grained, clast-poor crystalline lithology, its identification remains in doubt. It has never been allocated or subdivided.

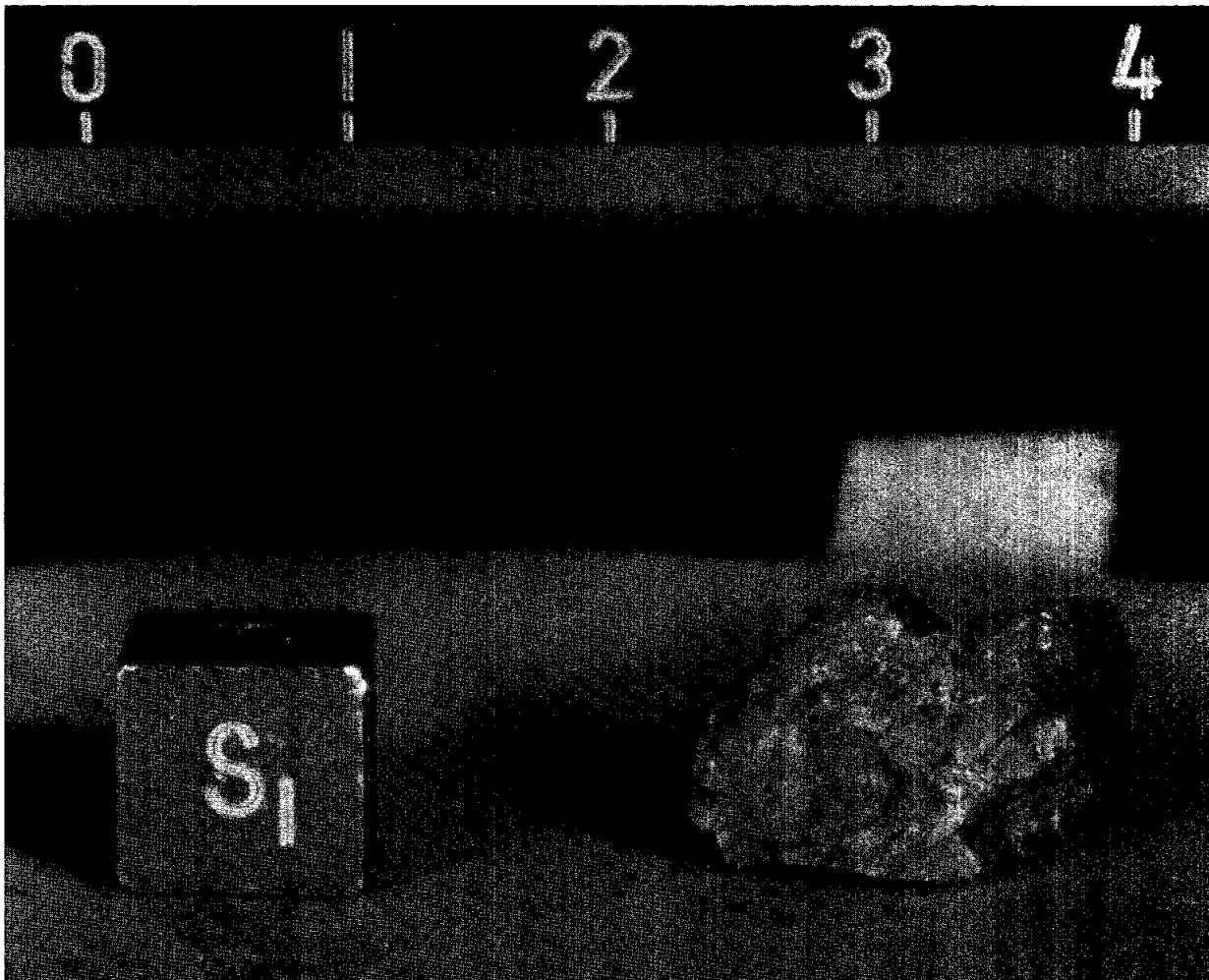


Figure 1: Sample 73156. Scale bar 1 centimeter. Part of S-73-17878.

73215

Aphanitic Impact Melt Breccia

St. 3, 1062 g

INTRODUCTION

73215 is a polymict breccia consisting largely of dark aphanitic impact melt and entrained clasts. It is characterized by structure indicating flow and shear during and after consolidation. Its composition is similar to other local aphanitic melt breccias in being a little higher in Al_2O_3 and a little lower in TiO_2 than the common low-K Fra Mauro basalt composition. Its melt appears to have crystallized close to 3.87 Ga ago, and the rock was exposed to radiation about 240 Ma ago.

73215 was collected from the landslide on the rim of the 10 m crater at Station 3. It is irregular in shape (Fig. 1), about 12 x 11 x 8.5 cm, and is blocky and tough. It has a few penetrative fractures. The rock is heterogeneous, with a light part that is pale yellow gray (5Y 8/1) and a dark part that is medium gray (N5). Flow gives the appearance of the light part, which occurs as lenses from 3 cm long down to minute veinlets, invading the dark part. The light part appears to be about 30% on the exterior, but the sawn interiors show rather less light material (Fig. 2). Most of the dark appears as

closely packed aphanitic clasts embedded in a matrix of similar appearance, with subtle color variations. One surface is irregularly knobby, most of the others irregular, and one is a broken surface. There are many zap pits on two sides, fewer on the others, and none on the broken surface. No cavities are apparent. 73215 has been extensively studied in a consortium led by O. James. The sample was sawn to produce a slab in 1973, and most allocations were made from slab pieces. A second slab parallel to the first was cut in 1989 and subdivided for further studies (Fig. 3).

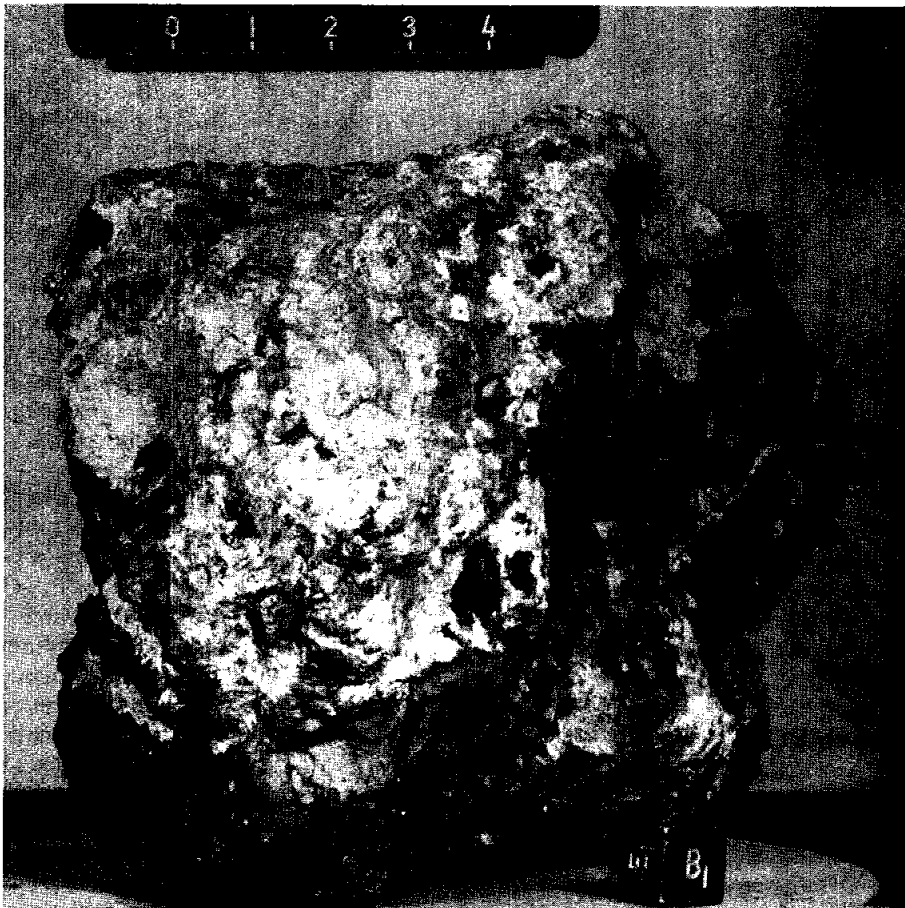


Figure 1: Pre-processing view of 73215, showing heterogeneous mix of light and dark banding. Cube and scale divisions are 1 cm. S-73-24270.

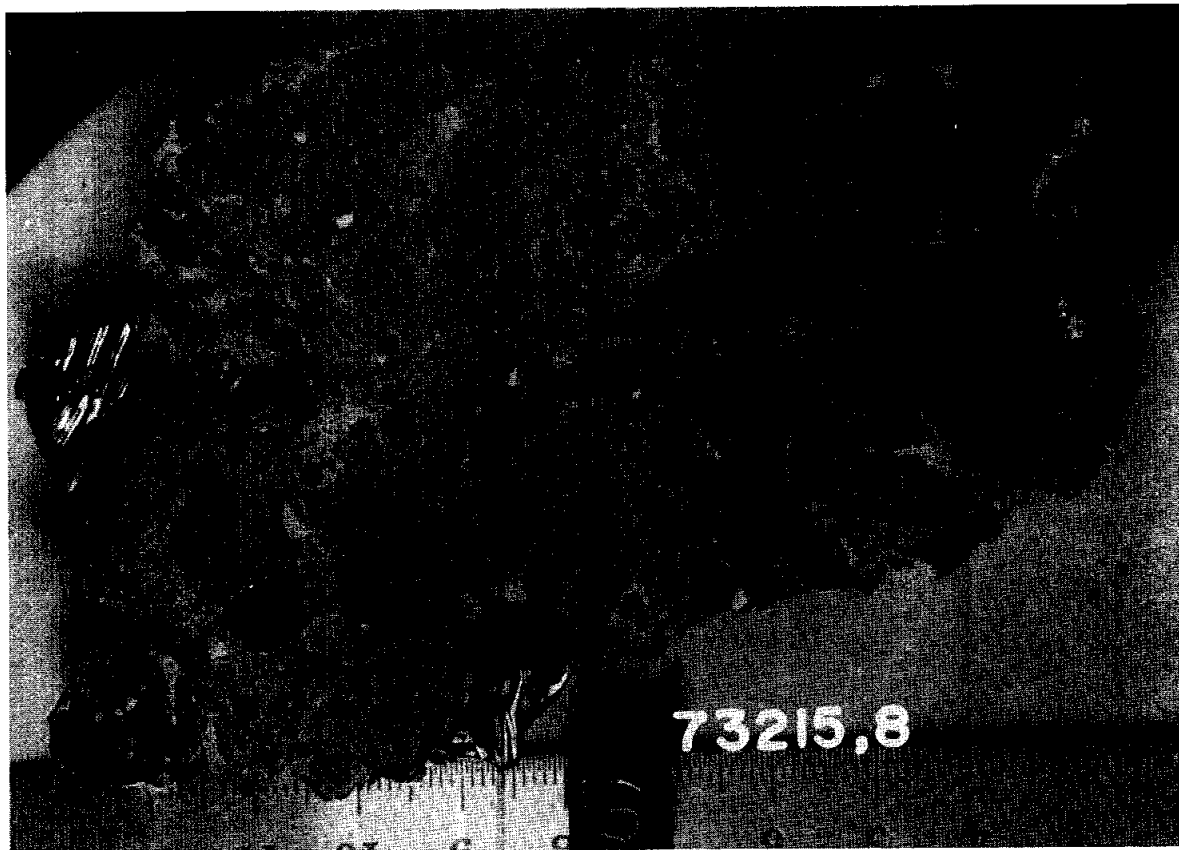


Figure 2: Sawn surface of end piece ,8, showing predominance of dark material and the apparent flow structures. Cube and scale divisions are 1 cm. S-76-26038.

PETROGRAPHY

The hand specimen is characterized by prominent structures, particularly flow banding, formed by differential flow or shear or both during and after aggregation and consolidation (James et al. 1975a,b). The bands are composed of several different kinds of gray to black aphanitic rock and different kinds of granulated clastic materials (Fig. 4). Locally, fault-like structures displace the banding. All types of aphanitic matrix consist of abundant small lithic and mineral fragments set in a dark groundmass (Fig. 5). The clasts are dominated by feldspathic impactites (granulites) and other feldspathic lithologies. Felsites are minor, and clasts with basaltic textures are rare.

Simonds et al. (1974) listed 73215 as granular, with matrix feldspars

and mafic minerals from 1 to 10 microns, and with about 50-60% feldspar. They found it to be one of the finest-grained of the micropoikilitic-subophitic-granular group, with the poorest development of tabular feldspar. They also noted the concentration of mineral clasts into vein-like segregations. Knoll and Stoffler (1976) classified 73215 as a dark, fine-grained, equigranular crystalline matrix breccia that partly contained areas of light-colored, coarser matrix, similar to 72215 and 72255. Dence et al. (1976) and Dence and Grieve (1976) described 73215 as genetically comparable with suevites, with the rock consisting of pods of dark breccia in a light porous clastic matrix. They noted the fine grain size of the dark material (1-2 microns in the finest areas) and the varied color. Shocked rounded plagioclases are conspicuous in it, and the clast

population consists of highland rock types. However, there is not so much strongly shocked material as in terrestrial suevites. 73215 seems to be more thoroughly mixed than suevites, perhaps because of lower viscosity. They interpret the dark matrix to be shock melted material, with unshocked material from the upper 25 km of the crust and shocked materials from deeper levels; they infer that the melt is of Serenitatis origin.

By far the greater amount of work on 73215 has been done under the auspices of the James consortium (e.g. James et al., 1975a,b; James and Blanchard, 1976). Consortium members also prefer a Serenitatis melt origin for the sample. James et al. (1976a,b) identified a distinct groundmass that binds the fragments together. James (1976) clearly distinguished "matrix" as a binocular-microscope designation for aphanitic bulk masses distinct

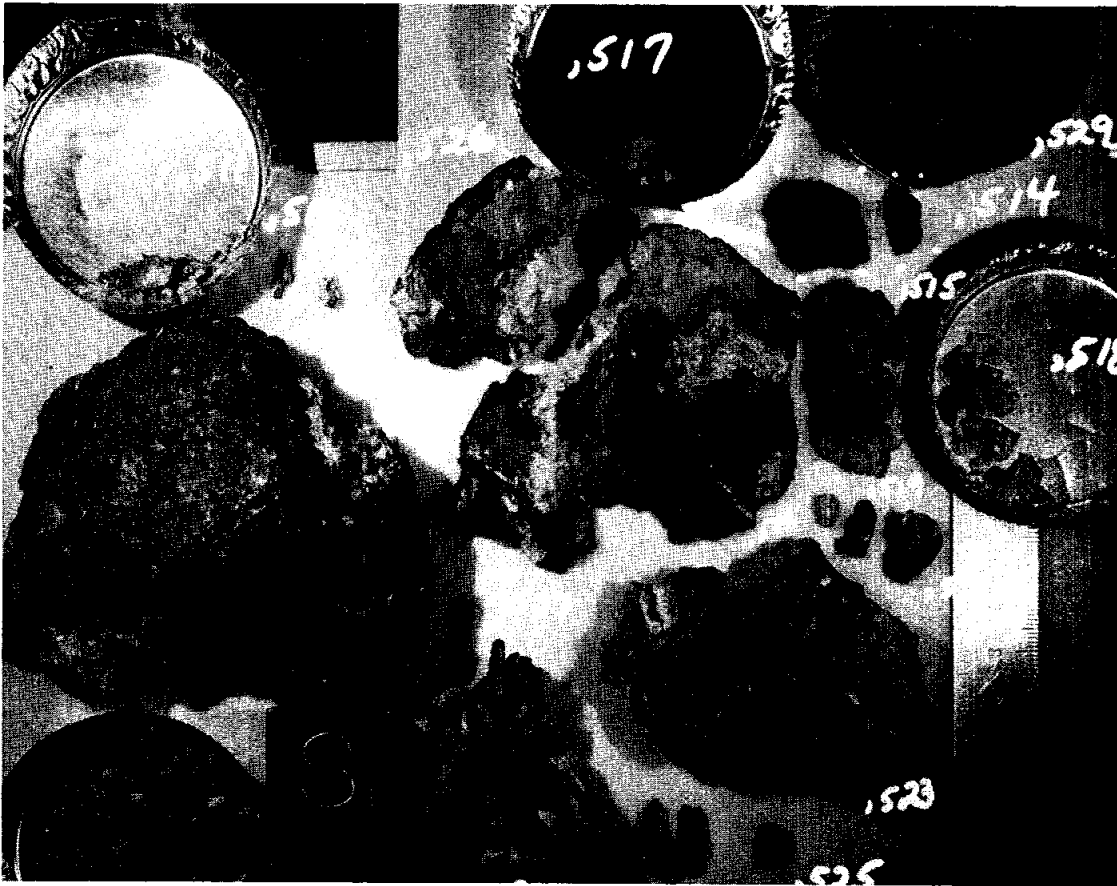
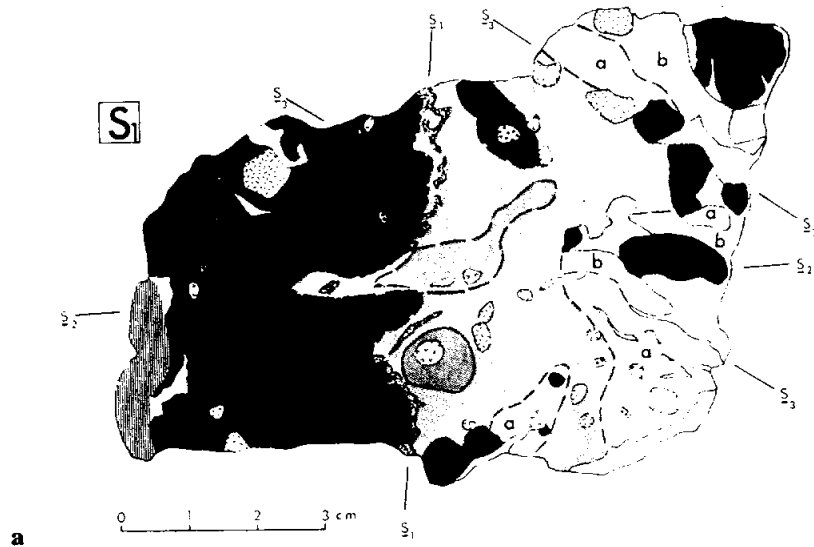


Figure 3: End piece ,9 and new pieces sawn from it. Cube is 2.5 cm. S-89-46188.

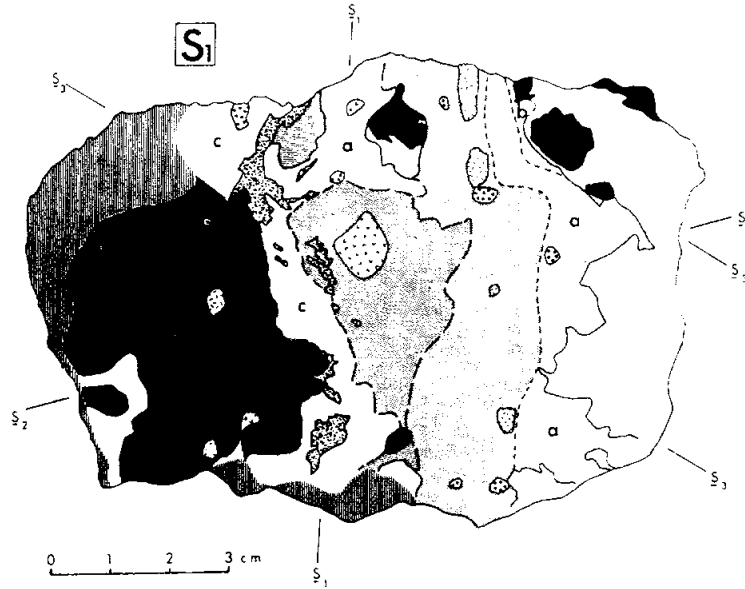
from separable clasts from "groundmass" as the fine-grained intergrowth that encloses even small clasts (Fig. 5b); that distinction will be followed here (this acceptance of the dark melt as matrix and the porous feldspathic materials as clasts is distinct from that of Dence et al., 1976, and Dence and Grieve, 1976, but is the status referred to by most workers). The dominant constituents of the groundmass are plagioclase and mafic minerals, with minor amounts of opaque oxides, and some Fe-metal and troilite. Generally felsic or silicic mesostasis is not apparent. The groundmass textures range from microintergranular to microsubophitic, and average grain size is from about 1 to 8 microns. The different aphanite types (color, coherency, etc.) relate to differences in groundmass grain-size and porosity, with the darkest aphanites being the least porous.

James et al. (1976a,b) identified the enclosed fragments as dominated by plagioclases, with the lithic fragments mainly being coarse and fine granular feldspathic impactites. Many of these exist as monomict schlieren. The clasts have had diverse shock histories, with many showing no visible shock-induced microstructures. They have also had diverse thermal histories, with some, particularly felsites, being melted but most showing little if any thermal effects from breccia formation. Few reaction rims are visible, except for very unstable minerals such as silica and spinel; although overgrowth rims are present on some mafic clasts. In many matrix samples, elongate fragments show weak to strong parallel preferred orientations. Intensely sheared areas seen on sawed surfaces have higher porosity; shear and groundmass crystallization appear to have been contemporaneous.

James (1976b,c), James et al. (1976) and Nord and James (1977) made a detailed study of the aphanitic matrix lithologies, which form the bulk of the rock. The rock formed as a mechanically mixed aggregate of crystalline clasts and silicate melt. The electron petrographic study of Nord and James (1977) confirms the melt origin of the groundmass, with microsubophitic laths of plagioclase clearly visible. While most of the aphanitic material is a matrix, similar material forms clast-like bodies, most commonly gray spheroids within the matrix, and black clasts within granulated feldspathic materials. The gray spheroids at least are probably equivalent to cogenetic accretionary lapilli. The black aphanites form both angular particles and rinds and they are the darkest and toughest aphanites. James (1976) described several different types of aphanite



a

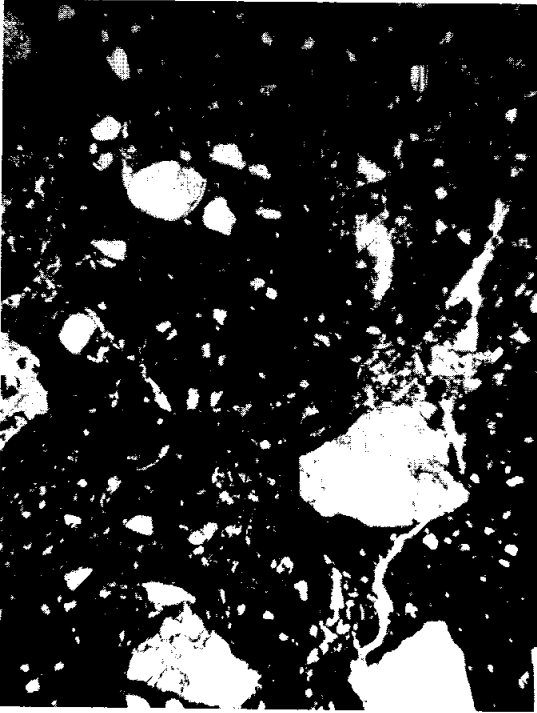


b

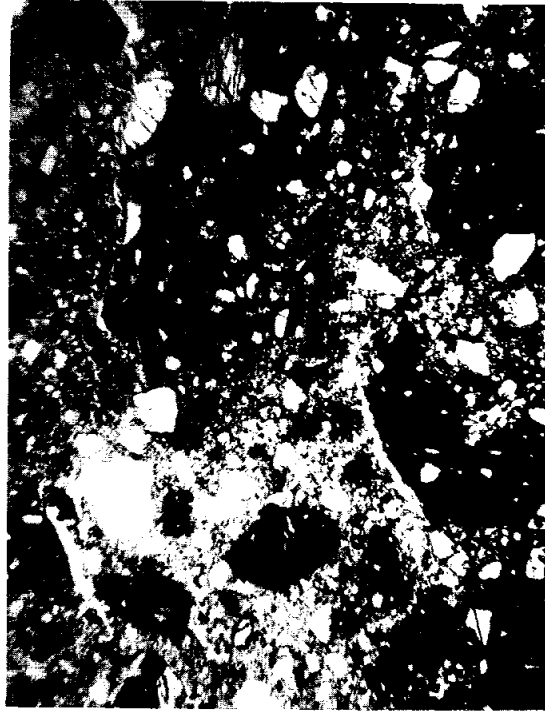
Map Symbol	Characteristics
	Broken or polished surface
Matrix lithologies	
	Black aphanitic matrix: homogeneous black aphanitic; faintly mottled appearance, cut by sparse minute light-colored shear traces; tends to be richer in felsic clasts than other types of matrix
	Heterogeneous black aphanitic: cut by abundant minute light-colored streaks; occurs as discontinuous bands bordering homogeneous black aphanitic matrix
	Mixed black aphanitic matrix: small clasts and patches of black aphanitic matrix in network of light-colored, intensely sheared material that may contain appreciable amounts of other types of matrix or granulated clasts
	Transitional gray aphanitic matrix: medium to dark gray aphanitic, with abundant schlieren, lenses, and patches of sheared feldspathic clasts; occurs in patches and discontinuous bands
	Gray aphanitic matrix: homogeneous gray aphanitic; homogeneous on millimeter scale, but on very fine scale is cut by abundant minute closely-spaced shear traces
	Light gray matrix: homogeneous light gray matrix; fine mineral clasts set in a matrix of finer grained mineral powder; softer and more friable than other types of matrix
	Light gray matrix rich in small clasts of black aphanite; separates areas of homogeneous light gray matrix from areas of granulated feldspathic clast materials
	Light gray matrix rich in troctolitic clasts

Class Lithologies	
Granulated:	
	Anorthositic and troctolitic anorthositic: aggregates of white to colorless to gray plagioclase fragments, with subordinate fragments of pale green olivine; fragments range in size from fine-grained irresolvable powder up to 0.5 mm; traces of relict textures indicate pre-granulation grain sizes up to 4 mm; locally contains concentrations of small clasts of black aphanite; relatively friable
	Olivine-rich troctolite: aggregates of pale green olivine fragments (about 75%) and colorless plagioclase fragments (about 25%) and trace red spinel fragments
	Black aphanite: darker than black aphanitic matrix; contains common small milky white clasts and schlieren and is locally cut by thin varieties of granulated feldspathic clast materials; is locally vesicular; is enclosed by granulated feldspathic clast materials
Competent:	
	Anorthositic, noritic, and troctolitic "hornfels": very fine grain size and sugary, cherty, or chalky appearance; some are inequigranular with scattered coarse plagioclase xenocrysts
	Troctolite: equigranular olivine plus plagioclase; grain size up to 3 mm; some of coarser-grained rocks are knobby (milky feldspar and cloudy olivine); some of finer-grained rocks contain accessory red spinel
	Plagioclase and olivine single crystals: olivine is clear, pale green, up to 2 mm size; plagioclase ranges from clear to cherty gray to milky white, up to 4 mm size, some have dark colored rinds
	Brown-pyroxene basalt and labbro and felsite: brown pyroxene or brown felsic glass are 50% or greater, plagioclase and olivine are subordinate, accessory black opaque

Figure 4: Maps of the lithologies in sawed faces of 73215, as mapped by James (James et al., 1976a). a) is face of butt end, 8 (as in Fig. 2). b) is one of the slab faces, parallel to but about 1.5 cm removed from a). James et al. (1975a).



a



b

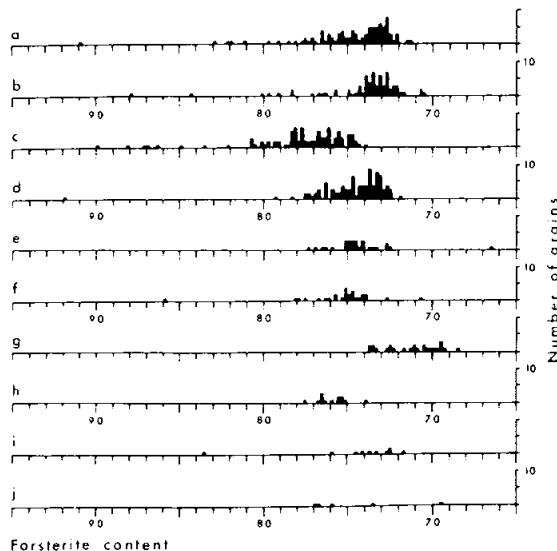
Figure 5: Photomicrographs of 73215,119. All plane transmitted light. a) general aphanitic matrix, with rounded and angular clasts, mainly plagioclases and feldspathic impactites. Field of view about 2 mm wide. b) mixed zone of aphanitic clasts and schlieren of porous feldspathic cataclasite with angular mineral fragments. Field of view about 2 mm. c) melt groundmass of the aphanite, showing distinction of fine-grained uniform melt from even small clasts. Field of view about 500 microns.



c

Table 1: Proportions of groundmass and clasts larger than 5 microns in various types of aphanite (vol %). (James, 1976).

	Area counted (mm ²)	Clasts > 5 μm			Groundmass
		Mafic minerals	Plagioclase	Lithic	
Gray aphanitic matrix (73215,245)	0.19	8.2	23.7	0	68.1
Black aphanitic matrix (73215,243)	0.21	5.1	20.5	3.3	71.1
Schlieren-rich gray aphanitic matrix (73215,103)	0.14	10.9	23.4	0	65.7
Gray aphanite spheroid .38,57 (73215,350)	0.35	13.8	22.2	3.2	60.8
Black aphanite clast .46,10 (73215,349)	0.35	7.9	23.4	0.1	68.8



Olivine compositions in 73215 aphanites. Sizes of the areas surveyed are: (a) 228 matrix—1.9 mm²; (b) 106 matrix—5 mm²; (c) 228 clast-poor aphanite—0.41 mm²; (d) 106 clast-poor aphanite—0.56 mm²; (e) 46,10 black clast—1.3 mm²; and (f) 38,57 gray spheroid—0.8 mm². (a) Clasts > 25 μm in schlieren-rich gray matrix (1,106). (b) Clasts > 25 μm in black matrix (2,228). (c) Clasts > 15 μm in gray spheroid (38,57 (3,350)). (d) Clasts > 15 μm in black clast (46,10 (3,349)). (e) Clasts > 10 μm in clast-poor aphanite in 1,106. (f) Clasts > 15 μm in clast-poor aphanite in 2,228. (g) Groundmass grains and 5–25 μm clasts in gray matrix (2,228), black matrix (2,243) and schlieren-rich gray matrix (1,103, 1,106). (h) 5–25 μm clasts in gray spheroid (38,57 (3,350)). (i) 5–25 μm clasts in black clast (46,10 (3,349)). (j) Grains with euhedral outlines.

Figure 6: Compositions of olivines in 73215 aphanites. James (1976b)

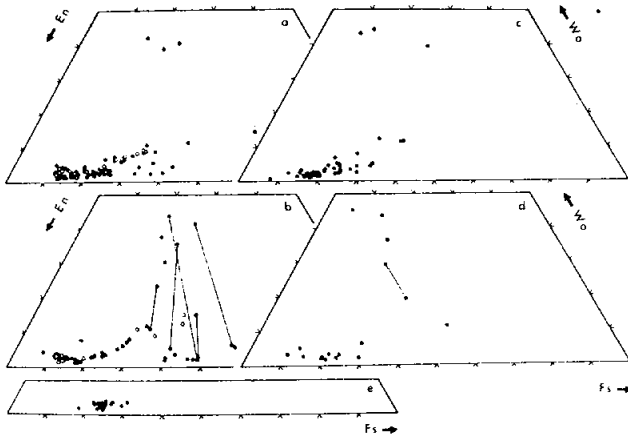
(differing in color, grain-size, and mode of occurrence) providing modal data (Table 1) and mineral chemistry for both clasts and groundmass phases (Figs. 6–10). The aphanites contain from 60 to 70% groundmass melt, with the darkest aphanites having the most groundmass (Table 1).

In the groundmass the dominant minerals are plagioclase (An₉₀₋₉₁) and low-Ca pyroxene (En₇₄Wo₃), with minor olivine (Fo₆₈₋₇₄) (Figs. 6–9). The clasts were derived from a more homogeneous source than those in regolith breccias and most were cool and unshocked. Larger olivine clasts tend to be more

magnesian than groundmass olivines. Pyroxene clasts too are more magnesian than groundmass pyroxenes. Most metal grains fall in the field appropriate for meteoritic metal. Most competent clasts were not deformed during or after breccia aggregation, although some devitrified maskelynites have outlines suggestive of plastic flow. Clasts of felsite show textures indicating plastic flow during incorporation. Other than felsites, few clasts show evidence of internal partial melting. A few clasts have overgrowth rims, and some mineral clasts much different from the groundmass have reacted or partly re-equilibrated, as described in detail in James (1976b).

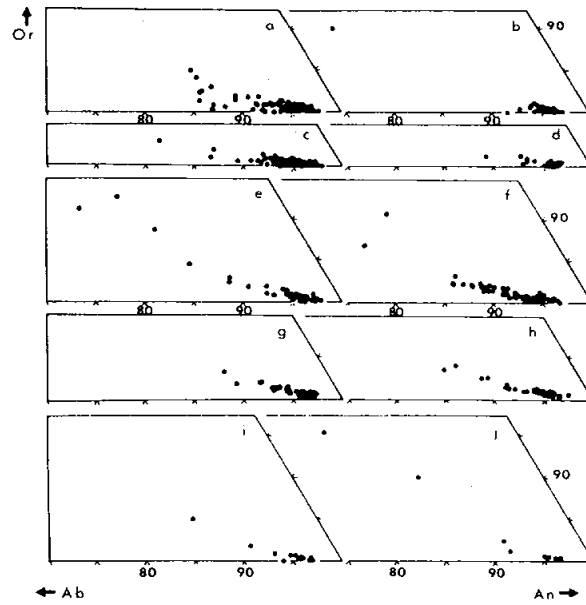
James (1976a,b) infers that the matrix aphanites were about 50% melt when it formed and the melt was fluid and superheated. During mixing with cold clasts in a debris cloud, the melt cooled and crystallized rapidly, producing lithologic banding as it flowed.

The most common clast-type is feldspathic impactite or granulite, commonly referred to as "anorthositic gabbro". Examples have been briefly described in the general consortium references; the most detailed descriptions are in James (1977a), James and



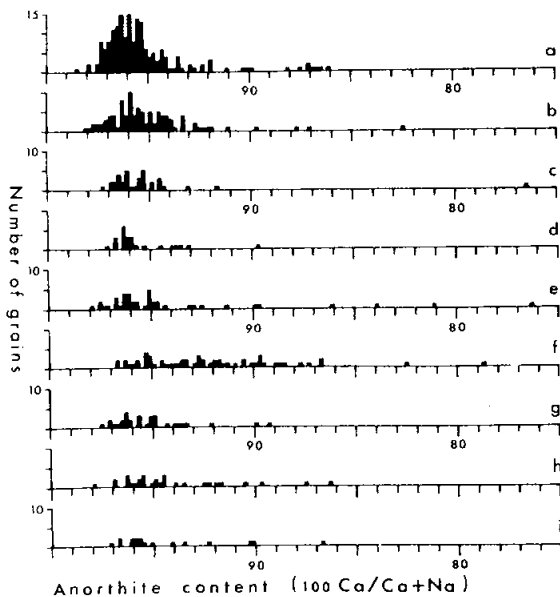
Wollastonite:enstatite:ferrosilite contents of pyroxenes in 73215 aphanites. Tie lines connect the compositions of pyroxenes co-existing in the same fragment, either as a patchy intergrowth of two phases or as host and exsolved lamellae. (a) Clasts in schlieren-rich gray matrix (.106). Filled circles are clasts $>25 \mu\text{m}$ in matrix; open circles are clasts $>10 \mu\text{m}$ in clast-poor aphanite. (b) Clasts in gray matrix (.228). Filled circles are clasts $>25 \mu\text{m}$ in matrix; open circles are clasts $>15 \mu\text{m}$ in clast-poor aphanite. (c) Clasts $>15 \mu\text{m}$ in gray spheroid .38.57 (.350). (d) Clasts $>15 \mu\text{m}$ in black clast .46.10 (.349). (e) Groundmass grains and 5-25 μm clasts in gray matrix (.228, .245), black matrix (.243), schlieren-rich gray matrix (.103), and gray spheroid .38.57 (.350).

Figure 7: Compositions of pyroxenes in 73215 aphanites. James (1976b).



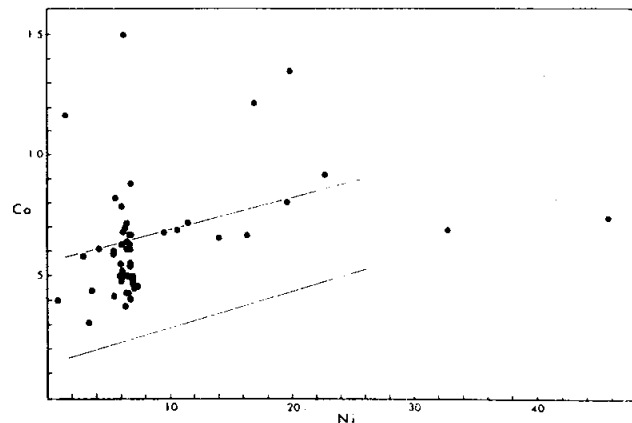
Orthoclase:albite:anorthite contents of feldspars in 73215 aphanites. (a) Clasts $>25 \mu\text{m}$ in schlieren-rich gray matrix (.106). (b) Clasts $>10 \mu\text{m}$ in clast-poor aphanite (.106). (c) Clasts $>25 \mu\text{m}$ in gray matrix (.228). (d) Clasts $>20 \mu\text{m}$ in clast-poor aphanite (.228). (e) 5-25 μm clasts and groundmass grains in gray matrix (.245) and schlieren-rich gray matrix (.103, .106). (f) 5-25 μm clasts in black matrix (.243). (g) 5-25 μm clasts in black clast .46.10 (.349). (h) 5-25 μm clasts in gray spheroid .38.57 (.350). (i) Euhedral clasts in matrix aphanites. (j) Euhedral grains in zones surrounding clasts of felsic glass.

Figure 8: Compositions of plagioclases in 73215 aphanites. James (1976b).



Plagioclase compositions in 73215 aphanites. (a) Clasts $>25 \mu\text{m}$ in schlieren-rich gray matrix (.106). (b) Clasts $>25 \mu\text{m}$ in gray matrix (.228). (c) Clasts $>10 \mu\text{m}$ in clast-poor aphanite in .106. (d) Clasts $>20 \mu\text{m}$ in clast-poor aphanite in .228. (e) Groundmass grains and 5-25 μm clasts in gray matrix (.245) and schlieren-rich gray matrix (.103, .106). (f) 5-25 μm clasts in black matrix (.243). (g) 5-25 μm clasts in black clast .46.10 (.349). (h) 5-25 μm clasts in gray spheroid .38.57 (.350). (i) Euhedral clasts.

Figure 9: Compositions of plagioclases in 73215 aphanites. James (1976b).

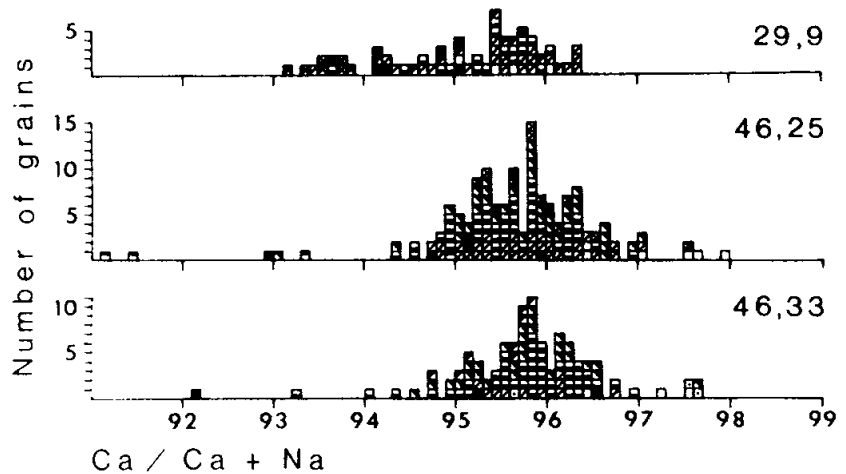


Compositions of metal particles in schlieren-rich gray matrix (.106). Particles analyzed were $>10 \mu\text{m}$ across and were isolated within matrix; none were within clasts or had attached silicate mineral grains. The band passing through the diagram marks the range of compositions of meteoritic metal.

Figure 10: Compositions of metals in 73215 gray matrix. James (1976b).

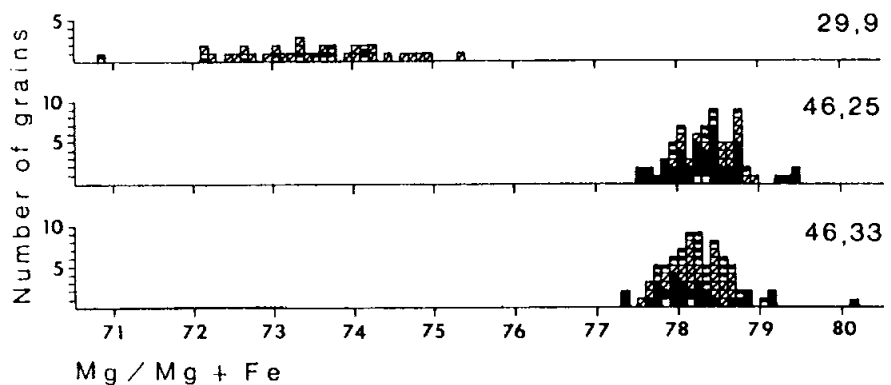
Hammarstrom (1977), and James and Hedenquist (1978). The three clasts described in detail by James and Hammarstrom (1977) and James (1977a) were also analyzed by other members of the consortium. The clasts are modally anorthositic norites; one (29,9) is coarse poikilitic, the other two (45,25 and 45,33) are finer-grained and have mosaic as well as poikilitic textures. All are fairly well equilibrated, as shown by the microprobe analyses (Figs. 11-14), and are similar except that the coarser-grained sample has a lower mg' (Figs. 12,13). The cores of the large plagioclases, which are commonly surrounded by olivine "necklaces" are probably relics of pre-existing rocks. The impactites also contain trace constituents including K-feldspar, K-Si-rich glass, apatite, whitlockite, ilmenite, chromite, Ni-Fe metal, and baddeleyite. The metal compositions fall squarely in fields appropriate for meteorite contaminated rocks (Fig. 14). James and Hammarstrom interpret the texture and mineral chemical variations as being the products of crystallization from melts and solid-state crystallization. 29,9 is inferred to be mainly from melt, 45,25 mainly from solid-state crystallization, and 45,33 from melt (poikilitic) and solid-state (mosaic). Thus an origin as heated, partly-melted and/or recrystallized polymict breccias appears most likely. All three samples show healed fractures that post-date the recrystallization events.

James and Hedenquist (1978) described a 5 mm clast of spinel-bearing troctolitic basalt that consists of patches of basaltic-textured rock enclosed by very fine-grained granoblastic material (also analyzed by other members of the consortium). The boundaries between the two textures vary from sharp to gradational. The granoblastic material, a mosaic of anhedral grains, has grain sizes from 5 to 270 microns. The basaltic material has plagioclase laths 75-100 microns long with subhedral



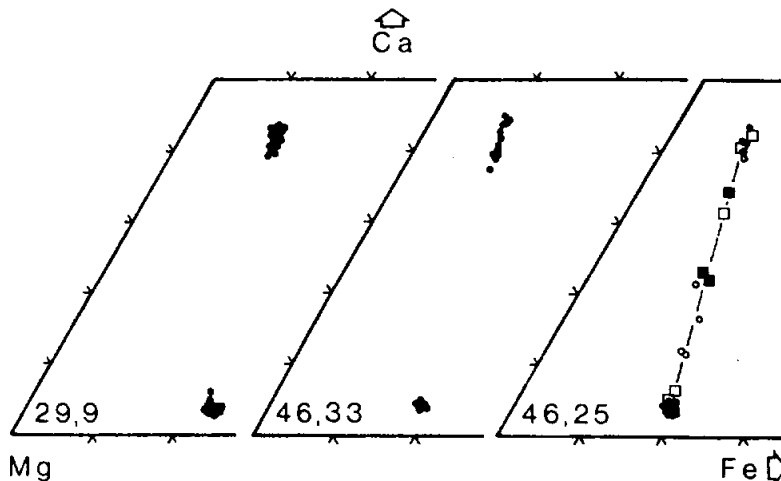
Histograms of $\text{Ca}/\text{Ca} + \text{Na}$ contents in plagioclase in anorthositic gabbros. Textures and occurrences of the individual grains analyzed are indicated by the following symbols in the boxes on the diagrams: filled, cores containing K-feldspar inclusions; empty, inclusion-free cores and cores containing bubbles; small dot, cores containing glass inclusions; diagonal lines, rims on large grains; filled lower half, grains in oikocrysts; filled upper right corner, grains in mosaics; filled upper half, small euhedral grains in oikocrysts; filled upper left corner, globules included in olivine (29,9) or deformed, recovered plagioclase in mosaics (46,33); crosses, grains in lathy aggregate (46,25) or grain margins (29,9).

Figure 11: Compositions of plagioclases in feldspathic impactites in 73215. James and Hammarstrom (1977).



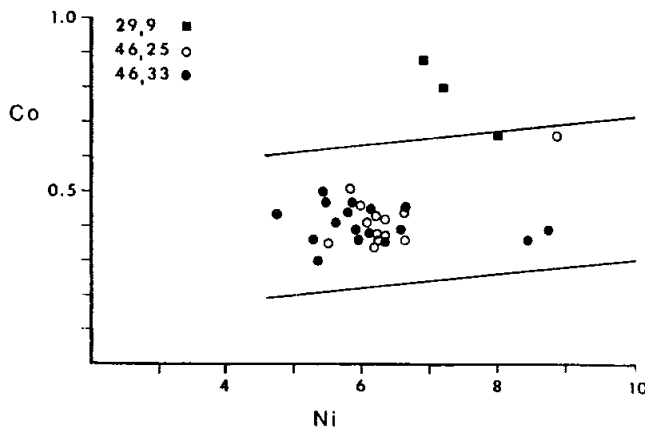
Histograms of $\text{Mg}/\text{Mg} + \text{Fe}$ contents in olivines in anorthositic gabbros. Textures and occurrences of the individual grains analyzed are indicated by the following symbols in the boxes on the diagrams: filled, grains in mosaics; empty, centers of large grains; diagonal lines, globules forming "necklaces" in plagioclase grains; filled upper half, grains in oikocrysts; filled lower half, grain margins.

Figure 12: Compositions of olivines in feldspathic impactites in 73215. James and Hammarstrom (1977).



Ca:Mg:Fe of pyroxenes in anorthositic gabbros. Filled circles, grains forming oikocrysts. Open circles, analyses attempted of exsolution lamellae. Squares indicate analyses of pyroxene globules included in plagioclase grains in 46,25; open squares are individual phases in these globules; filled squares are expanded-beam analyses of the bulk globules.

Figure 13: Compositions of pyroxenes in feldspathic impactites in 73215. James and Hammarstrom (1977).



Ni-Co contents (wt.%) in metal grains in anorthositic gabbros. The area within the lines is the range of compositions of "meteoritic" metal (Goldstein and Yakowitz, 1971).

Figure 14: Compositions of metal grains in feldspathic impactites in 73215. James and Hammarstrom (1977).

olivine and pyroxene (50-200 microns) and pink spinel (20-50 microns). Both domains have the same mineral compositions (Fog7-82, Eng4Wo4, En50Wo44) except for plagioclase (basaltic An95-84; granoblastic An99-90). The troctolitic melt must have cooled quickly (otherwise the spinel would have been absorbed) and then

partial granulation occurred. Subsequently the granulated areas were recrystallized. Several other clasts are like it.

Nord and James (1977) made electron petrographic investigations of 200 micron clast of "hornfelsic norite". The clast had a grain size of 5 to 50 microns. The texture

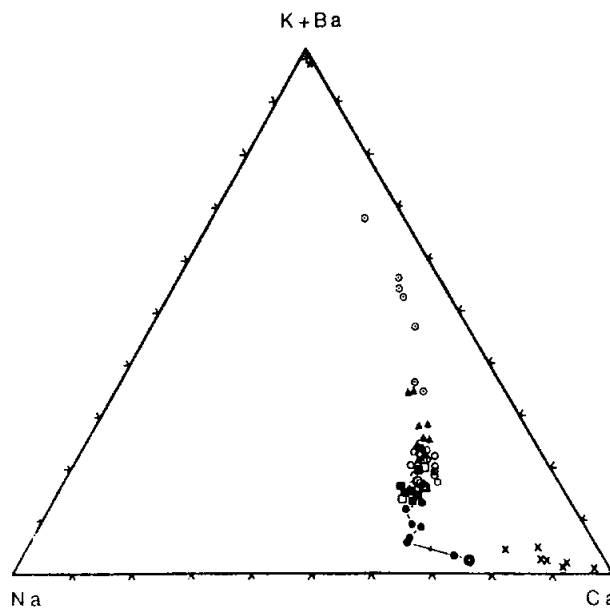
indicates that the clast was deformed and recrystallized prior to incorporation in the breccia. The transmission electron microscopy shows that recrystallization was extensive, producing straight contacts and triple junctions among small plagioclase grains. Antiphase domain boundaries are type (b) and probably formed by subsolidus recrystallization rather than from a phase transition during cooling. The orthopyroxenes have a moderate density of dislocations and a high density of linear defects (lamellae). The lamellae are clinopyroxene that are clinohypersthene, probably promoted by shock-induced shear. Hewins and Goldstein (1975a,b) analyzed metal in four clasts of "anorthositic hornfels" in 73215, fine-grained granoblastic materials. The metals are at the lower end of the meteoritic field. Two other clasts were analyzed: a devitrified shocked plagioclase has metal with high Co (2.2%) but low Ni (1%), and a light matrix breccia (presumably a porous feldspathic shlieren) has metal with low Ni (1-2%) but at the low end of the meteoritic field.

Neal et al. (1990d) reported preliminary data on a spinel troctolite assemblage in a clast in 73215, with olivine (Fo89-92), plagioclase (An91-96) and Mg-Al spinel with 8-11 wt % Cr₂O₃. Individual grains are unzoned. Eckert et al. (1991a,b,c) reported further on this clast, which appears to be a statically recrystallized cumulate rock. The mode is about 78% plagioclase, 21% olivine, 2% spinel, with minor high-Ca and low-Ca pyroxene, FeNi metal, and chromite (Eckert et al. 1991a). The pyroxene may not be in equilibrium with the rest of the assemblage. The olivines have very low CaO abundances, indicative of slow cooling. The mineral assemblage appears to have originated at relatively high pressure, deeper than about 25 km. Eckert et al. (1991b) also reported a cataclased dunite clast, with spinel and a glass mesostasis cored by an SiO₂

phase. The main silicates have ranges in composition: olivine Fo72-92, plagioclase An90-97.

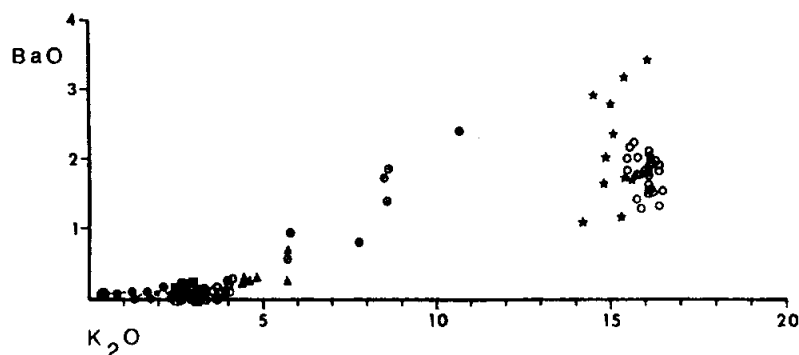
Hansen et al. (1979b) and Smith et al. (1980) reported some precise minor element data (microprobe) for olivines and low-Ca pyroxenes in a feldspathic impactite and an Mg-rich plutonic troctolitic rock. The reports are not very specific about the parent lithologies. The Mg-rich plutonic has olivine with Fo90-91 and plagioclase with An96, while the feldspathic impactite is more iron-rich (Fo76). Steele et al. (1980) reported ion probe data for plagioclase in the Mg-rich troctolite.

James and Hammarstrom (1976) and Nord and James (1977) gave a detailed description of a felsite clast that was also studied by other members of the consortium. The felsite comprises two components: crystalline felsite and veins of silicic glass. James and Hammarstrom (1976) detail the textures and the mineral and glass chemistry (Figs. 15-17; Table 2), and their genetic inferences therefrom. The crystalline felsite consists mainly of a vermicular intergrowth of quartz (40%) and K-feldspar (60%); minor plagioclase forms blebs associated with the quartz. Trace amounts of ilmenite, zircon, olivine, apatite, and whitlockite are present, and some mosaic patches include pyroxene. Some of the feldspars have an unusual ternary composition (Fig. 15); the electron petrographic studies show this ternary feldspar to be a homogeneous phase, with some probable initial attempts at phase separation apparent (Nord and James, 1977). The minerals do not show shock effects; dislocation density in the quartz is very low, and that in the K-feldspar not much higher. The felsic glass is varied in vesicularity, color, and relict mineral content; second generation minerals quenched from the glass are present. Most of the glass is brown, with abundant needle-like crystallites. Electron petrographic study shows that the bulk of this



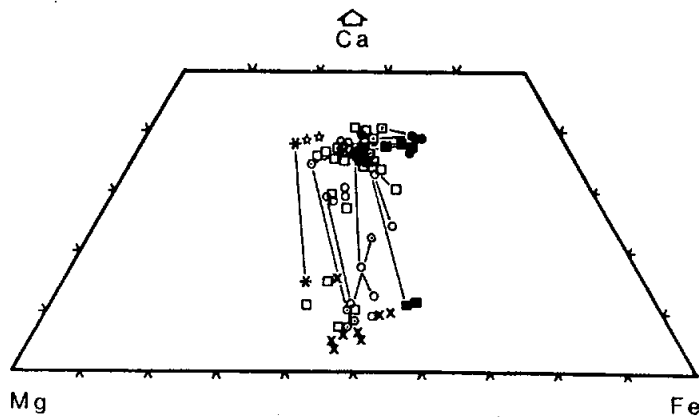
K + Ba:Na:Ca contents of feldspars in felsite clast. Large circle, average of 14 analyses in core of zoned plagioclase grain (Fig. 1d); small filled circles, traverse from inner to outer boundary of rim of zoned plagioclase grain (3 μ m steps, arrow indicates direction of traverse). Filled squares, points in equant 0.2 mm plagioclase grain. Open squares, plagioclase grains in mosaics. Small open circles, plagioclase grains in vermicular intergrowth. Filled triangles, centers of plagioclase relics in felsic glass. Small dotted circles, reacted and second-generation inclusion-rich plagioclase in felsic glass. Asterisk, average of 26 analyses of K-feldspar in vermicular intergrowth. Filled star, average of 11 analyses of second-generation K-feldspar in felsic glass. \times , small plagioclase grains in mixed material at edge of clast.

Figure 15: Compositions of feldspars in the felsite clast in 73215. James and Hammarstrom, 1977.



K₂O vs. BaO contents in feldspars in felsite clast. Symbols are as in Fig. 2, except: open circles indicate all analyses of plagioclase and K-feldspar in vermicular intergrowth; filled stars indicate all analyses of second-generation K-feldspar in felsic glass; plagioclase in mixed material is not shown.

Figure 16: Compositions of feldspars in the felsite clast in 73215. James and Hammarstrom, 1977.



Ca:Mg:Fe contents of pyroxenes in felsite clast. Filled circles, centers of pyroxene grains in crystalline felsite. Filled squares, centers of pyroxene relics in felsic glass. Open symbols are second-generation pyroxenes, as follows: dotted squares, edges of grains in crystalline felsite or edges of relics in felsic glass; circles, rims on olivine relics; squares, prismatic crystals; dotted circles, large blocky grains with associated Fe metal and troilite; stars, rims on ilmenite relics; asterisks, rim on olivine relic at edge of clast. ×, grains in mixed material at edge of clast. Tie lines connect compositions of points in the same grains.

Figure 17: Compositions of pyroxenes in the felsite clast in 73215. James and Hammarstrom, 1977.

material is uncrystallized (Nord and James, 1977). All the glasses are Si- and K-rich. The crystalline felsite clearly crystallized from a melt to produce a texture similar to terrestrial granophyres. The felsic glass forms veins and patches and was emplaced as dikelets, not by *in situ* melting. The fracturing and diking preceded incorporation of the clast into the breccia. Nonetheless, the parent of the glass, presumably shock produced, must have been from the same felsite body. The bulk clast was quite hot when it was incorporated in the breccia, because some of the glass it contains *did* form at that time by *in situ* melting. It was then rapidly cooled, precipitating second generation pyroxene and K-feldspar.

Miura (1988) reported the presence of "anomalous" plagioclases (i.e., deficient in Al, Na) in 73215 as is present in some lunar basalts. However, the plagioclases are not otherwise described. Bickel and Warner (1978a) listed 73215,234 in their study of plutonic and granulitic lunar samples, but did not

otherwise provide any data on such sample from 73215.

CHEMISTRY

Many chemical analyses have been made of bulk rock, aphanite samples, and clasts or schlieren. Both bulk rock/matrix and aphanite analyses are compiled in Table 3, with the rare earth elements plotted in Figure 18. Microprobe defocused beam analyses of the groundmass are reproduced as Table 4 and Figure 19. Clast analyses are compiled in Table 5, with the rare earth elements plotted in Figures 20 and 21. A guide to how some of the split numbers correspond with lithologies is shown in Figure 22 and Table 6 (from James and Blanchard, 1976). (The text of Bence et al. (1975) erroneously refers to 72315 where 73215 is intended.) Ehmman et al. (1975a,b) reported an O analysis of 47.2% for ,172 aphanite. James et al. (1975a) reported that no CH₄ or CD₄ in excess of 0.06 ug/g were found in interior or exterior samples.

The matrix and bulk sample analyses are dominated by the aphanitic phase. In general both black and gray aphanites have the same composition; however, at least some of the black materials appear to be higher in volatile and incompatible elements. Individual differences are probably a result of variation in included clasts (e.g. James et al., 1975a,b). All matrix and aphanite samples are aluminous, low-K Fra Mauro basalt compositions, distinguished from the typical Apollo 17 impact melt by the lower TiO₂ and higher Al₂O₃ of the 73215 materials. The incompatible elements show a range from about 70x chondrites to about 120 x chondrites, part or all of which is probably a reflection of varied clast contents (e.g., Blanchard et al., 1976) as well as the small sample sizes; similar considerations probably apply to variations in Co and Ni as well. The Zn is much lower than that found in typical soils or regolith breccia, lending weight to the argument that 73215 was not created from regolith, but from a larger event (James et al., 1975a). The meteoritic siderophiles in the aphanites fall into Group 2 of Morgan et al.(1976), attributed to Serenitatis, and distinct from the Boulder 1, Station 2 aphanites. Although one analyzed (38,57) appeared to be a group 6 (Morgan et al., 1976) a second analysis appeared quite normal; the reason for the first analysis being different remains a mystery (Morgan and Petrie, 1979a,b).

James (1976) made defocused beam microprobe analyses of the varied aphanites (with subtraction of clast compositions) to attempt to obtain the composition of the melt groundmass (Table 4). The groundmass composition is similar to that of the bulk aphanites and is fairly homogeneous.

**Table 2: Compositions of minor phases and glasses in felsite (wt%; electron microprobe analyses).
(James and Hammarstrom, 1977).**

	(1)	(2)	(3)	(4)	(5)	(6)	(7)	(8)	(9)
SiO ₂	0.22	0.28	—	—	74.2	78.2	76.7	76.8	78.1
TiO ₂	50.7	1.79	—	—	0.73	0.36	0.65	0.28	0.49
Al ₂ O ₃	0.13	22.2	—	—	13.4	12.9	13.1	13.4	12.6
FeO	45.4	31.8	1.81	0.34	1.24	0.61	0.81	0.38	0.40
MgO	1.15	1.89	2.29	0.07	0.04	0.01	0.04	0.03	0.03
CaO	0.09	0.09	38.7	53.4	0.62	0.64	0.79	0.75	0.77
Na ₂ O	—	—	—	—	0.10	0.14	0.21	0.17	0.30
K ₂ O	—	—	—	—	9.58	6.90	7.20	7.88	7.21
BaO	—	—	—	—	0.26	0.06	0.04	0.11	0.10
MnO	0.47	0.51	—	—	0.02	0.02	0.02	0.01	<0.01
Cr ₂ O ₃	0.38	38.1	—	—	0.03	0.01	0.02	0.01	0.02
Y ₂ O ₃	—	—	4.48	0.37	—	—	—	—	—
La ₂ O ₃	—	—	1.07	0.13	—	—	—	—	—
Ce ₂ O ₃	—	—	3.01	0.23	—	—	—	—	—
Nd ₂ O ₃	—	—	1.63	0.19	—	—	—	—	—
Sm ₂ O ₃	—	—	0.59	0.06	—	—	—	—	—
Gd ₂ O ₃	—	—	1.37	0.20	—	—	—	—	—
P ₂ O ₅	—	—	40.5	40.4	0.21	0.04	0.26	0.09	0.20
ZrO ₂	—	—	—	—	0.11	0.13	0.22	0.04	0.07
F	—	—	0.43	2.88	—	—	—	—	—
Cl	—	—	0.29	0.89	—	—	—	—	—
Total	98.54	96.66	96.17	99.16	100.54	100.02	100.06	99.95	100.29

(1) Ilmenite: average of 12 analyses of grains in felsic glass and crystalline felsite.

(2) Aluminous chromite: inclusion in ilmenite grain in crystalline felsite (low total due to small size of grain).

(3) Whitlockite: average of three analyses of grains in crystalline felsite (low total due to destruction of grains during analysis).

(4) Apatite: average of eight analyses of grains in felsic glass and crystalline felsite.

(5) Brown glass: average of 20 analyses.

(6) Uncrystallized colorless glass in felsic glass veins and patches: average of ten analyses.

(7) Uncrystallized colorless glass haloes around second-generation and relict mafic mineral grains: average of 12 analyses.

(8) Uncrystallized colorless glass selvages in vermicular intergrowth in crystalline felsite: average of five analyses.

(9) Uncrystallized colorless glass bands at contact of crystalline felsite and matrix: average of five analyses.

Table 3: Chemical analyses of bulk rock/matrix and aphanites in 73215.

Split wt%	.161	.161	.74	.184	.177	.186	.76	.170 .9006	.? bleckmx
SiO ₂	48.1		46.1	46.8	46.1	46.7			
TiO ₂	0.8		1.1	0.4	1.1	0.6			
Al ₂ O ₃	19.4		21.7	21.5	19.9	20.4			
Cr ₂ O ₃	0.168		0.200	0.230	0.221	0.46			
FeO	7.64		7.39	7.20	7.28				
MnO	0.123		0.104	0.099	0.119				
MgO	10.2		10.2	11.8	11.1	11.0			
CaO	11.0		12.2	11.8	12.3	11.5			
Na ₂ O	0.624		0.495	0.488	0.487				
K ₂ O	0.656		0.167	0.170	0.191	0.31			
P ₂ O ₅									
ppm									
Sc	14.3		14.4	13.5	14.1	23.7			
V									
Co	24.5		25.6	27.8	21.2	27.1			
Ni	200	152	150	190	150		163	118	
Rb	5.5	8.93			3.0	13.6	2.3	2.34	
Sr									
Y									
Zr									
Nb									
Hf	13.7		9.5	8.9	7.8	13.9			
Ba									
Th	7.5		3.7	4.2	3.6				4.332
U		2.2					1.2	1.1	1.207
Ca	0.18	0.56			0.123	0.57	0.164	0.107	
Ta	2.3		1.5	1.4	1.4				
Pb									2.556
La	41		25.5	25.6	24.3	36.1			
Ce	105		69	68	63	86			
Pr									
Nd	62				37.3	55			
Sm	18.6		11.9	12.2	10.7	16.8			
Eu	1.63		1.41	1.37	1.35	1.55			
Gd	20.6				13.0	15.0			
Tb	3.55		2.8	2.7	2.11	3.3			
Dy	23.5				14.6	20.0			
Ho									
Er									
Tm									
Yb	13.0		8.8	9.1	8.5	12.1			
Lu	1.91		1.2	1.35	1.1	1.84			
Li									
Be									
B									
C									
N									
S									
P									
Cl									
Br		0.106					0.026	0.0092	
Cu									
Zn	<5	2.5			2.5	2.0	1.9		
ppb									
Au		2.4					2.7	1.65	
Ir		4.3					4.9	3.49	
I									
At									
Ga	4160				5300	5300			
Ge		252					175	82	
As									
Se		72					72	39	
Mo									
Tc									
Ru									
Rh									
Pd									
Ag		0.73					0.91	20	
Cd		12.4					18.4	1.3	
In									
Sn									
Sb		1.2					0.95	0.89	
Te		4.9					5.9		
W									
Re		0.34					0.37	0.274	
Os									
Pt									
Hg									
Tl		5.0					4.3	2.8	
Bi		0.28					0.52	0.75	
	(1)	(1,8,10)	(1)	(1)	(1)	(1)	(1,8,10)	(1,8,10)	(1)(a)

References and methods:
 (1) James et al. (1975a); INAA, RNAA, AAS. (a) isotope dilution/mass spec.
 (8) Higuchi and Morgan (1975a,b); RNAA
 (10) Morgan et al. (1976); RNAA

Table 3 continued: Chemical analyses of bulk rock/matrix and aphanites in 73215.

Split wt%	.146 + .147	.139	.156	.273	Split wt%
SiO ₂					SiO ₂
TiO ₂					TiO ₂
Al ₂ O ₃					Al ₂ O ₃
Cr ₂ O ₃					Cr ₂ O ₃
FeO					FeO
MnO					MnO
MgO					MgO
CaO					CaO
Na ₂ O					Na ₂ O
K ₂ O					K ₂ O
P ₂ O ₅					P ₂ O ₅
BBB					BBB
Sc					Sc
V					V
Co					Co
Ni					Ni
Rb					Rb
Sr					Sr
Y					Y
Zr					Zr
Nb					Nb
Hf					Hf
Ba					Ba
Th					Th
U					U
Ca					Ca
Ta					Ta
Pb					Pb
La					La
Ce					Ce
Pr					Pr
Nd					Nd
Sm					Sm
Eu					Eu
Gd					Gd
Tb					Tb
Dy					Dy
Ho					Ho
Er					Er
Tm					Tm
Yb					Yb
Lu					Lu
Li					Li
Be					Be
B					B
C	32	27	24	13	C
N	<1.5	<1.5	<1.5	<1.5	N
S	234	199	183	284	S
P					P
Cl					Cl
Br					Br
Cu					Cu
Zn					Zn
BBB					BBB
As					As
Ir					Ir
I					I
At					At
Ga					Ga
Ge					Ge
As					As
Se					Se
Mo					Mo
Tc					Tc
Ru					Ru
Rh					Rh
Pd					Pd
Ag					Ag
Cd					Cd
In					In
Sn					Sn
Sb					Sb
Te					Te
W					W
Re					Re
Os					Os
Pt					Pt
Hg					Hg
Tl					Tl
Bi					Bi
	(1)	(1)	(1)	(1)	

References and methods: James et al. (1975a); combustion/mass spectrometry

Table 3 continued: Chemical analyses of bulk rock/matrix and aphanites in 73215.

Split wt%	.94	.49	.140	.32	.90	Avg. of 11	.81 black	.136 gray	Split wt%
SiO ₂	47.67	46.47	46.53	46.75	46.34	46.4			SiO ₂
TiO ₂	0.23	0.63	0.65	0.67	0.68	0.7			TiO ₂
Al ₂ O ₃	23.4	22.95	20.66	20.64	20.07	20.6			Al ₂ O ₃
Cr ₂ O ₃		0.118	0.204			0.25			Cr ₂ O ₃
FeO	5.39	6.58	7.73	7.56	7.79	7.3			FeO
MnO						0.104			MnO
MgO	9.16	9.39	11.47	11.16	11.79	11.6			MgO
CaO	12.81	13.25	12.10	12.2	11.79	11.9			CaO
Na ₂ O	0.83	0.49	0.58	0.42	0.80	0.50			Na ₂ O
K ₂ O	0.19	0.23	0.20	0.20	0.31	0.20			K ₂ O
P ₂ O ₅							0.33	0.21	P ₂ O ₅
ppm									ppm
Sc		11	16			14.7			Sc
V		39	52						V
Co		19	24			25.3			Co
Ni		160	200			165			Ni
Rb	1.99	4.73	2.2	1.4	7.7				Rb
Sr									Sr
Y	87	58	93	85	127				Y
Zr	400	208	300	354	665				Zr
Nb	25.6	16.8	23.6	23.5	42				Nb
Hf	9.90	6.1	8.41	8.0	14.5	9.5			Hf
Ba	300	211	315	350	432				Ba
Th	4.81	3.49	4.51	4.20	7.3	4.1			Th
U	1.23	0.87	1.24	1.08	1.76		1	1.9	U
Ce									Ce
Ta						1.4			Ta
Pb	2.79	2.42	2.86	2.17	5.15				Pb
La	26	16.6	25	24.5	37.2	27.0			La
Ce	68	41	71	68	99.6	70			Ce
Pr	9.0	5.9	9.8	8.96	13.3				Pr
Nd	38	22.2	39.9	36.3	55				Nd
Sm	11.0	6.42	11.1	9.55	15.6	12.5			Sm
Eu	1.39	1.25	1.45	1.19	1.59	1.43			Eu
Gd	11.0	8.14	13.9	10.7	18.3				Gd
Tb	2.28	1.45	2.35	1.98	3.24	2.6			Tb
Dy	14.2	8.80	14.5	12.9	21.3				Dy
Ho	3.12	2.12	3.30	2.90	4.61				Ho
Er	9.30	6.20	9.80	8.60	13.9				Er
Tm	1.43	0.91	1.44	1.24	2.05				Tm
Yb	8.67	5.34	8.73	7.51	12.4	9.1			Yb
Lu	1.34	0.86	1.35	1.16	1.93	1.30			Lu
Be									Be
B									B
C									C
N									N
S									S
P								80	P
Cl							6.1(a)	36.1(a)	Cl
Br							53(a)	217(a)	Br
Cu									Cu
Zn									Zn
ppb									ppb
As									As
Ir							2.2		Ir
I									I
At									At
Ga									Ga
Ge									Ge
As									As
Se									Se
Mo									Mo
Tc									Tc
Ru									Ru
Rh									Rh
Pd									Pd
Ag									Ag
Cd									Cd
In									In
Sn									Sn
Sb									Sb
Te									Te
W									W
Re									Re
Os									Os
Pt									Pt
Hg									Hg
Tl									Tl
Bi									Bi

References and methods:

- (2) Bence et al. (1975); EMP/spark source mass spectrometry
- (3) Blanchard et al (1976); INAA
- (12) Jovanovic and Reed (1976a,b, 1980a);neutron and photon activation analysis

Notes:

(a) combined leach and residue

Table 3 continued: Chemical analyses of bulk rock/matrix and aphanites in 73215.

Spill	.46,2	.46,7	.46,10	.46,10.5	.46,19	.46,19.4	.38,17	.38,32	.38,57	.38,57.6	.38,57
SiO ₂	a	a	a	a	a		b	b	b	b	b
TiO ₂		46.7	45.6		46.3		46.7	46.4	45.9		
Al ₂ O ₃		1.3	1.1		1.0		0.8	0.9	0.8		
Cr ₂ O ₃	0.24	0.28	0.25		0.25		0.23	0.23	0.21		
FeO	8.32	8.75	8.13		7.87		6.97	7.04	6.94		
MnO		0.121	0.106		0.111		0.089	0.108	0.093		
MgO		12.6	12.0		11.7		10.7	12.4	11.8		
CaO		11.1	11.5		11.7		12.3	11.6	11.4		
Na ₂ O	0.52	0.50	0.52		0.54		0.54	0.49	0.52		
K ₂ O		0.20	0.22		0.22		0.20	0.19	0.16		
P ₂ O ₅											
Sc	15.9	17.1	15.7		15.8		11.9	13.2	12.0		
V											
Co	22.7	33.6	36.0		24.9		26.6	26.7	30.0		
Ni	40.0	220	290	167	150	137	230	160	250	596	195
Rb				3.02		3.2				2.84	
Sr											
Y											
Zr											
Nb											
Hf	9.8	9.7	10.7		9.9		9.1	7.7	8.3		
Ba											
Tb	4.0	4.3	4.6		4.4		4.1	4.3	3.9		
U				1.100		1.130				1.040	1.380
Ca				0.110		0.141				0.109	
Ti	2.3	1.5	1.2		1.4		1.5	1.3	1.4		
Pb											
La	26.6	28.8	27.7		27.5		25.9	32.0	23.4		
Ce	69	78	74		73		67	86	65		
Pr											
Nd											
Sm	12.1	13.5	12.2		12.4		11.5	14.9	10.2		
Eu	1.44	1.38	1.41		1.41		1.49	1.53	1.44		
Gd											
Tb	2.7	2.9	2.9		2.7		2.9	3.8	2.6		
Dy											
Ho											
Er											
Tm											
Yb	9.1	9.7	9.4		9.3		8.4	10.3	7.9		
Lu	1.21	1.35	1.27		1.27		1.21	1.40	1.09		
Li											
Be											
B											
C											
N											
S											
P											
Cl											
Br				0.0358		0.023				0.250	
Cu											
Zn				1.9		1.9				2.3	2.9
Rh											
Au				2.01		2.0				5.63	3.4
Ir				3.24		3.5				27.3	5.4
I											
At											
Ga											
Ge				135		216				315	320
As											
Se				57		110				59	73
Mo											
Tc											
Ru											
Rh											
Pd				8.4		5.9				31.5	11.6
Ag				0.72		0.7				5.91	0.98
Cd				5.4		7.4				5.4	5.0
In				11.4		1.8				59.8*	<6
Su											
Sb				1.65						32.7	1.51
Te				7.2						8.7	
W											
Re				0.343		0.32				2.61	0.56
Os				3.56		3.1				34.1	6.3
Pt											
Hg											
Tl				1.7		2.5				2.1	2.7
Bi				0.59						0.62	0.46
	(3)	(3)	(3)	(9,10)	(3)	(10)	(3)	(3)	(3)	(9,10)	(11)

References and methods:

- (3) Blanchard et al. (1976); INAA,AAS
 (9) Groe et al. (1976); RNAA
 (10) Morgan et al. (1976); RNAA
 (11) Morgan and Petrie (1979a,b);RNAA

Notes:

- *doubtful value according to authors
 a black aphanitic clasts
 b gray aphanitic spheroids

Table 3 continued: Chemical analyses of bulk rock/matrix and aphanites in 73215.

Split wt%	.176 gray	.66 gray	.68 gray	.160 black	.163 black	.166 black	.172(†) gray	.0	.52	.155	.158	.401
SiO ₂	48.8											
TiO ₂												
Al ₂ O ₃	21.4											
Cr ₂ O ₃	0.250	0.200	0.206	0.210	0.191	0.200	0.234					
FeO	8.5	6.1	6.5	8.0	7.1	7.5	7.7*					
MnO	0.10											
MgO	18.1(a)											
CaO												
Na ₂ O	0.51											
K ₂ O								0.200				
P ₂ O ₅												
REM												
Sc	17	12	13	15	13	14	15					
V												
Co	33	25	30	28	25	25	34					
Ni												
Rb												
Sr												
Y												
Zr	563	362	411	866	613	743	486		271	331	337	576
Nb												
Hf	12.4	8.64	9.24	19.7	14.1	17.1	11.1		6.4	7.5	8.1	14.3
Ba												
Th												
U								4.05				
Cs								1.10				
Ta												
Pb												
La												
Ce												
Pr												
Nd												
Sm												
Eu	1.6	1.3	1.4	2.1	1.6	1.6	1*					
Gd												
Tb												
Dy												
Ho												
Er												
Tm												
Yb												
Lu												
Li												
Be												
B												
C												
N												
S												
F												
Cl												
Br												
Cu												
Zn												
REH												
Au												
Ir												
I												
At												
Ga												
Ge												
As												
Se												
Mo												
Tc												
Ru												
Rh												
Pd												
Ag												
Cd												
In												
Sa												
Sb												
Te												
W												
Re												
Os												
Pt												
Hg												
Tl												
Bi												
	(6)	(6)	(6)	(6)	(6)	(6)	(6)	(7)	(13)	(13)	(13)	(13)

References and methods:
 (6) Ehmann et al. (1975a,b); INAA, RNAA.; Zr values corrected for U fission (decreased less than 10 ppm) by Garg and Ehmann (1976a)
 (7) Eldridge et al. (1975a,b); Gamma ray spectroscopy.
 (13) Hughes and Schmitt (1985); INAA

Notes:
 (†) erroneous data from computational error reported in Ehmann et al. (1975b)
 (*) approximate
 (a) clearly erroneously high; major element oxides without CaO and TiO₂ total 97%

Table 4: Compositions of groundmass in aphanites, from defocused beam microprobe analyses and clast subtraction. James (1976).

	Black aphanitic matrix (73215,243)		Gray aphanitic matrix (73215,245)		Schlieren-rich gray aphanitic matrix (73215,103)		Clast-poor aphanitic (73215,103)		Black aphanite clast (73215,46,10)		Gray aphanite spheroid (73215,38,57)		Bulk black aphanite clast† (73215,46,10)		Bulk gray aphanite spheroid† (73215,38,57)	
	Average	Range	Average	Range	Average	Range	Average	Range	Average	Range	Average	Range	Average	Range	Average	Range
SiO ₂	46.4	45.5-47.3	46.5	45.2-45.9	46.9	46.0-47.6	46.3	47.7	47.3-48.3	46.8	46.6-47.5	46.4	45.6	45.9		
TiO ₂	1.00	0.78-1.15	1.09	1.02-1.14	1.04	0.88-1.15	0.86	0.96	0.87-1.03	0.95	0.77-1.18	0.7	1.1	0.8		
Al ₂ O ₃	19.0	18.1-20.2	19.0	18.7-19.3	18.0	17.3-18.7	18.0	18.1	16.9-19.2	20.0	18.8-20.8	20.6	19.8	20.7		
FeO	8.26	7.70-9.10	8.27	7.94-8.54	8.73	7.96-9.15	8.56	7.89	7.24-8.56	6.86	6.37-7.80	7.30	8.13	6.94		
MnO	0.10	0.08-0.12	0.09	0.07-0.11	0.13	0.12-0.15	0.08	0.09	0.07-0.11	0.07	0.04-0.09	0.104	0.106	0.093		
MgO	11.6	9.74-12.5	12.8	12.7-13.0	12.0	11.2-12.3	13.5	12.4	11.5-14.0	11.8	11.0-12.9	11.6	12.0	11.8		
CaO	12.0	11.6-12.5	11.9	11.7-12.2	11.8	11.3-12.2	11.4	11.6	11.0-12.2	12.2	11.6-12.6	11.9	11.5	11.4		
Na ₂ O	0.76	0.66-0.95	0.64	0.61-0.67	0.62	0.56-0.77	0.63	0.57	0.48-0.66	0.61	0.53-0.66	0.50	0.52	0.52		
K ₂ O	0.29	0.17-0.39	0.30	0.25-0.33	0.31	0.27-0.39	0.29	0.24	0.20-0.27	0.24	0.22-0.25	0.20	0.22	0.16		
Cr ₂ O ₃	0.15	0.07-0.20	0.16	0.14-0.20	0.19	0.15-0.23	0.17	0.22	0.19-0.24	0.15	0.14-0.16	0.25	0.25	0.21		
P ₂ O ₅	0.41	0.26-0.48	0.25	0.20-0.30	0.31	0.25-0.42	0.25	0.29	0.26-0.33	0.31	0.26-0.35	—	—	—		
Number of analyses in average	14		4		7		2	7		7		11				

*Derived from broad-beam microprobe analysis of 100 μm spots (analyzed by G. H. Conrad and K. Keil, University of New Mexico); contributions from all clasts $>5 \mu\text{m}$ across within each spot have been subtracted and the resulting corrected compositions have been normalized to 100%.

†Determined by atomic absorption spectrophotometry and instrumental neutron activation analyses (Blanchard *et al.*, 1976).

Table 5: Chemical analyses of clasts in 73215.

	.94	.32	.29,9	.29,9	.29,9	.29,9	.29,9	.46,25	.46,33	.43,3	.43 IV	.46,102	.46,102
	a	b	c	c	c	c	c	d	d	e	e	f	f
Spili													
wt%													
SiO ₂	44.47	44.71	45.9	46.6				44.1					
TiO ₂	0.08		0.69	0.58				0.23					
Al ₂ O ₃	30.99	31.2	25.6	25.4				25.6					
Cr ₂ O ₃			0.130	0.146				0.124	0.123	0.015			
FeO	3.03	3.05	4.44	5.14				5.82	5.1	2.98			
MnO			0.062	0.077				0.067					
MgO	3.42	3.42	8.36	8.42				9.41					
CaO	17.21	17.24	13.9	14.1				13.8					
Na ₂ O	0.44	0.47	0.430	0.403				0.356	0.375	0.194			
K ₂ O	0.10	0.036	0.121	0.097				0.088		7.0			
P ₂ O ₅													
EMM													
Sc			7.16	9.04				7.12	8.2	4.8			
V													
Co			13.7	13.2				30.7	32.7	2.10			
Ni			80	80	64			420	460				
Rb	1.88	0.29									255.5	1.77	1.76
Sr							2.43	2.48			158.0	154.3	154.8
Y	33.7	19.7					167.0	167.2					
Zr	184	79											
Nb	10.4	6.3											
Hf	3.15	1.96	3.1	2.2				1.5	1.4	25.6			
Ba	182	61											
Th	1.34	0.80	1.6	0.96				0.53	0.58	39.9			
U	0.33	0.36			0.360								
Ce			0.3	0.2				0.3	0.16	5.4			
Ta													
Pb	1.4	1.87											
La	10.1	4.2	8.70	6.24				2.61	3.52	42.9			
Ce	27	12	24.4	16.8				6.78	9.1	125			
Pr	3.2	1.54											
Nd	12.1	6.3											
Sm	3.40	1.82	3.88	3.08				1.04	1.53	19.0			
Eu	1.23	0.50	1.00	0.91				0.77	0.77	3.11			
Gd	4.12	2.05											
Tb	0.82	0.42	0.84	0.82				0.23	0.36	5.6			
Dy	5.60	2.71											
Ho	1.32	0.57											
Er	3.67	1.62											
Tm	0.61	0.27											
Yb	3.67	1.66	2.9	3.0				1.4	1.71	27.2			
Lu	0.57	0.26	0.413	0.405				0.225	0.273	5.3			
Li													
Be													
B													
C													
N													
S													
F													
Cl													
Br													
Cu													
Zn							2.0						
EMH													
As							0.58						
Ir							1.78						
I													
At													
Ga													
Ge							47						
As													
Se							40						
Mo													
Tc													
Ru													
Rh													
Pd							2.1						
Ag							0.74						
Cd							19.4						
In							3.2						
Sn													
Sb													
Te													
W													
Re							0.167						
Os							2.3						
Pt													
Hg													
Tl							2.64						
Bi							0.44						
	(2)	(2)	(4,5)	(4,5)	(11)	(14)	(14)	(4,5)	(4)	(4,5)	(14)	(14)	(14)

References and methods:
 (2) Bence et al. (1975); EMP/spark source mass spec.
 (4) Blanchard et al. (1977a); INAA, AAS
 (5) Blanchard et al. (1977b); INAA, AAS
 (11) Morgan and Petrie (1979a,b); RNAA
 (14) Compston et al. (1977a,b); ID/MS

Notes:
 a not characterized
 b spinel troctolite
 c coarse-grained anorthositic gabbro
 d fine-grained anorthositic gabbro
 e felsite
 f feldspathic polymict material

Table 5 continued: Chemical analyses of clasts in 73215.

	,38,18	,38,26	,38,45	,46,5	,38,5	,38,23	,38,33	170,9007	170,5	,46,25.6	,46,25	,46,25
Splitt												
wt%	a	a	a	a	b	c	c	d	c	e	e	e
SiO ₂		45.6	46.8	44.9	42.2				42.8			
TiO ₂		0.48	0.37	1.13	0.29				0.47			
Al ₂ O ₃		25.4	30.6	26.3	6.69				12.6			
Cr ₂ O ₃	0.130	0.117	0.042	0.127	0.197	0.186	0.19		0.152			
FeO	5.44	5.14	1.79	5.23	10.1	8.36	7.22		8.6			
MnO		0.052	0.026	0.073	0.089				0.087			
MgO		8.89	2.37	6.82	37.7				26.0			
CaO		13.8	16.0	14.2	3.47				8.17			
Na ₂ O	0.495	0.483	0.951	0.494	0.127	0.320	0.47		0.311			
K ₂ O		0.109	0.197	0.126	0.038				0.060			
P ₂ O ₅												
ppm												
Sc	7.83	7.55	2.66	9.71	3.64	4.09	10.1		3.7			
V												
Co	22.7	18.0	4.13	11.5	54.9	47.4	34.9		50.8			
Ni	150	130		70	360	185	280	247	360	463	2.21	2.31
Rb								0.297		2.15	143.4	143.5
Sr												
Y												
Zr												
Nb												
Hf	4.7	4.0	0.94	3.8	1.67	0.82	6.4		0.9			
Ba												
Tb	1.8	1.48	0.39	1.9	0.86	0.27	2.5		0.2			
U								0.023		0.195		
Ca								0.0075		0.113		
Ta	0.6	0.44		0.70	0.17		0.8					
Pb												
La	12.3	9.8	4.24	11.0	4.84	3.17	16.6		2.6			
Ce	32.5	26.8	10.9	29.3	14.0	17.8	45.5		7.0			
Pr												
Nd												
Sm	5.48	4.32	1.73	4.9	2.17	1.28	7.34		1.34			
Eu	1.23	1.15	0.64	1.22	0.301	0.656	1.08		0.75			
Gd												
Tb	1.18	1.05	0.320	1.14	0.51	0.320	1.70		0.30			
Dy												
Ho												
Er												
Tm												
Yb	4.2	3.21	1.07	3.9	1.54	1.00	5.70		1.06			
Lu	0.60	0.46	0.151	0.55	0.222	0.125	0.79		0.16			
Li												
Be												
B												
C												
N												
S												
F												
Cl												
Br								0.0141		0.034		
Ca												
Zn								6.2		2.0		
ppb												
Au								2.64		8.29		
Ir								1.02		20.3		
I												
At												
Ga												
Ge								109		403		
As												
Se								3.9		61		
Mo												
Tc												
Ru												
Rh												
Pd										29.6		
Ag										0.51		
Cd								127		15.6		
In								3.1		3.94		
Sn												
Sb								0.706		1.27		
Te								<2		23.6		
W												
Re								0.043		1.73		
Os										23.4		
Pt												
Hg												
Tl								1.04		2.6		
Bi								0.49		1.76		
	(4)	(4)	(4)	(4)	(4)	(4)	(4)	(8,10)	(4)	(9,10)	(14)	(14)

References and methods:
(4) Blanchard et al. (1977a); INAA, AAS
(8) Higuchi and Morgan (1975a,b); RNAA
(9) Gros et al. (1976); RNAA
(10) Morgan et al. (1976); RNAA
(14) Compston et al. (1977a,b)

Notes:
a granulated feldspathic materials
b granulated troctolite
c troctolitic basalts
d spinel troctolite
e gabbroic anorthositic

Table 6: Clast allocation types in 73215; see Figure 22. From James and Blanchard (1976).

Principal Investigator	Aphanitic lithologies							Rind on ANT-suite clast
	Gray matrix	Black matrix	Heterogeneous black matrix	Schlieren-rich gray matrix	Light-gray matrix	Gray spheroids	Black aphanite clasts	
Anders	76(3) 9006,170(3)	9003,161(4)				38,57(2)	46,10(2) 46,19(2)	
Eglinton	73(3)	82(4)		128(2)				
Burns (Braucher)	21(3) 65(3)	34(4) 85(4)						
Compston		38,49(2) 36,3(2)	157(2) 258(2)	178(2)	46,45(2)	38,57(2) 38,32(2)	46,10(2) 46,19(2)	
Haskin	74(3) 46,33(2)	161(4) 209(2) 262(2)	159(2) 184(2)	177(2)	186(2) 46,30(2) 170(2)	38,17(2) 38,32(2) 38,57(2)	46,2— 46,7(2) 46,10(2) 46,19(2)	46,25(2)
James	228(3) 245(3)	127(2) 243(4) 231(4)	282(2) 283(2)	103(2) 106(2) 107(2) 247(2) 238(2)	46,37(2)	38,17(2) 38,32(2) 38,57(2) 121(2)	46,2— 46,7(2) 46,10(2) 46,19(2) 118(2) 120(2)	46,25(2)
Kaplan			156(2) 273(2)					
Kirsten	9001,73(3)	41(2) 36,2(2)		9005,177(2)	46,44(2)	38,57(2) 38,32(2)	46,10(2) 46,7(2) 46,19(2)	
Marti	33(2)	260—1, 263—8(2)						
Price	72(3)	162(4)		92(2)	88(3)			
Reed†		81(4)		136(2)				
Silver		213(2)						
Ehmann†	66(3) 68(3) 172—	160(4) 163— 166(4)		176(2)				
Taylor, S. R.†		90(4)		94(2)	140(2)			

*Numbering system is as follows: samples numbered 29.X, 36.X, 38.X, and 46.X were obtained by chipping of large consortium pieces in air and distributed by D. P. Blanchard; samples numbered 900X.Y are from pieces obtained by chipping in the SSPL and then further subdivided in the lab of a consortium member—the initial recipient has retained the split with the original specific number Y; all other samples are listed by NASA-assigned specific numbers. The number in parentheses after the specific number indicates the figure on which the subsample appears.

†Investigators who are not members of the consortium but who have analyzed samples from the rock.

‡These are not all lithologically equivalent nor are they from the same area of the rock.

ANT-suite clasts					Surface samples			
Coarser-grained anorthositic gabbro	Finer-grained anorthositic gabbro	Granulated troctolite	Spinel-bearing troctolitic basalt	Granulated feldspathic clast material†	Felsite clast	Exposed top	Partly buried side	Buried bottom
29,9(2)	46,25(2)		9007,170(2)	46,103(2)		152(2)		
29,9(2)	46,25(2)			46,102(2)	43(2)			
29,9(2)	46,25(2) 46,33(2)	38,5—	170(2) 38,23(2) 38,33—	38,18(2) 38,20(2) 38,45— 46,5(2)	43(2)	151(2)	185(2)	
29,9(2)	46,25(2) 46,33(2)	121(2) 122(2) 124(2) 125(2) 38,39(2)	170(2) 38,23(2) 38,33—	118(2) 120(2) 46,5(2) 46,105(2) 46,13(2) 38,18(2) 38,45— 38,22(2)	43(2)			
29,9(2)	46,25(2) 46,33(2)	38,39(2)		46,6(2)	43(2)	146(2) 147(2)	139(2)	
	46,25(2)			46,101(2)		27(2)		87(2)
		32(2)		49(2)				

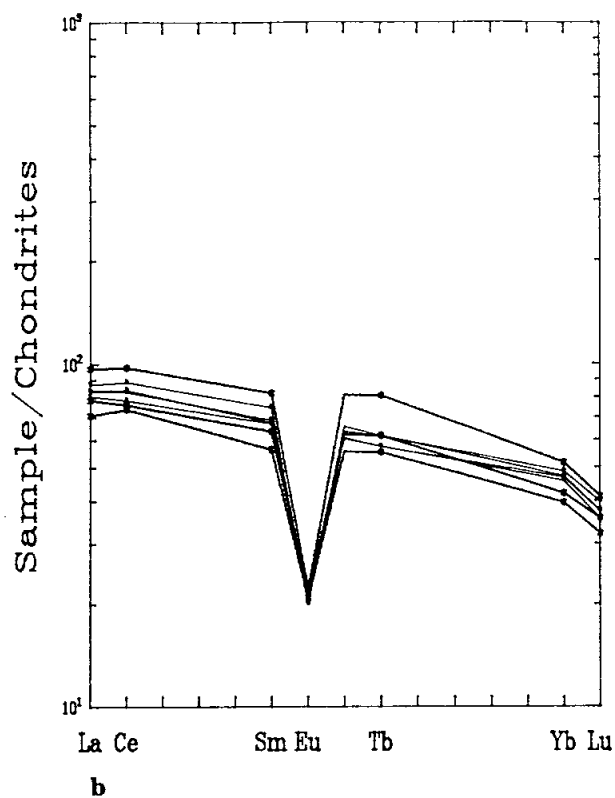
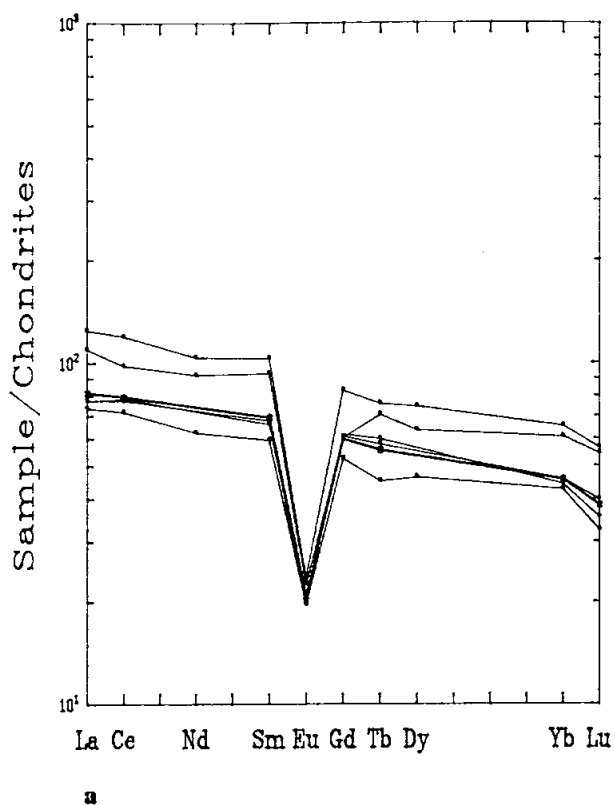
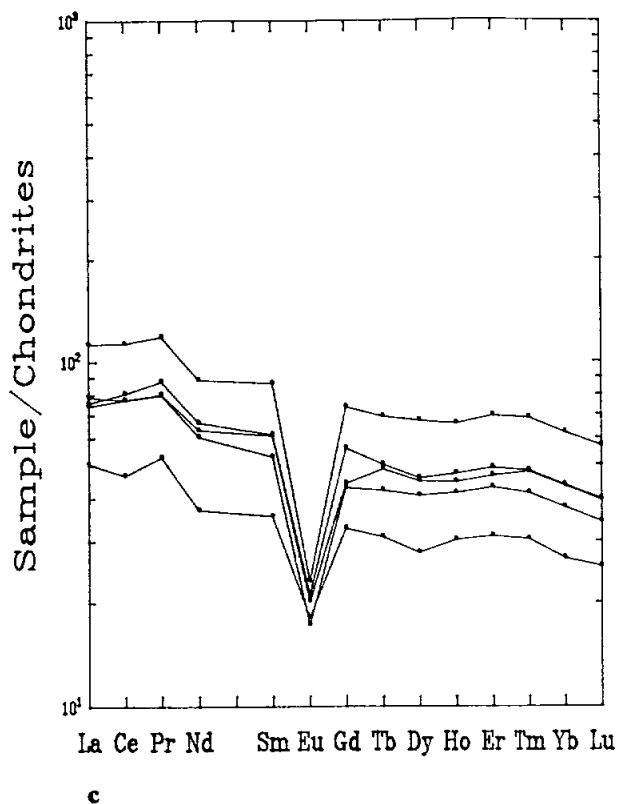


Figure 18: Chondrite-normalized plot of rare earth elements in bulk rock/matrix and aphanites in 73215. Data from Table 3.
 a) data of James et al. (1975a) and average of 11 samples by Blanchard et al. (1976).
 b) data for individual samples of Blanchard et al. (1976).
 c) data of Bence et al. (1975a).



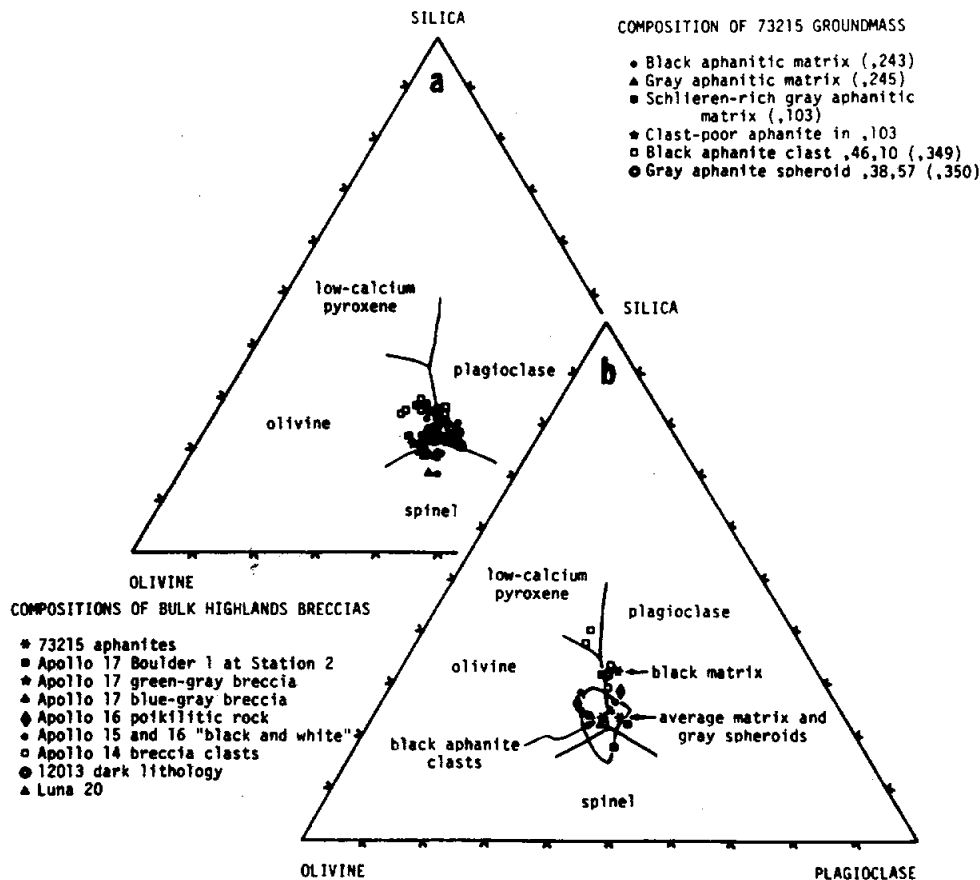


Figure 19: Compositions of groundmass melt in 73215 and other samples on silica-olivine-plagioclase plot. James (1976).

Several groups have reported analyses of "anorthositic gabbros" or feldspathic, granulitic impactite clasts in 73215. Blanchard et al. (1977a,b) reported that .46,25 and .46,33 were similar to each other and are similar to other feldspathic impactites such as 78155. They are somewhat different from .29,9, which has higher rare earth elements and a negative Eu anomaly (Fig. 20) and also has high Cd and Sb (Morgan and Petrie, 1988). Clast .45,25 is also high in meteoritic siderophiles (e.g., Ni more than 400 ppm), whereas .29,9 has much lower levels of meteoritic contamination. Gros et al. (1976) placed .46,25 in meteoritic Group

3L; sample .29,9 was also Group 3 (Morgan and Petrie, 1988). Some other analyses in Table 5 may also be of similar materials, but accurate descriptions have not been retrieved.

Blanchard et al. (1977a,b) reported analyses of other feldspathic breccias, some of which are probably polymict (Table 5, Figure 21). The high rare earths and continuous rare earth slopes of some samples are probably a result of matrix contamination. The fine-grained, igneous-textured spinel-bearing troctolite analyzed appears to have indigenous rather than meteoritic siderophiles (Higuchi

and Morgan, 1975a,b) and roughly matches the 72417 dunite in the siderophile relative abundances (Morgan and Wandless, 1988). Bence et al. (1975) reported data for a spinel troctolite clast of undescribed nature; it is certainly feldspathic with fairly low incompatible element abundances (Fig. 21). Eckert et al. (1991a,b) reported on the chemistry of an apparently cumulate spinel troctolite without tabulating the data. The sample has 28% Al_2O_3 and a positive Eu anomaly. The small dunite clast analyzed by the same group (Eckert et al., 1991b) has low rare earth element abundances with a fairly flat rare

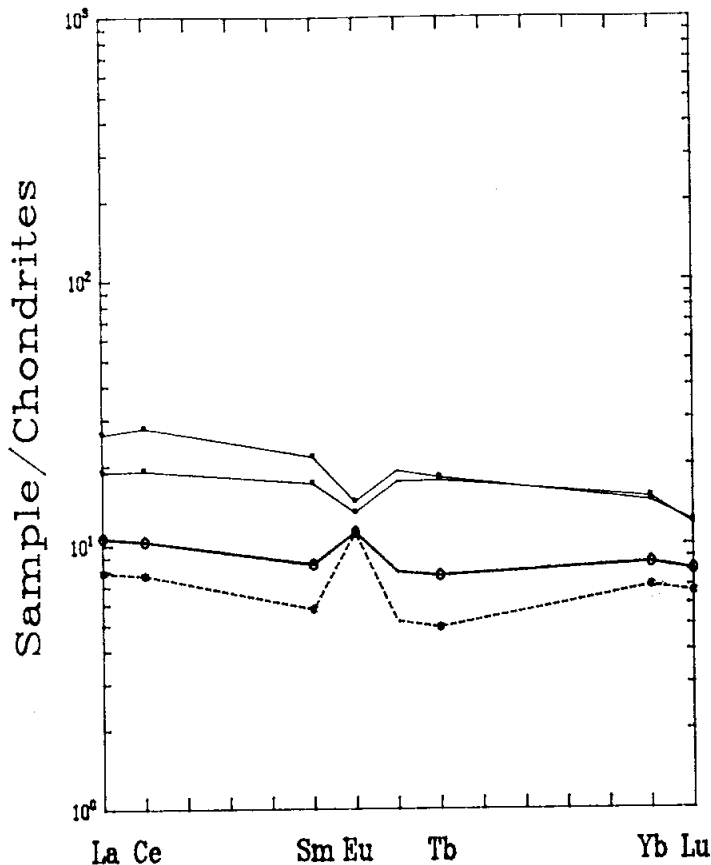


Figure 20: Chondrite-normalized plot of rare earth elements in feldspathic impactites (granulites, or "anorthositic gabbros") in 73215. Data from Table 5.

earth element pattern and only a small negative Eu anomaly; however, the mineral variability suggests that this sample is polymict, not pristine igneous. One of the two clasts analyzed by Bence et al. (1975) was described as spinel troctolite and is the most feldspathic of 73215 clasts analyzed; the other clast, not described, is similar but has twice the abundance of incompatible elements.

The felsite pieces analyzed were tiny (less than 14 mg). The sample is K-rich and poor in FeO and Na₂O, with high rare earth element abundances (La 130 x chondrites; Fig. 21). The pattern is V-shaped, and the chemistry suggestive of an origin that includes liquid immiscibility (Blanchard et al., 1977b).

STABLE ISOTOPES

Sulfur isotope data for matrix samples were reported by James et al. (1975a). The $\delta^{34}\text{S}$ ‰ values for two samples of interior heterogeneous matrix were 1.0 and 1.7 and for surface chips were 1.9 and 2.0. These values are like those of lunar crystalline rocks and unlike those of typical regoliths or regolith breccias.

RADIOGENIC ISOTOPES AND GEOCHRONOLOGY

Geochronological studies have been conducted on both aphanitic matrix and varied clasts in 73215. Because of the fine-grained nature of the aphanites, most of the work on them has been on the Ar-Ar system. The clasts and the melt

groundmass have not equilibrated with each other in any of the investigated systems. The argon data clearly demonstrate incomplete degassing during the breccia-forming event and Ar loss appears to have been varied depending on particular thermal histories and clast types. Both stepwise heating and laser Ar studies have been conducted on 73215 materials.

Jessberger et al. (1976a,b; 1977) and Staudacher et al. (1977) included several aphanitic matrix materials in their stepwise heating studies of 73215. They tabulated the data and produced release diagrams (Figs. 23 and 24; note the age axes use the "old" decay constants). The argon age data are summarized in Table 7, where the "new" decay constants are used. The results clearly demonstrate incomplete degassing, with the structure of the releases apparently resulting from combinations of old clastic material and melt. Few of the plateaus are very constant or very flat (Figs. 23, 24). Given that the age of the melt is probably best given by the age of the melted felsite clast within it (see below) and thus 3.87 ± 0.01 Ga, then even claimed good plateaus such as that of gray matrix 73.1, which produces an age of 4.09 ± 0.01 Ga must reflect undegassed clast material. None of the samples analyzed are pure groundmass melt, and thus the "ages" yield only upper limits of the events that formed them (Jessberger et al., 1976a). Although the aphanitic melt spheroids and clasts give old "ages", the petrographic and chemical data strongly imply that these clasts and the matrix aphanites all formed in the same event, and thus these "ages" of up to 4.18 Ga (new constants) also reflect incomplete degassing of clasts. There is a reasonable correlation among aphanite samples of decreasing "age" with increasing K content, which may reflect the content of better-degassed felsite clasts (Jessberger et al., 1976). Jessberger et al. (1977) find it at

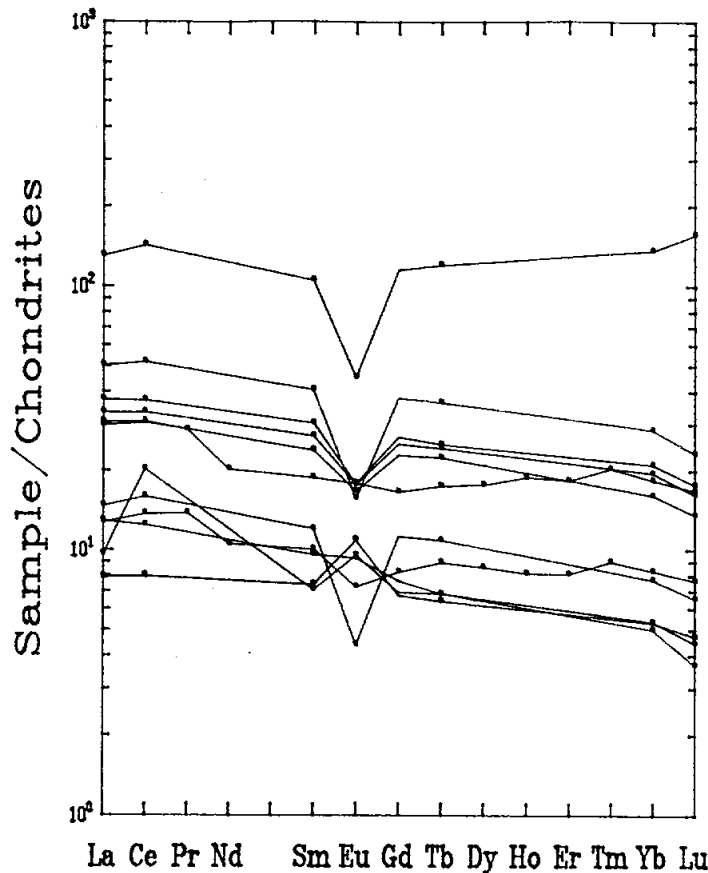


Figure 21: Chondrite-normalized plot of rare earth elements in felsite and feldspathic breccias in 73215. Data from Table 5.

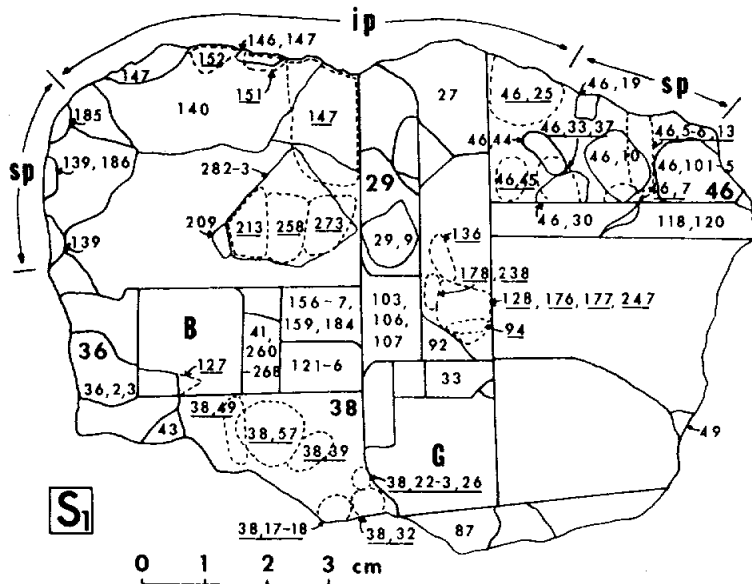


Figure 22: Map of slab sample locations and allocated material for 73215; see Table 6. (From James and Blanchard, 1976).

least conceivable, however, that the data can be interpreted in a straightforward manner and that some of these clasts are indeed old melts.

Muller et al. (1977a,b) and Eichorn et al. (1978a,b) conducted Ar isotopic studies on 73215 aphanitic materials using pulsed laser release of argon from polished surfaces. The method allows precise selection of the target through petrographic observation; the releases are from small areas (10-100 micron half-spheres) so individual small phases can be targeted. The method differs from step-wise heating in that all the gas is measured at once, because temperature control is not possible; thus the method is in essence K-Ar, not Ar-Ar. Pre-heating of the samples at 550-750°C (after irradiation, but before laser pulsing) was used to remove argon from unretentive phases and thus to single out gas from retentive phases that have greater chronological significance. Numerous small clasts in the matrix as well as groundmass melt were targeted. The data are reproduced in Tables 8 and 9, which are taken from Eichorn et al. (1978) who revised the older data from Muller et al. (1977a) with correction of the K/Ca ratios (Table 8). Fuller descriptions of the targets are given in the original papers.

Muller et al. (1977a,b) analyzed clasts and groundmass in two matrix chips (Table 8), one a schlieren-rich gray matrix, the other just gray matrix, with about 50% recognizable clasts in a microsubophitic melt. The data indicate clearly that during the breccia-forming event degassing of argon was incomplete on a scale of tens of microns. The three groundmass age determinations agree within error at 4.01 Ga, but plagioclase clasts show variedly older ages and some clasts, including felsites, have younger ages (about 3.90 Ga). The most likely of possible alternative explanations is that the younger ages represent an upper limit to the

Table 7: Summary of argon ages for 73215 materials, using new decay constants. Jessberger et al. (1978).

Subnumber	Sample	K-Ar Age AE	⁴⁰ Ar- ³⁹ Ar Plateau Age AE
43,3	felsite clast	3.83	3.87 ± .01
36,2	black	3.77	3.93 ± .01
41,1	black	3.93	3.99 ± .03
46,44	light gray	3.90	3.97 ± .01
73,1	gray	4.03	4.09 ± .01
177,1	schlieren-rich gray	4.04	4.07 ± .04
38,32,5	gray spheroid	3.98	4.03 ± .01
38,57,4	gray spheroid	4.05	4.10 ± .03
46,7,3	vesicular black clast	3.92	3.97 ± .01
46,19,5	non-vesicular black clast	3.97	4.03 ± .01
46,10,7	non-vesicular black clast	4.08	4.18 ± .01
46,6,1	dark gray clast	4.05	4.11 ± .07
38,39,1,1	troctolite vein	3.90	3.95 ± .06
38,39,1,1	feldspathic clast	4.13	{ 4.05 ± .05 4.22 ± .03 4.00 ± .02 4.18 ± .01
29,9,6	anorthositic gabbro clasts	4.10	{ 4.02 ± .01 4.20 ± .01 4.02 ± .01 4.16 ± .01
46,25,5		4.07	
46,33,4		4.09	

age of the breccia-forming melt event (and not a subsequent heating event), and older ages represent incomplete degassing during that event. The groundmass melt "age" of 4.01 Ga then has no real chronological significance, and represents incomplete degassing of even the silicate liquid phase, or a still-appreciable content of very tiny, undegassed clasts, or gain of argon by the melt from the clasts during cooling. Eichorn et al. (1978) analyzed aphanitic clast material that was black, and which had given an anomalously old age by Ar-Ar (Jessberger et al., 1976a). The purpose was to establish the ages of various components of clasts and melt groundmass (Table 9). The results strongly support the suggestion that the black aphanite clast is cogenetic with the main matrix samples; a felsic glass clast is the same age as that of other felsic clasts and the breccia-forming event, i.e. 3.89 Ga, and the groundmass itself gives a similar

age. The older age of Jessberger et al. (1976a) must clearly reflect the presence of undegassed clasts.

Compston et al. (1977a,b) reported Rb-Sr isotopic data on six bulk matrix and five aphanitic clasts in 73215 (Table 10). The range in Rb/Sr results principally from differences in the Rb contents and reflects mainly a variation in felsite clast content. At breccia formation (about 3.83 Ga, new constants) there were small differences in ⁸⁷Sr/⁸⁶Sr ratios; data for the matrices are correlated along a mixing line that passes near though not exactly through the felsite data. Mixing is evident, with the low Rb members consisting of feldspathic materials with low initial ⁸⁷Sr/⁸⁶Sr and material with higher initial ratios. The data shown in Fig. 25, which includes data for Boulder 1, Station 2, emphasizes such differences and demonstrates the lack of Sr isotope equilibration on a 1 cm to 1 mm scale. The age

of the breccia-forming event cannot be determined directly from the aphanite data, but must be inferred from clast data, particularly the felsites, which give an age of 3.83 ± 0.05 Ga (new constants). Figure 25 shows that many 73215 aphanites have model ages greater than 4.5 Ga; one possible explanation is volatile loss of Rb during melt formation, although it is not known whether the "excess"-age component is the melt phase or a clast phase. Compston et al. (1977a) note that if the older Ar ages result from incomplete degassing and the older Rb-Sr model ages result from Rb loss, then there should be a reciprocal relationship between the Ar age and the K content of aphanites, but such a correlation is in fact weak, and degassing and volatilization must be complex.

James et al. (1975) reported data from a U, Th, and Pb isotopic study of black matrix material. On a concordia diagram the 73215 data fall within the field defined by other Apollo 17 melt breccias such as Boulder 1, Station 2 and the North Massif melt boulders (Fig. 26). The data plot very roughly along a chord with intersections at 4.4-4.5 and 4.0 Ga, suggesting old components strongly modified by outgassing during the breccia-forming event. James et al. (1976) reported Nd isotopic data for a sample of black matrix (also plotted in a Figure in Lugmair et al., 1975). The ¹⁴³Nd/¹⁴⁴Nd of 0.51185 ± 0.00003 is lower than chondritic evolution, and the data require at least a two-stage evolution, with a stage very early in lunar history with Sm/Nd even lower than in the present breccia.

A fission track age for a whitlockite clast (James et al., 1975; Braddy et al. 1975a,b; and Goswami et al. 1976a,b) using a Lexan mapping technique is 4.05 (+0.05, -0.08) Ga, with uncertainties resulting from corrections for cosmic ray exposure. The age is in reasonable agreement as a compaction age for

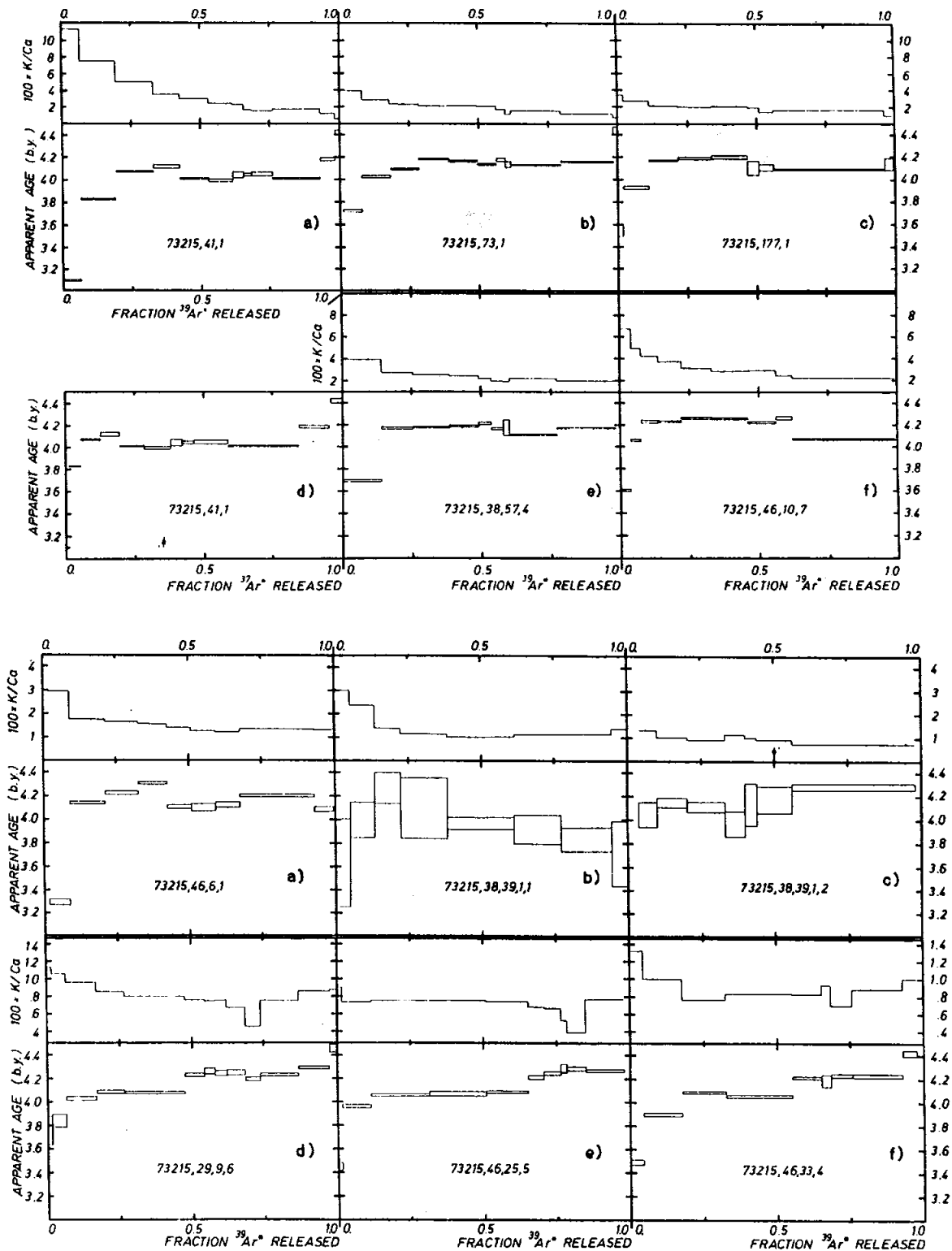


Figure 23: Ar release diagrams and ages for 73215 materials; ages are for old constants and should be reduced by about 0.06 Ga for new decay constants. Jessberger et al. (1977a). Key: Part 1, a) black matrix, b) gray matrix, c) shlieren-rich gray matrix, d) black matrix plotted against $^{37}\text{Ar}^*$, e) gray aphanite spheroid, f) black aphanite clast. Part 2, a) dark gray aphanite clast, b) olivine in troctolite vein, c) feldspathic clast, d)-f) feldspathic granulites ("anorthositic gabbros").

Figure 24: Ar release diagrams and ages for 73215 materials; ages are for old constants and should be reduced by about 0.06 Ga for new decay constants. Jessberger et al. (1977a).

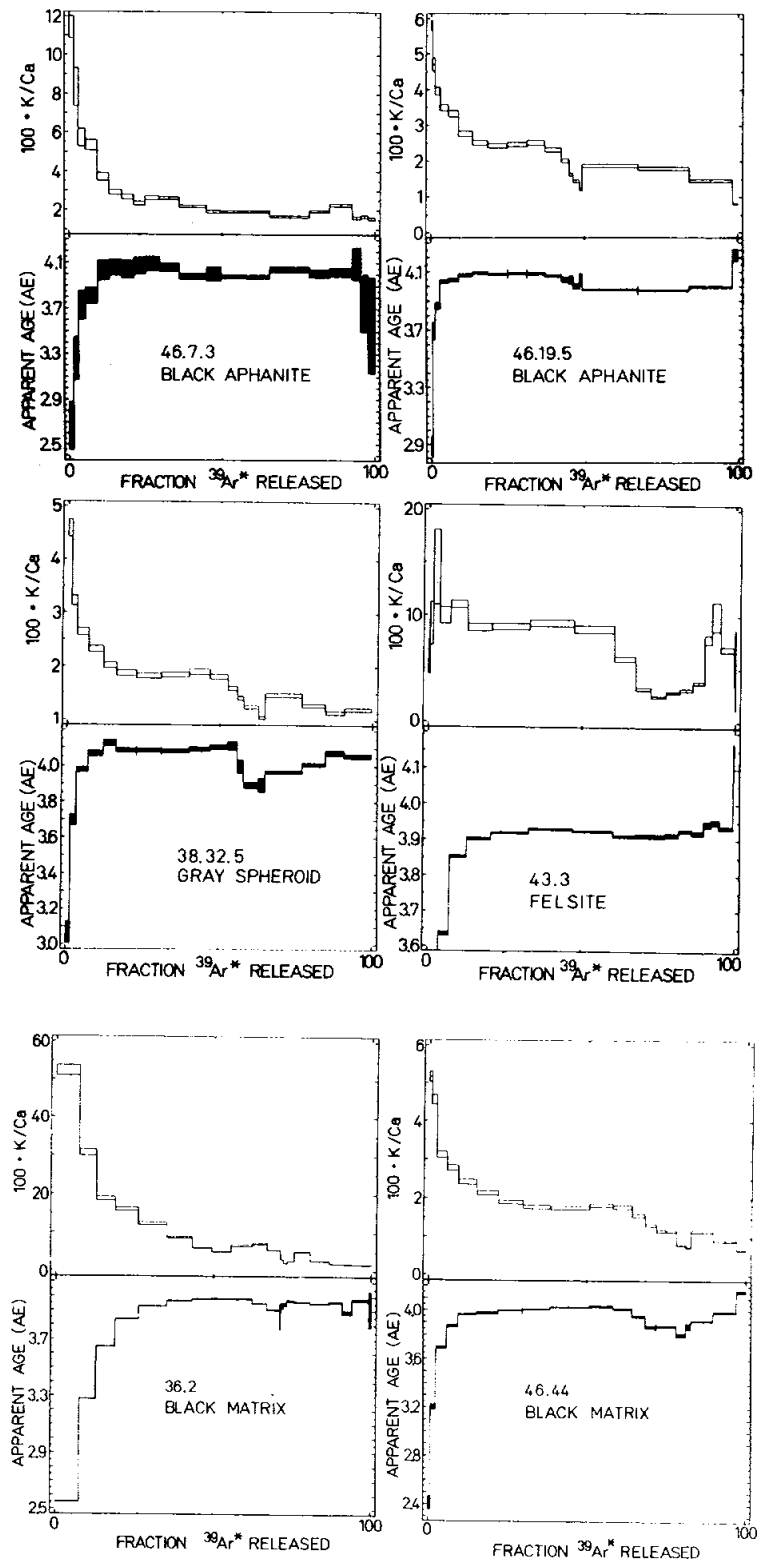


Table 8: Laser argon results for aphanitic matrix material in 73215; new decay constants.
Originally from Muller et al. (1977a,b), revised by Eichorn et al. (1978) in simplified form.

Material	K/Ca	$^{40}\text{Ar}_K/^{39}\text{Ar}_K$	Age (G.y.)
<u>Matrix sample 73215,177 unheated</u>			
Groundmass	.021 ±.001	77.00 ±1.57	3.96 ±.03
<u>Matrix sample 73215,177 preheated to 550°C</u>			
Groundmass	.021 ±.002	79.70 ±3.98	4.01 ±.07
Center of 0.28 mm plagioclase clast	.008 ±.001	87.56 ±5.29	4.17 ±.08
Centers of 29 40–125 μm plagioclase clasts	.011 ±.002	84.01 ±2.28	4.10 ±.04
0.24 mm clast of devitrified maskelynite	.012 ±.002	85.56 ±3.04	4.13 ±.05
<u>Matrix sample 73215,131 preheated to 550°C</u>			
Groundmass	.021 ±.001	76.63 ±1.22	3.93 ±.02
Groundmass in clast-poor matrix	.030 ±.001	79.57 ±1.88	3.99 ±.03
Granulated 0.4 mm core of 0.9 mm anorthosite clast	.007 ±.001	71.18 ±2.14	3.81 ±.04
Granulated 0.4 mm core of 0.9 mm anorthosite clast, repolished	.008 ±.001	65.87 ±2.03	3.69 ±.04
Recrystallized rim of 0.9 mm anorthosite clast	.009 ±.001	78.22 ±2.31	3.96 ±.04
0.4 mm clast of recrystallized anorthosite	.010 ±.001	79.00 ±3.06	3.98 ±.05
0.4 mm clast of recrystallized anorthosite, repolished	.011 ±.001	80.98 ±2.32	4.02 ±.04
0.15 mm clast of felsite (vermicular intergrowth of K-feldspar, quartz, and plagioclase)	1.328 ±1.328	82.34 ±5.44	4.04 ±.09
0.25 mm clast of felsic glass	2.788 ±.971	75.18 ±1.84	3.90 ±.03
0.25 mm clast of felsic glass, repolished	1.787 ±1.787	69.89 ±.63	3.78 ±.01
<u>Matrix sample 73215,131 preheated to 750°C</u>			
Granulated 0.4 mm core of 0.9 mm anorthosite clast	.007 ±.001	74.13 ±1.12	3.89 ±.02
0.25 mm clast of felsic glass	1.683 ±1.683	73.09 ±0.55	3.85 ±.01

¹Data from Müller *et al.* (1977) recalculated using "new" preferred values for the isotopic composition of K, the decay constants, and the monitor composition (see text). K/Ca values have also been revised because the previously published values were in error.

Table 9: Laser argon results for black aphanite clast material and inclusions. Eichorn et al. (1978a).

Analysis Number	Material	Number of Pulses	⁴⁰ Ar	³⁹ Ar*	³⁸ Ar*	³⁷ Ar	³⁶ Ar*	K/Ca	⁴⁰ Ar _K / ³⁹ Ar _K	Age (G.y.)
Black aphanite clast 73215,46,10 preheated to 650°C										
1. (09131)	Groundmass	~100	525.5 ±2.5	6.87 ±.12	3.91 ±.69	107 ±9	4.79 ±1.37	.034 ±.003	76.3 ±1.4	3.90 ±.03
2. (09133)	Groundmass	~100	554.0 ±2.6	7.45 ±.13	5.34 ±.32	116 ±4	7.81 ±.76	.034 ±.002	74.0 ±1.4	3.86 ±.03
3. (01212)	Center of 0.25 × 0.40 mm plagioclase clast A	~35	232.6 ±2.0	2.85 ±.24	1.61 ±.28	241 ±28	1.21 ±.49	.006 ±.001	81.7 ±6.8	4.01 ±.11
4. (01256)	Plagioclase clast A, repolished	60	777.4 ±5.6	9.58 ±.22	5.60 ±.39	612 ±72	2.69 ±.45	.008 ±.001	81.2 ±2.0	4.00 ±.03
5. (01252)	75 × 100 μm felsic glass clast	13	244.2 ±2.8	3.23 ±.23	.51 ±.15	92 ±61	.09 ±.09	.019 ±.013	75.7 ±5.4	3.89 ±.10
6. (01254)	130 μm clast of K-Ca-rich plagioclase	10	659.0 ±3.6	7.96 ±.23	.12 ±.12	19 ±19	.37 ±.37	.216 ±.216	82.8 ±2.4	4.03 ±.04
7. (02033)	130 μm clast of K-Ca-rich plagioclase, repolished	8	1139.8 ±6.1	13.53 ±.46	.34 ±.26	39 ±39	.08 ±.08	.185 ±.185	84.3 ±2.9	4.06 ±.05

*Information given in footnote to Table 1 applies to the data presented in this table as well. Blank levels for ⁴⁰Ar, ³⁹Ar, ³⁸Ar, ³⁷Ar, and ³⁶Ar were respectively: 4.8, .79, 28.0, 12.4, and 74.0 for measurements 1-2; and 6.8, 1.4, 2.5, 2.5, and 7.6 for the remaining measurements.

³⁹Ar, ³⁸Ar, and ³⁶Ar corrected for n-induced contributions from Ca; ³⁸Ar also corrected for n-induced contributions from K.

Table 10: Rb-Sr isotopic data for 73215 whole-rock chip aphanite samples. Compston et al. (1977a).

		Rb	Sr	⁸⁷ Rb/ ⁸⁶ Sr	⁸⁷ Sr/ ⁸⁶ Sr
46,10.6 Black clast	A	22.2	4.83	137.1	.1016
	B	10.1	5.02	143.7	.1007
38,57.5 Gray spheroid	A	17.7	2.94	155.4	.0546
	B	20.0	3.02	150.4	.0579
157 Heterogeneous black matrix	A	24.0	5.96	139.8	.1231
	B	25.4	5.67	138.6	.1179
258 Heterogeneous black matrix	A	43.1	3.01	145.8	.0595
	B	28.8	2.88	141.4	.0588
46,45 Light-gray matrix	A	21.2	2.26	139.3	.0467
	B	16.9	2.33	140.4	.0478
178 Schlieren-rich gray matrix	A	25.3	3.46	138.9	.0719
	B	23.5	3.24	139.9	.0669
38,49 Black matrix	A	16.6	8.20	146.9	.1612
	B	15.4	8.32	148.5	.1618
46,102 Gray aphanite clast	A	6.21	3.27	131.2	.0720
	B	6.77	3.45	133.3	.0747
38,32 Gray spheroid	A	15.7	7.16	147.2	.1405
	B	19.4	6.87	148.8	.1333
46,19 Black aphanite clasts		25.6	3.65	136.1	.0773
36,3 Black matrix	I	22.2	58.2	165.4	1.0214
	II	21.4	10.53	173.5	0.1753

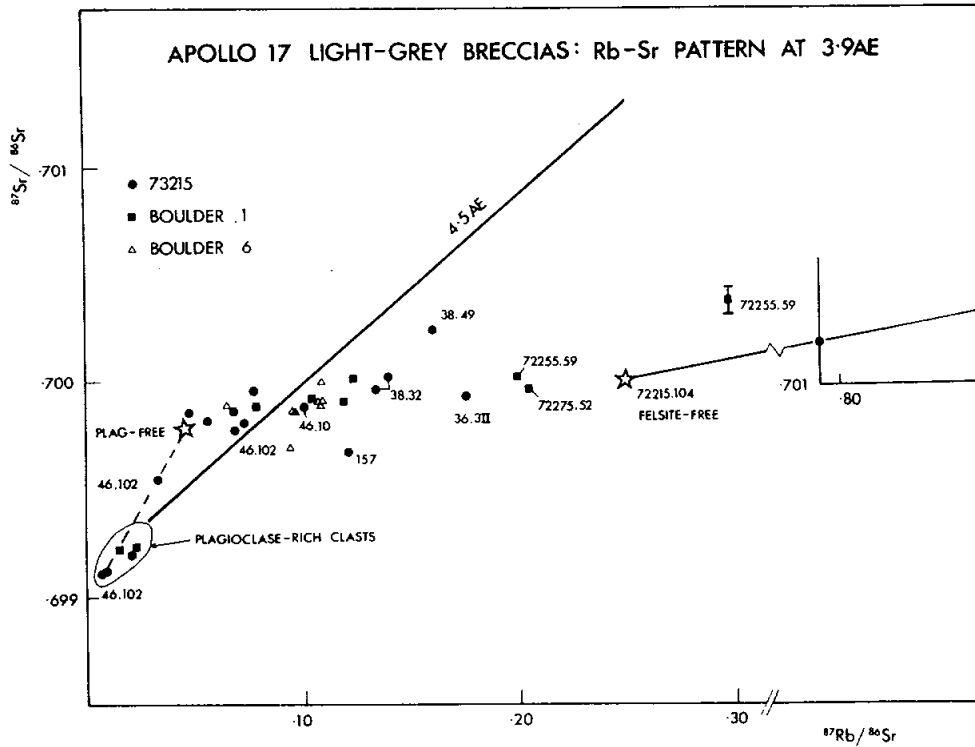


Figure 25: Sr evolution diagram for 73215 aphanite materials, after removal of radiogenic ^{87}Sr produced since 3.83 Ga (new constants). Compston et al. (1977a).

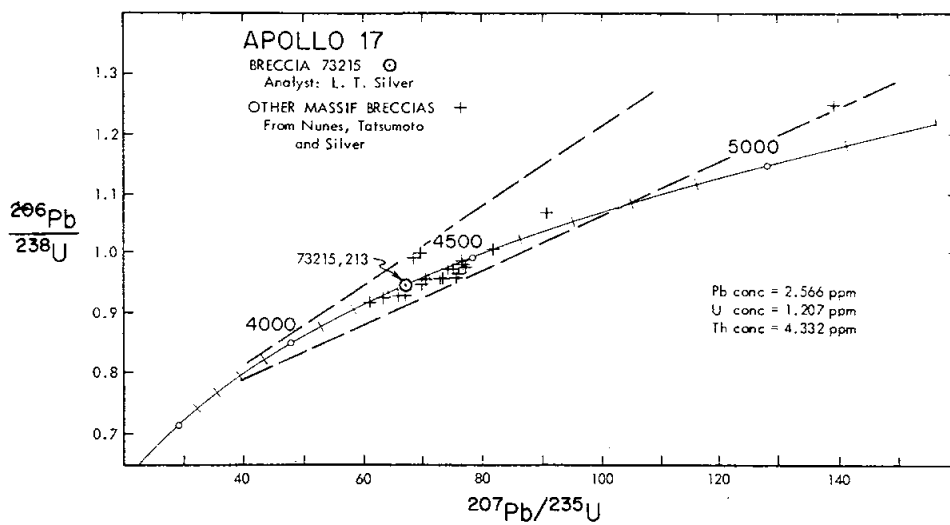


Figure 26: U-Pb concordia diagram for a 73215 matrix sample and other Apollo 17 breccia materials. James et al. (1975).

the breccia with results from the Ar and Sr systems.

The feldspathic impactite ("anorthositic gabbro") clasts were included in the argon studies of Jessberger et al. (1976a,b) and Eichorn et al. (1978a,b), and the strontium studies of Compston et al. (1977a,b). Jessberger et al. (1976a) stated that the releases (Fig. 23) for three samples had distinct two step plateaus: intermediate-temperature ones with ages of about 4.0 Ga (new constants) and high-temperature ones with ages of about 4.16-4.22 Ga (new constants). The K/Ca ratios do not show concomitant changes. The lower age corresponds roughly with the breccia-forming event age, and is interpreted by Jessberger et al. (1977a) as thermal resetting by that event that left some material incompletely degassed. The older ages are thus lower limits on the age of the parent material. Two of these clasts were also studied by laser release methods, which also show a range of ages (Tables 11 and 12) (Muller et al. 1977a; Eichorn et al., 1978a,b). For the laser release studies, the samples were pre-heated as for the aphanites (above) and the ages are K-Ar on the more retentive phases. Small spots (30-60 micron half-spheres) were targeted, and ranged from cores of large and small plagioclases to small interstitial phases and rims. Plagioclase was the dominant phase being outgassed. The tabulated results show that cores of plagioclase crystals have higher ages (4.11-4.28 Ga, new constants) and recrystallized and apparent melt products have younger ages (3.81-3.88 Ga). The pattern of dates is reasonably consistent with production by partial outgassing through grains and along grain boundaries when the clasts were incorporated in 73215, although not all of the observations fit such a process. The combined data for the two clasts set a lower limit of 4.26 Ga on the date of the high-temperature melting/recrystal-

lization that affected them. The alternative that the melting event in the clast took place at about 4.0 Ga and that incorporation into 73215 had only minor effects is an unpreferred alternative explanation.

Compston et al. (1977a,b) performed Rb-Sr isotopic studies on separates from two of the feldspathic granulites ("anorthositic gabbros") (Table 13, Fig. 27). Sample ,29,9 has enough dispersion among plagioclase, olivine, and bulk rock to define an imprecise isochron at 4.18 +/- 0.31 Ga (new constants) with an initial $^{87}\text{Sr}/^{86}\text{Sr}$ of 0.69918 +/- 0.0016. There is inadequate dispersion among the analyzed phases from ,45,25 to define an isochron, although the data is consistent with the ,29,9 isochron. Model ages based on BABI are about 4.3 Ga and supposedly constitute older limits on the age of the observed melting. If the systems were not entirely closed during incorporation into 73215, then the olivine model age of ,29,9 might be a better estimate of its age; such a model

age is 4.5 +/- .2 Ga, hence the impactite could be very old.

Other feldspathic and troctolitic clasts were analyzed in the argon and the strontium studies. Jessberger et al. (1976a) analyzed a feldspathic clast that gave results similar to those of the feldspathic impactites (Fig. 23), with an older, higher temperature plateau and a younger, lower temperature plateau. Olivines picked from a stringer or vein do not give a good plateau and the errors are large because of the small amount of K in the sample. The spectrum shows a steady decrease in ages with temperature, possibly a result of recoil from included material, and the overall age is low, less than 4.0 Ga. Several of the fragments in the melt analyzed using laser release by Muller et al. (1977a,b) were feldspars or feldspathic materials and gave a variety of ages from 4.17 Ga to 3.69 Ga (Table 8). The sample of feldspathic material analyzed for Rb-Sr isotopes by Compston et al. (1977a,b) (Table

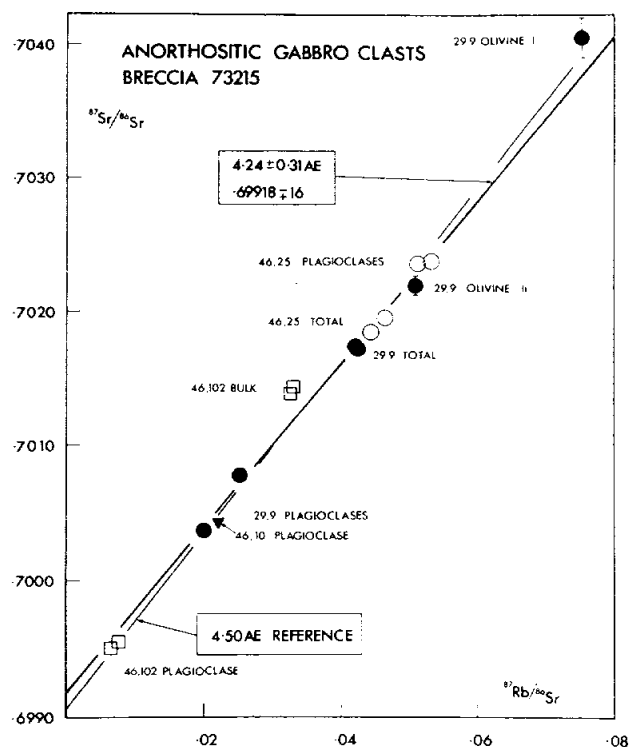


Figure 27: Strontium evolution diagram for feldspathic impactite and granulated feldspathic material in 73215. Calculated ages are for the old decay constants. Compston et al. (1977a).

Table 11: Laser argon release data for feldspathic impactite ,46,25 (new constants). Eichorn et al. (1978a).

Analysis Number	Material	Number of Pulses	⁴⁰ Ar	³⁹ Ar*	³⁸ Ar*	³⁷ Ar	³⁶ Ar*	K/Ca	⁴⁰ Ar _K / ³⁹ Ar _K	Age (G.y.)
Sample 73215,46,25 preheated to 650°C										
1. (10184)	Centers of two 0.3 mm relict cores, grains A + B	~80	938.4 ±4.4	9.69 ±0.09	4.36 ±0.39	264 ±27	7.10 ±6.7	.019 ±0.002	96.5 ±1.0	4.28 ±.01
2. (01181)	Intermediate zone in relict core of grain A (after repolishing)	36	431.8 ±2.8	4.76 ±.22	3.36 ±.45	362 ±62	2.28 ±.32	.007 ±.001	90.7 ±4.2	4.18 ±.06
3. (01191)	Intermediate zone in relict core of grain B (after repolishing)	34	508.4 ±3.5	5.70 ±.21	3.54 ±.45	412 ±46	2.37 ±.61	.007 ±.001	89.1 ±3.4	4.15 ±.05
4. (12222)	0.3 mm relict core of grain C	67	467.7 ±2.7	5.30 ±.21	3.52 ±.27	380 ±37	2.59 ±.39	.007 ±.001	88.2 ±3.6	4.14 ±.06
5. (10186)	Eight 0.13–0.20 mm relict cores, grains E-L	~100	1003.0 ±2.4	11.55 ±.15	7.90 ±.73	561 ±11	8.91 ±.52	.011 ±.001	86.7 ±1.2	4.11 ±.02
6. (01185)	Five 0.06–0.10 mm relict cores, grains M-Q	42	385.2 ±3.9	4.36 ±.22	2.79 ±.26	265 ±31	2.02 ±.50	.009 ±.001	88.2 ±4.6	4.14 ±.07
7. (01174)	Core-rim boundary of grain C (after repolishing)	~75	521.0 ±4.8	6.33 ±.24	4.24 ±.21	463 ±66	2.59 ±.50	.007 ±.001	82.4 ±3.2	4.03 ±.05
8. (01183)	Rim of grain A (after repolishing)	35	517.6 ±3.6	6.31 ±.21	4.27 ±.52	480 ±54	2.61 ±.68	.007 ±.001	82.0 ±2.8	4.02 ±.05
9. (01176)	Rim of grain C (after repolishing)	30	488.8 ±5.8	5.84 ±.23	3.38 ±.26	435 ±52	2.69 ±.27	.007 ±.001	83.7 ±3.4	4.05 ±.06
10. (01195)	Rims of five grains (M-Q) containing relict cores	~55	415.7 ±2.5	5.06 ±.22	2.84 ±.24	342 ±55	1.24 ±.22	.008 ±.001	82.2 ±3.6	4.02 ±.06
11. (10191)	Centers of 0.1 mm recrystallized grains plus rims of grains A and B	~100	838.7 ±3.6	10.43 ±.15	7.27 ±1.15	541 ±6	7.32 ±1.26	.010 ±.001	80.3 ±1.2	3.99 ±.02
12. (10193)	Edges of grains bordering olivine	~100	868.6 ±2.6	11.76 ±.15	10.19 ±.62	604 ±15	12.02 ±.67	.010 ±.001	73.6 ±1.0	3.85 ±.02
13. (01197)	Edges of grains bordering olivine	~55	1014.0 ±4.4	14.06 ±.43	8.73 ±.49	895 ±164	5.29 ±.61	.008 ±.002	72.1 ±2.2	3.81 ±.04
14. (10188)	Small grains plus pyroxene in oikocrysts	~120	499.0 ±3.2	6.60 ±.12	6.95 ±.73	438 ±14	7.62 ±.70	.008 ±.001	75.4 ±1.4	3.88 ±.03
15. (10182)	Small grains plus pyroxene in oikocrysts	100–120	1102.5 ±8.5	15.15 ±.19	16.72 ±.65	938 ±20	24.15 ±.74	.009 ±.001	72.3 ±1.2	3.82 ±.02
Sample 73215,46,25 preheated to 850°C										
16. (01262)	Edges of grain bordering olivine	68	726.3 ±3.7	8.75 ±.22	5.64 ±.21	498 ±57	3.27 ±.68	.009 ±.001	83.0 ±2.1	4.04 ±.04
Sample 73215,46,25 preheated to 900°C										
17. (02013)	Center of 0.25 mm relict core of grain D	59	787.1 ±2.9	9.12 ±.23	4.44 ±.26	493 ±94	2.77 ±.54	.010 ±.002	86.3 ±2.2	4.10 ±.03
18. (01311)	Edge of relict core of grain A (after second repolishing)	55	595.3 ±2.7	6.30 ±.24	4.00 ±.31	587 ±63	3.25 ±.43	.006 ±.001	94.4 ±3.7	4.25 ±.05
19. (02031)	Rim of grain A (after second repolishing)	42	263.6 ±2.5	2.88 ±.21	1.86 ±.28	161 ±49	1.31 ±.58	.009 ±.003	91.5 ±6.8	4.20 ±.10
20. (02015)	Rim of grain D	36	408.9 ±2.4	4.44 ±.22	2.06 ±.11	359 ±53	1.59 ±.56	.007 ±.001	92.0 ±4.6	4.21 ±.07
21. (01313)	Edges of grains bordering olivine	57	426.2 ±3.1	4.73 ±.21	4.44 ±.56	464 ±63	3.12 ±.54	.005 ±.001	90.1 ±4.1	4.17 ±.06
22. (02011)	Small grains plus pyroxene in oikocrysts	59	254.8 ±2.1	2.75 ±.22	2.43 ±.32	257 ±41	.55 ±.43	.006 ±.001	92.5 ±7.5	4.21 ±.11

*Values are in 10^{-12} cm³ STP; all values are corrected for blank. As the volume of material melted by each laser pulse is somewhat variable, we have not attempted to estimate gas concentrations in the rock sample (see text). Blank levels for ⁴⁰Ar, ³⁸Ar, ³⁷Ar, and ³⁶Ar were, respectively: 4.8, .79, 28.0, 12.4, and 74.0 for measurements 1, 5, 11, 12, 14, and 15; and 6.8, 1.4, 2.5, 2.5, and 7.6 for the remaining measurements. The blank is mainly the mass spectrometer tube background; the change in blank values was correlated with a change of the mass spectrometer multiplier and the accompanying bake outs. The blank for ⁴⁰Ar was variable by a factor of about 2; variation in the ³⁹Ar blank for the first set of measurements was $\pm 0.04 \times 10^{-12}$ cm³ STP and for the second set of measurements was $\pm 2 \times 10^{-12}$ cm³ STP. Gas samples in which the level of the ³⁹Ar from the rock was less than twice the blank level were found to give unreliable results so we have not reported analyses of such samples. Uncertainties reported in the ages are one standard deviation and indicate precision only, to facilitate intercomparison of the data; the absolute uncertainty is 0.02 G.y. (1 σ).

*³⁹Ar, ³⁸Ar, and ³⁶Ar corrected for n-induced contributions from Ca; ³⁸Ar also corrected for n-induced contributions from K.

**Table 12: Laser argon release data for feldspathic impactite ,29,9 (new constants).
Eichorn et al. (1978a). Data revised from Muller et al (1977a).**

Material	K/Ca	$^{40}\text{Ar}_k/^{39}\text{Ar}_k$	Age (G.y.)
Sample 73215.29.9 unheated			
~0.4 mm relict core of ~0.8 mm grain	.012 ±.001	90.16 ±1.97	4.21 ±.03
Sample 73215.29.9 preheated to 550°C			
~0.4 mm relict core of ~0.8 mm grain	.006 ±.001	98.53 ±5.62	4.36 ±.08
~0.4 mm relict core of ~0.8 mm grain	.006 ±.001	95.21 ±3.88	4.30 ±.06
~0.4 mm relict core of ~0.8 mm grain	.007 ±.001	97.75 ±5.84	4.35 ±.08
Three ~0.2 mm relict cores in ~0.6 mm grains	.010 ±.001	95.79 ±3.00	4.31 ±.04
Centers of 48 .075-.230 mm melt-derived grains	.008 ±.001	82.29 ±2.10	4.07 ±.03

⁴Data from Müller *et al.* (1977) recalculated using "new" preferred values for the isotopic composition of K, the decay constants, and the monitor composition (see text). K/Ca values have also been revised because the previously published values were in error.

Table 13: Rb-Sr data for clasts of feldspathic impactite (anorthositic gabbro), granulated feldspathic material, and the felsite from 73215. Compston et al. (1977a).

		Weight (mg)	Rb ppm	Sr ppm	$^{87}\text{Rb}/^{86}\text{Sr}$	$^{87}\text{Sr}/^{86}\text{Sr}$
A. 29,9	A	19.0	2.43	167.0	.0420	.70175 ± 5
1. total-rock	B	21.1	2.48	167.2	.0427	.70173 ± 5
2. plagioclase	A	5.0	1.45	208.6	.0201	.70038 ± 5
	B	6.2	1.63	185.9	.0253	.70078 ± 6
3. olivine	I	2.1	.40	15.45	.0755	.70406 ± 23
olivine	II	5.3	.70	39.2	.0510	.70220 ± 8
B. 46,25	A	16.8	2.21	143.4	.0444	.70185 ± 5
1. total-rock	B	21.1	2.31	143.5	.0465	.70195 ± 6
	A	5.6	3.55	193.1	.0531	.70238 ± 5
2. plagioclase	B	5.0	3.22	181.0	.0513	.70237 ± 8
C. 46,102 feldspathic material	A	23.7	1.77	154.3	.03316	.70144 ± 5
	B	25.9	1.76	154.8	.03278	.70139 ± 5
2. plagioclase	A	3.00	0.46	199.8	.00666	.69950 ± 5
	B	2.52	0.56	207.2	.00777	.69955 ± 5
D. 46,10 plagioclase fragment		4.1	1.55	202.4	.0221	.70043 ± 5
E. 43,IV felsite chip		1.62	255.5	158.0	4.666	.96616 ± 6
43,III glass concentrate		0.55	252.0	91.9	7.910	1.14662 ± 8
43,II grey fraction		1.19	290.0	156.4	5.350	1.00460 ± 8
43,I white fraction		0.84	342.8	213.4	4.634	.96423 ± 5

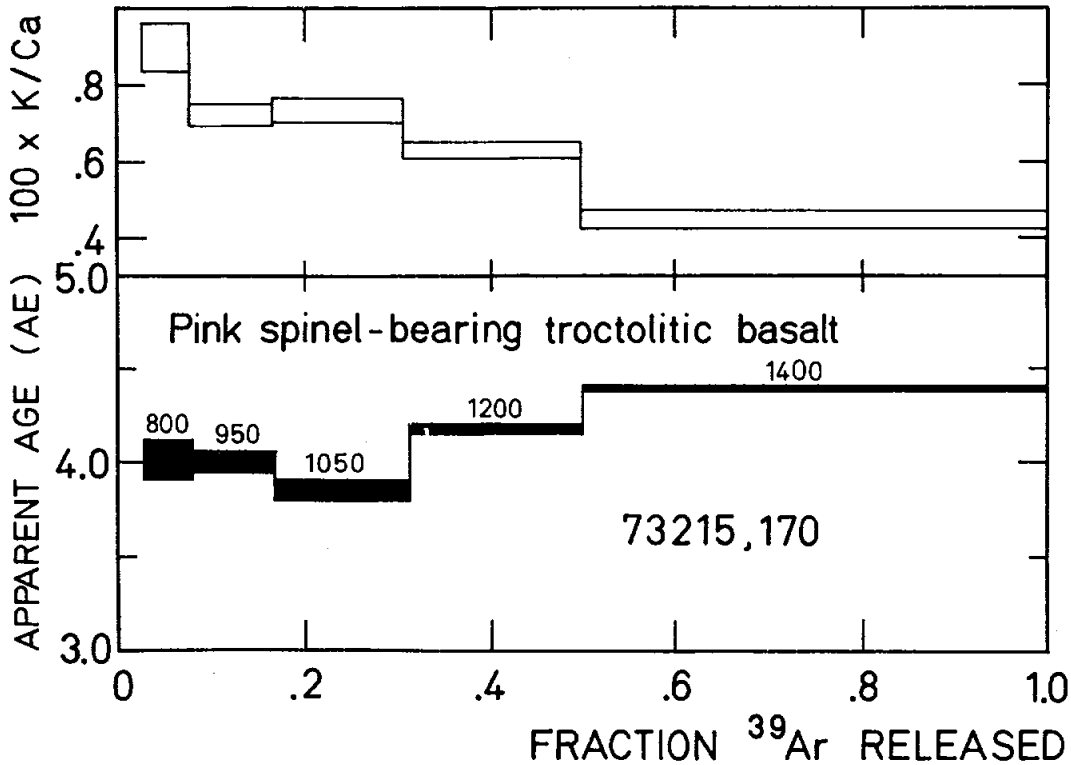


Figure 28: Apparent age and K/Ca spectra for a pink-spinel bearing troctolitic basalt in 73215. Jessberger et al. (1979).

12) is probably polymict and might contain some 73215 matrix material. Its bulk analysis falls significantly above the feldspathic impactite isochron, and even above the 4.44 Ga reference isochron through BABI. In contrast, separated plagioclase falls below the feldspathic impactite isochron.

Jessberger et al. (1979) reported argon temperature release data for a clast of pink spinel-bearing troctolitic basalt (Fig. 28). This clast has been interpreted to contain indigenous, not meteoritic, siderophiles, and to have first crystallized rapidly and later to have suffered partial granulations and recrystallization, and then fragmentation. The age spectrum shows a two-step pattern similar to that of the feldspathic impactites, with an upper age of 4.46 ± 0.04 Ga which must be a minimum age for the melting. The younger age of about 3.94 ± 0.07 Ga is in agreement with the age of breccia-formation.

The felsite clast ,43,3 was analyzed by stepwise argon release by Jessberger et al. (1977a,b), and gave a good plateau at 3.86 ± 0.01 Ga (new constants). The felsite was molten at the time of incorporation, so this age dates that of resetting of the felsite rather than its primary crystallization age; it is also the best definition of the age of the melt and breccia formation. Rb-Sr isotopic data (Compston et al., 1977a,b) for the same felsite (Table 13 and Figure 29) give an age of 3.84 ± 0.05 Ga (new constants), in good agreement with the argon age. The slope of the isochron is controlled largely by the melted brown glass, and the age is that of the aggregation. The Rb-Sr model age of a "total-rock" chip gives a maximum crystallization age of 3.94 Ga. Felsic glasses analyzed in the laser argon studies also give ages in the 3.85 ± 0.05 Ga range (Muller et al., 1977a,b; Eichorn et al., 1978a,b).

RARE GAS AND EXPOSURE

Rare gas analysis shows that trapped solar wind gases are essentially absent from 73215 (James et al., 1975a). Trapped Ne and Ar are less than 3×10^{-8} cc/g. James et al. (1975a) reported a Kr-Kr exposure age of 243 ± 7 Ma for black matrix (both Kr and Xe are dominantly from *in situ*-produced spallation and neutron-capture). ^{38}Ar exposure ages for three matrix chips reported in the same study are about the same: 185, 217, and 227 ± 30 Ma. A moderate amount of shielding during irradiation is indicated by the data, on average about 10-15 cm of rock or soil. The data can be interpreted as dominantly a simple exposure history with one irradiation of about 243 Ma, or a more complex multi-stage irradiation; the latter seems less likely.

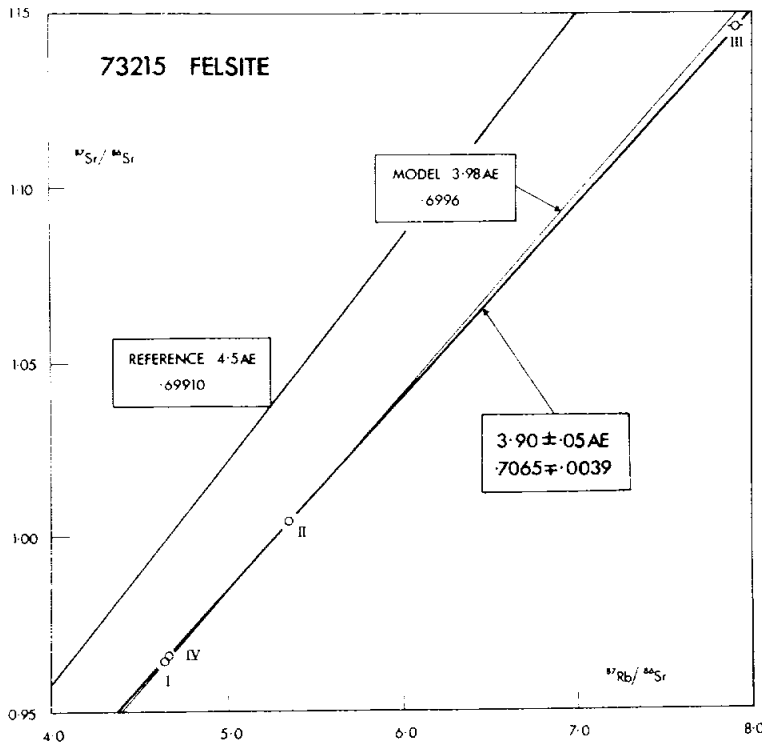


Figure 29: Internal Rb-Sr isochron for a felsite clast in 73215. Age stated is for old decay constants; new constant gives 3.84 ± 0.05 Ga for the age of the felsite. Compston et al. (1977a).

Jessberger et al. (1977a; 1978a) reported ^{38}Ar cosmic ray exposure ages for several matrix and clast samples, including aphanitic clasts, feldspathic impactite clasts, and the felsite. All have the same exposure within uncertainty and average 244 ± 9 Ma, very close to the reported Kr-Kr ages. The ^{38}Ar exposure age for the pink spinel troctolitic basalt reported by Jessberger et al. (1979) at 256 ± 10 Ma is also in agreement within uncertainty.

O'Kelley et al. (1974a,b) reported cosmogenic nuclide data for the bulk rock 73215, measured soon after splashdown. Their discussion mainly concerns the August 1972 solar flare event. 73215 appears to have been at least partly shielded from that flare, having low ^{54}Mn , ^{56}Co , and ^{46}Sc compared with other nuclides. Yokoyama et al. (1974) used the saturation of ^{26}Al and ^{22}Na data to determine that the rock had had an exposure of at least a few million years.

Hutcheon et al. (1974b) measured track densities in 73215 and suggested that it had had a very complex irradiation history. The exposed surfaces are saturated with impact pits (according to Horz), hence at least a million years of exposure is suggested; the bottom had no craters, so there was no turnover in that time frame. However, the track density profile from the top to the bottom is virtually flat: $5 \times 10^6/\text{cm}^2$ at 1.6 cm; $4.0 \times 10^6/\text{cm}^2$ at 4.8 cm; and $3.7 \times 10^6/\text{cm}^2$ at 6.7 cm. A long irradiation (more than 50 Ma) in a different orientation at a few centimeters depth is required, with the prediction of a long spallation age (which is in fact the case). Hutcheon et al. (1974b) found no solar flare track density gradient near the surface of the sample measured. Nord and James (1977a) also found track densities consistent with those of Hutcheon et al. (1974b); one quartz grain showed higher densities that are probably a result of an adjacent U-Th-rich

phase. Braddy et al. (1975a,b) and Goswami et al. (1976a,b) used such track data to estimate the compaction age of 73215 (see RADIOGENIC ISOTOPES AND GEOCHRONOLOGY section, above).

PHYSICAL PROPERTIES

Housley et al. (1976) made ferromagnetic resonance studies of 73215 and established that it did not have the FMR intensity characteristic of glassy agglutinates.

A detailed study of the magnetic properties of 73215 was made by Brecher (1975, 1976a,b,c; also partly reported in James et al. 1975a,b). She concluded that there are intimate interrelationships between the dominant petrographic features and the magnetization behaviour that she terms textural remanent magnetism. The samples used were two cubes (3.4 g and 1.9 g) from 5 centimeters apart and mutually oriented. Both were aphanitic matrix materials, one black and one gray. Small chips of similar material were subjected to thermomagnetic analysis. The average Fe^0 (0.121 and 0.15 wt%) and Fe^{2+} (6.31 and 6.35 wt%) of the cubes show the low degrees of reduction typical of crystalline highlands rocks and the sample show no evidence of a previous regolith history. Multi-domain metal grains dominate the magnetic behaviour and the thermomagnetic analyses establish that they have meteoritic Ni.

The initial magnetic moments (Natural Remanent Magnetization, or NRM) were similar in the cubes as received and decayed only a little in two months storage in a zero field; thus acquisition of a viscous remanence from earth's field is probably negligible. The cubes were subjected to standard AF demagnetization (Fig. 30); the NRM is rather soft. The microcoercivity spectra of both

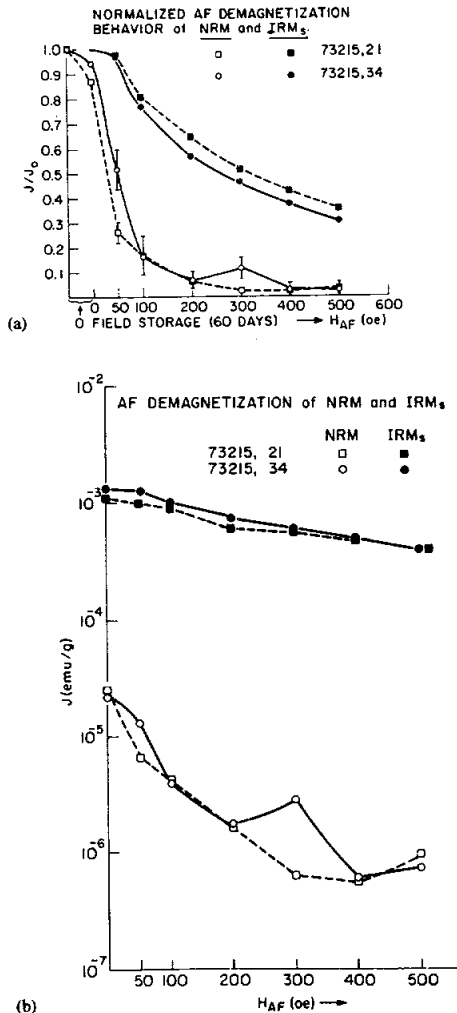


Figure 30: Absolute (a) and normalized (b) demagnetization curves of natural and saturation remanence in two cubes of 73215 matrix. (Brecher 1976b).

NRM and saturation remanence are similar in the two samples, with the saturation remanence about 50x the NRM. Figure 31 summarizes the directional changes. A stable and possibly primordial NRM should show directional convergence. The initial NRM directions of the two samples are different (points marked 0 in Fig. 31), in fact almost reversed. Cleaning in high fields results in oscillations with directions close to shear or other planes. Both the initial and convergence directions of magnetization are distinctly different in the two matrix cubes.

Thermomagnetic curves are reproduced as Figure 32. The samples were heated to 850 degrees C. The reproducible thermal hysteresis loops show that no chemical changes took place. The two samples are nearly identical, and the major phase is kamacite. The transformation temperature (gamma to alpha) corresponds with a Ni content of about 5%; the cooling behaviour indicates that only 1% of the metal is pure Fe⁰. Some low temperature inflections probably result from sulfides. Full magnetization curves and hysteresis loops were obtained for the two

cubes (Figure 33), from which the Fe₀ and Fe₂₊ contents are determined. The average values of the hysteresis parameters (Table 14) confirm the predominance of multi-domain magnetic grains.

Brecher (1976b) measured the magnetic anisotropy by three different methods to detect the presence of the magnetic fabric implied by the directional behaviour of the NRM. She used high-field anisotropy, where a comparison of the derived hysteresis loop parameters for the orthogonal directions indicates that both cubes are magnetically anisotropic. The anisotropy differs in sense and magnitude for each magnetic parameter. Anisotropy in the acquisition of anhysteretic remanent magnetization (ARM) indicates that both samples have anisotropy in the same sense but to different degrees; the actual value for the degree of anisotropy is probably meaningless. The qualitative conclusion may be drawn that the gray matrix sample has a more pronounced magnetic fabric. Low-field anisotropic susceptibility also shows that the two breccias are magnetically anisotropic, and probably as a result of a magnetic fabric mimetic to the observed rock fabric. Brecher (1976a,b,c) discusses in some detail the model of textural remanent magnetism.

PROCESSING AND SUBDIVISIONS

Following separation of a few small chips, 73215 was sawn in late 1973, producing end pieces (8, 140 g; and 9, 644 g) and a slab (10) about 1.5 cm thick (Fig. 2). Because of the complex structure of the rock, lithological maps were constructed to assist processing and allocation correlations (Figs. 4 and 22) for the consortium study led by O. James. The slab was greatly subdivided by sawing (Fig. 22). A large number of thin sections from several pieces were cut from this rock, and allocations for many

types of study were made. In 1989 a further slab was cut from end piece ,9, which is now 372 g. This slab piece broke into pieces and allocations were made of clasts for chemical and petrographic studies.

Figure 31: Directional behaviour of NRM and the orientation of the magnetic susceptibility ellipsoid relative to petrofabric features of the two cubes from 73215. Brecher (1976b).

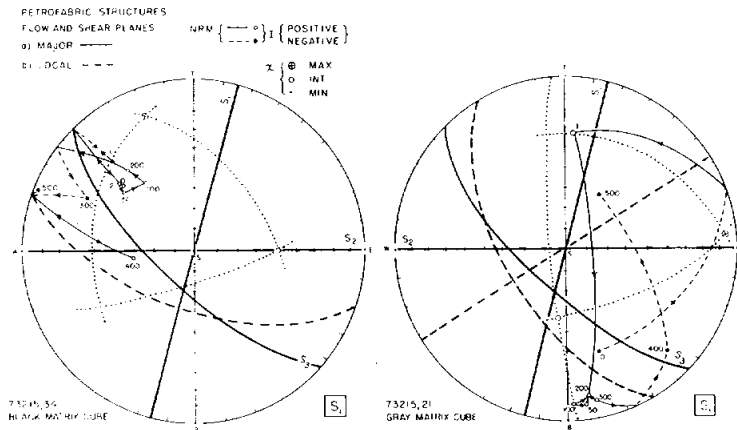


Figure 32: Thermomagnetic behaviour for the cubes from 73215; Curves (1) are heating and (2) are cooling. Brecher (1976b).

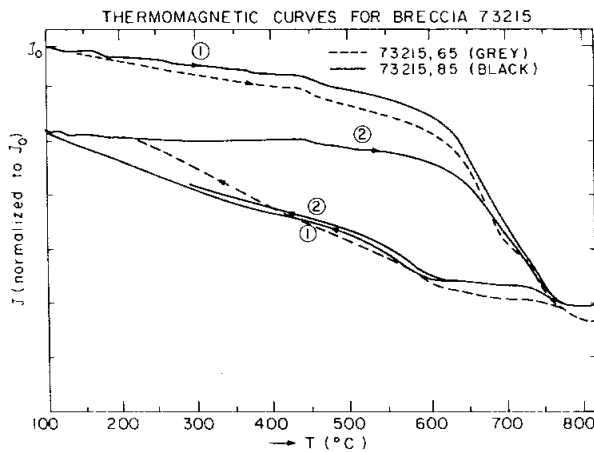


Figure 33: Sets of magnetization curves obtained with the magnetic field sequentially parallel to the cube axes. Brecher (1976b).

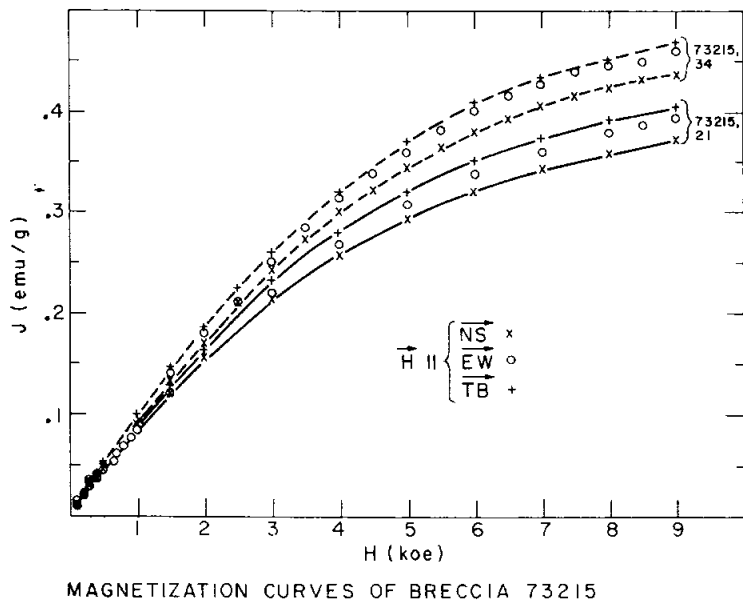


Table 14: 300° K hysteresis loop parameters for cubes 73215,21 and ,34. Brecher (1976b).

		J_s (e.m.u./g)	Fe° (wt.%)	$\langle J_{rs} \rangle$ (e.m.u./g) $\times 10^{-2}$	$\frac{\langle J_{rs} \rangle}{J_s}$	χ_p $\left(\frac{\text{e.m.u.}}{\text{Oe g}} \right)$ $\times 10^{-6}$	Fe ²⁺ (wt.%)	$\frac{\text{Fe}^\circ}{\text{Fe}^{2+}}$	H_c (Oe)	$\chi_a \times 10^{-4}$	J_s / χ_a
H NS	21	.263	.1195	.148	.0056	12	5.58	.0215	14	.85	3100
	34	.3095	.14	.151	.0049	14	6.59	.021	10	.925	3350
H EW	21	.267	.121	.0684	.0025	13.95	6.49	.0186	10	.8-.83	3300
	34	.338	.153	.177	.0052	13.18	6.13	.025	3	.966	3500
H TB	21	.271	.123	.12	.0044	14.7	6.87	.018	10	1	2700
	34	.346	.157	.2	.0058	13.6	6.33	.0247	38	1.2	2900

73216

Impact Melt Breccia

St. 3, 162.2 g

INTRODUCTION

73216 is a tan to olive gray (5Y5/1) tough breccia collected near the rim-crest of a 10-m crater. It is an impact melt breccia (originally described as metaclastic) that has a homogeneous groundmass and about 5% lithic clasts. The sample is subrounded and 7 x 5 x 3 cm. It has many zap pits on most sides (Fig. 1) and a thin glass film occurs as a small patch on one face. A few percent cavities, some spherical, others slit-like are present (Fig. 2) and some of these are crystal-lined. Following early allocations from chipping, the sample was sawn and broken for more detailed study in 1989.

PETROGRAPHY

No description of the groundmass has been published. It appears to be a crystalline impact melt containing angular mineral and lithic clasts, with the thin sections showing a fairly dark, fine-grained groundmass. It was described by Wolfe et al. (1981) as having a fine-grained granoblastic matrix.

A variety of small clasts were selected and studied by a group organized by L. Taylor (Neal et al., 1990e, d; 1992; Eckert et al., 1991b, c; Neal and Taylor, 1991). Neal et al. (1990d) and Eckert et al. (1991b) reported mineral composition data on four highlands

clasts (a troctolite, an anorthosite, a noritic anorthosite, and a gabbroic anorthosite) and a high-Ti basalt clast (Table 1; Fig. 3). Neal et al. (1990e) and Neal and Taylor (1991) reported whitlockite analyses from three of these clasts. Eckert et al. (1991b) interpreted the anorthosite ,57 as being monomict igneous with a striking cumulate texture and the noritic anorthosite ,36 also as igneous cumulate. They and Neal et al. (1992) interpreted the high-Ti basalt ,38 as being a plagioclase-rich polymict impact melt, and the troctolite ,42 similarly, because it has radiating acicular plagioclase in a melt matrix. The mineral compositions of four clast fall in the field of the

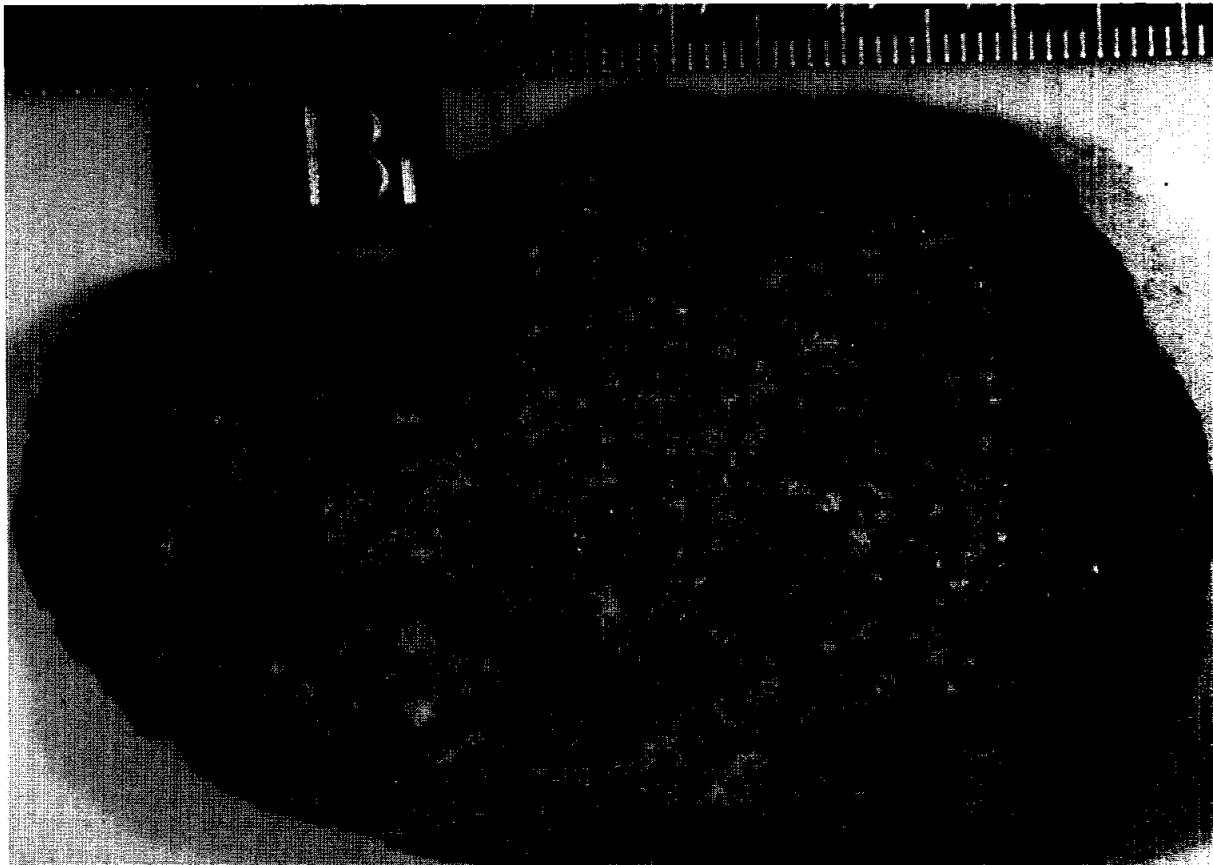


Figure 1: Unsawn face of butt end 73216,0, prior to breaking, showing patina and zap pits. Cube is 1 centimeter. S-89-46682.

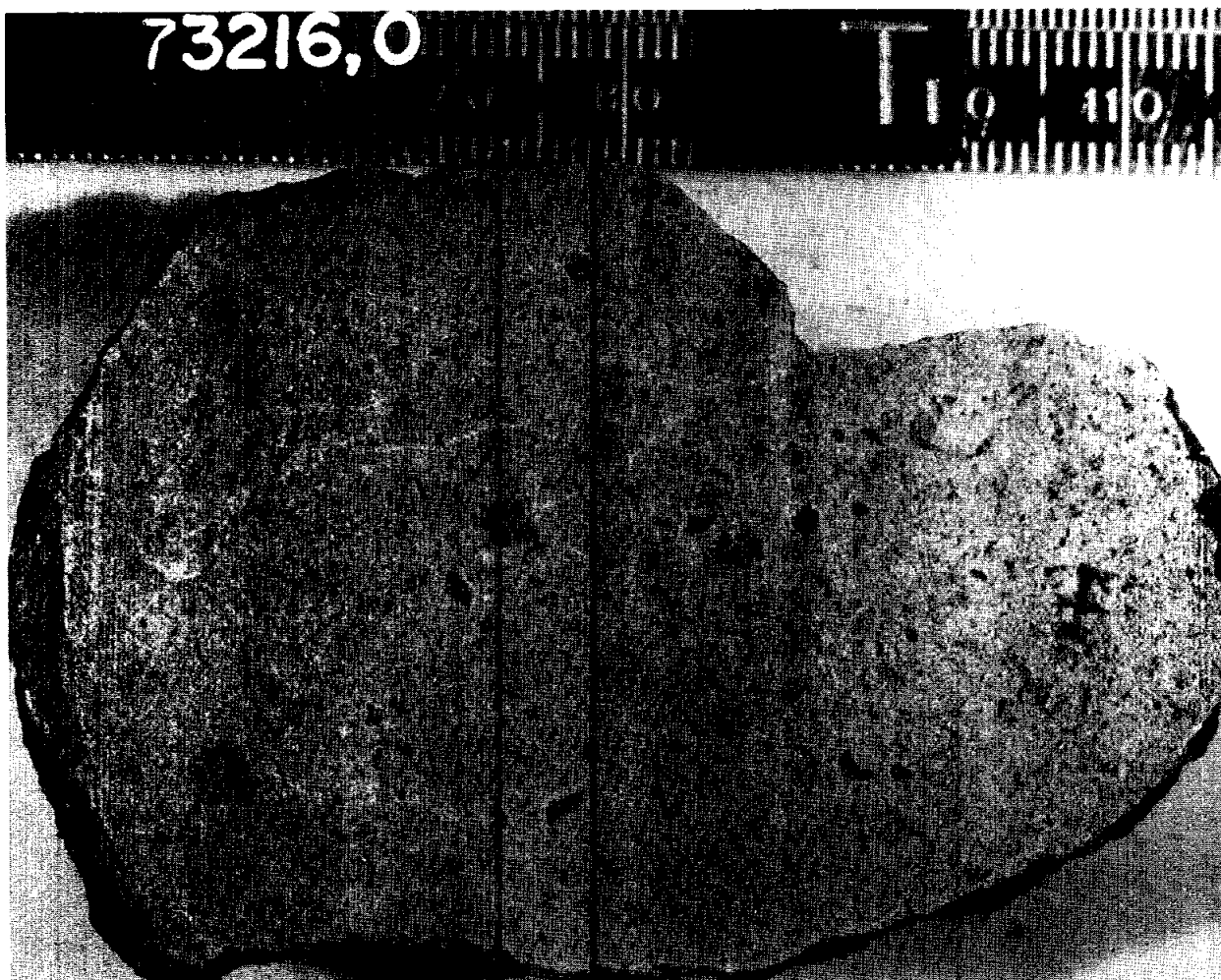


Figure 2: Sawn face of butt end 73216,0, prior to breaking. The surface shows the generally homogeneous nature of the groundmass, and the presence of small clasts and vesicles. Smallest scale divisions in millimeters. S-89-46683.

Mg-suite pristine rocks of the highlands; the anorthosite ,57 falls between the Mg-suite and the ferroan anorthosites. Neal et al. (1992) referred to the gabbroic anorthosite ,49 as a norite and to the noritic anorthosite ,36 as an anorthosite.

Studies of the whitlockites and numerical modeling of their origin are presented in Neal et al. (1990e) and Neal and Taylor (1991). The whitlockite compositions strongly influence the rock compositions, despite their small abundances. Models of metasomatism are preferred by the authors as being most consistent with the observations.

CHEMISTRY

Some chemical data by neutron activation for the five bulk clasts were presented (not tabulated) in Eckert et al. (1991b,c) and Neal et al. (1992). (Their sample numbers correspond with the petrographic descriptions as follows: ,36 =,66; ,38=,67; ,42=,68; ,49=,69; ,57=,70). All samples contain Ir and Au, including the anorthosite interpreted as monomict (pristine igneous) by Neal et al. (1992). They suggest the possibility of vapor transport of siderophiles during impact melting. This sample is the only one with low REEs and a positive Eu anomaly. The (noritic) anorthosite ,66 had matrix

chips included in the analyzed sample and has light rare earth elements about 30 x chondrites; it is feldspathic. The troctolite impact melt has light rare earth elements about 100 x chondrites with a negative Eu anomaly, as do the high-Ti basalt and the gabbroic anorthosite (norite), suggesting that they are polymict.

PROCESSING

Original allocations were minimal and made by picking. In 1989, the sample was sawn to produce two butt ends: ,0 (Fig. 1, 2) being about twice the size of ,30. End ,0 was broken into two subequal parts and ,30 into two non-equal parts.

During this processing samples of the five clasts were taken for petrographic and chemical work. End ,0 is now about 46 g and its broken subsample ,55 about 49 g. End ,30 is now about 40 g and its broken subsample ,45 about 9 g.

Table 1: Summary of mineral compositions in five clasts from 73216.
From Neal et al. (1990d).

	OLIVINE	PLAG.		PYROXENE			ILM	ARM
	Fo	An	Ab	Wo	En	MG#	MG#	MG#
73216,36	—	87-98	1-10	4-39	46-72	73-78	20-23	—
73216,38	68-71	83-95	4-13	4-39	46-76	74-80	22-26	—
73216,42	66-68	77-93	6-11	—————			23-31	45-48
73216,49	68-70	82-97	3-16	3-40	46-75	73-79	30-31	46-59
73216,57	—	93-98	1-7	3-41	46-73	74-79	—	—

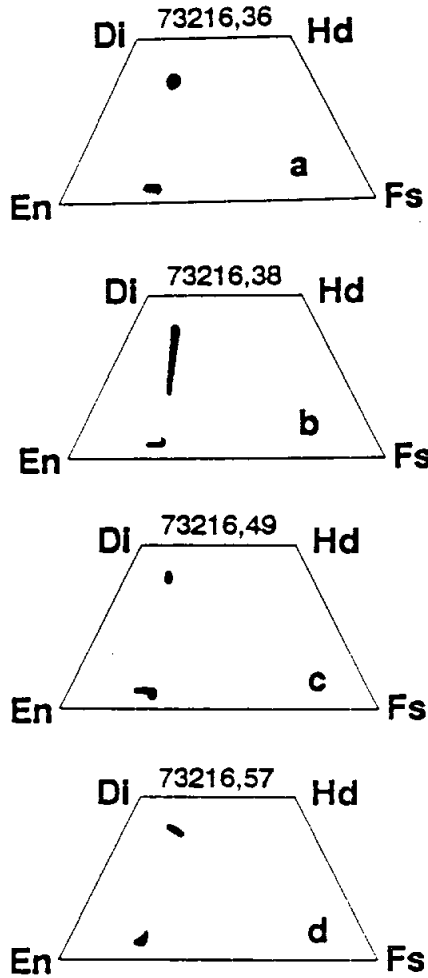


Figure 3: Pyroxene quadrilaterals for four clasts in 73216 a) noritic anorthosite ,36, b) high-Ti(?) impact melt ,38, c) gabbroic anorthosite. From Neal et al. (1990d).

73217

Impact Melt Breccia

St. 3, 138.8 g

INTRODUCTION

73217 is a tough impact melt; its bulk groundmass may be the low-K Fra Mauro basalt composition common at the Apollo 17 landing site but data is lacking. The rock contains a prominent white anorthosite clast (Fig. 1) as well as conspicuous and abundant fragments apparently derived from a plutonic gabbro with plagioclase, exsolved pyroxenes, and ilmenites. Brown silicic glass is conspicuous. Zircon clasts, probably part of the gabbro, have been dated as 4.36 Ga old. 73217 is medium gray (N5), subangular and blocky and has dimensions of 6.5 x 4.5 x 3.0 cm. The clast distribution is varied, with one face more rubbly with a

different lithology comprising 20% of the rock and consisting of clasts and matrix. Zap pits are irregularly distributed; the sample was collected from a half-buried position. Cavities and vesicles are uncommon except on the rubbly face. Allocations of 73217 have been made from chipped samples (e.g., Fig. 2).

PETROGRAPHY

Most published petrographic work has concentrated on the clasts and not on the general matrix of the breccia. Most of the thin sections consist of abundant mineral clasts in a fine-grained impact melt

groundmass (Fig. 3a). However, lithic clasts are present, particularly coarse granoblastic feldspathic impactites and the remains of a gabbro phase with feldspar, two pyroxenes (with complex exsolution) and ilmenite (Fig. 3b) with little host melt present. The rock and its clasts looks very similar to 73155. The augitic pyroxenes contain numerous inclusions very similar to those in 73155. Many mineral clasts have thin rims formed post-brecciation by overgrowth or reaction. Silicic brown glass is conspicuous particularly where the gabbro exists. Its petrographic nature is uncertain; in places it appears to be relict mesostasis of the gabbro, but

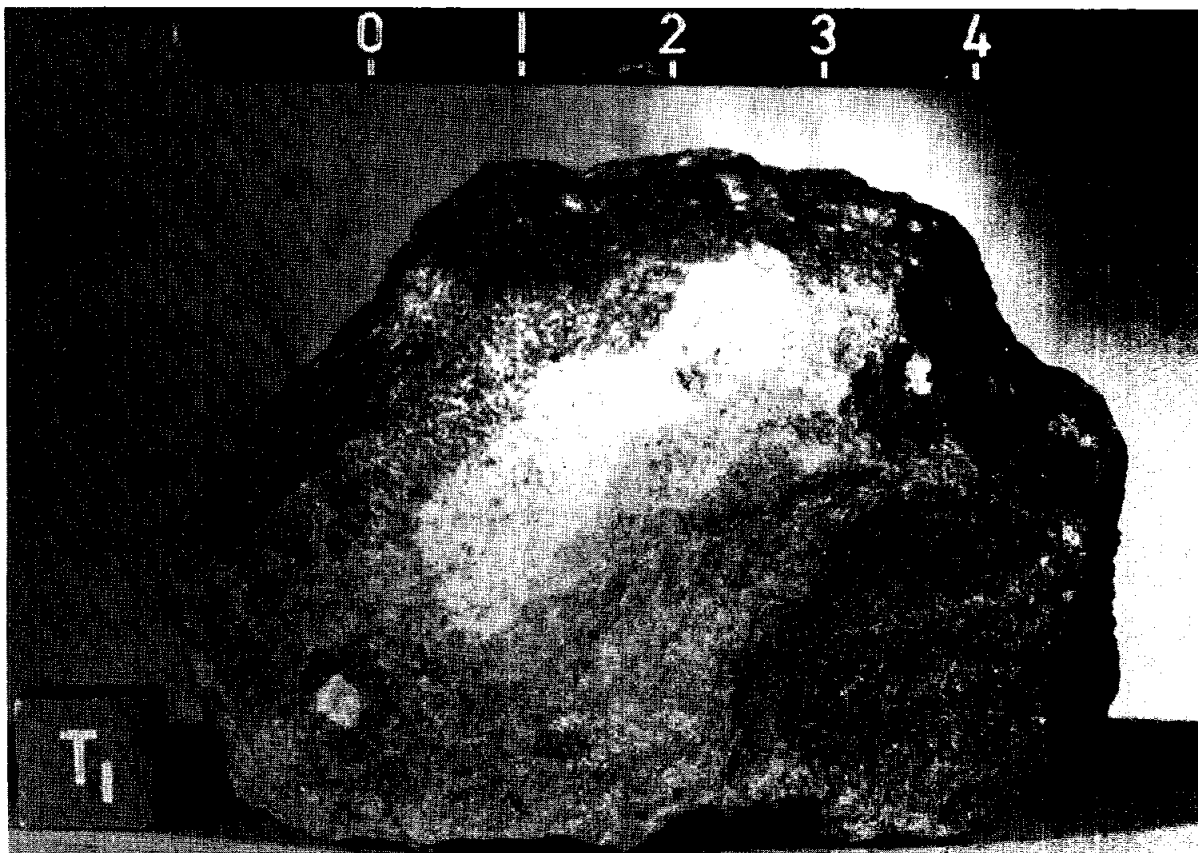


Figure 1: Pre-processing photograph of sample 73217. Scale divisions in centimeters. S-73-16786.

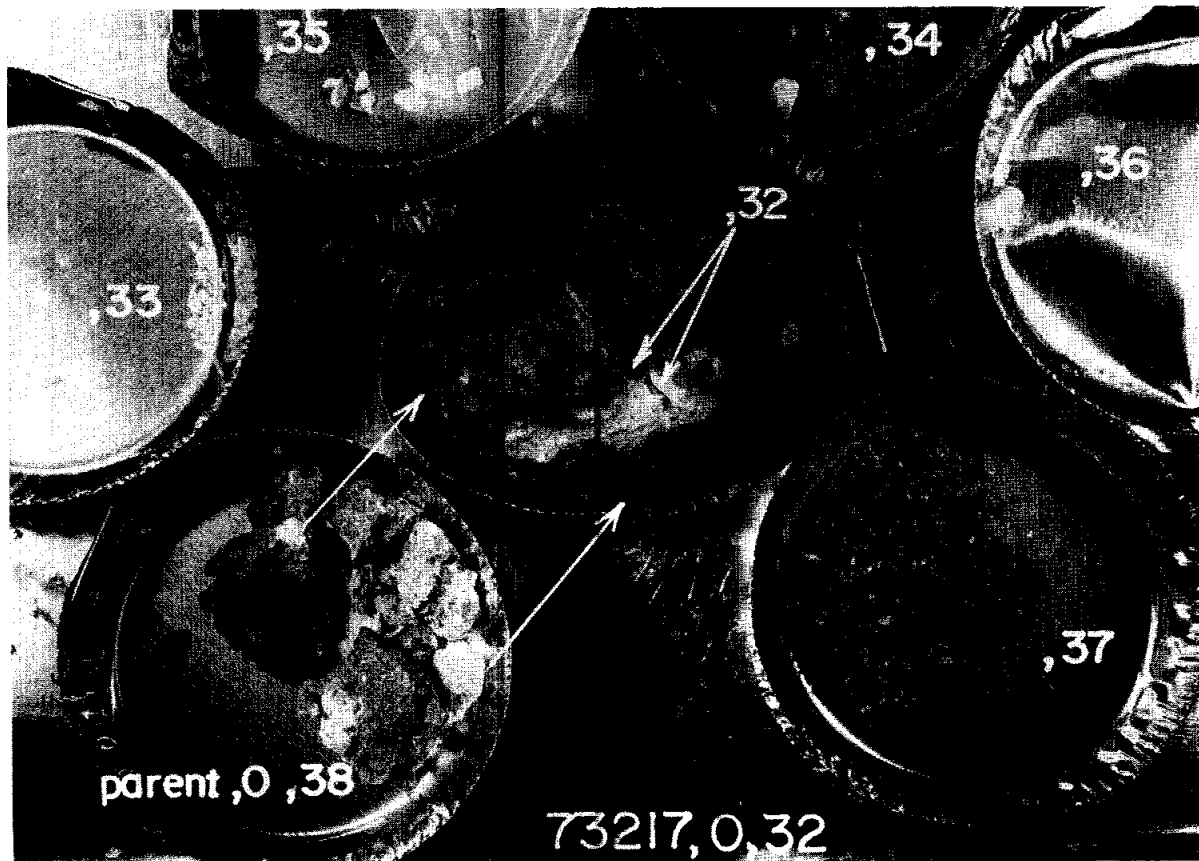


Figure 2: Processing to obtain the prominent white clast in 73217. S-81-25234

elsewhere appears to post-date the gabbro. Locally the brown glass is independent of the gabbro, and exists as patches in the groundmass, commonly with coronas, that might be residual melt or reacted clasts. The anorthosite clast is a finely ground, fairly pure cataclasized anorthosite with a broad reaction rim with the matrix.

Crawford (1975a, b) described the melt groundmass in 73217,15 as grading from a finely granulated aggregate of plagioclase with small amounts of pyroxene to a clear to pale brown glass. She noted an abundance of monomineralic clasts, particularly plagioclase, and proposed that the whole rock was generated by in situ partial melting of the clast population, which in turn had a plutonic, crustal origin. She described and depicted all phases, with microprobe data. The plagioclase is predominantly anorthitic (near An93), but grains

as sodic as An72 are reported. Common glass inclusions appear to be the same composition as the host anorthite. The sodic plagioclases show considerably more melting. Crawford (1975a, b) distinguished three classes of pyroxene: "plutonic" ortho- and clinopyroxenes with coarse exsolution lamellae; fine-grained pyroxene in coronas; and groundmass melt pyroxene. She diagrammed their compositions (Fig. 4). She interpreted the augite inclusions as products of exsolution during her proposed partial melting of the plutonic rock. The orthopyroxene exsolution suggests equilibration in the original plutonic environment at about 800 degrees centigrade. The brown glass is evolved (e.g. tabulated probe analysis of 81%SiO₂ and 4.4% K₂O) and its difference from bulk melt groundmass, she states, is the best evidence for the partial melting origin. Crawford (1975a) supposes

73217 to be the first convincing case supporting impact triggered partial melting on the Moon. She concludes that the product of such partial melting is not KREEP basalt.

Ishii et al. (1980, 1981, 1983) made a detailed study of the petrology and thermal history of 73217 from examination of the pyroxene crystallization sequence, pyroxene exsolution, and geothermometry. They used petrographic, microprobe, and x-ray diffraction methods. They too conclude that an early plutonic event was succeeded by a thermal event; however, they disagree with Crawford (1975) that the thermal event was one of in situ partial melting. Ishii et al. (1980, 1981, 1983) describe the breccia (as seen in 72317,26) as a calcic-plagioclase-rich breccia containing abundant angular mineral clasts which are rare lithic

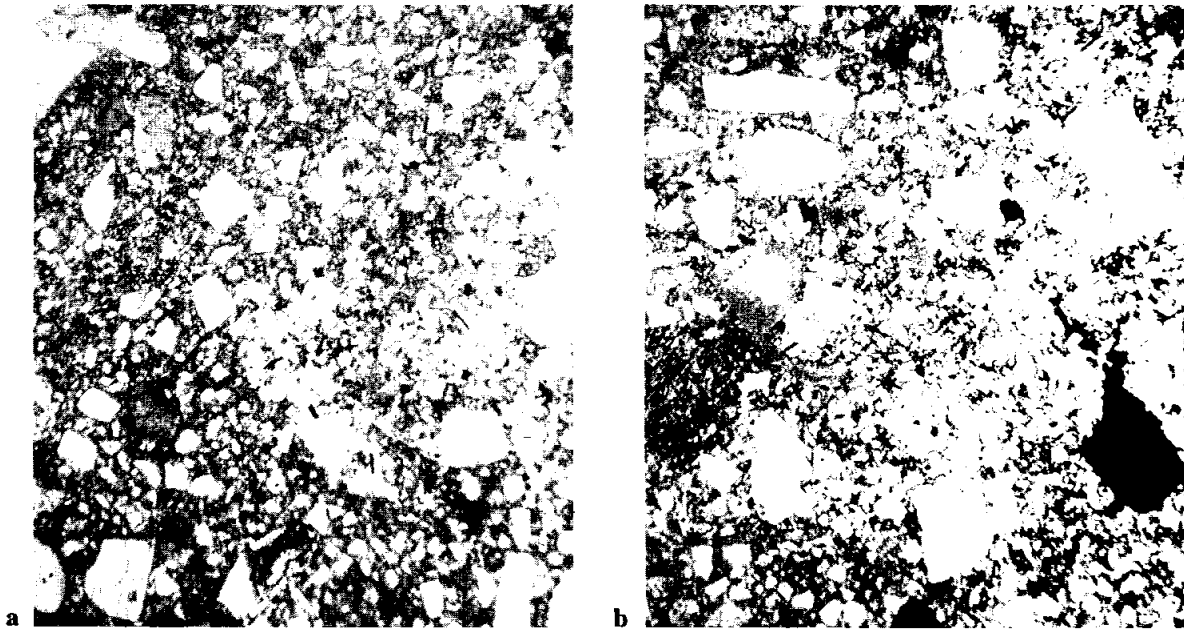


Figure 3: Photomicrographs of 73217,27. Plane transmitted light, fields of view about 2 mm wide. a) general view showing dark fine melt groundmass and abundant angular mineral clasts. b) view showing area dominated by gabbroic lithology with melt groundmass prominent only at top; remainder dominated by crushed gabbro, including plagioclase (white), ilmenite (black), and pyroxenes (pale to gray). Fuzzy phases are small patches of silicic brown glass.

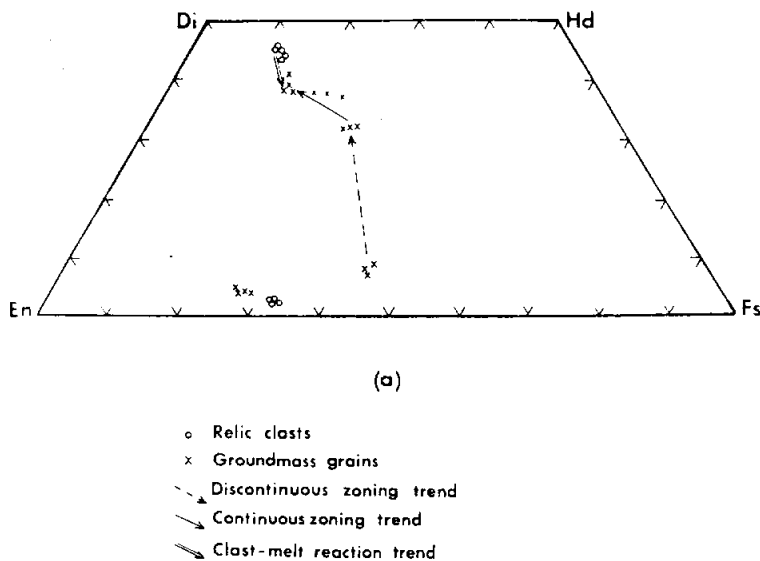


Figure 4: Pyroxene quadrilateral. (Crawford, 1975a).

clasts in a fine-grained, partially glassy matrix. It consists of two domains with a gradational boundary. Domain A contains coarse orthopyroxene clasts, whereas domain B contains coarse pigeonite clasts. The pyroxene trends are analogous to early (A) and late (B) fractionation stages of terrestrial intrusions. Some other small clasts are also described: a gabbroic lithic clast, a troctolitic lithic clast, and dusty augite clasts. The most detailed information on the pyroxenes is presented in Ishii et al. (1983), including tabulated and diagrammed microprobe data (Figs. 5-8), and crystallographic information (Table 1) including precession photographs. Minor element compositions for both high-Ca and low-Ca pyroxenes in both breccia domains vary continuously with Mg^1 . The optical and X-ray diffraction studies demonstrate a great variety of exsolution textures, but individual pyroxenes show relatively simple exsolution. None of pyroxene, plagioclase, or ilmenite

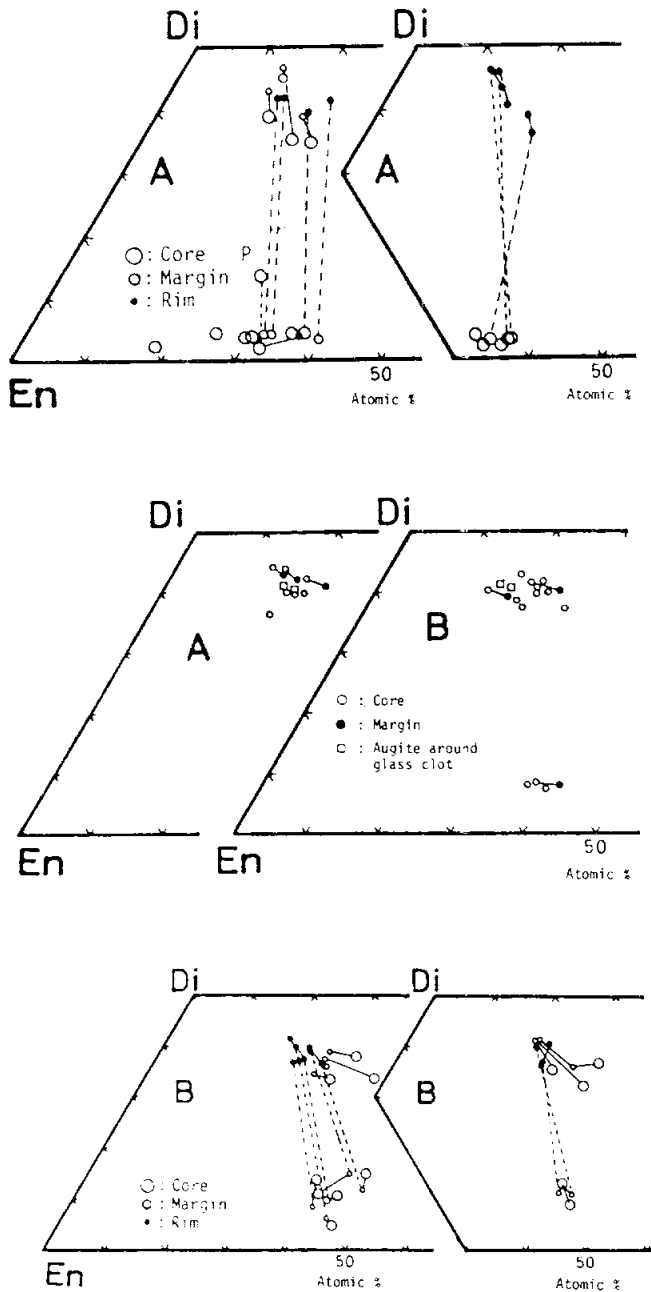


Figure 5: Pyroxene quadrilaterals. (Ishii et al., 1983)

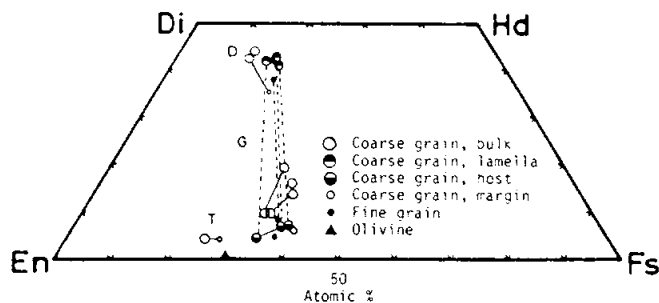


Figure 6: Pyroxene quadrilaterals. (Ishii et al., 1983)

compositions in domains A and B overlap. Ishii et al. (1983) conclude that both domains could be derived from a single pluton, A at the bottom (early, 1100 degrees C or so) and B at the top (later, a few tens of degrees lower temperature). (The troctolitic, etc., lithic clasts are unrelated to this sequence).

However, the pyroxene crystallization trend (Figs. 5, 6, 9) is so complicated that at least two or more episodes are required: an early plutonic/hypabyssal event, and a later thermal/annealing event. They propose a first event forming layered bodies, a second event mixing mineral only in the upper part of a pluton (B) and a third event that mixed lower (A) and upper (B). During the latter event temperatures rose to over 1000 degrees C and the rock was partially melted. The precise nature of this latter event is not clarified by Ishii et al. (1983).

Warren et al. (1982a, b) described the prominent white clast, estimated to weigh about 1.7 g. The boundary between the clast and the groundmass is extremely diffuse. The thin section studied (41) includes the boundary area. The central, matrix-free part is almost entirely plagioclase, whereas the diffuse area, presumably contaminated with matrix, contains about 40% pyroxene. The central anorthosite is fine-grained and cataclased. The plagioclase is $An_{90.2-95.4}$ with a mean of $An_{93.3}$. The pyroxene, about $En_{72}Wo_4$, may not even be part of the anorthosite. Warren et al. (1982a) refer to the clast as "quasi-pristine," i.e., it is likely to be essentially pristine but to have undergone subtle changes.

Compston et al. (1984a) described and depicted zircon grains and their associated assemblages from 73217, providing zircon microprobe analyses. They describe the host as a clast that has a granitic melt composition that contains seriate mineral clasts of anorthite, augite, hypersthene, ilmenite, and zircon. The zircons are inferred to

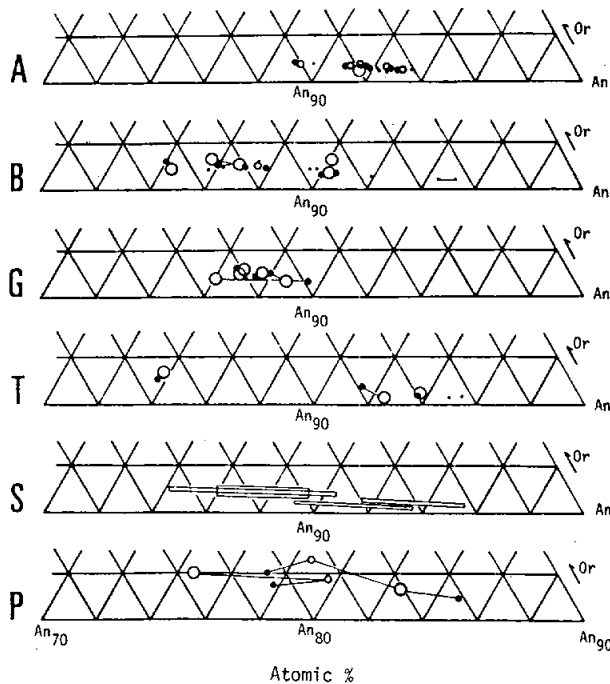


Figure 7: Plagioclase compositions. (Ishii et al., 1983)

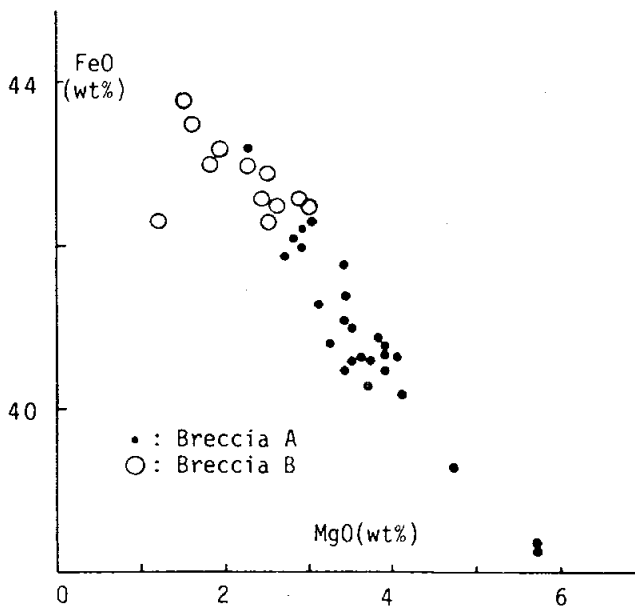


Figure 8: Ilmenite compositions. (Ishii et al., 1983)

be an integral part of the gabbroic igneous assemblage, one zircon being attached to ilmenite. (The zircons were used for ion-microprobe U-Pb isotopic studies). The zircons are anhedral and have evidence of resorption, presumably during the melting of the matrix, and have no overgrowths.

Bersch et al. (1988, 1991) reported precise minor element and major element compositions for some pyroxene grains in 73217,41; the pyroxene is most likely to derive from clasts in the matrix and not from the anorthosite itself.

CHEMISTRY

The only chemical analyses are two splits of the anorthosite clast, one at least of which is rather impure (Warren et al., 1982a, b). A single chip was handpicked to separate as much pure white clast as possible from groundmass. The analyses are presented in Table 2. The purer handpicked part appears to be a true anorthosite, as also indicated by the thin section. The pristine nature of the sample is ambiguous on the basis of Au at least, although Ir and Ni are both low. However, the impure separate has no more Au or Ni than the more pure separate. Possibly there has been some diffusion of elements across the boundary with the groundmass. The rare earth elements, while low, have a KREEP pattern (Fig. 10), also indicating some contamination. The sample, on the basis of plagioclase compositions and incompatible element abundances, is not an alkali anorthosite, but is at least close to the established range for ferroan anorthosites.

RADIOGENIC ISOTOPES AND GEOCHRONOLOGY

Four zircons were analyzed for U-Pb isotopes using high resolution ion microprobe techniques (Compston et al., 1984a, b) (Table 3). The zircons were analyzed in thin sections, and are probably part

Table 1: Crystallographic data for pyroxenes in 73217. (Ishii et al., 1983)

Group‡	Crystal number	Pyroxenes	a(Å)	b(Å)	c(Å)	β (°)	Space group	Analysis* number	Crystal† stage	Remarks
Ia	A 12	Host Augite	9.74	8.91	5.25	106.11	<i>C2/c</i>	19 Aug	Plutonic	50
		(001) Pigeonite	9.74	8.91	5.22	108.00	<i>P2₁/c</i>			20 (volume ratio)
		(100) Orthopyroxene	18.29	8.91	5.24	—	<i>Pbca</i>			20
IIa	K 13	Host Orthopyroxene	18.27	8.88	5.21	—	<i>Pbca</i>	23 Pig	Plutonic	Kintoki-san type
		(100) Augite	9.70	8.88	5.25	105.07	<i>C2/c</i>			
Ib	A 06	Host Augite	9.75	8.93	5.26	105.6	<i>C2/c</i>	05 Aug	A2	—
		(100) Orthopyroxene	18.4	8.9	5.2	—	<i>Pbca</i>			
IIb	B 10	Host Orthopyroxene	18.31	8.88	5.22	—	<i>Pbca</i>	13 Opx	A2	Bushveld type
		(100) Augite	9.73	8.88	5.22	105.40	<i>C2/c</i>			
III	A 11	Host Augite	9.74	8.94	5.26	106.29	<i>C2/c</i>	16 Aug	B1	Chemical zoning
		(001) Pigeonite	9.74	8.94	5.24	108.85	<i>P2₁/c</i>			

of the gabbroic assemblage (one is attached to ilmenite) whose exsolved pyroxenes are so prominent as clasts. The zircons show zoning that is visible microscopically and confirmed by electron- and ion-probe data. All four crystals show little loss of radiogenic Pb, and give U-Pb ages that are within 10% of concordance at $4356 \pm 23, -14$ Ma. (Fig. 11a, b). This age presumably is that of the igneous event that produced the gabbro, or whatever parent assemblage the zircons reflect. Two of the crystals show evidence of initial radiogenic lead that evolved in a source with $\mu = 2000$. The lower intersect on the concordia diagram is earlier than 1000 Ma, showing that lead loss was not a very recent event. However, the common 3900 Ma lunar event(s) does not show up in this zircon data.

PROCESSING

73217 has never been sawn. In 1973 chips were removed from one end (apparently typical rock) for early allocations including thin sections from potted butt ,11. No samples were taken of the rubbly lithology or of the white clast. 73217 was designated a posterity sample, hence temporarily denied

further processing. Nonetheless, eventually further chipping was carried out (1982) to obtain samples of the prominent white clast (Fig. 2) for chemical and petrographic studies. Further thin sections were cut from a chip (,10) that had been separated from adjacent ,11 in the original processing.

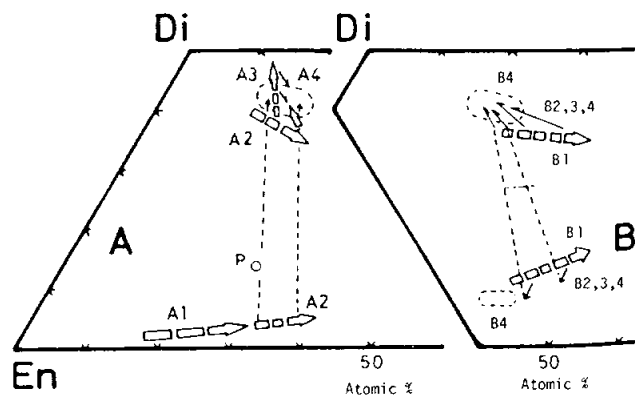


Figure 9: Summary of pyroxene crystallization trends. (Ishii et al., 1983).

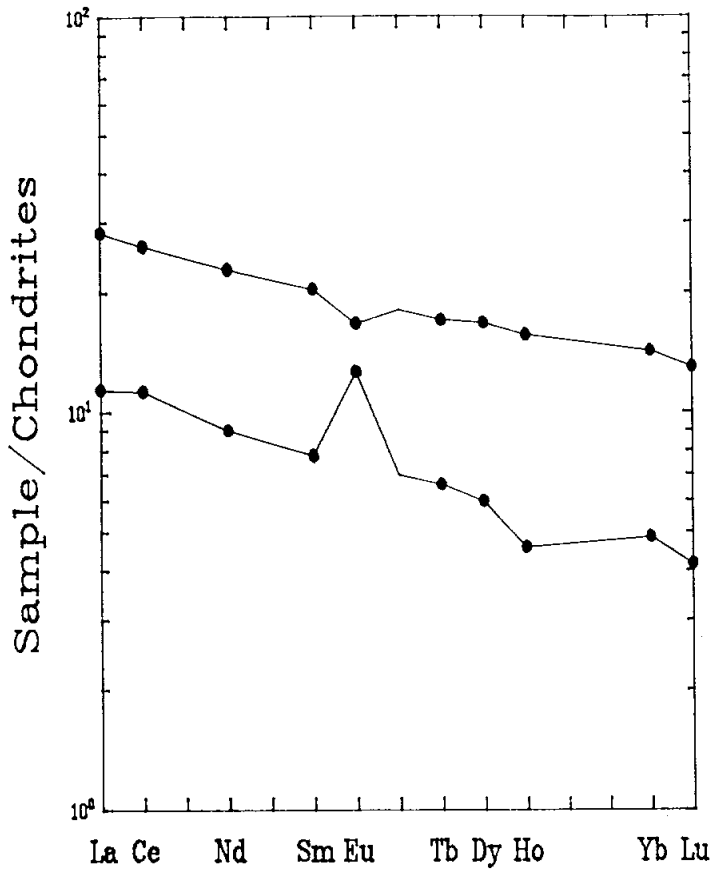


Figure 10: Rare earth elements in pure (lower) and impure (upper) anorthosite samples from prominent white clast in 73217 (from data of Warren et al., 1982a,b).

Table 2: Chemical analyses of pure (,35a) and impure (,35b) anorthositic samples from prominent white clast in 73217. (Warren et al., 1982 a, b).

	,35a	,35b
Split		
wt %		
SiO ₂	44.9	45.8
TiO ₂	.07	.25
Al ₂ O ₃	35.0	31.6
Cr ₂ O ₃	.020	.047
FeO	.77	2.67
MnO	.015	.047
MgO	0.75	2.1021.0
CaO	18.5	16.8
Na ₂ O	0.67	0.73
K ₂ O	0.04	0.115
P₂O₅		
ppm		
Sc	1.91	4.7
V		
Co	5.4	8.9
Ni	6.4	6.8
Rb		7.3
Sr		
Y		
Zr	121	240
Nb		
Hf	1.42	3.4
Ba	190	240
Th	1.10	2.65
U	0.40	0.69
Cs		0.56
Ta	0.16	0.71
Pb		
La	3.75	9.3
Ce	9.9	23.0
Pr		
Nd	5.4	13.7
Sm	1.41	3.69
Eu	0.87	1.15
Gd		
Tb	0.31	0.80
Dy	1.89	5.3
Ho	0.32	1.09
Er		
Tm		
Yb	0.97	2.84
Lu	0.141	0.44
Li		
Be		
B		
C		
N		
S		
F		
Cl		
Br		
Cu		
Zn	0.47	2.2
ppb		
Au	2.27	2.06
Ir	0.04	0.180
I		
At		
Ga	7200	8200
Ge	53	85
As		
Se		
Mo		
Tc		
Ru		
Rh		
Pd		
Ag		
Cd	124	1040
In		
Sn		
Sb		
Te		
W		
Re	<0.20	<0.35
Os		
Pt		
Hg		
Tl		
Bi		

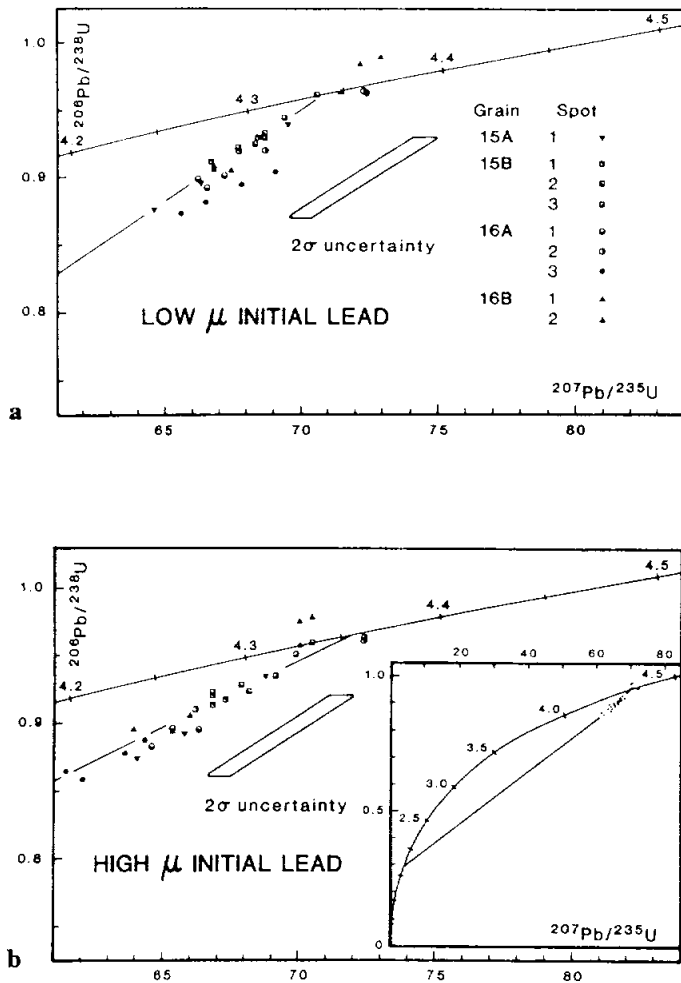


Figure 11: Concordia diagram showing analyses of 73217 zircons, corrected assuming evolution of initial lead in a low u source (a) and a high u source (b) (Compston et al., 1984a). Each point represents the mean of 10 observations of the isotopic composition. In most cases, three such determinations were made at a single spot. Line in a) is reference line for $^{207}\text{Pb}/^{206}\text{Pb}$ age of grains 15A, 15B, and 16B, 4340 Ma. Age of 16A is higher. Line in b) is best fit with intercepts of 4356 +23, -14 Ma, and 1680 +/- 580 Ma.

Table 3: Summary of ion microprobe data for 73217 zircons. (Compston et al., 1984a).

Spot	U*	Th*	Pb*	$^{232}\text{Th}/^{238}\text{U}$	$f_{\text{Pb}}\dagger$	$^{208}\text{Pb}_s/^{206}\text{Pb}_s$	$^{208}\text{Pb}_s/^{232}\text{Th}$	$^{207}\text{Pb}_s/^{206}\text{Pb}_s$	$^{206}\text{Pb}_s/^{238}\text{U}$	$^{207}\text{Pb}_s/^{235}\text{U}$
1	300 ± 10	103 ± 4	378 ± 20	0.333 ± 9	0.10 0.32	0.0852 ± 1	0.225 ± 4	0.5370 ± 8 0.5335 ± 6	0.903 ± 18 0.900 ± 18	66.8 ± 1.5 66.2 ± 1.4
1	307 ± 9	215 ± 6	415 ± 12	0.702 ± 3	0.04 0.37	0.1766 ± 6	0.231 ± 3	0.5338 ± 9 0.5294 ± 17	0.918 ± 5 0.917 ± 2	67.6 ± 0.5 67.0 ± 0.2
2	329 ± 8	240 ± 5	456 ± 14	0.728 ± 3	0.03 0.15	0.1818 ± 3	0.234 ± 3	0.5346 ± 7 0.5329 ± 12	0.938 ± 11 0.937 ± 11	69.2 ± 0.7 68.9 ± 0.8
3	396 ± 11	323 ± 8	551 ± 15	0.816 ± 2	0.01 0.00	0.2023 ± 6	0.231 ± 2	0.5345 ± 10 0.5319 ± 31	0.931 ± 7 0.936 ± 8	68.6 ± 0.5 68.6 ± 0.9
1	154 ± 6	136 ± 4	209 ± 8	0.885 ± 11	0.10 0.60	0.222 ± 6	0.224 ± 4	0.5394 ± 25 0.5320 ± 24	0.896 ± 2 0.891 ± 4	66.6 ± 0.3 65.4 ± 0.5
2-1	165	138	229	0.838	0.33 1.30	0.2084	0.228	0.5420	0.919	68.7
2-2	174 ± 4	168 ± 8	256 ± 7	0.971 ± 21	0.50 0.00	0.2355 ± 5	0.233 ± 1	0.5429	0.910	66.2
2-3								0.5453 ± 8	0.962 ± 1	72.3 ± 0.1
3	141 ± 10	137 ± 10	194 ± 14	0.977 ± 3	0.06 2.10	0.256 ± 3	0.233 ± 3	0.5455 ± 5 0.5493 ± 23	0.962 ± 1 0.888 ± 8	72.4 ± 0.1 67.2 ± 0.8
1	356 ± 49	213 ± 30	469 ± 64	0.597 ± 9	0.05 1.00	0.1547 ± 7	0.235 ± 3	0.5225 ± 26 0.5371 ± 22	0.872 ± 6 0.905 ± 1	62.8 ± 0.7 67.0 ± 0.2
2	373 ± 31	228 ± 18	532 ± 45	0.610 ± 3	0.05 0.80	0.1571 ± 8	0.252 ± 4	0.5251 ± 37 0.5353 ± 20	0.899 ± 3 0.978 ± 8	65.1 ± 0.6 72.2 ± 0.4
								0.5251 ± 33	0.970 ± 7	70.2 ± 0.1

73218

Impact Melt Breccia

St. 3, 39.7 g

INTRODUCTION

73218 is a greenish-gray gray (5GY 6/1) angular breccia (Fig. 1). It is a fine-grained impact melt with small clasts. Its chemical composition might be similar to the common low-K Fra Mauro basalt impact melts common at the site, but chemical data is lacking and it was originally described as anorthositic. The sample is tough, crystalline, and homogeneous, with dimensions of 4 x 3 x 2.5 cm. The matrix is dominated by plagioclases, although small mafic crystals are also visible macroscopically. Several surfaces are fresh fractures; the other side is rounded with some zap pits with pale gray glass. A few small drusy cavities (less than 1 mm) are present. Splits were taken from 73218 by chipping, mainly of matrix. A composite potted butt

from 4 particles was used to make 3 thin sections. No data has been published.

PETROGRAPHY

The thin sections of the four particles show a fine-grained impact melt groundmass (Fig. 2), with mineral and lithic clasts. The groundmass has plagioclase needles and ilmenite needles, demonstrating growth from a melt. The mineral clasts are predominantly plagioclase and olivine, some of the smaller of which have coronas. The larger clasts include recrystallized anorthositic breccias, feldspathic impactites, a coarse anorthosite with a metamorphic texture, and a single grain of multiply-exsolved and twinned pyroxene (presumably an inverted pigeonite).

PROCESSING

Most of 73218 is preserved in the parent ,0 (now 35.8 g). One large piece (,10; 1.97 g) was allocated, but no data have been published. Twelve small chips, labelled A-L and predominantly matrix, were chipped from varied locations. Eight are preserved as ,8. The others (A, typical matrix; B, olivine rich?; H, anorthositic plus typical matrix; and I, with brown mineral clasts were used to make make serial thin sections ,26-,28.

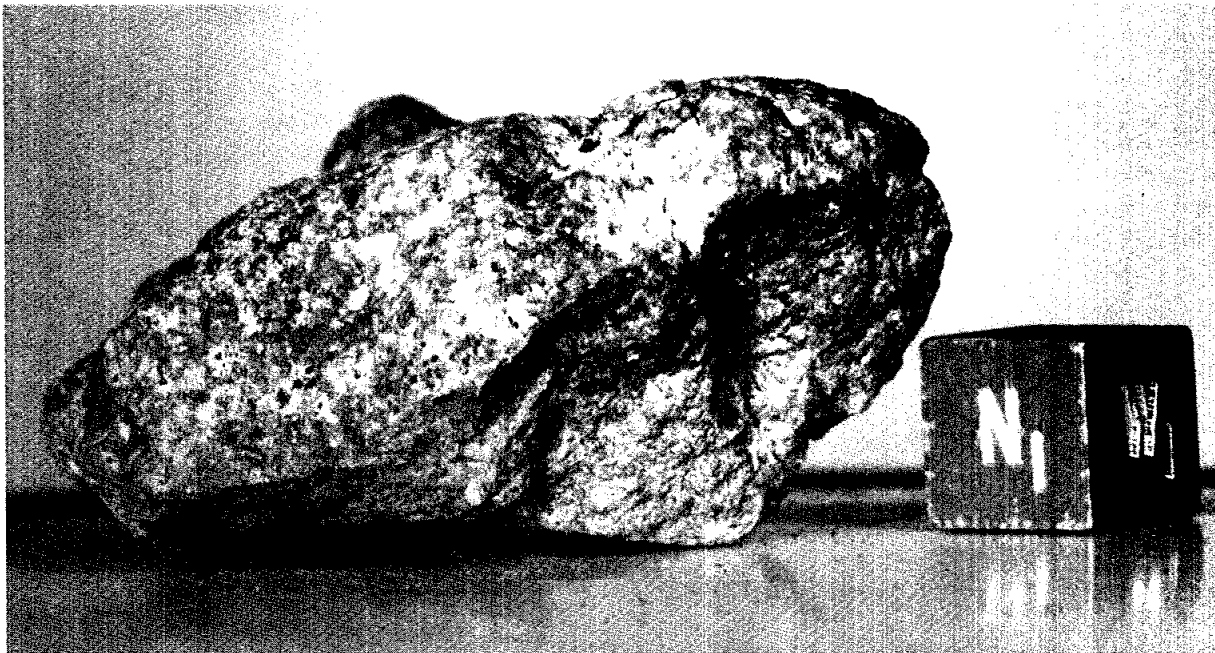


Figure 1: 73218, showing patina and zap pits on top left surface, broken surfaces below. Cube is 1 centimeter. S-73-24909.

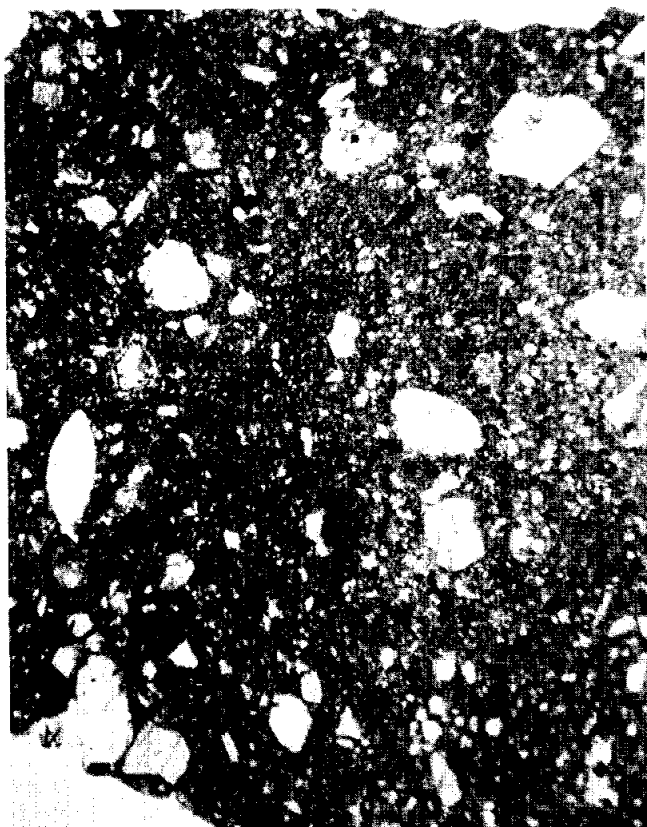


Figure 2: Photomicrograph of typical groundmass in 73218,26. Clasts are seriate, and dominantly plagioclases. Plane transmitted light, field of view about 2 mm wide.

73219**High-Ti Mare Basalt
St. 3, 2.88 g****INTRODUCTION**

73219 is a medium dark gray (N4), small blocky sample (Fig. 1) that is a high-titanium mare basalt, the only mare basalt as an individual rock fragment from the South Massif or landslide. It is olivine microporphyratic. The sample is coherent and measures 1.5 x 1.3 x 1.0 cm. It is holocrystalline (macroscopically microporphyratic, with obvious peridotite-green olivine), homogeneous, and with a hackly surface on a very fine scale. It has many zap pits on two surfaces, with few to none on others. There is about 1% of tiny drusy cavities, with the largest 0.2 mm. Small (2-4 mm) patches of dark glass suggest that 73219 might be locally vitrophyric. Five chips were taken (four from a single location) for one allocation.

PETROGRAPHY

Sample 73219 is a fine-grained olivine-bearing high-titanium mare basalt (Fig. 2). It was described with microprobe analyses of its mineral phases by Warner et al. (1975b, c, 1976a, b, 1978f). The microprobe analyses are diagrammed as Figure 3. Warner et al. (1976a) reported a mode of 3.5% olivine, 42.1% pyroxene, 30.5% plagioclase, 2.5% silica, 19.6% ilmenite, 1.0% armalcolite, and 0.6% of other (mainly opaque) phases. They described the groundmass as consisting of irregular titanite crystals separated by intrafasciculate pyroxene-plagioclase intergrowths, with the olivines being subequant and hollow or skeletal. The oxides include common prismatic, ilmenite-mantled armalcolite, and ilmenite microphenocrysts with an armalcolite morphology.

CHEMISTRY

A bulk analysis by neutron activation techniques was reported by Warner et al. (1975b, c, 1976a) and by Laul et al. (1975b). It is reproduced here as Table 1 and the rare earth elements are plotted as Figure 3. The sample is unexceptional, and its slightly high alumina (compared with other Apollo 17 basalts) might merely reflect unrepresentative sampling in that the analyzed mass was only 258 mg.

PROCESSING

Five chips, four from a single location, were combined for the single allocation in 1974 from which a thin section and the chemical analyses were produced.

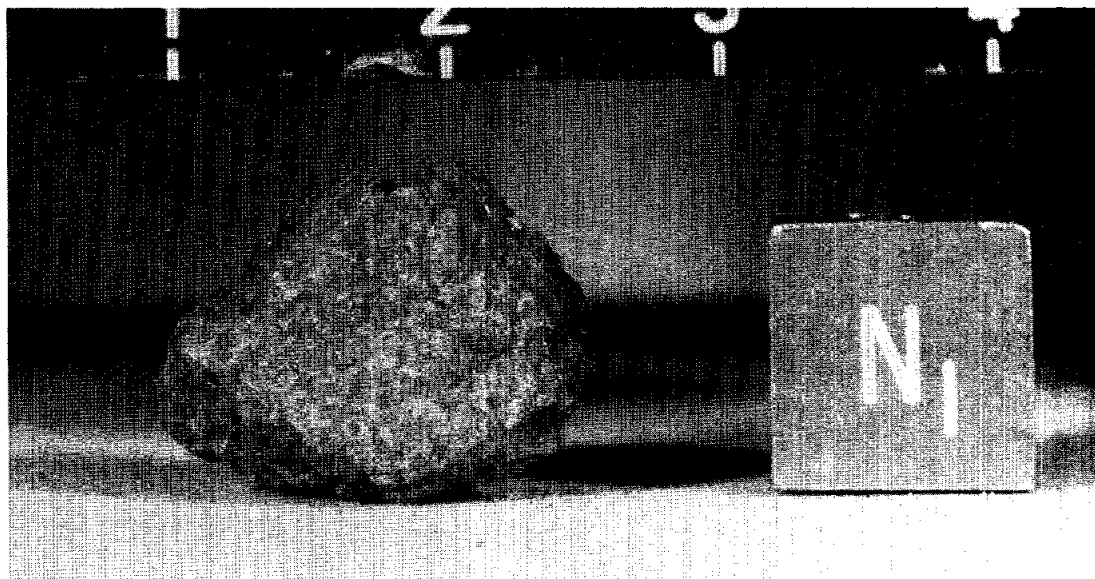


Figure 1: 73219, pre-processing. Cube and scale divisions are 1 centimeter. S-73-16963.



Figure 2: Photomicrograph of typical groundmass in 73219,26. Clasts are seriate, and dominantly plagioclases. Plane transmitted light, field of view about 2 mm wide.

Table 1: Chemical analysis of 73219, 258 mg whole-rock sample. (Warner et al., 1976a; Laul et al., 1976b)

Split	,1
wt %	
SiO ₂	12.4
TiO ₂	10.0
Al ₂ O ₃	0.360
Cr ₂ O ₃	19.3
FeO	0.244
MnO	7.0
MgO	11.2
CaO	0.33
Na ₂ O	0.04
K ₂ O	
P ₂ O ₅	
ppm	
Sc	80
V	90
Co	16.6
Ni	
Rb	
Sr	
Y	
Zr	
Nb	
Hf	7.2
Ba	
Th	
U	
Cs	
Ta	1.4
Pb	
La	4.7
Ce	20
Pr	
Nd	20
Sm	7.8
Eu	1.66
Gd	
Tb	2.1
Dy	13
Ho	
Er	
Tm	
Yb	7.5
Lu	1.1
	(1)

References and methods:
 (1) Laul et al. (1975b);
 Warner et al.,(1975b);INAA

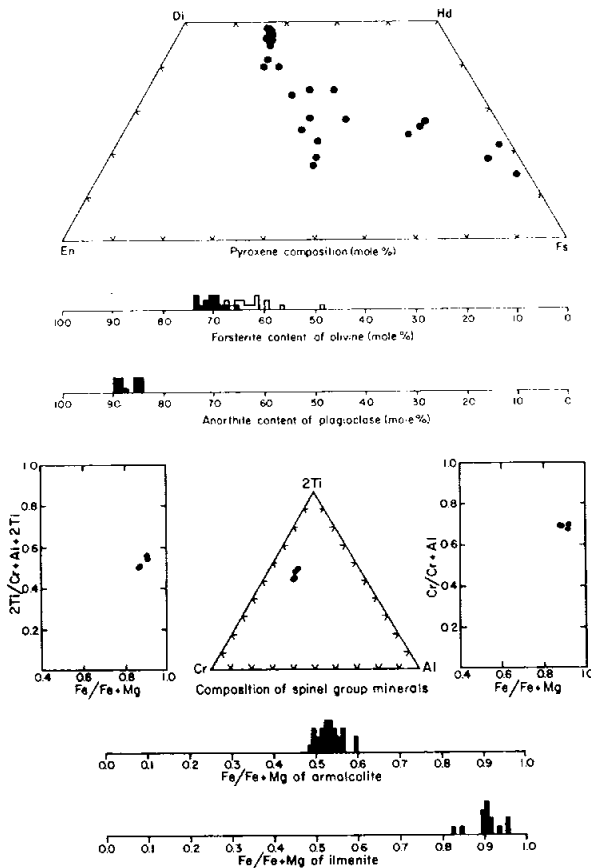


Figure 3: Rare earth elements in 73219; data of Warner et al. (1976a) and Laul et al. (1976b).

73225**Impact Melt Breccia (?)****St. 3, 3.66 g****INTRODUCTION**

73225 is a light gray (N5) breccia that is equant (Fig. 1). It is tough, crystalline, homogeneous, and originally described as meta-polymict breccia. It contains some larger plagioclases and is most likely to be an impact melt breccia; possibly a granoblastic impactite. The sample is 1.7 x 1.5 x

1.3 cm, and all its surfaces appear to be fracture surfaces. It has a few dark glass lined zap pits, possibly on all surfaces, and abundant vugs with projecting crystals of plagioclase. A thin vein of black glass penetrates the rock. 73225 was picked from a regolith sample collected from the upper part of a trench wall. It has never been subdivided or allocated.

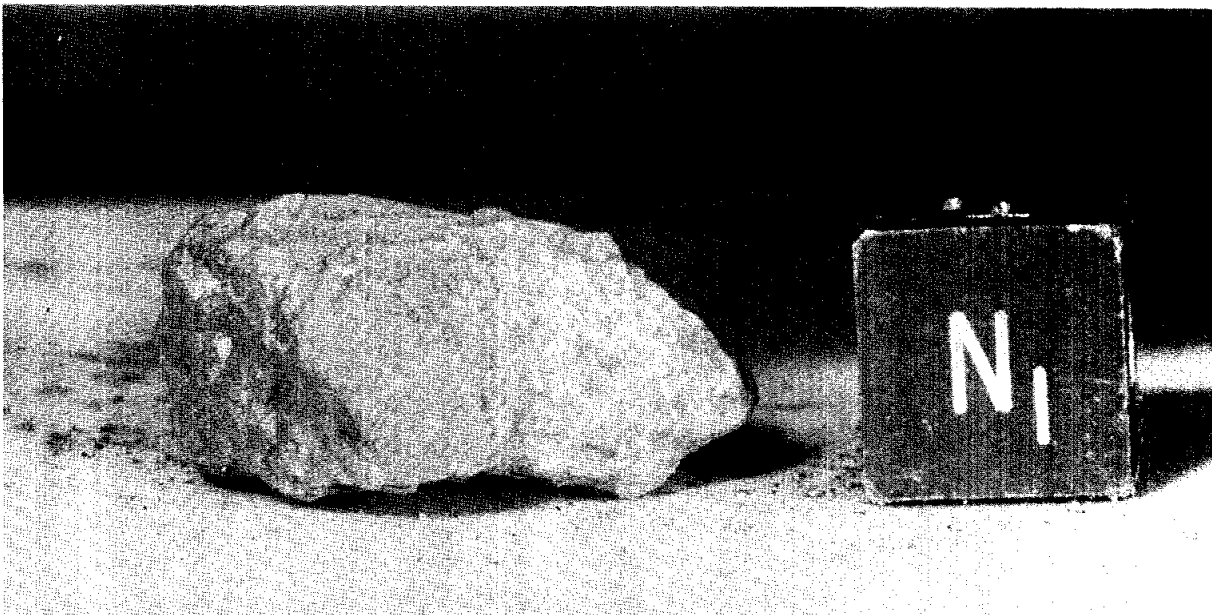


Figure 1: 73225, showing dust-covered rock. Cube is 1 centimeter. S-73-21764

73235**Aphanitic Impact Melt Breccia
St. 3, 878.3 g****INTRODUCTION**

73235 is a clast-rich aphanitic melt breccia with a variety of mineral and lithic clasts. It is similar in petrography and chemistry to the aphanitic melts of Boulder 1, Station 2 and other Station 3 aphanites. It has about 75% dense matrix, 10% lithic clasts larger than a few millimeters across, and 15% mineral clasts larger than about 0.5 mm. Poorly-defined Ar-Ar plateaus suggest an age of about 3.91 Ga. The sample was collected on the rim of a 10-m crater, near 73255. It is tough with several shallow fractures, homogeneous, and medium light gray (N6) with mottling. It is subangular to rounded (Fig. 1) and 12 x 10 x 8 cm. None of the surfaces are fresh.

There are many zap pits, with varied glass linings from dark gray to almost colorless, on most surfaces. Vugs and cavities are not apparent. The sample was sawn to produce a slab (Fig. 2); extensive allocations were made from the slab and one of the butt end pieces (.8).

PETROGRAPHY

73235 has a dense, aphanitic melt groundmass with a seriate clast distribution (Figs 3a, b), very similar to other South Massif aphanitic impact melt breccias. The fine-grained groundmass consists mainly of plagioclase and pyroxene with some opaque oxide phases. Lithic clasts include granoblastic

feldspathic impactites with a variety of grains sizes, shocked anorthosites, and cataclasized troctolites, and norites. Some ophitic/subophitic melt particles, probably of impact origin, and glassy/granitic fragments (Fig. 3a) are present. Many clasts are cataclasized and strung out as schlieren within the dense matrix (Fig. 3c). One prominent white clast is a cataclasized troctolite (Fig. 3d) that was large enough for separate allocation (see below). Mineral clasts include plagioclase, olivine, pyroxene, and rare pleonaste spinels. Shock features vary from non-existent to strong and most grains are at least a little rounded by resorption.

Brown et al. (1974) and Hodges and Kushiro (1974a, b) provided brief descriptions of 73235. Brown et al. (1974) described it as a polygenetic microbreccia with calcic plagioclase (An₉₄), zoned Mg-olivines (Fo₈₇₋₈₁ with low Cr₂O₃ that relates them to the 76535 allivalite), and bronzite. They also noted patches of potassic rhyolite and purple Cr-pleonastes. Hodges and Kushiro (1974a, b) described the sample as being a fine-grained, dark brown, slightly metamorphosed breccia with numerous mineral and lithic clasts. The mineral clasts exhibit a wide range of shock features. Hodges and Kushiro (1974a,b) provide some microprobe data for pyroxenes and olivines (Fig. 4) and spinels, noting that pyroxenes include grains zoned from pigeonite to subcalcic augite and that some augite show thin exsolution lamellae. The olivine clasts are more magnesian than those in the lithic clasts. The lithic clasts are described as relatively unshocked, consisting predominantly of gabbroic to anorthositic rocks, and lacking mare basalts. The clast population indicates a wide range

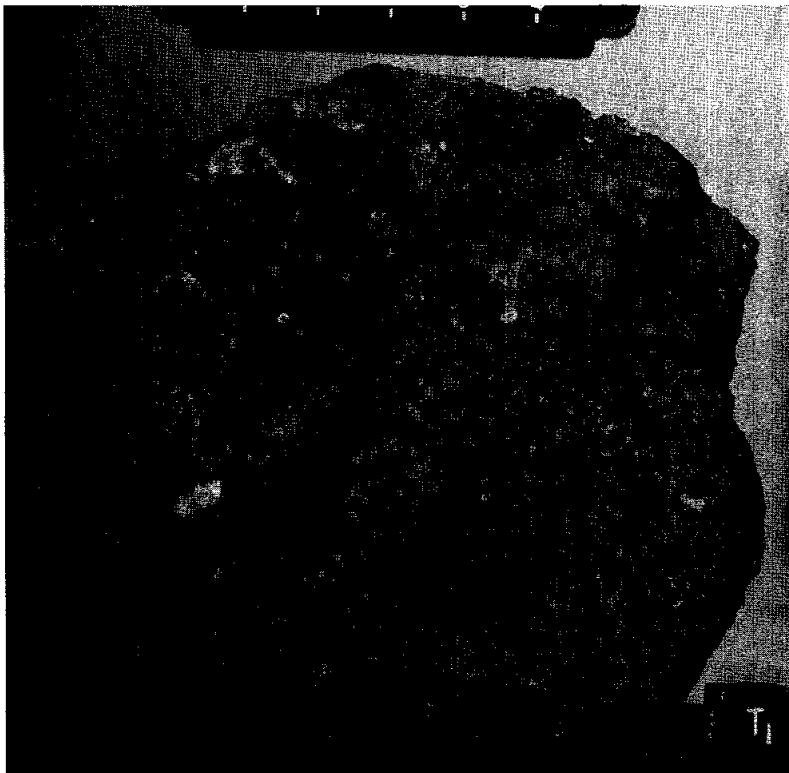


Figure 1: Pre-processing photograph of 73235, showing rounded surface with zap pits. Some white clasts are visible. Scale divisions and cube 1 cm S-73-19663.

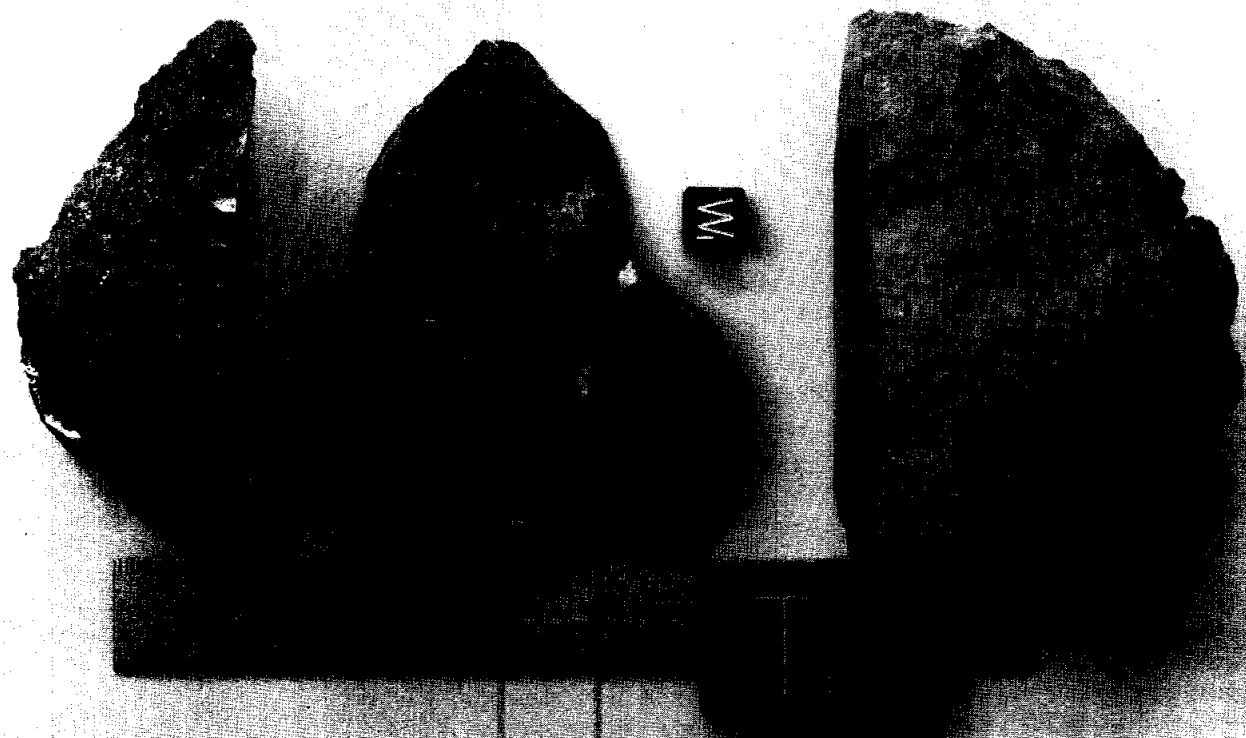


Figure 2: Post-sawing photograph of 73235, showing main subdivisions of the slab. End piece ,8 was subsequently substantially subdivided for allocations. Small cube is 1 cm. S-73-28684.

of sources. Warren and Wasson (1979) reported in diagram form microprobe analyses of olivine (Fo79-92) and plagioclase (An93-96) in the matrix of 73235 (Fig. 5).

Dence et al. (1976a, b) described 73235 as consisting of two lithologies, a coherent clast-rich dark matrix breccia interlayered with lighter more porous clastic breccia, with the former predominant. The light clastic material has irregular, locally sheared boundaries, and evidently is the material existing as schlieren described above. Dence et al. (1976a, b) describe the clast population as large and distinctive, as much as 50% and ranging down to very small sizes. No sorting of grain size is apparent. The clasts are typical highlands samples, including noritic microbreccias and granoblastic or crushed anorthositic and troctolitic fragments. Most of the lithic clasts, except for some coarse plagioclase-rich fragments,

display little shock effect, but mineral fragments have diverse shock effects. The light matrix materials consist of angular mineral fragments, especially plagioclase, but also pyroxene, olivine, and minor ilmenite. There is some loss of porosity along their contacts.

Hewins and Goldstein (1975a, b) analyzed iron metal grains in two clasts of "anorthositic hornfels" without discussion. The metals have about 5.5 to 7.5% Ni and 0.5 to 0.7% Co on the edge of the meteoritic field.

Engelhardt (1979) listed 73235 as having a granular matrix and with a paragenesis in which ilmenite, plagioclase, and pyroxene crystallized simultaneously. Knoll and Stoffler (1979) described the matrix as equigranular, with areas of light, coarser matrix. Smith et al. (1986) described a clast ("pomegranate") that consisted largely of zircons entirely enclosed

by bytownite (An80-85), as part of a geochronological study. The zircons, for which microprobe analyses are given, are 10-100 microns across and both they and the zircons were fractured at one time and later the zircons had overgrowth. Bickel and Warner (1978a) listed the sample in their study of plutonic and granulitic fragments, but presented no data or description. Simonds et al. (1974) listed 73535 as having a subophitic matrix with groundmass feldspars 5-15 microns long and pyroxene oikocrysts about 125 microns; this does not agree with the description given here and may be an erroneous tabulation.

Warren (1979) and Warren and Wasson (1979) described two clasts (with chemistry, below) from 73235. One (their c1), from a prominent white clast visible macroscopically, is extremely cataclastic (Fig. 3d) with no grain fragments more than about 1.3 mm

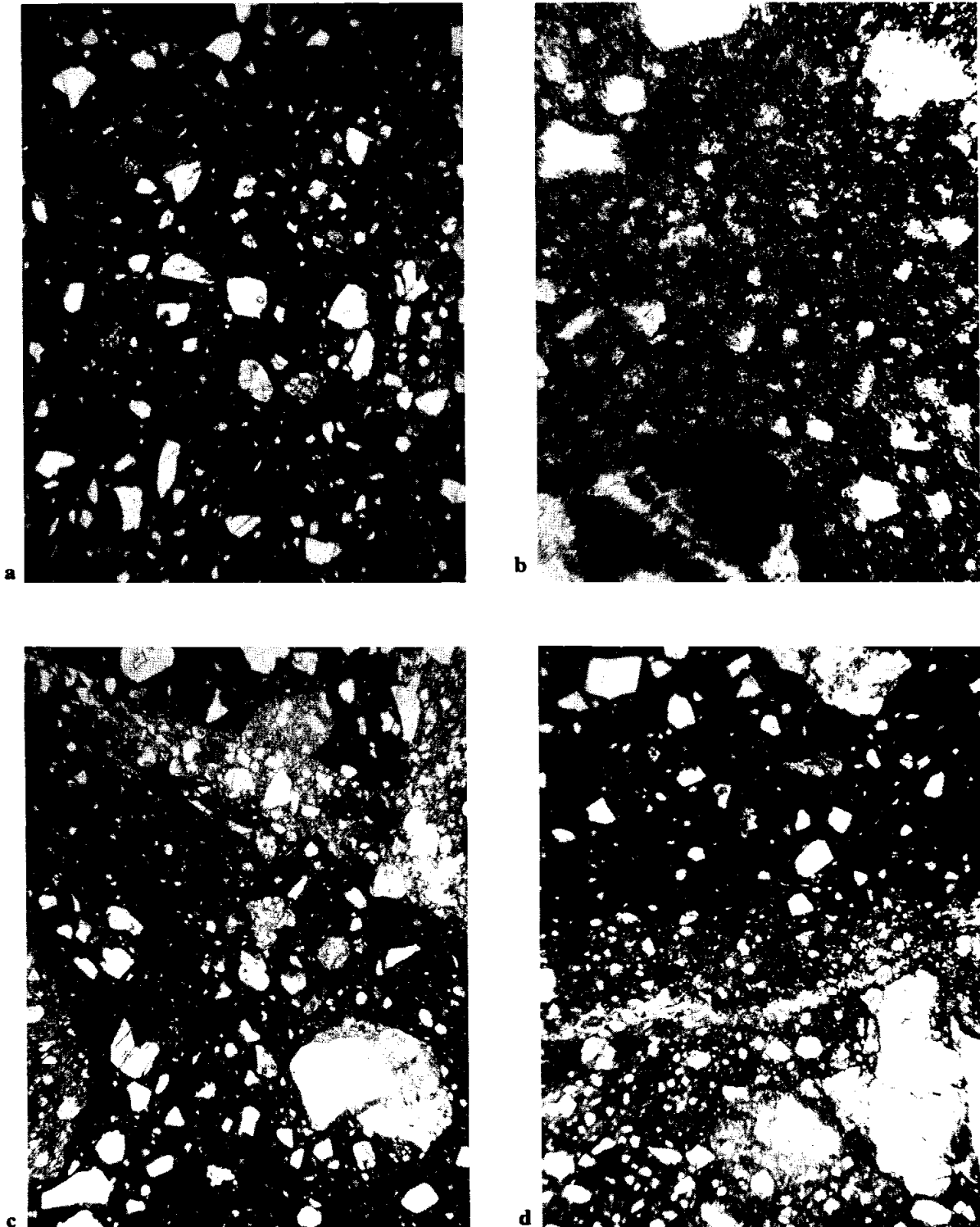


Figure 3: Photomicrographs of 73235, all plane transmitted light. Field of view 2mm except b) about 500 microns. All 73235,58 except d) 73235,83. a) general dense matrix with small mineral and lithic clasts ranging from angular to rounded. b) detail of groundmass and ragged edges of small clats. Clast in lower left is a glassy silicic particle. c) schlieren of cataclastic feldspathic impactite (across top) in general dense groundmass. d) boundary of impure cataclastic troctolite (bottom) and dense matrix (top).

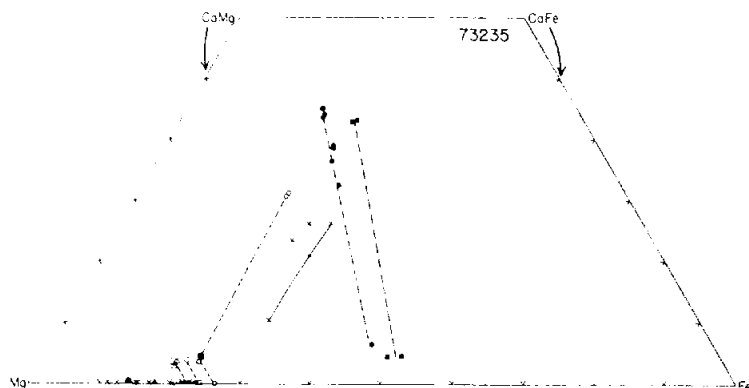


Figure 4: Plot of compositions of pyroxenes and olivines in 73235. Open symbols represent lithic clasts, closed symbols represent pyroxenes with exsolution lamellae, and x's represent monomineralic clasts. (Hodges and Kushiro, 1974a).

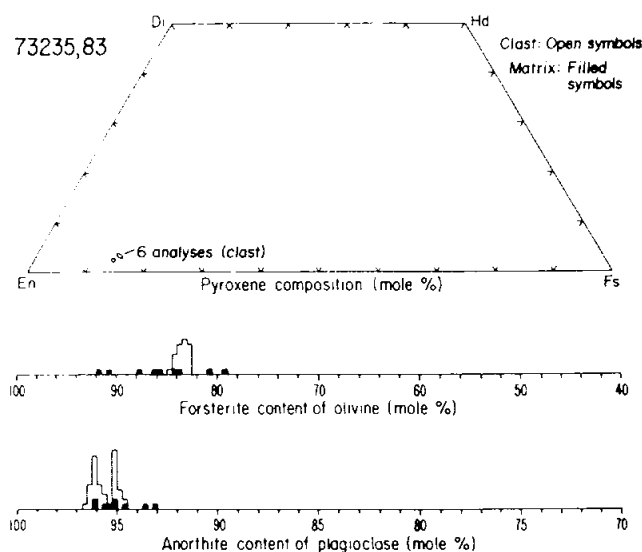


Figure 5: Plots of compositions of silicate mineral phases in 73235,83 troctolite (open symbols) and groundmass (filled symbols). (Warren and Wasson, 1979).

across. It contains about 60% plagioclase, 30% olivine, and 10% low-Ca pyroxene. Microprobe analyses are given in Figure 5, and show the troctolite to be a member of the Mg-suite of highlands rocks Warren and Wasson (1979) favor a pristine igneous origin on the basis of the restricted mineral chemistry. A second clast studied by Warren (1979) and Warren and Wasson (1979) (their c2) is also a brecciated troctolite, with about 2/3 plagioclase and 1/3 olivine, and

lacking pyroxene. The largest grain fragments are 0.7 mm across. Again mainly on the basis of restricted mineral chemistry (Fig. 6), Warren and Wasson (1979) favored a "probably pristine" igneous origin for the troctolite, which also is a member of the Mg-suite.

Bersch (1990) and Bersch et al. (1991) reported precise microprobe analyses of olivine and high-Ca pyroxene from thin section ,83

which contains the prominent white troctolite clast described by Warren and Wasson (1979). They also reported precise analyses of low- and high-Ca pyroxene, supposedly from a norite, from thin section ,136 which contains the other troctolite.

CHEMISTRY

Chemical analyses of the groundmass/matrix of 73235 are given in Table 1, with the rare earth elements plotted in Figure 7. Most of the analyses were presented by the authors with little specific comment, other than some note of its general similarity with other Apollo 17 highlands materials, including local soil. The chemistry is similar to that of other aphanitic melt breccias from the South Massif, but tends to be slightly more aluminous and with slightly lower abundances of incompatible trace elements. The sample clearly contains meteoritic contamination, but lacks regolith characteristics such as high C or S. The ratios of the meteoritic siderophiles place 73235 in a group 2 (Serenitatis) of Morgan et al. (1976) and Hertogen et al. (1977); however, the sample is slightly enriched in Br, Zn, and Cd compared with other "Serenitatis" melt rocks. Jovanovic and Reed (1974a, 1975c, 1980a) discussed the sample in terms of Cl (residual after leaching)/P₂O₅ ratios. Masuda et al. (1974) and Tanaka et al. (1974) noted the presence of positive Ce and Yb anomalies in their rare earth element plots, and even a small Dy anomaly, compared with the straight line fit (which they call "liquid-type pattern") of the other rare earth elements.

Analyses of clasts from 73235 are given in Table 2 with rare earth elements plotted in Figure 8. The two analyses of the prominent white clast, characterized by Warren and Wasson (1979) as a very probably pristine but cataclased troctolite (their c1) are acceptably similar. The rare earth

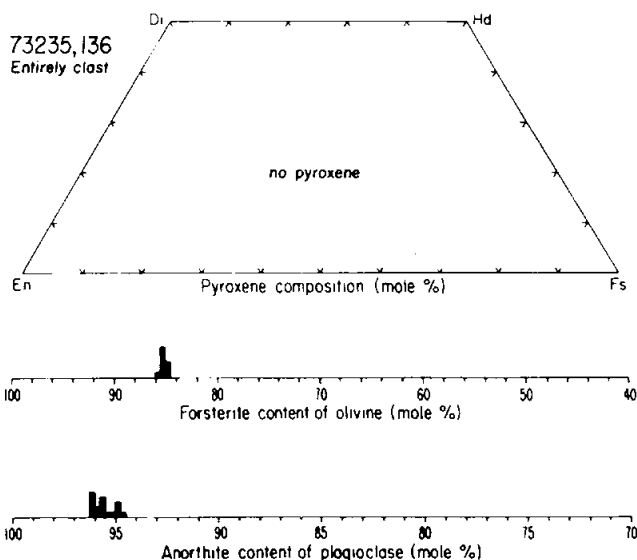


Figure 6: Plots of compositions of silicate mineral phases in 73235,136 troctolite. (Warren and Wasson, 1979).

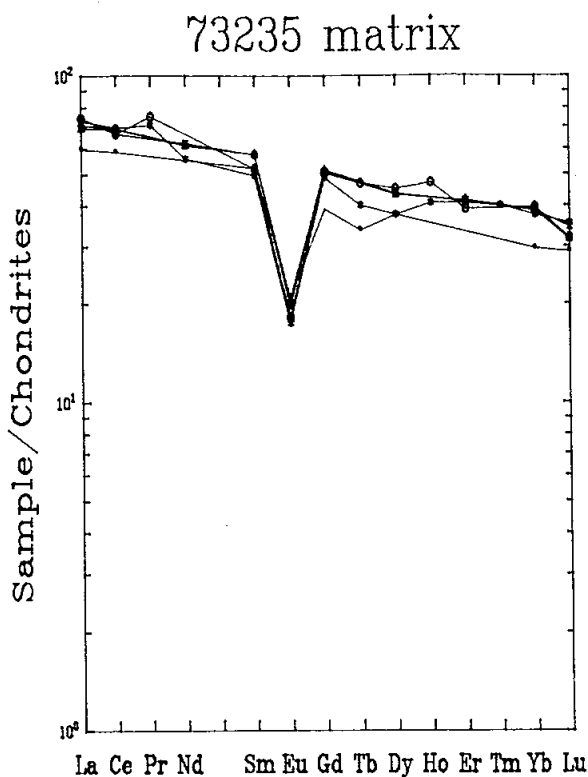


Figure 7: Chondrite-normalized plot of rare earth elements in bulk rock or groundmass for 73235. Data from Table 1.

elements, while in low abundance, are only slightly fractionated with respect to KREEP. The analyses probably include a little matrix contamination (clast boundaries are gradational), thus the details of trace element chemistry may not reflect the original pristine lithology. The "probably pristine" troctolite clast c2 of Warren and Wasson (1979) has slightly higher rare earth element abundances, again only mildly fractionated with respect to KREEP. Contamination with exterior (patina) surface might account for the fairly high siderophile abundances, which could alternatively reflect an indigenous component. The petrographic characters of the two clasts with very incomplete chemical data (Table 2) are unknown. The "anorthositic inclusion" has such low Fe and Sc as to suggest a true anorthosite or plagioclase separate; the "basaltic clast" is actually extremely similar to the melt groundmass of 73235 for all the reported elements.

STABLE ISOTOPES

Rees and Thode (1974a) reported a $(\delta) ^{34}\text{S}/\text{oo}$ of + 1.5, substantially lower than that in soils, and in the field of indigenous rocks, signifying that the bulk of the components of 73235 had no significant history of surface residence prior to their incorporation in the melt.

GEOCHRONOLOGY AND RADIOGENIC ISOTOPES

Nyquist et al. (1974a) presented Rb and Sr isotopic data for a bulk rock sample of 73235 (Table 3). The sample falls with other Apollo 17 noritic melt breccias on a 3.94 ± 0.10 Ga line (old constants 4.02 ± 0.10 Ga), whose age significance is uncertain. Oberli et al. (1978) also presented bulk rock Rb and Sr isotopic data, as well as data for a bulk clast (Table 3). The clast contains much less Rb than the

Table 1: Chemical compositions of bulk rock or groundmass for 73235.

Split	.52	.53	.55	.55	.88	.49	.91	.59	.54	.45	.89	.48	.46
wt%													
SiO ₂		45.96		46.20		46.4	46.7		47.7				
TiO ₂	0.75	0.60		0.67		0.63	0.65						
Al ₂ O ₃	22.2	22.57		21.28		21.2	20.5		20.79				
Cr ₂ O ₃	0.183	0.196	0.194			0.22	0.198						
FeO	6.6	6.68		7.32		7.33	7.40		7.9				
MnO	0.091	0.091		0.11			0.100		0.10				
MgO	10.6	9.61		11.05		10.7	11.6		12.9				
CaO	12.9	13.18		12.55		12.5	11.9		11.1				
Na ₂ O	0.47	0.44	0.51	0.48		0.47	0.456		0.47				
K ₂ O	0.173	0.200	0.210	0.20	0.197	0.18	0.197						
P ₂ O ₅		0.192		0.20			0.185						
ppm													
Sc	12.1					17	13.4						
V	51	40				58	50.7						
Co	23.7	22				33	26.3						
Ni	150	118				250	205			144			
Rb	4.1	5.6	5.13		5.26	3.1				4.7			
Sr	137	145	146.9		141		150						
Y		62.3				85	69						
Zr		315	341		366	350	343						
Nb		19.7				21.5	20.4						
Hf	7.7					6.5	7.85						
Ba	238	252	263		288	315		260					
Th	2.85		4.19			4.3	3.75						
U	0.75		1.14			1.1	1.05			1.060		1.2(a)	
Ca	0.17					0.15				0.198			
Ta	0.87						0.94						
Pb						3.0							
La	19.7		23.3			24	24.5		22.8				
Ce	51.5		60.6		58.4	61	58.5		60.4				
Pr						7.92	8.4						
Nd			37.0		37.3	33.5		36.7					
Sm	9.43		10.4		10.4	8.95	9.4	10.4					
Eu	1.43		1.37		1.35	1.20	1.25	1.42					
Gd			12.8		12.6	12.1	12.5	12.6					
Tb	1.58					1.88	2.2						
Dy	11.9		13.8		13.7	11.9	14.3	13.7					
Ho						2.85	3.3						
Er			8.2		8.27	8.15	7.8	8.28					
Tm						1.2							
Yb	5.9		7.7		7.69	7.47	7.9	7.74					
Lu	0.98				1.17	1.2	1.08	1.07					
Li			11.9		12.5		13.5					5.5	
Be													
B													
C													54
N													30
S		270		400							400		500
F							27						
Cl							20.0						
Br							0.11			0.09		30	
Cu	4.3	<2				1	3.8					(b)0.115	
Zn	3	<2								9.4			
ppb													
Au							3.2			2.31			
Ir										3.71			
I												1.9	
At													
Ga	3400						4000						
Ge							360			230			
As							130						
Se										53			
Mo													
Tc													
Ru												5.3	
Rh													
Pd													
Ag										1.0			
Cd										27			
In													
Sn												1.14	
Sb										4.3			
Te													
W	260						580						
Re										0.385			
Os												14	
Pt													
Hg													
Tl										2.1			
Bi										0.69			
	(1)	(2)	(3)	(4)	(5)	(6)	(7)	(8)	(9)	(10)	(11)	(12)	(13)

References and methods:

- (1) Brunfelt et al. (1974); INAA,XRF
- (2) Duncan et al. (1974a); XRF
- (3) Hubbard et al. (1974); Nyquist et al. (1974a); ID/MS, AA
- (4) Rhodes et al. (1974a,b); XRF, AA
- (5) Philpotts et al. (1974a); ID/MS
- (6) Taylor et al. (1974); Microprobe/Spark source MS
- (7) Wanke et al. (1974, 1977); INAA, RNA, XRF
- (8) Masuda et al. (1974), Tanaka et al. (1974); ID/MS
- (9) Ehmman et al. (1974), Miller et al. (1974); INAA
- (10) Morgan et al. (1974a,b; 1976), Hertogen et al. (1977); RNA
- (11) Rees and Thode (1974a); Chem.sep./gravimetry
- (12) Jovanovic and Reed (1974a,1975c); INAA, RNA
- (13) Moore et al. (1974a); Moore and Lewis (1976); Combustion
- (14) Oberli et al. (1978); ID/MS

Notes:

- (a) Value of 0.42 ppm also given
- (b) combined leach and residue

Table 2: Chemical compositions of clasts in 73235.

Split	,49 (a)	,54A (b)	,54B (c)	,127(d)	,135(e)
wt%					
SiO ₂	44.2			44.3	42.6
TiO ₂					.33
Al ₂ O ₃	23.1			24.9	21.9
Cr ₂ O ₃	0.09	0.006	0.197	0.103	0.157
FeO	5.06	0.65	6.7	4.5	6.2
MnO				0.05	0.07
MgO	14.0			12.5	17.8
CaO	12.7			13.7	11.1
Na ₂ O	0.30			0.275	.381
K ₂ O	0.06			0.056	0.077
P ₂ O ₅					
ppm					
Sc	5	0.8	13.2		
V	33				
Co	17	7	27	19.8	33
Ni	28			94	206
Rb					
Sr				200	210
Y	18				
Zr	85		365		
Nb	5.2				
Hf	1.53	0.21	8.03	1.6	2.1
Ba	100			110	130
Th	1.0			0.98	1.6
U	0.27				0.34
Cs					
Ta				0.23	0.26
Pb	1.2				
La	5.31		23	5.4	8.4
Ce	13.3			14	21
Pr	1.76				
Nd	7.33			8.4	13
Sm	2.17			2.43	4.1
Eu	0.79		1.6	1.0	1.0
Gd	2.73				
Tb	0.48			0.48	0.80
Dy	2.97				
Ho	0.67				
Er	1.85				
Tm	0.28				
Yb	1.72			1.7	2.5
Lu	0.27			0.23	0.34
Li					
Be					
B					
C					
N					
S					
F					
Cl					
Br					
Cu	1				
Zn				0.94	5.0
ppb					
Au				0.140	1.370
Ir				0.380	5.510
Ga				3500	3100
Ge				10.4	92
In				4.3	4.7
Re				0.029	0.410
	(1)	(2)	(2)	(3)	(3)

References and methods:

- (1) Taylor et al. (1974); Microprobe/Spark source MS
- (2) Ehmann and Chyi (1974), Chyi and Ehmann(1974), Garg and Ehmann (1976a), Miller et al. (1974); RNA
- (3) Warren and Wasson (1979), Warren (1979), Warren and Kallemeyn (1984); INAA, RNA, microprobe.

Notes:

- (a) white clast
- (b) "anorthositic inclusion"
- (c) "basaltic clast"
- (d) same clast as that of Taylor et al. (1974)
- (e) white troctolite clast

Table 3: Rb and Sr isotopic data for 73235.

Split	Rb/ ⁸⁶ Sr	⁸⁷ Sr// ⁸⁶ Sr	T _{Babi} (Ga) (I=0.69910)	T _{Luni} (Ga) (I=0.69903)	Reference
bulk:					
,55	0.1010+/-9	0.70539+/-6	4.35+/-0.08a 4.26+/-0.08b	4.39+/-0.08a 4.30+/-08b	(1)
,50B	0.1134	0.70606+/-5	4.35+/-0.04a 4.26+/-0.04b		(2)
clast:					
,50W	0.02159	0.70030+/-5	4.27+/-0.16a 4.18+/-0.16b		(2)

a) old decay constant, lamda (⁸⁷Rb) = 0.0139 Ga⁻¹

b) new decay constant, lamda (⁸⁷Rb) = 0.0142 Ga⁻¹.

(1) Nyquist et al. (1974a)

(2)

Table 4: Sm and Nd isotopic data for 73235.

Sample	¹⁴⁷ Sm/ ¹⁴⁴ Nd	¹⁴³ Nd/ ¹⁴⁴ Nd	T _{Juv} ^a	T _{Chur} ^b	Reference
,50B bulk	0.1688+/-1	0.511057+/-17	4.54+/-0.02	4.73+/-0.13	(1)
,50W clast	0.1656+/-1	0.510931+/-21	4.51+/-0.02	4.86+/-0.13	(1)

a) model age calculated from the initial ¹⁴³Nd/¹⁴⁴Nd of Juvinas

b) model age calculated from the intersection of sample evolution line with the chondritic evolution line.

(1) Oberli et al. (1978).

Table 5: Elastic wave velocities for 73235,18 . (Mizutani and Osako, 1974a, b)

Pressure Kb	0.0	0.5	1.0	2.0	3.0	5.0	7.0	9.0
V _p km/sec	5.42	6.02	6.39	6.72	6.88	7.08	7.12	7.14
V _s km/sec.	2.95	3.32	3.48	3.66	3.77	3.86	3.90	3.92

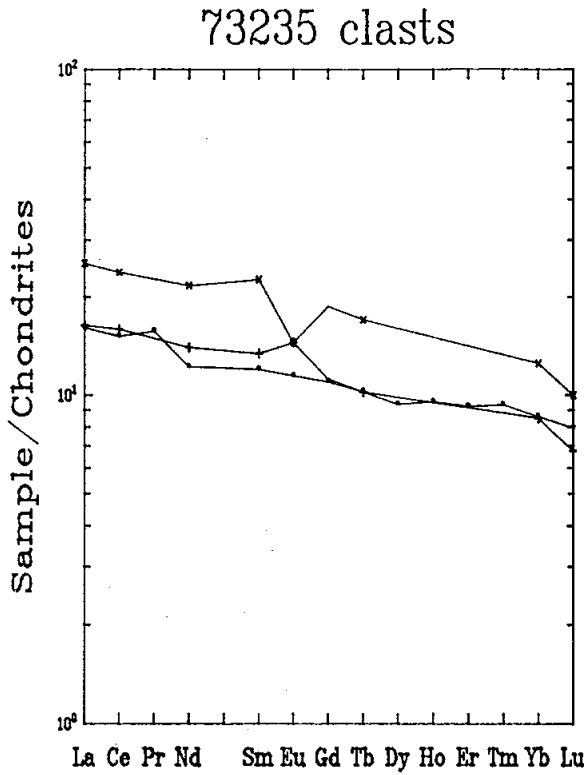


Figure 8: Chondrite-normalized plot of rare earth elements in clasts in 73235. Data from Table 2.

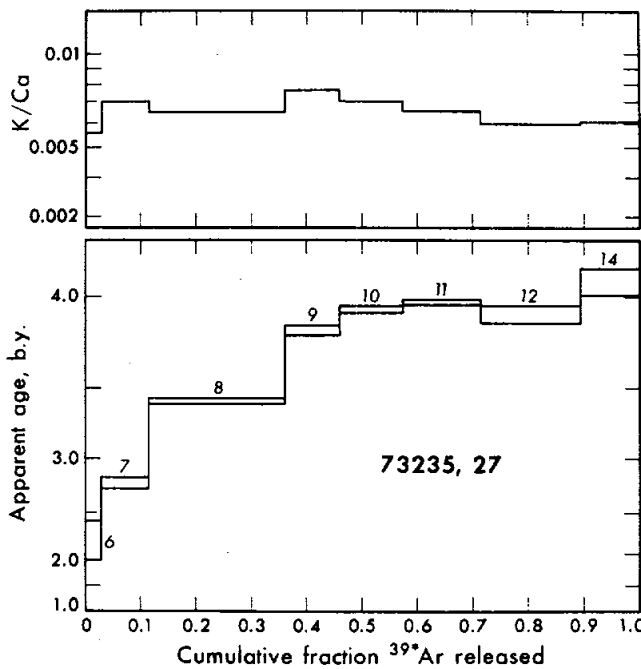


Figure 9: Ar release for 73235,27 (Phinney et al. 1975)

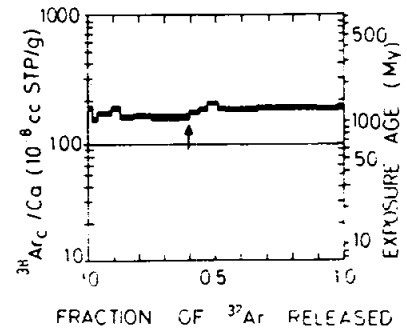
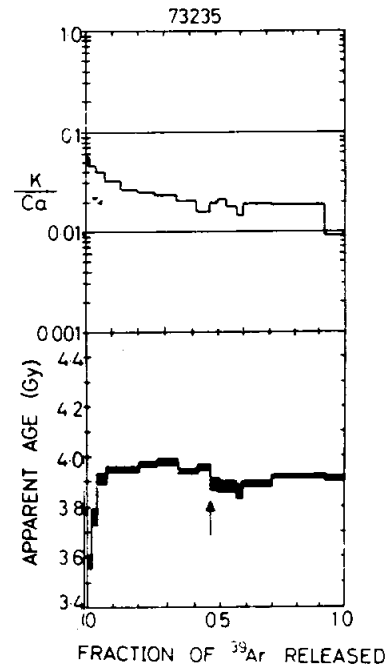


Figure 10: Ar release for 73235,30 (Turner and Cadogan 1975a).

groundmass and gives slightly younger model ages. The model ages require young crust formation (i.e. about 4.3 Ga) or remelting at less than 4.3 Ga of materials relatively rich in Rb that had been produced before 4.3 Ga; loss of Rb as a volatile does not explain the data.

Oberli et al. (1978) presented Sm and Nd isotopic data for a bulk rock sample of 73235, as well as for the same clast that was analyzed for Rb and Sr isotopes (Table 4). The model ages are older than those for the Rb system, demonstrating that there was no change in the Sm/Nd ratio while events might have been

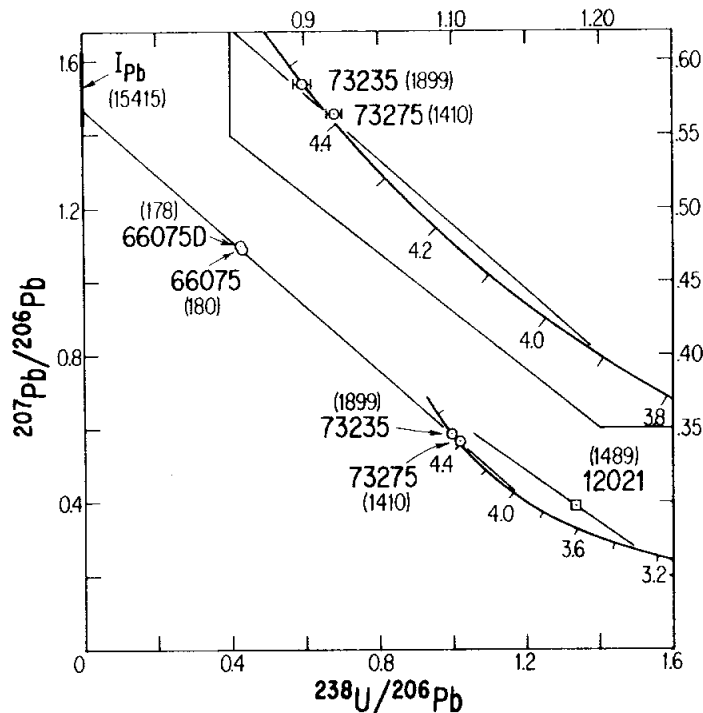


Figure 11: U-Pb evolution diagram for 73235 and some other lunar samples. The u values are given in parentheses. A reference line is drawn through points on concordia corresponding to 4.42 Ga and 3.90 Ga. 12021 is a mare basalt. (Oberli et al. 1978).

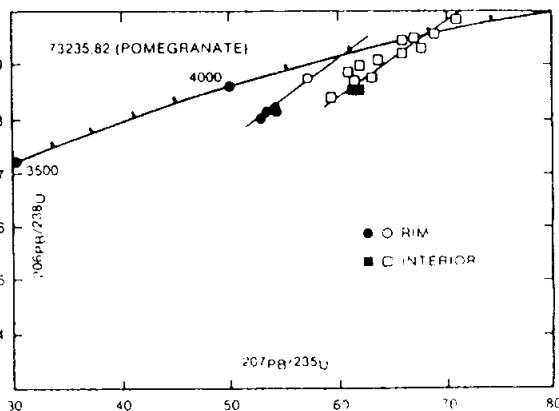


Figure 12: Concordia diagram for rim and interior of zircon assemblage in 73235,82. Open symbols = 1984 data, closed symbols = 1985 data.

increasing the Rb/Sr ratio in source materials.

Phinney et al. (1975) and Turner and Cadogan (1975a, b) presented bulk sample Ar-Ar stepwise heating isotopic data, depicted in Figures 9 and 10. Phinney et al. (1975) reported a plateau age of 3.92 ± 0.04 Ga (new decay constants; old decay age is 3.98 Ga), noting, however, that the plateau was at best "poorly developed" (Fig. 10). The release is dominated by ^{40}Ar loss over the first 50% of release, and the total Ar age is only 3.69 ± 0.03 Ga (new decay constants; old decay age is 3.74 Ga). The K/Ca ratio is fairly constant, implying well mixed Ca and K rather than release from a single mineral. The bulk K and the K/Ca ratio determined are much lower than either bulk rock or the Turner and Cadogan (1975a, b) samples. Turner and Cadogan (1975a, b) reported a plateau age of 3.91 ± 0.04 (new decay constants; old decay age is 3.96 Ga), but although the plateau is better defined than that of Phinney et al. (1975), it is not a good one (Fig. 10). It is bimodal with lower apparent ages at high temperatures (3.90 Ga) than at low (3.80-3.86 Ga) and perhaps reflects a recoil effect. The total Ar age is 3.87 Ga (no uncertainty stated).

Oberli et al. (1978) presented U, Th, and Pb isotopic data for the bulk rock sample of 73235 that they also analyzed for Rb-Sr and Sm-Nd isotopes. The U-Th-Pb data are concordant at 4.47 Ga within 0.1%. However, the near-tangential relationship of a discordant data array as represented by the reference line with the concordia curve (Fig. 11) provides poor discrimination between truly concordant and discordant data. The $^{207}\text{Pb}/^{206}\text{Pb}$ age is 4.470 ± 0.001 Ga; the $^{206}\text{Pb}/^{238}\text{U}$ age is $4.474 \pm 0.018/-0.022$ Ga; and the $^{208}\text{Pb}/^{232}\text{Th}$ age is $4.474 \pm 0.044/-0.047$ Ga.

Smith et al. (1986) used a high resolution ion microprobe to make Pb isotopic determinations and ages on zircons in a zircon-anorthite clast ("pomegranate") in thin section 73235,82 (Figure 12). The zircons have been through an original crystallization event at 4.310 Ga, were fractured, and then overgrown at 4.183 Ga i.e., the rims are 120 Ma years younger. The clast was emplaced in the groundmass (at about 3.9 Ga according to the Ar isotopic data) without either Pb loss or gain.

EXPOSURE

Phinney et al. (1975) calculated an Ar exposure age of 195 +/- 20 Ma for split ,27 which could be interpreted as the age of the light mantle if a single-stage model is appropriate. However, Phinney et al. (1975) are reluctant to assume a single stage model. A similarly-calculated Ar exposure age by Turner and Cadogan (1975a, b) is only 110 Ma (Fig. 10), similar to that of Boulder 1, Station 2 and some other South Massif samples. Horz et al. (1975) reported a 110 Ma exposure age for the sample, citing Reynolds (pers. comm.) as the source.

Padawer et al. (1974) attempted to obtain a hydrogen profile from the exterior to the interior of the sample, using LNM microanalysis with a Van de Graaf accelerator. However, for this sample, interferences were too great to obtain hydrogen concentrations.

PHYSICAL PROPERTIES

Mizutani and Osako (1974a, b), referring to the sample as a "fine-grained anorthositic breccia," reported elastic wave velocities, both compressional and shear wave, for 73235,18 (Table 5). The velocities are lower than those appropriate for the "lower layer" (25-65 km depth) of the lunar crust.

Watson et al. (1974) used thermomagnetic analysis (J_s v. T) and microscopy to identify the magnetic carriers in 73235. The carriers are mainly iron metals, some nickel free and others with up to 6% nickel. The total Fe^0 is 0.31 wt %, more than in basalts. The average NRM is 6×10^{-6} emu/gm, less than about a third that of basalts. The iron is fine-grained compared with basalts, and is partially oxidized (in the experiment) to Fe_3O_4 , even in fO_2 of 10^{-22} . Some of the iron is "newly-formed" iron, that is, produced in the impact event and not relict clasts.

PROCESSING

A small number of chips were initially taken from different parts of 73235 for allocations. Subsequently a slab (.11) was cut through the sample and itself subdivided (Fig. 2), providing interior and exterior samples. The sawing produced two butt ends, of which ,9 at over 500 g remains unprocessed. Butt end ,8 was completely subdivided such that its largest subsample (.35) is now 50 g. This butt end is the source of the conspicuous white troctolite clast. Four different chips from both the slab and the ,8 butt have been used for thin sections, of which a large number exist.

73245
Granoblastic Impactite(?)
St. 3, 1.60 g

INTRODUCTION

73245 is a medium gray (N6) tough sample that is probably a feldspathic granulite with a little adhering light brownish gray regolith breccia. The granulite may have been a clast in the breccia. 73245 is cuboidal with dimensions of 1 x 1 x 0.8 cm, and lacks fractures, zap pits, and cavities

(Fig. 1). The sample is homogeneous and fine-grained. The photomicrograph (Fig. 2) suggests that the sample is a metamorphosed, fine-grained, polymict breccia. Small chips representing average rock were taken from the same area for the thin section and for chemical analysis; no data has been published.

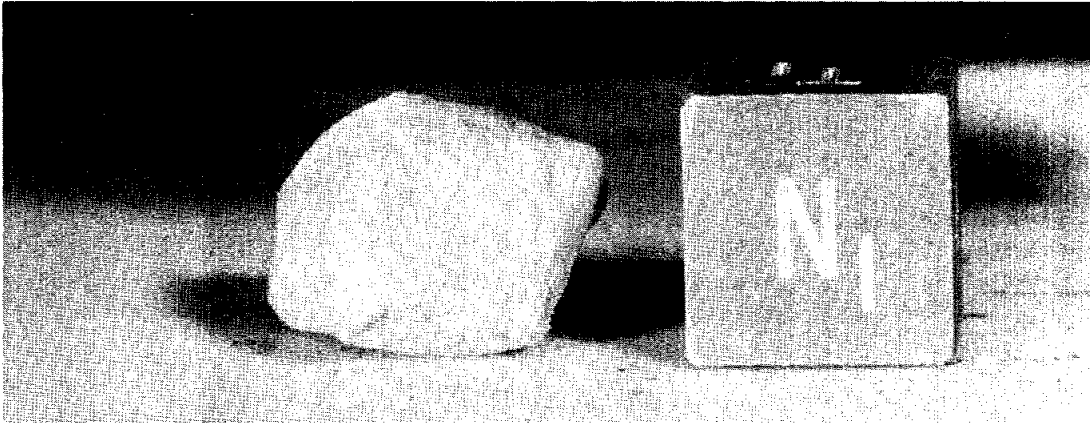


Figure 1: Pre-processing photograph of 73245, showing white friable blocky rock. Cube is 1 centimeter. S-73-21775



Figure 2: Photomicrograph of 73245, 4, transmitted light. Field of view 2.4 mm wide.

73255**Aphanitic Impact Melt Breccia
St. 3, 394.1 g****INTRODUCTION**

73255 is an aphanitic impact melt breccia that is unusual in being an oblate spheroid that has retained, to a large extent, the original shape and internal structures produced in the breccia-forming event. It is essentially an agglomeritic bomb with abundant clasts (Figs. 1-4). It consists of a clast-rich, non-vesicular, very fine-grained melt breccia core surrounded by a rind (up to 1 cm thick) of more vesicular, less clast-rich melt breccia that generally has a sharp contact with the interior (Figs. 3, 4). The core itself is an agglomeration of melt breccias. The chemical composition of the aphanitic melts is very similar to that of the common low-K Fra Mauro melt breccias that are

generally assumed to be the Serenitatis impact melt, although it has lower TiO_2 . The aphanitic melt crystallized at about 3.87 Ga, while older clasts such as pristine norites (one dated at 4.23 Ga), aluminous mare basalts, felsites, and feldspathic impactites are contained within it.

73255 was collected from the surface on the rim of a 10 m crater on the landslide at Station 3. Exposure appears to have occurred about 95 Ma ago, which is also the generally inferred age for the landslide itself. The sample is medium light gray (N5-N6), locally very light gray (N8), and is tough with a few penetrative fractures. It is 8 x 7.5 x 5 cm and subrounded. Its surface is rough and there are a few zap pits on most surfaces.

Original surface is apparently present in some locations; in others the vesicular rind has been broken off. Macroscopically the sample appears to consist of about 85% matrix (less than about 100 microns), 10% lithic clasts, and 5% mineral clasts. A slab was sawn through the rock and most allocations were made from it. The sample was studied in detail in a consortium led by O. James.

PETROLOGY

The structure and petrology of 73255 have been studied in some detail. It consists of a core of non-vesicular aphanitic melt breccias (Fig. 5a, b) enclosed in a rind of vesicular aphanitic melt breccia; all were created in a single impact

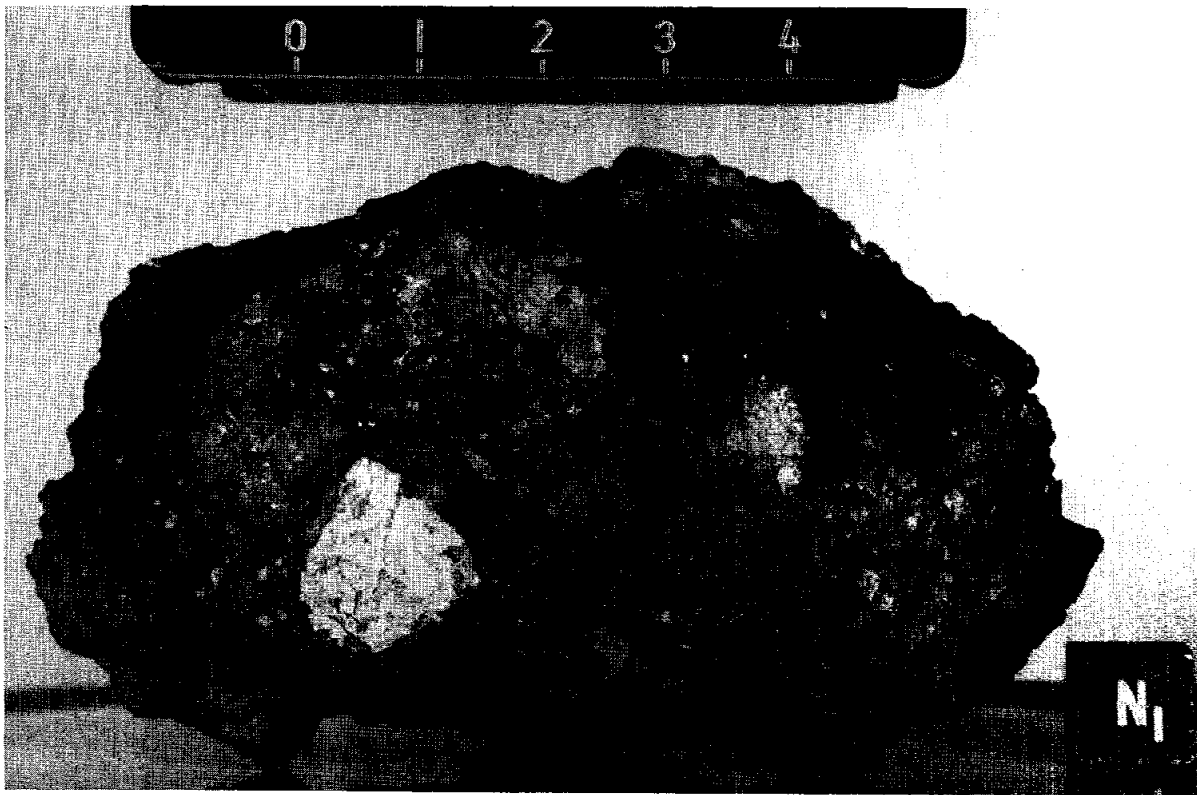
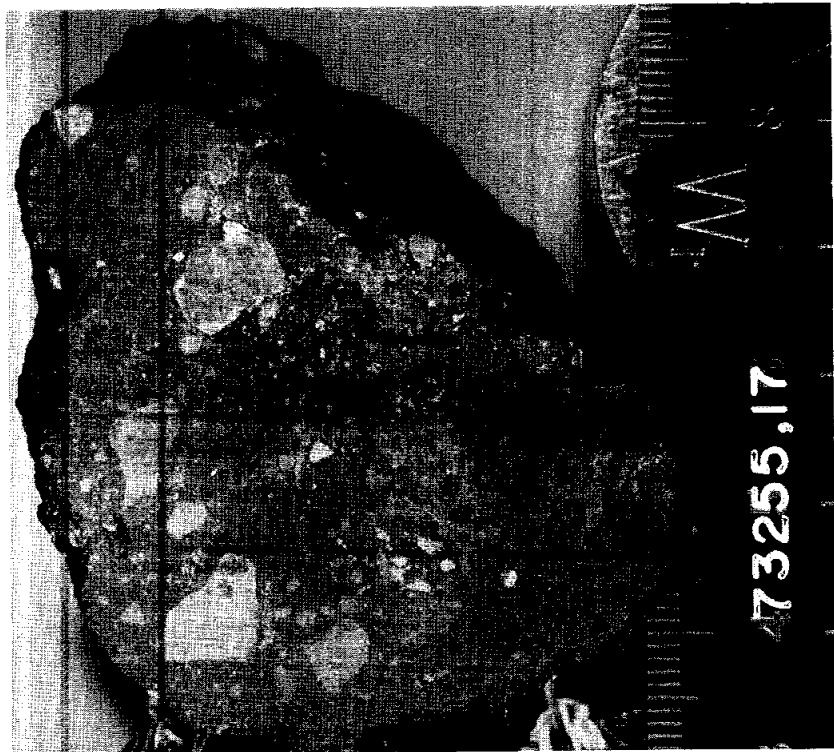


Figure 1: Pre-processing photograph of 73255, showing cindery appearance of vesicular rind, and prominent lithic clasts. Cube is 1 centimeter. S-73-24202.



Figure 2: Photograph of 73255, post-slabbing, showing end pieces ,12 and ,17 (and ,20 which was part of the end piece), and the slab piece, 27 which has been subdivided. Cube is 1 cm. S-74-22994.

Figure 3: Sawn surface of end piece ,17, showing large clasts and the distinct vesicular rind. Cube is 1 cm. S-76-25842.



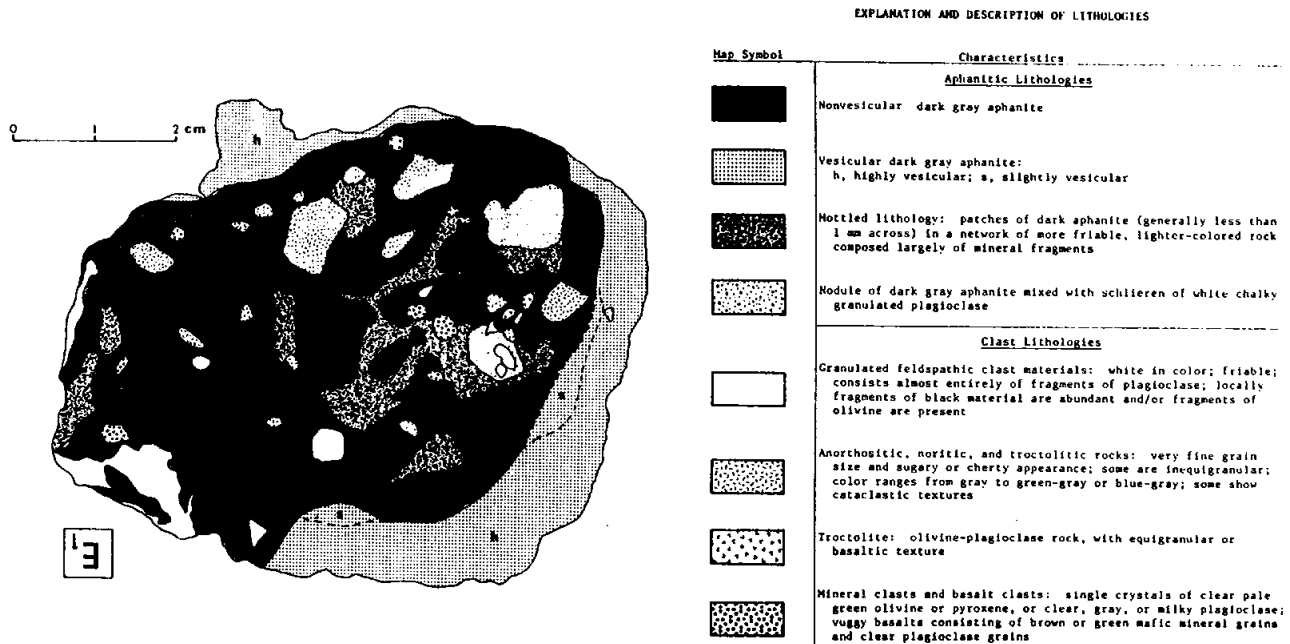


Figure 4: Lithologic map of one face of the slab cut through 73255, with key. From James et al. (1978).

event (James et al., 1978). All melt breccias contain mineral and lithic clasts, and the core aphanites include small cryptocrystalline globular masses. The core contains abundant coherent lithic and mineral clasts, patches of friable white granulated plagioclase-rich rock, and mottled areas, as mapped by James et al. (1978) (Fig. 4). The clasts are from about 1 cm across down to the limits of resolution.

The general structure of 73255 and the petrology of the aphanitic melt breccias have been described and discussed by James et al. (1978), James and Marti (1977), James and Hedenquist (1978a), and Nord and James (1978a, b), and were briefly discussed by Simonds et al. (1974) and Spudis and Ryder (1981). Two igneous norite clasts were described and discussed by James and McGee (1979a, b), and Nord and James (1979a, b). These two norites were described and used by James (1982) and James and Flohr (1982) as representatives of two main groups of pristine norites among lunar samples. Felsite clasts were

described by James and McGee (1980c) and Nord and James (1978a, b), and five mare basalt clasts were described by James and McGee (1980a, b). Brief descriptions of other clasts were given in James et al. (1978) and electron petrographic work on some anorthitic fragments was described in Nord and James (1978a, b).

James et al. (1978), James and Marti (1977), and James and Hedenquist (1978a) described the various lithologies, particularly the varied aphanitic melt breccias, and structure of 73255. They made a detailed study of four particular types of aphanitic melt breccia that dominate the rock: 1) non-vesicular core, 2) vesicular rind, 3) slightly vesicular material at the core-rind boundary, and 4) cryptocrystalline aphanitic melt that forms small particles within other aphanitic material in the core. The latter are most common in the mottled lithology of the core, in which the aphanites form irregular blebs and angular fragments. A summary of the characteristics of these four

types is given in Table 1. The groundmasses are mainly subophitic to ophitic, and consist of plagioclase and pyroxenes, mainly 1-5 microns in dimension (Simonds et al., 1974, listed 1-10 microns for both phases, and suggested an "almost granular" texture). The grain size of the groundmass is finer than rock 73215, another aphanitic melt breccia collected nearby. Table 1 shows that the groundmass volume is varied from 59-85 volume % (virtually all melt-derived; clasts smaller than 5 microns have not been identified), and its abundance is roughly inversely correlated with grain size. The abundance of vesicles and their size are positively correlated. Defocused beam microprobe analyses show that the melt is close to the same composition in all melts (see CHEMISTRY section). There are virtually no post-consolidation shock features except some fractures, with no evidence of post-consolidation heating or shear.

The origin of the groundmasses as rapidly-cooled melts is shown in

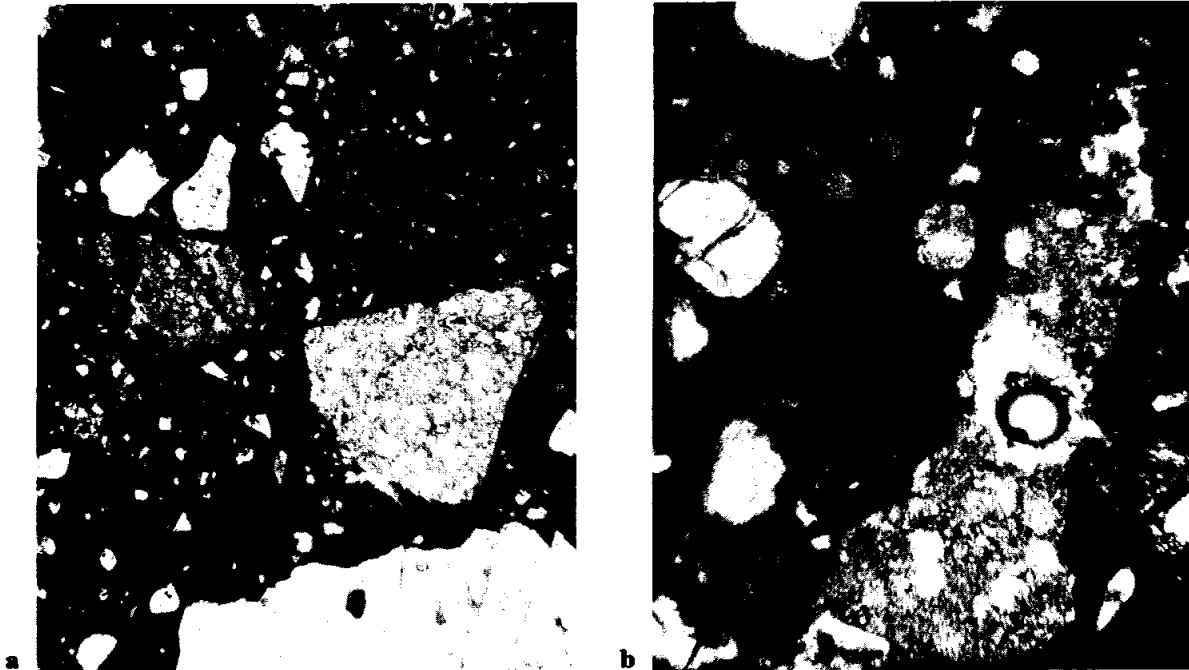


Figure 5: Photomicrographs of 73255,287, showing dense aphanitic groundmass and rounded to angular clasts. Plane transmitted light. a) large plagioclase clast (bottom) and fine-grained feldspathic impactite (center left). Field of view about 2 mm wide. b) elongated fine-grained feldspathic impactite. Field of view about 500 microns wide.

electron petrographic (TEM) studies (Nord and James, 1978 a, b), in which the fine-grained subophitic/ophitic textures, with lath-shaped plagioclases, are clear. The plagioclases are a little more blocky in the more vesicular samples. Electron diffraction characteristics establish the pyroxene as pigeonite. These studies also found minor augite, but there was no orthopyroxene, olivine, or silica in the groundmass in the pieces investigated. Exsolution in the groundmass pyroxenes is of two types, as established in the TEM studies, and demonstrates rapid subsolidus cooling of the melt, and the absence of significant reheating after crystallization. Neither are there any shock-induced microstructures in the groundmass minerals, so there has been no significant post-consolidation shock event (>25kb).

Two norite clasts have been interpreted as being pristine igneous rocks. One, ,27,80 was 1/2 cm across, the other ,27,45, almost

1 cm in maximum dimension. Norite ,27,80 is modally a pyroxene anorthosite with about 90% plagioclase and 10% orthopyroxene, but is probably an unrepresentative sample of a norite, whereas ,27,45 has only about 50% plagioclase. They are rather different in detail, and were used by James (1982) and James and Flohr (1982) as representatives of Mg-norites and Mg-gabbronorites respectively. Both cooled beneath the surface of the Moon, but in detail have different thermal and subsequent shock histories. They have been described in detail by James and McGee (1979a, b) and Nord and James (1979a, b) who provide petrographic (including TEM) descriptions and microprobe mineral analyses and have been subjected to other types of study (see CHEMISTRY and GEOCHRONOLOGY sections, below).

A thin section of pyroxene anorthosite ,27,80 consists of plagioclase (83%), orthopyroxene

(15%), about 1% augite, 1% quartz+cristobalite, and less than 1% trace phases (James and McGee 1979a,b). The trace phases are K-feldspar, chromite, rutile, iron metal, apatite, whitlockite, baddelyite, armalcolite, troilite, ilmenite, and zirkelite. The texture is igneous, with equant plagioclase and pyroxene with sizes of 0.3 to 2 mm (most about 1 mm). The plagioclases have cores with inclusions (most almost certainly exsolved) and the orthopyroxenes have sparse, widely spaced thin augite exsolution lamellae and some exsolved oxides. The plagioclases are fairly homogeneous (An_{93.1}; range An_{91.1-95.3}), as are the orthopyroxenes (En_{72.9}Wo_{2.2}) and clinopyroxenes (Fig. 6). The potash feldspars differ in composition from inclusions in plagioclase to interstitial phases (Fig. 7). The metal grains are extremely poor in Ni. The clast does have some well-developed shock-produced plastic deformation features, and the orthopyroxene has some patchy

Table 1: Characteristics of 73255 aphanites and 73215 aphanite. James et al. (1978).

	73255				73215 ³
	Cryptocrystalline	Nonvesicular	Slightly vesicular	Vesicular	Average of all types of matrix aphanite
Groundmass texture	Subophitic to devitrified-appearing; little intergranular porosity	Subophitic; locally variolitic or graphic; few percent intergranular porosity	Subophitic; locally variolitic or graphic; few percent intergranular porosity	Subophitic with blocky pyroxene grains; locally variolitic or graphic; few percent intergranular porosity	Subophitic to intergranular; locally graphic or variolitic; intergranular porosity highly variable
Groundmass grain size	<1 μm	average ~2 μm (1-5 μm)	average ~2 μm (1-5 μm)	average 4-5 μm	average ~4-5 μm (<1-8 μm)
Vesicle content (vol.%)	~1-4 ¹	~2 ²	~5 ²	21-34 ²	none
Vesicle size (mm)	average ~.01	average ~.01	average ~.02	average ~.04 range .01-1.0	—
Mode (vol.%, normalized to zero porosity)					
Groundmass	70-85 ¹	72.3 (71.4-73.8) ²	77.2 ²	66.4 (59.4-74.6) ²	68.3 (65.7-71.1)
Plagioclase clasts >5 μm	not estimated	13.3 (7.9-18.0) ²	10.3 ²	20.3 (11.6-25.4) ²	22.5 (20.5-23.7)
Mafic-mineral clasts >5 μm	not estimated	7.4 (6.3-9.2) ²	9.1 ²	9.6 (8.8-11.6) ²	8.1 (5.1-10.9)
Lithic clasts >5 μm	not estimated	7.0 (1.4-13.6) ²	2.8 ²	3.7 (2.7-6.3) ²	1.1 (0-3.3)
Other clasts	not estimated	—	0.6 ²	—	—
Number of areas counted		(3)	(1)	(4)	(3)

¹From visual estimates.

²From point counts on transparent overlays traced from reflected light photomicrographs of 0.6 × 1.4 mm areas.

³James (1976).

extinction. Fe-S rich glass veinlets have partly penetrated the clast during the 73255 breccia-forming event. Electron petrographic studies show heterogeneous microstructures in anorthites, the most striking of which are polygonal grains about 1 micron in diameter; other areas show recovery and defect-free patches. The potash feldspar inclusions have glass and some dislocations. The orthopyroxenes have 1000 angstrom-thick augite lamellae, and abundant stacking faults. The silica polymorphs show a wide range of shock features, including glass. The glasses in silica, anorthite, and K-feldspar indicate shock pressures of 250-450 Kb; only the glasses in anorthite devitrified later. The only subsolidus, post-crystallization events, apart from shock, are the exsolutions; the orthopyroxene exsolutions suggest equilibration to 800 degrees C. The norite appears to have crystallized from an indigenous melt, slowly beneath the surface of the Moon. There are no recognizable xenocrysts and the

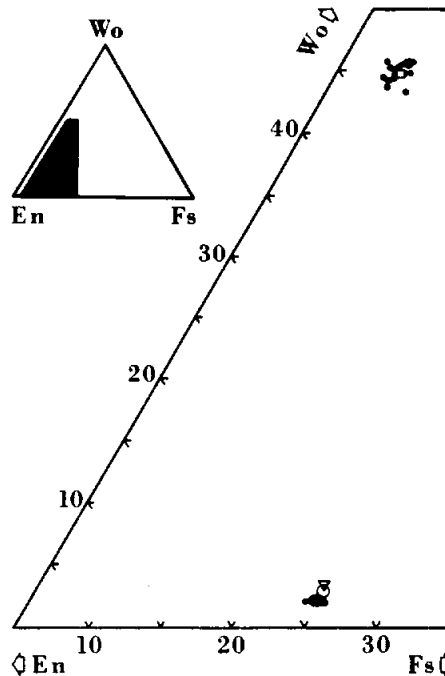


Figure 6: Compositions of pyroxenes in pyroxene anorthosite (norite) 27,80. See James and McGee (1979a) for details.

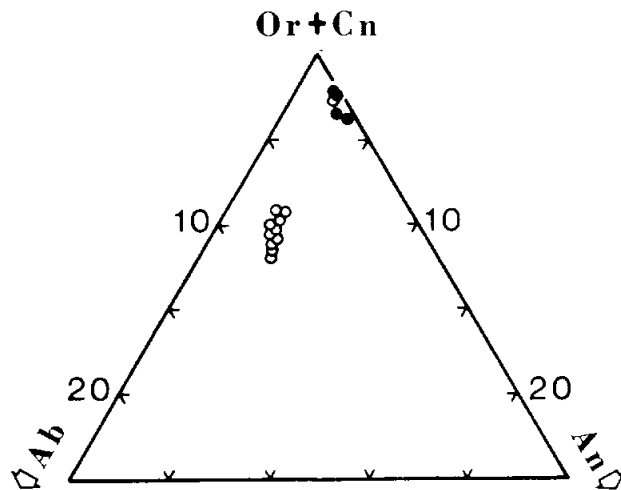


Figure 7: Compositions of potash feldspars in pyroxene anorthosite (norite) 27,80. Open circles are inclusions in plagioclase; filled are interstitial grains. James and McGee (1979a).

melt appears to have been rather evolved (to give an early plagioclase capable of exsolving K-spar and the many trace phases; see also CHEMISTRY). There may have been two generations of plagioclase growth.

Gabbronorite 27,45 did not retain an igneous texture, although a few relict grain boundaries are preserved; instead it has a granulated texture, with a regular variation of intensity across the clast. Most grains are angular. Grains up to 1.8 mm and monomineralic areas suggest an original grain size of about 2 mm. James and McGee (1979a, b) gave a mode of 53% plagioclase, 40% orthopyroxene, 5% augite, 0.5% ilmenite, and <1.5% all other phases. The trace phases are apatite, whitlockite, chromite, troilite, iron-metal, stanfieldite (Ca-Mg-rich phosphate), armalcolite, and rutile. Single grains of K-feldspar and K-Si-rich glass were also found. The plagioclases do not contain inclusions, but the orthopyroxenes do contain inclusions as well as thin, widely spaced exsolution lamellae. The augites contain abundant exsolution lamellae of low-Ca pyroxene. Plagioclase compositions are fairly

homogeneous (An88.6, range An86.7-90.5) and more sodic than in pyroxene anorthosite 27,80. The pyroxenes show significant correlation with texture, with exsolution lamellae differing from host grains of the same phase; individual grains are not zoned (Fig. 8). All of the iron metals, which seem to be part of injected veins, contain significant Ni (Fig. 9), unlike those in the pyroxene anorthosite 27,80. Electron petrographic studies show that the bytownite is mainly defect free, with a low density of antiphase domains. All pyroxenes contain exsolution, and orthopyroxenes have abundant stacking faults and Ca-enriched (GP) zones in varied density. The subsolidus effects indicate that the gabbronorite cooled at rates similar to the Bushveldt intrusion, down to 600 degrees C, and cooling to those temperatures in about 3000 years. This, with the compositional variation of pyroxenes, suggests cooling in the upper part of the lunar crust. The gabbronorite was shocked and granulated, with no significant production of theomorphous glass, at about 50Kb, substantially lower than the shock pressures of 27,80. This was accompanied by an Fe-S vapor.

Only slight modification by post-shock events occurred.

Two tiny felsite clasts were described with mineral analyses by James and McGee (1980c). One (27,3) consists of a vermicular intergrowth of quartz and K-feldspar, with optically continuous quartz as ribs 15-45 microns thick. Shock has converted K-feldspar largely to glass, but original textures are preserved. The clast is cut by a veinlet of host aphanitic melt breccia, with reddish brown glass at the contact that is higher in SiO₂ and K₂O than host breccia. The plagioclase is rich in both K and Na (An56.3Ab39.0Or4.7), and the K-feldspar is rich in Ba. Ca contents are higher in shock-vitrified K-spar than in non-vitrified K-feldspar. The other clast (253,24) is more strongly shocked, although it originally had a similar texture of vermicular intergrowth of quartz and K-feldspar. The K-feldspar was converted completely to glass by shock and flowed. The contact with the surrounding breccia is marked by a band of devitrified glass. Neither clast displays textures unequivocally igneous or metamorphic in origin, but by comparison with a clast in 73215 is almost certainly igneous. The shock event(s) occurred prior to the incorporation of the felsites into the breccia, and melted and injected material into the clasts. At the time of incorporation into the breccia the clasts were hot or were heated at that time. Electron petrographic work on a separate(?) felsite was reported by Nord and James (1978a, b), although this felsite is similar to the others in having the same textures and shock glass in K-feldspar. The TEM studies confirm glass at the grain boundaries and within K-feldspar and a lack of glass in quartz. No microstructures indicative of deformation, or deformation followed by recovery, were observed in either the K-feldspar or the quartz. Pigeonite grains contain antiphase domain boundaries, abundant twins, and exsolved augite lamellae. Some glass at

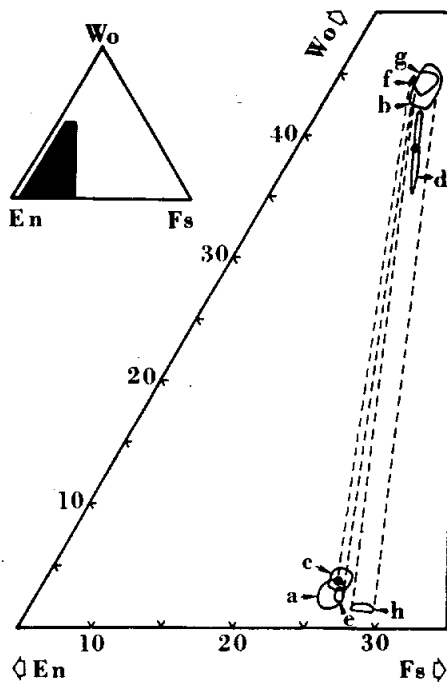


Figure 8: Compositions of pyroxenes in gabbronorite 27,45. For details see James and McGee (1979a).

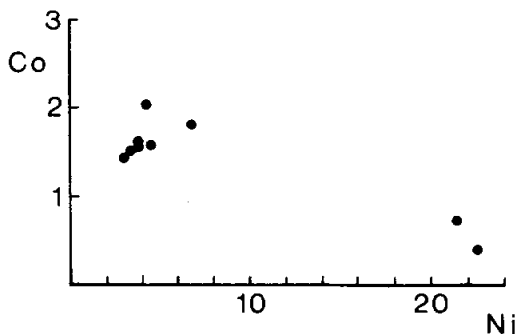


Figure 9: Ni-Co contents (wt%) of metal grains in gabbronorite 27,45. James and McGee (1979a).

grain boundaries was produced by heating within the breccia, not by direct shock heating, whereas K-feldspar glass shows characteristics indicative of both thermal and shock melting. Injection of veinlets and globules of mafic melt probably accompanied the shock event. The evidence suggests that the clast was heated to more than 990 degrees C after incorporation into the breccia.

James and McGee (1980a, b) extracted five small mare basalt clasts from 73255, describing them

and providing microprobe analyses. They are fractured and locally granulated; one is a collection of basalt fragments in a fine-grained matrix. The fragments are rounded and concentrated in the mottled lithology of the core. The basalts are generally subophitic but are all at least slightly different in grain size and texture; they probably form a sequence related by differentiation. The finest-grained fragment has some variolitic patches. Olivine and Cr-spinel crystallized first, followed by composite pyroxenes (pigeonite

cores to ferroaugite rims) and plagioclase. Pyroxene and olivine analyses are shown in Fig. 10; these phases are iron-rich (e.g. olivine Fo<66) as they are in mare basalts. The plagioclases are calcic, averaging about An93. The basalts are high-alumina mare basalts, petrographically most similar to high-alumina mare basalt 14053. The granulation of the fragments appears to have taken place before the basalts had finished crystallizing; because the granulation appears to be a result of the shock event that produced the breccia, the basalts are inferred to be about 3.87 Ga old. The fragment consisting of basalts in a fine-grained matrix also has some patches of very fine-grained melt that is aluminous like the host aphanite.

Nord and James (1978a,b) reported electron petrographic studies of an undeformed anorthite (An97; about 540 x 700 microns) and a shocked anorthite (An94, 450 x 200 microns). The undeformed anorthite showed no visible deformation in normal microscopy. The TEM studies showed a low dislocation density and unusually small type (c) antiphase domains; the former indicates no significant shock effects, the latter that the latest event was rapid cooling through 600 degrees C. The shocked anorthite had microscopically visible deformation lamellae and undulatory extinction. The TEM studies showed the presence of tiny crystallites, each with minute twin lamellae. The anorthite had been shocked into a glass and then devitrified, cooling rapidly, perhaps in two stages, to less than 840 degrees C.

The petrographic studies of the structure and lithologies of 73255 show that it crystallized from a mass of aphanitic melts of similar composition, including the vesicular rind, that contained numerous mineral and lithic clasts of varied shock history. All clasts were heated by the melt to above

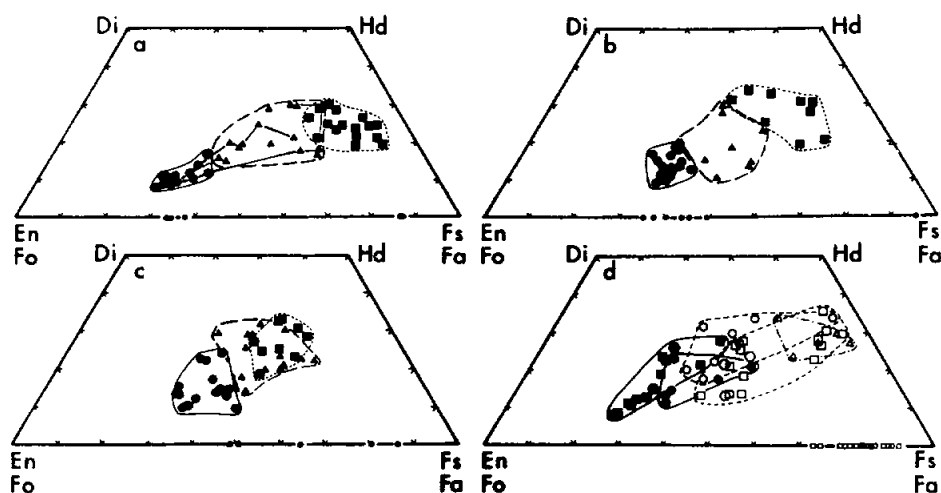


Figure 10: Compositions of pyroxenes and olivines in basalt clasts in 73255. Diagram d) contains data from 3 clasts; the others each are data from a single clast. James et al. (1980a).

900 degrees C and then cooled rapidly. Following crystallization, there were no significant shock effects.

CHEMISTRY

Major and trace element analyses of the bulk rock and aphanitic melt phases are compiled in Tables 2 and 3, with plots of the rare earth abundances in Fig. 11. A plot of rare earth abundances in comparative vesicular/non-vesicular aphanite pairs (James et al., 1978a) is given as Figure 12. Defocused beam microprobe analyses of the melt phase of the aphanitic melt phases are given in Table 4. Major and trace element analyses of separated clasts are given in Table 5, with a description of the clasts as analyzed by Blanchard and Budahn (1979a) given as Table 6. The rare earth element plots of Blanchard and Budahn (1979a) for different clast groups are presented as Fig. 13a-c. Mineral separates for pyroxene anorthosite (norite) 27,80, and not a bulk rock sample, were analyzed for trace elements by Blanchard and Budahn (1979a); the rare earth element plot for these separates and

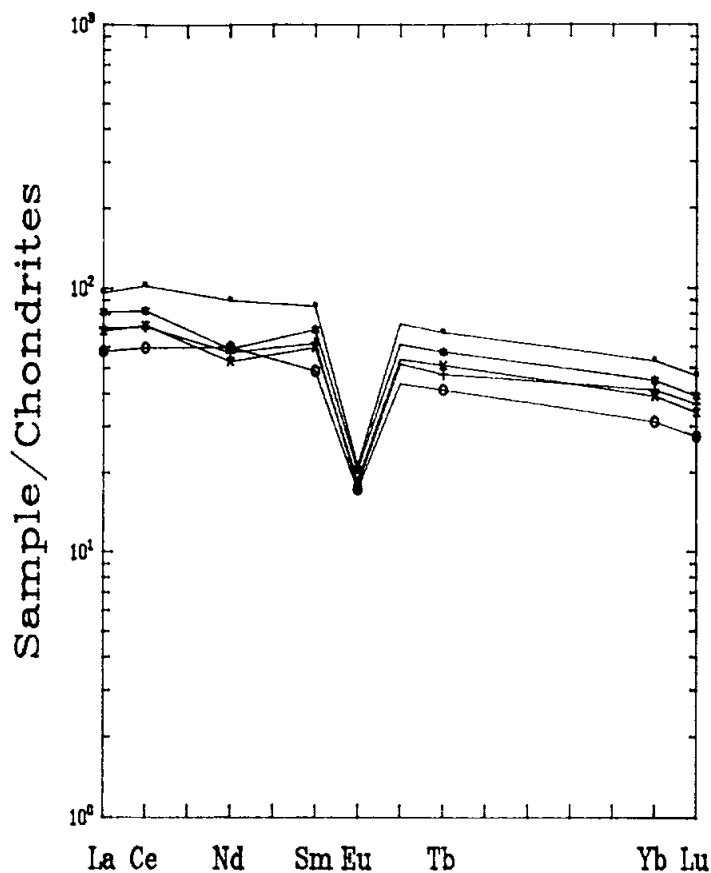


Figure 11: Rare earth elements in aphanites from 73255 (James et al., 1978).

VESICULAR/NONVESICULAR MATRIX FROM 73255

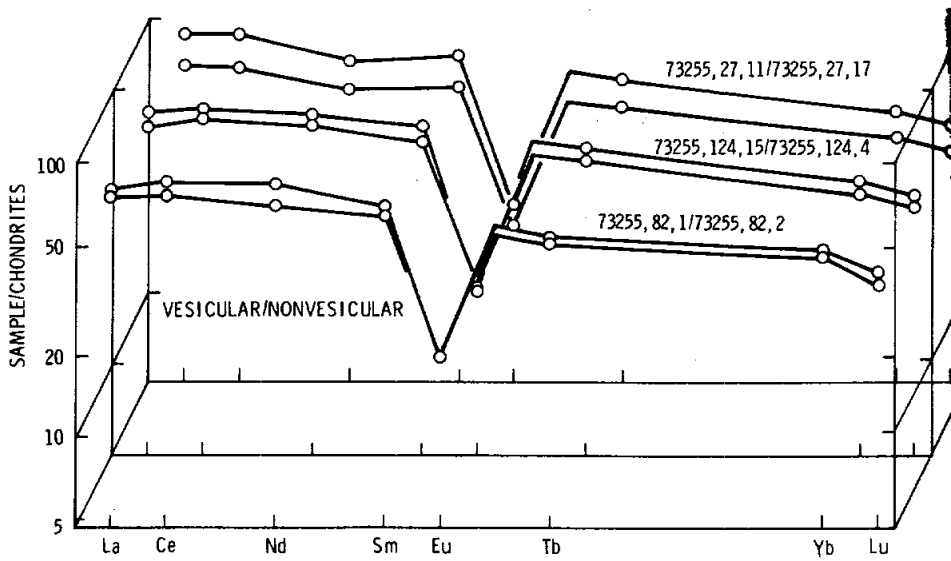
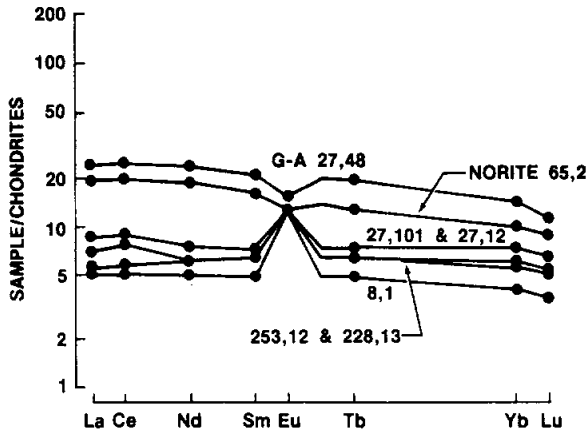
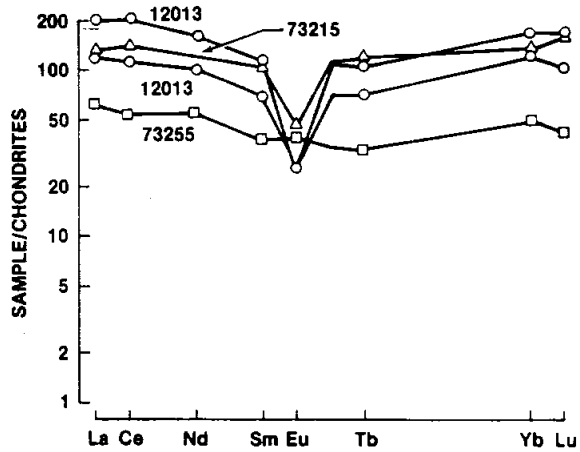


Figure 12: Comparison of rare earths in vesicular/non-vesicular aphanite pairs in 73255. (James et al. 1978).

ANT SUITE CLASTS FROM 73255



FELSITES FROM 73255, 73215, & 12013



BASALT CLASTS FROM 73255

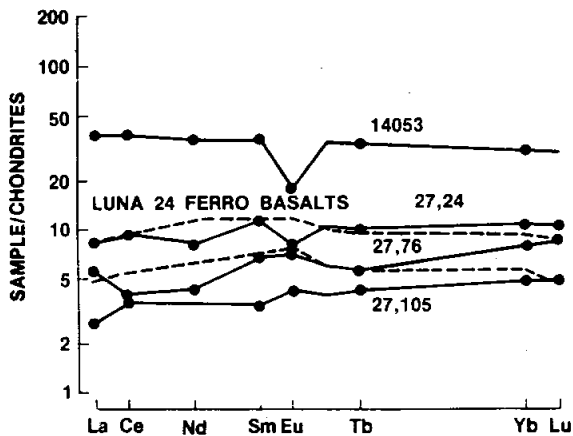


Figure 13: Rare earth element plots for different clast groups. (Blanchard and Budahn, 1979a).

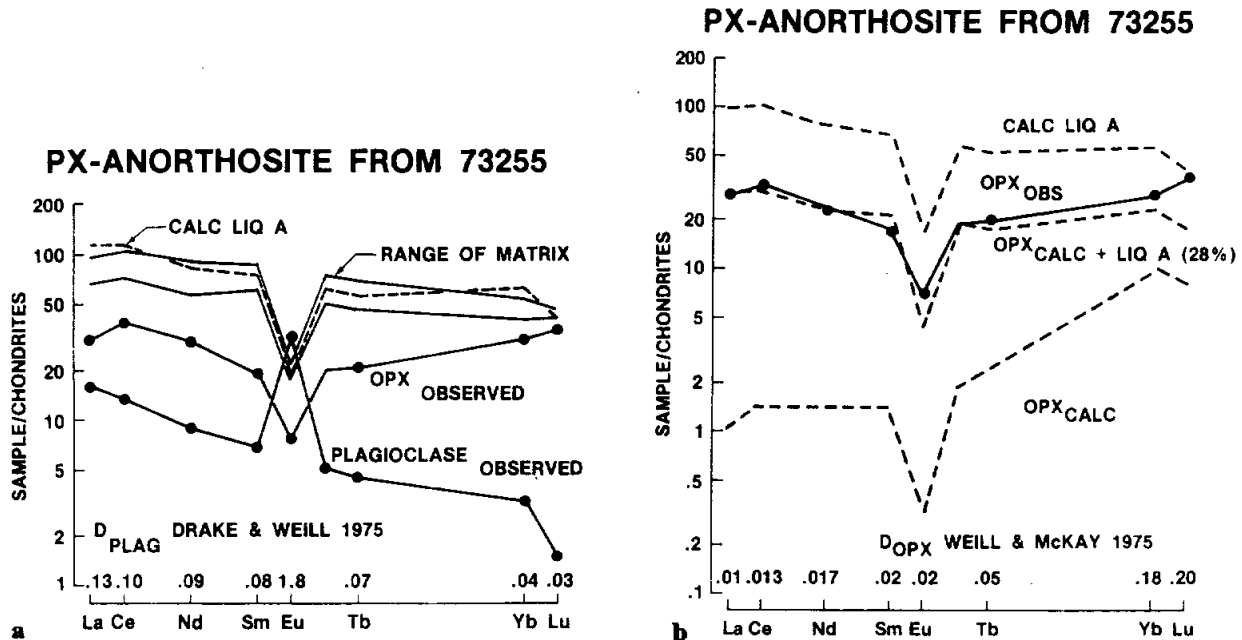


Figure 14: a) Rare earth element plots for mineral separates for pyroxene anorthosite (norite) ,27,80 and parent (LIQ A) calculated from plagioclase separate. b) Rare earth elements calculated for pure orthopyroxene and impure orthopyroxene separate for ,27,80. (Blanchard and Budahn, 1979a).

calculated parent melts are given as Fig. 14a, b. The aphanitic melt breccia data show that the compositions cluster very tightly, more so than those in 73215, and are rather similar to other Apollo 17 fragment-laden melts, such as the Station 6 and 7 boulders. However, the 73255 aphanites do have lower TiO_2 (James et al., 1978, Blanchard et al., 1978). The 73255 aphanitic melts differ from others such as 73215 and the Boulder 1 Station 2 samples in being less feldspathic and having a lower dispersion of Al_2O_3 and FeO among samples; however, most trace elements are virtually indistinguishable. The vesicular aphanites in 73255 appear to be slightly enriched in rare earth elements by about 10-30% compared with the non-vesicular aphanites (Table 3, Fig. 12). Other data suggests that the vesicular samples are enriched in some volatiles, such as Rb and Bi (Table 3). The aphanites are contaminated with meteoritic siderophiles and volatiles, corresponding with the Anders Group 2 assigned to Serenitatis rocks (Morgan and

Petrie, 1979a, b). Defocused beam microprobe analyses of the groundmass of the aphanites, avoiding clasts and thus corresponding with melt, indicate that the melt is fairly homogeneous and corresponds closely with bulk rock (Table 4). This indicates that the clast population has a bulk composition similar to that of the melt (James et al., 1978).

The gabbronorite clast 27,45 was analyzed as a tiny (10-12 mg) bulk samples (2 chips with different compositions) by Blanchard and Budahn (1979a, b) and for Sm and Nd by Carlson and Lugmair (1981). The coarse grain size makes these unrepresentative. The incompatible element contents are fairly low (Table 5, Fig. 13a) The norite has low enough Ni to be considered lacking in meteoritic contamination, although one of the subsamples has some black veins. The pyroxene anorthosite (norite) clast 27,80 was analyzed only for trace elements on mineral separates (Blanchard and Budahn, 1979a, b); the data indicates crystallization

from an evolved parent with incompatible trace elements not unlike the host aphanite breccia; however, clearly the norite did not crystallize in place from such a parent.

The felsite sample analyzed was tiny (2.0 mg) and can hardly be representative. It is similar in major elements to the 73215 felsite and to 12013; it lacks the negative Eu anomaly of these others (Fig. 13b). Blanchard and Budahn (1978a, b) find their data indicative of an origin by liquid immiscibility.

The three basalt fragments analyzed (Blanchard and Budahn, 1978a, b) have major element compositions similar to high-alumina mare basalts, particularly Apollo 14 examples such as 14053, but the rare earth elements are more similar to very low Ti mare basalts (Fig. 13c). The samples are generally similar but differ in detail; again, these are tiny analyzed pieces (less than 10 mg).

Table 2: Major and trace element chemistry of aphanite phases in 73255.

Split	.110 S	.148 N	.135,5 A	.253,13 B	.27,101 C	.122 V	.176 S	.245 N	.27,46 D	.0 E	Split
wt%											wt%
SiO ₂	(47.5)	(47.9)	(47.0)	(48.6)	(46.8)						SiO ₂
TiO ₂	1.02	1.01	1.00	0.85	0.82						TiO ₂
Al ₂ O ₃	18.5	18.2	18.4	18.0	19.0						Al ₂ O ₃
Cr ₂ O ₃	0.31	0.36	0.34	0.34	0.32						Cr ₂ O ₃
FeO	9.0	9.7	9.7	9.3	9.5						FeO
MnO	0.13	0.14	0.14	0.13	0.13						MnO
MgO	11.8	11.7	11.6	11.6	11.4						MgO
CaO	11.0	10.2	11.0	10.3	11.2						CaO
Na ₂ O	0.50	0.44	0.49	0.48	0.44						Na ₂ O
K ₂ O										0.191	K ₂ O
P ₂ O ₅											P ₂ O ₅
ppm											ppm
Sc	19.7	21.3	22.1	20.8	22.0						Sc
V	57	68	64	63	66						V
Co	28.2	33.7	30	33.1	29						Co
Ni	180	210	209	236	237				167		Ni
Rb											Rb
Rb (a)	9.93	5.31				9.85	5.54	5.28			Rb(a)
Sr	212	153	160	189	164						Sr
Sr (a)	126.1	122.8				128.6	125.4	118.1			Sr(a)
Y											Y
Zr											Zr
Nb											Nb
Hf	10.9	9.2	7.5	10.4	6.0						Hf
Ba	360	421	343	358	176						Ba
Th	5.6	4.0	3.9	4.6	2.9				1.310	3.47	Th
U										1.00	U
Ce											Ce
Ta	1.7	1.1	1.0	1.1	0.9						Ta
Pb											Pb
La	31.8	23.3	22.8	26.9	19.1						La
Ce	89.7	62.8	63.5	72.1	52.3						Ce
Pr											Pr
Nd	53.8	34.3	31.7	35.4	35.9						Nd
Sm	15.4	11.2	10.8	12.6	8.79						Sm
Eu	1.47	1.23	1.29	1.42	1.19						Eu
Gd											Gd
Tb	3.18	2.21	2.39	2.69	1.93						Tb
Dy											Dy
Ho											Ho
Er											Er
Tm											Tm
Yb	10.6	8.23	7.8	8.95	6.23						Yb
Lu	1.59	1.24	1.15	1.33	0.93						Lu
Li											Li
Be											Be
B											B
C											C
N											N
S											S
P											P
Cl											Cl
Br											Br
Cu											Cu
Zn									1.77		Zn
ppb											ppb
Au									3.0		Au
Ir									5.3		Ir
I											I
At											At
Ga											Ga
Ge									191		Ge
As											As
Se									87		Se
Mo											Mo
Tc											Tc
Ru											Ru
Rh											Rh
Pd									7.7		Pd
Ag									0.75		Ag
Cd									6.3		Cd
In									<2		In
Sn											Sn
Sb									2.0		Sb
Te											Te
W											W
Re									0.479		Re
Os									5.7		Os
Pt											Pt
Hg											Hg
Tl									1.99		Tl
Bi									<0.17		Bi
	(1)	(1)	(1)	(1)	(1)	(1)	(1)	(1)	(2)	(3)	

References and methods:
 (1) James et al. (1978): INAA; (a) from ID/MS (a) also in Blanchard et al. (1978)
 (2) Morgan and Petric (1979a,b): RNAA
 (3) Eldridge et al. (1974a,b): Gamma ray spectroscopy.

Notes:
 V = vesicular
 N = non-vesicular
 S = slightly vesicular, from core-rind contact
 A = large globule in mottled lithology
 B = coating on clast of granulated anorthositic
 C = black fraction of black and white nodules
 D = coating on granulated noritic clast
 E = bulk rock

Table 3: Major and trace element chemistry of comparative core-rind vesicular/non-vesicular aphanite melt phases in 73255 (James et al., 1978).

Split wt%	.82,1 V	.82,2 N	.124,15 V	.124,4 N	.27,11 V	.27,17 N	.130 V	.124 N	Split wt%
SiO ₂	(48.4)	(48.0)	(47.0)	(45.6)	(48.1)	(47.1)			SiO ₂
TiO ₂	0.87	0.92	0.96	1.06	0.94	1.02			TiO ₂
Al ₂ O ₃	17.3	18.4	17.1	17.9	18.5	18.3			Al ₂ O ₃
Cr ₂ O ₃	0.35	0.33	0.40	0.35	0.33	0.35			Cr ₂ O ₃
FeO	9.4	8.9	9.7	10.1	9.1	9.5			FeO
MnO	0.14	0.12	0.15	0.15	0.13	0.13			MnO
MgO	12.6	11.2	13.5	12.9	11.3	11.3			MgO
CaO	10.2	11.2	10.4	11.2	10.8	11.6			CaO
Na ₂ O	0.49	0.48	0.48	0.49	0.51	0.47			Na ₂ O
K ₂ O	0.25	0.34	0.27		0.27	0.14			K ₂ O
P ₂ O ₅									P ₂ O ₅
ppm									ppm
Sc	20.5	19.8	20.9	23.0	20.3	22.3			Sc
V	68	63	76	67	71	79			V
Co	27	26	27.4	28.2	25.2	29.2			Co
Ni	167	175	148	206	160	208	188	149	Ni
Rb									Rb
Rb(a)			(b)5.47	5.56					Rb(a)
Sr	131	145	140	150	140	160			Sr
Sr(a)			(b)126.0	127.3					Sr(a)
Y									Y
Zr									Zr
Nb									Nb
Hf	8.8	8.5	8.2	9.0	9.4	8.7			Hf
Ba	333	307	350	280	430	308			Ba
Th	4.3	4.1	4.3	4.3	4.8	3.6			Th
U							1.420	1.180	U
Cs									Cs
Ta	1.3	1.1	1.0	1.0	1.2	1.0			Ta
Pb									Pb
La	27.2	25.1	28.0	24.6	28.7	22.5			La
Ce	76.2	68.4	76.9	70.6	77.3	58.6			Ce
Pr									Pr
Nd	50.7	43.0	50	45	41.7	33			Nd
Sm	12.8	11.7	13.5	11.9	13.4	10.3			Sm
Eu	1.36	1.33	1.27	1.32	1.43	1.21			Eu
Gd									Gd
Tb	2.54	2.45	2.94	2.64	2.85	2.24			Tb
Dy									Dy
Ho									Ho
Er									Er
Tm									Tm
Yb	9.57	8.46	9.37	8.40	9.14	7.27			Yb
Lu	1.35	1.22	1.38	1.26	1.38	1.11			Lu
Li									Li
Be									Be
B									B
C									C
N									N
S									S
F									F
Cl									Cl
Br									Br
Cu									Cu
Zn							2.2	2.4	Zn
Pb									Pb
Au							3.2	2.4	Au
Ir							5.4	4.4	Ir
I									I
At									At
Ga									Ga
Ge							240	166	Ge
As									As
Se							91	81	Se
Mo									Mo
Te									Te
Ru									Ru
Rh									Rh
Pd							7.8	6.0	Pd
Ag							0.66	0.55	Ag
Cd							4.6	5.1	Cd
In							<3	<2	In
Su									Su
Sb							1.25	1.13	Sb
Te									Te
W									W
Re							0.482	0.383	Re
Os							5.6	5.2	Os
Pt									Pt
Hg									Hg
Tl							1.68	1.46	Tl
Bi							0.63	0.29	Bi
	(1)	(1)	(1)	(1)	(1)	(1)	(2)	(2)	

References and methods:

- (1) James et al. (1978); INAA (SiO₂ by difference); (a) ID/MS (a) also in Blanchard et al. (1978)
 (2) Morgan and Petric (1979a,b); RNAA

Notes:

- V = vesicular
 N = non-vesicular
 (b) analysis on slightly vesicular, core-rind contact

Table 4: Defocused beam microprobe analyses of clast-free groundmass areas of 73255. (James et al. (1978).

73255 ¹													
Section number	314(78)				9009(124)				280(171)			315 (158)	316 (265)
Analysis number Type	1 C	2 NV	3 SV	4 V	5 BFC	6 SV	7 V	8 V(VAR)	9 NV(F)	10 NV(M)	11 NV(C)	12 C	13 NV
SiO ₂	47.6	48.3	48.3	48.5	48.7	48.3	47.4	48.0	48.4	48.3	48.5	48.8	48.0
TiO ₂	0.87	1.01	1.07	0.96	0.83	1.21	1.50	1.46	0.99	1.02	1.05	0.98	1.07
Al ₂ O ₃	17.4	17.6	17.1	17.6	17.4	17.7	17.6	18.0	18.4	17.9	18.1	18.0	17.5
FeO	9.03	8.84	9.37	9.37	9.40	10.2	11.8	10.3	9.10	9.54	9.64	9.08	9.34
MnO	0.12	0.12	0.12	0.17	0.12	0.14	0.16	0.13	0.12	0.14	0.13	0.11	0.16
MgO	11.8	11.5	11.4	11.2	12.2	10.8	9.12	9.58	11.4	11.2	11.2	11.4	11.5
CaO	11.2	11.4	11.4	11.2	10.5	11.5	12.0	11.9	11.4	11.3	11.4	11.0	11.4
Na ₂ O	0.54	0.54	0.57	0.59	0.89	0.55	0.59	0.58	0.43	0.48	0.48	0.50	0.49
K ₂ O	0.30	0.38	0.40	0.47	0.57	0.36	0.37	0.38	0.27	0.26	0.29	0.33	0.32
Cr ₂ O ₃	0.27	0.26	0.27	0.27	0.29	0.29	0.27	0.23	0.25	0.31	0.29	0.28	0.26
P ₂ O ₅	0.20	0.21	0.23	0.22	0.17	0.16	0.16	0.22	0.21	0.21	0.25	0.22	0.19
Total	99.33	100.16	100.23	100.55	101.07	101.21	100.97	100.78	100.97	100.66	101.33	100.70	100.23
Number of spots analysed	15	11	15	8	4	10	10	10	11	10	12	7	3

73255 ¹											73215 ²		
Section number	286(265)			219(120)			Average C	Average NV	Average SV	Average V	Average black aphanitic matrix	Average gray aphanitic matrix	Average Schlieren-rich gray aphanitic matrix
Analysis number Type	14 C	15 NV	16 SV	17 SV	18 V	19 V(C)	(1 + 12 + 14)	(2 + 9 + 11 + 13 + 15)	(3 + 16 + 17)	(4 + 18)			
SiO ₂	47.6	47.7	48.1	48.7	48.5	48.7	48.0	48.2	48.4	48.5	47.6	46.7	48.1
TiO ₂	0.99	1.05	0.98	1.09	1.08	1.08	0.91	1.03	1.06	1.03	1.00	1.09	1.04
Al ₂ O ₃	18.3	17.5	17.5	18.3	17.4	18.7	17.6	17.8	17.6	17.5	19.0	19.0	18.0
FeO	9.49	9.71	9.27	9.37	9.52	8.61	9.08	9.41	9.35	9.45	8.26	8.27	8.73
MnO	0.13	0.13	0.11	0.13	0.14	0.17	0.12	0.13	0.12	0.15	0.10	0.09	0.13
MgO	11.5	11.5	11.2	10.4	11.1	9.49	11.7	11.4	11.1	11.2	10.5	11.7	10.9
CaO	11.4	11.0	11.0	11.6	11.3	12.0	11.1	11.3	11.3	11.3	12.0	11.9	11.8
Na ₂ O	0.49	0.49	0.48	0.55	0.57	0.60	0.52	0.48	0.54	0.58	0.76	0.64	0.62
K ₂ O	0.32	0.34	0.29	0.35	0.39	0.43	0.31	0.31	0.36	0.43	0.29	0.30	0.31
Cr ₂ O ₃	0.25	0.26	0.30	0.27	0.27	0.24	0.27	0.27	0.28	0.27	0.15	0.16	0.19
P ₂ O ₅	0.16	0.22	0.14	0.19	0.12	0.17	0.20	0.22	0.20	0.16	0.41	0.25	0.31
Total	100.63	99.90	99.37	100.95	100.39	100.19	99.81	100.55	100.31	100.57	100.07	100.10	100.13
Number of spots analysed	2	20	7	9	10	5	24	67	31	18	14	4	7

¹C—cryptocrystalline; NV—nonvesicular; SV—slightly vesicular; V—vesicular; (VAR)—variolitic; (F)—relatively fine grained; (M)—relatively medium grained; (C)—relatively coarse grained; BFC—within 60 μm of edge of felsite clast. Sample numbers are thin section numbers; parent piece for thin section is given in parentheses.

²From James (1976). Analyses were done at University of New Mexico by G. H. Conrad and K. Keil; SiO₂ and MgO values tabulated here have been corrected for systematic interlaboratory biases.

Table 5: Major and trace element chemistry of clasts in 73255.

Split	27,76,1 Bas	27,25,1 Bas	27,109 +100,1 Bas	8,1 Anor	27,101,7 Anor	253,12,1 Gab-an	228,13,5 An-gab	27,12,2 An-gab	27,48,7 An-gab	154,1,2 An-gab	27,65,2,1 Nor	27,65,2,2 Nor	27,45 Nor
wt%													
SiO ₂	(43.6)	(46.1)	(52.9)	(43.0)	(45.5)	(45.9)	(46.9)	(47.1)	(46.1)	(46.6)	(51.1)	(49.8)	
TiO ₂	2.1	1.54	0.34	0.02	0.27	0.10	0.26	0.18	0.28	1.47	0.68	0.52	
Al ₂ O ₃	14.2	13.8	14.2	31.3	27.4	29.7	25.0	25.5	28.1	19.9	9.5	15.0	
Cr ₂ O ₃	0.51	0.46	0.72	0.056	0.10	0.07	0.181	0.09	0.102	0.297	0.30	0.23	
FeO	16.6	17.1	15.4	3.24	7.9	4.4	6.7	6.6	6.3	9.4	12.1	9.2	
MnO	0.26	0.26	0.23	0.05	0.05	0.06	0.08	.06	0.055	0.127	0.18	0.14	
MgO	11.0	9.5	10.1	3.24	7.9	4.4	6.7	6.6	6.3	9.9	18.7	14.8	
CaO	11.5	11.0	10.0	18.7	14.0	15.9	14.8	14.9	14.5	11.6	7.1	9.8	
Na ₂ O	0.23	0.26	0.18	0.37	0.36	0.39	0.33	0.37	0.42	0.47	0.34	0.46	
K ₂ O				0.04						0.28		0.08	
P ₂ O ₅													
ppm													
Sc	52.9	63.4	51.5	5.44	5.7	7.7	11.7	8.0	7.9	22	21.9	15.9	
V	120	160	220				35	24	18	78	78	58	
Co	26.5	22	36	6.48	24	4.2	20	32	18	26	23	20	
Ni				24	320	50	190	440	115	130	35	35	
							154	511					
Rb													
Sr		50	95		220	180	130			190	140	135	
Y													
Zr													
Nb													
Hf	1.55	1.51	0.45	0.58	1.2	0.98	0.96	1.1	3.5	7.5	1.8	0.9	
Ba					65		40	60	100	210	80	50	
Th		0.28		0.27	1.0	0.63	0.55	0.9	2.5	3.2	1.4	0.37	
U							0.025	0.027					
Ca													
Ta		0.30			0.36		0.18	0.2	0.6	1.1	0.14	0.14	
Pb													
La	1.82	2.75	0.92	1.67	2.92	1.79	2.32	3.0	7.9	16.7	9.77	3.15	
Ce	3.5	8.2	3.0	4.6	7.8	5.2	6.9	7.9	21.8	46	27	8.7	
Pr													
Nd	3.2	4.8			4.4	3.6	3.7	4.7	14	28	18	4.4	4.27
Sm	1.28	2.03	0.62	0.88	1.26	1.15	1.11	1.33	3.8	8.2	4.24	1.48	1.68
Eu	0.49	0.62	0.29	0.83	0.86	0.83	0.77	0.82	1.03	1.2	0.75	1.09	
Gd													
Tb	0.27	0.47	0.20	0.23	0.34	0.30	0.30	0.35	0.91	1.6	0.84	0.37	
Dy													
Ho													
Er													
Tm													
Yb	1.58	2.23	0.95	0.83	1.47	1.13	1.21	1.45	2.85	6.5	2.61	1.49	
Lu	0.30	0.36	0.16	0.12	0.22	0.17	0.18	0.22	0.42	1.0	0.38	0.22	
Li													
Be													
B													
C													
N													
S													
P													
Cl													
Br													
Cu													
Zn							1.71	1.92					
ppb													
Au							2.7	9.3					
Ir							6.5	21					
I													
At													
Ga													
Ge							75	172					
As													
Se							33	62					
Mo													
Tc													
Ru													
Rh													
Pd							7.9	23					
Ag							0.56	0.77					
Cd							4.4	3.8					
In							<3	<2					
Sn													
Sb							2.5	1.68					
Te													
W													
Re							0.582	2.0					
Os							8.3	26					
Pt													
Hg													
Tl							0.89	1.35					
Bi							0.37	0.30					
	(1)	(1)	(1)	(1)	(1)	(1)	(1)	(1)	(1)	(1)	(1)	(1)	(2)

References and methods:
 (1) Blanchard and Budahn (1979a,b); INAA (SiO₂ by difference)
 except (a) Morgan and Petric (1979a,b); RNAA
 (2) Carlson and Lagmir (1981); ID/MS

Notes: The norites are all the same clast.

Table 6: Description of samples listed in Table 5.

Type sample number	Analyzed sample number	Sample descriptions
<i>Basalts</i>		
27,76	27,76,1	Single, clean piece of vuggy basalt (6.69 mg)
27,24	27,25,1	Basalt chip, black vuggy (9.33 mg)
27,105	(27,109) (110,1)	Coarser grained basalt, subophitic, vuggy (3.87 mg)
<i>Anorthosites</i>		
27,101	8,1 27,101,7	Anorthosite analyzed in 1974; major elements by AAS White material from the black and white nodule (see 27,101,10 for black) (9.96 mg)
<i>Gabbroic Anorthosite</i>		
253,12	253,12,1	3 plagioclase clasts (13.5 mg) from coherent gabbroic anorthosite clast
<i>Anorthositic Gabbros</i>		
228	228,13,5	Fine-grained, sugary clean piece of G-A (22.72 mg)
27,1	27,12,2	Fine-grained, sugary clean piece of G-A (30.70 mg)
27,48	27,48,7	Medium-grained, clean G-A (23.66 mg)
154,1	154,1,2	Very fine-grained G-A (8.32 mg)
<i>Norite</i>		
27,45	27,65,2,1	Clean sample of granulated, coarse-grained norite (12.91 mg)
27,45	27,65,2,2	Norite chip same as 27,65,2,1 but containing black veins (10.63 mg)
<i>Felsite</i>		
27,3	27,3	2 mg sample of hand picked, clean felsite and felsite and felsite glass
<i>Plagioclase</i>		
27,95	27,95,1	Pure plagioclase sample (3.9 mg)
27,80	27,80,1	Hand picked plagioclase separate from coarse grained pyroxene anorthosite—very clean (2.5 mg)
<i>Pyroxene</i>		
27,80	27,80,2	Hand picked pyroxene separate from coarse grained pyroxene anorthosite—probably not pure (0.7 mg)

The other highland breccia samples analyzed appear to be fairly typical lunar anorthositic breccias and feldspathic impactites, contaminated with meteoritic siderophiles. They have low rare earth abundances and positive Eu anomalies (Fig. 13a). One (154, not shown on Fig. 13a) is like a "very high alumina basalt" and appears to be an impact melt. Two of the feldspathic impactites ("anorthositic gabbros") were analyzed for meteoritic siderophiles and volatiles and appear to be different in total abundance but fall in the same group 3 inferred to be a pre-Serenitatis meteoritic component (Morgan and Petrie, 1979 a, b).

RADIOGENIC ISOTOPES AND GEOCHRONOLOGY

^{40}Ar - ^{39}Ar stepwise heating analyses on several samples of aphanitic melt breccias were conducted by Jessberger et al. (1978) and Staudacher et al. (1979a, b); a single sample was similarly analyzed by Eichorn et al. (1979a, b), who also included aphanitic melt phases in their laser pulsed Ar study of materials in 73255. Jessberger et al. (1978) analyzed four samples of different aphanitic types, summarized in Table 7 and Fig. 15. The apparent age spectra all show some structure, with clear low-temperature argon loss, then a low temperature "plateau" succeeded by a dip then a high-temperature "plateau". The low temperature "plateau" indicates

a slightly younger age than the high temperature one (Table 7). The preferred interpretation of the authors is that the high-temperature region dates clasts and the low temperature region the melt; the dip might be a recoil effect. There are no clear differences between the melt age for vesicular and non-vesicular samples, but the vesicular samples appear to contain clasts that are much more degassed than those in the non-vesicular melts. Jessberger et al. (1978) conclude that the age of the melt and breccia-forming event is 3.88 ± 0.03 Ga. Staudacher et al. (1979a, b) analyzed four more aphanitic melts (Tables 8 and 9 and Fig. 16), with similar results, and further discussed the significance of the structure in the temperature releases. The age inferred for the melt, i.e. the low-temperature

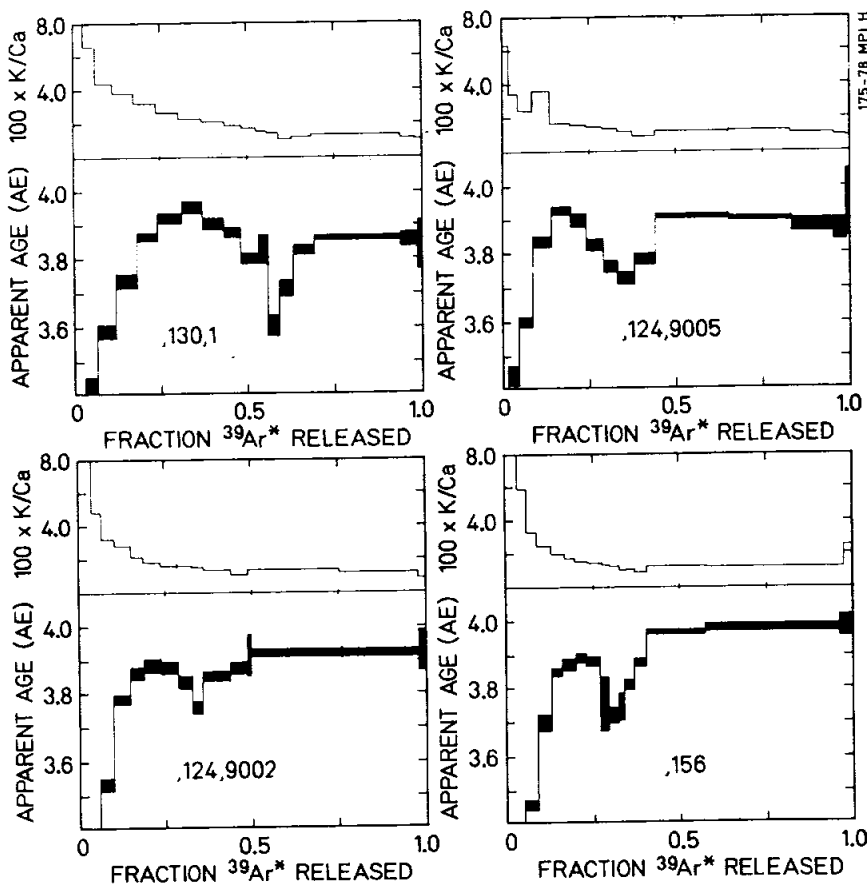


Figure 15: Ar-Ar and K/Ca release diagrams for 73255 aphanitic melts. Vesicularity decreases from top left to bottom right. Jessberger et al. (1978).

"plateau", depends on the model used to understand the structure, as listed in Table 9. In model A the dip is explained by gas loss from microclasts during breccia formation; in model B the dip results from recoil from the fine-grained groundmass and results in slightly younger ages for breccia formation. Eichorn et al. (1979a, b) analyzed one sample of aphanite and obtained a roughly similar release structure (Fig. 17), although the dip is not so prominent. The precise age of the melt is difficult to infer from this release.

Eichorn et al. (1979a, b) used laser release from polished surfaces to obtain gas for Ar analyses of various phases in 73255. Samples were pre-heated to remove low-temperature gas, and the data correspond with K-Ar ages of an assumed higher-temperature plateau (assuming therefore no structure in the high-temperature release) because temperature cannot be controlled in this experiment. The inferred age data for the aphanites (included in the summary Table 10) are varied and determination of the age of the breccia-forming event is difficult at best. Clearly much material did not

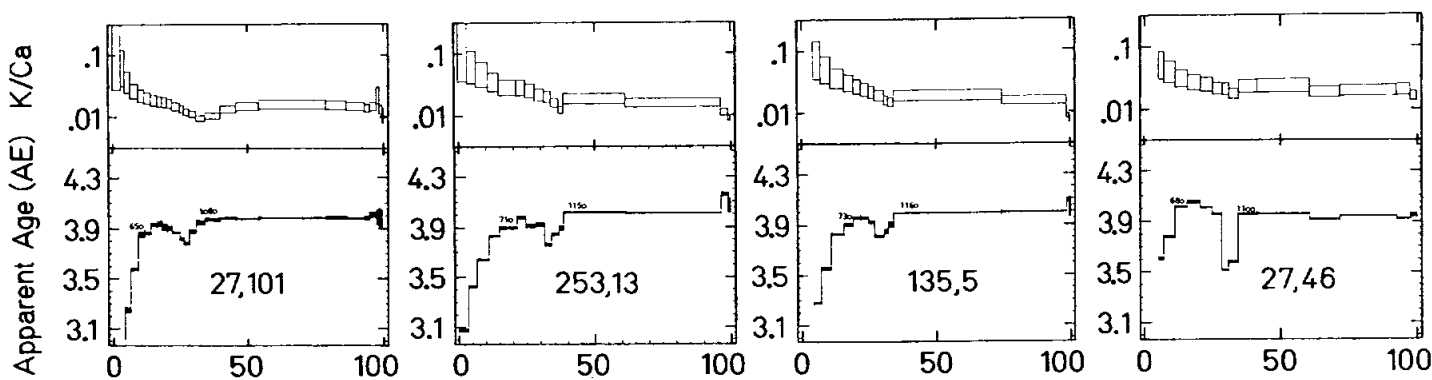


Figure 16: Ar-Ar and K/Ca release diagrams for 73255 aphanitic melts. Staudacher et al. (1979a).

Table 7: Summary of Ar-Ar release age data for 73255 aphanitic melts. ,156 is non-vesicular core; ,124,9002 is a less-vesicular core/rind boundary sample; ,124,9005 is a more-vesicular core/rind boundary; ,130,1 is vesicular rind. Jessberger et al. (1978).

Sample Subnumber	K [ppm]	Ca [%]	Exposure Age ^{a)} [m.y.]	K-Ar Age ^{b)} [AE]	⁴⁰ Ar- ³⁹ Ar Plateau Ages ^{c)}		Temperature Ranges
					Plateau 1	Plateau 2	
,156	1090	8.0	104	3.90	3.88 ± .02(670–810)	3.98 ± .01(1160–1440)	⁴⁰ Ar-loss corrected K-Ar Age 3.94 ± .03(670–1440)
,124,9002	1420	9.6	99	3.89	3.88 ± .02(700–820)	3.92 ± .01(1150–1400)	3.90 ± .02(700–1400)
,124,9005	1280	9.9	93	3.84	3.92 ± .02(720–780)	3.91 ± .01(1140–1410)	3.89 ± .03(720–1410)
,130,1	1350	7.7	86	3.80	3.90 ± .03(670–860)	3.86 ± .01(1160–1360)	3.86 ± .03(670–1360)

^{a)}Error is 15 m.y.

^{b)}Absolute uncertainty is 0.03 AE (1 σ).

^{c)}Uncertainties listed are 2 σ and appropriate for comparison of the results within this study. Plateau ranges are given in brackets.

Table 8: Summary of Ar-Ar release age data for 73255 aphanitic melts and clasts. Plateau 2 is the high-temperature region inferred to represent clasts. Staudacher et al. (1979a).

Sample subnumber		K [ppm]	Ca [%]	Exposure Age ^{a)} [m.y.]	K-Ar age ^{b)} [AE]	⁴⁰ Ar- ³⁹ Ar age ^{d)}	
						Plateau 1 ^{c)} [AE]	Plateau 2 [AE]
253,13	aphanite coating	1380	7.2	97	3.92		4.00 ± .01
135,5	aphanite in mottled lithology	1430	7.2	96	3.89		3.99 ± .01
27,101	aphanite from black and white nodule	1130	7.3	92	3.89		3.99 ± .01
27,46	aphanite coating	1670	7.4	94	3.87		3.94 ± .01
156 ⁺	nonvesicular core aphanite	1090	8.0	96	3.90		3.98 ± .01
124,9002 ⁺	less vesicular aphanite from core-rind contact	1420	9.6	91	3.89		3.92 ± .01
124,9005 ⁺	more vesicular aphanite from core-rind contact	1280	9.9	86	3.84		3.91 ± .01
130,1 ⁺	highly vesicular rind aphanite	1350	7.7	79	3.80		3.86 ± .01
228	} anorthositic gabbro clasts	450	9.7	92	3.95	3.96 ± .01	4.20 ± .01
27,1.2		600	9.2	94	3.90	3.93 ± .01	4.14 ± .02
27,1.1		630	10.1	88	3.85	3.91 ± .02	—
27,48		590	9.7	89	3.89	3.93 ± .02	—

^{a)} Error is 10 m.y.

^{b)} Absolute uncertainty is .03 AE

^{c)} Low temperature ages for aphanites are listed in Table 3.

^{d)} An absolute error of ±.03 AE is not included.

⁺ Results are taken from Jessberger *et al.* (1978).

Table 9: Model ages for low temperature regions of Ar-Ar release data for 73255 aphanitic melts. Temperature range for corresponding fractions given in parentheses. Staudacher et al. (1979a).

Sample subnumber	Model A Age Plateau 1 [AE]	Model B Age [AE]	³⁹ Ar redistribution in Region I [%]
73255,253,13	3.92 ± .02 (710–900)	3.89 ± .03 (710–1080)	1.2
135.5	3.93 ± .02 (730–880)	3.90 ± .02 (730–1090)	1.4
27,101	3.90 ± .02 (650–890)	3.88 ± .02 (650–1010)	1.1
27,46	4.01 ± .02 (680–890)	3.89 ± .09 (680–1030)	5.1
156	3.88 ± .02 (670–810)	3.83 ± .03 (670–1010)	1.7
124,9002	3.88 ± .02 (700–820)	3.85 ± .02 (700–1030)	.8
124,9005	3.92 ± .02 (720–780)	3.82 ± .04 (720–1060)	2.0
130,1	3.90 ± .03 (670–860)	3.85 ± .04 (670–1080)	2.2

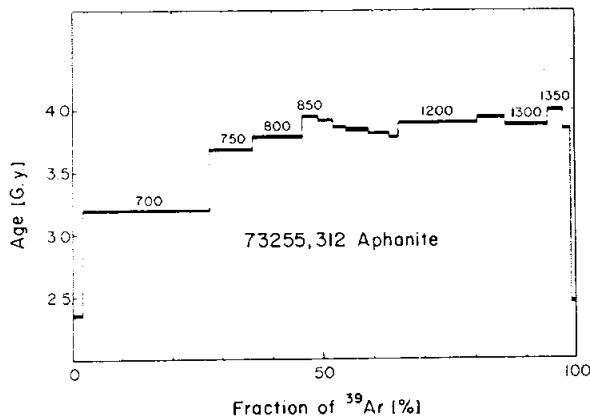


Figure 17: Ar-Ar release diagram for a 73255 aphanitic melt. Eichorn et al. (1979a).

completely degas at the time of melting, which is best inferred from the best-degassed clasts and the thermal releases (such as those of Staudacher et al. (1979a) which agree at 3.87 ± 0.03 Ga.

James et al. (1978) reported Rb and Sr isotopic data on 7 aphanitic melt phases from 73255.

Calculated to about 3.9 Ga, the data show that there were significant differences in ⁸⁷Sr/⁸⁶Sr at that time (Fig. 18), thus the melt did not then equilibrate over a scale of a few millimeters. The data indicate similarities with other aphanitic melts (Fig. 18) with the bulk data reflecting mixing of materials.

Staudacher et al. (1979a, b) conducted thermal release Ar-Ar studies on clasts in 73255: one felsite and three "anorthositic gabbros" (one duplicate). The data are summarized in Table 8 and the release diagrams shown as Fig. 19 (anorthositic gabbros) and Fig. 20 (felsite). Two of them (228 and one chip of 27,1 are stated to have a marked 2-step release, with low temperature release indicating lower ages. The other two show low temperature releases that rise more gradually to high-temperature, higher ages (Fig. 19). The felsite (Fig. 20) is the same clast analyzed by Blanchard and Budahn (1979a, b); it shows a high-temperature plateau age of 3.89 ± 0.03 Ga over the last 50% of Ar

release. This is inferred to date the melting and degassing of the felsite as it was incorporated into the melt, thus dating the melt event.

Eichorn et al. (1979a, b) used laser release from polished surfaces to obtain gas for Ar analyses of various phases in 73255. Samples were pre-heated to remove low-temperature gas and the data correspond with K-Ar ages of an assumed higher-temperature plateau (assuming, therefore, no structure in the high-temperature release) because temperature cannot be controlled in this experiment. The inferred age data for the clasts are summarized in Table 10. They show a wide variety of ages, including some that are rather younger than the inferred age of the host melt, e.g. felsites range from 3.48 to 3.98 Ga. Devitrified maskelynites give "ages" as old as 5.5 Ga (Table 12), hence maskelynites must be considered unreliable for determining ages. No other samples except some groundmasses suggest ages older than 4.0 Ga.

Carlson and Lugmair (1981) reported a Sm-Nd isotopic analysis of the pristine igneous gabbronorite 27,45 (Table 13, Fig. 21). The three-point isochron gives an age of 4.23 ± 0.05 Ga and is well defined. The T_{ICE} age is similar to the isochron age, thus the

**Table 10: Summary of laser Ar ages (Ga) in 73255, for melt and clasts (preheated samples).
Eichorn et al. (1979a).**

Sample	Preheating temperatures ⁽¹⁾		
	650°C	700°C	900°C
<i>Groundmass</i>			
73255,255			
nonvesicular	4.10 ± .01	4.09 ± .03*	4.21 ± .01*
(~ 2 μm grain size)	4.07 ± .01*		4.03 ± .01*
	4.00 ± .01		
cryptocrystalline			4.02 ± .01*
(< 1 μm grain size)			
73255,310			
highly vesicular	3.76 ± .01	3.78 ± .01*	3.86 ± .03*
(~ 4–5 μm grain size)	3.80 ± .01*		
	3.78 ± .01		
slightly vesicular			3.91 ± .02*
(~ 2 μm grain size)			
73255,309			
fine-grained (~ 1 μm)	3.91 ± .01	4.09 ± .01	4.07 ± .01
coarse-grained (5–10 μm)	3.80 ± .01	3.81 ± .01	3.70 ± .02
<i>Felsic clast material</i>			
73255,255			
glass A	3.77 ± .01	3.72* ± .01	3.73* ± .01
	3.58* ± .01		
K-feldspar A	3.96 ± .01	3.93* ± .01	3.92* ± .01
	3.98* ± .01		
K-feldspar C	3.94 ± .02		
K-feldspar B			3.73 ± .03
73255,310			
partly melted			
vermicular intergrowth C	3.72 ± .01		3.97 ± .02*
	3.69* ± .01		
partly melted			
vermicular intergrowth I	3.77 ± .01	3.82 ± .02*	
glass H	3.69 ± .01		3.87 ± .02*
plagioclase H	3.87 ± .03		
partly melted			
vermicular intergrowth D			3.86 ± .02*
vermicular intergrowth F			3.48 ± .03*
73255,312			
glass D	3.59† ± .01		
<i>Lithic clasts</i>			
ANT-suite fine-grained anorthositic gabbro			
73255,310			
shocked clast M	3.81 ± .01		
small plagioclases in clast J	3.74 ± .01	3.84* ± .02	
large plagioclases in clast J	3.93 ± .01		

Table 10: Continued.

Sample	Preheating temperatures ⁽¹⁾		
	650°C	700°C	900°C
<i>Lithic clasts</i>			
73255,309 clast B	3.67 ± .01	3.77 ± .05	
73255,312 clast B	3.73† ± .01		
ANT-suite coarse-grained pyroxene anorthosite			
73255,309 relict plagioclase of clast D	3.66 ± .02		} 3.92 ± .08
shattered plagioclase of clast D	3.62 ± .02		
Fine-grained quenched basalt			
73255,309 Groundmass A1	3.84 ± .01	3.81 ± .01	
Groundmass A2			3.99 ± .01
<i>Devitrified maskelynite clasts</i>			
73255,255 Centers of two 0.5-mm clasts	3.99 ± .01		
73255,310 center of 0.3-mm clast A	3.99 ± .01		
center of 0.5-mm clast B	4.82 ± .02		
	4.96* ± .05		
intermediate zone within 0.5-mm clast B	4.34 ± .03		
	4.36* ± .04		
centers of 5 0.2-mm clasts	3.89 ± .01		
73255,309 center of 0.3-mm clast	4.14 ± .02	4.20 ± .02	

⁽¹⁾ Samples were preheated for 1.5 hours at each temperature successively. Ages marked with an * were obtained on samples that were preheated twice, for a total of 3 hours, at 650°C. Ages marked with a † were obtained on a sample that was not preheated.

Table 11: Rb-Sr isotopic data for 73255 aphanites. James et al. (1978).

Sample	Rb (ppm)	Total Sr (ppm)	⁸⁷ Rb/ ⁸⁶ Sr	⁸⁷ Sr/ ⁸⁶ Sr
Vesicular rind aphanite				
122	9.85	128.6	0.2214	0.71251
Slightly vesicular aphanite, at core-rind contact				
9006 (110)	9.93	126.1	0.2276	0.71287
9004 (124)	5.47	126.0	0.1254	0.70705
Nonvesicular aphanite				
9003 (124)	5.56	127.3	0.1261	0.70698
9007 (148)	5.31	122.8	0.1248	0.70679
176	5.54	125.4	0.1276	0.70701
9008 (245)	5.28	118.1	0.1291	0.70723

Table 12: Summary of laser-released Ar studies of a 1.4 mm clast of devitrified maskelynite in 73255. Eichorn et al. (1979a).

	Center	Zone 4	Zone 3	Zone 2	Edge
Surface 1	4.20 ± .05	4.03 ± .01	4.49 ± .02	4.51 ± .02 4.20 ± .01	4.13 ± .01
Surface 2	3.99 ± .02	4.39 ± .02	4.26 ± .01	4.96 ± .02	4.02 ± .02
Surface 3	3.99 ± .01	4.01 ± .01	3.99 ± .02	5.53 ± .01	5.68 ± .02

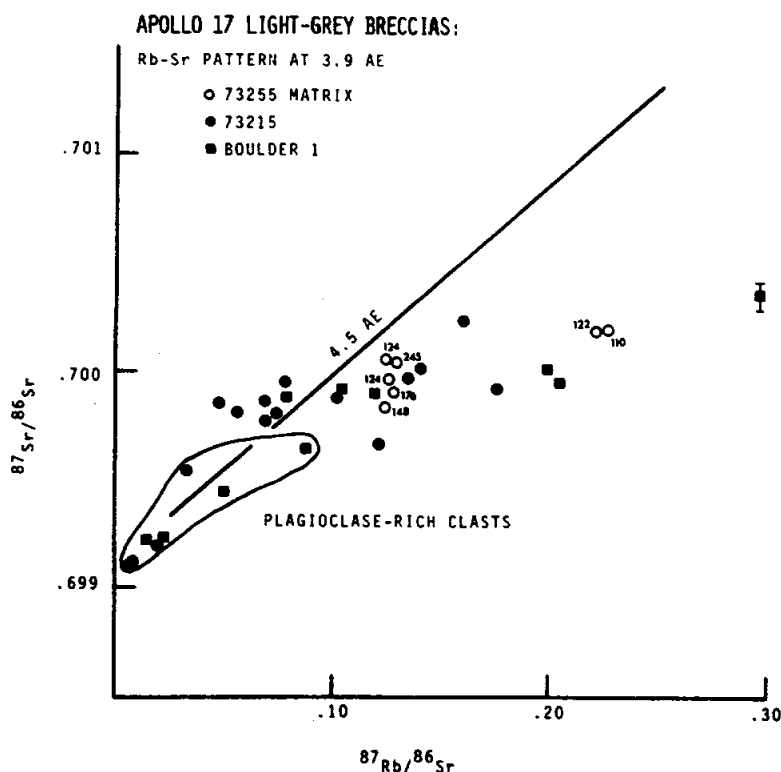
Table 13: Sm-Nd isotopic data for mineral separates and whole rock of 27.45 gabbronorite. (Carlson and Lugmair, 1981)

Sample	Weight (mg)	[Sm] (ppm)	[Nd] (ppm)	¹⁴⁷ Sm/ ¹⁴⁴ Nd ^a	¹⁴³ Nd/ ¹⁴⁴ Nd ^a	T _{ICE} ^b
Pl-1	14.2	0.841	4.52	0.1124 2	0.510393 42	
TR	12.3	1.68	4.27	0.2380 2	0.513899 45	4.23 =17
Px-1	18.3	0.523	0.976	0.3237 9	0.516332 55	

^a See footnote for Table 1.

^b ICE = "intercept with chondritic evolution" line; model parameters are: (¹⁴³Nd/¹⁴⁴Nd)_{JUV} = 0.512636, (¹⁴⁷Sm/¹⁴⁴Nd)_{JUV} = 0.1936.

Figure 18: Modified Sr evolution diagram for samples from Apollo 17 aphanitic melt rocks. The diagram shows how the pattern would have appeared if measured just after the breccias formed about 3.90 Ga ago. James et al. (1978).



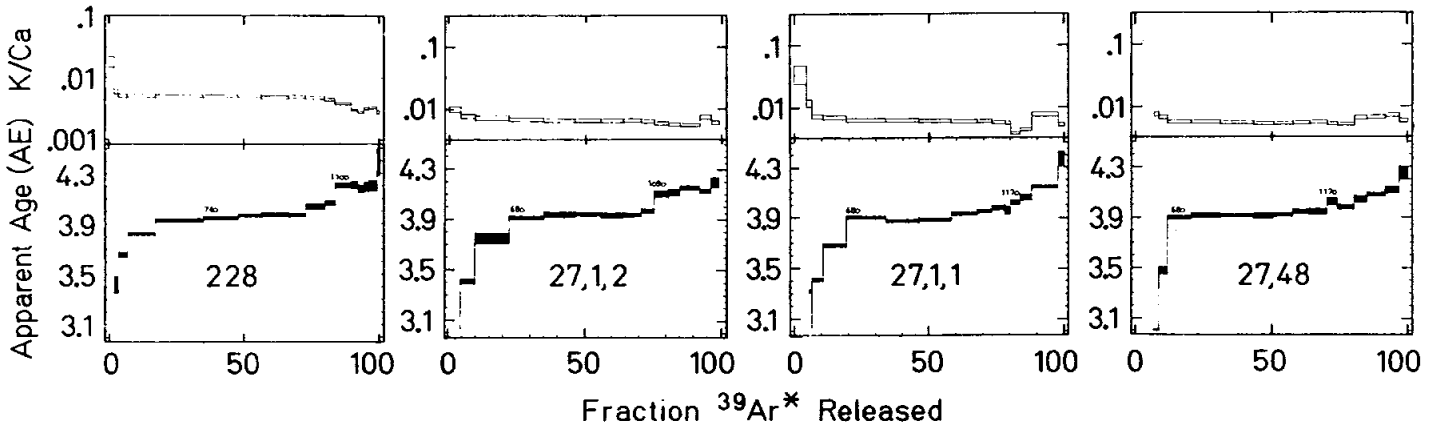


Figure 19: Ar-Ar and K/Ca release diagrams for "anorthositic gabbro" clasts in 73255, including 2 splits of a single sample. Staudacher et al. (1979a).

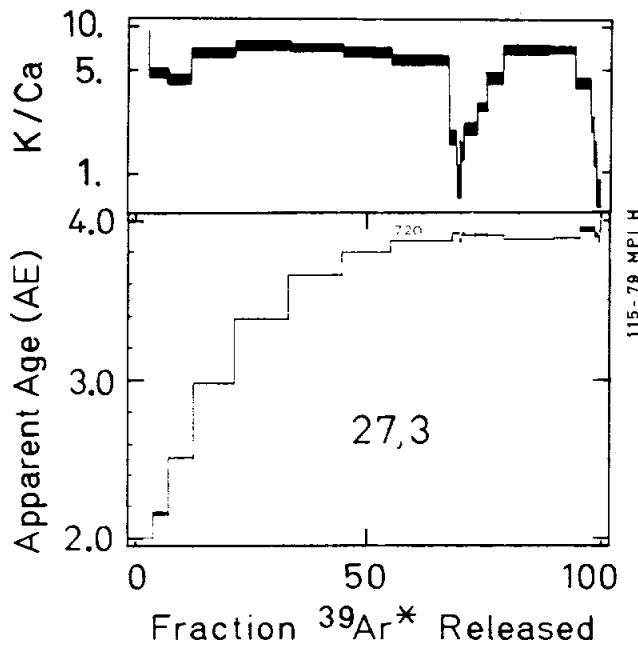


Figure 20: Ar-Ar and K/Ca release diagram for a felsite clast in 73255. Staudacher et al. (1979a).

granulation and breccia formation did not disturb the Sm-Nd system. Sources at 4.23 Ga had not sufficiently fractionated Sm/Nd or had not existed long enough to evolve a Nd isotopic signature reasonably different from the assumed chondritic reference. This implies that liquids with highly fractionated relative rare earths were crystallizing to produce melts of the Mg-suite 4.2 to 4.3 Ga ago.

EXPOSURE AGES

Microcraters on the surface of 73255 are sparse and tiny on all surfaces, and nowhere approach saturation. The uniform coverage shows that the sample must have been tumbled at least once (James and Marti, 1977).

Exposure ages have been determined from the Ar isotopic studies. Staudacher et al. (1979a, b)

listed exposure ages for clasts and aphanitic melts (Table 8) that include revisions (apparently corrected for Ti- and Fe-contributions to the $^{38}\text{Ar}_C$ production) of the exposure ages reported for four aphanitic melts by Jessberger et al. (1978). These exposure ages average 91 Ma with a range from 71 Ma to 97 Ma. The laser study of Eichorn et al. (1979a) produced a similar range of Ar exposure ages for clasts and aphanitic melts (86-104 Ma, average about 97 Ma). The stepwise heating experiment on a single sample of aphanitic melt produced a similar exposure age. This age has occurred for other landslide samples and is inferred to be the age of the landslide.

James and Marti (1977) reported an ^{81}Kr - ^{83}Kr age of 149 Ma for an interior, non-vesicular aphanitic melt. This age is substantially older than the Ar exposure ages. The high spallation $^{78}\text{Kr}/^{83}\text{Kr}$ suggests little shielding during exposure and the xenon isotopes too suggest that the entire radiation took place within a few centimeters of the surface.

Yokoyama et al. (1974) found that 73255 was saturated with both ^{22}Na and ^{26}Al , thus the sample has been exposed for at least a few million years.

PROCESSING

Following separation of a few small pieces for preliminary study, a slab about 1.5 cm thick was sawn through 73255 (Figs. 2, 4) in 1974 for the consortium study led by O. James. Butt end piece ,17 (Fig. 3) remains intact at 102 g. Some further processing of butt end piece ,12 (Fig. 2) was done but its mass too remains close to the original at 127 g. The slab piece, consisting mainly of ,27; ,20; and ,29 has been extensively subdivided and many allocations made from both interior and exterior parts. More than 100 thin sections or probe mounts have been made from many different pieces of 73255.

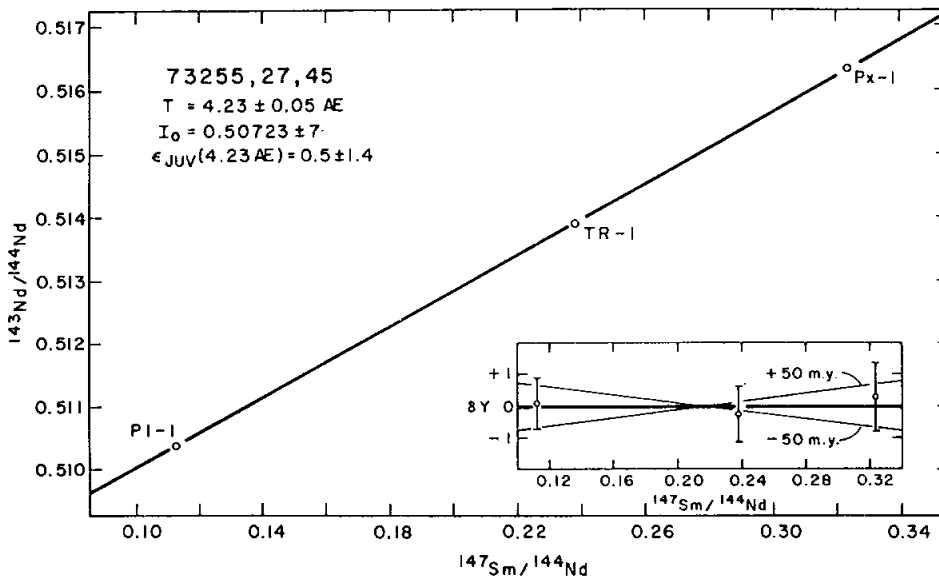


Figure 21: Sm-Nd isochron for gabbro sample, 27,45. Carlson and Lugmair (1981).

73275**Micropoikilitic Impact Melt Breccia
St. 3, 429.6 g****INTRODUCTION**

73275 is a clast-bearing micropoikilitic impact melt breccia that has a chemical composition similar to the low-K Fra Mauro melts common at the site and generally presumed to represent the Serenitatis impact melt. An Ar-Ar age of about 3.90 Ga has been determined and it had a multi-stage exposure history. 73275 was collected from the surface on the rim of the 10-m crater at Station 3. The sample is light gray, tough

with no penetrative fractures, and is homogeneous. Matrix material smaller than about 100 microns constitutes about 95% of the rock. It is 10 x 7 x 7 cm and blocky or subangular. Its surface is uneven, with many zap pits on most sides, but one area has a fresh fracture surface (Fig. 1). It has 2-3% vugs up to 6 mm in dimension, ranging in shape from near-hemispherical to slit-like; some have drusy linings. A slab was sawn through the rock (Fig. 2) and provided most but not all of the allocated subsamples.

PETROGRAPHY

No detailed description of 73275 has been published. It is a clast-bearing impact melt with a micropoikilitic texture (Fig. 3a, b, c). It is a homogeneous melt with an appearance very much like that of finer-grained "Serenitatis" melts. Large clasts are uncommon in the thin sections; those lithic clasts present are dominantly granoblastic impactites and coarse-grained feldspar-rich samples with plutonic igneous textures. Mineral

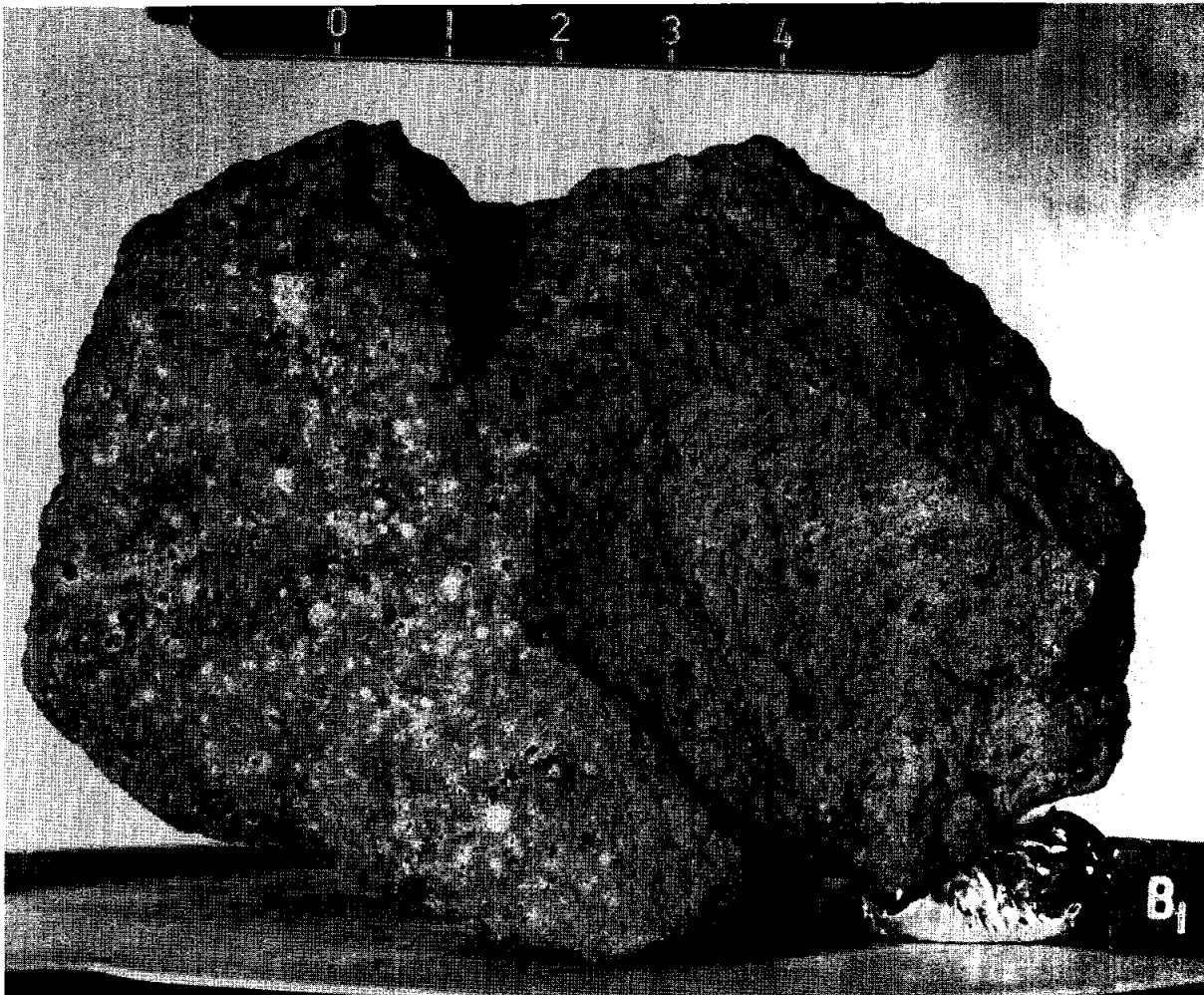


Figure 1: Pre-processing photograph of 73275, showing common eroded surface with patina and zap pits (left) and fresh broken surface (right). Scale divisions 1 cm S-73-16929

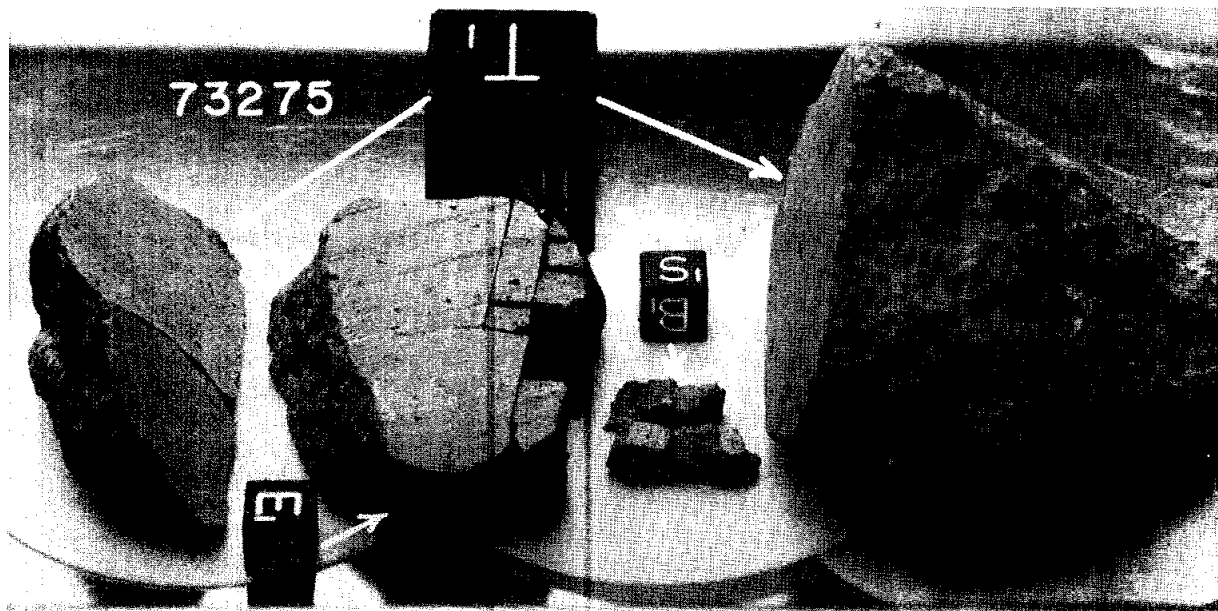


Figure 2: Slab cut of 73275. Small butt end ,2 (left) was partly broken. Large butt end ,1 (right, 274 g) was retained intact .The slab piece (center) is ,3. Further subsample numbers not shown. Small cubes are 1 cm. S-73-34459.

clasts are dominantly plagioclase, with nonetheless conspicuous olivine and some pyroxene. The groundmass consists of tiny equant plagioclases and larger but still small (less than 150 micron, generally) oikocrysts of pyroxene; ilmenite is prominent as lathy to equant grains (Fig. 3a, b). In a few areas, tiny clasts are less abundant and the groundmass consists of elongated plagioclases optically enclosed in more clearly visible pyroxenes (Fig. 3c).

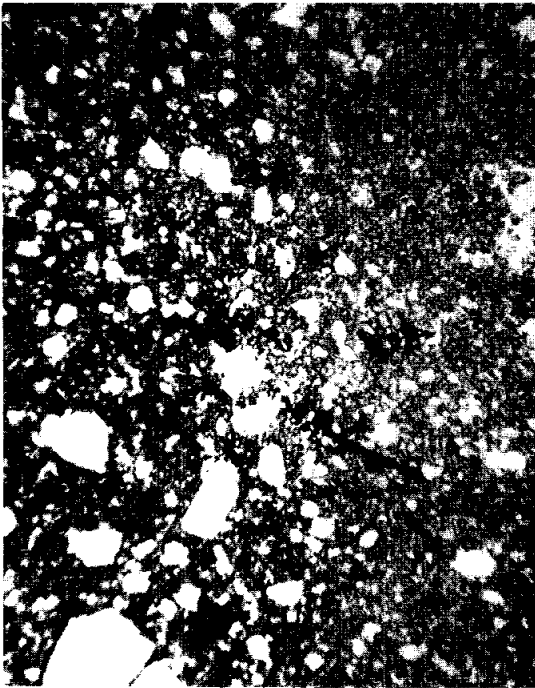
Simonds et al. (1974) listed 73275 as a rock with 50-60% feldspar and a subophitic-micropoikilitic texture. The tabulated matrix feldspar as 10-50 microns and matrix mafic grains as 10-100 microns in dimension. Their pyroxene and olivine analyses (Fig. 4) are similar to those of the other common melt rocks at Apollo 17, although some of the groundmass pyroxenes are of more magnesian composition (as much as Mg' 86). Engelhardt (1979) tabulated the paragenesis as one having ilmenite crystallization entirely post-date that of pyroxene. Heuer et al. (1974) and Radcliffe et al. (1974) described 73275 as a

recrystallized breccia with low porosity. They found that the rock consisted of large clasts of plagioclase (0.3-1.00 mm), with smaller olivines (0.05-0.2 mm) and orthopyroxenes (0.1-0.2 mm) in a fine-grained recrystallized groundmass of the same phases. Many of the plagioclases have rims separated from the clasts by a ring of dark inclusions; the clasts are more calcic (An₉₀₋₉₇) than the presumed overgrowth rims (An₈₅₋₉₀). Electron transmission studies showed that there were dislocation substructures in plagioclases and are associated with pores; there is some evidence of recovery. These authors provide electron transmission photographs. There are well-developed type (b) antiphase domains in plagioclase, and features due to movement of disassociated dislocations. In clinopyroxenes there are thin widely-spaced exsolution lamellae suggestive of prolonged annealing. Goldstein et al. (1976a,b) described the rock as having a fine-grained groundmass with plagioclase laths enclosed by poikilitic pyroxenes 0.1-0.5 mm across. Most of the clast are single crystal, but there are

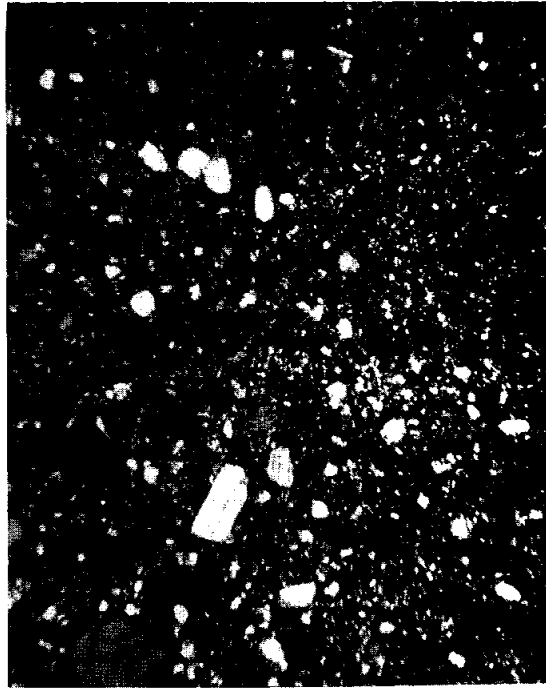
also coarse-grained granulites and devitrified plagioclase glasses. The focus of the study by Goldstein et al. (1976a, b), however, was the presence of the carbide phase cohenite ((Fe,Ni)₃C) which occurs with kamacite interstitial to silicates. They depicted an example and made microprobe analyses across grains (Fig. 5).

CHEMISTRY

Chemical analyses are given in Table 1. Most of these were originally published with little specific comment, other than the general similarity with typical "Serenitatis" melt rocks. The little available rare earth element data are consistent with that similarity. The analyses demonstrate the similarity with common meteorite-contaminated melt rocks such as the Station 6 boulder and not with the aphanitic melt rocks, which have higher alumina and lower titania. Morgan et al. (1976) assign the sample to their Group 2, the "Serenitatis" group, on the basis of meteoritic siderophile ratios.

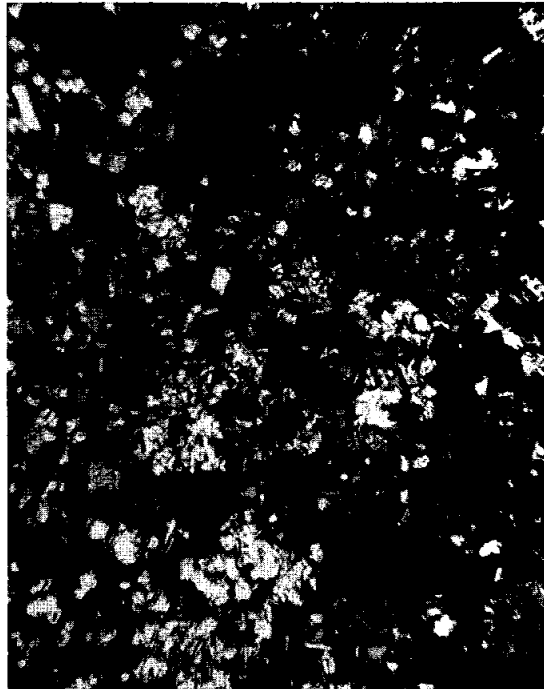


a



b

Figure 3: Photomicrographs of 73275,62. a,b) Same view with plane transmitted light (a) and crossed polarizers (b) of general clast-bearing micropoikilitic groundmass. Small clasts are obvious. Field of view about 2 mm wide. c) detail of ophitic, clast-poor area with lathy plagioclases. Crossed polarizers; field of view about 500 microns wide.



c

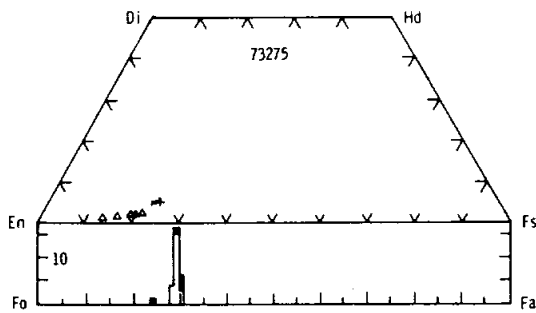


Figure 4: Microprobe analyses of pyroxenes and olivines in 73275,60. Open symbols and dots are groundmass phases; closed symbols are clasts. Simonds et al. (1974).

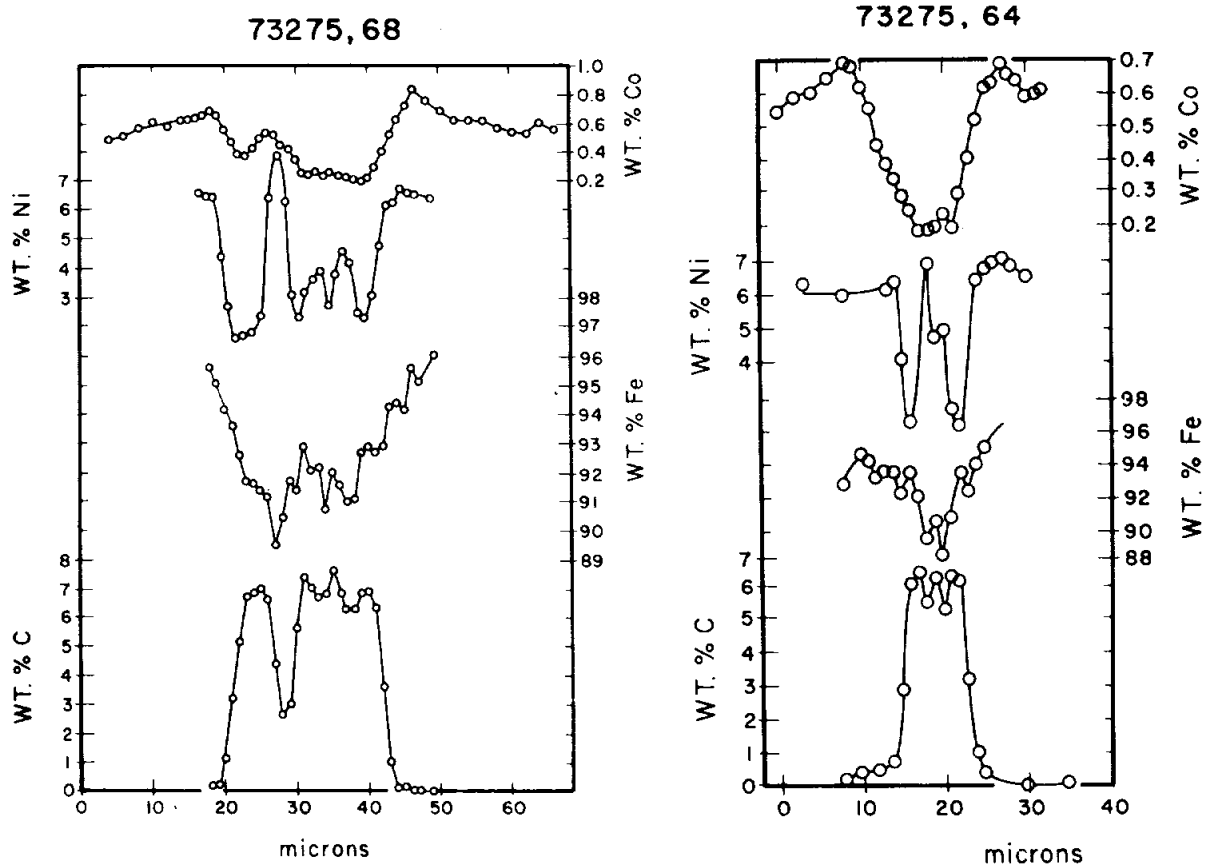


Figure 5: Profiles across Fe-metal/cohenite grains in thin sections of 73275. Goldstein et al. (1976a).

Table 1: Chemical analyses of bulk samples of 73275.

Split	,30	,0	,23	,24	,27	,28	,22
wt %							
SiO ₂	46.16						
TiO ₂	1.43						
Al ₂ O ₃	18.49						
Cr ₂ O ₃							
FeO	9.05						
MnO	0.13						
MgO	11.54						
CaO	11.30						
Na ₂ O	0.67						10.5
K ₂ O	0.27	0.269					0.28
P ₂ O ₅	0.26						
ppm							
Sc							
V							
Co							
Ni			182				
Rb	6.62		6.9			9.11	
Sr	171.8					185.5	
Y							
Zr							
Nb							
Hf							
Ba							
Th		4.53				4.97	
U		1.20	0.136		1.1	1.31	
Cs			0.270				
Ta							
Pb						2.8	
La							
Ce							
Pr							
Nd						50.67	
Sm						14.30	
Bu							
Gd							
Tb							
Dy							
Ho							
Er							
Tm							
Yb							
Lu							
Li					9.4		
Be							
B							
C							
N							
S	800			927			
F					30		
Cl					(a)11.89		
Br			0.073		(a)0.115		
Cu							
Zn			2.5				
pph							
Au			3.34				
Ir			5.71				
I					0.9		
At							
Ga							
Ge			265				
As							
Se			92				
Mo							
Tc							
Ru							
Rh							
Pd							
Ag			0.74				
Cd			4.1				
In							
Sn							
Sb			1.19				
Te			5.5				
W							
Re			0.494				
Os							
Pt							
Hg							
Tl			1.60				
Bi			0.16				
	(1)	(2)	(3)	(4)	(5)	(6)	(7)

References and methods:
 (1) Rhodes et al. (1974a,b), Nyquist et al. (1974a);XRF, AA, IS/MS
 (2) Eldridge et al. (1974a,b); Gamma-ray spectroscopy
 (3) Morgan et al. (1974a,b, 1976); RNAA
 (4) Gibson and Moore (1974a,b)
 (5) Jovanovic and Reed (1974a,b,c, 1980a); RNAA
 (6) Oberli et al. (1978); ID/MS
 (7) Turner and Cadogan (1974a); from Ar-Ar irradiation

Notes:
 (a) Combined leach and residue.

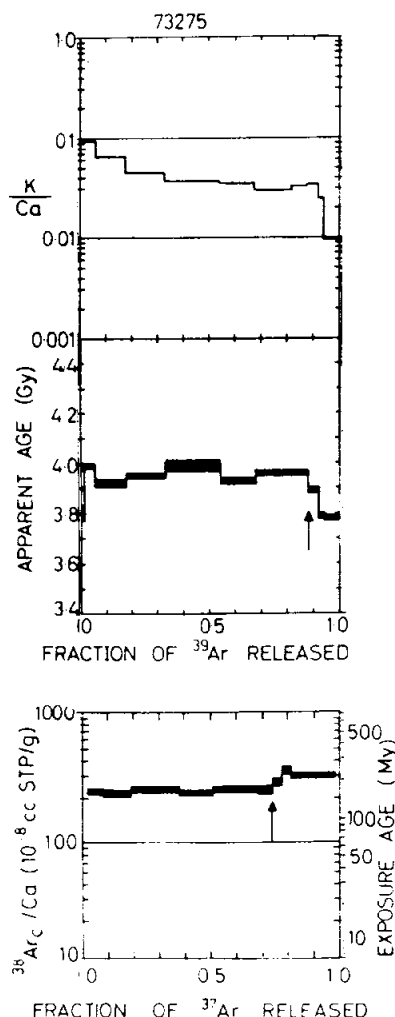


Figure 6: Ar release and apparent age with K, Ca, and Ar exposure age of 73275, 22. (Turner and Cadogan (1975a).

GEOCHRONOLOGY AND RADIOGENIC ISOTOPES

Turner and Cadogan (1974a, b) reported Ar-Ar release data. The data provide an extended plateau (Fig. 6) with a small high-temperature release. However, there is a fine structure in the plateau which is real and outside of experimental error. The apparent age is 3.90 ± 0.05 Ga (new decay constants; old decay constants 3.96 Ga), and the total Ar age is identical.

Nyquist et al. (1974a) provided Rb and Sr isotopic data that is similar

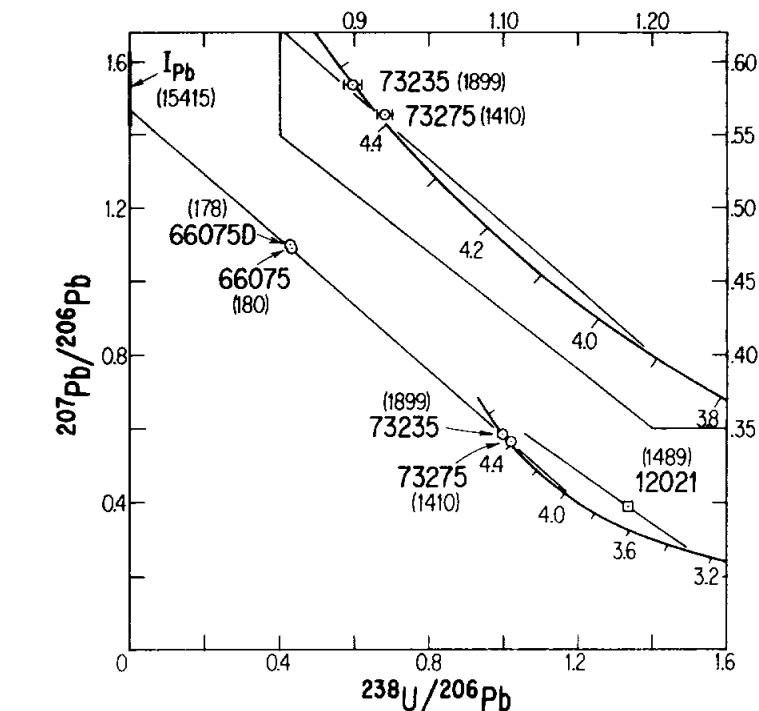


Figure 7: U-Pb evolution diagram for 73275, 28 and other samples. The u values are given in parentheses. A reference line is drawn through points corresponding with 4.42 and 3.9 Ga. Oberli et al. (1978).

to the other "noritic breccias" that they analyzed, falling on the same 3.96 Ga (new decay constants) line of unclear significance. The $^{87}\text{Rb}/^{86}\text{Sr} = 0.1112 \pm 10$ and the $^{87}\text{Sr}/^{86}\text{Sr} = 0.70619 \pm 5$. These data provide T_{Babi} of 4.39 ± 0.07 Ga (new decay constants) and T_{Luni} of 4.42 ± 0.07 Ga. Oberli et al. (1978) provided corresponding isotopic ratios of 0.1598 and 0.70870 ± 5 , and T_{Babi} of 4.18 ± 0.03 Ga (new decay constants). As for sample 73235, the young Rb-Sr model ages imply that either crust formation occurred at these late model ages or that remelting of materials relatively rich in Rb/Sr took place then.

Oberli et al (1978) also provided Sm-Nd and U-Th-Pb isotopic data. The $^{147}\text{Sm}/^{144}\text{Nd}$ of 0.1708 ± 1 and the $^{143}\text{Nd}/^{144}\text{Nd}$ of 0.511092 ± 19 give T_{Juv} of 4.51 ± 0.02 Ga and T_{Chur} of 4.91 ± 0.15 Ga. As for sample 73235,

these model ages are older than the Rb-Sr model ages, implying that the events that lead to Rb/Sr increases in the history of these samples were not accompanied by changes in the Sm/Nd ratio. The U-Th-Pb isotopic data are marginally concordant at 4.42 Ga. (Figure 7). However, the tangential relationship (again, like 73255) is poorly suited to discriminating a discordant array. The $^{207}\text{Pb}/^{206}\text{Pb}$ age is 4.418 ± 2 Ga, the $^{206}\text{Pb}/^{238}\text{U}$ age is $4.404 \pm 16/-17$ Ga, and the $^{208}\text{Pb}/^{232}\text{U}$ age is 4.379 ± 41 Ga.

RARE GASES AND EXPOSURE

It is apparent that 73275 had a multi-stage exposure history. Turner and Cadogan (1974a) derived a nominal exposure age of 160 Ma from $^{38}\text{Ar}/\text{Ca}$ data (Figure 5). Crozaz et al. (1974a, b) reported Kr isotopic data and

spallation spectra. They derived an exposure age of 139 +/-5 Ma. This Kr data and also xenon isotopic data was also discussed by Arvidson et al. (1976). The relatively high $(^{131}\text{Xe}/^{126}\text{Xe})_c$ of 5.7 and the fact that the $(^{80}\text{Kr}/^{83}\text{Kr})_c$ and $(^{82}\text{Kr}/^{83}\text{Kr})_c$ are the highest among the samples they analysed indicates substantial shielding and is inconsistent with a simple surface history. They suggest that the Kr age of 139 Ma overestimates the true surface residence time.

Crozaz et al. (1974a, b) also reported nuclear track data for 73275, giving 4.7 +/-1 Ma for a single point determination at 2.9 +/-0.4 cm depth, which provides a maximum surface exposure. They suggest (using soil radiation data also) that the age of Ballet Crater is 5 to 20 Ma. Goswami and Lal (1974) also studied track densities, giving a "sun tan" age of 1.2 Ma and a subdecimeter age of about 8 Ma. The "sun tan" age suggests frequent chipping of the rock. The flattening of the track profiles at depths greater than 1 cm clearly show a multiple exposure history. No pre-irradiated components were found among feldspar clasts.

Yokoyama et al. (1974) found the sample to be saturated in ^{22}Na and ^{26}Al , the latter requiring exposure of at least 2 or 3 Ma.

PHYSICAL PROPERTIES

Huffman et al. (1974a) and Huffman and Dunphyre (1975) used Mossbauer and magnetic methods to understand the state of iron in various phases of 73275. 96.1% of the total Fe is in silicates (66.3% in pyroxenes, 29.8% in olivines), 3.2% in ilmenite, 0.7% in FeS, and 0.735% as Fe^0 . The total Fe^{2+} is 8.5%. They were conducting low-temperature Mossbauer studies of superparamagnetic clustering of Fe^{2+} spin in lunar olivines.

Nagata et al. (1974a, b, 1975a) tabulated some magnetic data for 73275,15 (Table 2) in a study that was partly meant to elucidate the origin of lunar iron. Housley et al. (1976) found no FMR intensity (unlike soils) in their magnetic study of 73275,25.

PROCESSING

A sawn slab (,3) was produced in 1973, with exterior and interior pieces. Several chips were taken from exterior areas for exposure and other studies (Fig. 2). Two of these (,4, and , 6) were made into potted butts for thin sections. Some subdivisions and allocations were made from end piece ,2, which is now 26 g. Further chipping from the subsamples was conducted in 1975. The large end piece ,1 is now 274 g, and the largest remaining slab piece (,3) is 69 g. The three large pieces account for all but about 60 g of the original sample.

Table 2: Magnetic data for 73275,25. Nagata et al. (1974a).

Parameter	73275-15 (Br)	Unit
I_n	13.4	$\times 10^{-4}$ emu/g
I_0	1.1	$\times 10^{-6}$ emu/g
\dot{H}_0	105	Oe · rms
h	13	Oersteds
\dot{H}'_0	3	Oe · rms
$\Delta I / I$	0.08	
Stability of NRM	(3)	

73285

Glass-Coated Polymict Breccia
St. 3, 2.58 g

INTRODUCTION

73285 is a friable polymict breccia that is dusty and partly coated with dark vesicular glass (Figure 1). It was picked from the regolith sample 73280 taken from a trench on the rim of a 10 m crater at Station 3. The sample is medium light gray (N6) and barely coherent.

It is of very irregular shape with approximate dimensions of 1 x 1 x 2.5 cm. The glass is not uniformly distributed, being more common on one highly fragmented end of the sample, where it partly veins the breccia. The glass has a smooth surface. The breccia is fine-grained (mainly less than 0.1 mm) and consists of white plagioclase and

somewhat less abundant pale gray and yellow mafic minerals. Anorthositic clasts, possibly granulites, up to a few millimeters across are present. There are a few zap pits on one end, and cavities in the shattered part. No subdivisions of 73285 have been made.

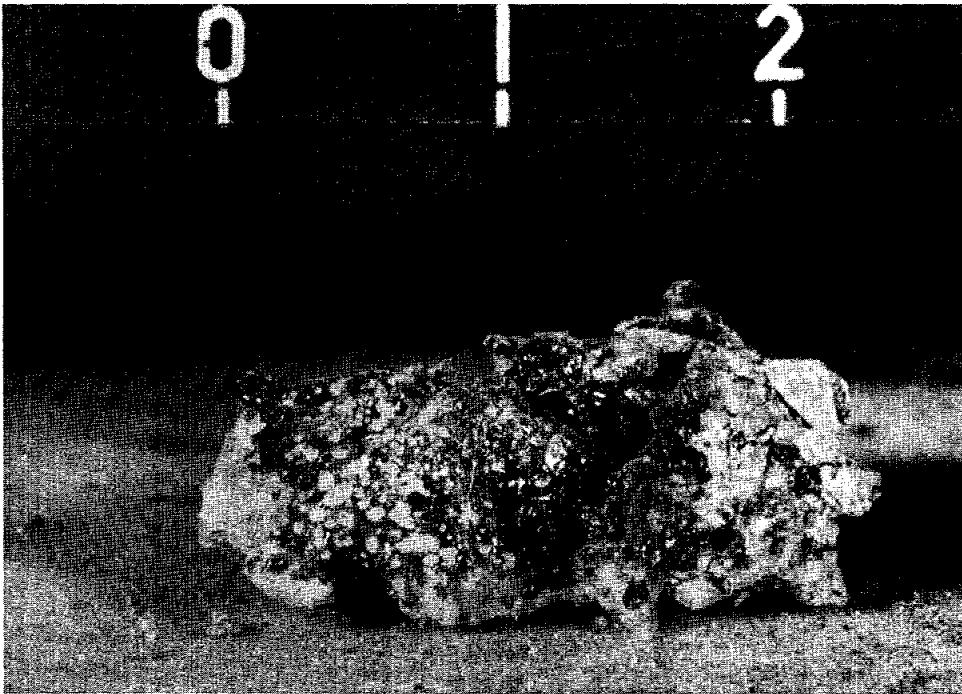


Figure 1: Photograph of 73285, showing dark glass and paler gray breccia. Scale divisions 1 cm S-73-19445.

74115

Friable Regolith Breccia

LRV-5, 15.4 g

INTRODUCTION

74115 is a rounded, very friable sample of regolith breccia, collected from the light mantle 700 m northwest of Station 3. It is a light gray polymict breccia. The sample is the largest of 5 similar pieces picked from regolith sample 74110 that was collected as light mantle material. LRV-5 is on the ejecta blanket of a 15-m crater and 74115 probably represents ejecta, possibly lithified by the impact. The fragments were observed during preliminary examination to contain about 10% white clasts and

a trace of dark clasts in a light gray matrix. All the samples are rounded and shed fine-grained material.

PETROLOGY

74115 has a fine-grained matrix consisting of angular mineral and glass fragments (Fig. 1). Some of the larger clasts are lithic fragments including very dark glassy breccias, granulites, feldspathic breccias and feldspathic impact melts, as well as some high-Ti mare basalts. Orange glass balls and shards are conspicuous.

PROCESSING AND SUBDIVISIONS

Little was originally done with the 5 samples (74115-74119) following their original separation from the regolith sample because they were so friable. 74115 was partly subdivided in 1984 to produce subchip ,1 (then 0.91g) and some smaller pieces. ,1 was made into a potted butt and partly used for four thin sections. Other splits were allocated for analyses but no data has been reported.

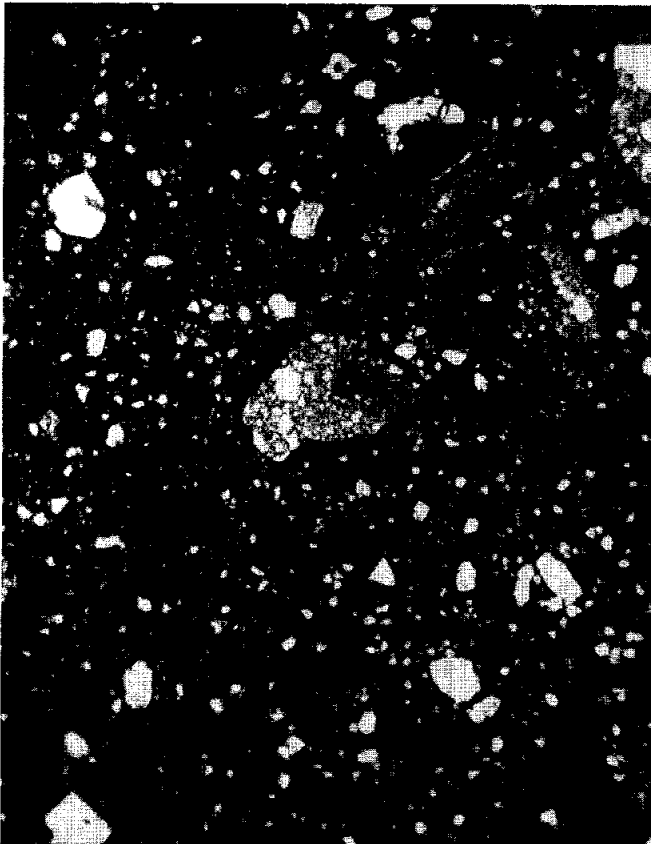


Figure 1: Photomicrograph of thin section 74115,8, showing dense matrix and mineral clasts. At top is a dense glassy breccia clast; center is a granulite. Plane polarized light. Field of view about 2 mm wide.

74116

Friable Regolith Breccia

LRV-5, 12.8 g

INTRODUCTION

74116 is a rounded, very friable sample of regolith breccia, collected from the light mantle 700 m northwest of Station 3. It is a light gray polymict breccia. The sample is the second largest of 5 similar pieces picked from regolith sample 74110 that was collected as light mantle material. LRV-5 is on

the ejecta blanket of a 15-m crater and 74116 probably represents ejecta, possibly lithified by the impact. The fragments were observed during preliminary examination to contain about 10% white clasts and a trace of dark clasts in a light gray matrix. All the samples are rounded and shed fine-grained material. No subdivisions of 74116 have been made.

74117

Friable Regolith Breccia

LRV-5, 3.69 g

INTRODUCTION

74117 is a rounded, very friable sample of regolith breccia, collected from the light mantle 700 m northwest of Station 3. It is a light gray polymict breccia. The sample is one of the smallest of 5 similar pieces picked from regolith sample 74110 that was collected as light mantle material. LRV-5 is on

the ejecta blanket of a 15-m crater and 74117 probably represents ejecta, possibly lithified by the impact. The fragments were observed during preliminary examination to contain about 10% white clasts and a trace of dark clasts in a light gray matrix. All the samples are rounded and shed fine-grained material. No subdivisions of 74117 have been made.

74118
Friable Regolith Breccia
LRV-5, 3.59 g

INTRODUCTION

74118 is a rounded, very friable sample of regolith breccia, collected from the light mantle 700 m northwest of Station 3. It is a light gray polymict breccia. The sample is among the smallest of 5 similar pieces picked from regolith sample 74110 that was collected as light mantle material. LRV-5 is on

the ejecta blanket of a 15-m crater and 74118 probably represents ejecta, possibly lithified by the impact. The fragments were observed during preliminary examination to contain about 10% white clasts and a trace of dark clasts in a light gray matrix. All the samples are rounded and shed fine-grained material. No subdivisions of 74118 have been made.

74119

Friable Regolith Breccia

LRV-5, 1.79 g

INTRODUCTION

74119 is a rounded, very friable sample of regolith breccia, collected from the light mantle 700 m northwest of Station 3. It is a light gray polymict breccia. The sample is the smallest of 5 similar pieces picked from regolith sample 74110 that was collected as light mantle material. LRV-5 is on the

ejecta blanket of a 15-m crater and 74119 probably represents ejecta, possibly lithified by the impact. The fragments were observed during preliminary examination to contain about 10% white clasts and a trace of dark clasts in a light gray matrix. All the samples are rounded and shed fine-grained material. No subdivisions of 74119 have been made.

REFERENCES

- Adams J.B. and Charette M.P. (1975) Spectral reflectance of highland rock types at Apollo 17: Evidence from Boulder 1, Station 2. *The Moon* 14, 483-489.
72215 72255 72275 76315 77017 77135 78155 79215
- Aeschlimann U., Eberhardt P., Geiss J., Grogler N., Kurtz J., and Marti K. (1982) On the age of cumulate norite 78236. LPS XIII, 1-2.
78236
- Ahrens T.J. and Watt J.P. (1980a) Dynamic properties of mare basalts: Relations of equations of state to petrology. Proc. Lunar Planet. Sci. Conf. 11th, 2059-2074.
70215
- Ahrens T.J. and Watt J.P. (1980b) Dynamic properties of mare basalts: Relation of equations of state to petrology. LPS XI, 60-8.
70215
- Ahrens T.J., Jackson I., and Jeanloz R. (1977) Shock compression and adiabatic release of a titaniferous lunar basalt. Proc. Lunar Sci. Conf. 8th, 3437-3455.
70215
- Ahrens T.J., Jackson I., and Jeanloz R. (1977) Dynamic properties of ilmenite-rich mare basalt and the relative ages of lunar cratered surfaces. LPS XVIII, 1-3.
70215
- Albee A.L., Gancarz A.J., and Chodos A.A. (1973) Metamorphism of Apollo 16 and 17 and Luna 20 metaclastic rocks at about 3.95 AE: Samples 61156, 64423,14-2, 65015, 67483,15-2, 76055, 22006, and 22007. Proc. Lunar Sci. Conf. 4th, 569-595.
76055
- Albee A.L., Chodos A.A., Dymek R.F., Gancarz A.J., Goldman D.S., Papanastassiou D.A., and Wasserburg G.J. (1974a) Dumite from the lunar highlands: petrography, deformational history, Rb-Sr age. LS V, 3-5.
72415 72417
- Albee A.L., Chodos A.A., Dymek R.F., Gancarz A.J., and Goldman D.S. (1974b) Preliminary investigation of Boulders 2 and 3, Apollo 17, Station 2: Petrology and Rb-Sr model ages. LS V, 6-8.
72315 72335 72355 72375 72395
- Albee A.L., Dymek R.F., and DePaolo D.J. (1975) Spinel symplectites: High pressure solid-state reaction or late-stage magmatic crystallization? LS VI, 1-3.
72415 76535
- Allen R.O., Jovanovic S., and Reed G.W., Jr. (1975) Heavy element affinities in Apollo 17 samples. *Earth Planet. Sci. Lett.* 27, 163-169.
72275 76315
- Allen R.O., Jr., Jovanovic S., and Reed G.W., Jr. (1977) Volatile metals - mode of transport. LPS XVIII, 22-24.
74275 75075
- Alvarez R. (1974a) Electrical properties of sample 70215. Proc. Lunar Sci. Conf. 5th, 2663-2671.
70215
- Alvarez R. (1974b) Electrical properties of sample 70215 in the temperature range of 100° to 373° K. LS V, 15-17.
70215

- Andersen D.J. and Lindsley D.H. (1979) The olivine-ilmenite thermometer. Proc. Lunar Planet. Sci. Conf. 10th, 493-507.
78155 79215
- Andersen D.J. and Lindsley D.H. (1982) Application of a two- pyroxene thermometer. LPS XIII, 15-16.
76255 77215
- Arvidson R., Drozd R., Guinness E., Hohenberg C., Morgan C., Morrison R., and Oberbeck V. (1976) Cosmic ray exposure ages of Apollo 17 samples and the age of Tycho. Proc. Lunar Sci. Conf. 7th, 2817-2832.
70135 71055 72535 73275 75015 75035 71135 71569
- Ashwal L.D. (1975) Petrologic evidence for a plutonic igneous origin of anorthositic norite clasts in 67955 and 77017. Proc. Lunar Sci. Conf. 6th, 221-230.
77017
- Baedecker P.A., Chou C.-L., Sundberg L.L., and Wasson J.T. (1974) Volatile and siderophile trace elements in the soils and rocks of Taurus-Littrow. Proc. Lunar Sci. Conf. 5th, 1625-1643.
71055 79135 79155
- Baker M.B. and Herzberg C.T. (1980a) Spinel cataclasites in 15445 and 72435: Petrology and criteria for equilibrium. Proc. Lunar Planet. Sci. Conf. 11th, 535-553.
72435 77517
- Baker M.B. and Herzberg C.T. (1980b) Spinel cataclasites in 15445 and 72435: Petrography, mineral chemistry, and criteria for equilibrium. LPS XI, 52-54.
72435
- Banerjee S.K. and Mellema J.P. (1976a) Early lunar magnetism. *Nature* 260, 230-231.
72215
- Banerjee S.K. and Mellema J.P. (1976) A solar origin for the large lunar magnetic field at 4.0×10^9 yr ago? Proc. Lunar Sci. Conf. 7th, 3259-3270.
72215
- Banerjee S.K. and Mellema J.P. (1976b) A solar origin for the large lunar magnetic field at 4.0×10^9 yrs ago? LS VII, 29-31.
72215
- Banerjee S.K. and Swits G. (1975) Natural remanent magnetization studies of a layered breccia boulder from the lunar highland region. *The Moon* 14, 473-481.
72215 72255 72275
- Banerjee S.K., Hoffman K., and Swits G. (1974a) Remanent magnetization directions in a layered boulder from the South Massif. Proc. Lunar Sci. Conf. 5th, 2873-2881.
72255 72275
- Banerjee S.K., Hoffman K., and Swits G. (1974b) Reversed polarity remanent magnetization in a layered boulder near South Massif. LS V, 32-34.
72255 72275
- Bansal B., Wiesmann H., and Nyquist L. (1975) Rb-Sr ages and initial $^{87}\text{Sr}/^{86}\text{Sr}$ ratios for Apollo 17 mare basalts. In Papers presented to the Conference on Origins of Mare Basalts and Their Implications for Lunar Evolution (Lunar Science Institute, Houston), 1-5.
70035 70017 70135 70215 74255 74275 75075
- Becker R.H. and Clayton R.N. (1975) Nitrogen abundances and isotopic compositions in lunar samples. Proc. Lunar Sci. Conf. 6th, 2131-2149.
70019

- Becker R.H. and Epstein S. (1981) Carbon isotopic ratios in some low-d¹⁵N lunar breccias. *Proc. Lunar Planet. Sci. Conf. 12th*, 289-293.
79035 79135
- Bell P.M. and Mao H.K. (1975) Cataclastic plutonites: Possible keys to the evolutionary history of the early Moon. *LS VI*, 34-35.
72415
- Bell P.M., Mao H.K., Roedder E., and Weiblen P.W. (1975) The problem of the origin of symplectites in olivine-bearing lunar rocks. *Proc. Lunar Sci. Conf. 6th*, 231-248.
70275 74255 72415 72417 76535
- Bence A.E., Papike J.J., Sueno S., and Delano J.W. (1973) Pyroxene poikiloblastic rocks from the lunar highlands. *Proc. Lunar Sci. Conf. 4th*, 597-611.
77135
- Bence A.E., Taylor S.R., Muir P.M., Nance W.B., Rudowski R., and Ware N. (1975) Chemical and petrologic relations among highland rock types. *LS VI*, 36-38.
73215
- Benkert J.P., Baur H., Pedroni A., Wieler R., and Signer P. (1988) Solar He, Ne and Ar in regolith minerals: All are mixtures of two components. *LPS XIX*, 59-60.
79035
- Benkert J.P., Kerridge J.F., Kim J.S., Kim Y., Marti K., Signer P., and Wieler R. (1991) Evolution of isotopic signatures in lunar regolith nitrogen: Noble gases and N in ilmenite grain-size fractions from regolith breccia 79035. *LPSC XXII*, 85-86.
79035
- Bersch M.G., Taylor G.J., and Keil K. (1988) Ferroan anorthosites and the magma ocean: Searching for trends in the Sea of Confusion. *LPS XIX*, 67-68.
73217 73235
- Bersch M.G., Taylor G.J., Keil K. and Norman M.D. (1991) Mineral compositions in pristine lunar highland rocks and the diversity of highland magmatism. *Geophys. Res. Letters* 18, 2085 - 2088.
- Bhandari N. (1977a) Solar flare exposure ages of lunar rocks and boulders based on ²⁶Al. *Proc. Lunar Sci. Conf. 8th*, 3607-3615.
75035 79215
- Bhandari N. (1977b) Solar flare induced Al-26 in short exposure age rocks. *LPS XVIII*, 100-102.
75035
- Bhandari N., Bhattacharya S.K., and Padia J.T. (1976a) Solar proton fluxes during the last million years. *Proc. Lunar Sci. Conf. 7th*, 513-523.
79215
- Bhandari N., Bhattacharya S.K., and Padia J.T. (1976b) Solar flare records in lunar rocks. *LS VII*, 49-51.
79215
- Bickel C.E. (1977) Petrology of 78155: An early, thermally metamorphosed polymict breccia. *Proc. Lunar Sci. Conf. 8th*, 2007- 2027.
78155
- Bickel C.E. and Warner J.L. (1977) Petrology of 78155: An early, thermally metamorphosed polymict breccia. *LPS XVIII*, 109-111.
78155

- Bickel C.E. and Warner J.L. (1978a) Survey of lunar plutonic and granulitic lithic fragments. Proc. Lunar Planet. Sci. Conf. 9th, 629-652.
73155 73215 73235 77035 77115 77135 77215
- Bickel C.E. and Warner J.L. (1978b) Textural-mineralogical relationships in a population of ANT samples. LPS IX, 82-84.
77017 78155 79215
- Bickel C.E., Warner J.L., and Phinney W.C. (1976a) Petrology of 79215: Brecciation of a lunar cumulate. Proc. Lunar Sci. Conf. 7th, 1793-1819.
79215
- Bickel C.E., Warner J.L., and Phinney W.C. (1976b) 79215: A unique, early lunar breccia. LS VII, 55-57.
79215
- Blanchard D.P., Brannon J.C., Jacobs J.W., and Haskin L.A. (1977) Major and trace element abundances in anorthositic gabbro clasts and a clast of K-rich felsite from consortium breccia 73215. LPS XVIII, 124-126.
73215
- Blanchard D.P., Budahn J.R., Kerridge J.F., and Compston W. (1978) Consortium breccia 783255: Rare-earth-element, light-element, and Rb-Sr chemistry of aphanitic lithologies. LPS IX, 103-105.
73215 73255
- Blanchard D.P. and Budahn J.R. (1979a) Remnants from the ancient lunar crust: Clasts from consortium breccia 73255. Proc. Lunar Planet. Sci. Conf. 10th, 803-816.
73215 73255
- Blanchard D.P. and Budahn J.R. (1979b) Clasts from Consortium breccia 73255: Remnants from the early lunar crust? LPS X, 134-136.
73255 73215
- Blanchard D.P. and McKay G.A. (1981) Remnants from the ancient lunar crust III: Norite 78236. LPS XII, 83-85.
78236
- Blanchard D.P., Haskin L.A., Jacobs J.W., and Brannon J.C., and Korotev, R.L. (1975) Major and trace element chemistry of Boulder 1 at Station 2, Apollo 17. *The Moon* 14, 359-371.
72215 72235 72255 72275
- Blanchard D.P., Jacobs J.W., Brannon J.C., and Haskin L.A. (1976) Major and trace element compositions of matrix and aphanitic clasts from consortium breccia 73215. Proc. Lunar Sci. Conf. 7th, 2179-2187.
73215
- Blanchard D.P., Jacobs J.W., and Brannon J.C. (1977) Chemistry of ANT-suite and felsite clasts from consortium breccia 73215 and of gabbroic anorthosite 79215. Proc. Lunar Sci. Conf. 8th, 2507-2524.
73215 79215
- Blanford G.E., Fruland R.M., McKay D.S., and Morrison D.A. (1974a) Lunar surface phenomena: Solar flare track gradients, microcraters, and accretionary particles. Proc. Lunar Sci. Conf. 5th, 2501-2526.
76015
- Blanford G.E., McKay D., and Morrison D. (1974b) Accretionary particles and microcraters. LS V, 67-69.
75035 79115
- Blank H., Nobiling R., Traxel K., and El Goresy A. (1981) Partitioning of trace elements among coexisting opaque oxides in Apollo 17 basalts using a proton probe microanalyzer. LPS XII, 89-91.
70215 72015

- Blank H., El Goresy A., Janicke J., Nobiling R., and Traxel. K. (1984) Partitioning of Zr and Nb between coexisting opaque phases in lunar rocks - determined by quantitative proton microprobe analysis. *Earth Planet. Sci. Letters* **68**, 19-33.
70215
- Bogard D.D. and Nyquist L.E. (1974) 76535: An old lunar rock? LS V, 70-72.
76535
- Bogard D.D., Nyquist L.E., Bansal B.M., Wiesmann H., and Shih C.Y. (1975) 76535: An old lunar rock. *Earth Planet. Sci. Lett.* **26**, 69-80.
76535
- Boynton W.V., Baedeker P.A., Chou C.-L., Robinson K.L., and Wasson J.T. (1975a) Mixing and transport of lunar surface materials: Evidence obtained by the determination of lithophile, siderophile, and volatile elements. Proc. Lunar Sci. Conf. 6th, 2241-2259.
71055 75055 79155 72155 77035
- Boynton W.V., Chou C.-L., Bild R.W., and Wasson J.T. (1975b) Surface correlation of volatile elements in Apollo-16 soils. LS VI, 74-76.
71055 72155 75055 79155 77035
- Braddy D., Hutcheon I.D., and Price P.B. (1975a) Crystal chemistry of Pu and U and concordant fission track ages of lunar zircons and whitlockites. Proc. Lunar Sci. Conf. 6th, 3587-3600.
73215 76535
- Braddy D., Hutcheon I.D., and Price P.B. (1975b) Crystal chemistry of Pu and U and concordant fission track ages of lunar zircons and whitlockites. LS VI, 77-79.
72215 72255 73215
- Brecher A. (1974) Inferences from comparative magnetic studies of some Apollo 17 basalts, breccias and soils. LS V, 83-85.
70017 71055 72275 74275 77017 77135
- Brecher A. (1975) Textural remanence: A new model of lunar rock magnetism. LS VI, 83-85.
72415 73215 74275 76315 77017 77035
- Brecher A. (1976a) Textural remanence: A new model of lunar rock magnetism. *Earth Planet. Sci. Lett.* **29**, 131-145.
72415 73215 74275 76315 77017 77035
- Brecher A. (1976b) The magnetic characteristics of highland breccia 73215: Evidence for tectural control of magnetization. Proc. Lunar Sci. Conf. 7th, 2217-2231.
73215
- Brecher A. (1976c) Textural control of magnetization in lunar, meteoritic and terrestrial rocks. LS VII, 91-93.
73215
- Brecher A. (1977a) Interrelationships between magnetization directions, magnetic fabric and oriented petrographic features in lunar rocks. Proc. Lunar Sci. Conf. 8th, 703-723.
70135 75035 77035 77135
- Brecher A. (1977b) New evidence for textural magnetization (TXM) in lunar rocks synthetic analogs and meteorites. LPS XVIII, 142-144.
70135 77135
- Brecher A., Menke W.H., and Morash K.R. (1974) Comparative magnetic studies of some Apollo 17 rocks and soils and their implications. Proc. Lunar Sci. Conf. 5th, 2795-2814.
72275 77017 77135 70017 71005 74275

- Brecher A., Menke W.H., Adams J.B., and Gaffey M.J. (1975) The effects of heating and subsolidus reduction on lunar materials: An analysis by magnetic methods, optical, Mossbauer, and X-ray diffraction spectroscopy. *Proc. Lunar Sci. Conf. 6th*, 3091-3109.
77017 77135
- Brett R. (1976) Reduction of mare basalts by sulfur loss. *Geochim. Cosmochim. Acta* 40, 997-1004.
70017 70035 70215 74275 75035 75055 72275 72415 72435 76055 76315 77017 77135 78155
- Brown G.M., Peckett A., Emeleus C.H., and Phillips R. (1974) Mineral-chemical properties of Apollo-17 mare basalts and terra fragments. *LS V*, 89-91.
70017 70035 70215 71055 73235 74275 75035 76535 77017
- Brown G.M., Peckett A., Emeleus C.H., Phillips R., and Pinsent R.H. (1975) Petrology and mineralogy of Apollo 17 mare basalts. *Proc. Lunar Sci. Conf. 6th*, 1-13.
70017 70035 70135 70185 70215 70255 70275 70315 71035 71055 71075 71135 71155 71175 71569 72135 72155 74235 74245 74255 74275 75015 75035 75055 75075 76136 78135 78505 78506 79155
- Brown G.M., Peckett A., Phillips R., and Emeleus C.H. (1975b) Mineralogy and petrology of Apollo 17 basalts. *LS VI*, 95-97.
70017 70035 70135 70185 70215 70255 70275 70315 71035 71055 71075 71135 71155 71175 71569 72135 72155 74235 74245 74255 74275 75015 75035 75055 75075 76136 78135 78505 78506 79155
- Brunfelt A.O., Heier K.S., Nilssen B., Steinnes E., Sundvoll B. (1974) Elemental composition of Apollo 17 fines and rocks. *Proc. Lunar Sci. Conf. 5th*, 981-990.
70017 70215 71055 74275 75035 73235
- Butler P. and Dealing T.E. (1974) The dissection and consortium allocation of Apollo 17 lunar rocks from the boulder at Station 7. *Earth Planet. Sci. Lett.* 23, 429-434.
77075 77115 77135 77215
- Cadogan P.H. and Turner G. (1976) The chronology of the Apollo 17 Station 6 boulder. *Proc. Lunar Sci. Conf. 7th*, 2267-2285.
76015 76215 76235 76255 76275 76295 76315
- Caffee M., Hohenberg C., and Hudson B. (1981a) Troctolite 76535: A study in the preservation of early isotopic records. *LPS XII*, 120-122.
76535
- Caffee M., Hohenberg C.M., and Hudson B. (1981b) Troctolite 76535: A study in the preservation of early isotopic records. *Proc. Lunar Planet. Sci. Conf. 12th*, 99-115.
76535
- Carlson R.W. and Lugmair G.W. (1979) Early history recorded by norite 78236. In *Papers Presented to the Conference on the Lunar Highlands Crust. LPI Contr.* 394, 9-11.
78235 78236
- Carlson R.W. and Lugmair G.W. (1980) 78236, a primary, but partially senile, lunar norite. *LPS XI*, 125-128.
78236
- Carlson R.W. and Lugmair G.W. (1982) Time and duration of lunar highlands crust formation. *Earth Planet. Sci. Letters* 52, 227-238.
73255 78236
- Carr L.P., Wright I.P., and Pillinger C.T. (1985) Nitrogen abundance and isotopes in lunar breccias - a progress report. *LPS XVI*, 115-116.
70175 70295 74246
- Carter J.L., Clanton U.S., Fuhrman R., Laughton R.B., McKay D.S., and Usselman T.M. *Proc. Lunar Sci. Conf. 6th*, 719-728.
76015 76215

- Chao E.C.T. (1973a) The petrology of 76055,10, a thermally metamorphosed fragment-laden olivine micronorite hornfels. *Proc. Lunar Sci. Conf. 4th*, 719-732.
76055
- Chao E.C.T. (1973b) 76055, a fragment-laden contact-metamorphosed magnesian hornfels. *EOS* 54, 584.
76055
- Chao E.C.T. and Minkin J.A. (1974a) Preliminary description of Apollo 17 station 7 boulder consortium rocks. *LS V*, 109-111.
77075 77115 77135 77215
- Chao E.C.T. and Minkin J.A. (1974b) The petrogenesis of 77135, a fragment-laden pigeonite feldspathic basalt - a major highland rock type. *LS V*, 112-114.
72435 76315 77135
- Chao E.C.T., Minkin J.A., and Thompson C.L. (1974) Preliminary petrographic description and geologic implications of the Apollo 17 Station 7 Boulder Consortium samples. *Earth Planet. Sci. Lett.* 23, 413-428.
77135 77115 77075 77215
- Chao E.C.T., Minkin J.A., Thompson C.L., and Heubner J.S. (1975a) The petrogenesis of 77115 and its xenocrysts: Description and preliminary interpretation. *Proc. Lunar Sci. Conf. 6th*, 493-515.
77075 77115 77135 77215
- Chao E.C.T., Minkin J.A., and Thompson C.L. (1975b) The petrogenesis of 77115 and its xenocrysts: Description and preliminary interpretation. *LS VI*, 134-136.
77115 77135
- Chao E.C.T., Minkin J.A., and Thompson C.L. (1976a) The petrology of 77215, a noritic impact breccia. *Proc. Lunar Sci. Conf. 7th*, 2287-2308.
77215
- Chao E.C.T., Minkin J.A., and Thompson C.L. (1976b) The petrology of 77215, a noritic impact ejecta breccia. *LS VII*, 129-131.
77215
- Charette M.P. and Adams J.B. (1975) Mare basalts: Characterization of compositional parameters by spectral reflectance. In *Papers presented to the Conference on Origins of Mare Basalts and their Implications for Lunar Evolution* (Lunar Science Institute, Houston), 25-28.
70017 70215 71055 74235 74275 75035 75055
- Charette M.P. and Adams J.B. (1977) Spectral reflectance of lunar highland rocks. *LPS XVIII*, 172-174.
72215 72275 72395 76015 76535 77017 79215
- Chen H.-K., Delano J.W., and Lindsley D.H. (1982) Chemistry and phase relations of VLT volcanic glasses from Apollo 14 and Apollo 17. *Proc. Lunar Planet. Sci. Conf. 13th*, A171-A181.
79135
- Chen J.H., Tilton G.R., Mattinson J.M., and Vidal P. (1978a) Lead isotope systematics of mare basalt 75075. *Proc. Lunar Planet. Sci. Conf. 9th*, 509-521.
75075
- Chen J.H., Mattinson J.M., Tilton G.R., and Vidal P. (1978b) Lead isotope systematics of mare basalt 75075. *LPS IX*, 160-162.
75075
- Chen J.H., Tilton G.R., and Mattinson J.M. (1979) Lead isotope systematics of three Taurus-Littrow mare basalts. *LPS X*, 195-197.
70017 75075 71055

- Chen J.H. and Wasserburg G.J. (1980) The isotopic composition of U in meteorites and lunar samples. LPS XI, 131-133.
75055
- Church S.E. and Tilton G.R. (1975) Lead isotope systematics of soils and soil breccias from Taurus-Littrow. LS VI, 143-145.
70019 79135
- Chyi L.L. and Ehmann W.D. (1974) Implications of Zr and Hf abundances and their ratios in lunar materials. LS V, 118-120.
73235
- Cirlin E.H. and Housley R.M. (1977) An atomic absorption study of volatile trace metals in lunar samples. LPS XVIII, 184-186.
75035
- Cisowski S.M. and Fuller M. (1983) Lunar sample magnetic stratigraphy. LPS XIV, 115-116.
79135
- Cisowski C.S., Dunn J.R., Fuller M., Rose M.F., and Wasilewski P.J. (1974) Impact processes and lunar magnetism. Proc. Lunar Sci. Conf. 5th, 2841-2858.
79135
- Cisowski S.M., Hale C., and Fuller M. (1977) On the intensity of ancient lunar fields. Proc. Lunar Sci. Conf. 8th, 725-750.
70017 70019 70215 72215 79155
- Cisowski S.M., Collinson D.W., Runcorn S.K., Stephenson A., and Fuller M. (1983) A review of lunar paleointensity data and implications for the origin of lunar magnetism. Proc. Lunar Planet. Sci. Conf. 13th, A691-A704.
70035 70135 77017 77115 77135 78505 79155
- Clanton U.S. and Fletcher C.R. (1976) Sample size and sampling errors as the source of dispersion in chemical analyses. Proc. Lunar Sci. Conf. 7th, 1413-1428.
70017
- Clanton U.S. and Morrison D.A. (1979) Hypervelocity impact craters less than 1000A diameter. LPS X, 212-214.
76015
- Clanton U.S., Carter J.L., and McKay D.S. (1975) Vapor-phase crystallization of sulfides? LS VI, 152-154.
76015
- Clayton R.N. and Mayeda T.K. (1975a) Genetic relations between the moon and meteorites. Proc. Lunar Sci. Conf. 6th, 1761-1769.
72275 72417 79155
- Clayton R.N. and Mayeda T.K. (1975b) Genetic relations between the Moon and meteorites. LS VI, 155-157.
72275 72417 79155
- Clayton R.N., Mayeda T.K., and Hurd J.M. (1974) Loss of oxygen, silicon, sulfur, and potassium from the lunar regolith. Proc. Lunar Sci. Conf. 5th, 1801-1809.
70019
- Collinson D.W., Runcorn S.K., and Stephenson A. (1975) On changes in the ancient lunar magnetic field intensity. LS VI, 158-160.
70017 70215
- Compston W., Foster J.J., and Gray C.M. (1975) Rb-Sr ages of clasts from within Boulder 1, Station 2, Apollo 17. *The Moon* 14, 445-462.
72215 72255 72275

- Compston W., Foster J.J., and Gray C.M. (1977a) Rb-Sr systematics in clasts and aphanites from consortium breccia 73215. Proc. Lunar Sci. Conf. 8th, 2525-2549.
73215
- Compston W., Foster J.J., and Gray C.M. (1977b) Rb-Sr systematics in clasts and aphanites from consortium breccia 73215. LPS XVIII, 199-201.
73215
- Compston W., Williams I.S., and Meyer C. (1984) U-Pb geochronology of zircons from lunar breccia 73217 using a sensitive high mass-resolution ion microprobe. Proc. Lunar Planet. Sci. Conf. 14th, B525-B534.
73217
- Compston W., Williams I.S., and Meyer C., Jr. (1983) U-Pb geochronology of zircons from breccia 73217 using a Sensitive High Mass-Resolution Ion Microprobe (Shrimp). LPS XIV, 130-131.
73217
- Crawford M.L. (1973) Crystallization of plagioclase in mare basalts. Proc. Lunar Sci. Conf. 4th, 705-717.
70035
- Crawford M.L. (1975a) Magma genesis by in situ melting within the lunar crust. Proc. Lunar Sci. Conf. 6th, 249-261.
73217
- Crawford M.L. (1975b) Closed system partial melting of a K-rich highlands rock. LS VI, 164-166.
73217
- Cripe J.D. and Moore C.B. (1975) Total sulfur contents of Apollo 15, 16 and 17 samples. LS VI, 167-169.
72135 72395 78235 78505
- Crozaz G., Drozd R., Hohenberg C., Morgan C., Ralston C., Walker R., and Yugas D. (1974a) Lunar surface dynamics: Some general conclusions and new results from Apollo 16 and 17. Proc. Lunar Sci. Conf. 5th, 2475-2499.
75035 73275 76015 76315 76535 77135
- Crozaz G., Drozd R., Hohenberg C., Morgan C., Walker R., and Yugas D. (1974b) Lunar surface dynamics: Some general conclusions and new results from Apollo 16 and 17. LS V, 157-159.
73275 75035 76315 76535 77135
- Dankwerth P.A., Hess P.C., and Rutherford M.J. (1979) The solubility of sulfur in high-TiO₂ mare basalts. Proc. Lunar Planet. Sci. Conf. 10th, 517-530.
74275
- Delaney J.S. and Sutton S.R. (1991) Fe-Mn-Mg in plagioclase from lunar basalt and highland samples. LPSC XXII, 299-230.
70035 78235
- Delaney J.S., Sutton S.R., Bajt S., and Smith J.V. (1992) In situ microXANES determination of ferrous/ferric ratio in terrestrial and extraterrestrial plagioclase: First reconnaissance. LPSC XXIII, 299-300.
70035
- Delano J.W. (1977) Experimental melting relations of 63545, 76015, and 76055. Proc. Lunar Sci. Conf. 8th, 2097-2123.
76055 76015
- Delano J.W. (1980) Constraints on the chemical nature of magmas parental to pristine highland cumulates. LPS XI, 216-218.
72415 76535 78235

- Delano J.W. and Lindsley D.H. (1982) Chromium, nickel, and titanium abundances in 74275 olivines: More evidence for a high- pressure origin of high-titanium mare basalts. LPS XIII, 160-161.
74275
- Delano J.W. and Lindsley D.H. (1983a) Mare volcanic glasses from Apollo 17. LPS XIV, 156-157.
79135
- Delano J.W. and Lindsley D.H. (1983b) Mare glasses from Apollo 17: Constraints on the Moon's bulk composition. Proc. Lunar Planet. Sci. Conf. 14th, B3-B16.
79135
- Dence M.R. and Grieve R.A.F. (1976) Secondary impact mixing in the formation of Apollo 17 grey breccias. LS VII, 196-198.
73215 73235
- Dence M.R., Grieve R.A.F., and Plant A.G. (1976) Apollo 17 grey breccias and crustal composition in the Serenitatis Basin region. Proc. Lunar Sci. Conf. 7th, 1821-1832.
73215 73235
- Des Marais D.J. (1978a) Carbon, nitrogen and sulfur in Apollo 15, 16 and 17 rocks. Proc. Lunar Planet. Sci. Conf. 9th, 2451-2467.
70215 75035
- Des Marais D.J. (1978b) Carbon isotopes, nitrogen and sulfur in lunar rocks. LPS IX, 247-249.
70215 75035
- Des Marais D.J. (1980) Six lunar rocks have little carbon and nitrogen and some rocks have detectable spallogenic ¹³C. LPS XI, 228-230.
70017 74275
- Dickinson T., Bild R.W., Taylor G.J., and Keil K. (1988) Late- stage enrichment of Ge in the magma ocean: Evidence from lunar basalts. LPS XIX, 277-278.
70017 70135 70215 71055 74275
- Dickinson T., Taylor G.J., Keil K., and Bild R.W. (1989) Germanium abundances in lunar basalts: Evidence of mantle metasomatism. Proc. Lunar Planet. Sci. 19th, 189-198.
70017 70135 70215 71055 74275
- Dowty E., Keil K., and Priinz M. (1974) Plagioclase twin laws in lunar highland rocks; possible petrogenetic significance. *Meteoritics* 9, 183-197.
76535
- Drake M.J. and Consolmagno G.J. (1976) Critical review of models for the evolution of high-Ti mare basalts. Proc. Lunar Sci. Conf. 7th, 1633-1657.
75075
- Drozd R.J., Hohenberg C.M., Morgan C.J., Podosek F.A., and M.L. Wroge (1977) Cosmic-ray exposure history at Taurus-Littrow. Proc. Lunar Sci. Conf. 8th, 3027-3043.
70035 70185 70215 70275 78135 78155 78235 78505
- Duncan A.R., Erlank A.J., Willis J.P., Sher M.K., and Ahrens L.H. (1974a) Trace element evidence for a two-stage origin of some titaniferous mare basalts. Proc. Lunar Sci. Conf. 5th, 1147-1157.
70017 70215 73235 74275
- Duncan A.R., Erlank A.J., Willis J.P., Sher M.K., and Ahrens L.H. (1974b) Trace element evidence for a two-stage origin of high- titanium mare basalts. LS V, 187-189.
70017 70215 74275

- Duncan A.R., Erlank A.J., Willis J.P., and Sher M.K. (1974c) Compositional characteristics of the Apollo 17 regolith. LS V, 184-186.
73235
- Duncan A.R., Erlank A.J., Sher M.K., Abraham Y.C., Willis J.P., and Ahrens L.H. (1976a) Proc. Lunar Sci. Conf. 7th, 1659-1671.
70135 75035
- Duncan A.R., Sher M.K., Abraham Y.C., Erlank A.J., Willis J.P., and Ahrens L.H. (1976b) Source region constraints for lunar basalt types inferred from trace element chemistry. LS VII, 218-220.
70135 75035
- Dymek R.F., Albee A.L., and Chodos A.A. (1975a) Comparative mineralogy and petrology of Apollo 17 mare basalts: Samples 70215, 71055, 74255, and 75055. Proc. Lunar Sci. Conf. 6th, 49-77.
70215 71055 74255 75055
- Dymek R.F., Albee A.L., and Chodos A.A. (1975b) Comparative petrology of lunar cumulate rocks of possible primary origin: Dunitite 72415, troctolite 76535, norite 78235, and anorthosite 62237. Proc. Lunar Sci. Conf. 6th, 301-341.
72415 72417 72435 76535 78235
- Dymek R.F., Albee A.L., and Chodos A.A. (1976a) Petrology and origin of Boulders #2 and #3, Apollo 17 Station 2. Proc. Lunar Sci. Conf. 7th, 2335-2378.
72315 72335 72355 72375 72395 72435
- Dymek R.F., Albee A.L., and Chodos A.A. (1976b) Petrographic investigation of lunar sample 72435 with emphasis on the nature of its clasts. LS VII, 227-229.
72435
- Dymek R.F., Albee A.L., and Chodos A.A. (1976c) Chemical and mineralogical homogeneity of Boulder #2, Apollo 17 Station #2. LS VII, 230-232.
72315 72335 72355 72375 72395
- Eberhardt P., Eugster O., Geiss J., Graf H., Grogler N., Guggisberg S., Jungk M., Maurer P., Morgeli M., and Stettler A. (1974) Solar wind and cosmic radiation history of Taurus-Littrow regolith. LS V, 197-199.
70035 74275
- Eberhardt P., Eugster O., Geiss J., Graf H., Grogler N., Morgeli M., and Stettler A. (1975) Kr^{81} -Kr exposure ages of some Apollo 14, Apollo 16 and Apollo 17 rocks. LS VI, 233-235.
74235 74255 74275 77135
- Ebihara M., Wolf R., Warren P.H., and Anders E. (1992) Trace elements in 59 mostly highland moon rocks. *Proc. Lunar Planet. Sci.* 22, 417-426.
72315 72395 76536 77115 77215
- Eckert J.O., Taylor L.A., and Neal C.R. (1991a) Spinel troctolite from Apollo 17 breccia 73215: Evidence for petrogenesis as deep-seated lunar crust. LPS XXII, 329-330.
73215
- Eckert J.O., Taylor L.A., Neal C.R., and Schmitt R.A. (1991b) Cumulate lithologies and melt rocks from Apollo 17 breccias: Correlations of whole-rock and mineral chemistry. LPSC XXII, 333-334.
73215 73216 77035
- Eckert J.O., Taylor L.A., Neal C.R., and Patchen A.D. (1991c) Anorthosites with negative Eu anomalies in Apollo 17 breccias: Further evidence for "REEP" metasomatism. LPSC XXII, 331-332.
73215 73216 77035
- Ehmann W.D. and Chyi L.L. (1974) Abundances of the group IVB elements, Ti, Zr, and Hf and implications of their ratios in lunar materials. Proc. Lunar Sci. Conf. 5th, 1015-1024.
73235

- Ehmann W.D., Miller M.D., Ma M.-S., and Pacer R.A. (1974) Compositional studies of the lunar regolith at the Apollo 17 site. *LS V*, 203-205.
70017 73235 74275
- Ehmann W.D., Chyi L.L., Garg A.N., Hawke B.R., Ma M.-S., Miller M.D., James W.D. Jr., and Pacer R.A. (1975a) Chemical studies of the lunar regolith with emphasis on zirconium and hafnium. *Proc. Lunar Sci. Conf. 6th*, 1351-1361.
73215 77035
- Ehmann W.D., Chyi L.L., Hawke B.R., Ma M.-S., Miller M.D., and Pacer R.A. (1975b) Chemical studies of the lunar regolith with emphasis on zirconium and hafnium. *LS VI*, 236-238.
73215 77035
- Eichhorn G., James O.B., Schaeffer O.A., and Muller H.W. (1978a) Laser ^{39}Ar - ^{40}Ar dating of two clasts from consortium breccia 73215. *Proc. Lunar Planet. Sci. Conf. 9th*, 855-876.
73215
- Eichhorn G., James O.B., Schaeffer O.A., and Muller H.W. (1978b) Laser-probe ^{39}Ar - ^{40}Ar dating of two clasts from consortium breccia 73215. *LPS IX*, 279-281.
73215
- Eichhorn G., McGee J.J., James O.B., and Schaeffer O.A. (1979a) Consortium breccia 73255: Laser ^{39}Ar - ^{40}Ar dating of aphanite samples. *Proc. Lunar Planet. Sci. Conf. 10th*, 763-788.
73255
- Eichhorn G., James O.B., McGee J.J., and Schaeffer O.A. (1979b) Consortium breccia 73255: Preliminary ^{39}Ar - ^{40}Ar laser dating of aphanite samples. *LPS X*, 346-348.
73255
- Eldridge J.S., O'Kelley G.D., and Northcutt K.J. (1974a) Primordial radioelement concentrations in rocks and soils from Taurus-Littrow. *Proc. Lunar Sci. Conf. 5th*, 1025-1033.
70135 70185 70215 71135 71136 71175 71566 73215 73255 73275 76295 78597 79155
- Eldridge J.S., O'Kelley G.D., and Northcutt K.J. (1974b) Primordial radioelement concentrations in rocks and soils from Taurus-Littrow. *LS V*, 206-208.
70135 70185 70215 71135 71136 71175 73215 73255 73275 76295 78597 79155
- Eldridge J.S., O'Kelley G.D., and Northcutt K.J. (1975a) Primordial and cosmogenic radionuclides in Descartes and Taurus-Littrow materials: extension of studies by nondestructive x-ray spectrometry. *Proc. Lunar Sci. Conf. 6th*, 1407-1418.
70315 71546 72155 74275
- Eldridge J.S., O'Kelley G.D., and Northcutt K.J. (1975b) Primordial radioelements and cosmogenic nuclides in rocks and soils from Descartes and Taurus-Littrow. *LS VI*, 242-244.
70315 72155 74275
- El Goresy A. and Ramdohr P. (1975a) Subsolidus reduction of lunar opaque oxides: Textures, assemblages, geochemistry, and evidence for a late-stage endogenic gaseous mixture. *Proc. Lunar Sci. Conf. 6th*, 729-745.
70017 70035 70135
- El Goresy A. and Ramdohr P. (1975b) Subsolidus reduction of lunar opaque oxides: Evidence, assemblages, geochemical relevance, and evidence for a late-stage reducing gaseous mixture. *LS VI*, 245-247.
70035 70135
- El Goresy A. and Ramdohr P. (1975c) Taurus-Littrow TiO_2 -rich basalts: Opaque mineralogy and geochemistry. *LS VI*, 248-250.
70035 70135 79155

- El Goresy A. and Ramdohr P. (1977a) Apollo 17 TiO₂-rich basalts: Reverse spinel zoning as evidence for the subsolidus equilibration of the spinel-ilmenite assemblage. Proc. Lunar Sci. Conf. 8th, 1611-1624.
70017 70035 70215 71155
- El Goresy A. and Ramdohr P. (1977b) Apollo 17 TiO₂-rich basalts: Spinel chemical bimodality in the two major basalt types and genetic significance of inverted zoning in chromian ulvospinel. LPS XVIII, 281-283.
70017 70035 70215
- El Goresy A., Ramdohr P., Medenbach O., and Bernhardt H.-J. (1974) Taurus-Littrow TiO₂-rich basalts: Opaque mineralogy and geochemistry. Proc. Lunar Sci. Conf. 5th, 627-652.
70017 70035 70215 72015 74275 75055 79155
- El Goresy A., Ramdohr P., Medenbach O., and Bernhardt H.-J. (1974) Taurus-Littrow crystalline rocks: Opaque mineralogy and geochemistry. LS V, 209-211.
70215 72015 79155
- El Goresy A., Engelhardt W.v., Arndt J., and Mangliers D. (1976) Shocked norite 78235: Primary textures and shock features. LS VII, 239-241.
78235
- Engelhardt W. von (1979) Ilmenite in the crystallization sequence of lunar rocks. Proc. Lunar Planet. Sci. Conf. 10th, 677-694.
70215 71055 72315 72335 72355 72395 72518 72535 72536 72539 72548 72549 72558 72735 72736 72738
73235 73275 74279 76015 76255 76275 76295 76315 77075 77115 77135 77515 77518 77539 77545 78155
- Eugster O., Eberhardt P., Geiss J., Grogler N., Jungck M., and Morgeli M. (1977) The cosmic-ray exposure history of Shorty Crater samples; the age of Shorty Crater. Proc. Lunar Sci. Conf. 8th, 3059-3082.
74235 74255 74275
- Eugster O., Eberhardt P., Geiss J., Grogler N., and Schwaller H. (1984) Cosmic ray exposure histories and ²³⁵U-¹³⁶Xe dating of Apollo 11, Apollo 12, and Apollo 17 mare basalts. Proc. Lunar Planet. Sci. Conf. 15th, C171-C181.
77135
- Evensen N.M., Murthy V. Rama, and Coscio M.R. (1973a) Rb-Sr ages of some mare basalts and the isotopic and trace element systematics in lunar fines. Proc. Lunar Sci. Conf. 4th, 1707-1724.
70035
- Evensen N.M., Murthy V.R., and Coscio M.R. (1973b) Taurus-Littrow: Age of mare volcanism; chemical and Rb-Sr isotopic systematics of the dark mantle soil. EOS 54, 587-588.
70035
- Fechtig H., Hartung J.B., Nagel K., Neukum G., and Storzer D. (1974a) Lunar microcrater studies, derived meteoroid fluxes, and comparison with satellite-borne experiments. Proc. Lunar Sci. Conf. 5th, 2463-2474.
70215 74275 77135 79155
- Fechtig H., Hartung J.B., Nagel K., Neukum G., and Storzer D. (1974b) Microcrater studies, derived meteoroid fluxes and comparison with satellite-borne experiments. LS V, 22-224.
70215 74275 79155
- Filleux C., Tombrello T.A., and Burnett D.S. (1977) Direct measurement of surface carbon concentrations. Proc. Lunar Sci. Conf. 8th, 3755-3772.
70019
- Filleux C., Spear R.H., Tombrello T.A., and Burnett D.S. (1978) Direct measurement of surface carbon concentrations for lunar soil breccias. Proc. Lunar Planet. Sci. Conf. 9th, 1599-1617.
70019 79135

- Filleux C., Spear R., Tombrello T.A., and Burnett D.S. (1978b) Carbon depth distributions for soil breccias. LPS IX, 317-319.
70019
- Finnerty A.A. and Rigden S.M. (1981) Olivine barometry: Application to pressure estimation for terrestrial and lunar rocks. LPS XII, 279-281.
72415 76535
- Fredriksson K., Brenner P., Nelen J., Noonan A., Dube A., and Reid A. (1974) Comparative studies of impact glasses and breccias. LS V, 245-247.
70019 79035
- Frick U., Becker R.H., and Pepin R.O. (1987) Solar wind record in the lunar regolith: nitrogen and noble gases. Proc. Lunar and Planet. Sci. Conf. 18th, 87-120.
79035
- Fruchter J.S., Rancitelli L.A., and Perkins R.W. (1975) Primordial radionuclide variations in the Apollo 15 and 17 deep core samples and in Apollo 17 igneous rocks and breccias. Proc. Lunar Sci. Conf. 6th, 1399-1406.
71155 72235 72255 76215 77115 78135 79215
- Fruchter J.S., Rancitelli L.A., Evans J.C., and Perkins R.W. (1978a) Lunar surface processes and cosmic ray histories over the past several million years. Proc. Lunar Planet. Sci. Conf. 9th, 2019-2032.
70019
- Fruchter J.S., Evans J.C., Rancitelli L.A., and Perkins R.W. (1978b) Lunar surface processes and cosmic ray histories over the past several million years. LPS IX, 350-352.
70019
- Fruchter J.S., Evans J.C., Reeves J.H., and Perkins R.W. (1982) Measurement of ^{26}Al in Apollo 15 core 15008 and ^{22}Na in Apollo 17 rock 74275. LPS XIII, 243-244.
74275
- Gamble R.P. and Taylor L.A. (1979) The effects of kinetics on crystal-liquid partitioning in augite. LPS X, 419-421.
75055
- Garg A.N. and Ehmann W.N. (1976a) Zr-Hf fractionation in chemically defined lunar rock groups. Proc. Lunar Sci. Conf. 7th, 3397-3410.
70017 70215 70315 71055 73215 73235 74275 75035 75055 76535 77035 79035
- Garg A.N. and Ehmann W.N. (1976b) Chemical fractionation in the lunar crust with emphasis on zirconium and hafnium. LS VII, 281-283.
70017 70215 71055 74275 75035
- Garner E.L., Machlan L.A., and Barnes I.L. (1975) The isotopic composition of lithium, potassium, and rubidium in some Apollo 11, 12, 14, 15, and 16 samples. Proc. Lunar Sci. Conf. 6th, 1845-1855.
70215
- Ghose W.A., Strangway D.W., and Pearce G.W. (1978) Origin of magnetization in lunar breccias: An example of thermal overprinting. *Earth Planet. Sci. Lett.* 38, 373-384.
76015 76215 76255 76275 76315 76295 76307
- Gibson E.K. and Moore G.W. (1974a) Sulfur abundances and distributions in the valley of Taurus-Littrow. Proc. Lunar Sci. Conf. 5th, 1823-1837.
70035 70215 72275 72415 72435 73275 74275 75035 75055 76015 76055 76315 77017 77135 78155 79135
- Gibson E.K. and Moore G.W. (1974b) Total sulfur abundances and distributions in the valley of Taurus-Littrow: Evidence of mixing. LS V, 267-269.
70035 70215 72275 72415 72435 73275 74275 75035 75055 76055 76315 77017 77135 78155 79135

- Gibson E.K., Chang S., Lennon K., Moore G.W., and Pearce G.W. (1975a) Sulfur abundances and distributions in mare basalts and their source magmas. *Proc. Lunar Sci. Conf. 6th*, 1287-1301.
70035 70215 74275 75035 75055
- Gibson E.K., Chang S., Lennon K., Moore G.W., and Pearce G.W. (1975b) Carbon, sulfur, hydrogen and metallic iron abundances in Apollo 15 and Apollo 17 basalts. *LS VI*, 290-292.
70035 70215 74275 75035 75055
- Gibson E.K., Usselman T.M., and Morris R.V. (1976a) Sulfur in the Apollo 17 basalts and their source regions. *Proc. Lunar Sci. Conf. 7th*, 1491-1505.
70035 70135 70185 70215 70275 71035 71135 71136 71175 71546 71566 71567 71569 71577 72155 74235
74245 74255 74275 75015 75035 75055 75075 76136 76537 76539 77535 78135 78506 78597 78599 79155
- Gibson E.K., Morris R.V., and Usselman T.M. (1976b) Nature of the sulfur in the Apollo 17 basalts and their source regions. *LS VII*, 290-292.
70035 70135 70185 70215 70275 71035 71135 71136 71175 71546 71566 71567 71569 71577 72155 74235
74245 74255 74275 75015 75035 75055 75075 76136 76537 76539 77535 78135 78506 78597 78599 79155
- Gibson E.K., and Andrawes F.F. (1978) Nature of the gases released from lunar rocks and soils upon crushing. *Proc. Lunar Planet. Sci. Conf. 9th*, 2433-2450.
74275 75035 78505
- Gibson E.K., Bustin R., Skaugset A., Carr R.H., Wentworth S.J., and McKay D.S. (1987) Hydrogen distributions in lunar materials. *LPS XVIII*, 326-327
70035 70215 74255 74275 75035 75055 72415 76015 76055 76215 77135 78155 78505 79135
- Goel P.S., Shukla P.N., Kothari B.K., and Garg A.N. (1975) Total nitrogen in lunar soils, breccias, and rocks. *Geochim. Cosmochim. Acta* **39**, 1347-1352.
70215
- Gold T., Bilson E., and Baron R.L. (1976a) The surface chemical composition of lunar samples and its significance for optical properties. *Proc. Lunar Sci. Conf. 7th*, 901-911
76315 79135
- Gold T., Bilson E., and Baron R.L. (1976b) Electrical properties of Apollo 17 rock and soil samples and a summary of the electrical properties of lunar material at 450 MHz frequency. *Proc. Lunar Sci. Conf. 7th*, 2593-2603.
76315 79135
- Gold T., Bilson E., and Baron R.L. (1976c) Electrical properties of Apollo 17 rock and soil samples and a summary of the electrical properties of lunar material at 450 MHz frequency. *LS VII*, 298-300.
76315 79135
- Goldberg R.H., Burnett D.S., and Tombrello T.A. (1975a) Fluorine surface films on lunar samples: Evidence for both lunar and terrestrial origins. *Proc. Lunar Sci. Conf. 6th*, 2189-2200.
76215
- Goldberg R.H., Burnett D.S., Tombrello T.A., and Weller R.A. (1975b) Hydrogen, carbon and teflon on the surfaces of lunar samples. *LS VI*, 299-301.
76215
- Goldstein J.I., Hewins R.H., and Romig A.D. Jr. (1976a) Carbides in lunar soils and rocks. *Proc. Lunar Sci. Conf. 7th*, 807-818.
72215 73275
- Goldstein J.I., Hewins R.H., and Romig A.D. Jr. (1976b) Carbides in lunar soils and rocks. *LS VII*, 310-312.
72215 73275
- Gooley R., Brett R., Warner J., and Smyth J.R. (1974) A lunar rock of deep crustal origin: Sample 76535. *Geochim. Cosmochim. Acta* **38**, 1329-1339.
76535

- Gose W.A., Strangway D.W., and Pearce G.W. (1976) Origin of magnetization in lunar breccias: An example of thermal overprinting. *LS VII*, 322-324.
76015 76215 76255 76275 76295 76307
- Gose W.A., Strangway D.W., and Pearce G.W. (1978) Origin of magnetization in lunar breccias: An example of thermal overprinting. *Earth Planet. Sci. Letters* **38**, 373-384.
76015 76215 76255 76275 76295 76307 76315
- Goswami J.N. and Hutcheon I.D. (1975) Cosmic ray exposure history and compaction age of Boulder 1 from Station 2. *The Moon* **14**, 395-405.
72215 72255 72275
- Goswami J.N. and Lal D. (1974) Cosmic ray irradiation pattern at the Apollo 17 site: implications to lunar regolith dynamics. *Proc. Lunar Sci. Conf. 5th*, 2643-2662.
70215 74275 79215 73275
- Goswami J.N., Braddy D., and Price P.B. (1976a) Microstratigraphy of the lunar regolith and compaction ages of lunar breccias. *Proc. Lunar Sci. Conf. 7th*, 55-74.
72255 72275 72435 73215
- Goswami J.N., Braddy D., and Price P.B. (1976b) Microstratigraphy of the lunar regolith and compaction ages of lunar breccias. *LS VII*, 328-330.
72255 72275 72435 73215 76535
- Green D.H., Ringwood A.E., Ware N.G., and Hibberson W.O. (1974) Petrology and petrogenesis of Apollo 17 basalts and Apollo 17 orange glass. *LSV*, 287-289.
70215 74275
- Green D.H., Ringwood A.E., Hibberson W.O., and Ware N.G. (1975a) Experimental petrology of Apollo 17 mare basalts. *Proc. Lunar Sci. Conf. 6th*, 871-893.
70215 72135 74275
- Green D.H., Ringwood A.E., Ware N.G., and Hibberson W.O. (1975b) Experimental petrology and petrogenesis of Apollo 17 mare basalts. *LS VI*, 311-313.
70215 74275
- Gros J., Takahashi H., Hertogen J., Morgan J.W., and Anders E. (1976) Composition of the projectiles that bombarded the lunar highlands. *Proc. Lunar Sci. Conf. 7th*, 2403-2425.
73215 76255 76275 76315
- Grossman L., Clayton R.N., and Mayeda T.K. (1974) Oxygen isotopic constraints on the composition of the Moon. *Proc. Lunar Sci. Conf. 5th*, 1207-1212.
70019
- Haggerty S.E. (1973a) Armalcolite and genetically associated opaque minerals in the lunar samples. *Proc. Lunar Sci. Conf. 4th*, 777-797.
70035
- Haggerty S.E. (1973b) Apollo 17: Armalcolite paragenesis and subsolidus reduction of chromian-ulvospinel and chromian-picroilmenite. *EOS* **54**, 593-594.
70035
- Haggerty S.E. (1973c) Ortho and para-armalcolite samples in Apollo 17. *Nature Phys. Sci.* **242**, 123-125.
70035
- Haggerty S.E. (1974) Apollo 17 Orange glass: Textural and morphological characteristics of devitrification. *Proc. Lunar Sci. Conf. 5th*, 193-205.
79035 79135

- Haggerty S.E. (1975) Geochemistry of opaque oxides in troctolites and basalts from Taurus Littrow. LS VI, 321-323.
76535 79215
- Hale C.J., Fuller M., and Bailey R.C. (1978) On the application of microwave heating to lunar paleointensity determination. Proc. Lunar Planet. Sci. Conf. 9th, 3165-3179.
77115 77135
- Hansen E.C., Steele I.M., and Smith J.V. (1979a) Lunar highland rocks: Element partitioning among minerals 1: Electron microprobe analyses of Na, K, and Fe in plagioclase; mg partitioning with orthopyroxene. Proc. Lunar Planet. Sci. Conf. 10th, 627-638.
76535 78235
- Hansen E.C., Steele I.M., and Smith J.V. (1979b) Minor elements in plagioclase from lunar highland rocks: New data, especially for granulitic impactites. In Papers Presented to the Conference on the Lunar Highlands Crust. *LPI Contr.* 394, 39-41.
72255 73215 76255 76535 77077 77115 78235 79215
- Hansen E.C., Steele I.M., and Smith J.V. (1979c) Minor elements in plagioclase and mafic minerals from lunar plagioclase-rich rocks. LPS X, 497-499.
76535 78235
- Hansen E.C., Smith J.V., and Steele I.M. (1980) Minor elements in lunar olivine: Electron probe analyses of Na, Al, P, Ca, Rb, Cr, Mn, and Ni. LPS XI, 391-393.
73215 76255 76535 77135 79215
- Hapke B.W., Partlow W.D., Wagner J.K., and Cohen A.J. (1978) Reflectance measurements of lunar materials in the vacuum ultraviolet. Proc. Lunar Planet. Sci. Conf. 9th, 2935-2947.
70017
- Hargraves R.B. and Dorety N.F. (1975) Remanent magnetism in two Apollo 16 and two Apollo 17 rock samples. LS VI, 331-333.
70215 78155
- Harrison W.J. and Horz F. (1981) Experimental shock metamorphism of calcic plagioclase. LPS XII, 395-397.
75035
- Hartung J.B. and Storzer D. (1974) Lunar microcraters and their solar flare track record. Proc. Lunar Sci. Conf. 5th, 2527-2541.
72315
- Haselton J.D. and Nash W.P. (1975a) A model for the evolution of opaques in mare lavas. Proc. Lunar Sci. Conf. 6th, 747-755.
75035
- Haselton J.D. and Nash W.P. (1975b) Observations on titanium in lunar oxides and silicates. LS VI, 343-345.
70215 74275
- Haskin L.A., Shih C.-Y., Bansal B.M., Rhodes J.M., Wiesmann H. and Nyquist L.E. (1974a) Chemical evidence for the origin of 76535 as a cumulate. Proc. Lunar Sci. Conf. 5th, 1213-1225.
76535
- Haskin L.A., Shih C.-Y., Bansal B.M., Rhodes J.M., Wiesmann H. and Nyquist L.E. (1974b) Chemical evidence for the origin of 76535 as a cumulate. LS V, 313-315.
76535
- Hazen R.M., Mao H.K., and Bell P.M. (1977) Effects of compositional variation on absorption spectra of lunar olivines. Proc. Lunar Sci. Conf. 8th, 1081-1090.
70017

- Hazen R.M., Bell P.M., and Mao H.K. (1978) Effects of compositional variation on absorption spectra of lunar pyroxenes. Proc. Lunar Planet. Sci. Conf. 9th, 2919-2934.
70017 74275
- Heiken G. H. and Vaniman D.T. (1989) Petrography of lunar ilmenite resources. LPSC XX, 400-401.
70017 70215 74275 78505
- Heavilon C.F. and Crozaz G. (1989) REE and selected minor and trace element microdistributions in some pristine lunar highlands rocks. LPSC XX, 398-399.
76535
- Helz R.T. and Appleman D.E. (197) Poikilitic and cumulate textures in rock 77017, a crushed anorthositic gabbro. LS V, 322- 324.
77017
- Hertogen J., Janssens M.-J., Takahashi H., Palme H, and Anders E. (1977) Lunar basins and craters: Evidence for systematic compositional changes of bombarding population. Proc. Lunar Sci. Conf. 8th, 17-45.
72215 72235 72255 72275 72415 72417 73215 73235 73275 76015 76215 76235 76255 76275 76295 76315 76535 77017 77075 77135 77215 78155 78235 79215
- Herzberg C.T. (1979) Identification of pristine lunar highland rocks: Criteria based on mineral chemistry and stability. LPS X, 537-539.
72415 76535
- Herzberg C. (1978) The bearing of spinel cataclasites on the crust-mantle structure of the Moon. Proc. Lunar Planet. Sci. Conf. 9th, 319-336.
72435
- Herzberg C.T. and Baker M.B. (1980) The cordierite- to spinel- cataclasite transition: Structure of the lunar crust. Proc. Conf. Lunar Highlands Crust, 113-132.
72435
- Hess P.C., Rutherford M.J., Guillemette R.N., Ryerson F.J., and Tuchfeld H.A. (1975) Residual products of fractional crystallization of lunar magmas: An experimental study. Proc. Lunar Sci. Conf. 6th, 895-909.
70017 75055
- Heuer A.H., Christie J.M., Lally J.S., and Nord G.L., Jr. (1974) Electron petrographic study of some Apollo 17 breccias. Proc. Lunar Sci. Conf. 5th, 275-286.
73275 79035
- Hewins R.H. and Goldstein J.I. (1975a) The provenance of metal in anorthositic rocks. Proc. Lunar Sci. Conf. 6th, 343-362.
73215 73235 76535 77135 78155 78235 78238
- Hewins R.H. and Goldstein J.I. (1975b) The provenance of metal in anorthositic rocks. LS VI, 358-360.
73215 73235 76535 77017 77135 78155 78238
- Hewins R.H. and Goldstein J.I. (1975c) Comparison of silicate and metal geothermometers for lunar rocks. LS VI, 356-358.
76535
- Higuchi H. and Morgan J.W. (1975a) Ancient meteoritic component in Apollo 17 boulders. Proc. Lunar Sci. Conf. 6th, 1625-1651.
72215 72235 72255 72275 72415 72417 73215 76015 76215 76235 76295 77135 77215 78235 79215
- Higuchi H. and Morgan J.W. (1975b) Ancient meteoritic component in Apollo 17 boulders. LS VI, 364-366.
72415 72417 73215 76015 76215 76295

- Hintenberger H., Weber H.W., and Schultz L. (1974a) Solar, spallogenic, and radiogenic rare gases in Apollo 17 soils and breccias. Proc. Lunar Sci. Conf. 5th, 2005-2022.
79035 79135
- Hintenberger H., Weber H.W., and Schultz L. (1974b) Solar, spallogenic, and radiogenic rare gases in Apollo 17 soils and breccias. LS V, 334-336.
79035 79135
- Hintenberger H., Schultz L., and Weber H.W. (1975a) A comparison of noble gases in lunar fines and soil breccias: Implications for the origin of soil breccias. Proc. Lunar Sci. Conf. 6th, 2261- 2270.
79035 79135
- Hintenberger H., Schultzt L., and Weber H.W. (1975b) Rare gases in ilmenite and bulk samples of Apollo 17 soils and breccias. LS VI, 370-372.
79035 79135
- Hinthorne J.R., Conrad R.L., and Andersen C.A. (1975) Lead-lead and trace element abundances in lunar troctolite, 76535. LS VI, 373-375.
76535
- Hinthorne J.R., Conrad R.L., and Church S.E. (1977) Lead-lead age and rare earth element determinations in lunar norite 78235. LPS XVIII, 444-446.
78235
- Hodges F.N. and Kushiro I. (1974a) Apollo 17 petrology and experimental determination of differentiation sequences in model Moon compositions. Proc. Lunar Sci. Conf. 5th, 505-520.
70017 73235 74275
- Hodges F.N. and Kushiro I. (1974b) Apollo 17 petrology and experimental determination of differentiation sequences in model Moon compositions. LS V, 340-342.
70017 73235 74275
- Hohenberg C.M., Hudson B., Kennedy B.M., and Podosek F.A. (1980) Fission xenon in troctolite 76535. Proc. Conf. Lunar Highlands Crust, 419-439.
76535
- Horai K. and Winkler J. (1975) Thermal diffusivity of three Apollo 17 rock samples: 70215,18, 77035,44 and 70017,77. LS VI, 390-392.
70017 70215 77035
- Horai K. and Winkler J.L., Jr. (1976) Thermal diffusivity of four Apollo 17 rock samples. Proc. Lunar Sci. Conf. 7th, 3183-3204.
70017 70215 72395 77017 77035
- Horai K. and Winkler J.L., Jr. (1980) Thermal diffusivity of two Apollo 11 samples, 10020,44 and 10065,23: Effect of petrofabrics on the thermal conductivity of porous lunar rocks under vacuum. Proc. Lunar Planet. Sci. Conf. 11th, 1777-1788.
70017 70215
- Horn P., Jessberger E.K., Kirsten T., and Richter H. (1975) ^{39}Ar - ^{40}Ar dating of lunar rocks: Effects of grain size and neutron irradiation. Proc. Lunar Sci. Conf. 6th, 1563-1591.
75075
- Horz F. and Schaal R.B. (1979) Glass production in massive versus porous basalts via shock. LPS X, 573-575.
75035
- Horz F., Gibbons R.V., Gault D.E., Hartung J.B., and Brownlee D.E. (1975). Some correlation of rock exposure ages and regolith dynamics. Proc. Lunar Sci. Conf. 6th, 3495-3508.
70017 70035 70215 74275 75075 73235 73275 76535 77017 79215

- Housley R.M., Cirlin E.H., Goldberg I.B., and Crowe H. (1976) Ferromagnetic resonance studies of lunar core stratigraphy. Proc. Lunar Sci. Conf. 7th, 13-26.
72275 73215 73275 76315 79035
- Hubbard N.J., Rhodes J.M., Wiesmann H., Shih C.Y., and B.M. Bansal (1974) The chemical definition and interpretation of rock types from the non-mare regions of the Moon. Proc. Lunar Sci. Conf. 5th, 1227-1246.
72255 72275 72435 73235 76015 76055 76315 77017 77135 78155
- Huebner J.S. (1976) Diffusively rimmed xenocrysts in 77115. LS VII, 396-398.
77115
- Huebner J.S., Ross M., and Hickling N. (1975a) Significance of exsolved pyroxenes from lunar breccia 77215. Proc. Lunar Sci. Conf. 6th, 529-546.
77215
- Huebner J.S., Ross M., and Hickling N.L. (1975b) Cooling history and significance of exsolved pyroxene in lunar noritic breccia 77215. LS VI, 408-410.
77215
- Hughes S.S. and Schmitt R.A. (1985) Zr-Hf-Ta fractionation during lunar evolution. Proc. Lunar Planet. Sci. Conf. 16th, D31-D45.
70017 70035 70215 70255 71035 73215 74245 74255 74275 75055 76136 76539 77035 78526
- Huffman G.P. and Dunmyre G.R. (1975) Superparamagnetic clusters of Fe²⁺ spins in lunar olivine: Dissolution by high-temperature annealing. Proc. Lunar Sci. Conf. 6th, 757-772.
73275 77135
- Huffman G.P., Schwerer F.C., Fisher R.M., and Nagata T. (1974a) Iron distributions and metallic-ferrous ratios for Apollo lunar samples: Mossbauer and magnetic analyses. Proc. Lunar Sci. Conf. 5th, 2779-2794.
70017 70215 73275 76315 77017 77135
- Huffman G.P., Schwerer F.C., Fisher R.M., and Nagata T. (1974b) Iron distributions and metallic-ferrous ratios for Apollo lunar samples: Mossbauer and magnetic analyses. LS V, 372-374.
70017 77017
- Hughes S.S. and Schmitt R.A. (1988) Confirmation of Zr-Hf fractionation in lunar petrogenesis--an interim report. LPS XV, 385-386.
73215 77035
- Huneke J.C. (1978) ⁴⁰Ar-³⁹Ar microanalysis of single 74220 glass balls and 72435 breccia clasts. Proc. Lunar Planet. Sci. Conf. 9th, 2345-2362.
72435
- Huneke J.C. and Wasserburg G.J. (1975) Trapped ⁴⁰Ar in troctolite 76535 and evidence for enhanced ⁴⁰Ar-³⁹Ar age plateaus. LS VI, 417-419.
76535
- Huneke J.C. and Wasserburg G.J. (1978) ⁴⁰Ar-³⁹Ar ages of single orange glass balls and highland breccia phenocrysts. LPS IX, 567-569.
72435
- Huneke J.C., Jessberger E.K., Podosek F.A., and Wasserburg G.J. (1973) ⁴⁰Ar/³⁹Ar measurements in Apollo 16 and 17 samples and the chronology of metamorphic and volcanic activity in the Taurus-Littrow region. Proc. Lunar Sci. Conf. 4th, 1725-1756.
75055 76055
- Huneke J.C., Radicati di Brozolo F., and Wasserburg G.J. (1977) ⁴⁰Ar-³⁹Ar measurements on lunar highlands rocks with primitive ⁸⁷Sr/⁸⁶Sr. LPS XVIII, 481-483.
72435

- Hutcheon I.D. (1975) Microcraters in oriented vugs - evidence for an anisotropy in the micrometeoroid flux. LS VI, 420-422. 71055 74255
- Hutcheon I.D., MacDougall D., and Price P.B. (1974a) Improved determination of the long-term average Fe spectrum from 1 to 460 MeV/amu. Proc. Lunar Sci. Conf. 5th, 2561-2576. 72315
- Hutcheon I.D., MacDougall D., and Stevenson J. (1974b) Apollo 17 particle track studies: surface residence times and fission track ages for orange glass and large boulders. Proc. Lunar Sci. Conf. 5th, 2597-2608. 72255 72275 72315 72395 73215
- Hutcheon I.D., MacDougall D., and Price P.B. (1974c) Rock 72315: A new lunar standard for solar flare and micrometeorite exposure. LS V, 378-380. 72315
- Irving A.J. (1975) Chemical, mineralogical, and textural systematics of non-mare melt rocks: implications for lunar impact and volcanic processes. Proc. Lunar Sci. Conf. 6th, 363-394. 72275 76055
- Irving A.J. (1977) Chemical and experimental constraints on the genesis of Apollo 15 and Apollo 17 KREEP basalts. LPS XVIII, 493- 495. 72275
- Irving A.J., Merrill R.B., and Singleton D.E. (1978) Experimental partitioning of rare earth elements and scandium among armalcolite, olivine, and mare basalt liquids. Proc. Lunar Planet. Sci. Conf. 9th, 601-612. 74275
- Ishii T., Miyamoto M., and Takeda H. (1976) Pyroxene geothermometry and crystallization, subsolidus equilibration temperatures of lunar and achondritic pyroxenes. LS VII, 408-410. 72415 76535 78235
- Ishii T., McCallum I.S., and Ghose S. (1980) Multiple impact history of a genomict breccia 73217 as inferred from pyroxene crystallization sequences. LPS XI, 499-501. 73217
- Ishii T., Ghose S., and McCallum I.S. (1981) Inversion, decomposition, and exsolution phenomena of lunar pyroxenes observed in breccia 73217. LPS XII, 494-496. 73217
- Ishii T., McCallum S., and Ghose S. (1983) Petrological and thermal histories of a lunar breccia 73217 as inferred from pyroxene crystallization sequences, exsolution phenomena, and pyroxene geothermometry. Proc. Lunar Planet. Sci. Conf. 13th, A631-A644. 73217
- Jackson E.D., Sutton R.L., and Wilshire H.G. (1975) Structure and petrology of a cumulus norite boulder sampled by Apollo 17 in Taurus-Littrow valley, the Moon. *Geol. Soc. Am. Bull.* 86, 433- 442. 78235 78236 78238 78255
- Jagodzinski H. and Korekawa M. (1975) Diffuse scattering by domains in lunar and terrestrial plagioclases. LS VI, 429-431. 75035
- Jagodzinski H., Korekawa M., Muller W.F., and Schropfer L. (1975a) X-ray diffraction and electron microscope studies of clinopyroxenes from lunar basalts 75035 and 75075. Proc. Lunar Sci. Conf. 6th, 773-778. 75035 75075

- Jagodzinski H., Korekawa M., Muller W.F., and Schropfer L. (1975b) X-ray study of clinopyroxenes of lunar basalts 75035 and 75075. LS VI, 432-434.
75035 75075
- James O.B. (1975) Petrography of the matrix of light gray (consortium) breccia 73215. LS VI, 438-440.
73215
- James O.B. (1976a) Petrology of aphanitic lithologies in consortium breccia 73215. Proc. Lunar Sci. Conf. 7th, 2145-2178.
73215
- James O.B. (1976b) Petrology of aphanitic lithologies in consortium breccia 73215. LS VII, 420-422.
73215
- James O.B. (1977a) Petrology of four clasts from consortium breccia 73215. LPS XVIII, 502-504.
73215
- James O.B. (1982) Subdivision of the Mg-suite plutonic rocks into Mg-norites and Mg-gabbronorites. LPS XIII, 360-362
72255 72415 72417 73255 76255 76535 77215 78235 78238
- James O.B. and Blanchard D.P. (1976) Consortium studies of light-gray breccia 73215: Introduction, subsample distribution data, and summary of results. Proc. Lunar Sci. Conf. 7th, 2131- 2143.
73215
- James O.B. and Flohr M.K. (1983) Subdivision of the Mg-suite noritic rocks into Mg-gabbronorites and Mg-norites. Proc. Lunar Planet. Sci. Conf. 13th, A603-A614.
73255 76255 78235 78238 78255 77035 72255 77215 77075 77077 72415 76535
- James O.B. and Hammarstrom J.G. (1977) Petrology of four clasts from consortium breccia 73215. Proc. Lunar Sci. Conf. 8th, 2459- 2494.
73215
- James O.B. and Hedenquist J.W. (1978a) Consortium breccia 73255: Petrology of aphanitic lithologies. LPS IX, 585-587.
73255
- James O.B. and Hedenquist J.W. (1978b) Spinel-bearing troctolitic basalt 73215,170: Texture, mineralogy, and history. LPS IX, 588- 590.
73215
- James O.B. and Marti K. (1977) Consortium breccia 73255: Matrix petrography and exposure history. LPS XIII, 505-507.
73255
- James O.B. and McGee J.J. (1979a) Consortium breccia 73255: Genesis and history of two coarse-grained "norite" clasts. Proc. Lunar Planet. Sci. Conf. 10th, 713-743.
73255
- James O.B. and McGee J.J. (1979b) Consortium breccia 73255: Genesis and history of two coarse-grained "norite" clasts. LPS X, 616-618.
73255
- James O.B. and McGee J.J. (1980a) Petrology of mare-type basalt clasts from consortium breccia 73255. Proc. Lunar Planet. Sci. Conf. 11th, 67-86.
73255
- James O.B. and McGee J.J. (1980b) Petrology of ancient mare-type basalt clasts from breccia 73255. LPS XI, 505-507.
73255

- James O.B. and McGee J.J. (1980c) Petrology of felsite clasts from Consortium breccia 73255. LPS XI, 508-510. 73255
- James O.B., Brecher A., Blanchard D.P., Jacobs J.W., Brannon J.C., Korotev R.L., Haskin L.A., Higuchi H., Morgan J.W., Anders E., Silver L.T., Marti K., Braddy D., Hutcheon I.D., Kirsten T., Kerridge J.F., Kaplan I.R., Pillinger C.T., and Gardiner L.R. (1975a) Consortium studies of matrix of light gray breccia 73215. Proc. Lunar Sci. Conf. 6th, 547-577. 73215
- James O.B., Marti K., Braddy D., Hutcheon I.D., Brecher A., Silver L.T., Blanchard D.P., Jacobs J.W., Brannon J.C., Korotev R.L., and Haskin L.A. (1975b) Consortium studies of matrix of light gray breccia 73215. LS VI, 435-437. 73215
- James O.B., Blanchard D.P., Jacobs J.W., Brannon J.C., Haskin L.A., Brecher A., Compston W., Marti K., Lugmair G.W., Gros J., Takahashi H., and Braddy D. (1976) Consortium studies of aphanitic lithologies and two anorthositic gabbro clasts in breccia 73215. LS VII, 423-525. 73215
- James O.B., Hedenquist J.W., Blanchard D.P., Budahn J.R., and Compston W. (1978) Consortium breccia 73255: Petrology, major- and trace element chemistry, and Rb-Sr systematics of aphanitic lithologies. Proc. Lunar Planet. Sci. Conf. 9th, 789-819. 73215 73255
- Jeanloz R.F. and Ahrens T.J. (1976) Alkali mobility in shocked basalt. LS VII, 428-430. 70215
- Jerde E.A., Warren P.H., Morris R.V., Heiken G.H., and Vaniman D.T. (1987) A potpourri of regolith breccias: "New" samples from the Apollo 14, 16, and 17 landing sites. Proc. Lunar Planet. Sci. Conf. 17th, E526-E536. 78515 78516 78555 79115
- Jessberger E.K. (1979) Ancient pink-spinel-bearing troctolitic basalt in Apollo 17 breccia 73215. LPS X, 625-627. 73215
- Jessberger E.K., Horn P., and Kirsten T. (1975) ^{39}Ar - ^{40}Ar -dating of lunar rocks: A methodical investigation of mare basalt 75075. LS VI, 441-443. 75075
- Jessberger E.K., Kirsten T., and Staudacher T. (1976a) Argon-argon ages of consortium breccia 73215. Proc. Lunar Sci. Conf. 7th, 2201-2215. 73215
- Jessberger E., Kirsten T., and Staudacher T. (1976b) Ages of plutonic clasts in consortium breccia 73215. LS VII, 431-433. 73215
- Jessberger E.K., Kirsten T., and Staudacher T. (1977) One rock and many ages- further K-Ar data on consortium breccia 73215. Proc. Lunar Sci. Conf. 8th, 2567-2580. 73215
- Jessberger E.K., Staudacher T., Dominik B., and Kirsten T. (1978) Argon-argon ages of aphanite samples from consortium breccia 73255. Proc. Lunar Planet. Sci. Conf. 9th, 841-854. 73215 73255
- Jost D.T. and Marti K. (1982) Pu-Nd-Xe dating: Progress towards a "solar system" Pu/Nd ratio. LPS XIII, 371-372. 78236 76535

- Jovanovic S. and Reed G.W. (1974a) Labile and nonlabile element relationships among Apollo 17 samples. Proc. Lunar Sci. Conf. 5th, 1685-1701.
72275 72395 72417 73235 73275 74275 75075 76315 76535 77035
- Jovanovic S. and Reed G.W. (1974b) Labile trace elements in Apollo 17 samples. LS V, 391-393.
72275 73275 74275 75075 76315 76535
- Jovanovic S. and Reed G.W. (1975a) Cl and P₂O₅ systematics: Clues to early lunar magmas. Proc. Lunar Sci. Conf. 6th, 1737-1751.
70019 70135 72215 72255 72275 72395 72417 76535
- Jovanovic S. and Reed G.W. (1975b) Soil breccia relationships and vapor deposits on the moon. Proc. Lunar Sci. Conf. 6th, 1753- 1759.
70019 70135 72215 72255 72275
- Jovanovic S. and Reed G.W. (1975c) History of Boulder 1 at Station 2, Apollo 17 based on trace element interrelationships. *The Moon* 14, 385-393.
72215 72255 72275 72395 72417 73235 73275 76315 77035
- Jovanovic S. and Reed G.W. (1975d) Studies on regolith processes: Apollo 15 and 17 labile trace element implications. LS VI, 451- 453.
70019 70135 72215 72255 72275
- Jovanovic S. and Reed G.W. (1976a) Chemical fractionation of Ru and Os in the Moon. Proc. Lunar Sci. Conf. 7th, 3437-3446.
70135 72417
- Jovanovic S. and Reed G.W. (1976b) Convection cells in the early lunar magma ocean: trace-element evidence. Proc. Lunar Sci. Conf. 7th, 3447-3459.
73215 76535
- Jovanovic S. and Reed G.W. (1977) Trace element geochemistry and the early lunar differentiation. Proc. Lunar Sci. Conf. 8th, 623-632.
71055 75035 79215 70135 74275
- Jovanovic S. and Reed G.W. (1978) Trace element evidence for a laterally inhomogeneous Moon. Proc. Lunar Planet. Sci. Conf. 9th, 59-80.
70017 70019 71055 74275 75035 75055 75075 78526 79155
- Jovanovic S. and Reed G.W. (1980a) Candidate samples for the earliest lunar crust. Proc. Conf. Lunar Highlands Crust, 101-111.
70017 70019 70135 71055 72395 74275 75035 75055 75075 78526 79115 72215 72255 72275 73235 73275 77035 76315 73215 76535
- Jovanovic S. and Reed G.W. (1980b) P₂O₅, U and Br associated with mineral separates from a low and a high Ti mare basalt. Proc. Lunar Planet. Sci. Conf. 11th, 125-134.
75055
- Jovanovic S. and Reed G.W. (1980c) Cl, P₂O₅, Br and U partitioning among mineral separates from mare basalt 75055. LPS XI, 517-519.
75055
- Jovanovic S. and Reed G.W. (1981) Chlorine and phosphorus-bearing phases in lunar samples: The significance of Cl/P₂O₅ ratios: A response. LPS XII, 516-519.
75055
- Jovanovic S. and Reed G.W. (1983) The role of phosphorus in lunar samples—a chemical study. Proc. Lunar Planet. Sci. Conf. 13th, A705-A712.
70315 75055

- Jovanovic S., Jensen K.J., and Reed G.W. (1976) Trace elements and the evolution of lunar rocks. LS VII, 437-439.
70135 73215
- Jovanovic S., Jensen K.J., and Reed G.W. (1977) Further insights into the evolution of the early Moon: I. Convection cells, II. Ru-Os partitioning and mixing. LPS XVIII, 516-518.
71055 71569 75035 79155 79215
- Keith J.E., Clark R.S. and Bennett L.J. (1974a) Determination of natural and cosmic ray induced radionuclides in Apollo 17 lunar samples. Proc. Lunar Sci. Conf. 5th, 2121-2138.
70019 70175 70255 70275 71155 72255 72315 72355 72415 76215 76535 78135 78235 78255 78505
- Keith J.E., Clark R.S., and Bennett L.J. (1974b) Determination of natural and cosmic ray induced radionuclides in Apollo 17 lunar samples. LS V, 402-404.
70019 70175 70255 70275 71155 72255 72315 72355 72415 76215 76535 78135 78235 78255 78505
- Kerridge J.F., Kim J.S., Kim Y., and Marti K. (1992) Evolution of isotopic signatures in lunar-regolith nitrogen: Noble gases and nitrogen in grain-size fractions from regolith breccia 79035. *Proc. Lunar Planet. Sci.* 22, 215-224.
79035
- Kesson S.E. (1975a) Mare basalt petrogenesis. In Papers presented to the Conference on Origins of Mare Basalts and their Implications for Lunar Evolution (Lunar Science Institute, Houston), 81-85.
70215
- Kesson S.E. (1975b) Mare basalts: melting experiments and petrogenetic interpretations. Proc. Lunar Sci. Conf. 6th, 921- 944.
70215
- Kesson S.E. (1975c) Melting experiments on synthetic mare basalts and their petrogenetic implications. LS VI, 475-477.
70215
- Kirsten T. and Horn P. (1974a) Chronology of the Taurus-Littrow region III: ages of mare basalts and highland breccias and some remarks about the interpretation of lunar highland rock ages. Proc. Lunar Sci. Conf. 5th, 1451-1475.
70215 79155 75055 76055 77017
- Kirsten T. and Horn P. (1974b) ^{39}Ar - ^{40}Ar -chronology of the Taurus Littrow region II: A 4.28 b.y. old troctolite and ages of basalts and highland breccias. LS V, 419-421.
70215 77017
- Kirsten T., Horn P., Heymann D., Hubner W., and Storzer D. (1973) Apollo 17 crystalline rocks and soils: Rare gases, ion tracks, and ages. *EOS* 54, 595-597.
75055 76055
- Klein J., Middleton R., Fink D., Dietrich J.W., Aylmer D., and Herzog G.F. (1988) Beryllium-10 and aluminum-26 contents of lunar rock 74275. LPS XIX, 607-608.
74275
- Klein L., Onorato P.I.K., Uhlmann D.R., and Hopper R.W. (1975a) Viscous flow, crystallization behaviour, and thermal histories of lunar breccias 70019 and 79155. Proc. Lunar Sci. Conf. 6th, 579- 593.
70019 79155
- Klein L., Uhlmann D.R., and Hopper R.W. (1975b) Viscous flow, crystallization behaviour and thermal history of lunar breccias 70019 and 79155. LS VI, 481-483.
70019 79155
- Klein L.C. and Uhlmann D.R. (1976) The kinetics of lunar glass formation, revisited. Proc. Lunar Sci. Conf. 7th, 1113-1121.
70019

- Knoll H.-D. and Stoffler D. (1979) Characterization of the basic types of lunar highland breccias by quantitative textural analysis. LPS X, 673-675.
76255 72215 72255 73215 73235 77135 79215
- Korotev R.L. and Haskin L.A. (1975) Inhomogeneity of trace element distributions from studies of the rare earths and other elements in size fractions of crushed basalt 70135. In Papers presented to the Conference on Origins of Mare Basalts and their Implications for Lunar Evolution (Lunar Science Institute, Houston), 86-90.
70135
- Kratschmer W. and Gentner W. (1976) The long-term average of the galactic cosmic-ray iron group composition studied by the track method. Proc. Lunar Sci. Conf. 7th, 501-511.
75035
- Kridelbaugh S.J. (1973) The mineralogy and petrology of ilmenite basalt 75055. *EOS* 54, 597-598.
75055
- Lally J.S., Christie J.M., Nord G.L., and Heuer A.H. (1976) Deformation, recovery, and recrystallization of lunar dunite 72417. Proc. Lunar Sci. Conf. 7th, 1845-1863.
72415 72417
- Lally J.S., Christie J.M., Heuer A.H., and Nord G.L. (1976b) Electron microscopy of lunar dunite 72417. LS VII, 468-470.
72417
- Laul J.C., and Schmitt R.A. (1973) Chemical composition of Apollo 15, 16, and 17 samples. Proc. Lunar Sci. Conf. 4th, 1349-1367.
78155
- Laul J.C. and Schmitt R.A. (1974a) Chemical composition of boulder-2 rocks and soils, Apollo 17, Station 2. *Earth Planet. Sci. Lett.* 23, 206-219.
72315 72335 72355 72375 72395
- Laul J.C. and Schmitt R.A. (1974b) Chemical composition of Apollo 17 boulder-2 rocks and soils. LS V, 438-440.
72315 72335 72355 72375 72395
- Laul J.C. and Schmitt R.A. (1974c) Siderophile and volatile trace elements in Apollo 17 boulder-2 rocks and soils. LS V, 441-443.
72315 72335 72355 72375 72395
- Laul J.C. and Schmitt R.A. (1975a) Dunite 72417: A chemical study and interpretation. Proc. Lunar Sci. Conf. 6th, 1231-1254.
72417
- Laul J.C. and Schmitt R.A. (1975b) Dunite 72417: A chemical study. LS VI, 495-497.
72417
- Laul J.C. and Schmitt R.A. (1975c) Chemical composition of Apollo 17 samples: Boulder breccias (2), rake breccias (8), and others. LS VI, 489-491.
72235 72535 77515 77538 77539 77545 78526 78527 78535 78546 78547 78548 78549
- Laul J.C., Hill D.W., and Schmitt R.A. (1974) Chemical studies of Apollo 16 and 17 samples. Proc. Lunar Sci. Conf. 5th, 1047-1066.
70135 72155 72315 72335 72355 72375 72395 75035 77017 79035
- Laul J.C., Murali A.V., Schmitt R.A., and Wakita H. (1975a) Apollo 17 basalts and lunar evolution constraints. In Papers presented to the Conference on Origins of Mare Basalts and their Implications for Lunar Evolution (Lunar Science Institute, Houston), 91-93.
72417 70135 75035 70017

- Laul J.C., Schmitt R.A., Robyn M., and Goles G.G. (1975b) Chemical composition of 18 Apollo 17 rake basalts and one basalt-breccia. LS VI, 492-494.
71515 71559 71566 71567 71569 71577 71578 71587 71588 71596 73219 77516 77535 78569 78575 78578
78586 78597 78598
- Leich D.A., Goldberg R.H., Burnett D.S., and Tombrello T.A. (1974) Hydrogen and fluorine in the surfaces of lunar samples. Proc. Lunar Sci. Conf. 5th, 1869-1884.
70019 75075
- Leich D.A., Kahl S.B., Kirschbaum A.R., Niemeyer S., and Phinney D. (1975a) Rare gas constraints on the history of Boulder 1, Station 2, Apollo 17. *The Moon* 14, 407-444.
72215 72255 72275
- Leich D.A., Kahl S.B., Kirschbaum A.R., Niemeyer S., and Phinney D. (1975b) Rare gas studies on Boulder 1, Station 2, Apollo 17. LS VI, 501-503.
72255 72275
- Levsky L.K., Verchovski A.B., and Chorev A.N. (1981) Argon and xenon adsorption on mineral surfaces: Cosmochemical and geochemical consequences. LPS XII, 613-615.
72555 72775 75535
- Lindstrom M.M. (1985) Compositional distinctions among lunar granulites. LPS XVI, 491-492.
73215 77017 78155 79215
- Lindstrom M.L. and Lindstrom D.J. (1986) Lunar granulites and their precursor anorthositic norites of the early lunar crust. Proc. Lunar Planet. Sci. Conf. 16th, D263-D276.
77017 78155 79215
- Longhi J. (1990) Silicate liquid immiscibility in isothermal crystallization experiments. Proc. Lunar Planet. Sci. Conf. 20th, 13-24.
75055
- Longhi J., Walker D., Grove T.L., Stolper E.M., and Hays J.F. (1974) The petrology of the Apollo 17 mare basalts. Proc. Lunar Sci. Conf. 5th, 447-469.
70017 70215 71569 75035
- Longhi J., Walker D., and Hays J.F. (1974) Fe and Mg in plagioclase. Proc. Lunar Sci. Conf. 7th, 1281-1300.
70017 75035
- Longhi J., Walker D., and Hays J.F. (1978) The distribution of Fe and Mg between olivine and lunar basaltic liquids. *Geochim. Cosmochim. Acta* 42, 1545-1558.
70215 70017 71569 71255 72135 74275 75035
- LSPET (The Lunar Sample Preliminary Examination Team) (1973) Preliminary examination of lunar samples. Apollo 17 Preliminary Science Report. NASA SP-330, 7-1--7-46.
70035 70135 70175 70185 70215 70255 70275 71035 71155 72255 72275 72355 72415 72435 74235 75055
76015 76055 76215 76315 76255 76275 76295 77017 77135 78135 78155 78235 78236 79135 79155
- LSPET (The Lunar Sample Preliminary Examination Team) (1973) Apollo 17 lunar samples: Chemical and petrographic description. *Science* 182, 659-672.
70035 70215 72135 72255 72275 72415 72435 73235 74235 75055 76055 76255 76315 76535 77017 77135
78155 78235 79135
- Lugmair G.W. (1975) Sm-Nd systematics of some Apollo 17 basalts. In Papers presented to the Conference on Origins of Mare Basalts and their Implications for Lunar Evolution (Lunar Science Institute, Houston), 107-110.
70017 75055 75075

- Lugmair G.W. and Marti K. (1978) Lunar initial $^{143}\text{Nd}/^{144}\text{Nd}$: Differential evolution of the lunar crust. *Earth Planet. Sci. Lett.* **39**, 349-357.
75075 75035 75055 70017 76535
- Lugmair G.W., Scheinin N.B., and Marti K. (1975a) Sm-Nd age and history of Apollo 17 basalt 75075: Evidence for early differentiation of the lunar interior. *Proc. Lunar Sci. Conf.* 6th, 1419-1429.
75075
- Lugmair G.W., Scheinin N.B., and Marti K. (1975b) Sm-Nd age of Apollo 17 basalt 75075: Two-stage igneous processes. *LS VI*, 531- 533.
75075
- Lugmair G.W., Marti K., Kurtz J.P., and Scheinin N.B. (1976a) History and genesis of lunar troctolite 76535 or: How old is old? *Proc. Lunar Sci. Conf.* 7th, 2009-2033.
76535
- Lugmair G.W., Kurtz J.P., Marti K., and Scheinin N.B. (1976b) The low Sm/Nd region of the Moon: Evolution and history of a troctolite and a KREEP basalt. *LS VII*, 509-511.
76535
- Ma M.-S., Schmitt R.A., Warner R.D., Taylor G.J., and Keil K. (1979) Composition, petrography, and genesis of Apollo 17 high-Ti mare basalts. *LPS X*, 765-767.
70075 70136 70137 70315 71037 71045 71046 71065 71066 71067 71068 71069 71085 71086 71155 71156
71505 71506 74248 74247 74249 75085 78507 78509 78577 78585 79516 79515
- MacDougall D., Hutcheon I.D., and Price P.B. (1974) Irradiation records in orange glass and two boulders from Apollo 17. *LS V*, 483-485.
72255 72315 72335 72395
- Mao H.K., El Goresy A., and Bell P.M. (1974a) Evidence of extensive chemical reduction in lunar regolith samples from the Apollo 17 site. *Proc. Lunar Sci. Conf.* 5th, 673-683.
70017 70019 79155
- Mao H.K., El Goresy A., and Bell P.M. (1974b) Orange glasses: Reaction of molten liquids with Apollo 17 soil breccia (70019) and gabbro (79155). *LS V*, 489-491.
70019 79155
- Mao H.K., Bell P.M., and Haggerty S.E. (1975) Chemical reduction of glasses in breccia 70019,93: The most reduced Apollo sample. *LS VI*, 548-549.
70019
- Marti K. (1983) Recoils: New opportunities to study and date early solar system processes. *LPS XIV*, 462-463.
78236
- Marvin U.B. (1975) The Boulder. *The Moon* **14**, 315-326.
72215 72235 72255 72275
- Masuda A., Tanaka T., Nakamura N., and Kurasawa H. (1974) Possible REE anomalies of Apollo 17 REE patterns. *Proc. Lunar Sci. Conf.* 5th, 1247-1253.
70215 75075 73235
- Mattinson J.M., Tilton G.R., Todt W., and Chen J.H. (1977) Lead isotope studies of mare basalt 70017. *Proc. Lunar Sci. Conf.* 8th, 1473-1487.
70017 75035 75055 75075
- Mayeda T.K., Shearer J., and Clayton R.N. (1975) Oxygen isotope fractionation of Apollo 17 rocks. *Proc. Lunar Sci. Conf.* 6th, 1799-1802.
70017 71055 72155 75055 75075 79155 72275 72417 76315 77017 78235

- McCallum I.S. (1983) Formation of Mg-rich pristine rocks by crustal metasomatism. LPS XIV, 473-474.
72415 78235
- McCallum I.S. and Charette M.P. (1977) Partitioning of Zr between crystals and coexisting high-Ti mare basalt melt. LPS XVIII, 637- 639.
75035
- McCallum I.S. and Charette M.P. (1978) Zr and Nb distribution coefficients: Further constraints on the genesis of high-Ti mare basalts and KREEP. LPS IX, 711-713.
75035
- McCallum I.S. and Mathez E.A. (1975) Petrology of noritic cumulates and a partial melting model for the genesis of Fra Mauro basalts. Proc. Lunar Sci. Conf. 6th, 395-414.
78235 78238
- McCallum I.S., Mathez E.A., Okamura F.P., and Ghose S. (1974a) Petrology and crystal chemistry of poikilitic anorthositic gabbro 77017. Proc. Lunar Sci. Conf. 5th, 287-302.
77017
- McCallum I.S., Okamura F.P., Mathez E.A., and Ghose S. (1974b) Pyroxene relations in highland plutonic and high grade metamorphic rocks. LS V, 472-474.
77017
- McCallum I.S., Okamura F.P., Mathez E.A., and Ghose S. (1975) Petrology of noritic cumulates: Samples 78235 and 78238. LS VI, 534-536.
78235 78238
- McGee J.J., Bence A.E., Eichhorn G., and Schaeffer O.A. (1978a) Feldspathic granulite 79215: Limitations on T-fO₂ conditions and time of metamorphism. Proc. Lunar Planet. Sci. Conf. 9th, 743-772.
79215
- McGee J.J., Bence A.E., and Schaeffer O.A. (1978b) Feldspathic granulite 79215: Conditions of metamorphism and age. LPS IX, 720-722.
79215
- McGee J.J., Nord G.L., Jr., and Wandless M.-V. (1980a) Comparative thermal histories of matrix from Apollo 17 Boulder 7 fragment-laden melt rocks: An analytical transmission electron microscopy study. Proc. Lunar Planet. Sci. Conf. 11th, 611-627.
77075 77115 77135
- McGee J.J., Nord G.L., Jr., and Wandless M.-V. (1980b) Comparative thermal histories of matrix from Apollo 17 Boulder 7 fragment-laden melt rocks. LPS XI, 700-702.
77075 77115 77135
- McKay D.S., Wentworth S.J., and Basu A. (1988) Core 79001/2: An example of extreme mixing in the lunar regolith. LPS XIX, 758- 759.
79115
- McKay G., Wiesmann H., and Bansal B. (1979) The KREEP-magma ocean connection. LPS X, 804-806.
72415 72417
- Mehta S. and Goldstein J.I. (1980a) Metallic particles in the glassy constituents of three lunar highland samples 65315, 67435, and 78235. Proc. Lunar Planet. Sci. Conf. 11th, 1713-1725.
78235
- Mehta S. and Goldstein J.I. (1980b) Metallic particles in the glass coatings of lunar highland samples 65315, 67435, and 78235. LPS XI, 720-722.
78235

- Merlivat L., Lelu M., Nief G., and Roth E. (1974a) Deuterium, hydrogen, and water content of lunar material. Proc. Lunar Sci. Conf. 5th, 1885-1895.
70215 75035
- Merlivat L., Lelu M., Nief G., and Roth E. (1974b) Deuterium content of lunar material. LS V, 498-500.
75035
- Merlivat L., Lelu M., Nief G., and Roth E. (1976) Spallation deuterium in rock 70215. Proc. Lunar Sci. Conf. 7th, 649-658.
70215
- Meyer C.E. and Wilshire H.G. (1974) "Dunite" inclusion in lunar basalt 74275. LS V, 503-505.
74275
- Meyer C., Anderson D.H., and Bradley J.G. (1974) Ion microprobe mass analysis of plagioclase from "non-mare" lunar samples. LS V, 506-508.
76535
- Meyer H.O.A. and Boctor N.Z. (1974a) Opaque mineralogy: Apollo 17, rock 75035. Proc. Lunar Sci. Conf. 5th, 707-716.
75035
- Meyer C., Williams I.S., and Compston W. (1989) $^{207}\text{Pb}/^{206}\text{Pb}$ ages of zircon-containing rock fragments indicate continuous magmatism in the lunar crust from 4350 to 3900 million years. LPSC XX, 691-692.
73217 73235
- Meyer H.O.A. and Boctor N.Z. (1974b) Opaque minerals in basaltic rock 75035. LS V, 512-514.
75035
- Meyer C., Jr. (1979) Trace elements in plagioclase from the lunar highlands. In Papers Presented to the Conference on the Lunar Highlands Crust. *LPI Contr.* 394, 111-113.
74235 76215 77135 78315
- Miller M.D., Pacer R.A., Ma M.-S., Hawke B.R., Lookhart G.L., and Ehmann W.D. (1974) Compositional studies of the lunar regolith at the Apollo 17 site. Proc. Lunar Sci. Conf. 5th, 1079-1086.
70017 70215 71055 73235 74275 75035 79035
- Minkin J.A., Thompson C.L., and Chao E.C.T. (1978) The Apollo 17 Station 7 boulder: Summary of study by the International Consortium. Proc. Lunar Planet. Sci. Conf. 9th, 877-903.
77075 77115 77135 77215
- Misra K.C., Walker B.M., and Taylor L.A. (1976a) Textures and compositions of metal particles in Apollo 17, Station 6 boulder samples. Proc. Lunar Sci. Conf. 7th, 2251-2266.
76015 76215 76275 76295 76315
- Misra K.C., Walker B.M., and Taylor L.A. (1976b) Native FeNi metal particles in Apollo 17 Station 6 boulder. LS VII, 565-567.
76015 76215 76275 76295 76315
- Miura Y. (1982) A new indicator of formation process based on bulk An and Or contents of terrestrial and extraterrestrial plagioclases with or without exsolution. LPS XIII, 524-525.
70017
- Miura Y. (1988) Normal and anomalous compositions of lunar feldspars - I. Lunar plagioclases. LPS XIX, 794-795.
70017 73215 75055 76535 77515
- Mizutani H. and Osako M. (1974a) Elastic-wave velocities and thermal diffusivities of Apollo 17 rocks and their geophysical implications. Proc. Lunar Sci. Conf. 5th, 2891-2901.
70215 73235 74275 77017

- Mizutani H. and Osako M. (1974b) Elastic wave velocities and thermal diffusivities of Apollo 17 rocks. LS V, 518-519.
70215 73235 74275 77017
- Moore C.B., Lewis C.F., and Cripe J.D. (1974a) Total carbon and sulfur contents of Apollo 17 lunar samples. Proc. Lunar Sci. Conf. 5th, 1897-1906.
70215 71055 72275 72395 73235 75035 77017 78155 79135
- Moore C.B., Lewis C.F., Cripe J.D., and Volk M. (1974b) Total carbon and sulfur contents of Apollo 17 lunar samples. LS V, 520-522.
70215 71055 72275 72395 73235 75035 77017 78155 79135
- Moore C.B. and Lewis C.F. (1976) Total nitrogen contents of Apollo 15, 16 and 17 lunar rocks and soils. LS VII, 571-573.
70215 71055 72135 72275 72385 73235 75035 77017 78155 78235 78505 79135
- Morgan J.W. and Petrie R.K. (1979a) Breccias 73215 and 73255: Siderophile and volatile trace elements. Proc. Lunar Planet. Sci. Conf. 10th, 789-801.
73215 73255
- Morgan J.W. and Petrie R.K. (1979b) Siderophile and volatile trace elements in breccias 73215 and 73255 and in core 74001. LPS X, 852-854.
73215 73255
- Morgan J.W. and Wandless G.A. (1979) Terrestrial upper mantle: Siderophile and volatile trace element abundances. LPS X, 855-857.
72415 72417
- Morgan J.W. and Wandless G.A. (1988) Lunar dunite 72415-72417: Siderophile and volatile trace elements. LPS XIX, 804-805.
72415 72417 73215
- Morgan J.W., Ganapathy R., Higuchi H., Krahenbuhl U., and Anders E. (1974) Lunar basins: Tentative characterization of projectiles, from meteoritic elements in Apollo 17 boulders. Proc. Lunar Sci. Conf. 5th, 1703-1736.
70215 72255 72275 73235 73275 75035 76315 76535 77017 77075 77135 78155 79035 79155
- Morgan J.W., Ganapathy R., Higuchi H., Krahenbuhl U., and Anders E. (1974b) Lunar basins: Tentative characterization of projectiles, from meteoritic elements in Apollo 17 boulders. LS V, 526-528.
70215 72255 72275 73235 73275 75035 76315 76535 77017 77075 77135 78155 79035
- Morgan J.W., Higuchi H., and Anders E. (1975) Meteoritic material in a boulder from the Apollo 17 site: Implications for its origin. *The Moon* 14, 373-383.
72215 72235 72255 72275
- Morgan J.W., Gros J., Takahashi H., and Hertogen J. (1976) Lunar breccia 73215: siderophile and volatile elements. Proc. Lunar Sci. Conf. 7th, 2189-2199.
73215 73235 73275
- Morgeli M., Eberhardt P., Eugster O., Geiss J., Grogler N., and Jungck M. (1977) The age of Shorty Crater. LPS XVIII, 679-681.
74235 74255 74275
- Mori H. and Takeda H. (1980) Thermal and deformational history of diogenites and a lunar norite, as determined by electron microscopy and crystallography. LPS XI, 743-745.
72255
- Mori H., Takeda H., and Miyamoto M. (1982) Comparison of orthopyroxenes in lunar norites and diogenites. LPS XIII, 540-541.
72255 78236

- Morrison D.A. and Zinner E. (1975) Studies of solar flares and impact craters in partially protected crystals. Proc. Lunar Sci. Conf. 6th, 3373-3390. 76015 76215
- Morrison D.A. and Zinner E. (1977a) 12054 and 76215: New measurements of interplanetary dust and solar flare fluxes. Proc. Lunar Sci. Conf. 8th, 841-863. 76215
- Morrison D.A. and Zinner E. (1977b) Microcraters and solar cosmic ray tracks. LPS XVIII, 691-693. 76215
- Morrison D.A. and Clanton U.S. (1979) Properties of microcraters and cosmic dust of less than 1000 Å dimensions. Proc. Lunar Planet. Sci. Conf. 10th, 1649-1663. 76015
- Muan A., Lofall T., and Ma C.-B. (1974) Liquid-solid equilibria in lunar rocks from Apollo 15, 16 and 17, and phase relations in parts of the system $\text{CaMgSi}_2\text{O}_6$ - $\text{CaFeSi}_2\text{O}_6$ - Fe_2SiO_4 - $\text{CaAl}_2\text{Si}_2\text{O}_8$. LS V, 529-530. 71055 75075
- Muhich T., Vaniman D., and Heiken G. (1990) Ilmenite in high-Ti Apollo 17 basalts: Variations in composition with degree of exsolution. LPSC XXI, 817-819. 70035 70215 71055 78505
- Muller H.W., Plieninger T., James O.B., and Schaeffer O.A. (1977a) Laser probe ^{39}Ar - ^{40}Ar dating of materials from consortium breccia 73215. Proc. Lunar Sci. Conf. 8th, 2551-2565. 73215
- Muller H.W., Plieninger T., James O.B., and Schaeffer O.A. (1977b) Laser probe ^{40}Ar - ^{39}Ar dating of materials from consortium breccia 73215. LPS XVIII, 697-699. 73215
- Muller O. (1974a) Solar wind nitrogen and indigenous nitrogen in Apollo 17 lunar samples. Proc. Lunar Sci. Conf. 5th, 1907-1918. 70215 77017 79155
- Muller O. (1974b) Solar wind- and indigenous nitrogen in Apollo 17 lunar samples. LS V, 534-536. 70215 77017 79155
- Muller O., Grallath E., and Tolg G. (1976a) Nitrogen in lunar igneous rocks. Proc. Lunar Sci. Conf. 7th, 1615-1622. 70215 77017 79155
- Muller O., Grallath E., and Tolg G. (1976b) Nitrogen in lunar igneous rocks. LS VII, 580-582. 70215 77017 79155
- Murali A.V., Ma M.-S., Laul J.C., and Schmitt R.A. (1977a) Chemical composition of breccias, feldspathic basalt and anorthosites from Apollo 15 (15308, 15359, 15382 and 15362), Apollo 16 (60618 and 65785), Apollo 17 (72434, 72536, 72559, 72735, 72738, 78526, and 78527) and Luna 20 (22012 and 22013). LPS XVIII, 700-702. 72435 72536 72559 72735 72738 78526 78527
- Murali A.V., Ma M.-S., Schmitt R.A., Warner R.D., Keil K., and Taylor G.J. (1977b) Chemistry of 30 Apollo 17 rake basalts; 71597 a product of partial olivine accumulation. LPS XVIII, 703-705. 71507 71508 71525 71526 71527 71528 71529 71535 71536 71537 71538 71539 71545 71547 71548 71549 71555 71556 71568 71575 71576 71579 71586 71589 71595 71597 78579 78588 78589 78596
- Murthy V.R. (1976) Rb-Sr studies of A-17 mare basalts and some general considerations early terrestrial and lunar evolution. LS VII, 585-587. 74255 75035 75075

- Murthy V.R. (1978) Considerations of lunar initial strontium ratio. LPS IX, 778-780.
77035 78155 79215
- Murthy V.R. and Coscio C., Jr. (1976) Rb-Sr ages and isotopic systematics of some Serenitatis mare basalts. Proc. Lunar Sci. Conf. 7th, 1529-1544.
70017 70035 70135 71055 74255 74275 75035 75075 75055
- Murthy V.R. and Coscio C., Jr. (1977) Rb-Sr isotopic systematics and initial Sr considerations for some lunar samples. LPS XVIII, 706-708.
74275 77035 78155
- Nagata T., Sugiura N., Fisher R.M., Schwerer F.C., Fuller M.D., and Dunn J.R. (1974a) Magnetic properties of Apollo 11-17 lunar materials with special reference to effects of meteorite impact. Proc. Lunar Sci. Conf. 5th, 2827-2839.
70017 70215 73275 74275 77017 78155
- Nagata T., Sugiura N., Fisher R.M., Schwerer F.C., Fuller M.D., and Dunn J.R. (1974b) Magnetic properties and natural remanent magnetization of Apollo 16 and 17 lunar samples. LS V, 540-542.
70017 70215 77017
- Nagata T., Fisher R.M., Schwerer F.C., Fuller M.D., and Dunn J.R. (1975a) Effects of meteorite impact on magnetic properties of Apollo lunar materials. Proc. Lunar Sci. Conf. 6th, 3111-3122.
70017 70215 74275 73275 76315 77017 77135 78155
- Nagata T., Fisher R.M., Schwerer F.C., Fuller M.D., and Dunn J.R. (1975b) Basic magnetic properties of Apollo 17 basaltic and anorthositic lunar materials. LS VI, 584-586.
73275 74275 76315 77135 78155
- Nagle J.S. (1982) Evidence of subcrater lithification and hot ejecta deposition in lunar polymict regolith breccias and achondrites. LPS XIII, 568-569.
76545 79135
- Nakamura N. and Tatsumoto M. (1977) The history of the Apollo 17 Station 7 boulder. Proc. Lunar Sci. Conf. 8th, 2301-2314.
77075 77135 77115 77215
- Nakamura N., Tatsumoto M., Nunes P.D., Unruh D.M., Schwab A.P., and Wildeman T.R. (1976) 4.4. b.y.-old clast in Boulder 7, Apollo 17: A comprehensive chronological study by U-Pb, Rb-Sr, and Sm-Nd methods. Proc. Lunar Sci. Conf. 7th, 2309-2333.
77075 77115 77135 77215
- Nash W.P. and Haselton J.D. (1975) Proc. Lunar Sci. Conf. 6th, 119-130.
70017 70215 74275
- Nautiyal C.M., Padia J.T., Rao M.N., and Venkatesan T.R. (1981a) Solar and galactic cosmic ray records of noble gases in lunar rock 79215. LPS XII, 753-755.
79215
- Nautiyal C.M., Padia J.T., Rao M.N., and Venkatesan T.R. (1981b) Solar flare neon: Clues from implanted noble gases in lunar soils and rocks. Proc. Lunar Sci. Conf. 12th, 627-637.
79215
- Nava D.F. (1974a) Chemical compositions of some soils and rock types from the Apollo 15, 16, and 17 lunar sites. Proc. Lunar Sci. Conf. 5th, 1087-1096.
70017 76055
- Nava D.F. (1974b) Chemistry of some rock types and soils from the Apollo 15, 16 and 17 lunar sites. LS V, 547-549.
70017 76055

- Neal C.R. and Taylor L.A. (1989a) The nature of barium partitioning between immiscible melts: A comparison of experimental and natural systems with reference to lunar granite petrogenesis. Proc. Lunar Planet. Sci. Conf. 19th, 209-218.
73215 73255
- Neal C.R. and Taylor L.A. (1989b) The barium problem in silicate liquid immiscibility: Influence of melt composition and structure on elemental partitioning. LPSC XX, 770-771.
73255
- Neal C.R. and Taylor L.A. (1991) Evidence for metasomatism of the lunar highlands and the origin of whitlockite. *Geochim. Cosmochim. Acta* 55, 2965-2980.
73216
- Neal C.R., Taylor L.A., Hughes S.S., and Schmitt R.A. (1990a) The significance of fractional crystallization in the petrogenesis of Apollo 17 Type A and B high-Ti basalts. *Geochim. Cosmochim. Acta* 54, 1817-1833.
70138 70139 70145 70146 70147 70148 70155 70156 70157 70165 71047 71048 71049 71087 71088 71089
71095 71096 71097 71157 74286 75065 75086 75087 76037 79265
- Neal C.R., Paces J.B., Taylor L.A., and Hughes S.S. (1990ba) Two new Type C basalts: Petrogenetic implications for source evolution and magma genesis at the Apollo 17 site. LPSC XXI, 855- 856.
71095 74245 74247 74255 74275 74285 74287
- Neal C.R., Taylor L.A., Hughes S.S., and Schmitt R.A. (1990c) The importance of fractional crystallization in the petrogenesis of Apollo 17 Type A and B high-Ti basalts. LPSC XXI, 857-858.
71095
- Neal C.R., Taylor L.A., and Patchen A.D. (1990d) An Apollo 17 safari: Exciting new clat from breccia "pull apart" efforts. LPSC XXI, 859-860.
73215 73216
- Neal C.R., Taylor L.A., and Patchen A.D. (1990e) The dichotomy between primitive highland cumulates and evolved interstitial whitlockites: The process of "REEP-fraction" metasomatism. LPSC XXI, 863-864.
73216
- Neal C.R., Taylor L.A., Schmitt R.A., and Liu Y.-G. (1992) The recognition of monomict and polymict clasts from Apollo 17 breccias. LPSC XXIII, 979-980.
73215 73216 77035
- Nehru C.E., Warner R.D., Keil K., and Taylor G.J. (1978) Metamorphism of brecciated ANT rocks: Anorthositic troctolite 72559 and norite 78527. Proc. Lunar Planet. Sci. Conf. 9th, 773-788.
72559 78527
- Newsome H.E. (1984) The abundance of molybdenum in lunar samples, new evidence for a lunar metal core. LPS XV, 605-606.
75035
- Niederer F.R., Papanastassiou D.A., and Wasserburg G.J. (1980) Titanium abundances in terrestrial, lunar and meteoritic samples. LPS XI, 809-811.
75055
- Niemeyer S. (1977a) Exposure histories of lunar rocks 71135 and 71569. Proc. Lunar Sci. Conf. 8th, 3083-3093.
71135 71569
- Niemeyer S. (1977b) Exposure histories of lunar rocks 71135 and 71569. LPS XVIII, 729-731.
71135 71569
- Nord G.L. (1976) 76535: Thermal history deduced from pyroxene precipitation in anorthite. Proc. Lunar Sci. Conf. 7th, 1875- 1888.
76535

- Nord G.L. and James O.B. (1977) Aphanitic matrix, an ANT-suite clast and a felsite clast in consortium breccia 73215: An electron petrographic study. *Proc. Lunar Sci. Conf. 8th*, 2495-2506.
73215
- Nord G.L. and James O.B. (1978a) Consortium breccia 73255: Thermal and deformational history of bulk breccia and clasts, as determined by electron petrography. *Proc. Lunar Planet. Sci. Conf. 9th*, 821-839.
73255
- Nord G.L. and James O.B. (1978b) Consortium breccia 73255: Electron petrography of aphanitic lithologies and anorthite clasts. *LPS IX*, 814-816.
73255
- Nord G.L. and McGee J.J. (1979a) Thermal and mechanical history of granulated norite and pyroxene anorthosite clasts in breccia 73255. *Proc. Lunar Planet. Sci. Conf. 10th*, 817-832.
73255
- Nord G.L. and McGee J.J. (1979b) Thermal and mechanical history of granulated norite and pyroxene anorthosite clasts in breccia 73255. *LPS X*, 919-921.
73255
- Nord G.L., Lally J.S., Heuer A.H., Christie J.M., Radcliffe S.V., Fisher R.M., and Griggs D.T. (1974) A mineralogical study of rock 70017, an ilmenite-rich basalt, by high voltage electron microscopy. *LS V*, 556-558.
70017
- Nord G.L., Heuer A.H., Lally J.S., and Christie J.M. (1975) Substructures in lunar clinopyroxene as petrologic indicators. *LS VI*, 601-603.
70017
- Nord G.L., Ross M., and Huebner J.S. (1976) Lunar troctolite 76535: Mineralogical investigations. *LS VII*, 628-630.
76535
- Nord G.L., Heubner J.S., and Ross M. (1977) Structure, composition, and significance of "G-P" zones in 76535 orthopyroxene. *LPS XVIII*, 732-734.
76535
- Norris S.J., Swart P.K., Wright I.P., Grady M.M., and Pillinger C.T. (1983) A search afor correlatable, isotopically light carbon and nitrogen components in lunar soils and breccias. *Proc. Lunar Planet. Sci. Conf. 14th*, B200-B210
70019 79135
- Nunes P.D. (1975) Pb loss from Apollo 17 glassy samples and Apollo 16 revisited. *Proc. Lunar Sci. Conf. 6th*, 1491-1499.
70019
- Nunes P.D. and Tatsumoto M. (1975a) U-Th-Pb systematics of selected samples from Apollo 17, Boulder 1, Station 2. *The Moon 14*, 463-471.
72215 72255 72275
- Nunes P.D. and Tatsumoto M. (1975b) Pb loss from Apollo 17 glassy samples and Apollo 16 revisited. *LS VI*, 604-606.
70019
- Nunes P.D. and Tatsumoto M. (1975c) U-Th-Pb systematics of anorthositic gabbro 78155. *LS VI*, 607-609.
78155
- Nunes P.D., Tatsumoto M., and Unruh D.M. (1974a) U-Th-Pb and Rb- Sr systematics of Apollo 17 Boulder 7 from the North Massif of the Taurus-Littrow valley. *Earth Planet. Sci. Lett. 23*, 445-452.
77135 77115 77075 77215

- Nunes P.D., Tatsumoto M., and Unruh D.M. (1974b) U-Th-Pb systematics of some Apollo 17 lunar samples and implications for a lunar basin excavation chronology. *Proc. Lunar Sci. Conf. 5th*, 1487-1514.
71569 72155 72255 72275 74235 74255 74275 75035 75055 77017 78155 79155
- Nunes P.D., Tasumoto M., and Unruh D.M. (1974c) U-Th-Pb systematics of some Apollo 17 samples.
LS V, 562-564.
74275 75035 75055 77017 78155 79155
- Nunes P.D., Tatsumoto M., and Unruh D.M. (1975a) U-Th-Pb systematics of anorthositic gabbros 78155 and 77017-implications for early lunar evolution. *Proc. Lunar Sci. Conf. 6th*, 1431-1444.
77017 78155
- Nunes P.D., Nakamura N., and Tatsumoto M. (1976) 4.4 B.y.-old clast in Boulder 7, Apollo 17. *LS VII*, 631-632.
77137 77215
- Nyquist L.E., Bansal B.M., Wiesmann H., and Jahn B.-M. (1974a) Taurus-Littrow chronology: some constraints on early lunar crustal development. *Proc. Lunar Sci. Conf. 5th*, 1515-1539.
70035 72275 72435 73235 73275 76015 76055 76315 77017 77135 78155 79135
- Nyquist L.E., Bansal B.M., Wiesmann H., and Jahn B.M. (1974b) Taurus-Littrow chronology: Implications for early lunar crustal development. *LS V*, 565-567.
70035 72275 72435 76055 76315 77017 77135 78155
- Nyquist L.E., Bansal B.M., and Wiesmann H. (1975a) Rb-Sr ages and initial $^{87}\text{Sr}/^{86}\text{Sr}$ for Apollo 17 basalts and KREEP basalt 15386. *Proc. Lunar Sci. Conf. 6th*, 1445-1465.
70017 70135 70215 70275 71135 72155 74235 74255 75055 75075 79155 76537 76539
- Nyquist L.E., Bansal B.M., and Wiesmann H. (1975b) Rb-Sr ages and initial $^{87}\text{Sr}/^{86}\text{Sr}$ for Apollo 17 basalts and KREEP basalt 15386. *LS VI*, 610-612.
70017 70135 75075
- Nyquist L.E., Bansal B.M., and Wiesmann H. (1976a) Sr isotopic constraints on the petrogenesis of Apollo 17 mare basalts. *Proc. Lunar Sci. Conf. 7th*, 1507-1528.
70017 75075 70135 70035 70185 70215 70255 71035 71136 71175 71546 71567 71569 71577 74245 74255 74275 75015 76136 77535 78135 78506 78597 78599
- Nyquist L.E., Bansal B.M., and Wiesmann H. (1976b) Sr isotopic constraints on the petrogenesis of Apollo 17 mare basalts. *LS VII*, 636-638.
70215 70255 71136 71577 74245 74255 74275 75015 76136 78597
- Nyquist L.E., Shih C.-Y., Wooden J.L., Bansal B.M., and Wiesmann H. (1979) The Sr and Nd isotopic record of Apollo 12 basalts: Implications for lunar geochemical evolution. *Proc. Lunar Planet. Sci. Conf. 10th*, 77-114.
70135 75075
- Nyquist L.E., Reimold W.U., Wooden J.L., Bansal B.M., Wiesmann H., and Shih C.-Y. (1981a) Sr and Nd cooling ages of cumulate norite 78236. *LPS XII*, 782-784.
78236
- Nyquist L.E., Reimold W.U., Bogard D.D., Wooden J.L., Bansal B.M., Wiesmann H., and Shih C.-Y. (1981b) A comparative Rb-Sr, Sm-Nd, and K-Ar study of shocked norite 78236: Evidence of slow cooling in the lunar crust? *Proc. Lunar Planet. Sci. Conf. 12th*, 67-97.
78236
- Oberli F., McCulloch M.T., Tera F., Papanastassiou D.A., and Wasserburg G.J. (1978) Early lunar differentiation constraints from U-Th-Pb, Sm-Nd and Rb-Sr model ages. *LPS IX*, 832-834.
73235 73275

- Oberli F., Huneke J.C., and Wasserburg G.J. (1979) U-Pb and K-Ar systematics of cataclysm and precataclysm lunar impactites. LPS X, 940-942.
78155 79215
- O'Hara M.J., Biggar G.M., Humphries D.J., and Saha P. (1974) Experimental petrology of high titanium basalt. LS V, 571-573.
70017
- O'Hara M.J. and Humphries D.J. (1975) Armalcolite crystallization, phenocryst assemblages, eruption conditions and origin of eleven high titanium basalts from Taurus Littrow. LS VI, 619-621.
70017 70215 70275 71055 71569 72135 74235 74255 74275 75035 75075
- O'Kelley G.D., Eldridge J.S., and Northcutt K.J. (1973) Solar flare induced radionuclides and primordial radioelement concentrations in Apollo 17 rocks and fines - preliminary results. LS IV, 572-574.
70135 76295 79155
- O'Kelley G.D., Eldridge J.S., and Northcutt K.J. (1974a) Cosmogenic radionuclides in samples from Taurus-Littrow: Effects of the solar flare of August 1972. Proc. Lunar Sci. Conf. 5th, 2139-2147.
70135 70185 71135 71136 71175 71566 73215 73255 73275 76295 78597 79155
- O'Kelley G.D., Eldridge J.S., and Northcutt K.J. (1974b) Concentrations of cosmogenic radionuclides in Apollo 17 samples: Effects of the solar flare of August, 1972. LS V, 577-579.
70135 70185 71135 71136 71175 73215 73255 73275 76295 78597 79155
- Onorato P.I.K., Uhlmann D.R., and Simonds C.H. (1976) Heat flow in impact melts: Apollo 17 Station 6 Boulder and some applications to other breccias and xenolith laden melts. Proc. Lunar Sci. Conf. 7th, 2449-2467.
76015 76215 76275 76295 76315
- Osborne M.D., Parkin K.M., and Burns R.G. (1978) Temperature- dependence of Fe-Ti spectra in the visible region: implications to mapping Ti concentrations of hot planetary surfaces. Proc. Lunar Planet. Sci. Conf. 9th, 2949-2960.
70017 70135
- Paces J.B., Nakai S., Neal C.R., Taylor L.A., Halliday A.N., Lee D.-C., and McKinney M.C. (1990a) Resolution of ages and Sm-Nd isotopic characteristics in Apollo 17 high-Ti basalts. LPSC XXI, 924-925.
70017 70035 70135 70138 70139 70215 70255 71055 71069 71095 71097 71539 71545 71576 74247 74255 74275 74285 74287 75035 75055 75075 77516 78586 79155
- Paces J.B., Neal C.R., Nakai S., Taylor L.A., and Halliday A.N. (1990b) Open- and closed-system magma evolution of Apollo 17 high-Ti basalts and origin of source heterogeneities at 4.1 Ga: Sr-Nd isotopic evidence. LSC XXI, 926-927.
70138 70139 71069 71095 71097 71539 71545 71576 74247 74255 74275 74285 74287 77516 78586
- Paces J.M., Nakai S., Neal C.R., Taylor L.A., Halliday A.N., and Lee D.C. (1991) A strontium and neodymium isotopic study of Apollo 17 high-Ti mare basalts: Resolution of ages, evolution of magmas, and origin of source heterogeneities. *Geochim. Cosmochim. Acta* 55, 2025-2043.
70138 70139 71069 71095 71097 71539 71545 71576 74247 74255 74275 74285 74287 77516 78586
- Padawer G.M., Kamykowski E.A., Stauber M.C., D'Agostino M.D., and Brandt W. (1974) Concentration-versus-depth profiles of hydrogen, carbon, and fluorine in lunar rock surfaces. Proc. Lunar Sci. Conf. 5th, 1919-1937.
73235
- Palme H. and Wlotzka F. (1977) Trace element fractionation during crystallization of lunar rock 75035. LPS XVIII, 747-749.
75035

- Palme H., Baddenhausen H., Blum K., Cendales M., Dreibus G., Hofmeister H., Kruse H., Palme C., Spettel B., Vilcsek E., and Wanke H. (1978) New data on lunar samples and achondrites and a comparison of the least fractionated samples from the earth, the moon, and the eucrite parent body. Proc. Lunar Planet. Sci. Conf. 9th, 25-57.
72215 72255 76015 76055
- Palme H., Spettel B., Wanke H., Bischoff A., and Stoffler D. (1984a) The evolution of the lunar magma ocean: Evidence from trace elements in plagioclase. LPS XV, 625-626.
78235
- Palme H., Spettel B., Wanke H., Bischoff A. and Stoffler D. (1984b) Early differentiation of the Moon: Evidence from trace elements in plagioclase. Proc. Lunar Planet. Sci. Conf. 15th, C3-C15.
78235
- Papanastassiou D.A. and Wasserburg G.J. (1975a) Rb-Sr study of a lunar dunite and evidence for early lunar differentiates. Proc. Lunar Sci. Conf. 6th, 1467-1489.
72417 72435
- Papanastassiou D.A. and Wasserburg G.J. (1975b) A Rb-Sr study of Apollo 17 boulder 3: Dunite clast, microclasts, and matrix. LS VI, 631-633.
72417 72435
- Papanastassiou D.A. and Wasserburg G.J. (1976a) Rb-Sr age of troctolite 76535. Proc. Lunar Sci. Conf. 7th, 2035-2054.
76535
- Papanastassiou D.A. and Wasserburg G.J. (1976b) Early lunar differentiates and lunar initial $^{87}\text{Sr}/^{86}\text{Sr}$. LS VII, 665-667.
72417 76535
- Papike J.J., Bence A.E., and Lindsley D.H. (1974) Mare basalts from the Taurus-Littrow region of the Moon. Proc. Lunar Sci. Conf. 5th, 471-504.
70035
- Pearce G.W. and Chou C.-L. (1977) On the origin of sample 70019 and its suitability for lunar magnetic field intensity studies. Proc. Lunar Sci. Conf. 8th, 669-677.
70019
- Pearce G.W., Strangway D.W., and Gose W.A. (1974a) Magnetic properties of Apollo samples and implications for regolith formation. Proc. Lunar Sci. Conf. 5th, 2815-2826.
70035 70215 74275 75035 75055 79135 72275 72415 72435 76015 76315 77017 77135 78155
- Pearce G.W., Gose W.A., and Strangway D.W. (1974b) Magnetism of the Apollo 17 samples. LS V, 590-592.
70035 70215 72275 72415 72435 74275 75035 75055 76015 76055 76315 77017 77135 78155 79135
- Pearce G.W., Chou C.-L., and Wu Y. (1977) Chemical compositions and magnetic properties in separated glass and breccia fractions of 70019. LPS XVIII, 759-761.
70019
- Pearce T.H. and Timms C. (1992) Interference imaging of plagioclase in lunar materials. LPSC XXIII, 1045.
70017 74255 74275
- Petrowski C., Kerridge J.F., and Kaplan I.R. (1974) Light element geochemistry of the Apollo 17 site. Proc. Lunar Sci. Conf. 5th, 1939-1948.
77017 77035 77135 70017 70019 70215 74275 75035 75075
- Philpotts J.A., Schuhmann S., Schnetzler C.C., Kouns C.W., Doan A.S., Wood F.M., Bickel A.L., and Lum Staab R.K.L. (1973) Apollo 17: Geochemical aspects of some soils, basalts, and breccia. EOS 54, 603-604.
76055 79135

- Philpotts J.A., Schumann S., Koons C.W., Lum R.K.L., and Winzer S. (1974a) Origin of Apollo 17 rocks and soils. *Proc. Lunar Sci. Conf. 5th*, 1255-1267
70017 71055 75035 79135 73235 76055
- Philpotts J.A., Schumann S., Koons C.W., and Lum R.K.L. (1974b) Lithophile trace elements in Apollo 17 soils. *LS V*, 599-601.
70017 76055 79135
- Phinney D., Kahl S.B., and Reynolds J.H. (1975) ^{40}Ar - ^{39}Ar dating of Apollo 16 and 17 rocks. *Proc. Lunar Sci. Conf. 6th*, 1593-1608.
70017 73235 77017
- Phinney W.C., McKay D.S., Simonds C.H., and Warner J.L. (1976a) Lithification of vitric- and clastic-matrix breccias: SEM photography. *Proc. Lunar Sci. Conf. 7th*, 2469-2492.
76506 76545 76548 76567
- Phinney W.C., McKay D.S., Warner J.L., and Simonds C.H. (1976b) Lithification of fragmental and vitric matrix breccias. *LS VII*, 694-696.
76567
- Phinney W.C., Warner J.L., and Simonds C.H. (1977) Petrologic evidence for formation and solidification of impact melts. *LPS XVIII*, 770-772.
76015 76215 76255 76295
- Pieters C.M. and Taylor G.J. (1989) Millimeter petrology and kilometer mineral exploration of the Moon. *Proc. Lunar Planet. Sci. Conf. 19th*, 115-125.
72415 78235
- Pieters C.M., Pratt S.F., and Sunshine J.M. (1990) Petrology of the olivine mountains at Copernicus. *LPSC XXI*, 962-963.
72415 78235
- Premo W.R. (1991) Rb-Sr and Sm-Nd ages for lunar norite 78235/78236: Implications on the U-Pb isotopic systematics in this high-Mg rock. *LPSC XXII*, 1089-1090.
78235 78236
- Premo W.R. and Tatsumoto M. (1990) Pb isotopes in norite 78235. *LPSC XXI*, 977-978.
78235
- Premo W.R. and Tatsumoto M. (1991) Pb isotopes in troctolite 76535. *LPSC XXII*, 1093-1094.
76535 78235
- Premo W.R. and Tatsumoto M. (1991b) U-Th-Pb isotopic systematics of lunar norite 78235. *Proc. Lunar Planet. Sci. Conf. 21st*, 89-100.
78235
- Premo W.R. and Tatsumoto M. (1992a) U-Th-Pb, Rb-Sr, and Sm-Nd isotopic systematics of lunar troctolite cumulate 76535: Implications on the age and origin of this early lunar, deep-seated cumulate. *Proc. Lunar Planet. Sci.* **22**, 381-397.
76535 78235
- Premo W.R. and Tatsumoto M. (1992b) Acid leaching of apatite: Implications for U-Th-Pb systematics of lunar highland plutonic rocks. *LPSC XXIII*, 1101-1102.
72415 76535 78235
- Premo W.R. and Tatsumoto M. (1992c) U-Pb isotopes in dunite 72415. *LPSC XXIII*, 1103-1104.
72415 76535 78235

- Radcliffe S.V., Christie J.M., Nord G.L., Lally J.S., Heuer A.H., Griggs D.T., and Fisher R.M. (1974) Electron petrographic evidence concerning the origin and lithification of the lunar breccias. *LS V*, 613-615.
73275 79035
- Rancitelli L.A., Perkins R.W., Felix W.D., and Wogman N.A. (1973) Preliminary analysis of cosmogenic and primordial radionuclides in Apollo 17 samples. *LS IV*, 612-614.
75055 76255 77135 78135
- Rancitelli L.A., Perkins R.W., Felix W.D., and Wogman N.A. (1974a) Solar flare and lunar surface process characterization at the Apollo 17 site. *Proc. Lunar Sci. Conf. 5th*, 2185-2203.
71035 71155 75055 76255 76275 76295 77135
- Rancitelli L.A., Perkins R.W., Felix W.D., and Wogman N.A. (1974b) Anisotropy of the August 4-7, 1972 solar flares at the Apollo 17 site. *LS V*, 618-620.
71035 71155 75055 76255 76275 76295 78135
- Reed G.W., Allen R.O., and Jovanovic S. (1977) Volatile metal deposits on lunar soils-relation to volcanism. *Proc. Lunar Sci. Conf. 8th*, 3917-3930.
74275 75075
- Rees C.E. and Thode H.G. (1974a) Sulfur concentrations and isotope ratios in Apollo 16 and 17 samples. *Proc. Lunar Sci. Conf. 5th*, 1963-1973.
70215 73235 74275 79135
- Rees C.E. and Thode H.G. (1974b) Sulphur concentrations and isotope ratios in Apollo 16 and 17 samples. *LS V*, 621-623.
79135
- Ridley W.I. (1973) Petrogenesis of basalt 70035: A multi-stage cooling history. *EOS 54*, 611-612.
70035
- Ridley W.I., Reid A.M., Warner J.L., Brown R.W., Gooley R., and Donaldson C. (1973) Glass compositions in Apollo 16 soils 60501 and 61221. *Proc. Lunar Sci. Conf. 4th*, 309-321.
78155
- Rhodes J.M. (1973) Major and trace element analyses of Apollo 17 samples. *EOS 54*, 609-610.
72415
- Rhodes J.M. and Blanchard D.P. (1983) New analyses of mare basalts. *LPS XIV*, 640-641.
70315 78585
- Rhodes J.M. and Rodgers K.V. (1975) Major element chemistry, classification and fractionation of Apollo 17 mare basalts. In *Papers presented to the Conference on Origins of Mare Basalts and their Implications for Lunar Evolution* (Lunar Science Institute, Houston), 140-143.
70017 70035 70215 74245 74255 74275 75035 75055 75075
- Rhodes J.M., Rodgers K.V., Shih C., Bansal B.M., Nyquist L.E., Wiesmann H., and Hubbard N.J. (1974a) The relationships between geology and soil chemistry at the Apollo 17 landing site. *Proc. Lunar Sci. Conf. 5th*, 1097-1117.
70017 70019 70215 72275 72415 73235 73275 75075 76015 76055 76315 77135 76535 79135
- Rhodes J.M., Rodgers K.V., Shih C., Bansal B.M., Nyquist L.E., Wiesmann H. (1974b) The relationship between geology and soil chemistry at the Apollo 17 landing site. *LS V*, 630-632.
70017 70019 70215 73235 73275 75075 76315 76535 77135
- Rhodes J.M., Hubbard N.J., Wiesmann H., Rodgers K.V., Brannon J.C., and Bansal B.M. (1976a) Chemistry, classification, and petrogenesis of Apollo 17 mare basalts. *Proc. Lunar Sci. Conf. 7th*, 1467-1489.
70017 70035 70135 70185 70215 70255 70275 71035 71135 71136 71175 71546 71566 71567 71569 71577 72155 74235 74245 74255 74275 75015 75055 75075 76136 76537 76539 77535 78135 78506 78597 78599 79155

- Rhodes J.M., Hubbard N.J., Wiesmann H., Rodgers K.V., and Bansal B.M. (1976b) Chemistry, classification and petrogenesis of Apollo 17 mare basalts. *LS VII*, 730-732.
70017 70215 74275 75015 75035 76136
- Richter D., Simmons G., and Siegfried R. (1976a) Microcracks, micropores, and their petrologic interpretation for 72415 and 15418. *Proc. Lunar Sci. Conf. 7th*, 1901-1923.
72415
- Richter D., Siegfried R., and Simmons G. (1976b) Unusual cracks and pores in breccia 15418 and lunar dunite 72415. *LS VII*, 736-738.
72415
- Roedder E. (1979a) Melt inclusions in 75075 and 78505—the problem of anomalous low-K inclusions in ilmenite revisited. *Proc. Lunar Planet. Sci. Conf. 10th*, 249-257.
75075 78505
- Roedder E. (1979b) Melt inclusions in 75075—the problem of anomalous low-K inclusions in ilmenite revisited. *LPS X*, 1033-1035.
75075
- Roedder E. and Weiblen P.W. (1975a) Anomalous low-K silicate melt inclusions in ilmenite from Apollo 17 basalts. *Proc. Lunar Sci. Conf. 6th*, 147-164.
70017 70035 70135 71175 75035 75075 79155
- Roedder E. and Weiblen P.W. (1975b) Anomalous low-K silicate melt inclusions in ilmenite from Apollo 17 basalts. *LS VI*, 683-685.
70017 70035 70135 71175 75035 75075 79155
- Roedder E. and Weiblen P.W. (1977) Compositional variation in late-stage differentiates in mare lavas, as indicated by silicate melt inclusions. *Proc. Lunar Sci. Conf. 8th*, 1767-1783.
71135 78505
- Rose H.J., Cuttitta F., Berman S., Brown F.W., Carron M.K., Christian R.P., Dwornik E.J., and Greenland L.P. (1974a) Chemical composition of rocks and soils at Taurus-Littrow. *Proc. Lunar Sci. Conf. 5th*, 1119-1133.
70017 70215 71055 75075 72275 79135
- Rose H.J., Brown F.W., Carron M.K., Christian R.P., Cuttitta F., Dwornik E.J., and Ligon D.T. (1974b) Composition of some Apollo 17 samples. *LS V*, 645-647.
70017 79135
- Rose H.J., Baedeker P.A., Berman S., Christian R.P., Dwornik E.J., Finkelman R.B., and Schnepfe M.M. (1975a) Chemical composition of rocks and soils returned by the Apollo 15, 16, and 17 missions. *Proc. Lunar Sci. Conf. 6th*, 1363-1373.
70135 74235 74255 74275 75035 79155
- Rose H.J., Christian R.P., Dwornik E.J., and Schnepfe M.M. (1975b) Major elemental analysis of some Apollo 15, 16 and 17 samples. *LS VI*, 686-688.
70135 74235 74255 74275 75035 79155
- Runcorn S.K., Collinson D.W., and Stephenson A. (1974) Magnetic properties of Apollo 16 and 17 rocks - interim report. *LS V*, 654-654.
70017 70215 76315
- Russell W.A., Papanastassiou D.A., Tombrello T.A., and Epstein S. (1977a) Ca isotope fractionation on the Moon. *Proc. Lunar Sci. Conf. 8th*, 3791-3805.
70215 75055

- Russell W.A., Papanasatassiou D.A., Tonmbrello T.A., and Epstein S. (1977b) Search for Ca isotopic fractionation and correlation of Ca and O effects. LPS XVIII, 823-825.
70215 75055
- Rutherford M.J. and Hess P.C. (1975) Origin of lunar granites as immiscible liquids. LS VI, 696-698.
70135 75055
- Rutherford M.J., Hess P.C., and Daniel G.H. (1974a) Experimental liquid line of descent and liquid immiscibility for basalt 70017. Proc. Lunar Sci. Conf. 5th, 569-583.
70017
- Rutherford M.J., Hess P.C., and Daniel G.H. (1974b) Liquid lines of descent and liquid immiscibility in high Ti lunar basalt. LS V, 657-659.
70017
- Ryder G. (1982) Apollo 17 ol-plag vitrophyres, 76035, and the Serenitatis melt sheet: Another brick in the wall. LPS XIII, 669- 670.
76035
- Ryder G. (1983) Nickel in olivines and parent magmas of lunar pristine rocks. Workshop on Pristine Highlands Rocks and the Early History of the Moon (Longhi J. and Ryder G., Eds.) LPI Tech Rept. 83-02. The Lunar and Planetary Institute, Houston, 66-68.
72415 76335 76535 76536
- Ryder G. (1984a) Most olivine in the lunar highlands is of shallow origin. LPS XV, 707-708.
76015 76035 72255
- Ryder G. (1984b) Olivine in lunar dunite 72415, a rather shallow- origin cumulate. LPS XV, 709-710.
72415 72417 76535
- Ryder G. (1992a) Chemical variation and zoning of olivine in lunar dunite 72415: Near-surface accumulation. Proc. Lunar Planet. Sci. Conf. 22nd, 373-380.
72415 73215 76255 76535 77135
- Ryder G. (1992b) Lunar highlands totality from bits and pieces: A whole-rock-chemistry-free characterization of an evolved hypabyssal igneous gabbro schlieren from the Apollo 17 landing site. LPSC XXIII, 1195-1196.
73155
- Ryder G. and Norman M. (1979) Catalog of pristine non-mare materials Part 1. Non-anorthosites. Revised. NASA-JSC Curatorial Facility Publ. JSC 14565, Houston. 147pp.
76536
- Ryder G., Stoesser D.B., Marvin U.B., and Bower J.F. (1975a) Lunar granites with unique ternary feldspars. Proc. Lunar Sci. Conf. 6th, 435-449.
72215 72235 72255 72275
- Ryder G., Stoesser D.B., Marvin U.B., Bower J.F., and Wood J.A. (1975b) Boulder 1, Station 2, Apollo 17: Petrology and petrogenesis. *The Moon* 14, 327-357.
72215 72235 72255 72275
- Ryder G., Stoesser D.B., and Wood J.A. (1977) Apollo 17 KREEPy basalt: A rock type intermediate between mare and KREEP basalts. *Earth Planet. Sci. Lett.* 35, 1-13.
72275
- Ryder G. and Spudis P. (1980) Volcanic rocks in the lunar highlands. Proc. Conf. Lunar Highlands Crust, 353-375.
72275 73255
- Ryder G. and Taylor G.J. (1976) Did mare-type volcanism commence early in lunar history? Proc. Lunar Sci. Conf. 7th, 1741-1755.
72235 72275

- Ryder G., Norman M.D., and Score R.A. (1980a) The distinction of pristine from meteorite-contaminated highlands rocks using metal compositions. Proc. Lunar Planet. Sci. Conf. 11th, 471-479.
72415 76335 76535 72255
- Ryder G., Norman M.D., and Score R.A. (1980b) Ni, Co content of metal grains for the identification of indigenous rocks. LPS XI, 968-970.
72255 79215
- Salpas P.A. and Taylor L.A. (1985) Basalt clasts in breccia 72275: Examples of pre-mare volcanism. LPS XVI, 728-729.
72275
- Salpas P.A., Taylor L.A., and Lindstrom M.M. (1986a) Apollo 17 KREEPy basalts: Pristine basaltic breccias. LPS XVII, 748-749.
72275
- Salpas P.A., Taylor L.A., and Lindstrom M.M. (1986b) The first Apollo 17 ferroan anorthosite: Its significance relative to Mg- suite highland clasts. LPS XVII, 752-753.
72275
- Salpas P.A., Lindstrom M.M., and Taylor L.A. (1987) Highland materials at Apollo 17: contributions from 72275. Proc. Lunar and Planet. Sci. Conf. 18th, 11-19.
72275
- Salpas P.A., Taylor L.A., and Lindstrom M.M. (1987) Apollo 17 KREEPy basalts: Evidence for Nonuniformity of KREEP. Proc. Lunar Planet. Sci. Conf. 17th, E340-E348.
72275
- Sanford R.F. and Huebner J.S. (1979) Reexamination of diffusion processes in 77115 and 77215. LPS X, 1052-1054.
77115 77215
- Sanford R.F. and Heubner J.S. (1980) Model thermal history of 77115 and implications for the origin of fragment-laden basalts. Proc. Conf. Lunar Highlands Crust, 253-269.
77075 77115 77135
- Sato M. (1976a) Oxygen fugacity and other thermochemical parameters of Apollo 17 high-Ti basalts and their implications on the reduction mechanism. Proc. Lunar Sci. Conf. 7th, 1323-1344.
70017 74275
- Sato M. (1976b) Oxygen fugacity values of some Apollo 16 and 17 rocks. LS VII, 758-760.
70017 70019 74275
- Schaal R.B. and Horz F. (1977a) Shock metamorphism of lunar and terrestrial basalts. Proc. Lunar Sci. Conf. 8th, 1697-1729.
75035 79155
- Schaal R.B. and Horz F. (1977b) Shock effects in some lunar basalts. LPS XVIII, 832-834.
75035 79155
- Schaal R.B., Horz F., and Bauer J.F. (1978) Shock experiments on particulate lunar basalt - a regolith analogue. LPS IX, 999-1001.
75035
- Schaal R.B., Horz F., Thompson T.D., and Bauer J.F. (1979a) Shock metamorphism of granulated lunar basalt. Proc. Lunar Planet. Sci. Conf. 10th, 2547-2571.
75035

- Schaal R.B., Thompson T.D., Horz F., and Bauer J.F. (1979b) Experimentally shocked lunar basalt: Massive and particulate. LPS X, 1055-1057.
75035
- Schaeffer G.A. and Schaeffer O.A. (1977) ^{39}Ar - ^{40}Ar ages of lunar rocks. Proc. Lunar Sci. Conf. 8th, 2253-2300.
70255
- Schaeffer G.A. and Schaeffer O.A. (1977) ^{39}Ar - ^{40}Ar ages of lunar rocks. LPS XVIII, 840-842.
70255
- Schaeffer O.A., Warasila R., and Labotka T.C. (1982) Ages of Serenitatis breccias. Lunar breccias and soils and their meteoritic analogs. LPI Tech. Rept. 82-02, 123-125.
72215 72255
- Schaeffer O.A., Muller H.W., and Grove T.L. (1977a) Laser ^{39}Ar - ^{40}Ar study of Apollo 17 basalts. Proc. Lunar Sci. Conf. 8th, 1489-1499.
70215 70017 75035
- Schaeffer O.A., Muller H.W., and Grove T.L. (1977b) Laser ^{39}Ar - ^{40}Ar study of Apollo 17 basalts. LPS XVIII, 837-839.
70017 70215 75035
- Schaeffer O.A., Warasila R., and Labotka T.C. (1982) Ages of Serenitatis breccias. LPS XIII, 685-686.
72215 72255
- Schmitt H.H. (1975) Geological model for Boulder 1 at Station 2, South Massif, Valley of Taurus-Littrow. *The Moon* 14, 491-504.
72215 72235 72255 72275
- Schonfeld E. (1973) Determination by non-destructive gamma-ray counting of radionuclides produced by the August 1972 solar flare. LS IV, 659.
76015
- Schwerer F.C. and Nagata T. (1976) Ferromagnetic- superparamagnetic granulometry of lunar surface materials. Proc. Lunar Sci. Conf. 7th, 759-778.
70017 70215 78155
- Schreiber E. (1977) The Moon and Q. Proc. Lunar Sci. Conf. 8th, 1201-1208.
70215
- Sclar C.B. and Bauer J.F. (1975a) Shock-induced subsolidus reduction-decomposition of orthopyroxene and shock-induced melting of norite 78235. Proc. Lunar Sci. Conf. 6th, 799-820.
78235
- Sclar C.B. and Bauer J.F. (1975b) Shock-induced subsolidus reduction-decomposition of orthopyroxene and shock-induced melting in norite 78235. LS VI, 730-731.
78235
- Sclar C.B. and Bauer J.F. (1976) Subsidius reduction phenomena in lunar norite 78235: Observations and interpretations. Proc. Lunar Sci. Conf. 7th, 2493-2508.
78235
- Sclar C.B. and Bauer J.F. (1976b) Redox reactions involving nonvolatile ionic species as a mechanism of shock-induced subsolidus reduction of Fe^{+2} in plagioclase and orthopyroxene: Indications from lunar norite 78235. LS VII, 791-793.
78235
- Shaw D.M. and Middleton T.A. (1987) Lunar boron: A preliminary study. LPS XVIII, 912-913.
70017

- Shaffer E., Brophy J.G., and Basu A. (1990) La/Sm ratios in mare basalts as a consequence of mafic cumulate fractionation from an initial lunar magma. LPSC XXI, 1130-1131.
70215
- Shearer C.K., Papike J.J., Galbreath K.C., and Shimizu N. (1991) Exploring the lunar mantle with secondary ion mass spectrometry: A comparison of lunar picritic glass beads from the Apollo 14 and Apollo 17 sites. *Earth Planet. Sci. Lett.* **102**, 134-147.
70017 70295 74115 78546 79035 79135
- Shih C.-Y., Haskin L.A., Wiesmann H., Bansal B.M., and Brannon J.C. (1975a) On the origin of high-Ti mare basalts. Proc. Lunar Sci. Conf. 6th, 1255-1285.
70017 70035 70135 70215 70275 71135 72155 74235 74255 75055 75075 76537 76539 79155
- Shih C.-Y., Wiesmann H.W., and Haskin L.A. (1975b) On the origin of high-Ti mare basalts. LS VI, 735-737.
70017 70035 70135 70215 72155 75055 75075 76537 76539
- Shih C.-Y., Nyquist L.E., Dasch E.J., Bansal B.M., and Wiesmann H. (1989) Ages of pristine lunar plutonic rocks and their petrogenetic implications. LPSC XX, 1004-1005.
73255 76535 78236
- Shih C.-Y., Bansal B.M., Wiesmann H., and Nyquist L.E. (1990a) Rb-Sr and Sm-Nd isotopic studies of an Apollo 17 KREEPy basalt. LPSC XXI, 1148-1149.
72275
- Shih C.-Y., Nyquist L.E., Bansal B.M., and Wiesmann H. (1992) Rb-Sr and Sm-Nd chronology of an Apollo 17 KREEP basalt. *Earth Planet. Sci. Lett* **108**, 203-215.
72275
- Sill G.T., Nagy B., Nagy L.A., Hamilton P.B., McEwan W.S., and Urey H.C. (1974) Carbon compounds in Apollo 17 lunar samples: Indications of cometary contribution to breccia 78155? LS V, 703-705.
71055 78155
- Simmons G., Siegfried R., and Richter D. (1975a) Characteristics of microcracks in lunar samples. Proc. Lunar Sci. Conf. 6th, 3227-3254.
70215 71569 75035 75055 77035 78235
- Simmons G., Richter D., and Siegfried R. (1975b) Characterization of microcracks in lunar igneous rocks. LS VI, 741-743.
75055
- Simon S.B., Papike J.J., Laul J.C., Hughes S.S., and Schmitt R. A. ((1989) Comparative petrology and chemistry of Apollo 17 regolith breccias and soils. LPSC XX, 1014-1015.
70175 74115 76565
- Simon S.B., Papike J.J., Gosselin D.C., Laul J.C., Hughes S.S., and Schmitt R.A. (1990) Petrology and chemistry of Apollo 17 regolith breccias: A history of mixing of highland and mare regolith. Procl. Lunar Planet. Sci. 20th, 219-230.
70019 70175 70295 74115 74246 76565 78546 79035 79135 79175
- Simonds C.H. (1975) Thermal regimes in impact melts and the petrology of the Apollo 17 Station 6 boulder. Proc. Lunar Sci. Conf. 6th, 641-672.
76015 76215 76235 76255 76275 76295 76315
- Simonds C.H. and Warner J.L. (1981) Petrochemistry of Apollo 16 and 17 samples. LPS XII, 993-995.
76275 76295 76506 76555 76556 76557 76559 76569 76575 76576 76577 76295 76538 76539 76537 76568 76536 76255 76565 76545 76505
- Simonds C.H., Warner J.L., and Phinney W.C. (1973) Petrology of Apollo 16 poikilitic rocks. Proc. Lunar Sci. Conf. 4th, 613-632.
72275 72435 76315 77135

- Simonds C.H., Phinney W.C., and Warner J.L. (1974) Petrography and classification of Apollo 17 non-mare rocks with emphasis on samples from the Station 6 boulder. Proc. Lunar Sci. Conf. 5th, 337-353.
72215 72235 72255 72275 72315 72335 72355 72395 72415 72435 73215 73235 73255 73275 76015 76055
76215 76235 76255 76275 76295 76315 76535 77017 77035 77075 77115 77135 77215 78155 78235 79215
- Simonds C.H., Phinney W.C., Warner J.L., and Heiken G.H. (1975) Thermal regimes in crater debris as deduced from the petrology of the Apollo 17 Station 6 boulder and rake samples. LS VI, 747-749.
76015 76215 76275 76295 76315 76505 76545 76548 76565 76567
- Simonds C.H., Warner J.L., Phinney W.C., and McGee P.E. (1976a) Thermal model for impact breccia lithification: Manicouagan and the moon. Proc. Lunar Sci. Conf. 7th, 2509-2528.
76015 76275
- Simonds C.H., Warner J.L., and Phinney W.C. (1976b) Clast-melt interactions in lunar and terrestrial impact melts. LS VII, 812-814.
76015 76215 76275 76295
- Simonds C.H., Phinney W.C., Warner J.L., McGee P.E., Geeslin J., Brown R.W., and Rhodes M.J. (1977) Apollo 14 revisited, or breccias aren't so bad after all. Proc. Lunar Sci. Conf. 8th, 1869-1893.
76015 76215 76255 76275 76295
- Smith J.M., Meyer C., Jr., Compston W., and Williams I.S. (1986) 73235,82 (pomegranate): An assemblage of lunar zircon with unique overgrowth. LPS XVII, 805-806.
73235
- Smith J.V., Hansen E.C., and Steele I.M. (1980) Lunar highland rocks: Element partitioning among minerals II: Electron microprobe analyses of Al, P, Ca, Ti, Cr, Mn and Fe in olivine. Proc. Lunar Planet. Sci. Conf. 11th, 555-569.
73215 79215 76255 76535 77135
- Smyth J.R. (1975) Intracrystalline cation order in a lunar crustal troctolite. Proc. Lunar Sci. Conf. 6th, 821-832.
76535
- Smyth J.R. (1986) Crystal structure refinement of a lunar anorthite, An₉₄. Proc. Lunar Planet. Sci. Conf. 17th, E91-E97.
76535
- Snee L.W. and Ahrens T.J. (1975a) Shock-induced deformation features in terrestrial peridot and lunar dunite. Proc. Lunar Sci. Conf. 6th, 833-842.
72415
- Snee L.W. and Ahrens T.J. (1975b) Shock-induced deformation features in terrestrial olivine and lunar dunite. LS VI, 759-761.
72415
- Spudis P.D. and Ryder G. (1981) Apollo 17 impact melts and their relation to the Serenitatis basin. Multi-ring basins. Proc. Lunar Planet. Sci. 12A, 133-148.
72215 72235 72275 72315 73215 73235 73255 76015 76055 76215 77075
- Stanin F.T. and Taylor L.A. (1979a) Armalcolite/ilmenite: Mineral chemistry, paragenesis, and origin of textures. Proc. Lunar Planet. Sci. Conf. 10th, 383-405.
70017 74275
- Stanin F.T. and Taylor L.A. (1979b) Ilmenite/armalcolite: Effects of rock composition, oxygen fugacity, and cooling rate. LPS X, 1160-1162.
70017 74275

- Stanin F.T. and Taylor L.A. (1980a) Armalcolite: an oxygen fugacity indicator. Proc. Lunar Planet. Sci. Conf. 11th, 117-124.
70017 74245
- Stanin F.T. and Taylor L.A. (1980b) An oxygen geobarometer for lunar high-titanium basalts. LPS XI, 1079-1081.
70017 74275
- Staudacher T., Jessberger E.K., and Kirsten T. (1977) ^{40}Ar - ^{39}Ar age systematics of consortium breccia 73215. LPS XVIII, 896-898.
73215
- Staudacher T., Dominik B., Jessberger E.K., and Kirsten T. (1978) Consortium breccia 73255: ^{40}Ar - ^{39}Ar dating. LPS IX, 1098-1100.
73255
- Staudacher T., Jessberger E.K., Flohs I., and Kirsten T. (1979a) ^{40}Ar - ^{39}Ar age systematics of consortium breccia 73255. Proc. Lunar Planet. Sci. Conf. 10th, 745-762.
73255
- Staudacher T., Dominik B., Flohs I., Jessberger E.K., and Kirsten T. (1979b) New ^{40}Ar - ^{39}Ar ages for aphanites and clasts of consortium breccia 73255. LPS X, 1163-1165.
73255
- Steele I.M. and Smith J.V. (1976) Mineralogy and petrology of complex breccia 14063,14. Proc. Lunar Sci. Conf. 7th, 1949-1964.
72415 76535
- Steele I.M. and Smith J.V. (1980) Ion-probe determination of Li, Na, Mg, Ti, Sr and Ba in lunar plagioclase. LPS XI, 1085-1087.
73155 73215 76535 78235 79215
- Steele I.M., Hutcheon I.D., and Smith J.V. (1980) Ion microprobe analysis and petrogenetic interpretations of Li, Mg, Ti, K, Sr, Ba in lunar plagioclase. Proc. Lunar Planet. Sci. Conf. 11th, 571-590.
73155 73215 76255 76535 77115 77135 78235 79215
- Stephenson A., Collinson D.W., and Runcorn S.K. (1974) Lunar magnetic field paleointensity determinations on Apollo 11, 16, and 17 rocks. Proc. Lunar Sci. Conf. 5th, 2859-2871.
70017 70215 (erroneously listed as 72015 in INTRO), 76315 77035
- Stephenson A., Runcorn S.K., and Collinson D.W. (1975) On changes in intensity of the ancient lunar magnetic field. Proc. Lunar Sci. Conf. 6th, 3049-3062.
70215 78505
- Stephenson A., Runcorn S.K., and Collinson D.W. (1977) Paleointensity estimates from lunar samples 10017 and 10020. Proc. Lunar Sci. Conf. 8th, 679-687.
78505
- Stettler A., Eberhardt P., Geiss J., Grogler N., and Maurer P. (1973) Ar^{39} - Ar^{40} ages and Ar^{37} - Ar^{38} exposure ages of lunar rocks. Proc. Lunar Sci. Conf. 4th, 1865-1888.
70035
- Stettler A., Eberhardt P., Geiss J., and Grogler N. (1974) ^{39}Ar - ^{40}Ar ages of samples from the Apollo 17 Station 7 boulder and implications for its formation. *Earth Planet. Sci. Lett.* 23, 453-461.
77215 77075 77135
- Stettler A., Eberhardt P., Geiss J., Grogler N., and Guggisberg S. (1975) Age sequence in the Apollo 17 Station 7 boulder. LS VI, 771-773.
77115 77135

- Stettler A., Eberhardt P., Geiss J., Grogler N., and Guggisberg S. (1978) Chronology of the Apollo 17 Station 7 Boulder and the South Serenitatis impact. LPS IX, 1113-1115.
77075 77115 77135 77215
- Stoeser D.B., Marvin U.B., and Bower J.F. (1974) Petrology and Petrogenesis of Boulder 1. CI2, L.S.I. Contr. No. 211D, 1-59
72215 72235 72275
- Stoeser D.B., Marvin U.B., Wood J.A., Wolfe R.W., and Bower J.F. (1974a) Petrology of a stratified boulder from South Massif, Taurus-Littrow. Proc. Lunar Sci. Conf. 5th, 355-377
72215 72235 72255 72275
- Stoeser D.B., Wolfe R.W., Marvin U.B., Wood J.A., and Bower J.F. (1974b) Petrographic studies of a boulder from the South Massif. LS V, 743-745.
72255 72275
- Stoeser D.B., Wolfe R.W., Wood J.A. and Bower J.F. (1974) Petrology and Petrogenesis of Boulder 1. CI1, L.S.I. Contr. No. 210D, 35-109.
72255 72275
- Stoeser D.B., Ryder G., and Marvin U.B. (1975) Lunar granite clasts with unique ternary feldspars. LS VI, 780-782.
72215 72235 72255 72275
- Stoffler D., Knoll H.-D., and Maerz U. (1979) Terrestrial and lunar impact breccias and the classification of lunar rocks. Proc. Lunar Planet. Sci. Conf. 10th, 639-675.
72215 72415 78235 76535 78527 79135 76255 77135 78526 79215
- Storey W.C., Humphries D.J., and O'Hara M.J. (1974) Experimental petrology of sample 77135. *Earth Planet. Sci. Lett.* 23, 435-438.
77135
- Storzer D., Poupeau G., and Kratschmer W. (1973) Track-exposure and formation ages of some lunar samples. Proc. Lunar Sci. Conf. 4th, 2363-2377.
75055 76055
- Sugiura N. and Strangway D.W. (1980a) Comparisons of magnetic paleointensity methods using a lunar sample. Proc. Lunar Planet. Sci. Conf. 11th, 1801-1813.
70019 70215
- Sugiura N. and Strangway D.W. (1980b) Thellier paleointensity: Studies of lunar samples. LPS XI, 1111-1113.
70019 70215
- Sugiura N., Strangway D.W., and Pearce G.W. (1978) Heating experiments and paleointensity determinations. Proc. Lunar Planet. Sci. Conf. 9th, 3151-3163.
75035 77035
- Sugiura N., Wu Y.M., Strangway D.W., Pearce G.W., and Taylor L.A. (1979a) A new magnetic paleointensity value for a "young lunar glass." Proc. Lunar Planet. Sci. Conf. 10th, 2189-2197.
70019
- Sugiura N., Wu Y.M., Strangway D.W., Pearce G.W., and Taylor L.A. (1979b) Paleointensity studies on 70019, a young glass sample from Apollo 17. LPS X, 1195-1197.
70019
- Sung C.-M., Abu-Eid R.M., and Burns R.G. (1974a) Ti^{3+}/Ti^{4+} ratios in lunar pyroxenes: implications to depth of origin of mare basalt magma. Proc. Lunar Sci. Conf. 5th, 717-726.
70017 71055 74275

- Sung C.-M., Abu-Eid R.M., and Burns R.G. (1974b) A search for trivalent titanium in Apollo 17 pyroxenes. LS V, 758-760.
70017 71055 74275
- Takeda H. and Ishii T. (1975) Typical processes of exsolution, decomposition and inversion of pyroxenes and its bearing on thermal history of lunar rocks. LS VI, 795-797.
72255 77135
- Takeda H. and Miyamoto M. (1976) Characterization of crust formation on a parent body of achondrites and the Moon by pyroxene crystallography and chemistry. LS VII, 846-848.
72255 76015
- Takeda H. and Miyamoto M. (1977a) Inverted pigeonites from lunar breccia 76255 and pyroxene-crystallization trends in lunar and achondritic crusts. Proc. Lunar Sci. Conf. 8th, 2617-2626.
76255
- Takeda H. and Miyamoto M. (1977b) Inverted pigeonites from lunar breccia 76255 and pyroxene-crystallization trends in lunar and achondritic crusts. LPS XVIII, 922-924.
76255
- Takeda H., Miyamoto M., Ishii T. and Reid A.M. (1976) Characterization of crust formation on a parent body of achondrites and the Moon by pyroxene crystallography and chemistry. Proc. Lunar Sci. Conf. 7th, 3535-3548.
72255 76015 77215
- Takeda H., Mori H., and Miyamoto M. (1982) Comparison of thermal history of orthopyroxenes between lunar norites 78236, 72255, and diogenites. Proc. Lunar Planet. Sci. Conf. 13th, A124-A130.
72255 78236
- Takeda H., Miyamoto M., and Ishii T. (1983) Mineralogical comparison of lunar and chondritic vesicular melt breccias. LPS XIV, 771-772.
77135 78236
- Tanaka T., Masuda A., Kurasawa H., and Nakamura N. (1974) Determination of REE and Ba in five Apollo 17 samples. LS V, 772-774.
70215 73235
- Tatsumoto M., Nunes P.D., Knight R.J., Hedge C.E., and Unruh D.M. (1973) U-Th-Pb, Rb-Sr, and K measurements of two Apollo 17 samples. EOS 54, 614
75055
- Tatsumoto M., Nunes P.D., Knight R.J., and Unruh D.M. (1974) Rb- Sr and U-Th-Pb systematics of boulders 1 and 7, Apollo 17. LS V, 774-776.
72275 77135 77215
- Taylor G.J., Warner R.D., Keil K., Ma M.-S., and Schmitt R.A. (1980) Silicate liquid immiscibility, evolved lunar rocks, and the formation of KREEP. Proc. Conf. Lunar Highlands Crust, 339- 352.
77538
- Taylor H.P., Jr., and Epstein S. (1973) O^{18}/O^{16} and Si^{30}/Si^{28} studies of some Apollo 15, 16, and 17 samples. Proc. Lunar Sci. Conf. 4th, 1657-1679.
75055 76055
- Taylor L.A. and Williams K.L. (1974a) Formational history of lunar rocks: applications of experimental geochemistry of the opaque minerals. Proc. Lunar Sci. Conf. 5th, 585-596.
70017 75035 77017
- Taylor L.A. and Williams K.L. (1974b) Formational history of lunar rocks: applications of experimental geochemistry of the opaque minerals. LS V, 783-785.
70017 75035 77017

- Taylor, L.A. (1979) Paleointensity determinations at elevated temperatures: Sample preparation technique. Proc. Lunar Planet. Sci. Confer. 10th, 2183 - 2187.
- Taylor L.A., McKay D.S., Patchen A., Wentworth S., Oder R., and Jerde E. (1992) Magnetic beneficiation of high-Ti mare basalts: Petrographic analyses. LPSC XXIII, 1415-1416.
71055
- Taylor S.R. and Bence A.E. (1975) Trace element characteristics of the mare basalt source region: Implications of the cumulate versus primitive source model. In Papers presented to the Conference on Origins of Mare Basalts and their Implications for Lunar Evolution (Lunar Science Institute, Houston), 159-163.
74275
- Taylor S.R., Gorton M., Muir P., Nance W., Rudowski R., and Ware N. (1974) Lunar highland composition. LS V, 789-791.
72275 73235 76315
- Tera F. and Wasserburg G.J. (1974) U-Th-Pb systematics on lunar rocks and inferences about lunar evolution and the age of the Moon. Proc. Lunar Sci. Conf. 5th, 1571-1599.
75055 76535
- Tera F. and Wasserburg G.J. (1975) The evolution and history of mare basalts as inferred from U-Th-Pb systematics. LS VI, 807- 809.
75055
- Tera F. and Wasserburg G.J. (1976) Lunar ball games and other sports. LS VII, 858-860.
75055
- Tera F., Papanastassiou D.A., and Wasserburg G.J. (1974a) Isotopic evidence for a terminal lunar cataclysm. *Earth Planet. Sci. Lett.* **22**, 1-21.
72315 72335 72355 73275 76055 75055
- Tera F., Papanastassiou D.A., and Wasserburg G.J. (1974b) The lunar time scale and a summary of isotopic evidence for a terminal lunar cataclysm. LS V, 792-794.
71055 7217 76535
- Thomber C.R. and Huebner J.S. (1980) An experimental study of the thermal history of fragment-laden "basalt" 77115. Proc. Conf. Lunar Highlands Crust, 233-252.
77115
- Tilton G.R. and Chen J.H. (1979) Lead isotope systematics of three Apollo 17 mare basalts. Proc. Lunar Planet. Sci. Conf. 10th, 259-274.
70017 71055 75075
- Tittmann B.R., Curnow J.M., and Housley R.M. (1975a) Internal friction quality factor $Q > 3100$ achieved in lunar rock 70215,85. Proc. Lunar Sci. Conf. 6th, 3217-3226.
70215
- Tittman B.R., Housley R.M., and Abdel-Gawad M. (1975b) Internal friction quality factor > 3100 achieved in lunar rock 70215,85. LS VI, 812-814.
70215
- Tittman B.R., Ahlberg L., and Curnow J. (1976) Internal friction and velocity measurements. Proc. Lunar Sci. Conf. 7th, 3123-3132.
70215
- Tittman B.R., Ahlberg H., Nadler H., Curnow J., Smith T., and Cohen E.R. (1977) Internal friction quality-factor Q under confining pressure. Proc. Lunar Sci. Conf. 8th, 1209-1224.
70215

- Tittman B.R., Nadler H., Richardson J.M., and Ahlberg L. (1978) Laboratory measurements of p-wave seismic Q on lunar and analog rocks. Proc. Lunar Planet. Sci. Conf. 9th, 3627-3635.
70215
- Trice R., Warren N., and Anderson O.L. (1974) Rock elastic properties and near-surface structure of Taurus-Littrow. Proc. Lunar Sci. Conf. 5th, 2903-2911.
71055
- Turner G., Cadogan P.H., and Yonge C.J. (1973a) Argon selenochronology. Proc. Lunar Sci. Conf. 4th, 1889-1914.
75055 76055
- Turner G., Cadogan P.H., and Yonge C.J. (1973b) Apollo 17 age determinations. *Nature* **242**, 513-515.
75035 76055
- Turner G. and Cadogan P.H. (1974) Possible effects of ^{39}Ar recoil in ^{40}Ar - ^{39}Ar dating. Proc. Lunar Sci. Conf. 5th, 1601-1615.
75035
- Turner G. and Cadogan P.H. (1975a) The history of lunar bombardment inferred from ^{40}Ar - ^{39}Ar dating of highland rocks. Proc. Lunar Sci. Conf. 6th, 1509-1538.
75035 73235 73275 76315 77135 78155
- Turner G. and Cadogan P.H. (1975b) The history of lunar basin formation inferred from ^{40}Ar - ^{39}Ar dating of highland rocks. LS VI, 826-828.
73235 73275 75035 77135 78155
- Uhlmann D.R. and Onorato P.I.K. (1979) A simplified model for glass formation. LPS X, 1250-1252.
70019 79155
- Uhlmann D.R. and Yinnon H. (1981) Simplified model evaluation of cooling rates for glass-containing lunar compositions. LPS XII, 1103-1105.
77017
- Uhlmann D.R., Klein L., Onorato P.I.K., and Hopper R.W. (1975) The formation of lunar breccias: sintering and crystallization kinetics. Proc. Lunar Sci. Conf. 6th, 693-705.
70019
- Uhlmann D.R., Onorato P.I.K., and Scherer G.W. (1979) A simplified model for glass formation. Proc. Lunar Planet. Sci. Conf. 10th, 375-381.
70019 79155
- Uhlmann D.R., Yinnon H., and C.-Y. Fang (1981) Simplified model evaluation of cooling rates for glass-containing lunar compositions. Proc. Lunar Planet. Sci. Conf. 12th, 281-288.
77017
- Unruh D.M., Stille P., Oatchett P.J., and Tatsumoto M. (1984) Lu-Hf and Sm-Nd evolution in lunar mare basalts. Proc. Lunar Planet. Sci. Conf. 14th, B459-B477.
75055 75075 70017
- Usselman T.M. (1975) Ilmenite chemistry in mare basalts, an experimental study. In Papers presented to the Conference on Origins of Mare Basalts and their Implications for Lunar Evolution (Lunar Science Institute, Houston), 164-168.
70035
- Usselman T.M. and Lofgren G.E. (1976a) The phase relations, textures, and mineral chemistries of high-titanium mare basalts as a function of oxygen fugacity and cooling rate. Proc. Lunar Sci. Conf. 7th, 1345-1363.
74275

- Usselman T.M. and Lofgren G.E. (1976b) Phase relations of high-titanium mare basalts as a function of oxygen fugacity. *LS VII*, 888-890.
74275
- Usselman T.M., Lofgren G.E., Donaldson C.H., and Williams R.J. (1975) Experimentally reproduced textures and mineral chemistries of high-titanium mare basalts. *Proc. Lunar Sci. Conf. 6th*, 997-1020.
70017 70035 70149 70215 70255 71055 71135 71569 74235 74245 74255 74275 75035 75075 76136 76539
78505
- Vaniman D.T. and Papike J.J. (1980) Lunar highland melt rocks: Chemistry, petrology, and silicate mineralogy. *Proc. Conf. Lunar Highlands Crust*, 271-337.
77135
- Venkatesan T.R., Nautiyal C.M., Padia J.T., and Rao M.N. (1981) Compositional characteristics of solar wind and solar flare neon in the past using lunar soils and rocks. *LPS XII*, 1112-1114.
79215
- Venkatesan T.R., Nautiyal C.M., Padia J.T., and Rao M.N. (1982) SCR-proton produced xenon isotopes in lunar rocks. *LPS XIII*, 821-822.
79215
- Walker D., Longhi J., Stolper E., Grove T., and Hays J.F. (1974) Experimental petrology and origin of titaniferous lunar basalts. *LS V*, 814-816.
70017 70215
- Walker D., Longhi J., and Hays J.F. (1975a) Heterogeneity in titaniferous lunar basalts. In *Papers presented to the Conference on Origins of Mare Basalts and their Implications for Lunar Evolution* (Lunar Science Institute, Houston), 169-173.
70215 71569 74275 75035
- Walker D., Longhi J., Stolper E.M., Grove T.L., and Hays J.F. (1975b) Origin of titaniferous lunar basalts. *Geochim. Cosmochim. Acta* **39**, 1219-1235
70017 70215 75035 71569
- Walker D., Longhi J., and Hays J.F. (1976) Heterogeneity in titaniferous lunar basalts. *Earth Planet. Sci. Lett.* **30**, 27-36.
70215 74275
- Wanke H., Palme H., Baddenhausen H., Dreibus G., Jagoutz E., Kruse H., Spettel B., Teschke F., and Thacker R. (1974) Chemistry of Apollo 16 and 17 samples: bulk composition, late-stage accumulation and early differentiation of the Moon. *Proc. Lunar Sci. Conf. 5th*, 1307-1335.
73235 79035 79135 74275
- Wanke H., Palme H., Baddenhausen H., Dreibus G., Jagoutz E., Kruse H., Palme C., Spettel B., Teschke F., and Thacker R. (1975a) New data on the chemistry of lunar samples: Primary matter in the lunar highlands and the bulk composition of the moon. *Proc. Lunar Sci. Conf. 6th*, 1313-1340.
70019 70215 71569 72155 75035 79155 72395 77035
- Wanke H., Palme H., Baddenhausen H., Dreibus G., Jagoutz E., Kruse H., Spettel B., Teschke F., and Thacker R. (1975b) New data on the chemistry of lunar samples and about the major element composition of KREEP. *LS VI*, 844-846.
70215 71569 72155 72395 75035 77035 79155
- Wanke H., Palme H., Kruse H., Baddenhausen H., Cendales M., Dreibus G., Hofmeister H., Jagoutz E., Palme C., Spettel B., and Thacker R. (1976) Chemistry of lunar highland rocks: a refined evaluation of the composition of the primary matter. *Proc. Lunar Sci. Conf. 7th*, 3479-3499.
78155

- Wanke H., Baddenhausen H., Blum K., Cendales M., Dreibus G., Hofmeister H., Kruse H., Jagoutz E., Palme C., Spettel B., Thacker R., and Vilcsek E. (1977) On the chemistry of lunar samples and achondrites. Primary matter in the lunar highlands: A re-evaluation. *Proc. Lunar Sci. Conf. 8th*, 2191-2213.
73235 77035 78155 72155 75035
- Warner J.L., Simonds C.H., Phinney W.C., and Gooley R. (1973) Petrology and genesis of two "igneous" rocks from Apollo 17 (76055 and 77135). *EOS* 54, 620-621.
76055 77135
- Warner J.L., Simonds C.H., and Phinney W.C. (1976a) Apollo 17, Station 6 boulder sample 76255: Absolute petrology of breccia matrix and igneous clasts. *Proc. Lunar Sci. Conf. 7th*, 2233-2250.
76255
- Warner J.L., Simonds C.H., and Phinney W.C. (1976b) Genetic distinction between anorthosites and Mg-rich plutonic rocks. *LS VII*, 915-917.
76255
- Warner J.L., Phinney W.C., Bickel C.E., and Simonds C.H. (1977) Feldspathic granulitic impactites and pre-final bombardment lunar evolution. *Proc. Lunar Sci. Conf. 8th*, 2051-2066.
76235 77017 78155 79215
- Warner R., Keil K., Murali A.V., and Schmitt R.A. (1975a) Petrogenetic relationships among Apollo-17 basalts. In *Papers presented to the Conference on Origins of Mare Basalts and their Implications for Lunar Evolution* (Lunar Science Institute, Houston), 179-183.
70185 70135 70255 71136 71175 71509 71559 71569 74245 75015 75115 75088 75089 77516 77536 78505 78595 78598
- Warner R.D., Keil K., Prinz M., Laul J.C., Murali A.V., and Schmitt R.A. (1975) Mineralogy, petrology, and chemistry of mare basalts from Apollo 17 rake samples. *Proc. Lunar Sci. Conf. 6th*, 193-220.
71546 71557 71558 71559 71565 71566 71567 71569 71577 71578 71585 71587 71588 71596 73219 77516 77535 77536 78569 78575 78576 78578 78586 78587 78597 78598 78599
- Warner R., Prinz M., and Keil K. (1975c) Mineralogy and petrology of mare basalts from Apollo 17 rake samples. *LS VI*, 850-852.
71546 71557 71558 71559 71565 71566 71567 71569 71577 71578 71585 71587 71588 71596 73219 77516 77535 77536 78569 78575 78576 78578 78586 78587 78597 78598 78599
- Warner R.D., Warren R.G., Mansker W.L., Berkley J.L., and Keil K. (1976a) Electron microprobe analyses of olivine, pyroxene and plagioclase from Apollo 17 rake sample mare basalts. *Spec. Publ. # 15*, UNM Institute of Meteoritics, Albuquerque. 158 pp.
71509 71546 71557 71558 71559 71565 71566 71567 71569 71577 71578 71585 71587 71588 71596 73219 77516 77535 77536 78569 78575 78576 78578 78586 78587 78595 78597 78598 78599
- Warner R.D., Berkley J.L., Mansker W.L., Warren R.G., and Keil K. (1976b) Electron microprobe analyses of spinel, Fe-Ti oxides and metal from Apollo 17 rake sample mare basalts. *Spec. Publ. #16*, UNM Institute of Meteoritics, Albuquerque. 114 pp.
71509 71546 71557 71558 71559 71565 71566 71567 71569 71577 71578 71585 71587 71588 71596 73219 77516 77535 77536 78569 78575 78576 78578 78586 78587 78595 78597 78598 78599
- Warner R.D., Keil K., and Taylor G.J. (1977a) Coarse-grained basalt 71597: A product of partial olivine accumulation. *Proc. Lunar Sci. Conf. 8th*, 1429-1442.
71597
- Warner R.D., Taylor G.J., and Keil K. (1977b) Petrology of crystalline matrix breccias from Apollo 17 rake samples. *Proc. Lunar Sci. Conf. 8th*, 1987-2006.
72535 72536 72539 72738 72548 72549 72736 72558 72735 77515 77539 77545 77518

- Warner R.D., Taylor G.J., and Keil K. (1977c) Petrology of breccias from Apollo 17 rake samples. LPS XVIII, 985-987.
72535 72536 72539 72738 72548 72549 72558 72559 72735 72736 77515 77517 77518 77538 77539 77545
78527 78535 78537 78546 78547 78548 78549 78555 78567 78568
- Warner R.D., Taylor G.J., Keil K., Planner H.N., Nehru C.E., Ma M.-S., and Schmitt R.A. (1978a) Green glass vitrophyre 78526: an impact melt of very low-Ti mare basalt composition. Proc. Lunar Planet. Sci. Conf. 9th, 547-563.
78526
- Warner R.D., Taylor G.J., Mansker W.L., and Keil K. (1978b) Clast assemblages of possible deep-seated (77517) and immiscible melt (77538) origins in Apollo 17 breccias. Proc. Lunar Planet. Sci. Conf. 9th, 941-958.
77517 77538
- Warner R.D., Keil K., Taylor G.J., and Nehru C.E. (1978c) Petrology of recrystallized ANT rocks from Apollo 17 rake samples: 72558 (anorthositic troctolite) and 78527 (norite). LPS IX, 1220-1222.
72559 78527
- Warner R.D., Taylor G.J., and Keil K. (1978d) Clasts in breccias 77517 and 77538: Evidence for deep-seated and immiscible melt origins. LPS IX, 1222-1224.
77517 77538
- Warner R.D., Taylor G.J., Keil K., and Nehru C.E. (1978e) Green glassy rock 78526: An impact melt rock of very low-Ti mare basalt? LPS IX, 1225-1227.
78526
- Warner R.D., Keil K., Nehru C.E., and Taylor G.J. (1978f) Catalogue of Apollo 17 rake samples from Stations 1a, 2, 7 and 8. Spec. Publ. #18, UNM Institute of Meteoritics, Albuquerque. 88pp.
71507 71508 71509 71515 71525 71526 71527 71528 71529 71535 71536 71537 71538 71539 71545 71546
71547 71548 71549 71555 71556 71557 71558 71559 71565 71566 71567 71568 71569 71575 71576 71577
71578 71579 71585 71586 71587 71588 71589 71595 71596 71597 72535 72536 72539 72548 72549 72558
72559 72735 72736 72738 73219 77515 77516 77517 77518 77535 77536 77538 77539 77545 78505 78526
78527 78535 78537 78546 78547 78548 78549 78555 78567 78568 78569 78575 78576 78578 78579 78586
78587 78588 78589 78595 78596 78597 78598 78599
- Warner R.D., Nehru C.E., and Keil K. (1978g) Opaque oxide mineral crystallization in lunar high-titanium basalts. Submitted to Amer. Min.
- Warner R.D., Taylor G.J., Conrad G.H., Northrop H.R., Barker S., Keil K., Ma M.-S., and Schmitt R. (1979a) Apollo 17 high-Ti mare basalts: New bulk compositional data, magma types, and petrogenesis. Proc. Lunar Planet. Sci. Conf. 10th, 225-247.
71067 74249 71156 74248 70075 71066 71065 79516 71069 78585 71046 71086 71037 71506 71505 71155
74247 71085 71068 70315 75085 71045 78509 78577 70137 78507 70136 79515
- Warner R.D., Taylor G.J., and Keil K. (1979b) Composition of glasses in Apollo 17 samples and their relation to known lunar rock types. Proc. Lunar Planet. Sci. Conf. 10th, 1437-1456.
71515 78535 78537 78546 78567 78568 78547 78548 78549 78555
- Warner R.D., Taylor G.J., and Keil K. (1979c) Composition of glasses in Apollo 17 soil breccias. LPS X, 1298-1300.
71515 78527 78535 78537 78546 78547 78548 78549 78555 78567 78568
- Warner R.D., Taylor G.J., Wentworth S.J., Huss G.R., Mansker W.L., Planner H.N., Sayeed U.A., and Keil K. (1979d) Electron microprobe analyses of glasses from Apollo 17 rake sample breccias and Apollo 17 drill core. UNM Spec. Publ. #20, Albuquerque, 20pp.
71515 78535 78537 78546 78547 78548 78549 78555 78567 78568
- Warren N., Trice R., and Stephens J. (1974) Ultrasonic attenuation: Q measurements on 70215,29. Proc. Lunar Sci. Conf. 5th, 2927-2938
70215

- Warren P.H. (1979) The quest for pristine nonmare rocks: A new crop of Toisons d'Or. LPS X, 1301-1303.
72705 73146 73235 76536 77035 78255
- Warren P.H., Mittlefehldt D.W., Boynton W.V., and Wasson J.T. (1977) In quest of primary highlands rocks. LPS XVIII, 988-990.
77545
- Warren P.H., McEwing C.E., Afiattalab F., and Wasson J.T. (1978) The quest for pristine non-mare rocks: Nine nonmare samples free of meteoritic siderophiles. LPS IX, 1228-1230.
76255 76286 76335 76576 77075
- Warren P.H., Taylor G.J., Keil K., Kallemeyn G.W., Rosener P.S., and Wasson J.T. (1982) Foraging for pristine nonmare rocks: Four more from the west. LPS XIII, 841-842
73217 78527
- Warren P.H. and Kallemeyn G.W. (1984) Pristine rocks (8th foray): Plagiophile element ratios, crustal genesis, and the bulk composition of the Moon. Proc. Lunar Planet. Sci. Conf. 15th, C16-C24.
72705 73146 73235 76255 76335 76536 77035 77075 77077 78255 78527
- Warren P. and Wasson J.T. (1977) Pristine nonmare rocks and the nature of the lunar crust. Proc. Lunar Sci. Conf. 8th, 2215-2235.
76335
- Warren P.H. and Wasson J.T. (1979) The compositional-petrographic search for pristine nonmare rocks: Third foray. Proc. Lunar Planet. Sci. Conf. 10th, 583-610.
72705 73146 73235 76536 77035 78255
- Warren P.H. and Wasson J.T. (1980) Early lunar petrogenesis, oceanic and extraoceanic. Proc. Conf. Lunar Highlands Crust, 81- 99.
76335
- Warren P.H. and Wasson J.T. (1978) Compositional-petrographic investigation of pristine nonmare rocks. Proc. Lunar Planet. Sci. Conf. 9th, 185-217.
72559 76255 76286 76335 76576 77075 77077 78255
- Warren P.H., Taylor G.J., Keil K., Kallemeyn G.W., Rosener P.S., and Wasson J.T. (1983) Sixth foray for pristine non-mare rocks and an assessment of the diversity of lunar anorthosites. Proc. Lunar Planet. Sci. Conf. 13th, A615-A630.
73217 78527 76565
- Warren P., Kallemeyn G.W., and Wasson J.T. (1984a) Pristine rocks (8th foray): Genetic distinctions using Eu/Al and Sr/Al ratios. LPS XV, 894-895.
76255
- Warren P.H., Jerde E.A., and Kallemeyn G.W. (1987) Pristine moon rocks: A large felsite and a metal-rich ferroan anorthosite. Proc. Lunar Planet. Sci. Conf. 17th, E303-E313.
73255 73215 78235 76535
- Warren P.H., Shirley D.N., and Kallemeyn G.W. (1986) A potpourri of pristine moon rocks, including a VHK mare basalt and a unique, augite-rich Apollo 17 anorthosite. Proc. Lunar Planet. Sci. Conf. 16th, D319-D330.
76255
- Warren P.H., Jerde E.H., and Kallemeyn G.W. (1991) Pristine moon rocks: Apollo 17 anorthosites. Proc. Lunar Planet. Sci. Conf. 21st, 51-61.
77539
- Wasson J.T., Warren P.H., Kallemeyn G.W., McEwing C.E., Mittlefehldt D.W., and Boynton W.V. (1977) SCCR, a major component of highlands rocks. Proc. Lunar Sci. Conf. 8th, 2237- 2252.
77545

- Watson D.E., Larson E.E., and Reynolds R.L. (1974) Microscopic and thermomagnetic analysis of Apollo 17 breccia and basalt: feasibility of obtaining meaningful paleointensities of the lunar magnetic field. *LS V*, 827-829.
71055 73235
- Weiblen P.W. (1977) Examination of the liquid line of descent of mare basalts in the light of data from melt inclusions in olivine. *Proc. Lunar Sci. Conf. 8th*, 1751-1765.
71135 78505
- Weiblen P.W. and Roedder E. (1976) Compositional interrelationships of mare basalts from bulk chemical and melt inclusions. *Proc. Lunar Sci. Conf. 7th*, 1449-1466.
70215 71135 71669 78505
- Weigand P.W. (1973) Petrology of a coarse-grained Apollo 17 ilmenite basalt. *EOS* 54, 621-622.
70035
- Wieler R., Etique P., Signer P., and Poupeau G. (1983) Decrease of the solar flare/solar wind flux ratio in the past several aeons deduced from solar neon and tracks in lunar soil plagioclases. *Proc. Lunar Planet. Sci. Conf. 13th*, A713-A724.
79035 79135
- Wiens R.C., Burnett D.S., Neugebauer M., and Pepin R.O. (1991) A comparison of solar wind and solar system xenon abundances. *LPSC XXII*, 1503-1504.
79035
- Wiens R.C., Burnett D.S., Neugebauer M., and Pepin R.O. (1992) A comparison of solar wind and estimated solar system xenon abundances: A test for solid/gas fractionation in the solar nebula. *Proc. Lunar Planet. Sci.* 22, 153-159.
79035
- Willis K.J. (1985) Three lithologic units of 72275. *LPS XVI*, 910-911.
72275
- Winzer S.R., Nava D.F., Schuhmann S., Kouns C.W., Lum R.K.L., and Philpotts J.A. (1974) Major, minor and trace element abundances in samples from the Apollo 17 Station 7 boulder: Implications for the origin of early lunar crustal rocks. *Earth Planet. Sci. Lett.* 23, 439-444.
77115 77135 77075 77215
- Winzer S.R., Nava D.F., Schuhmann S., Lum R.K.L., and Philpotts J.A. (1975a) Origin of the Station 7 boulder: A note. *Proc. Lunar Sci. Conf. 6th*, 707-710.
72215 72255 72275 73215 76015 76315 77075 77115 77135
- Winzer S.R., Nava D.F., Lum R.K.L., Schuhmann S., Schuhmann P., and Philpotts J.A. (1975b) Origin of 78235, a lunar norite cumulate. *Proc. Lunar Sci. Conf. 6th*, 1219-1229.
78235
- Winzer S.R., Lum R.K.L., Schumann S., and Philpotts J.A. (1975c) Large ion lithophile trace element abundances in phases from 78235,34, a lunar norite cumulate. *LS VI*, 872-873.
78235
- Winzer S.R., Nava D.F., Schuhmann P.J., Schuhmann S., Lindstrom M.M., Lum R.K.L., Lindstrom D.J., and Philpotts J.A. (1976) Origin of melts, breccias and rocks from the Apollo 17 landing site. *LS VII*, 941-943.
77135 77215
- Winzer S.R., Nava D.F., Schuhmann P.J., Lum R.K.L., Schuhmann S., Lindstrom M.M., Lindstrom D.J., and Philpotts J.A. (1977) The Apollo 17 "melt sheet": Chemistry, age, and Rb/Sr systematics. *Earth Planet. Sci. Lett.* 33, 389-400.
77135 77215

- Wolf R., Woodrow A., and Anders E. (1979) Lunar basalts and pristine highland rocks: Comparison of siderophile and volatile elements. *Proc. Lunar Planet. Sci. Conf.* 10th, 2107-2130.
75055 72255 72275 76255 76535 77215
- Wood J.A. (1975) The nature and origin of Boulder 1, Station 2, Apollo 17. *The Moon* 14, 505-517.
72215 72235 72255 72275 72435 76055 76315 77135
- Yokoyama Y., Reyss J.L., and Guichard F. (1974) ^{22}Na - ^{26}Al chronology of lunar surface processes. *Proc. Lunar Sci. Conf.* 5th, 2231-2247
70017 70019 70135 70175 70185 70255 70275 71035 71135 71136 71155 71175 75035 75055 79155 72255
72415 72315 73215 73255 73275 76215 76255 76275 76295 77135 78135 78235 78505
- Zinner E., Walker R.M., Chaumont J., and Dran J.C. (1976a) Ion probe analysis of artificially implanted ions in terrestrial samples and surface enhanced ions in lunar sample 76215,77. *Proc. Lunar Sci. Conf.* 7th, 953-984.
76215
- Zinner E., Walker R.M., Chaumont J., and Dran J.C. (1976b) Ion probe analysis of artificially implanted ions in terrestrial samples and solar wind implanted ions in lunar surface samples. *LS VII*, 965-967.
76215
- Zinner E., Walker R.M., Chaumont J., and Dran J.C. (1977a) Ion microprobe surface concentration measurements of Mg and Fe and microcraters in crystals from lunar rock and soil samples. *Proc. Lunar Sci. Conf.* 8th, 3859-3883.
76215
- Zinner E., Walker R.M., Chaumont J., and Dran J.C. (1977b) Surface enhanced elements and microcraters in lunar rock 76215. *LPS XVIII*, 1044-1046.
76215